

A study on aromatic carboxylic acids as ligands and receptors

*A Dissertation submitted to the
Indian Institute of Technology Guwahati as
partial fulfillment for the Degree of
Doctor of Philosophy in Chemistry*

Submitted by

Anirban Karmakar



Department of Chemistry

Indian Institute of Technology Guwahati

March 2009





Dedicated to My Parents...



Statement

I hereby declare that this thesis entitled “**A study on aromatic carboxylic acids as ligands and receptors**” is the outcome of research work carried out by me under the supervision of Prof. Jubaraj B. Baruah, at the Department of Chemistry, Indian Institute of Technology Guwahati, India.

In keeping with the general practice of reporting scientific observations, due acknowledgement has been made whenever work described here has been based on the findings of other investigators.

IIT Guwahati
March 19, 2009

Anirban Karmakar



Certificate

This is to certify that Anirban Karmakar has been working under my supervision since July, 2005 as a regular registered Ph. D. student. I am forwarding his thesis entitled “**A study on aromatic carboxylic acids as ligands and receptors**” being submitted for the Ph. D. (Science) Degree of this Institute.

I certify that he has fulfilled all the requirements according to the rules of this Institute regarding the investigations embodied in his thesis and this work has not been submitted elsewhere for a degree.

IIT Guwahati
March 19, 2009

Prof. Jubaraj B. Baruah



CERTIFICATE OF COURSE WORK

This is to certify that Anirban Karmakar has satisfactorily completed all the courses required for the Ph.D degree program. These courses include

CH 603:	Applied X-ray Crystallography
CH 627:	New Reagents for Organic Chemistry
CH 630:	Physical Methods in Chemistry
CH 632:	Bioinorganic chemistry

Anirban Karmakar has successfully completed his Ph.D qualifying examination in May 2006.

Prof. A. T. Khan
Head, Department of Chemistry
I. I. T. Guwahati

Dr. T. Punniyamurthy
Secretary, DPPC
I. I. T. Guwahati



Acknowledgements

The enlightening experience of doing science under the guidance of Prof. Jubaraj B. Baruah can hardly be described in words. The numerous discussions and interactions I had with him expanded my horizons to hitherto unknown frontiers of science and knowledge. I am indebt to this wonderful person for all that he has given me and above all for motivating me towards scientific research.

I would like to acknowledge my sincere gratitude to all my doctoral committee members, Dr. G. Krishnamoorthy, Dr. Gopal Das and Dr. Utpal Bora for their insightful advices and valuable suggestions. I am also grateful to the entire faculty and staff in the Department of Chemistry, Indian Institute of Technology Guwahati for providing a wonderful work atmosphere throughout this period.

I would like to thank my group members Rupam, Marjit, debendra, dip, Babulal Das and other group members Avijit, Harisadhan, Siva, Saitanya for their timely help, support and for the wonderful time we shared during this period. No words can express my thankfulness for giving me their time and companionship, which made the time spent in the laboratory pleasant and memorable. I would like to give my special thanks to my lab seniors Dr. Rupam Jyoti Sarma and Dr. Nilotpal Barooah with whom I had an opportunity to work.

I would like to thank Indian Institute of Technology for the research fellowship. The financial support from Council of Scientific and Industrial Research (CSIR), New Delhi in the form of SRF is duly acknowledged.

Finally, my Ph. D. endeavor could not be completed without the endless love, unending support, tolerance and blessings from my family. I wish to express my sincere gratitude to my parents, my brothers and sisters. They are the main soul and inspiration for each and every step that I achieve in my life.



Preview

Coordination chemistry of metal carboxylates are of great interest due to its potential applications in material and biological chemistry. Supramolecular architecture of metal carboxylates can be directly constructed with metal ions in various coordination geometries in combination with multifunctional ligands. The directional and molecular recognition properties of carboxylic acids and its derivatives are controlled by supramolecular interaction like hydrogen bonding, π - π stacking, weak electrostatic interactions and van der Waals forces. The thesis deals with the synthesis, characterization and structural aspects of some first row transition metal carboxylates along with the study of molecular/anion recognition properties of carboxylic acid derivatives. Thus, the research work carried out is basically focused on the synthesis, characterization, and structural elucidation along with understanding of physical properties such as fluorescence emission. The structural features are investigated with an objective to understand the factors, which control the formation of basic carboxylate frameworks or secondary building block units.

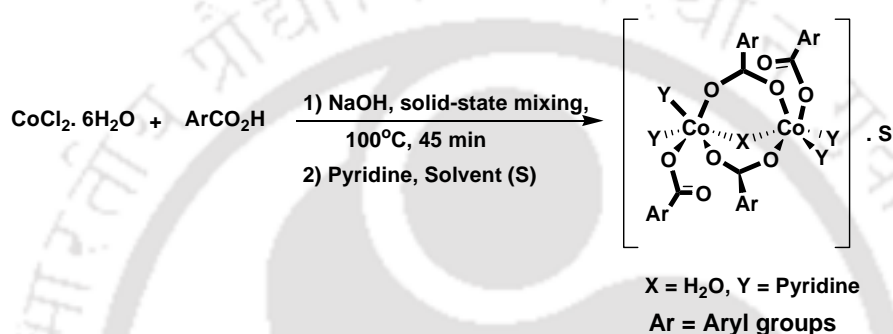
The content of the thesis is divided into six chapters which are described below.

Chapter 1: Introduction

In this chapter, a general state-of-art of the existing literature on various aspects related to the synthesis, structure and properties of various metal carboxylates are presented. This chapter also features discussion on several coordination polymers based on carboxylates, which are employed to design new open framework structures. Some biologically important metalloenzymes with carboxylate frameworks in its active sites are discussed. The gas storage, gas separation, molecular recognition, magnetic, and catalytic properties of porous metal organic framework having carboxylate ligands are also described. The challenging scope in carboxylate chemistry is to design multifunctional materials with predictable structures and properties, which is being emphasized in this chapter to make a perspective projection in the scope of work.

Chapter 2: Synthesis, structure and polymorphism in cobalt carboxylate complexes

Chapter 2 contains synthesis, characterization and structural studies of mono, di and tetranuclear cobalt(II) carboxylate complexes. To understand the synthetic and supramolecular behaviour of cobalt(II) carboxylate complexes, a series of carboxylate complexes are synthesized through solid and solution state synthetic paths (Scheme 1) and characterized them by different spectroscopic techniques along with single crystal X-ray crystallography.



Scheme 1

To understand the effect of synthetic methods on product formation, the structures of cobalt(II) carboxylate complexes obtained via solid state route with those obtained from solution state synthesis are compared. This study also leads to some important observations regarding the formation of three polymorphs of an aqua bridged dinuclear cobalt(II) complex with 2-nitrobenzoic acid. The polymorphism occurs in the complexes due to the relative orientations of the 2-nitrobenzoate groups, which are coordinated to the cobalt(II) centers.

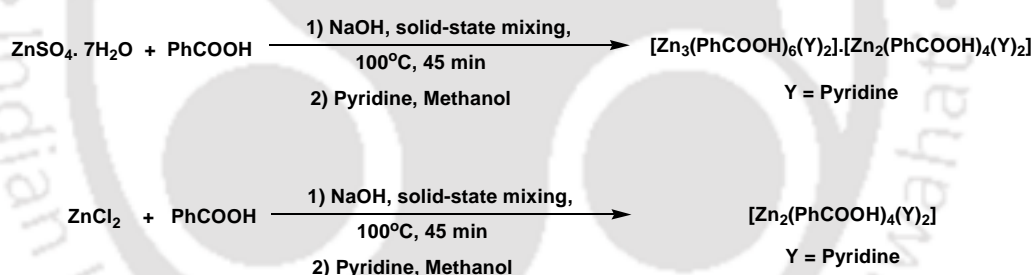
Chapter 3: Synthesis and structures of dinuclear nickel carboxylate complexes

This chapter of the thesis deals with the synthesis, characterization and structural features of different aqua bridged dinuclear nickel(II) carboxylate complexes. The synthesis of aqua bridged dinuclear nickel(II) carboxylate complexes are important due to its structural resemblance with certain biological metalloenzymes and these complexes are also used as secondary building block units of metal organic frameworks. With these objectives a variety of aqua bridged dinuclear nickel(II) carboxylate complexes through solid state synthetic procedure are synthesized. All

these complexes are also characterized by single crystal X-ray diffraction. The structural study on these aqua-bridged complexes reveals the inclusion of different types of solvent molecules in the complexes which leads to the formation of different pseudo-polymorphs. The role of substituent on the aromatic ring during the solid state synthesis of nickel carboxylate complexes is envisaged.

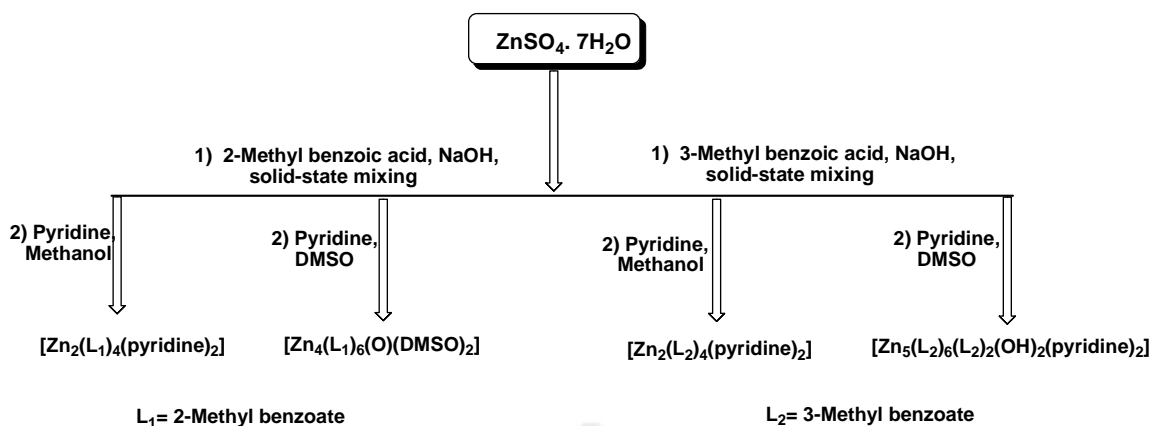
Chapter 4: Synthesis and characterization of zinc carboxylate complexes through solid state reactions

This chapter describes the synthesis and structure of zinc carboxylate complexes obtained via solid state strategy. Zinc carboxylate complexes are important for their relevance to biological system and some of them can also be used as effective catalysts for organic transformations. Mono, di and multinuclear zinc carboxylate complexes are synthesized by applying similar solid state synthetic procedure. This study enabled us to unearth the effect of salt, substituent on the aromatic ring and solvent of crystallization.



Scheme 2

The reactions of benzoic acid or sodium salt of substituted benzoic acids with zinc(II) sulphate heptahydrate or zinc(II) chloride followed by dissolution of the reaction mixture in methanol or dimethyl sulphoxide in the presence of pyridine leads to different zinc carboxylate complexes. The solid state reaction of zinc(II) sulphate heptahydrate with benzoic acid in presence of pyridine leads to a self-assembled dinuclear and trinuclear zinc benzoate complex (Scheme 2). Polar and protic solvent like methanol leads to paddle-wheel dinuclear zinc(II) carboxylate complexes. Polar and aprotic solvent like dimethyl sulphoxide leads to tetra and pentanuclear zinc carboxylates complexes (Scheme 3).



Scheme 3

Chapter 5: Structural studies and metal complexation of flexible carboxylic acid and its derivative

The synthesis of metal carboxylate with flexible aromatic carboxylic acid systems are described in chapter 5.

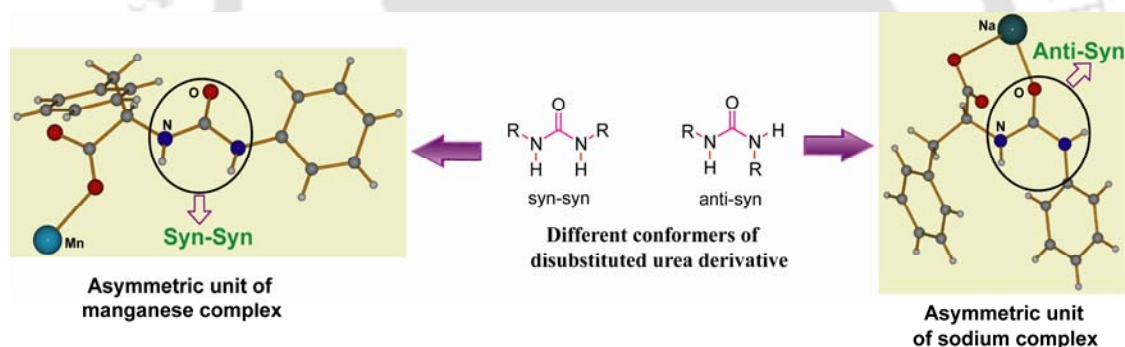


Figure 1

Synthesis of 3-phenyl-2-(3-phenyl-ureido)-propionic acid, containing urea unit is described in this chapter. It is found that in sodium complex the urea part of the ligand orient in an anti-syn conformation but in manganese complex it is in syn-syn orientation as shown in Figure 1. Such anti-syn conformation occurs due to the puckering of the ligand on co-ordination to the metal.

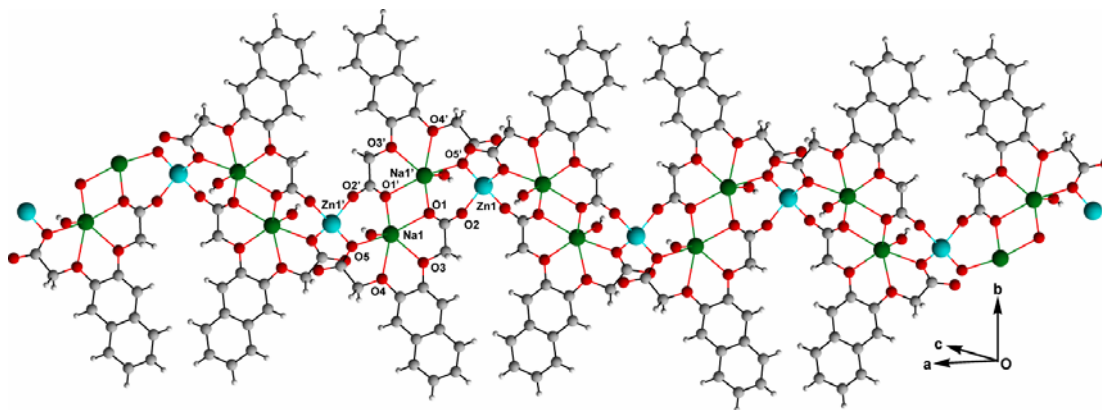


Figure 2

The role of weak intermolecular interactions in the polymorphic behavior of (3-methoxycarbonylmethoxy-naphthalen-2-yloxy) acetic acid and its methyl ester are described. The coordination chemistry of zinc with (3-carboxymethoxynaphthalen-2-yloxy) acetic acid in presence or absence of auxiliary ligands leading to one dimensional co-ordination polymer or dinuclear zinc carboxylate complexes which binds sodium ions due to formation of macrocycle like structure (Figure 2) are presented. Besides these, preparation of different types of mononuclear complexes, one dimensional coordination polymers and tetranuclear zinc metallamacrocycle by changing the reaction conditions are described.

Chapter 6: Structural aspects and acid/anion recognition properties of carboxylic acid derivatives

Acid or anion recognition is an important process in nature, being involved in the catalytic activity of enzymes, in the transfer of genetic information, and in ion transport through membrane channels etc. Characterization of some 8-hydroxyquinoline based amides and study of their structural and acid recognition properties in solid and solution state are described in chapter 6. The acid binding properties of three amides (Figure 3) namely N-cyclohexyl-2-(quinolin-8-yloxy) acetamide, N-(2,6-dimethylphenyl)-2-(quinolin-8-yloxy) acetamide, N-[2-(4-methoxy-phenyl)-ethyl]-2-(quinolin-8-yloxy)acetamide are presented.

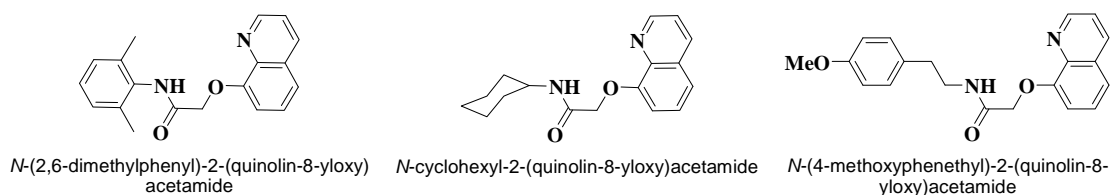


Figure 3

The receptor molecules namely *N*-(2,6-dimethylphenyl)-2-(quinolin-8-yloxy)acetamide and *N*-cyclohexyl-2-(quinolin-8-yloxy)acetamide lead to the formation of self-assembled dimers (assemblies) in the presence of suitable guest molecules. The head-to-tail and head-to-head orientations of the host molecules can describe the structure of these assemblies. *N*-cyclohexyl-2-(quinolin-8-yloxy)acetamide in presence of mineral acid such as sulphuric acid, hydrochloric acid, and perchloric acid led to the formation of gel and analogous compounds are self-assembled to give hydrogen bonded assembly in the presence of water or a suitable guest anion such as sulphate or perchlorate but does not lead to gels. The gel formation is facilitated by non-planar anions. The planar anions such as nitrate and carboxylate are not suitable for gelation in these cases. We have also synthesized and characterized various pseudo-polymorphs of *N*-[2-(4-methoxy-phenyl)-ethyl]-2-(quinolin-8-yloxy)acetamide. A clear distinction between the protonated and hydrogen bonded state of *N*-[2-(4-methoxy-phenyl)-ethyl]-2-(quinolin-8-yloxy)acetamide is made by fluorescence spectroscopy.

Contents

Statement

Certificate

Acknowledgements

Preview

Chapter 1: Introduction	1
Chapter 2: Synthesis, structure and polymorphism in cobalt carboxylate complexes	55
Chapter 3: Synthesis and structures of dinuclear nickel carboxylate complexes	89
Chapter 4: Synthesis and characterisation of zinc carboxylate complexes through solid state reactions	105
Chapter 5: Structural studies and metal complexation of flexible carboxylic acids and its derivative	121
Chapter 6: Structural aspects and acid/anion recognition properties of carboxylic acid derivatives	157
Appendix	203
References	233
List of Publications	

Chapter 1

Introduction

1.1 General features of carboxylic acids

The carboxyl group containing compounds are called carboxylic acids and they are widely studied in chemistry¹. They have found important place in biology², supramolecular chemistry³ and material science⁴. Depending on the alkyl or aryl groups present, they are classified as aliphatic or aromatic carboxylic acid (Figure 1.1).

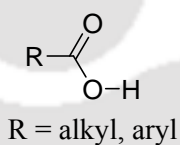
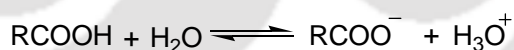


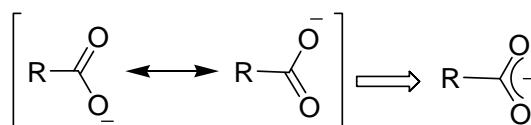
Figure 1.1

Carboxylic acids are widespread in nature and are typically weak acids. They partially dissociate into H_3O^+ cations and RCOO^- anions in aqueous solution, as shown in Equation 1.1.



Equation 1.1

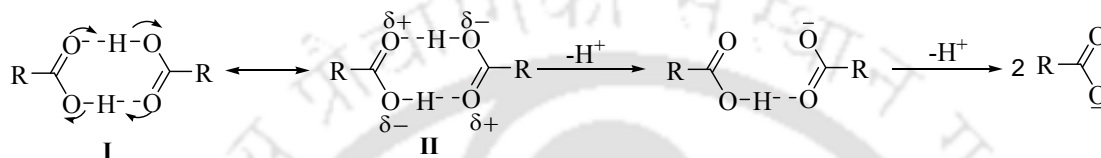
The conjugate base of carboxylic acids, namely carboxylate anions, is stabilized by inductive or resonance effects (Scheme 1.1). The resonance effect is also useful to explain the inherent acidity of carboxylic acids. Each of the carbon-oxygen bonds of carboxylate anion has partial double-bond character. Since the conjugate base is stable, the equilibrium in Equation 1.1 lies more towards the right.



Scheme 1.1

The acidity of carboxylic acids can also be attributed to the two electronegative oxygen atoms attached to carbon centers which distorts the electron clouds around the O–H bond and weakens the O–H bond. Due to the weak O–H bond strength the hydrogen atom attached to oxygen is labile and it dissociates easily to give the H^+ ion.

In solid state or in a concentrated solution, carboxylic acids adopt dimeric structure due to strong hydrogen bonding⁵⁻⁶. Such dimers can be sequentially deprotonated by supramolecular interactions leading to carboxylate anion⁷ (Equation 1.2).



Equation 1.2

The exceptionally strong hydrogen bonding in carboxylic acids can be explained by the large contribution of the ionic canonical form II. Carboxylic acids are easily characterized by infrared spectroscopy⁸. The C=O group in monomers of saturated aliphatic carboxylic acids appears near 1760 cm^{-1} and in dimeric saturated aliphatic acids it appears at $1720\text{-}1706\text{ cm}^{-1}$. Aromatic carboxylic acids show absorption for dimer in the $1710\text{-}1680\text{ cm}^{-1}$ region. Carboxylic acid dimers display very broad, intense O–H stretching absorption in the region $3300\text{-}2500\text{ cm}^{-1}$. The C–O stretching band for monomers and dimers appears at $1320\text{-}1210\text{ cm}^{-1}$ and $1315\text{-}1280\text{ cm}^{-1}$ respectively. In-plane C–O–H bending absorption appears at $1440\text{-}1395\text{ cm}^{-1}$. The carboxylate anion has two strongly coupled carbon oxygen bonds with bond strengths intermediate between C=O and C–O. Such phenomenon is reflected in appearance of two bands in the IR spectra; a strong asymmetric stretching band near $1650\text{-}1550\text{ cm}^{-1}$ and a weak symmetric stretching band near 1400 cm^{-1} .

1.2 Coordination modes of carboxylic acids

The carboxylate ligand binds to metal ions in various binding modes viz. monodentate, bridging bidentate, symmetric chelating, bidentate chelate bridging etc. The different binding modes of carboxylate anion with metal ions are illustrated in Figure 1.2. Versatile binding modes of carboxylates make them attractive. It is a challenge to make different metal carboxylate motifs in a predictable manner⁹⁻¹⁰. Several structural motifs based on carboxylates are employed to design new open framework structures¹¹⁻¹³. Due to multiple possibilities of

coordination the simplest carboxylic acids, such as formic acid and acetic acid can be used to construct complicated high dimensional frameworks¹⁴⁻¹⁵. Some of the commonly observed structural motifs are shown in Figure 1.3. Carboxylate ligands can provide rigid frameworks due to its ability to aggregate metal ions into M-O-C polynuclear units, which are referred to as secondary building units (SBU). Yaghi and coworkers have shown that the secondary building units, can be used as molecular building blocks to construct well defined orientations¹⁶.

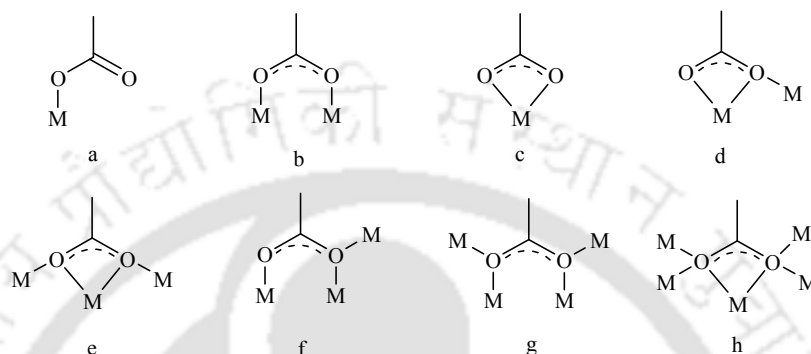
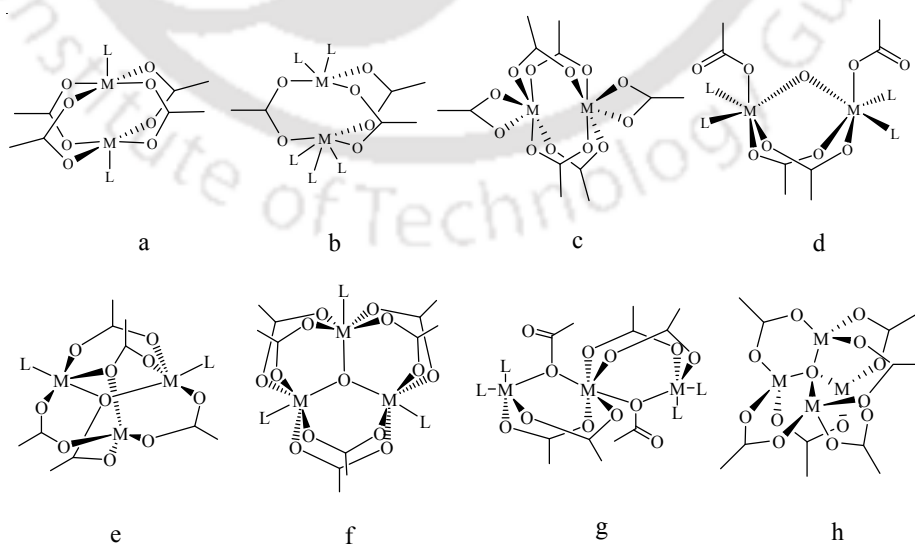


Figure 1.2 Different binding modes of carboxylate anion

The secondary building units are sufficiently rigid because the metal ions are locked into their positions by the carboxylates. Thus, instead of using one transition metal ion at a network vertex, the SBUs serve as large rigid vertices to produce extended frameworks of high structural stability. Several cluster motifs shown in Figure 1.3 serve as secondary building units. The core structure of secondary building units are defined by the atoms present therein and the extension of secondary building units to well defined orientations are dependent upon the linker.



Where M= Metal ions and L= Ligand

Figure 1.3 Some commonly observed structural motifs of metal carboxylates

Moreover the atoms in core structure define the underlying geometry of the secondary building units; they are relevant in predicting the overall topology of the modular network. In this chapter we will take examples of first row transition metal carboxylates with a systematic description of mononuclear to polynuclear carboxylate complexes.

1.3 Mono and multinuclear carboxylate complexes of first row transition metals

Mono as well as polynuclear carboxylate complexes of first row transition metals are widely investigated. These transition metal complexes are used as biomimetic models of some enzymes¹⁷. Some polynuclear carboxylate complexes behave as single-molecule magnets at low temperature. Besides that 1D, 2D, or 3D magnetic ordering takes place in carboxylate containing compounds. The carboxylate complexes catalyze different organic reactions by providing sites for organic substrates to coordinate in polymetallic centers, causing activation of functional groups of the substrate¹⁸⁻¹⁹. Due to the wide diversity of mono and polynuclear carboxylates, some specific examples of mono and multinuclear carboxylates are presented below.

1.3.1 Mononuclear metal carboxylates:

Mononuclear carboxylates of first row transition metals are well known. In mononuclear complexes monodentate and chelating binding modes of carboxylate are commonly observed. A mononuclear complex $[\text{Co}(\text{bpee})_2(6\text{-me-2,3-pyrdcH})_2]$ (**1.1**), where bpee is 1,2-bis(4-pyridyl) ethylene and 6-me-2,3-pyrdcH₂ is 6-methyl-2,3-pyridine dicarboxylic acid, was prepared by the reaction of cobalt(II) nitrate with 6-methyl-2,3-pyridine dicarboxylic acid and 1,2-bis(4-pyridyl) ethylene²⁰.

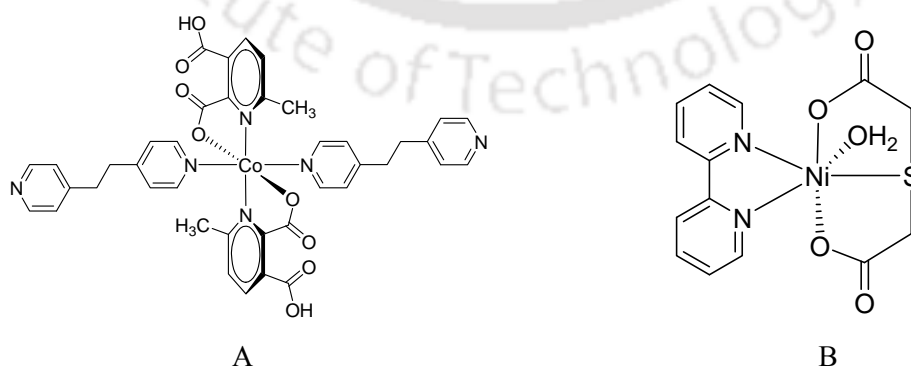


Figure 1.4 A) Mononuclear cobalt complex (**1.1**) of 6-methyl-2,3-pyridine dicarboxylic acid, B) Structure of mononuclear nickel complex (**1.2**) with thiodiglycolate

In this complex one proton of 6-methyl-2,3-pyridine dicarboxylic acid is deprotonated and the deprotonated carboxylate anion is coordinated to the cobalt center (Figure 1.4A). The free carboxylic acid group is involved in hydrogen bonding with nitrogen atoms of 1,2-bis(4-pyridyl) ethylene leading to a two dimensional rectangular grid with dimension of 12.8 X 16.3 Å.

The reaction of $[\text{Ni}(\text{tdga})(\text{H}_2\text{O})_3]$ with 2,2'-bipyridine gives a mononuclear nickel complex with composition $[\text{Ni}(\text{tdga})(\text{H}_2\text{O})(2,2'\text{-bipyridine})].4\text{H}_2\text{O}$ (**1.2**), where tdga is thiodiglycolate anion²¹. The nickel center in the complex has distorted octahedral geometry (Figure 1.4B). Similar type of zinc complex with thiodiglycolic acid is reported in literature²².

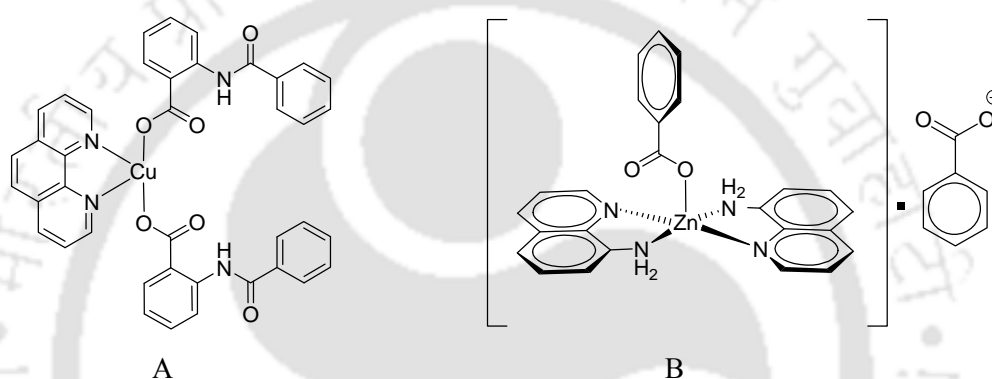


Figure 1.5 A) Copper complex (**1.3**) with N-benzoylanthranilic acid and 1,10-phenanthroline, B) Penta co-ordinated mononuclear zinc complex (**1.4**)

The reaction of $\text{Cu}(\text{OCH}_3)_2$ with N-benzoylanthranilic acid and 1,10-phenanthroline leads to a mononuclear complex $[\text{Cu}(\text{N-benzoylanthranilate})_2(1,10\text{-phenanthroline})]$ (**1.3**). In this complex the overall geometry around the four-coordinate copper ion has a distorted tetragonal geometry²³ as shown in Figure 1.5A. A penta co-ordinated mononuclear $[\text{Zn}(\text{8-aminoquinoline})_2(\text{benzoato})].\text{benzoate}$ (**1.4**) complex is reported (Figure 1.5B). In this complex one of the benzoate groups is coordinating and other benzoate group is a free anion. The complex has a square pyramidal geometry with a benzoate anion outside the coordination sphere²⁴. Similar type of penta coordinated zinc complex with 2-nitrobenzoic acid and 8-aminoquinoline is also reported in literature²⁵.

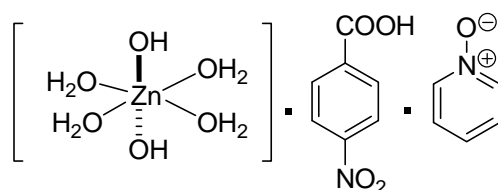


Figure 1.6 Three components molecular complex of zinc (**1.5**)

The reaction of zinc acetate with 4-nitrobenzoic acid and pyridine *N*-oxide gives a three component molecular complex $[\text{Zn}(\text{H}_2\text{O})_4(\text{OH})_2] \cdot 4\text{-NO}_2\text{C}_6\text{H}_5\text{COOH} \cdot \text{C}_6\text{H}_5\text{NO}$ (**1.5**). In this complex the zinc center has octahedral geometry and the complex is stabilised by extensive hydrogen bonding with carboxylic acid and pyridine *N*-oxide²⁶ (Figure 1.6).

1.3.2 Dinuclear metal carboxylates:

Various types of dinuclear metal carboxylates are reported in literature. Some examples are described in the following subsection. Dinuclear metal carboxylates are important from structural, magnetic and biological point of view. For example, oxobis(carboxylato)-bridged dimanganese(III) complex, $[\text{Mn}_2\text{O}(\text{O}_2\text{CCH}_3)_2\{\text{HB}(\text{pz})_3\}_2]$ (**1.6**), where $\text{HB}(\text{pz})_3^-$ is hydrotris(1-pyrazolyl)borate, has a di-manganese(III) core. This complex is important from biological point of view²⁷. In this complex two six-coordinated manganese sites are bridged by a μ -oxo and two μ -acetato groups. The remaining coordination sites are capped by two tridentate $\text{HB}(\text{pz})_3^-$ ligands (Figure 1.7A). This complex shows antiferromagnetic coupling among the two manganese(III) centers. Similar type of core has been obtained by the use of 1,4,7-triazacyclononan instead of hydrotris(1-pyrazolyl)borate²⁸.

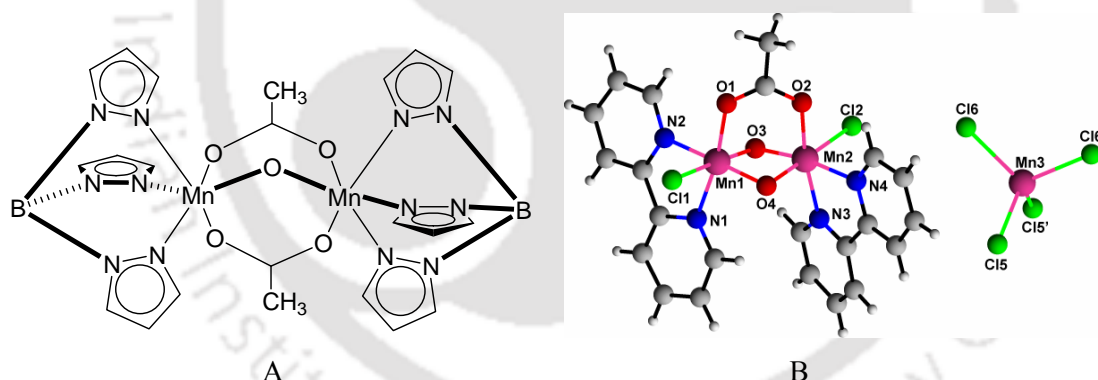


Figure 1.7 A) Dinuclear oxo bridged manganese carboxylate complex (**1.6**), B) Crystal structure of di-oxo acetate bridged dinuclear manganese complex (**1.7**)

Dinuclear manganese(IV) complex containing the $[\text{Mn}^{\text{IV}}_2(\mu\text{-O})_2(\mu\text{-O}_2\text{CMe})]^{3+}$ core with halide ions as terminal ligands are reported in literature. An example of such complex is $[\text{Mn}_2\text{O}_2(\text{O}_2\text{CMe})\text{Cl}_2(2,2'\text{-bipyridine})_2]_2[\text{MnCl}_4]$ (**1.7**). It has an oxo and carboxylate bridged dimeric core²⁹ (Figure 1.7B). Et_4N^+ salts of the $[\text{Fe}_2(\text{AcO})_5(\text{H}_2\text{O})(\text{pyridine})_2]^-$ (**1.8**), belongs to a class of asymmetric μ -aqua bis(μ -acetato) bimetallic complexes³⁰. The anion of complex **1.8** has an asymmetric dinuclear core with two bridging acetate ligands and a bridging water molecule (Figure 1.8A). Similar types of dimetallic cores are also obtained with

manganese(II) and cobalt(II) salts. A large number of dinuclear complexes having aqua and carboxylate bridges are known in literature³¹⁻³³. One typical example is $[\text{Co}_2(\mu\text{-H}_2\text{O})(\mu\text{-OOCCH}_3)_4(\text{tmen})_2]$ (**1.9**), where tmen is N,N,N',N'-tetramethylethane-1,2-diamine³⁴. In this complex apart from the two bridging carboxylates, two monodentate carboxylates are also present. The bidentate tmen ligand completes the octahedral geometry around each metal ion. The bridging aqua ligand is involved in intramolecular hydrogen bonding with carboxylate oxygen.

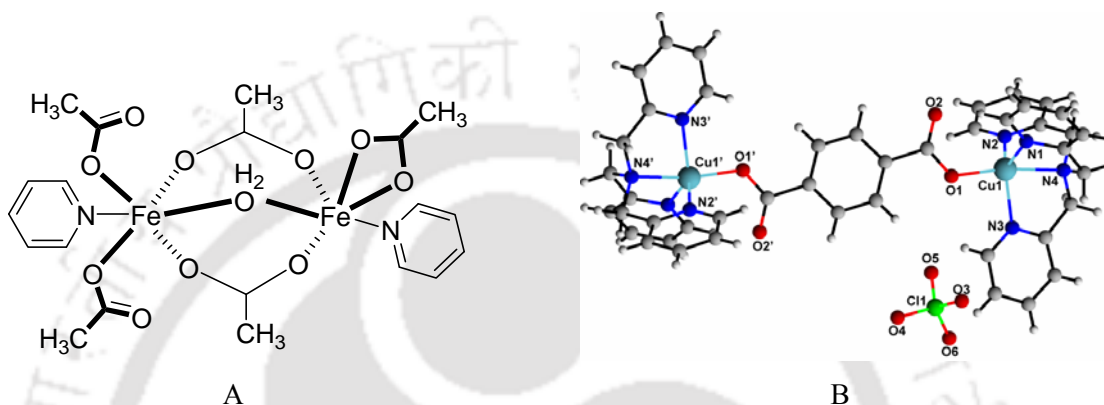


Figure 1.8 A) Aqua bridged dinuclear iron carboxylate complex (**1.8**), B) Dimeric copper(II) complex (**1.10**) with bridging terephthalate dianion

Apart from aquo, hydroxo and oxo bridged dimetallic carboxylate complexes are also well-established. A hydroxo bridged dinuclear copper(II) complex can be prepared by the reaction of copper(II) benzoate with N,N,N',N'-tetramethylethane-1,2-diamine (tmen) in methanol followed by addition of NH_4PF_6 . The copper atoms in the complex are bridged by a hydroxo and two carboxylate groups. The other coordination sites are occupied by the bidentate chelating tmen. The copper ions have distorted square-pyramidal geometry³⁵.

The structure of the complex $[\text{Cu}_2(\text{tpa})_2(\mu\text{-tp})](\text{ClO}_4)_2 \cdot \text{H}_2\text{O}$ (**1.10**), where tp is terephthalate dianion and tpa is tris(2-pyridylmethyl) amine, consist of bridging terephthalate dianion between two copper(II) centers in a bis(monodentate) bonding fashion. The coordination geometry around the copper(II) ions in this compound is distorted trigonal bipyramidal (Figure 1.8B). Four of the coordination sites are occupied by nitrogen atoms of tris(2-pyridylmethyl) amine and one by the oxygen atom of carboxylate ligand³⁶. The dinuclear copper complex having aqua and hydroxyl bridging ligand, can be prepared by the reaction of copper(II) salt with ethyl acetic acid and 2,2'-bipyridine. In this complex the coordination environment around each copper(II) ion is distorted square pyramidal³⁷. Similar type of copper(II) dinuclear core having both aqua and halogen bridge are reported in literature³⁸.

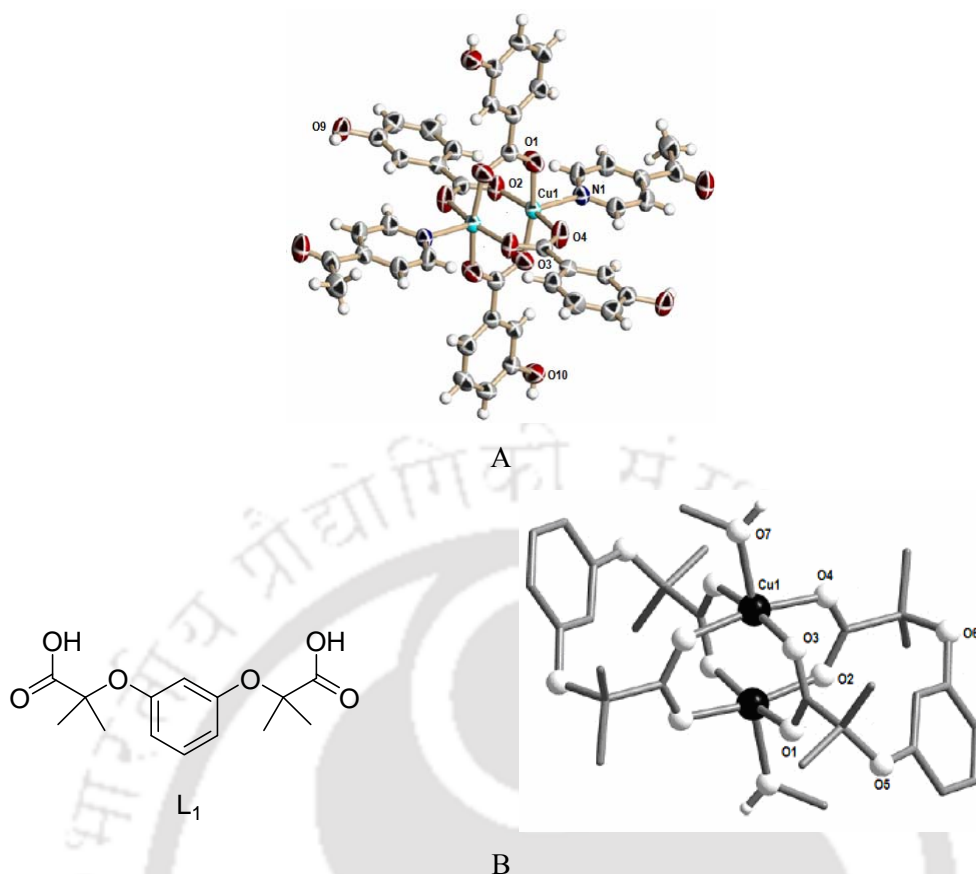


Figure 1.9 A) Paddle-wheel copper complex (**1.11**) with 3-hydroxybenzoic acid, B) Bischelate dinuclear complex (**1.12**) of copper with the ligand L₁

Paddle-wheel geometry is one of the most common geometry in dinuclear carboxylate complexes, the simplest example of such complex is copper(II) acetate. The reaction of Cu(BF₄)₂ with 3-hydroxybenzoic acid in presence of 4-acetyl pyridine gives a paddle-wheel dinuclear complex [Cu₂(μ-O₂CC₆H₄OH)₄(4-acpy)₂].6H₂O (**1.11**), where 4-acpy is 4-acetyl pyridine. The structure consists of centro-symmetric dinuclear paddle-wheel units with square pyramidal coordination geometry around the copper centers³⁹ (Figure 1.9A). Reaction of copper(II) acetate with 2-[3-(1-carboxy-1-methylehoxy)-phenoxy]-2-methyl-propionic acid (L₁) leads to a bischelate complex [Cu₂(L₁)₂].2MeOH (**1.12**) with normal paddle-wheel structure⁴⁰ as shown in Figure 1.9B. A dicarboxylic acid (L₂) having bolaamphiphile-like aromatic head groups and diol spacer react with copper(II) acetate to give a paddle-wheel complex [Cu(L₂).EtOH]₂ (**1.13**). Each metal center in the dimeric unit has a square-pyramidal geometry with the square base provided by carboxylate oxygen atoms and the apical coordination is provided by ethanol molecules⁴¹ (Figure 1.10B). Many other paddle-wheel copper(II) carboxylate complexes with different acids are reported in literature⁴²⁻⁴³.

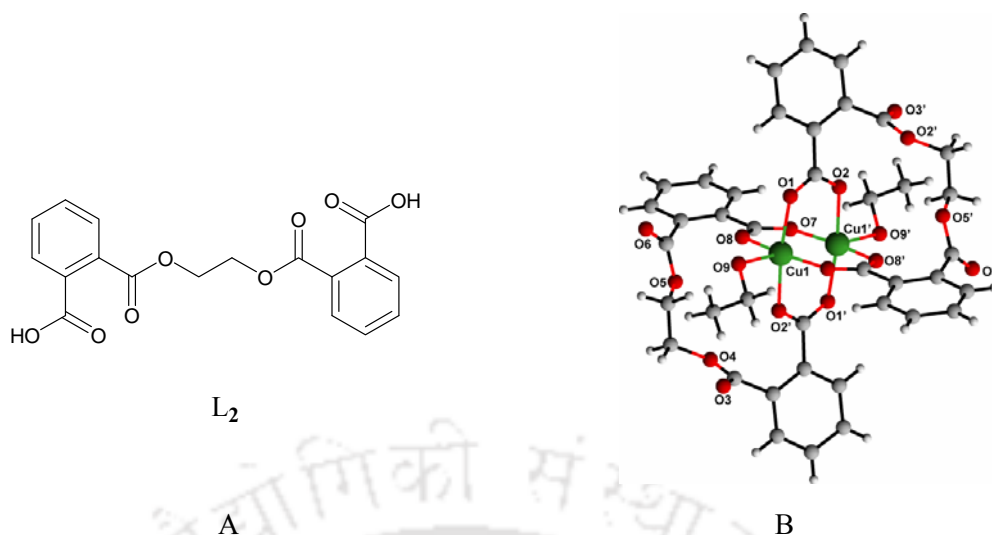


Figure 1.10 A) Structure of dicarboxylic acid (L_2), B) Crystal structure paddle-wheel dinuclear copper complex (**1.13**)

Several dinuclear zinc carboxylate complexes are models for phosphodiesterase. For example, the complex obtained from the reaction of 2,6-bis{[(2-pyridylmethyl)(2-hydroxyethyl)amino]methyl}-4-methylphenol with zinc acetate gives a model complex⁴⁴, which contains a μ -acetato- μ -cresolato-dizinc(II) core. The core has quasi-trigonal bipyramidal zinc and distorted octahedral zinc centers. The distance between two zinc centers in the complex is 3.421 Å which is close to the di-zinc distance in related natural metalloenzymes. Paddle-wheel zinc carboxylate complex is prepared by the solid state reaction of zinc(II) acetate with 2-nitrobenzoic acid and 2-aminopyridine²⁵. A square pyramidal geometry is formed around each zinc atom. The distance between the two zinc centers in this paddle-wheel structure is 3.01 Å.

1.3.3 Trinuclear metal carboxylates:

Trinuclear metal carboxylates of first row transition metals have extensive application in the field of magnetic materials. As for example, triangular manganese(II) core in $[Mn_3(Me_3CCO_2)_6(Me_3CCO_2H)_5] \cdot 2(Me_3CCO_2H)$ (**1.14**), is prepared by the reaction of manganese (II) carbonate with pivalic acid. The structure consists of a triangle of hexa-coordinate manganese(II) ions bridged by two pivalates. The edges of the triangle are bridged by three other pivalates. The remaining positions of Mn(II) site are occupied by two molecules of pivalic acid (Figure 1.11A). The magnetic exchange within the triangle in the complex is extremely weak and the complex shows antiferromagnetic behaviour⁴⁵.

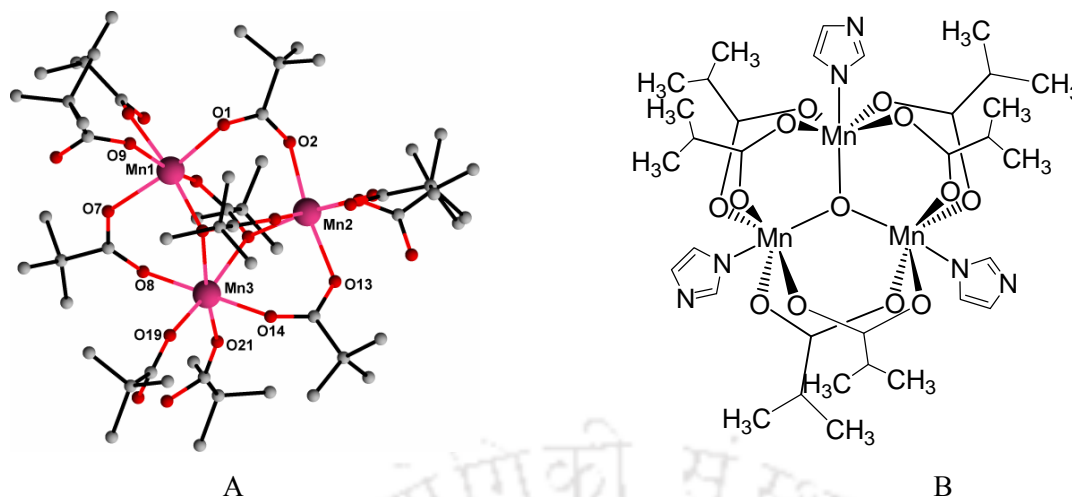


Figure 1.11 A) Trinuclear manganese(II) complex (**1.14**) with pivalic acid, B) Oxo centred trinuclear manganese complex (**1.15**)

Mixed-valence carboxylato bridged oxo-centered trinuclear manganese complexes can be prepared by reaction of mononuclear manganese(III) carboxylate complex with pyridine or pyridine derivatives⁴⁶⁻⁴⁸. The complex, $[\text{Mn}_3\text{O}(\text{Pr}^i\text{COO})_6(\text{imidazole})_3] \cdot 3\text{Pr}^i\text{COOH}$ (**1.15**), is an example of oxo-centred trinuclear cluster of manganese containing imidazole ligand⁴⁹. This complex has manganese in slightly distorted octahedron geometry. Four oxygen atoms from bridging isobutyrate groups, one bridging oxo group and a terminal imidazole nitrogen atom makes the hexa coordination environment around each metal centers (Figure 1.11B).

Oxo-centered single-valence manganese(III) carboxylate cluster $[\text{Mn}_3\text{O}(\text{O}_2\text{CMe})_3(\text{mpko})_3](\text{ClO}_4)$ (**1.16**), is prepared from the reaction of $[\text{Mn}_3\text{O}(\text{O}_2\text{CMe})_6(\text{pyridine})_3](\text{ClO}_4)$ with methyl 2-pyridyl ketone oxime (mpkoH). This complex shows ferromagnetic exchange interactions between the three Mn(III) ions. The structure of the complex⁵⁰ is shown in Figure 1.12A. By multi-high-frequency single-crystal EPR study⁵¹, it is recently shown that this complex is a single-molecule magnet with a spin ground state of $S = 6$.

The reaction of iron(II) acetate with bidentate nitrogen donor ligands like phenanthroline affords a trinuclear complex. This complex has a linear structure, with one monodentate and two bridging bidentate carboxylate ligands spanning each pair of metal atoms⁵². The trinuclear complex $[\text{Co}_3(\text{C}_6\text{H}_5\text{COO})_6(\text{pyridine})_2]$ (**1.17**), is prepared by the reaction of cobalt(II) nitrate with benzaldehyde in presence of pyridine⁵³. The structure of this complex consists of a centrosymmetric trimetallic unit with the central cobalt ion on an inversion center in an octahedral coordination sphere, and coordinated by six oxygens from six benzoate ions acting as bridging ligands. The peripheric cobalt ions are surrounded by four

oxygen atoms and one nitrogen atom and have distorted bipyramidal geometry (Figure 1.12B). Similar trinuclear cobalt(II) carboxylate complexes with acetate, crotonate and benzoate are also reported in literature⁵⁴⁻⁵⁷.

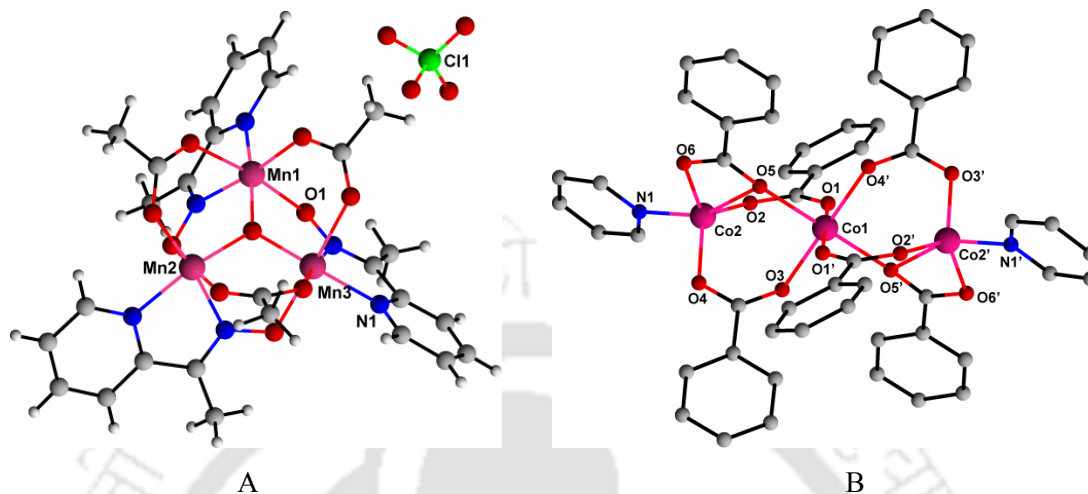


Figure 1.12 A) Structure of oxo-centered single valence manganese carboxylate cluster (**1.16**), B) Crystal structure of trinuclear cobalt(II) carboxylate complex (**1.17**)

1.3.4 Tetranuclear metal carboxylates:

Tetranuclear metal carboxylates are of great importance because they have substantial impetus for developments in several fields, including bioinorganic chemistry, magnetochemistry, material chemistry and solid-state physics. In the bioinorganic area, tetranuclear manganese clusters are integral components in the photosystem II which is the reaction center of green plants. Tetranuclear manganese $[\text{Mn}_4(\mu_3\text{-O})_2]^{8+}$ core bound to carboxylates, can be prepared by various synthetic procedures⁵⁸⁻⁵⁹. These cores consist of four manganese atoms, present in butterfly orientation and the carboxylate groups are coordinated to manganese atoms in bridging and chelating modes. The $[\text{Mn}_4\text{O}_3(\text{O}_2\text{C-C}_6\text{H}_4\text{-CH}_3)_4(\text{dibenzoylmethane})_3]$ (**1.18**), is prepared by controlled potential electrolysis⁶⁰ (Figure 1.13A). By applying controlled potential electrolysis a complex containing $[\text{Mn}_4(\mu_3\text{-O})_2]^{8+}$ core can be converted to a complex containing $[\text{Mn}_4(\mu_3\text{-O})_3]^{7+}$ core⁶¹. Tetranuclear manganese complexes with mixed-valence states are well known. For example, $[\text{Mn}_4\text{O}_2(2\text{-chlorobenzoato})_7(2,2'\text{-bipyridine})_2]$ (**1.19**) complex which contains one manganese (II) and three manganese(III) metal centers in to its core. In this complex manganese ion has distorted octahedral geometry⁶² as shown in Figure 1.13B. The complex having $[\text{Mn}_4\text{O}_3]$ core with halogen are also known in literature⁶³.

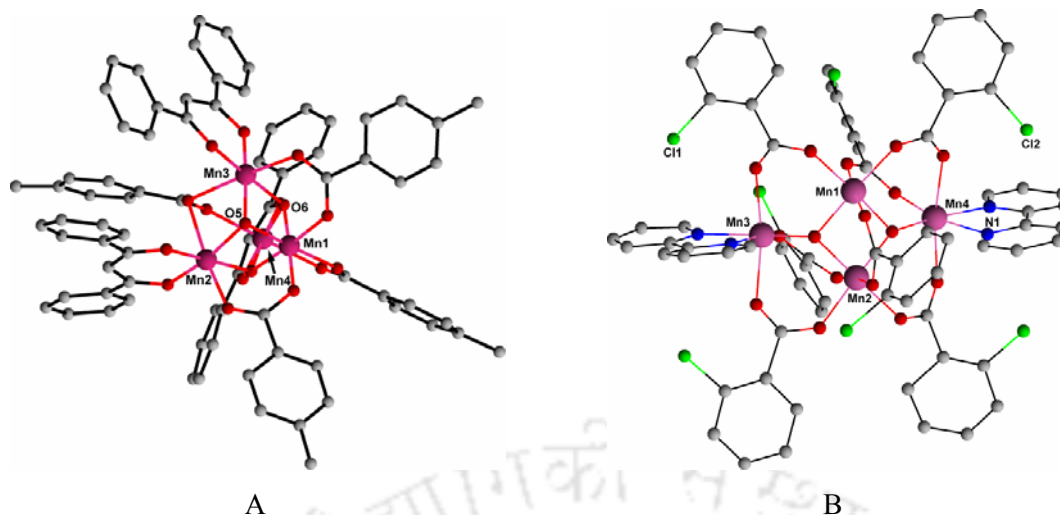


Figure 1.13 A) Structure of tetranuclear manganese carboxylate complex (**1.18**), B) Mixed-valence tetranuclear manganese complex (**1.19**), with 2-chlorobenzoic acid and 2,2'-bipyridine

The reaction between $\text{Fe}(\text{ClO}_4)_3 \cdot 6\text{H}_2\text{O}$, sodium acetate and 1,10-phenanthroline leads to a complex $[\text{Fe}_4(\text{OHO})(\text{OH})_2(\text{O}_2\text{CMe})_4(1,10\text{-phenanthroline})_4](\text{ClO}_4)_3$ (**1.20**). One oxo group and two acetate ligands form bridge between the metal centers (Figure 1.14A). The iron(III) centers are also bridged by a single OH^- group and a chelating phenanthroline molecule completes a distorted octahedral coordination at each metal ion⁶⁴. A good numbers of tetranuclear iron(III) carboxylate complexes with different carboxylate ligands are also reported in literature⁶⁵⁻⁶⁸.

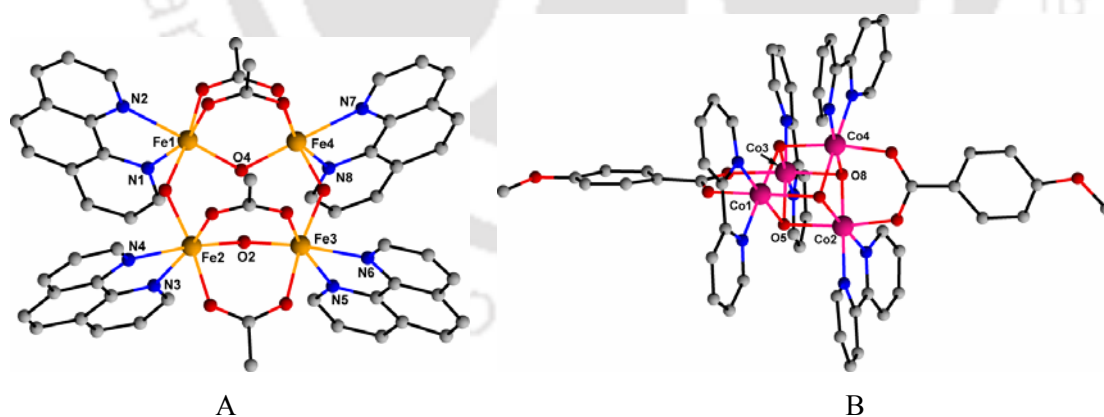


Figure 1.14 A) Crystal structure of tetranuclear iron(III) carboxylate complex (**1.20**) with acetate bridged, B) Tetranuclear cobalt(III) complex (**1.21**) with cubane type geometry

Tetranuclear cobalt(III) cores with cubane type geometry are formed with the aid of carboxylates. They have potential application in photochemical water oxidation. The complex $[\text{Co}_4\text{O}_2(\text{OH})_2(\text{O}_2\text{CC}_6\text{H}_4\text{-}p\text{-OMe})_2(2,2'\text{-bipyridine})_4](\text{ClO}_4)_4$ (**1.21**), contains distorted-cubane

type of core⁶⁹. In this complex the peripheral ligation is provided by chelating 2,2'-bipyridine and bridging carboxylate groups. The cobalt(III) atom has hexa-coordinate octahedral geometry (Figure 1.14B). Different types of tetranuclear cobalt(III) complexes containing a complete cubane cores such as $[\text{Co}_4\text{O}_4]^{4+}$ and $[\text{Co}_4\text{O}_3(\text{OH})]^{4+}$ are reported in literature⁷⁰⁻⁷². A tetranuclear cobalt(II) carboxylate complex can be prepared by the reaction of cobalt(II) acetate with di-2-pyridyl ketone $[(\text{py})_2\text{CO}]$. This complex has tetranuclear cubane like structure. The alternating non-metal vertices of the cube are occupied by four deprotonated oxygen atoms of $(\text{py})_2\text{C}(\text{OH})\text{O}^-$. A monodentate acetate group completes a distorted octahedral coordination environment of the cobalt(II) centers⁷³. Similar type of tetranuclear cages of cobalt(II) with di-2-pyridyl ketone and azide are also reported⁷⁴.

Tetranuclear copper(II) carboxylate complexes can be prepared by the reaction of copper(II) nitrate trihydrate with N-(2-hydroxypropyl)aminopropionic acid and nitrilodi(propionic acid)acetic acid⁷⁵. Similar type of copper(II) complex with succinic acid and N,N',N'',N'''-tetrakis-(2-pyridyl- methyl)-1,4,8,11-tetraazacyclotetradecane is reported, which has regular square pyramidal geometry around the copper center⁷⁶. Tetranuclear copper(I) carboxylate cluster, $[\text{Cu}_4\{\text{O}_2\text{C}(\text{3-F})\text{C}_6\text{H}_4\}_4]$ (**1.22**) shows solid state photoluminescence property⁷⁷. The complex **1.22** contains planar Cu_4 -core with carboxylate bridges positioned above and below the plane (Figure 1.15A).

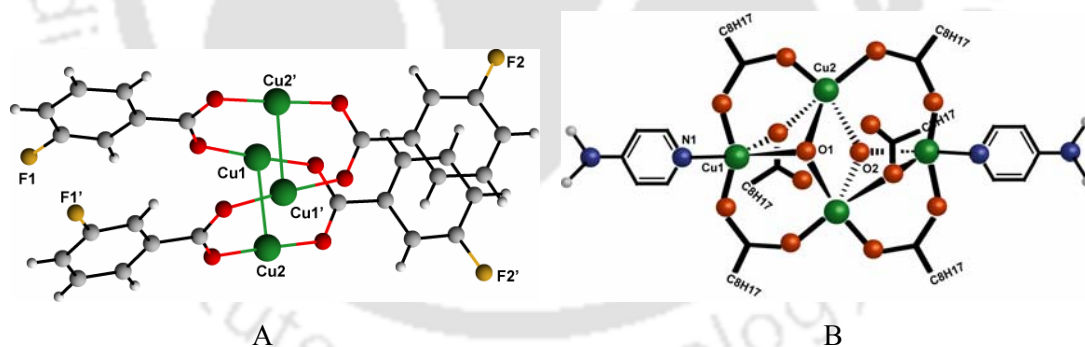


Figure 1.15 A) Tetranuclear copper(I) carboxylate cluster (**1.22**), B) Tetranuclear copper(II) complex of 4-aminopyridine and octanoate

The reaction of 4-aminopyridine with Cu(II) octanoate leads to a tetranuclear copper(II) complex. It is a centrosymmetric tetranuclear complex. The copper centers have distorted square pyramidal geometry. This complex contains bidentate bridging as well as monoatomic bridging carboxylate groups. Besides this, it has triply bridging hydroxyl groups and 4-aminopyridine as a terminal ligand as shown in Figure 1.15B. 4-aminopyridine is coordinated through the endo-cyclic nitrogen atom only⁷⁸. The tetranuclear zinc cluster with composition

$[\text{Zn}_4\text{O}(\text{OCOFCF}_3)_6]$ are structurally characterised and serves as catalyst for conversion reaction of esters to oxazolines⁷⁹.

1.3.5 Pentanuclear metal carboxylates:

First row transition metal carboxylates having pentanuclear core are known. A pentanuclear cobalt(II) complex is obtained from the reaction of cobalt(II) acetate and 3,5-bis(6-methyl-2-pyridyl)pyrazole. The complex is a centrosymmetric pentanuclear cobalt(II) complex with two 3,5-bis(6-methyl-2-pyridyl)pyrazole ligands, eight acetate anions and two H_2O molecules. The central cobalt atom is linked to the four neighbouring cobalt atoms by four μ_2 -acetate and two μ_3 -acetate ligands. The other coordination sites are fulfilled by 3,5-bis(6-methyl-2-pyridyl)pyrazole and water molecules⁸⁰.

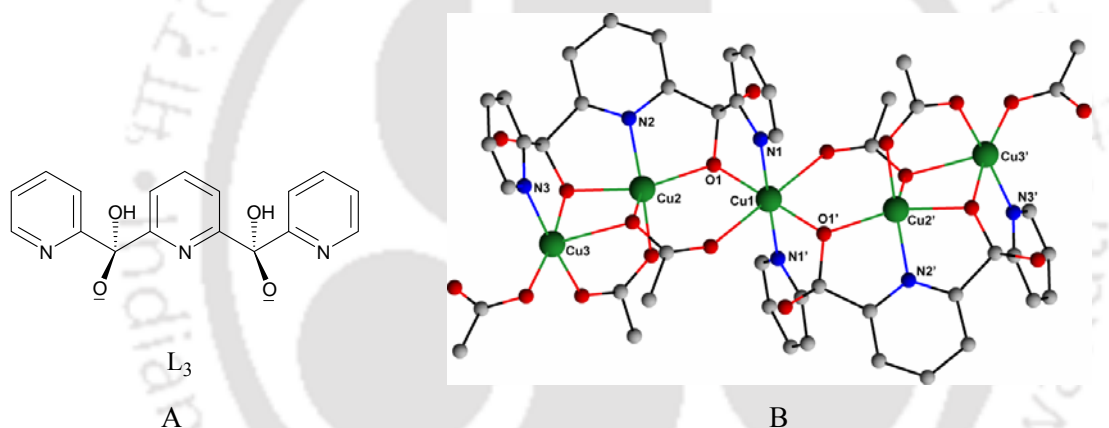


Figure 1.16 A) Structure of ligand L_3 , B) Pentanuclear carboxylate complex (**1.23**) of copper

Dihydroxo bridged pentanuclear nickel(II) complex can be prepared by the reaction of nonanuclear nickel complex with bis[3,5-(dimethylpyrazolyl)]-1,2,4,5-tetrazine. In this complex the five nickel atoms construct a planar spirane type metal core. The metal centers are connected through hydroxy groups. In addition to that, the metal atoms are also bridged by two trimethylacetate and bis[3,5-(dimethylpyrazolyl)]-1,2,4,5-tetrazine groups⁸¹. The reaction of copper(II) acetate with 2,6-di-(2-pyridylcarbonyl)-pyridine leads to a pentanuclear complex having composition $[\text{Cu}_5(\text{O}_2\text{CMe})_6(L_3)_2]$ (**1.23**). The structure of the complex consists of five copper atoms in an “S” like configuration. One copper center has distorted octahedral geometry, whereas the other four copper centers have square pyramidal geometry⁸² (Figure 1.16B).

1.3.6 Hexanuclear metal carboxylates:

In the foregoing subsections we have described few examples of mono to pentanuclear metal carboxylates of first row transition metals. Besides that many hexa-nuclear metal carboxylates are also known in literature. For example hexa-nuclear manganese complex $[\text{Mn}_6(\text{O}_2\text{CET})_8(\text{L}_4)(\text{MeOH})_4(\text{H}_2\text{O})_2]$ (**1.24**) where L_4 is an octadentate ligand (Figure 1.17A), can be obtained by the reaction of 1,3,5-trihydroxybenzene with four equivalents of $\text{Mn}(\text{O}_2\text{CET})_2$ in MeOH. The core consist of six manganese ions arranged as a dimer of two $[\text{Mn}_3(\mu_3\text{-OR})]$ triangles linked together by the bulky octadentate ligand L_4 (Figure 1.17B)⁸³.

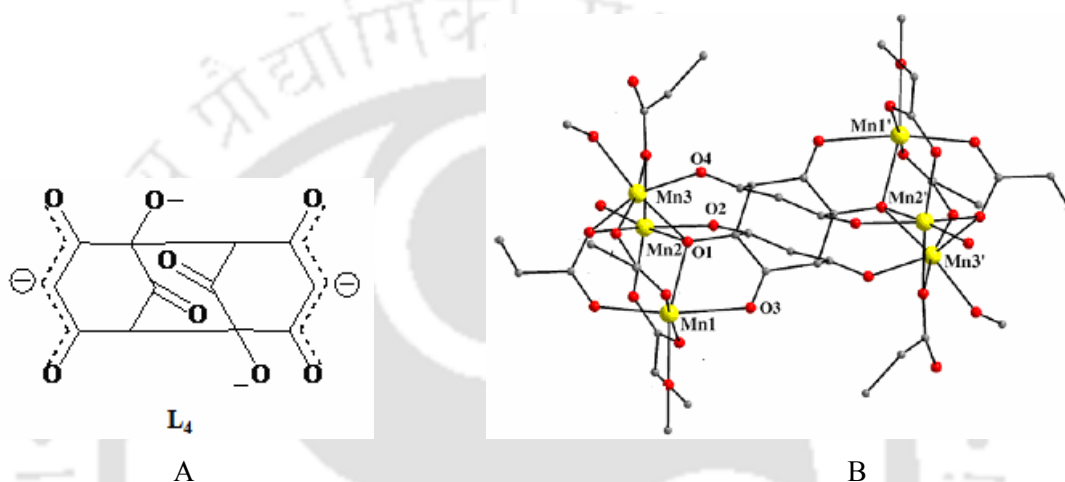


Figure 1.17 A) Structure of an octadentate ligand (L_4), B) Hexanuclear manganese complex (**1.24**) with the octadentate ligand L_4

Hexanuclear cobalt complex having composition $[\text{Co}_6(\text{OH})_2(\text{PhCOO})_{10}(\text{PhCOOH})_4].3\text{PhCH}_3$ (**1.25**) is prepared by the reaction of cobalt(II) nitrate with benzaldehyde⁵³. The structure of the complex consists of a centrosymmetric hexametallc unit. This unit is made up of four cobalt ions in a distorted octahedral geometry and two cobalt ions in tetrahedral coordination geometry.

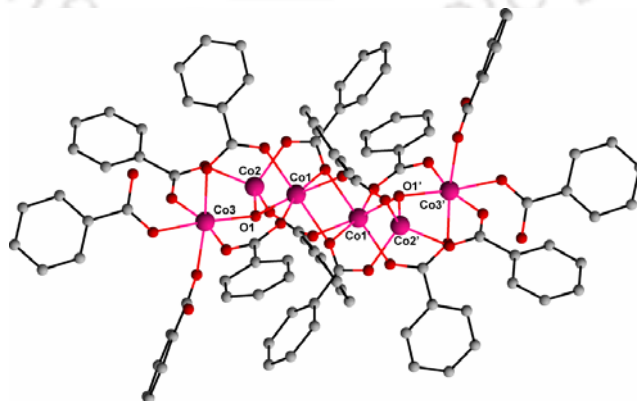


Figure 1.18 Structure of hexanuclear cobalt complex (**1.25**)

The coordination sphere is made up of ten benzoate anions, four molecules of benzoic acid, and two hydroxy groups (Figure 1.18). Hexanuclear cobalt(II) complex formed in by hydrothermal reaction of cobalt(II) nitrate with phenylcinnamic acid and sodium hydroxide. The complex consists of two edge-sharing octahedral $[\text{CoO}_6]$ and four tetrahedral $[\text{CoO}_4]$ units linked through μ -carboxylate ligands and μ -hydroxide ions⁸⁴. A polymeric trimethylacetate complex $[\text{Co}(\text{OH})(\text{OCCMe}_3)]_n$ can be transformed into hexa-nuclear cluster by recrystallization⁸⁵.

1.3.7 Heptanuclear metal carboxylates:

Transition metal based heptanuclear carboxylate clusters have potential applications in fields such as material science, catalysis etc. For example, heptanuclear zinc(II) complexes are effective catalyst for coupling reactions of carbon dioxide and epoxies. A heptanuclear manganese(II) complex is obtained by the reaction of manganese(II) perchlorate and ferrocene-1,1'-dicarboxylic acid. The complex $[\text{Mn}_7\text{O}_3(\text{OCH}_3)(\text{ferrocene-1,1'-dicarboxylate})_6(\text{H}_2\text{O})_3].3\text{DMF}.3\text{MeOH}$ (**1.26**) has a $[\text{Mn}_7(\mu_4\text{-O})_3(\mu_3\text{-OCH}_3)]$ core (Figure 1.19A)⁸⁶.

Hydrothermal reactions of *N*-(phosphonomethyl)-*N*-methylglycine (L) with zinc(II) acetate leads to the formation of a heptanuclear zinc carboxylate-phosphonate complex. The structure contains a heptanuclear zinc phosphonate cluster anion, $\{\text{Zn}_6\text{L}_6(\text{Zn})\}^{4-}$, in which seven zinc(II) cations form an unusual $\text{Zn}_6(\text{Zn})$ centered octahedron with six of its Zn_3 triangle faces each further capped by a phosphonate group. The Zn(II) cations of the Zn_6 octahedron are five-coordinated whereas the centered Zn(II) cation is octahedrally coordinated. Packing of these cluster anions create micropores that are occupied by the hydrated zinc(II) cations and lattice water molecules⁸⁷. The structural skeleton of this complex is retained after the removal of the lattice water molecules. The reaction between $\text{Zn}(\text{bis-trimethylsilyl amide})_2$ with 2,6- $\text{F}_2\text{C}_6\text{H}_3\text{COOH}$ in tetrahydrofuran (THF) leads to $[(2,6\text{-difluorobenzoate})_{10}\text{O}_2\text{Zn}_7](\text{THF})_2$ (**1.27**). The complex crystallizes from tetrahydrofuran as heptanuclear zinc cluster, where the metal atoms are interconnected by a combination of bridging benzoates and oxo ligands⁸⁸ (Figure 1.19B).

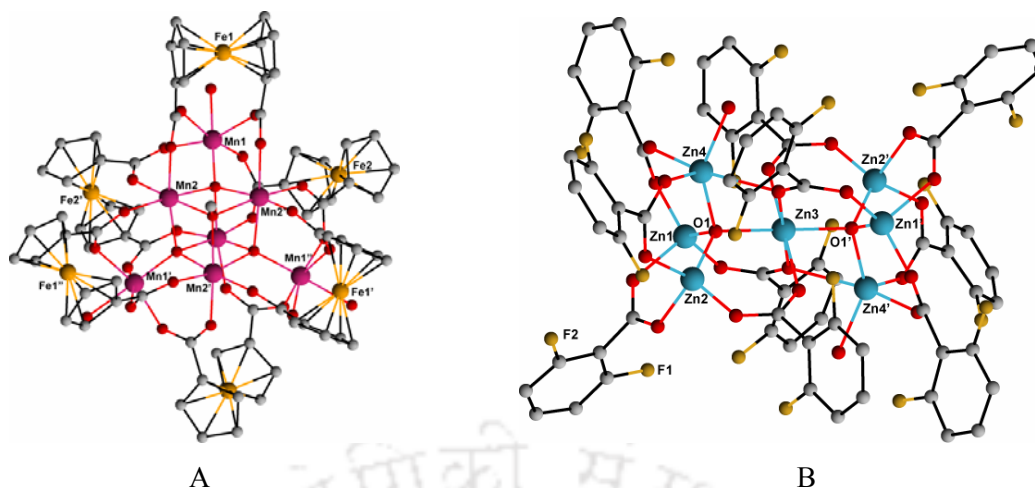


Figure 1.19 A) Heptanuclear manganese(II) complex (**1.26**) with ferrocene-1,1'-dicarboxylic acid, B) Oxo centered heptanuclear zinc carboxylate complex (**1.27**) of 2,6-difluorobenzoic acid

A heptanuclear zinc(II) complex having $[\text{Zn}_7(\mu_4\text{-O}_2)]^{10+}$ core can be prepared by the reaction of zinc(II) acetate with $\text{Ph}_2\text{P}(3\text{-OCH}_2\text{C}_5\text{H}_4\text{N})$. The complex has slightly distorted capped trigonal prismatic arrangement. Each of the two tetrahedrons of zinc contains an interstitial $\mu_4\text{-O}$ and metal centers are bridged by acetate ligands⁸⁹. Similar types of hepta-nuclear core using 1-methylimidazole are also reported in literature⁹⁰.

1.3.8 Higher nuclearity metal clusters:

Numerous examples of high-nuclearity transition metal carboxylates are known. They have interesting structural, spectroscopic and magnetic properties. Mixed-valence octanuclear manganese carboxylate complexes are reported in literature^{58,91}. Octanuclear complex of manganese containing $[\text{Mn}_4^{\text{III}}(\mu_4\text{-O}_4)]^{4+}$ core, derived from ferrocen-1,1'-dicarboxylic acid are also known⁸⁶. Oxo and carboxylate bridged nonanuclear manganese cluster are viewed as two "butterfly" type Mn_4O_2 units, interconnected through manganese atoms. The coordination environments around the manganese are best described as distorted square pyramidal⁹².

Dodecanuclear manganese cluster can be obtained by reaction of manganese(II) acetate with benzoic acid and $\text{NBu}^n_4\text{MnO}_4$. It is a mixed-valence Mn_8^{III} , Mn_4^{IV} complex and consists of a central $[\text{Mn}_4\text{O}_4]^+$ core. The cubane like $[\text{Mn}_4\text{O}_4]^+$ core are held within a nonplanar ring of eight manganese(III) atoms by eight $\mu_3\text{-O}^{2-}$ ions. Peripheral ligation is provided by $16\mu_2\text{-O}_2\text{CPh}^-$ and four terminal H_2O groups⁹³. This complex acts as molecular magnet at very low temperature⁹⁴⁻⁹⁵.

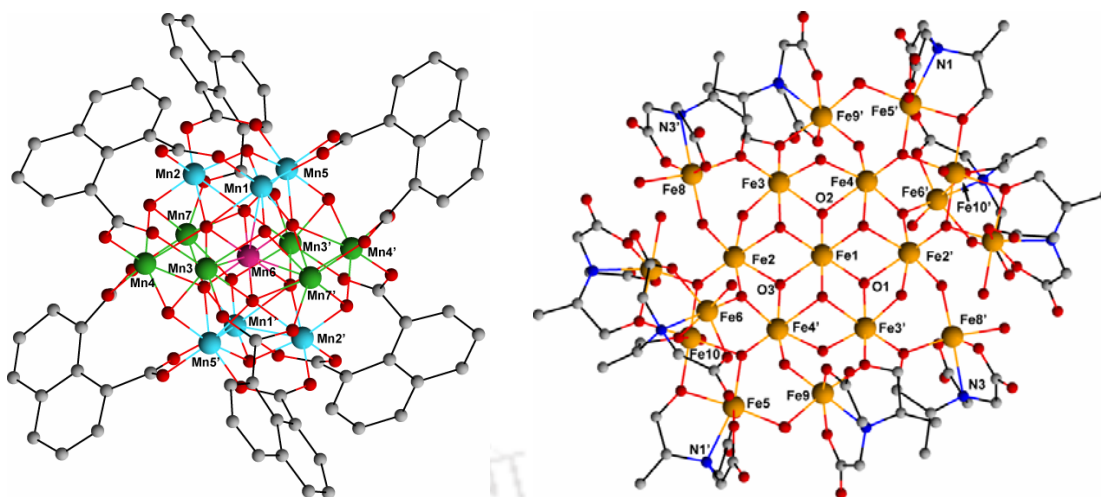


Figure 1.20 A) Mn_{13} cluster (**1.28**) with 1,8-naphthalenedicarboxylate, B) Fe_{19} cluster (**1.29**) of iron(III) with *N*-(1-Hydroxymethylethyl)iminodiacetic acid

$[\text{Mn}_{13}\text{O}_8(\text{OH})_6(1,8\text{-naphthalenedicarboxylate})_6]\cdot 8\text{DMF}\cdot \text{H}_2\text{O}$ (**1.28**), is prepared by the reaction of manganese(II) acetate with 1,8-naphthalenedicarboxylic acid in DMF⁹⁶. The core of the cluster contains one Mn^{IV} , six Mn^{II} and six Mn^{III} ions. The core is held together by six $\mu_5\text{-O}^{2-}$, two $\mu_3\text{-O}^{2-}$, and six $\mu_3\text{-OH}^-$ ions. Peripheral ligation is provided by six 1,8-naphthalenedicarboxylate groups whose carboxylate arms bridge two Mn atoms (Figure 1.20A). The same type Mn_{13} core has also been observed with benzoate or ferrocen-1,1'-dicarboxylate ligation^{97,86}. Other high-nuclearity manganese carboxylate complexes such as Mn_{21} , Mn_{30} , and Mn_{84} clusters are reported in literature⁹⁹⁻¹⁰¹.

A Fe_{19} cluster $[\text{Fe}_{19}(\text{methedi})_{10}(\text{OH})_{14}(\text{O})_6(\text{H}_2\text{O})_{12}]\text{NO}_3\cdot 24\text{H}_2\text{O}$ (**1.29**) is obtained by the reaction of iron(III) nitrate with *N*-(1-Hydroxymethylethyl)iminodiacetic acid ($\text{H}_3\text{methedi}$) as shown in Figure 1.20B¹⁰². Similar type of Fe_{19} cluster with *N*-(1-Hydroxyethyl)iminodiacetic acid are also known¹⁰³.

The oxidation of cobalt benzoate leads to octanuclear cluster consisting of a central $[\text{Co}^{\text{III}}_4\text{O}_4]^{4+}$ cubane unit with bridging $\mu_3\text{-O}^{2-}$ ions. These oxo anions also attach to a cobalt(II) center to give a $[\text{Co}_8\text{O}_4]^{12+}$ core. Twelve benzoate groups bridge between cobalt(II) and cobalt(III) centers¹⁰⁴. $[\text{Co}_{13}(\text{OH})_2(\text{phthalate})_2(6\text{-chloro-2-pyridonate})_{20}]$ (**1.30**) can be prepared by the reaction of cobalt(II) chloride with sodium phthalate and sodium salt of 6-chloro-2-pyridonate. Tridecanuclear cage of this complex can be described as a dimer of the heptanuclear cobalt cages with a common cobalt center (Figure 1.21). The asymmetric unit of this complex contains square pyramidal geometry. Ten crystallographically distinct pyridonate groups are present in this structure; two of them bind to cobalt centers through the

N-donor, and bridge two further metals through the oxygen. Of the remaining ligands, six ligands are chelating to one metal and bridging to a second through the oxygen, while the final two pyridonates are chelating to one cobalt and bridging to two further metal centres through the oxygen¹⁰⁵.

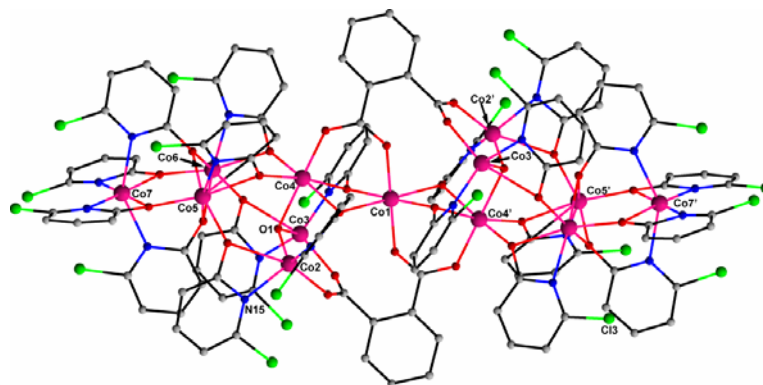


Figure 1.21 Crystal structure of **1.30**

The reaction of nickel(II) sulphate, citric acid and tetramethylammonium hydroxide at ambient temperature produces $(\text{NMe}_4)_{10}[\text{Ni}_8(\text{cit})_6(\text{OH})_2(\text{H}_2\text{O})_2]$ (**1.31**), where $\text{H}_4\text{cit} = \text{C}(\text{OH})(\text{CO}_2\text{H})(\text{CH}_2\text{CO}_2\text{H})_2$ (Figure 1.22A). If the crystallisation is done at higher temperature, it produces $(\text{NMe}_4)_{10}[\text{Ni}_8(\text{cit})_6(\text{OH})_2]$ (**1.32**), which is almost iso-structural with complex **1.31**¹⁰⁶. Ni_{24} cluster of acetate and 3-methyl-3-pyrazolin-5-one (Hmpo), consists of an octamer of chemically equivalent trinuclear building blocks $\{\text{Ni}_3(\text{OH})(\text{mpo})_2(\text{O}_2\text{CMe})_3(\text{Hmpo})_2\}$ ¹⁰⁷. Nickel centers are bridged by carboxylate and oxygen atoms and each nickel centers has distorted octahedral geometry. Besides this Ni_{10} , Ni_{11} and Ni_{12} core containing carboxylate clusters are reported in literature¹⁰⁸.

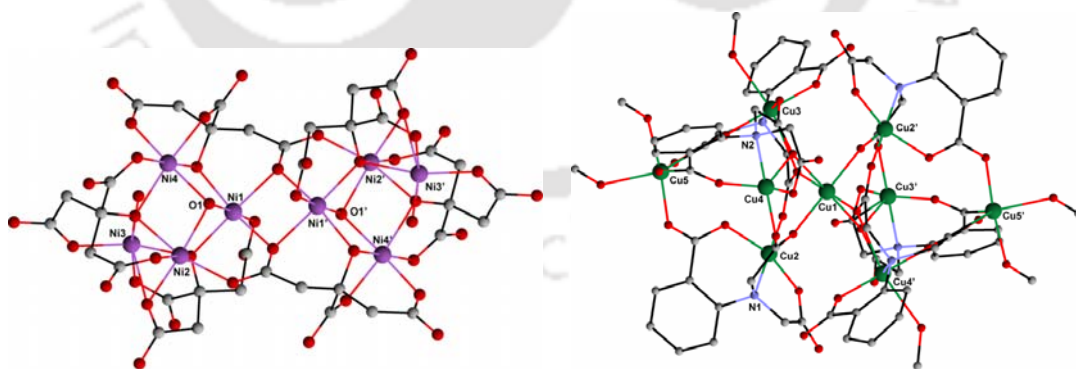


Figure 1.22 A) Octanuclear nickel complex (**1.31**) of citric acid, B) Nona-nuclear copper(II) carboxylate cluster (**1.34**)

A series of octanuclear copper(II) complexes with carboxylates and 2-pyridonate ligands are synthesized from the reaction of copper(II) acetate with 6-chloro-2-pyridonate. The octanuclear cluster with composition $[\text{Cu}_8\text{O}_2(\text{O}_2\text{CMe})_4(6\text{-chloro-2-pyridonate})_8]$ (**1.33**),

contains an edge-sharing Cu_6O_2 bi-tetrahedral core. The core is surrounded by two $[\text{Cu}(6\text{-chloro-2-pyridonate})_4]$ units. This complex shows a large antiferromagnetic exchange coupling within the Cu_6O_2 core¹⁰⁹. The nonanuclear copper(II) carboxylate with composition $[\text{Cu}_9\{2\text{-(carboxyphenyl)imino diacetate}\}_6(\text{MeOH})_6]\cdot 6(\text{MeOH})$ (**1.34**), has copper(II) ions with five-coordinate distorted square pyramidal geometry¹¹⁰ (Figure 1.22B).

1.3.9 Mixed-metal carboxylate complexes:

The polynuclear mixed metal complexes are of interest for understanding the nature of the magnetic exchange interactions between metal ions, and they can possibly be used as magnetic materials, and high temperature superconductors. Some mixed-metal carboxylate complexes such as $[\text{Ce}^{\text{IV}}\text{Mn}^{\text{III}}_8\text{O}_8(\text{O}_2\text{CMe})_{12}(\text{H}_2\text{O})_4]\cdot 4\text{H}_2\text{O}$ (**1.35**) behave as single molecular magnet. This complex consists of nonplanar saddle-like $[\text{Mn}_8\text{O}_8]^{8+}$ loops attached to the central Ce^{4+} via the O^{2-} ions. Additional peripheral ligation are provided by doubly or triply bridged acetate group and by water molecules¹¹¹ (Figure 1.23A).

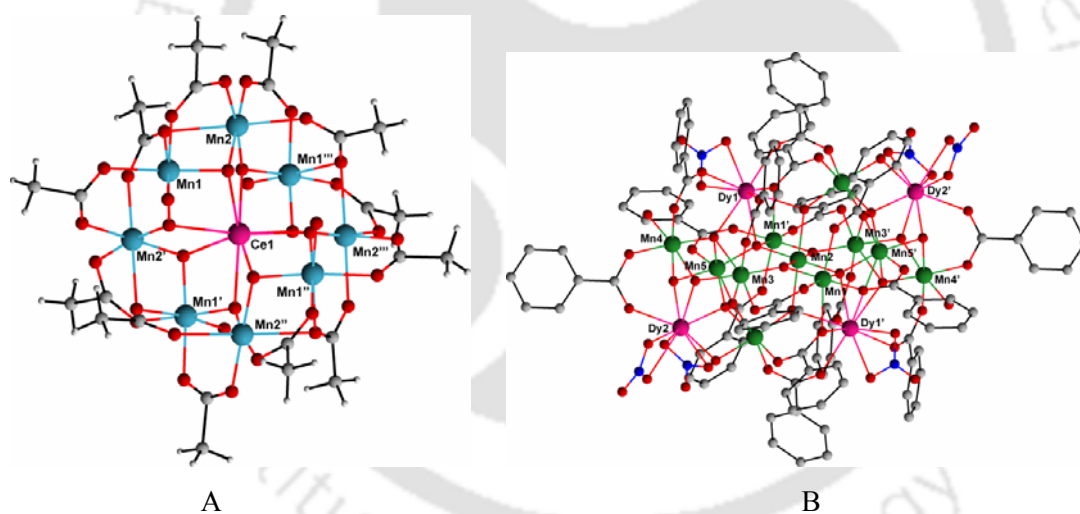


Figure 1.23 A) Cerium and manganese based mixed metal complex (**1.35**), B) Dysprosium and manganese based mixed metal carboxylate complex (**1.36**)

Another mixed-metal complex $[\text{Mn}_{11}\text{Dy}_4\text{O}_8(\text{OH})_6(\text{OMe})_2(\text{O}_2\text{CPh})_{16}(\text{NO}_3)_5(\text{H}_2\text{O})_3]\cdot 15\text{MeCN}$ (**1.36**) is obtained from the reaction of $[\text{Mn}_3\text{O}(\text{O}_2\text{CPh})_6(\text{pyridine})_2(\text{H}_2\text{O})]$ with $\text{Dy}(\text{NO}_3)_3$. The structure of this complex consists of a $[\text{Mn}_{11}\text{Dy}_4]^{45+}$ core and held together by bridged O^{2-} , OH^- and MeO^- ions. Peripheral ligation is provided by bridged benzoate groups and chelating NO_3^- groups on the dysprosium ions¹¹² (Figure 1.23B). Mixed metal complexes of thorium (IV) and manganese(IV) are also reported¹¹³. Hexanuclear mixed-metal carboxylate complex having general formula $[\text{Mn}_2\text{M}^{\text{II}}_4\text{O}_2(\text{PhCOO})_{10}(\text{DMF})_4]$, with M as Ni(II) or Co(II) are

reported in literature¹¹⁴. These complexes have $[\text{Mn}_2\text{M}^{\text{II}}_4\text{O}_2]$ core and the coordination sites are completed by bridged benzoato ligand and dimethyl formamide molecules. Similar type of hexanuclear $\text{Co}^{\text{II}}_2\text{-Ni}^{\text{II}}_4$ carboxylate complex is also reported⁵³. A tetranuclear mixed-metal carboxylate of $\text{Cu}^{\text{II}}_2\text{Ln}^{\text{III}}_2$ has Cu(II) ion quadruply bridged to a Ln(III) atom by the bridging carboxylate groups into a dinuclear subunit, and a pair of such dinuclear subunits is bridged by two carboxylate groups to form a tetranuclear cation. In the tetranuclear cation, each copper(II) atom have square pyramidal geometry. The copper atoms are coordinated by four carboxy oxygen atoms at the basal positions and by one aqua ligand at the apical position whereas each Ln(III) atom is coordinated in a monocapped square antiprism by six carboxy oxygen atoms and three aqua ligands¹¹⁵. The mixed-metal complexes of dysprosium and zinc are also known¹¹⁶.

1.4 Carboxylate based coordination polymers

Coordination polymers have infinite frameworks constructed from metal ions and organic ligands via coordination bonds and other weak interactions. These compounds are also named metallorganic coordination networks or metal-organic frameworks (MOF) in the case of ordered structures¹¹⁷.

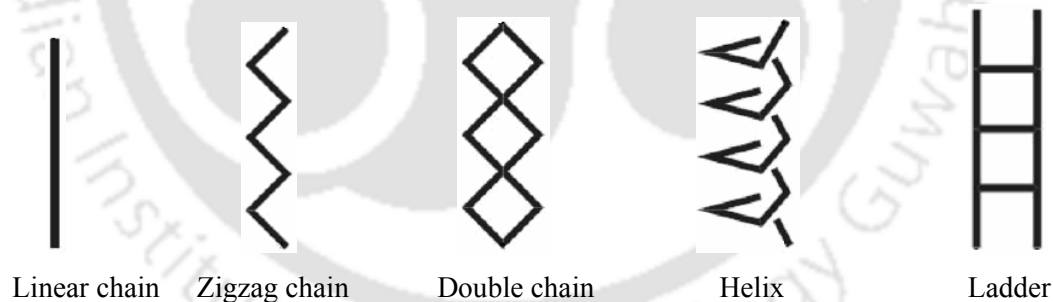


Figure 1.24

A wide range of network can be constructed from coordination polymers by using building-block methodologies¹¹⁸. Molecular architectures in coordination networks consist of metal ions (and metal clusters) that functions as nodes and organic ligands act as spacer. These building blocks together can lead to metal-organic frameworks of different dimensionalities such as one-, two- or three-dimensional architectures.

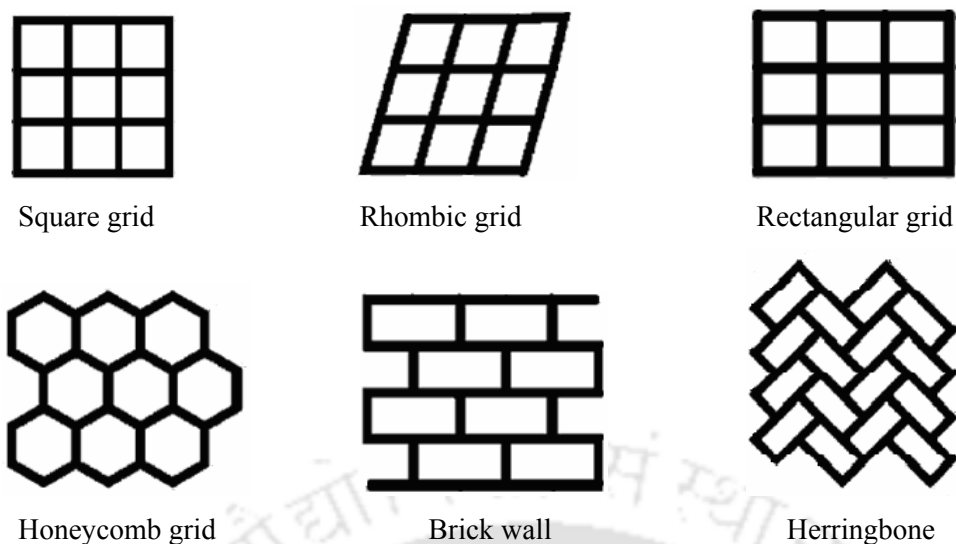


Figure 1.25

In one dimensional polymer each metal ion is coordinated to two ligand molecules to make infinite chains of metal and ligands. Two-dimensional structures are obtained from three or four ligands coordinating to each metal ion and the elementary motif expands in two directions. Metal ions having higher coordination numbers (tetrahedral or octahedral nodes), can lead to three-dimensional structures. The framework structures are primarily dependent on the coordination preferences of the metal-unit and the functionality of the ligands¹¹⁹.



Figure 1.26

The common way to classify coordination polymers are by their dimensionalities. The motifs presented in Figure 1.24-1.26 are the most typical ones. Over and above the metal to ligand interactions also play important roles in the formation of the coordination polymers. To illustrate the wide diversity of coordination polymers of first row transition metal some examples of metal-organic frameworks are presented in the next sections.

1.4.1 One dimensional coordination polymers

The main factors which influence the structural variety of the coordination polymers constructed from poly-carboxylato ligands are: (i) the number of the carboxylate groups, (ii) the spatial orientation of the carboxylato groups, (iii) the coordination modes of carboxylate groups, (iv) ancillary ligands in the coordination sphere of the metal ions. So, depending on these factors, coordination polymers may adopt different structures. Various examples of one dimensional coordination polymers are presented in the next subsections.

1.4.1.1 Linear chain:

Linear chain is the simplest and commonly observed one dimensional motif. For instance, one dimensional coordination polymer $[\text{Ni}(\text{cyclam})(2,2'\text{-bipyridyl-4,4'-dicarboxylate})]_n \cdot 5n\text{H}_2\text{O}$ (**1.37**) can be prepared by the reaction of 2,2'-bipyridyl-4,4'-dicarboxylic acid and macrocyclic $[\text{Ni}(\text{cyclam})]^{2+}$. This belongs to an important class of linear carboxylate bridged co-ordination polymer. In this coordination polymer the dicarboxylic acid is coordinated to $[\text{Ni}(\text{cyclam})]^{2+}$ (Figure 1.27A) and form a linear coordination polymer (Figure 1.27B). These polymeric chains are assembled by weak C–H $\cdots\pi$ interaction leading to triangular channels by overlapping triangular array of linear coordination polymer chains¹²⁰. The packing generates 1D channels with honeycomb like porous and robust structures. The frameworks are retained after several cycles of dehydration and rehydration processes. Many other interesting examples of linear chain coordination polymers are reported in literature¹²¹⁻¹²².

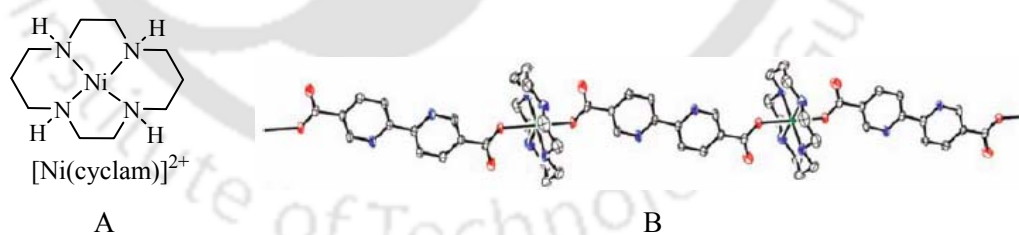


Figure 1.27 A) Schematic presentation of $[\text{Ni}(\text{cyclam})]^{2+}$, B) Structure of 1-D coordination polymer (**1.37**) constructed through $[\text{Ni}(\text{cyclam})]^{2+}$ and 2,2'-bipyridyl-4,4'-dicarboxylic acid

Coordination polymer **1.38** is the combination of a linear dimetallic spacer, $\text{Cu}_2(\text{O}_2\text{CMe})_4$, and a linear bidentate ligand, 1,3-di-4-pyridylpropane (Figure 1.28). The combined use of a long, linear ligand with a dimetallic fragment possessing linearly arranged binding sites to produce a porous channel-containing coordination polymer framework capable of including different guest species like methanol, acetic acid and ethylene glycol¹²³. Interestingly this type

of coordination polymer could also be prepared mechanochemically by grinding solid copper(II) acetate dihydrate with 1,3-di-4-pyridylpropane¹²⁴. One dimensional linear chain of copper(II) with terephthalate dianions and ammonia has square-planar geometry around the copper atoms. The coordination sites are fulfilled by two ammonia and two terephthalate molecules. Terephthalate molecules are coordinated in monodentate fashion, leading to a trans-arrangement of the ligands and linear chains¹²⁵.

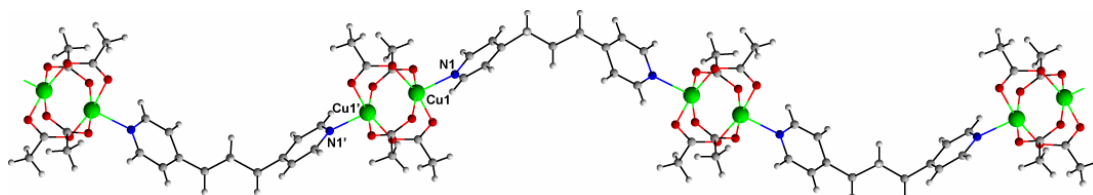


Figure 1.28 Structure of one dimensional coordination polymer **1.38**

The use of *N*-(4-carboxyphenyl)iminodiacetic acid with copper(II) leads to linear chain coordination polymer¹²⁶. The one-dimensional chain formation seems to be simple, but they show interesting packing pattern with unique physical property.

1.4.1.2 Zig-zag chain:

The formation of zig-zag chains can be induced in coordination polymers by controlling the shape of the ligand molecules. The complex $[\text{Mn}(\text{fumarate})(2,2'\text{-bipyridine})(\text{H}_2\text{O})]_n$ (**1.39**) has a zigzag polymeric chain connected by the flexible fumarate ligands and 2,2'-bipyridine. In this polymer each manganese(II) ion is seven-coordinated comprising of 2,2'-bipyridine, two bidentate carboxylates and one aqua ligand. Pair of chains are linked by hydrogen bonds, involving aqua ligands on one chain and two oxygen atoms of fumaric acid ligands on the other chain¹²⁷. Hydrothermal reactions of copper(II) chloride with 1,4-dicyanobenzene in the presence of 1,10-phenanthroline results in the hydrolysis of 1,4-dicyanobenzene to terephthalic acid. The dicarboxylic acid formed in situ leads to the formation of zig-zag polymeric complex, $[\text{Cu}(\text{terephthalate})(1,10\text{-phenanthroline})]_n$ (**1.40**). The metal environment can best be described as highly distorted square planar geometry with two nitrogen atoms from phenanthroline, two carboxylato-oxygen atoms from different terephthalic acid ligands and one oxygen atom from the coordinated water molecule. Similar types of complexes are also obtained in the case of cobalt and zinc (Figure 1.29)¹²⁸.

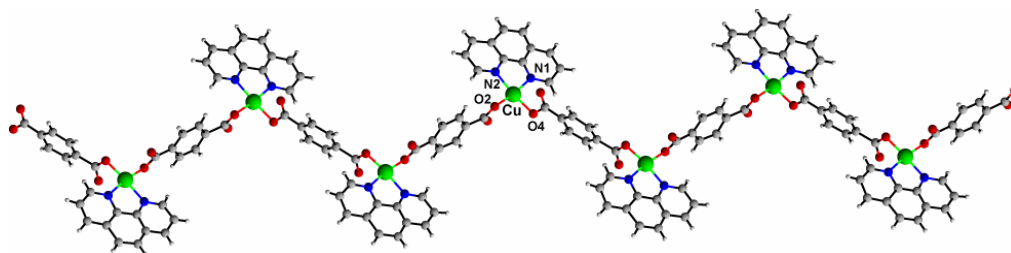


Figure 1.29 Zig-zag structure of one dimensional coordination polymer (**1.40**) of copper

The $[\text{Cu}(5\text{-hydroxyisophthalate})(\text{NEt}_3)(\text{H}_2\text{O})]_n$ (**1.41**), has an infinite zig-zag chain constructed by the copper-trimethyl amine node with 5-hydroxy isophthalic as spacer¹²⁹. Similar type of zig-zag coordination polymer are also obtained by the reaction of 2,5-dihydroxy terephthalic acid and 5-nitro isophthalic acid instead of 5-hydroxy-isophthalic acid with copper. In all cases one dimensional zig-zag coordination polymer, with a distorted octahedral geometry or a strongly distorted square-pyramidal geometry of copper (II) centers, are observed (Figure 1.30).

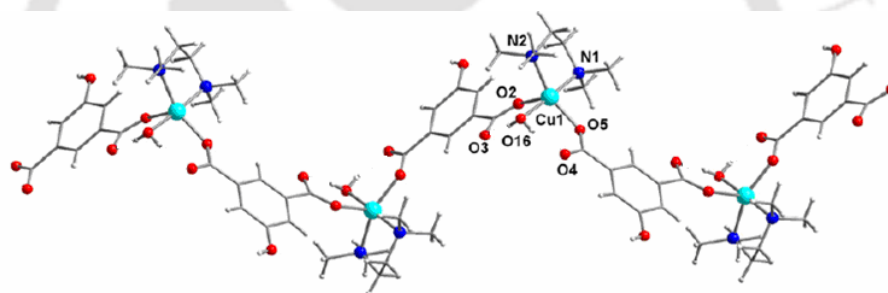


Figure 1.30 Crystal structure of $[\text{Cu}(5\text{-hydroxy-isophthalate})(\text{NEt}_3)(\text{H}_2\text{O})]_n$ (**1.41**)

Reaction of zinc salt with imidazole and 1,2-benzenedicarboxylic acid leads to a one dimensional zig-zag type coordination polymer. The carboxylate groups of the phthalate dianion are coordinated to zinc centers in a bridging fashion and form one dimensional zig-zag chain like structure¹³⁰. The presence of the bipyridine and phenanthroline ligands lowers the tendency of metal complexes to form high-dimensional carboxylate bridged complexes.

The reaction of $[\text{Zn}(\text{MeCO}_2)_2] \cdot \text{H}_2\text{O}$ with 1,4-benzenedicarboxylic acid in the presence of 2,2'-bipyridine leads to one dimensional infinite zig-zag chain. The one dimensional chains are connected by weak $\text{C-H} \cdots \text{O}$ hydrogen bonds and aromatic $\pi \cdots \pi$ stacking interactions, which makes them to assemble into a 3D network. The structural features shows the presence of nano-sized channels, capable of clathrating free 2,2'-bipyridine molecules. When the guest molecules are removed from the channels by heating, the evacuated framework is stable up to 340°C ¹³¹.

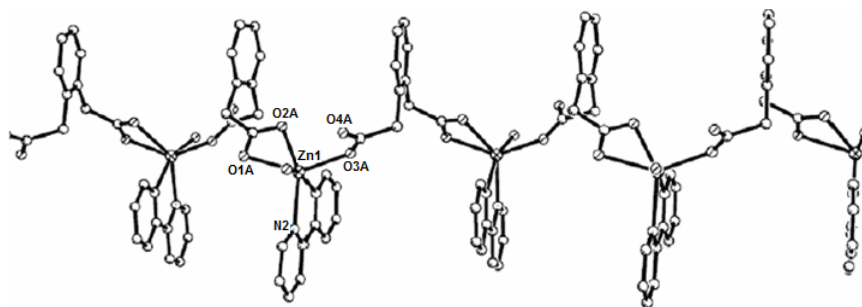


Figure 1.31 One dimensional infinite zig-zag chain of coordination polymer **1.42**

Another example of one dimensional zig-zag coordination polymer is, $[\text{Zn}(2,2'\text{-bipyridine})(1,2\text{-phenyldiacetato})_2(\text{H}_2\text{O})]_n$, (**1.42**) obtained from zinc(II) nitrate and 1,2-phenyldiacetic acid in the presence of 2,2'-bipyridine. The zinc(II) ion in the polymer has a distorted octahedron coordination environment. Strong $\pi \cdots \pi$ stacking interactions (face to face distance is 3.49 Å) exist between the bipyridine ligands and phenyl rings of phenyldiacetic acid on adjacent chains (Figure 1.31)¹³².

1.4.1.3 Double chain:

Double chain type carboxylate polymers are formed by different metal ions, in which the ligands have an appropriate geometry to form a chain like structure by occupying axial and equatorial positions of distorted octahedral geometry. Double chain coordination polymers of 1,2,7,8-benzenetetracarboxylic acid with manganese(II) ions in presence of 4,4'-bipyridine are structurally characterised. In this polymer the acid molecules act as tridentate ligands to manganese(II) ion, the octahedral coordination sphere of manganese(II) ion is completed by two water molecules and one protonated 4,4'-bipyridine molecule¹³³.

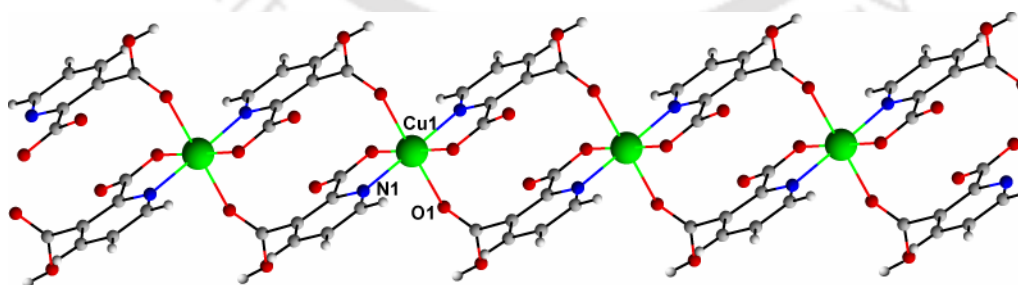


Figure 1.32 Double chain structure of $[\text{Cu}(2,3\text{-pyridine dicarboxylate})_2]_n$ (**1.43**)

Double chain motif $[\text{Cu}(2,3\text{-pyridine dicarboxylate})_2]_n$ (**1.43**) of copper(II) with 2,3-pyridine dicarboxylic acid can be synthesised by high-dilution synthesis¹³⁴. The repeating units of this coordination polymer are metallacycles, two ligands bridges two copper ions in the chain

(Figure 1.32). Each copper(II) centers has a distorted octahedral coordination geometry. The apical positions of the octahedron are occupied by the oxygen atoms of the non-deprotonated 3-carboxyl groups and the equatorial one are occupied by two nitrogen atoms and two oxygen atoms of the deprotonated 2-carboxyl groups. Similar type of double chain structure of zinc(II) with 2,3-pyridine dicarboxylic acid is reported in literature. Reaction of zinc(II) acetate with 2,3-pyridine dicarboxylic anhydride in presence of 4,4'-bipyridine leads to hydrolysis of the anhydride into 2,3-pyridine dicarboxylic acid and forms coordination polymer with double-chain structure¹³⁵.

1.4.1.4 Ladder:

Great advances have been achieved for construction of infinite ladder like coordination polymers through the metal-directed self assembly method. Few examples of ladder like coordination polymers are described in this section. The reaction of cobalt(II) nitrate with nicotinic acid in the presence of sodium salt of dicynamide leads to a co-ordination polymer $\{[\text{Co}_3(\text{dicynamide})_2(\text{nicotinate})_4(\text{H}_2\text{O})_8].2\text{H}_2\text{O}\}_n$, (**1.44**) with ladder type structure. The one dimensional polymer contains bridging dicynamide anions, bridging and terminal nicotinate anions and two interstitial water molecules (Figure 1.33).

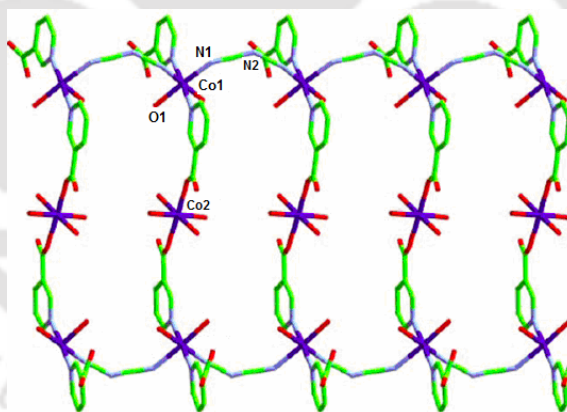


Figure 1.33 Ladder-like one dimensional coordination polymer (**1.44**) of cobalt

Due to the angular nature of the bridging nicotinic acid ligands the ladders are not flat, they have a 'Z'-shaped structure. The interior of the layers are hydrophilic and contain extensive hydrogen bonding interactions which connect the ladders together¹³⁶. Different types of ladder like architecture of copper(II) are also reported in literature. The reaction of copper (II) nitrate with maleic acid in presence of 2,2'-bipyridine leads to ladder-like one-dimensional coordination polymer. The two carboxylate groups of the dianion of maleic acid exhibit two different coordination modes in the complex. One acts as a bridge in syn-anti conformation,

while the other exhibits monodentate coordination mode¹³⁷. Similar types of molecular ladders are also formed by the reaction of trans-1,2,3-propenetricarboxylic acid with copper (II) nitrate¹³⁸. Hydrothermal reactions of metal acetates such as copper(II) acetate and zinc(II) acetate with 4,4'-bipyridine leads to 1D molecular ladder of the respective metals. The copper complex, $\{[\text{Cu}(4,4'\text{-bipyridine})(\text{OOCCH}_3)_2] \cdot 2.5\text{H}_2\text{O}\}_n$, (**1.45**) consists of a symmetric copper(II) dimer with bridging between copper centres furnished by mono-atomic acetate. Further coordination about copper is provided by two trans 4,4'-bipyridine ligands and a terminally bound mono-dentate acetate, the resulting complex has square pyramidal geometry around metal centers¹³⁹ (Figure 1.34).

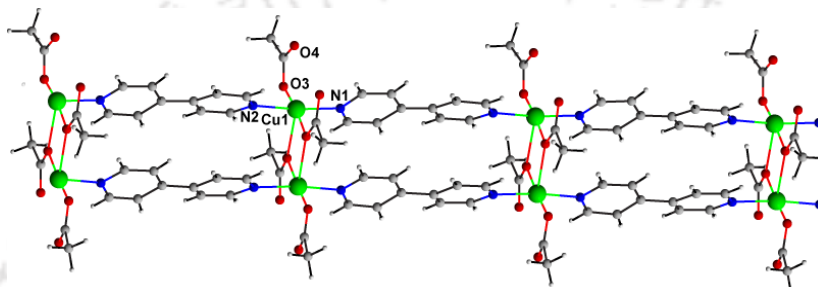


Figure 1.34 Crystal structure of the complex **1.45**

The zinc complex, $[\text{Zn}(4,4'\text{-bipyridine})(\text{OOCCH}_3)_2]_n$, (**1.46**) consists of a dimeric core. A quite irregular six coordinate geometry around zinc(II) is formed by a bidentate acetate which forms a four membered chelate ring¹³⁹. Two trans 4,4'-bipyridine rigid ligands are situated above and below the core, and two syn-syn bridging acetate groups complete the coordination sphere (Figure 1.35).

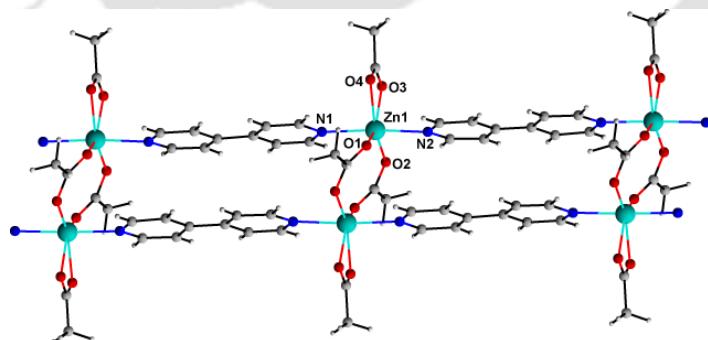


Figure 1.35 Ladder type coordination polymer (**1.46**) of zinc

Zinc complex with diphenic acid $[\text{Zn}(\text{diphenate})(\text{H}_2\text{O})]_n$, (**1.47**) is a one-dimensional coordination polymer that consists of parallel ladder-like chains¹⁴⁰. One carboxylate group of the diphenic acid coordinate with two zinc atoms and forms a dinuclear unit which composes

the steps of the ladder. The other carboxylate is connected to a zinc ion in the next step of the ladder. The fourth coordination site on the distorted tetrahedrally coordinated zinc ions is occupied by water molecule (Figure 1.36).

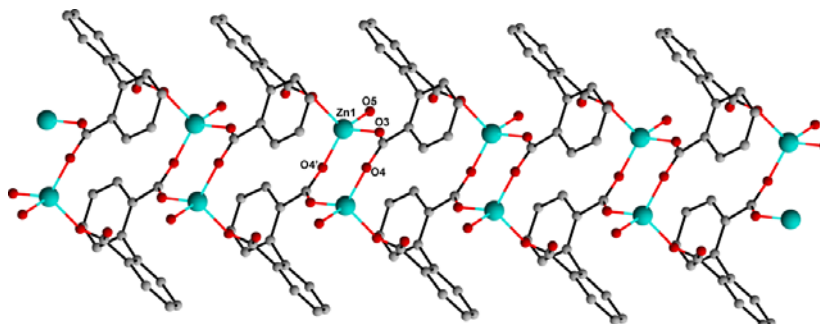


Figure 1.36 One-dimensional coordination polymer **1.47** of zinc with diphenic acid that consists of parallel ladder-like chains

1.4.1.5 Helix:

Among different first row transition metal complexes having helical structure the complex $[\text{Co}(\text{C}_{14}\text{H}_8\text{O}_5)(\text{C}_{12}\text{H}_8\text{N}_2)(\text{H}_2\text{O})]_n$ (**1.48**), is an example of a neutral double-strand helix¹⁴¹. The V-shaped 4,4'-oxybis(benzenecarboxylic acid) ligand acts as a bridge to connect two adjacent cobalt ions. The helical nature depends upon the capacity to form V-shaped configuration of the bridging dicarboxylate ligands. The cobalt polymer has two adjacent chains that interacts through hydrogen bonds between the non-coordinating carboxylate oxygen atoms and the aqua ligand to generate a double-stranded chain, as shown in Figure 1.37A. The phenanthroline ligands are attached to one side of the double stranded chain. Additionally, supramolecular interactions viz. strong aromatic π - π stacking between the phenanthroline ligands and hydrogen bonds between the aqua molecules from two adjacent chains, makes the double-stranded chains to remain in layers. Helical, multinuclear assemblies mediated by metal–ligand coordination are well documented in the literature¹⁴². The double stranded helix of copper (II) with 4,4'-oxybis(benzenecarboxylic acid) and phenanthroline is also reported in literature¹⁴³.

Helical coordination polymer of cobalt with 1,4-cyclohexanedicarboxylic acid and phenanthroline $[\text{Co}(1,4\text{-cyclohexanedicarboxylate})_2(1,10\text{-phenanthroline})_2(\text{H}_2\text{O})_2]_n$ (**1.49**), is structurally characterised¹⁴⁴. Each metal center of this complex is coordinated by one phenanthroline ligand, also with three oxygen atoms from two 1,4-cyclohexanedicarboxylic acid ligands and one aqua ligand. The repeated units propagate along the crystallographic 2₁-

screw axis (Figure 1.37B). The right-handed and left-handed helices are alternately packed through further interlinking via hydrogen bonds between the carboxylate and aqua ligands into a centrosymmetric 2D network.

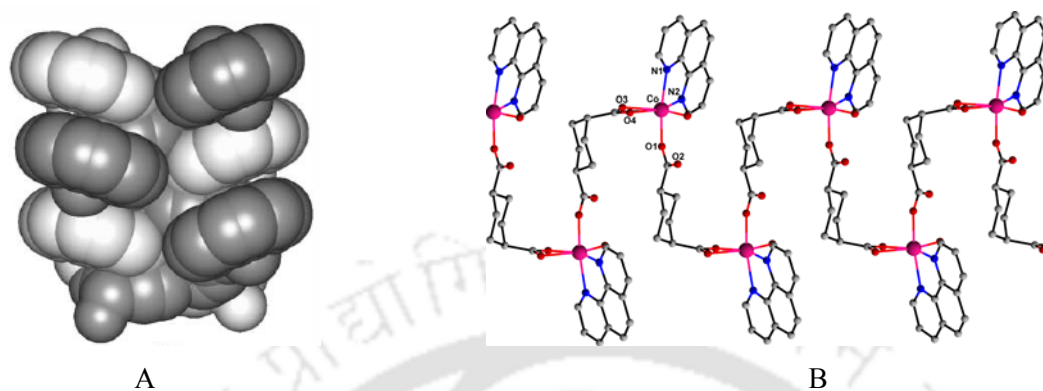


Figure 1.37 A) Neutral double-stranded helix of $[\text{Co}(\text{C}_{14}\text{H}_8\text{O}_5)(\text{C}_{12}\text{H}_8\text{N}_2)(\text{H}_2\text{O})]_n$ (**1.48**), B) Structure of helical coordination polymer **1.49** of cobalt with 1,4-cyclohexanedicarboxylic acid and 1,10-phenanthroline

The self-assembly of cobalt (II) ions with 2,2'-bipyridyl-3,3'-dicarboxylic acid in aqueous solution leads to one-dimensional (1D) helical coordination polymers **1.50**. Crystal structure of the compound shows that each metal center displays a distorted octahedral coordination geometry including three water oxygen atoms; one oxygen atom of the carboxylate of a 2,2'-bipyridyl-3,3'-dicarboxylic acid belongs to the adjacent metal ion and two nitrogen atoms from the 2,2'-bipyridyl-3,3'-dicarboxylic acid act as a chelating ligand.

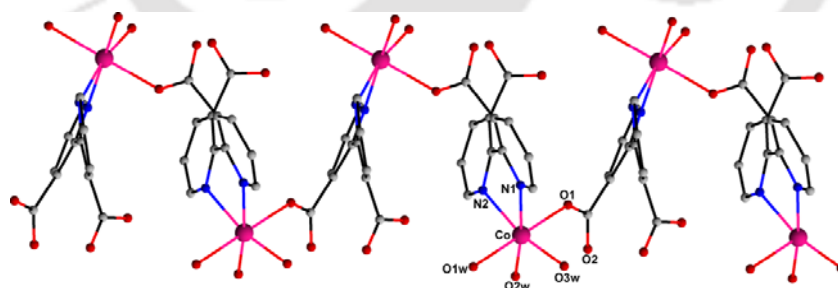


Figure 1.38 Structure of 1D helical coordination polymers **1.50**

One carboxylate oxygen atom of coordinated 2,2'-bipyridyl-3,3'-dicarboxylic acid binds to the neighbouring metal ions, which give rise to 1D helical coordination polymers (Figure 1.38). The helical chains are linked by the hydrogen bonding interactions between the oxygen atoms of carboxylate and the water molecule of the adjacent helical chain, which leads to 2D networks¹⁴⁵. Similar type of one dimensional helical coordination polymer of nickel with 2,2'-

bipyridyl-3,3'-dicarboxylic acid is also reported in literature¹⁴⁶. The reaction of copper (II) salt with 1,3-benzenedicarboxylic acid in the presence of 2,2'-bipyridine leads to a helical one dimensional coordination polymer, $\{[\text{Cu}(1,3\text{-benzenedicarboxylate})(2,2'\text{-bipyridine})].2\text{H}_2\text{O}\}_n$ (**1.51**). In this complex each copper(II) ion is coordinated by two oxygen atoms from two bidentate carboxylate ligands and two nitrogen atoms from 2,2'-bipyridine. A distorted square-planar geometry around copper is observed. The helical chains are assembled through π - π interaction between the bipyridine molecules and a zipper-like arrangement is attained in the lattice¹⁴³. Similar types of helical one dimensional chains of different metals with different dicarboxylic acids in presence of 2,2'-bipyridine are also reported¹⁴⁷⁻¹⁴⁸.

1.4.2 Two dimensional coordination polymers

In previous subsections we have described various one dimensional coordination polymers that are reported in literature. Besides that different types of two dimensional coordination polymers having a variety of architecture are also possible. In the next subsections syntheses and structural properties of different types of two dimensional coordination polymers are discussed.

1.4.2.1 Square grid:

One of the most common architecture in two dimensional polymers is the square grid network. The self-assembly of 1,1'-biphenyl-2,2',6,6'-tetracarboxylic acid with $[\text{Ni}(\text{cyclam})]^{2+}$ provides a square grid network of composition $\{[\text{Ni}(\text{cyclam})]_2(1,1'\text{-biphenyl-2,2',6,6'\text{-tetracarboxylate})\}.2\text{H}_2\text{O}$ (**1.52**). The crystal structure (Figure 1.39A), shows that the two phenyl rings of a 1,1'-biphenyl-2,2',6,6'-tetracarboxylate unit are twisted almost perpendicularly with respect to each other. Thus, each carboxylic acid acts as the planar four-connecting organic building block to anchor four nickel(II) macrocyclic complexes. The size of the square compartment in the square grid network is $10\text{\AA} \times 11\text{\AA}$. The guest molecules such as water are intercalated between the layers instead of the inside space in the square compartments¹⁴⁹.

Hydrothermal reaction of cobalt (II) salts with 4-(imidazol-1-yl)-benzoic acid leads to a 2D square grid having composition $[\text{Co}\{4\text{-}(\text{imidazol-1-yl})\text{-benzoate}\}_2]_n$ (**1.53**). Dimension of the square boxes in the structure are $11.42\text{\AA} \times 11.42\text{\AA}$ (Figure 1.39B). The central cobalt ion has a distorted tetrahedral geometry. The coordination sphere is completed by two oxygen atoms of carboxylate and two nitrogen atoms of imidazole groups¹⁵⁰. Similar type of square grid

structures are also obtained in polymers formed from the reaction of cobalt(II) salt with cinnamic acid and 4-carboxycinnamic acid¹⁵¹.

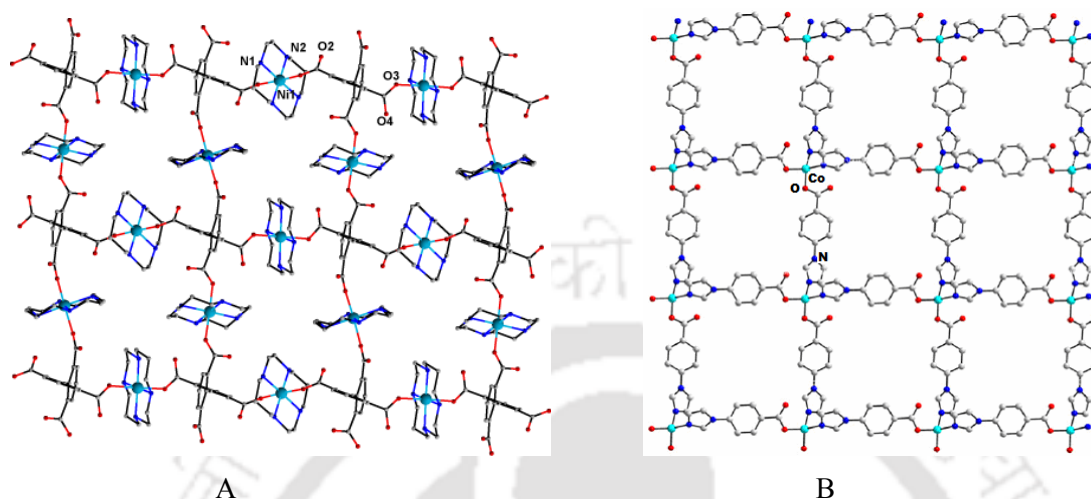


Figure 1.39 A) 2D coordination network constructed by 1,1'-biphenyl-2,2',6,6'-tetracarboxylic acid with $[\text{Ni}(\text{cyclam})]^{2+}$ (**1.52**), B) Structure of 2D square grid of $[\text{Co}\{4\text{-(imidazol-1-yl)benzoate}\}_2]_n$ (**1.53**)

Two dimensional square grid structure of copper(II) having composition $[\text{Cu}_4(\text{H}_2\text{O})_4(\text{N},\text{N}'\text{-bis[3-(dimethylamino)propyl]oxamide})_2(1,2,4,5\text{-benzenetetracarboxylate})]_n \cdot 10n\text{H}_2\text{O}$ (**1.54**) is prepared by the reaction of copper(II) salts with N,N'-bis[3-(dimethylamino) propyl] oxamide and 1,2,4,5-benzenetetracarboxylic acid. The two dimensional grid has dimension of $13.56 \text{ \AA} \times 15.62 \text{ \AA}$ (Figure 1.40). The environment around the copper(II) ion can be described as distorted square-pyramidal geometry. An overall three-dimensional channel-like framework is formed from the assembly of the 2D structure via H-bonding interactions¹⁵².

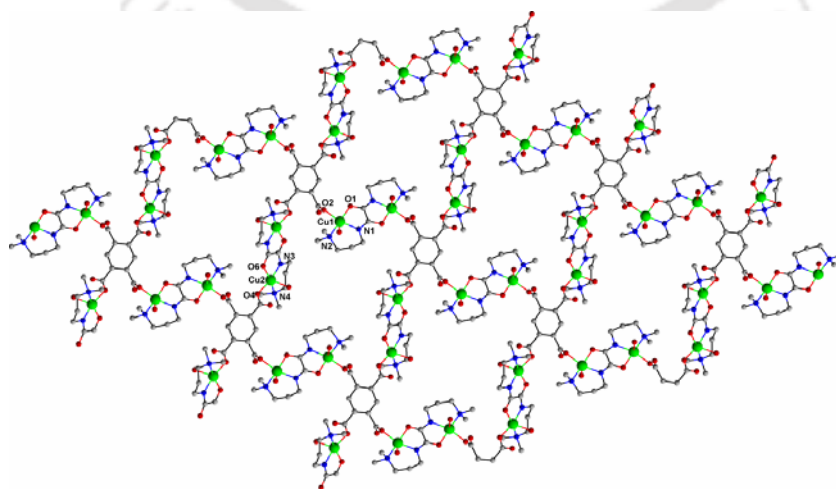


Figure 1.40 Two dimensional square grid structure of complex **1.54**

Square grid complex is also constructed by zinc(II) and 1,4-dicarboxylic acid. It has paddle-wheel units containing zinc(II) and 1,4-benzenediacrylate. The paddle-wheel units of zinc acts as secondary building block unit. Similar type of network also exists for 2-amino-1,4-benzenedicarboxylic acid¹⁵³. Two-dimensional coordination polymer of zinc with nicotinic acid has been synthesized under hydrothermal reaction conditions. Structure of the complex has self-assembled stacked square-grid nets. The zinc atoms in the complex are in distorted tetrahedral geometry¹⁵⁴.

1.4.2.2 Rhomboid grid:

Frameworks with specific topologies such as rhombic grids and cages have been obtained by the assembly of suitable metal ions with rationally designed carboxylate ligands. Two-dimensional layered complex of manganese with glycine having rhombic grid are reported in literature. The manganese ion is in a special position with half occupancy and is octahedrally surrounded by four oxygen atoms of bridging glycine molecules and two water molecules in a trans fashion¹⁵⁵. The glycine molecule, present in the zwitterionic form, bridges the Mn centers to form layers with a (4,4)-net topology parallel to the *bc* plane of the unit cell. The water molecules and the amine end of the glycine molecules project out from the layer, forming hydrogen bonds with the bromine atoms present in the interlamellar region. The rhombus grid has dimensions 5.4 Å x 5.4 Å.

A puckered rhombus grid $[\text{Ni}(4\text{-sulfanylmethyl-4'-phenylcarboxylate pyridine})_2]_n$ (**1.55**), is prepared by hydrothermal reaction of nickel(II) acetate with 4-sulfanylmethyl-4'-phenylcarboxylate pyridine. The rhombus grid (Figure 1.41A) has dimensions 11.72 Å x 11.09 Å. Each ligand acts as a single bridge linking two nickel ions through its nitrogen atom and carboxylate group and each nickel ion connects four ligands to form an infinite two-dimensional structure¹⁵⁶. Two dimensional rhombic grids such as $[\text{Ni}(\text{C}_{10}\text{H}_8\text{O}_4)(4,4\text{'-dipyridylamine})(\text{H}_2\text{O})]_n$ (**1.56**), can be constructed from both 4,4'-dipyridylamine and aromatic dicarboxylates (1,2-phenylenediacetic acid) with one or more flexible pendant arms (Figure 1.41B). In this complex each of the nickel(II) center display distorted octahedral coordination geometry, where the two trans-disposed nitrogen donor atoms belong to the two nitrogen atoms of 4,4'-dipyridylamine. The equatorial plane of each octahedron is occupied by two oxygen atoms of a chelating carboxylate terminus of a 1,2-phenylenediacetate ligand, one oxygen atom from a monodentate carboxylate group of 1,2-phenylenediacetate ligand, and an aqua ligand¹⁵⁷.

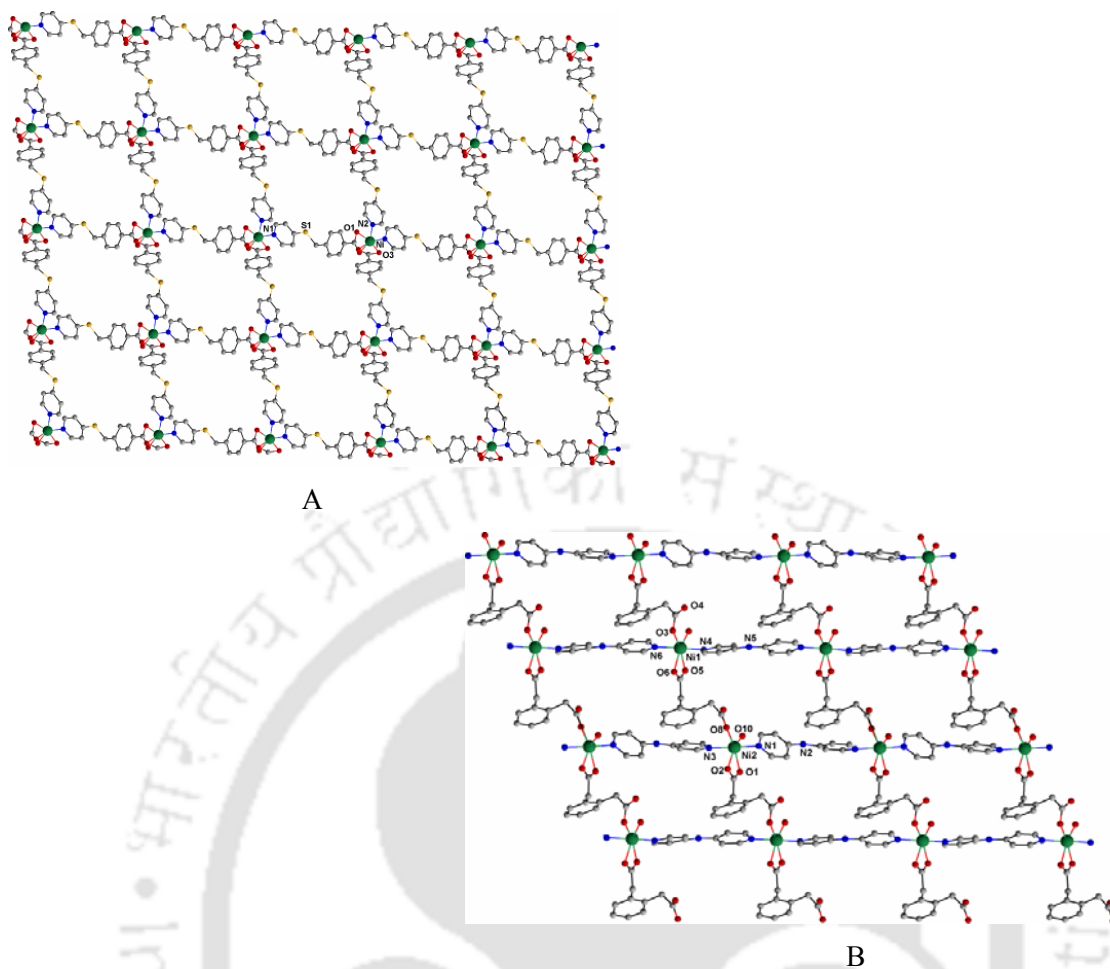


Figure 1.41 A) Rhombus grid like structure of $[\text{Ni}(4\text{-sulfanylmethyl-4'-phenylcarboxylate pyridine})_2]_n$ (**1.55**), B) Two dimensional rhombic grid of the complex **1.56**

Hydrothermal reaction of $\text{Ni}(\text{NO}_3)_2 \cdot 6\text{H}_2\text{O}$ with isophthalate dianion and a flexible organodiimine $\text{N,N}'\text{-bis}(4\text{-pyridylmethyl})\text{piperazine}$ leads to a 2D coordination polymer $[\text{Ni}\{\text{N,N}'\text{-bis}(4\text{-pyridylmethyl})\text{piperazine}\}(\text{isophthalate})\text{H}_2\text{O}]_n \cdot \text{H}_2\text{O}$ (**1.57**), with rhombic grid structure. In the complex the nickel center have octahedral geometry with nitrogen donors from two different $\text{N,N}'\text{-bis}(4\text{-pyridylmethyl})\text{piperazine}$ ligands arranged in a trans fashion and three equatorial oxygen donors belonging to two carboxylate donor and one coordinated water molecule. The junction of neighbouring nickel atoms through the amine and bis-bridging chelating/monodentate isophthalate ligands forms rhomboid grids with (4,4) topology¹⁵⁸. The dimension of each rhomboid void is $14.32 \text{ \AA} \times 19.10 \text{ \AA}$ (Figure 1.42A).

Arm-shaped two-dimensional layered complex of copper has been prepared by hydrothermal reaction of copper nitrate, 1,2,4-benzenetricarboxylic acid and triethylamine at 160°C . The two-dimensional layer of the complex consists of regular rhombic cavities and it also possesses pseudo-helical-shaped channels¹⁵⁹. In addition, the hydrogen-bonding and $\pi\text{-}\pi$

stacking interactions between layers extend into a three-dimensional supramolecular architecture with two differently oriented fashions. The dimension of the rhombic cavity is $6.90\text{Å} \times 6.90\text{Å}$ (Figure 1.42B).

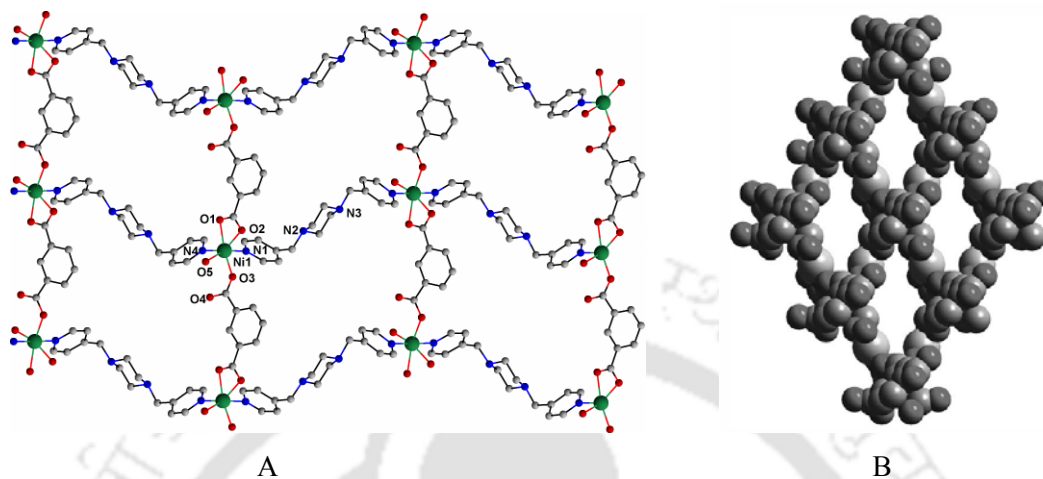


Figure 1.42 A) Rhombic grid structure of complex **1.57**, B) Rhombic cavities of a Two dimensional complex of copper

1.4.2.3 Rectangular Grid:

A good numbers of two-dimensional networks based on square grid, rectangular grid and rhombic grid motifs are found in literature. Hydrothermal reaction of cobalt(II) chloride hexahydrate with 3,5-dinitrobenzoic acid in presence of 4,4'-bipyridine leads to a 2D rectangular grid. The cobalt(II) centers display distorted octahedral geometries¹⁶⁰. The four oxygen atoms from four 3,5-dinitrobenzoic acid ligands are ligated in the equatorial positions and the trans axial sites are occupied by two nitrogen atoms from two 4,4'-bipyridine ligands. The cavity size of the rectangular grid is $5.05 \times 11.34 \text{Å}$. The reaction of cobalt(II) chloride hexahydrate with pyrazine and disodium terephthalate in water results in the formation of a neutral cavity-containing rectangular grid of the complex $[\text{Co}(\text{terephthalate})(\text{pyrazine})(\text{H}_2\text{O})_2]_n$ (**1.58**). The complex contains pyrazine molecule as aromatic guest¹⁶¹. The dimension of the cavities in the complex is $7.2 \times 11.3 \text{Å}$. Each cobalt site has slightly distorted octahedral coordination environment provided by two pyrazine ligands, two terephthalate ions, and two water molecules (Figure 1.43A).

Similar type of rectangular grid of cobalt(II) with pyridine-4-carboxylic acid and 4,4'-bipyridine is also reported in literature¹⁶². Rectangular grid from nickel isophthalate with 4,4'-bipyridine is also reported, where the nickel centers have distorted octahedral geometries.

There are two trans-related bridged 4,4'-bipyridine ligands at the axial positions. Two oxygen atoms from the chelate carboxylate and two oxygen atoms from the bridging carboxylate of the isophthalic acid ligands complete the near octahedral geometry¹⁶³.

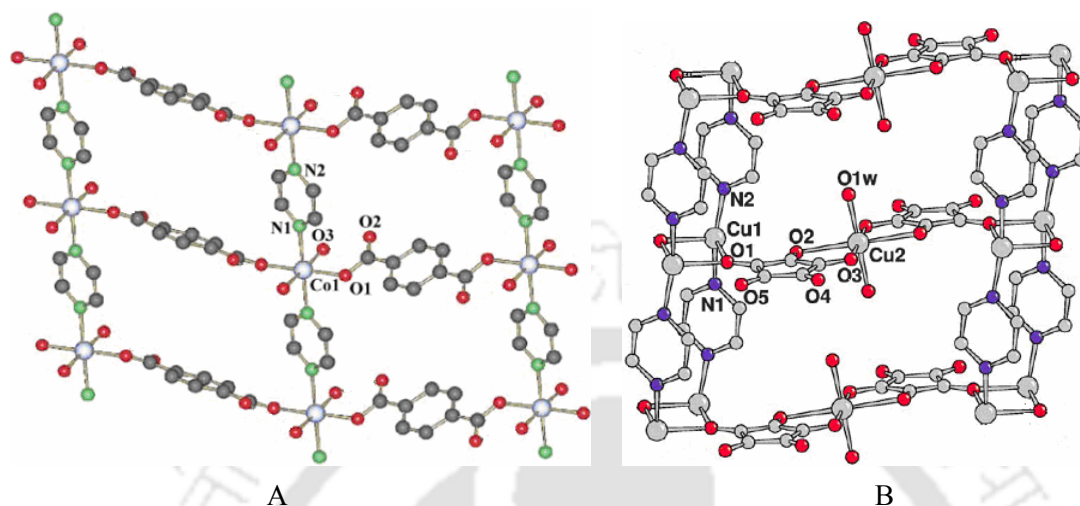


Figure 1.43 A) Structure of $[\text{Co}(\text{terephthalate})(\text{pyrazine})(\text{H}_2\text{O})_2]_n$ (**1.58**) containing rectangular grid into its structure, B) Two dimensional coordination polymer of copper having grid like structure

Two dimensional rectangular grid-like mixed-valence coordination polymer of copper(II) and copper(I) are reported in literature. Hydrothermal reaction of $\text{Cu}(\text{NO}_3)_2$, pyrazine and disodium crotonate leads to two dimensional coordination polymer. The octahedral coordination environment of copper(II) comprises of two chelating crotonate anions and two water molecules (Figure 1.43B). The structure extends to a 3D supramolecular network through H-bonding¹⁶⁴.

1.4.2.4 Honeycomb:

Metal organic framework having honeycomb type of structure can be prepared by multifunctional ligands with metal ions. For example, honeycomb like 2D coordination polymer of manganese(II) oxalate with pyrimidine-2-carboxylate are known¹⁶⁵. The oxalate ligand assumes the usual bis(chelating) bridging mode, but pyrimidine-2-carboxylate serves as a tridentate bridge with one of the pyrimidyl nitrogens remaining uncoordinated. The two different bridges collaborate to generate 2D layer and the layers are closely packed in parallel manner through π - π interactions.

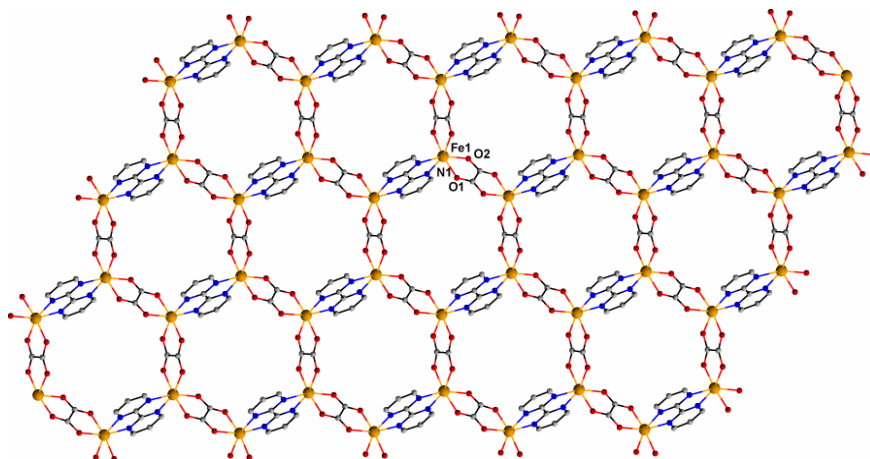


Figure 1.44 Honeycomb like 2D coordination polymer (**1.59**) of iron

The two-dimensional complex of iron(II), $\{[\text{Fe}_2(2,2'\text{-bipyrimidine})(\text{oxalate})_2]\cdot 5\text{H}_2\text{O}\}_n$ (**1.59**), is obtained by reaction of oxalic acid, iron(II) chloride and 2,2'-bipyrimidine in aqueous solution¹⁶⁶. Structure of the complex has oxalato-bridged iron(II) chains cross-linked by bis-chelating bipyrimidine affording a honeycomb type lattice (Figure 1.44). Similar types of honeycomb like heterodimetallic and homodimetallic oxalato complex with other metal ions are also reported in literature¹⁶⁷⁻¹⁶⁹.

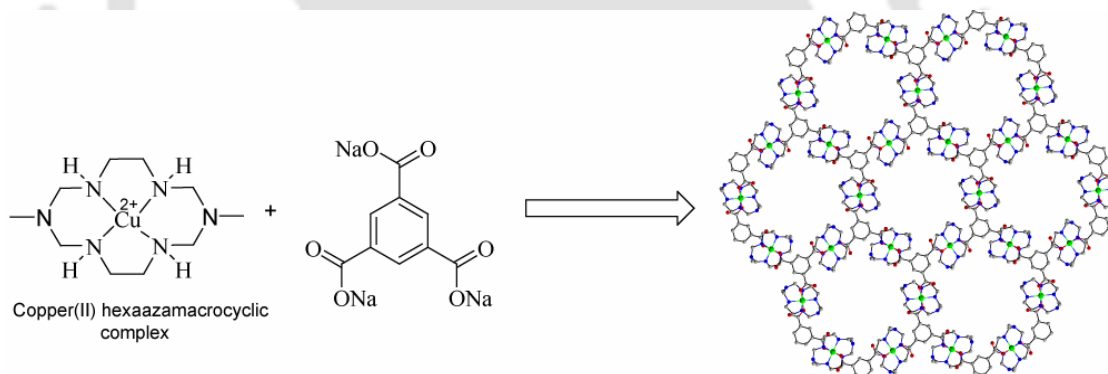


Figure 1.45 Two dimensional metal-organic open framework (**1.60**) of copper(II) having honeycomb like structure

Two dimensional metal-organic open framework of copper (**1.60**), can be prepared by copper(II) hexaazamacrocyclic complex with sodium 1,3,5-benzenetricarboxylate. The X-ray crystal structure indicates that each copper(II) macrocyclic unit binds two tricarboxylate ions in trans position and each benzenetricarboxylate ion is coordinated to three copper(II) macrocyclic complexes to form 2D coordination polymer layers with honeycomb cavities (effective size 8.1 Å). The layers are packed to generate 1D channels perpendicular to the 2D layers¹⁷⁰ (Figure 1.45).

1.4.2.5 Herringbone:

If the metal ions are only coordinated with three ligand molecules giving a “T-shape” around the node, layers are formed and the motifs are called herringbone motifs. Nickel-based two dimensional coordination polymer, $\{[\text{Ni}(\text{phthalate})(4,4'\text{-dipyridylamine})] \cdot 1.33\text{H}_2\text{O}\}_n$ (**1.61**), has a herringbone type architecture. The structure is constructed from both 4,4'-dipyridylamine and homophthalate (Figure 1.46A). The large asymmetric unit of the complex **1.61** consists of three crystallographically unique nickel atoms, homophthalate dianions and 4,4'-dipyridylamine ligands, along with four water molecules of crystallization. All the nickel atoms adopt distorted octahedral geometries, with nitrogen donors disposed at cis orientation to each other¹⁵⁷.

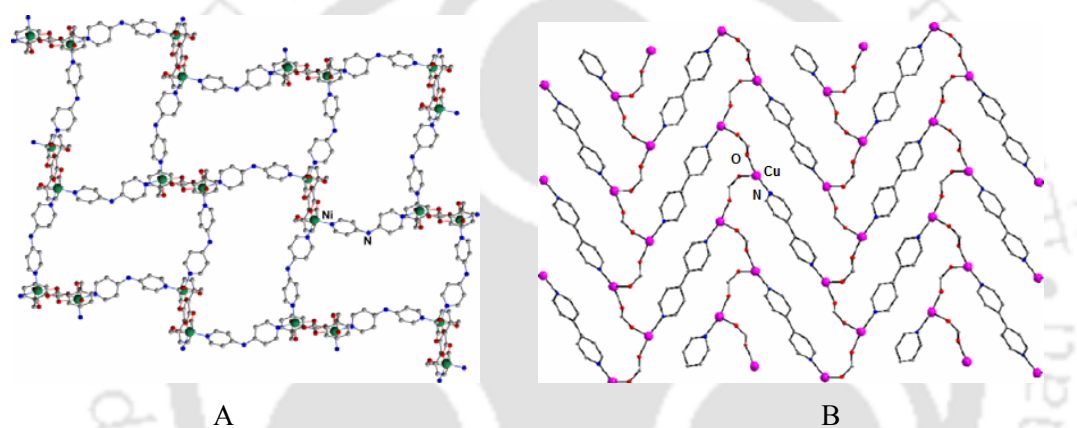


Figure 1.46 A) Herringbone architecture of nickel-based 2D coordination polymer (**1.61**), B) 2D herringbone network of copper (**1.62**) with 3,5-dinitrosalicylic acid and 4,4'-bipyridine

Hydrothermal reaction of $\text{CuCl}_2 \cdot \text{H}_2\text{O}$ with 3,5-dinitrosalicylic acid and 4,4'-bipyridine leads to a two dimensional herringbone type network of the complex $[\text{Cu}_2(\text{C}_7\text{H}_2\text{N}_2\text{O}_7)_2(\text{C}_{10}\text{H}_8\text{N}_2)(\text{H}_2\text{O})_2]_n$ (**1.62**). The copper atom possesses square-pyramidal geometry (Figure 1.46B). Penta-coordination of copper are fulfilled by three oxygen atoms from two different 3,5-dinitrosalicylates, one nitrogen atom from a 4,4'-bipyridine and an oxygen atom from a coordinated water molecule¹⁷¹.

1.4.2.6 Brickwall:

The reaction of 1,3,5-benzenetricarboxylate anion with nickel macrocyclic complex (Figure 1.47A) gives a complex **1.63**, that has brickwall structure (Figure 1.47B). Tetragonally distorted octahedron geometry is observed around nickel. The effective cavity size of the two dimensional complex is $6.7 \times 13 \text{ \AA}$. The cavities are filled with guest molecules. The host

structures assembled are greatly affected even by the partial change of the guest molecules. In the presence of pyridine the structures of complex change to honeycomb from brickwall motif¹⁷².

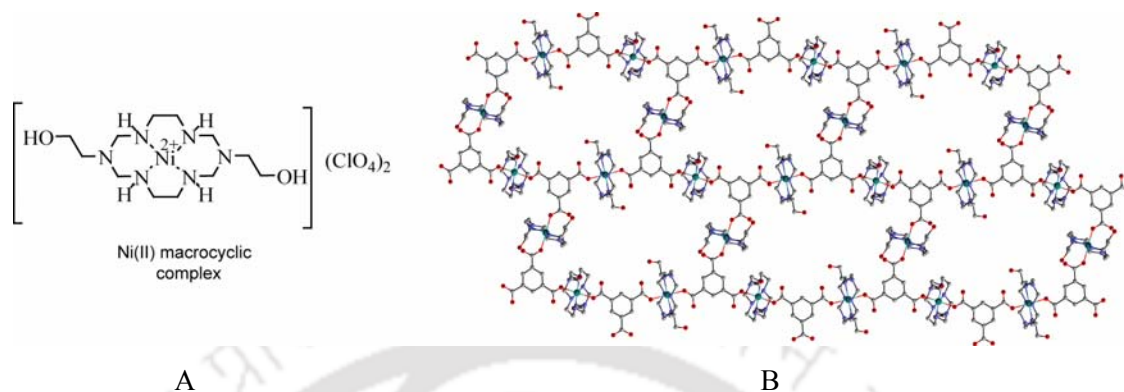


Figure 1.47 A) Structure of nickel(II) macrocyclic complex, B) Brickwall type structure of complex **1.63** constructed by nickel macrocycle and 1,3,5-benzenetricarboxylate

Similar type of brickwall motifs with macrocyclic nickel complex and 1,3,5-benzenetricarboxylic acid are reported¹⁷³. Different types of network are obtained from the reaction of copper(II) salts with trimesic acid in presence S,S'-diphenylsulfimide. When the copper complex is crystallised in the presence of pyridine a brickwall network with composition $[\text{Cu}_3(\text{Ph}_2\text{SNH})_6\{\text{trimesate}\}_2]$ (**1.64**), is obtained. In this complex each copper centre exhibits square planar coordination geometry (Figure 1.48). Each ring of the brickwall network composed with six metal centres and six trimesate anions¹⁷⁴.

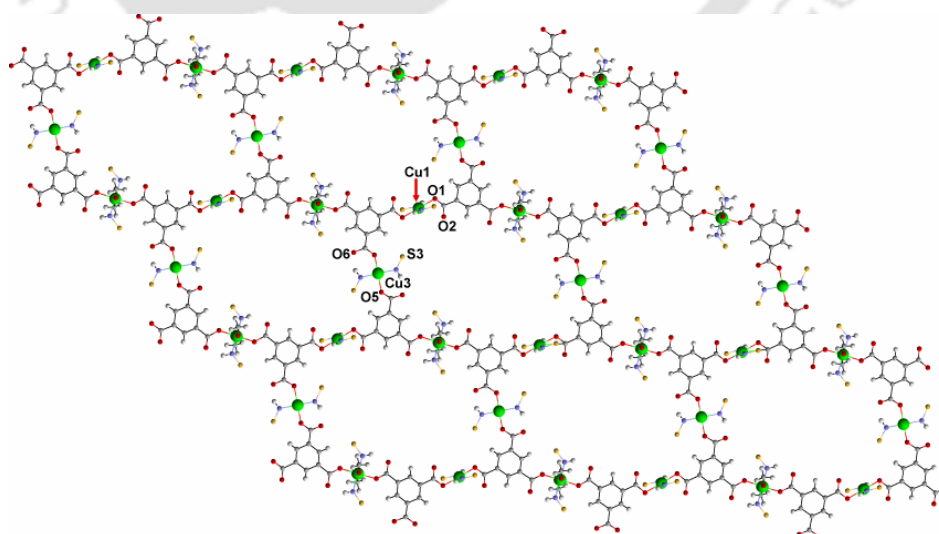


Figure 1.48 Brickwall type network of copper (**1.64**) with trimesic acid

1.4.3 Three dimensional coordination polymers

It is useful to know how three dimensional structures are formed by metal centers, multidentate ligands and auxiliary ligands bound to the metal centers. Some 3D networks which are common in literature are described below.

1.4.3.1 Diamondoid net:

One of the well-known and frequently found three dimensional metal carboxylate motifs is the diamondoid network. In this motif each node is connected to four bridging ligands in a tetrahedral manner, which leads to a three-dimensional diamond-like network. The hydrothermal reaction of zinc nitrate with urocanic acid leads to a novel fourfold-interpenetrated diamondoid network with 1D open channels in which the water molecules are trapped. The zinc(II) centers adopt tetrahedral geometries by coordinating to two imidazolyl nitrogen atoms and two carboxyl oxygen atoms of four separate urocanic acid ligands (Figure 1.49A). The compound exhibits a strong blue-fluorescent emission in the solid state¹⁷⁵.

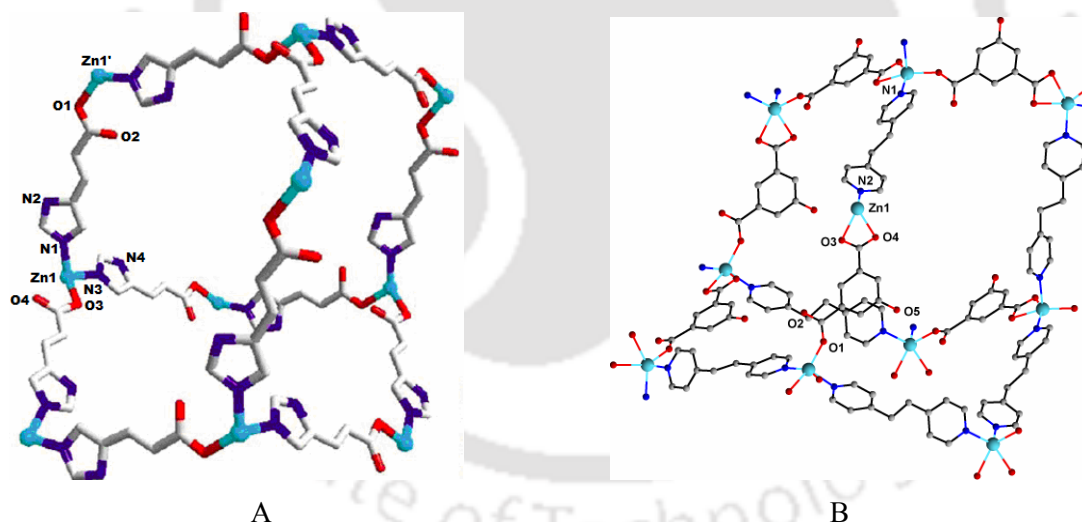


Figure 1.49 A) Structure of 3D diamond-like network constructed by zinc with urocanic acid, B) An interpenetrating 3D diamondoid zinc(II) complex

Adamantanoid cages are formed when tetrahedral organic building blocks are connected to nickel(II) macrocyclic complexes. The self assembly of $[\text{Ni}(\text{cyclam})]^{2+}$ and sodium salt of tetrakis[4-(carboxyphenyl)-oxamethyl]methane results in an 8-fold interpenetrating diamondoid network (Figure 1.50). Each nickel(II) ion exhibits a distorted octahedral coordination geometry. The diamondoid network comprises of large adamantanoid cages of

size 49.2 Å x 50.8 Å x 44.3 Å. Despite the high-fold interpenetration, the network generates 1D channel with an effective window size of 6.7 Å x 4.7 Å. The network exhibits a flexible behavior; it becomes nonporous on removal of the guest molecules¹⁷⁶.

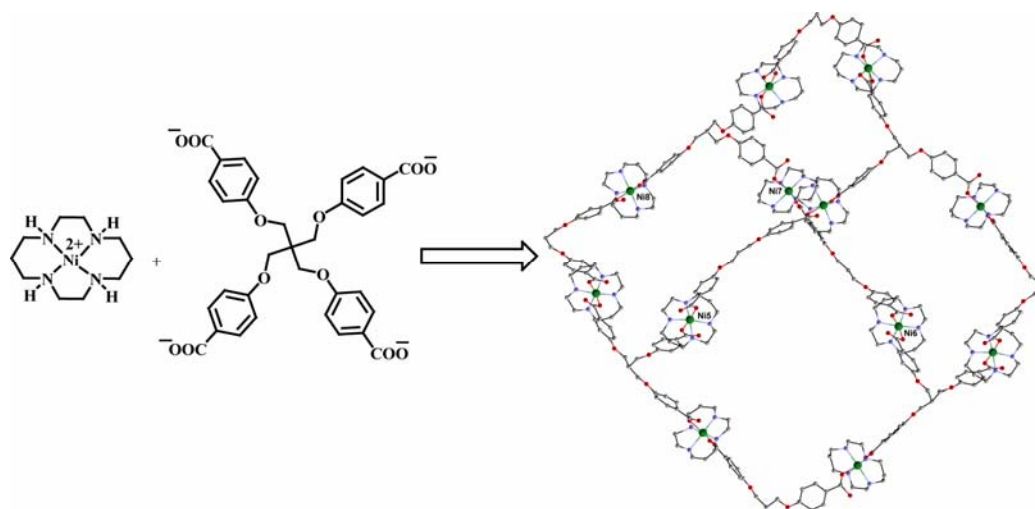


Figure 1.50

An interpenetrating 3D diamondoid zinc(II) compound is prepared solvothermally by assembly of 5-hydroxyisophthalic acid, zinc(II) nitrate hexahydrate with 1,2-bis(4-pyridyl)ethane. Single crystal X-ray diffraction analyses revealed that it has a 5-fold interpenetrating diamondoid network. By the use of 1,2-di(4-pyridyl)ethylene or 1,3-bi(4-pyridyl)propane instead of 1,2-bis(4-pyridyl)ethane leads to a 4-fold interpenetrating diamondoid structures with encapsulated guest molecules and water molecules¹⁷⁷ (Figure 1.49B). By self-assembling of zinc with fumaric acid and 1,1'-(1,4-butanediyl)bis(imidazole-2-phenyl), a 3-fold interpenetrating diamondoid network of zinc can be obtained¹⁷⁸. Several carboxylate based three-dimensional interpenetrating diamondoid networks are reported in literature¹⁷⁹⁻¹⁸³.

1.4.3.2 Octahedral net:

Octahedral motifs are based on the extension of the framework in the three directions from octahedral nodes. It is very difficult to coordinate six polydentate ligand molecules around one metal center due to steric reason. The apical positions of the octahedral metal ions are occupied by water molecules, other solvent molecules or counter anions, and results in network of low dimensionality. The construction of octahedral motifs is also possible if the nodes are made from binuclear subunits. The reaction of cobalt (II) nitrate hexahydrate with terephthalic acid and 4,4'-bipyridine gives [Co(terephthalate)(4,4'-bipyridine)]_n (**1.65**) shown

in Figure 1.51. The bipyridine molecules are linked to the cobalt(II) cations through the apical positions for the expansion of the structure in the third direction¹⁸⁴. The dimension of 2D rectangular sheets of metal and terephthalate is 10.30 x 11.37 Å.

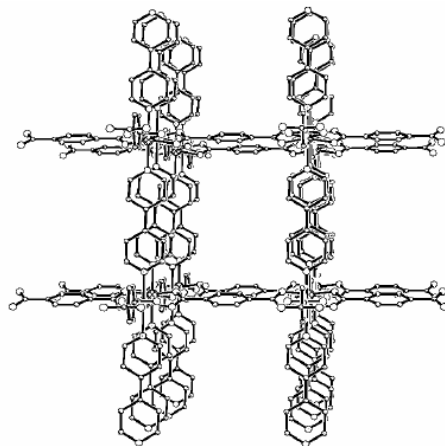


Figure 1.51 Octahedral net of cobalt with terephthalic acid and 4,4'-bipyridine (1.65)

1.5 Biological role of carboxylic acids and carboxylates

Carboxylic acids are important in biology. Carboxylic acid group is widely present in biological molecules like metalloproteins, enzymes and proteins. The amino acids are the most important constituent of biological molecules. Several metalloproteins and metalloenzymes contain dinuclear carboxylate bridged metal complexes in their active sites. Enzymes having multi-metal active sites control various biological processes. Many such enzymes contain two or more metal atoms connected by at least one endogenous carboxylate bridge. Active sites of metalloenzymes with the first row transition metal ions regulate Lewis acidities and hydrolytic activity of enzymes. Metalloenzymes containing carboxylate bridged dinuclear metal centers catalyze diverse reactions such as the degradation of DNA, RNA, phospholipids, and polypeptides¹⁸⁵⁻¹⁸⁹. They also play important roles in carcinogenesis, tissue repair, hormone level regulation, cell-cycle control, and protein degradation processes¹⁹⁰⁻¹⁹¹. Some metalloenzymes containing carboxylate bridged ligands are discussed in the next subsections.

1.5.1 Nickel containing metalloenzyme: Urease

Urease is a nickel-containing enzyme which catalyzes the conversion of urea into ammonia and carbon dioxide. It also hydrolyzes small amides such as formamide and acetamide to their corresponding carboxylic acids^{187, 192-193}. The enzyme contains two nickel (II) ions separated

by a distance of about 3.5 Å. The nickel ions are coordinated by two histidine residues and bridged by a carbamylated lysine residue¹⁹⁴⁻¹⁹⁵. One of the nickel ions is coordinated by an aspartate residue. In addition to these, the two nickel centers are bridged by one water molecule or hydroxide ion. An additional water molecule binds terminally to each metal ion. This results in an asymmetric coordination active sites, with one nickel ion in a pseudo-octahedral coordination environment and the other in a square pyramidal geometry. The active site of urease isolated from *Klebsiella aerogenes* is shown in Figure 1.52.

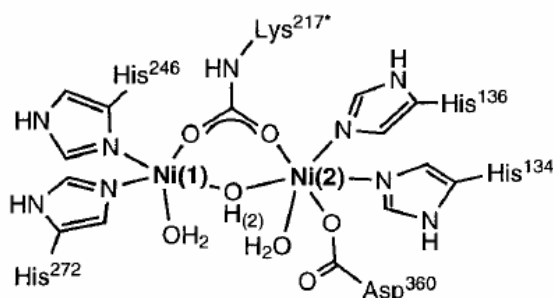
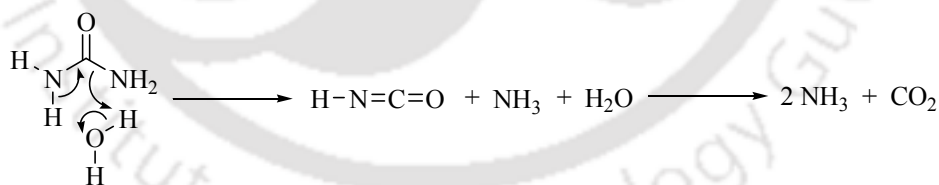
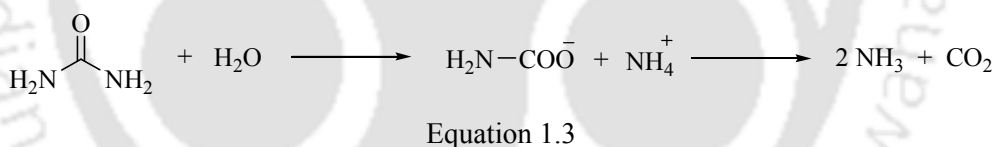


Figure 1.52 Active site of urease isolated from *Klebsiella aerogenes*

It is proposed that the urea hydrolysis by urease occurs via two pathways. They are either by nucleophilic attack of a coordinated water molecule at the carbonyl carbon atom of a bound urea molecule, to produce ammonium carbamate which spontaneously decomposes to ammonia and carbon dioxide¹⁹⁶⁻¹⁹⁹ (Equation 1.3).



Equation 1.4

Alternatively, the hydrolysis of urea passes through elimination of ammonia to form cyanate, which is further hydrolyzed to ammonia and carbon dioxide²⁰⁰⁻²⁰¹ (Equation 1.4).

1.5.2 Cobalt and zinc containing Metalloenzymes: Aminopeptidases

Aminopeptidases²⁰² are exopeptidases that hydrolyses a wide range of N-terminal amino acid residues of proteins and polypeptides. They play significant roles in protein maturation, protein degradation, regulation of hormone level and in cell-cycle control. So far, three

aminopeptidases have been crystallographically characterized. Among them bovine lens leucine aminopeptidase²⁰³⁻²⁰⁴ contains a (μ -hydroxo) bis(μ -carboxylato) dizinc (II) core with terminal carboxylates at each metal site along with a peptide backbone carbonyl and a lysine amine nitrogen bound to one of the zinc(II) ions²⁰⁵⁻²⁰⁸.

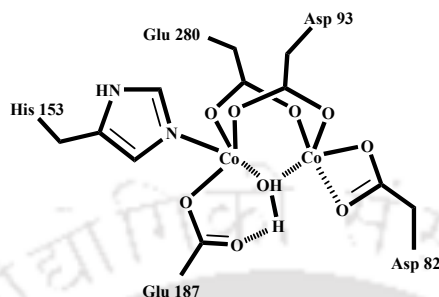


Figure 1.53 Active site structure of methionine aminopeptidase isolated from *Escherichia coli*

On the other hand, methionine aminopeptidase from *Escherichia coli* contains a bis (μ -carboxylato) dicobalt(II) core with terminal carboxylates at each metal site along with a histidine residue at the second Co(II) site²⁰⁹. Each cobalt(II) ion resides in a distorted octahedral environment with the remaining coordination sites filled by water molecules. In both leucine aminopeptidase and methionine aminopeptidase the metal-metal distance is 2.9 Å²¹⁰. A schematic representation of the active site of methionine aminopeptidase from *Escherichia coli* is shown in Figure 1.53.

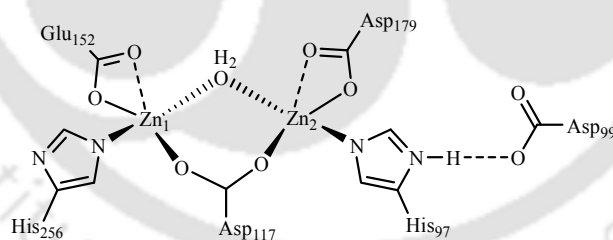


Figure 1.54 Active site structure of aminopeptidase isolated from *Aeromonas proteolytica*

The third aminopeptidase isolated from *Aeromonas proteolytica* possesses a (μ -aqua)(μ -carboxylato) dizinc(II) core with one terminal carboxylate and one histidine residue at each metal site²¹¹. Both Zn (II) are in distorted tetrahedral coordination geometry with a Zn-Zn distance of 3.5 Å. An oxygen atom of Glu151 forms a hydrogen bond with the bridging water molecule while the second oxygen atom is 3.4 Å apart from the nitrogen of His97 which is a ligand to Zn1. A schematic representation of the active site of aminopeptidase from *Aeromonas proteolytica* is shown in Figure 1.54.

1.5.3 Heterodinuclear metalloenzyme: Purple Acid Phosphatases

Purple acid Phosphatases catalyze hydrolysis of phosphomonoesters *in vitro* under acidic conditions (optimum pH of 4.9-6.0). They contain two irons (or one iron and another divalent metal ion), and exhibit a characteristic purple color ($\lambda_{\text{max}} \sim 550$ nm) in their inactive oxidized form and a pink color ($\lambda_{\text{max}} \sim 510$ nm) in their active reduced form²¹²⁻²¹³. They are isolated from mammals, plants and fungi. The structures of several enzymes from different sources have been determined by X-ray crystallography.

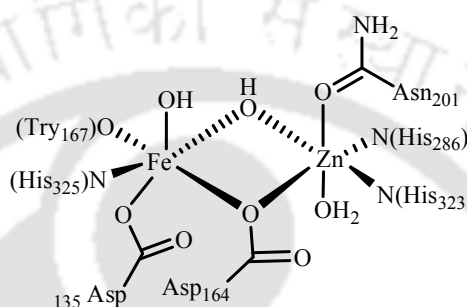


Figure 1.55 Active site structure of heterodinuclear metalloenzyme Purple acid Phosphatases

Two different coordination environments are present around the trivalent and the divalent metal ions. Iron (III) is coordinated by an aspartate, a histidine and a deprotonated tyrosine residue (Figure 1.55). The latter stabilizes the iron at +3 oxidation state and gives rise to the intense LMCT band around 560 nm. This is responsible for the colour of these enzymes. The two metal centers are bridged by a hydroxide and an aspartate residue. Other zinc (II) is further coordinated by two histidines and one asparagine. The octahedral coordination sites are occupied by one water and one hydroxide. There are also a few other non-coordinating amino acid residues in the active site that helps in binding and activation of the substrate by hydrogen bonding²¹⁴⁻²¹⁵.

1.6 Porous carboxylate networks

The advantage of introducing organic molecules in metal-organic frameworks is to control the material design, architecture choice, functionality of a porous material and increasing its selectivity^{16,216}. Gas storage is one of the applications for these materials. Yaghi et al. reported many robust carboxylate networks, which showed permanent porosity with large pore volume and large surface area²¹⁷. Representative examples are cubic porous networks constructed from the octahedral $\text{Zn}_4\text{O}(\text{CO}_2)_6$ secondary building unit and linear dicarboxylate linkers²¹⁸⁻²¹⁹. The channel sizes can be tuned by the use of appropriate ligand

molecules. The metal organic framework obtained by the reaction of zinc(II) salt with 1,4-benzenedicarboxylate has a cubic three-dimensional extended porous structure and able to adsorb hydrogen (Figure 1.56). These types of porous coordination polymers are applicable as hydrogen storage materials²²⁰⁻²²¹. The Zn₄O-based metal organic frameworks, which have high porosity and large surface area, are well known for their application to fuel gas storage. The spherical pore size of the metal organic framework constructed by zinc and 1,4-benzenedicarboxylic acid is about 15Å in diameter.

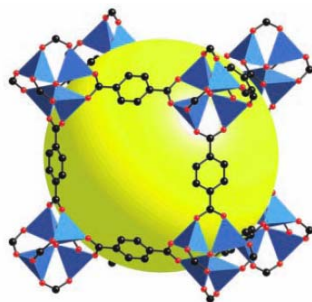


Figure 1.56 3D metallo-organic framework of zinc with 1,4-benzenedicarboxylate

Some of the metal organic frameworks based on Zn₄O network topology are shown in Figure 1.57. The structures are made up of oxo-centered Zn₄O tetrahedron residing at the edges of the cube and bridged by six carboxylate units to give octahedron shaped secondary building units (SBUs). These SBUs are further linked by the bridging dicarboxylate groups to form the 3D cubic networks. The pore size can be controlled by using carboxylate linkers of varying lengths such as biphenyl, tetrahydropyrene, pyrene, and terphenyl moieties. Additionally, various functional groups such as -Br, -NH₂, -OC₃H₇, -OC₅H₁₁, -C₂H₄ and -C₄H₄ can be incorporated into the frameworks that are orientated towards the pores. The resulting networks are highly porous with very low crystal densities²¹⁸.

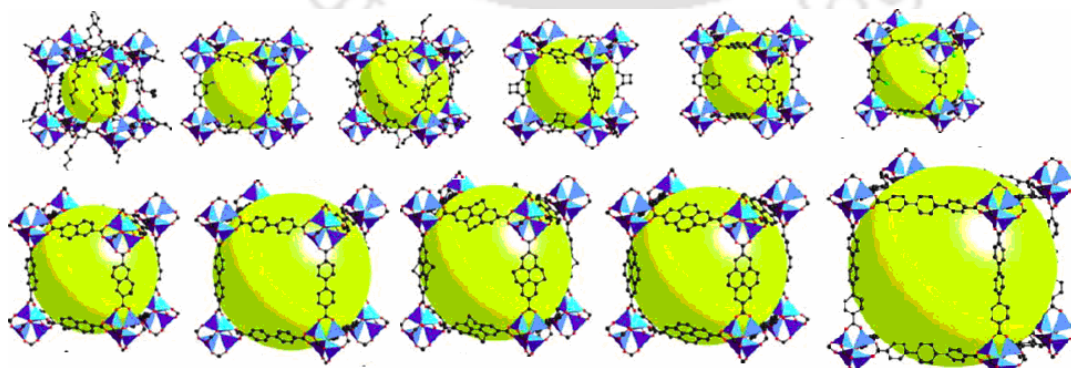


Figure 1.57 Metal organic frameworks obtained by using different dicarboxylate linkers

Different types of 3D metallo-organic frameworks of zinc(II) with 4,4'-biphenylcarboxylic acid are reported in literature²²². The asymmetric unit of these complexes have three crystallographically unique zinc atoms bridged by four carboxylate groups, each from different biphenylcarboxylate units. The zinc ions are also bound to two hydroxy groups to give two tetrahedral and one octahedral zinc center arranged in coplanar fashion. The infinite Zn-O-C columns are stacked in parallel and connected in the [110] direction by the biphenyl links to give one-dimensional (1D) rhombic channels of 12.2 Å along an edge and 16.6 Å along the diagonal (Figure 1.58A). Similar type of motifs are also obtained in the zinc complexes of 2,6-naphthalenedicarboxylic acid.

Other coordination polymers, based on bis- and tris-bidentate carboxylate linkers are copolymerized with different transition metals to construct stable porous materials. The sorption processes of these compounds are well studied affording efficient and robust materials for gas storage or liquid separation^{216, 223-226}. The hydrothermal reaction of copper nitrate with 3,3',5,5'-biphenyl tetracarboxylic acid leads to 3D metallorganic frameworks. The $\text{Cu}_2(\text{CO}_2)_4$ core is a secondary building unit, which is connected through biphenyl rings to construct 3D framework (Figure 1.58B).

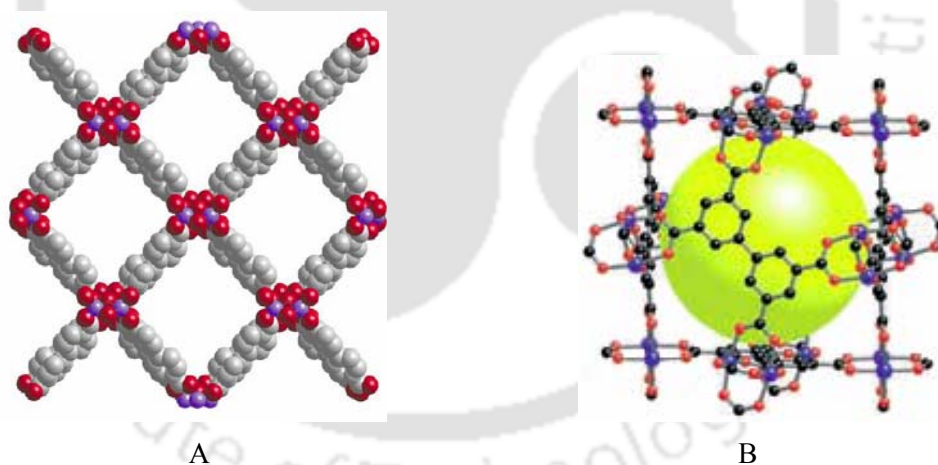


Figure 1.58 A) 3D metallo-organic frameworks of zinc(II) with 4,4'-biphenylcarboxylic acid, B) Structure of 3D metallorganic frameworks of copper with biphenyl tetracarboxylate

The carboxylate functionalities of the biphenyl tetracarboxylate ligand are nearly coplanar with the biphenyl rings. This metallo-organic framework has two kinds of pores, and possesses permanent porosity with high capacity for hydrogen adsorption²²⁷. Similar type of copper motifs with 4,4',4''-benzene-1,3,5-triyl-tribenzoic acid is also reported²²⁸. Many porous network solids with very large pore size and surface areas are known²²⁹⁻²³¹. Fourfold interpenetrated 3D networks, of zinc with 6,6'-dichloro-2,2'-diethoxy-1,1'-binaphthyl-4,4'-

dibenzoic acid and 6,6'-dichloro-2,2'-dibenzyloxy-1,1'-binaphthyl-4,4'-dibenzoic acid generates 3D channels and exhibit permanent porosity. These motifs are good for hydrogen uptake at room temperature²³².

1.6.1 Gas separation by carboxylate frameworks

The carboxylate MOF can be designed to distinguish multiple gases and also for potential gas absorption. Octanuclear nickel(II) cluster are useful for the separation of different gases. It is prepared by using tert-butyl-1,3-benzenedicarboxylic acid to form a trilayer, in which a hydrophilic cluster layer is sandwiched by two hydrophobic tert-butyl-1,3-benzenedicarboxylate layers (Figure 1.59). The network is flexible, and can separate commercially relevant gases such as H₂/N₂, H₂/CO, N₂/O₂, N₂/CH₄, CH₄/C₂H₄, and C₂H₄/C₃H₆. The gas separation capability of the network comes from the hydrophobic tert-butyl-1,3-benzenedicarboxylate gate in the hydrophilic/hydrophobic interface, which opens at higher temperatures due to thermal vibration of hydrophobic tert-butyl-1,3-benzenedicarboxylate groups²³³.

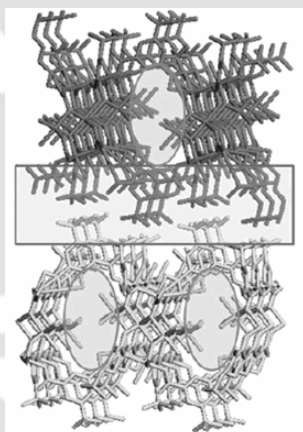


Figure 1.59 Octanuclear nickel(II) cluster with tert-butyl-1,3-benzenedicarboxylic acid

Microporous complexes of copper with 4,4'-(hexafluoroisopropylidene)-bis(benzoic acid), are able to separate hydrocarbons²³⁴. The complex consists of [Cu₂(COO)₄] paddle-wheel in the equatorial plane and 4,4'-(hexafluoroisopropylidene)-bis(benzoic acid) ligand in the axial sites to construct a 3D network. Another example of a doubly interpenetrated framework of zinc with 1,4-benzenedicarboxylic acid and 4,4'-bipyridine has 1D channels (channel size, 4.0 Å x 4.0 Å)²³⁵. This compound is able to separate n-pentane from n-hexane, branched 2-methylbutane from n-pentane, and 2-methylpentane, 2,2-dimethylbutane from n-hexane, respectively. In addition, the mixture of 2-methylbutane, n-pentane, 2,2-dimethylbutane, 2-

methylpentane, and n-hexane can be easily separated with different retention times. The selective separation of alkanes is attributed to their different van der Waals interactions with the host. Mixed alkyl aromatic compounds can be separated by using a MOF having composition $[\text{V}^{\text{III}}(\text{OH})(\text{O}_2\text{C}-\text{C}_6\text{H}_4-\text{CO}_2)_2 \cdot 0.75 (\text{HO}_2\text{C}-\text{C}_6\text{H}_4-\text{CO}_2\text{H})]^{236}$. This compound is able to separate p-xylene, m-xylene, o-xylene, and ethylbenzene.

1.6.2 Selective guest binding in carboxylate networks

The 3D network $\{[\text{Ni}(\text{L})(\text{H}_2\text{O})_2]_3[\text{BTC}]_2\}_n \cdot 24n\text{H}_2\text{O}$ (**1.66**) (where BTC= benzene tricarboxylate, L = 1,4,8,11-tetraazacyclotetradecane), selectively binds D-glucose into the channels over maltose. It has 1D channels of honeycomb aperture whose effective window size is 10.3 Å in diameter²³⁷ (Figure 1.60A).

A mixed metal framework of Cu(II) and Hg(II) constructed from $[(\text{Cu}(2\text{-pyrazinecarboxylato})_2)]$ building block and HgI_2 as linkers (Figure 1.60B). In this framework each copper(II) centers have distorted octahedral coordination geometry. It has cuboidal framework structure, possesses rectangular channels with dimension 7.24 x 7.24 Å. Interestingly uncoordinated linear HgI_2 molecules are encapsulated in the voids²³⁸.

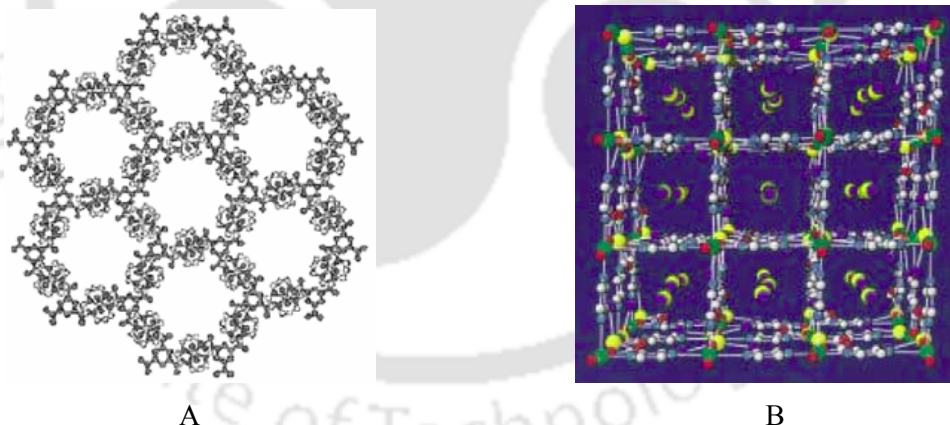


Figure 1.60 A) 3D network of $\{[\text{Ni}(\text{L})(\text{H}_2\text{O})_2]_3[\text{BTC}]_2\}_n \cdot 24n\text{H}_2\text{O}$ (**1.66**), B) Three dimensional network of Cu(II) and Hg(II) which encapsulate HgI_2 molecules in the voids

A microporous coordination polymer, of copper with pyrazine-2,3-dicarboxylic acid and 4,4'-bipyridine shows a reversible structural change on sorption/desorption of benzene²³⁹. The framework undergoes a deformation so that the channel cavities suit benzene molecules very well. This results in an appreciable difference in the channel shape with and without benzene. The channel without benzene has nearly a rectangular shape of dimensions of 5.6Å x 7.2 Å;

whereas that with a benzene has a “Z” shaped shown in Figure 1.61. In the absence of benzene, the geometry around the copper ion is square pyramidal, while that with benzene shows a square planar geometry. Eventually, the deformation produces a large contact area to the benzene plane.

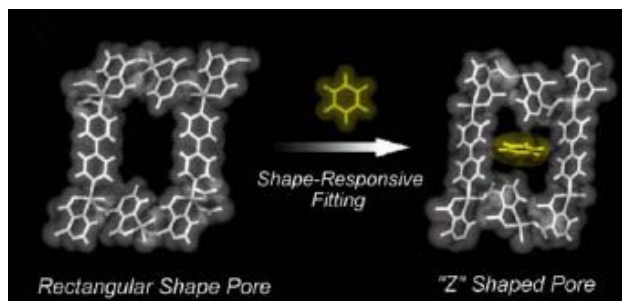


Figure 1.61

A chromium (III) complex with 1,4-benzenedicarboxylic acid exhibits a 3D framework with a 1D pore channel system²³⁹⁻²⁴¹. The transition between the hydrated form and anhydrous solid is reversible and followed by a high breathing effect, the pores being clipped in the presence of water molecules and re-opened when the channels are empty. No acetone or ethanol could be incorporated instead of water, whereas dimethyl formamide is incorporated into the pore instead of H₂O. This selectivity is attributed to the higher capability of dimethyl formamide toward the formation of strong hydrogen bonds with the hydroxyl groups of the framework (Figure 1.62).

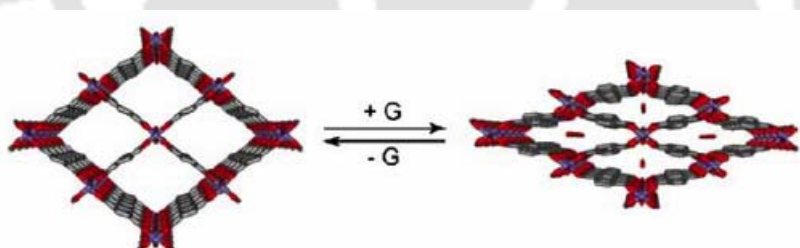


Figure 1.62 Structural transformation of chromium (III) complex after guest encapsulation

Microporous coordination polymers are one of the most reasonable candidates for the formation of specific molecular arrays because of their highly designable nature and pore homogeneity. Example of such type of framework is $[\text{Cu}_2(\text{pzdc})_2(\text{pyz})]$ (**1.67**), where pzdc is pyrazine-2,3-dicarboxylate and pyz is pyrazine. The alignment of oxygen molecules in the channels of this complex is observed²⁴². The confinement effect and the restricted geometry of 1D nanochannels leads to a 1D ladder-like structure of oxygen dimer (Figure 1.63). These types of metallo-organic frameworks are able to absorb CO₂ and acetylene molecules.

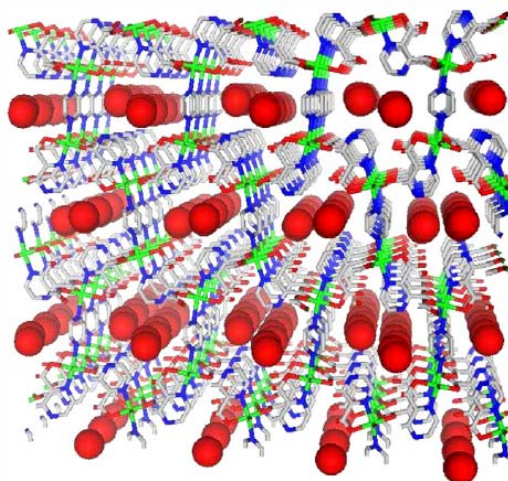


Figure 1.63 1D ladder-like structure of oxygen dimer encapsulated into the voids of 3D network of copper (**1.67**) with pyrazine-2,3-dicarboxylate

1.6.3 Carboxylate frameworks for enantioselective transformations

The first example of asymmetric catalysis using a homochiral metal-organic network is achieved by a zinc complex of a enantiopure bridging ligand with both carboxylic and pyridyl functional groups. In this complex three zinc ions are held together by six carboxylate groups of the chiral ligand and bridging oxo oxygen, to form a trinuclear unit. The complex contains chiral channels with edge lengths of about 13 Å as shown in Figure 1.64. The porous structure is stable in the presence of solvents. The trans-esterification reactions are carried out in the presence of size selectivity. With a racemic mixture of a chiral alcohol (1-phenyl-2-propanol) a slight enantiomeric excess (8% ee) was observed in the product ester²⁴³.

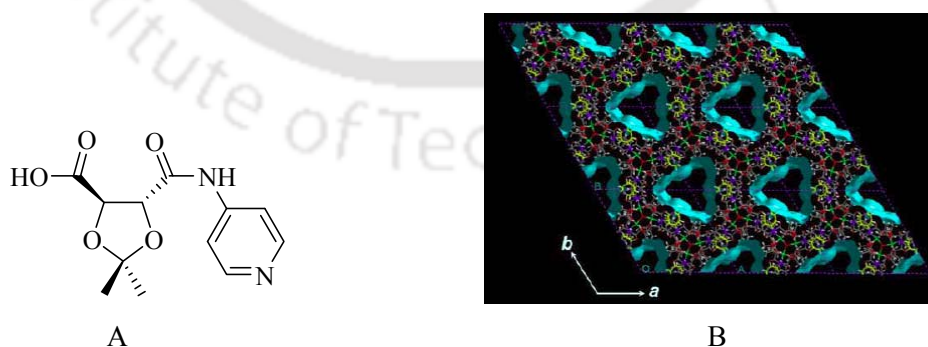


Figure 1.64 A) Enantiopure bridging ligand with both carboxylic acid and pyridyl functional groups, B) Homochiral metal-organic network of zinc that catalyzes trans-esterification reactions

1.7 Carboxylic acids and its derivatives as receptors

Unlike transition-metal coordination, the binding of anions or neutral molecules with synthetic receptors falls into the area of “supramolecular chemistry”, i.e. interactions between molecular or ionic species in the absence of covalent bond formation. Binding affinities between guest and their hosts are mostly attributed to hydrogen-bonding or electrostatic interactions.

As for example, cyclic hexapeptide, **1.68** (Figure 1.65A) composed of alternating L-proline and 3-aminobenzoic acid subunits with substituents on the aromatic subunits that contain free carboxylate groups are able to bind monosaccharide molecules. The free carboxylate groups are able to bind the monosaccharide molecules through hydrogen bonding. The binding selectivity of these peptides depends on the structure of the substituents on the aromatic subunits²⁴⁴. Enantioselective recognition of carboxylates has important implications in asymmetric synthesis and drug discovery²⁴⁵.

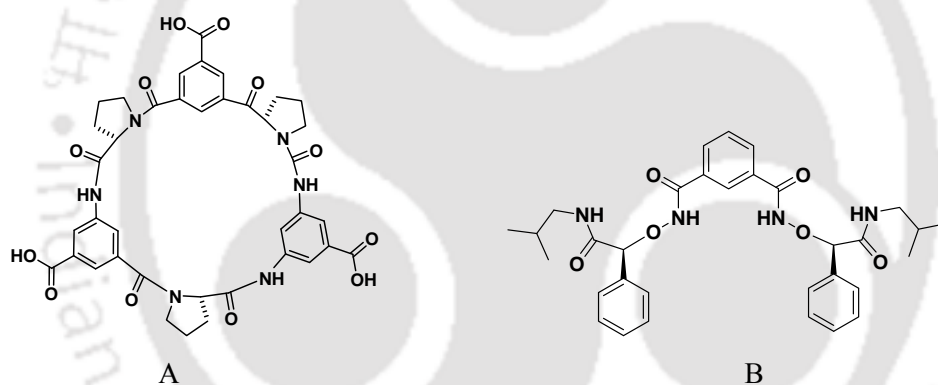


Figure 1.65 A) Cyclic hexapeptide (**1.68**) having free carboxylic acid groups, B) Receptor (**1.69**) for carboxylate anions

Many enantioselective carboxylate receptors have shown their application in chiral resolution²⁴⁶. An amide based C_2 -symmetric receptor (**1.69**) shows excellent ability to discriminate the enantiomers of a broad variety of carboxylic acids in solution²⁴⁷ (Figure 1.65B). A chiral fluorescent receptor **1.70**, based on cholic acid is also known in literature. The receptor **1.70** shows significant enantioselective ability to the enantiomers of the mandelate anion (Figure 1.66A). It binds S-mandelate anion more selectively rather than R-mandelate anion²⁴⁸. Tripodal guanidinocarbonyl pyrrole based receptor **1.71**, which binds citrate and other tricarboxylates with unprecedented high association constants in water (Figure 1.66B). The tricarboxylates are bound within the inner cavity of receptor **1.71** by ion

pairing between the carboxylate groups and the guanidiniocarbonyl pyrrole moieties. Hence, receptor can be considered as a molecular flytrap²⁴⁹.

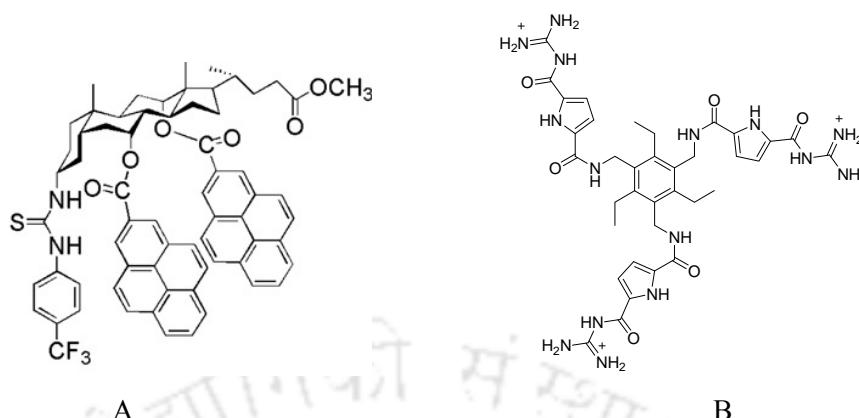


Figure 1.66A) Chiral fluorescent receptor (**1.70**) for mandelate anions, B) Molecular flytrap (**1.71**) for tricarboxylate anions

In the case of the aromatic tricarboxylate, additional aromatic interactions further strengthen the complex. The complexes with the tricarboxylates are so strong that even the presence of a large excess of competing anions or buffer salts does not significantly affect the association constant.

1.8 Scope of the present work

In foregoing subsections we have discussed about the various types of metal carboxylates and their application in material science²⁵⁰ and in biology²⁵¹. Metallo-organic framework having carboxylate ligands are used as storage material²⁵², sensor²⁵³, molecular recognition²⁵⁴, molecular magnetic material²⁵⁵, and also have prospective applications in catalysis²⁵⁶. Metal carboxylates have potential application in preparation of new non-linear optical materials²⁵⁷, and design of porous solids with novel inclusion properties²³⁸. Metal-organic materials having nano channels with tailorable chemical functionality are of primary interest for the manipulation and transformation of a wide range of molecules. So the size and geometry of the building blocks control the topology, spatial dimensionality and porosity of networks.

Crystal engineering of metal carboxylates, especially coordination polymers has been greatly developed in the past decade²⁵⁸. Supramolecular architecture of metal carboxylates can be directly constructed by using metal ions existing in various coordination geometries combined with multifunctional ligands²⁵⁹⁻²⁶⁰. The directional and molecular recognition properties of metal organic framework are controlled by the supramolecular interaction like hydrogen

bonding²⁹⁵, π - π stacking²⁶¹, weak electrostatic interactions and van der Waals forces. Metal-organic network are assembled by coordination bonds and/or supramolecular interactions allow for more predictable control over directional assemblies and packing arrangements in the solid state.

One of the most challenging aspects of carboxylate chemistry is to design multifunctional materials with predictable structures and properties²⁶⁰. In 1970s, A.F.Wells focused on the overall structures of inorganic compounds and abstracted crystal structures in terms of their topology by reducing them to a series of points of a certain geometry that are linked to a fixed number of other points²⁶²⁻²⁶³. The resulting structures, which can also be calculated mathematically, can be either discrete (zero-dimensional) polyhedra or infinite (one-, two-, and three dimensional) periodic nets. In early 1990s, R. Robson developed and extrapolated Wells' work into the realm of metal-organic compounds and coordination supramolecular chemistry¹¹⁸. In this context, the resulting "node and spacer" approach has been remarkably successful at producing predictable network architectures.

Majority of the polymeric and polynuclear species are synthesised by hydrothermal or solvothermal condition at high temperature and pressure. This leads to loss of information on the formation and the nucleation process of carboxylate complexes. Apart from this, in biological systems the reactions take place in mild and ambient condition. Thus there is scope to study the ligand exchange reactions of metal carboxylates to make various complexes in solid and solution state chemistry. Such study would enable one to design molecular assemblies in a more systematic and predictable manner. The binding ability of carboxylic acid to biologically related amide derivatives are of great value to understand drug delivery. With this background the synthesis, characterisation of metal carboxylate complexes through ligand exchange reaction and their binding abilities to organic substrates are studied. The results are presented in the following chapters.

Chapter 2

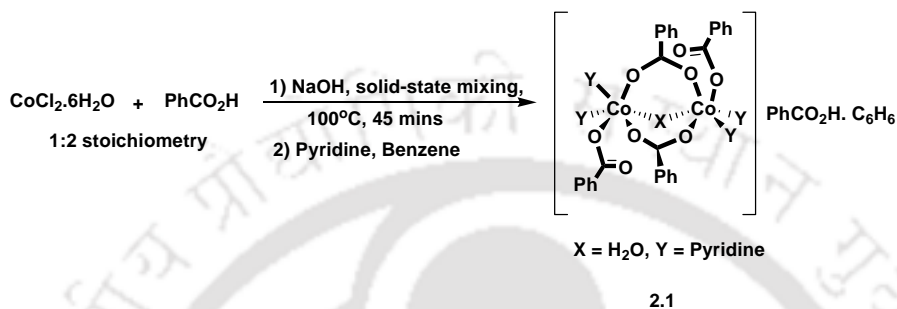
Synthesis, structure and polymorphism in cobalt carboxylate complexes

The dinuclear aqua bridged cobalt(II) carboxylate complexes are important because of their structural resemblance with metalloenzymes like methionine aminopeptidase and leucine aminopeptidase. The coordination environment around the metal ions in these binuclear active sites involves the oxygen atoms of the carboxylate groups in bridging positions, whereas the nitrogen coordination originates from imidazole group of a histidine residue. The carboxylates are coordinated to the cobalt centers of the metalloenzymes either in monodentate or in bridging bidentate fashion. Thus the transition metal complexes with bridging groups such as oxo²⁶⁴, hydroxo²⁶⁵ and aqua⁵⁵ are important. Depending on the reaction conditions, different types of cobalt(II) carboxylate complexes were prepared⁵³. So, the synthetic procedures also play a crucial role in the syntheses of cobalt(II) carboxylate complexes. On the other hand, the weak interactions are essential for the supramolecular assembly of metal carboxylates which in turn controls certain molecular property. In order to understand the synthetic and supramolecular behaviours of cobalt(II) carboxylate complexes, a systematic structural study is required. So, we have synthesized and characterised a series of cobalt(II) carboxylate complexes through both solid and solution state synthetic route to understand their structural aspects and supramolecular behaviour.

2.1 Synthesis and characterisation of dinuclear aqua bridged cobalt carboxylates

In this subsection, we have described the synthesis of some dinuclear aqua bridged cobalt(II) carboxylates. The reaction of cobalt(II) chloride hexahydrate, benzoic acid and sodium hydroxide in the solid-state, followed by addition of pyridine led to a dinuclear aqua bridged complex (Scheme 2.1). Recrystallization of the complex from benzene afforded pink plate type crystals having composition $\{[\text{Co}_2(\text{L})_4(\text{Pyridine})_4(\text{H}_2\text{O})] \cdot \text{LH} \cdot \text{Benzene}\}$ (**2.1**) where LH is benzoic acid. The structure of the complex is determined by X-ray crystallography. The complex has a dinuclear cobalt (II) core (Figure 2.1A), where each of the cobalt centres has distorted octahedral geometry. The dinuclear structure of the complex contains two benzoate

ligands in bridging mode along with a bridging water molecule. It may be pointed out that the complex has a close structural similarity to the biologically relevant enzyme aminopeptidase²⁰³⁻²⁰⁴. Each cobalt(II) center in the complex, **2.1** is coordinated to two pyridine molecules and one monodentate benzoate group thereby completing the octahedral coordination environment around the cobalt ion. This aqua-bridged dinuclear cobalt(II) benzoate complex **2.1** has uncoordinated benzoic acid as well as benzene in the crystal lattice.



Scheme 2.1

The Co1–O9_{aqua} and Co2–O9_{aqua} bond distances in this complex are 2.135(3) and 2.129(3) Å respectively and Co1–O_{aqua}–Co2 bond angle is 115.0(12)°. The benzoic acid molecules are held in the lattice through intermolecular O10–H···O2 [*d*_{O10···O2} 2.721 Å, <D–H···A 164.9°] hydrogen bonding interactions to one of the bridging benzoate ligand of the complex. Weak aromatic C–H···π interactions [*d*_{C···π} 3.87 Å] involving the C60–H of the benzene molecule as donor and the aromatic ring of the benzoic acid molecule as acceptor stabilises the solid-state assembly of **2.1** (Figure 2.1B).

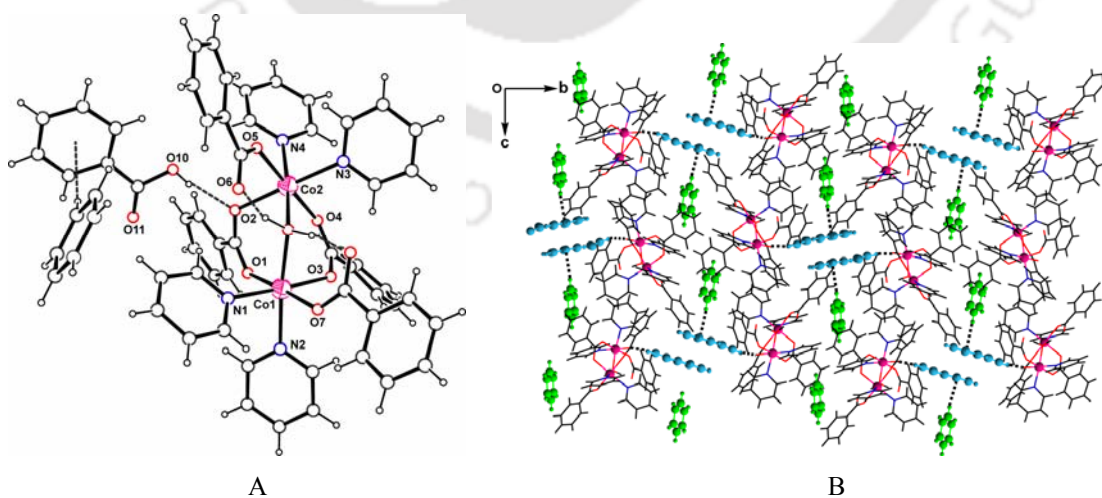


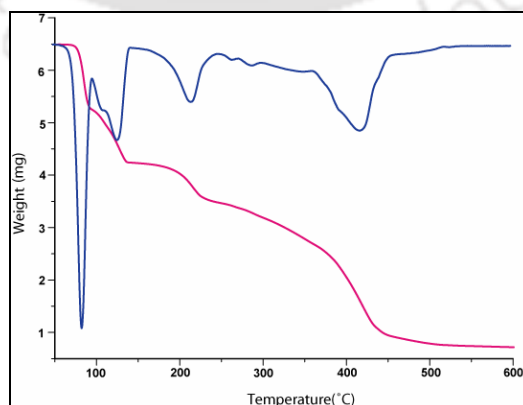
Figure 2.1 A) Crystal structure of **2.1**, B) Crystal packing of complex **2.1** showing inclusion of benzoic acid and benzene molecules in the crystal lattice

The monodentate benzoate groups are intramolecularly hydrogen bonded to the coordinated water molecule through O9–H \cdots O8 [$d_{\text{O9}\cdots\text{O8}}$ 2.583 Å, $\angle\text{D–H}\cdots\text{A}$ 169.3°] and O9–H \cdots O6 [$d_{\text{O9}\cdots\text{O6}}$ 2.545 Å, $\angle\text{D–H}\cdots\text{A}$ 163.4°] interactions. The uncoordinated oxygen atoms of monodentate benzoate groups are involved in weak C–H \cdots O interactions such as C36–H \cdots O8 [$d_{\text{C36}\cdots\text{O8}}$ 3.342 Å, $\angle\text{D–H}\cdots\text{A}$ 152.3°] and C46–H \cdots O6 [$d_{\text{C46}\cdots\text{O6}}$ 3.393 Å, $\angle\text{D–H}\cdots\text{A}$ 139.8°] with the hydrogen atoms of coordinated pyridine molecules (Table 2.1).

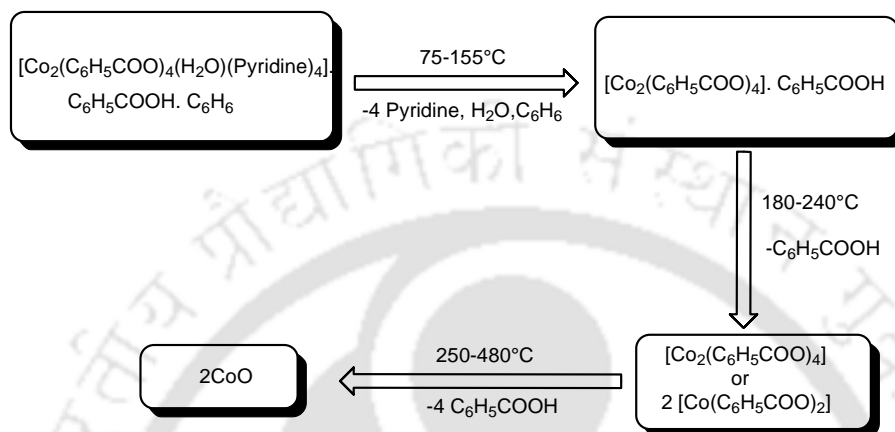
Table 2.1: Hydrogen bond geometry(Å, °) in **2.1**

D–H \cdots A	$d(\text{D–H})$	$d(\text{H}\cdots\text{A})$	$d(\text{D}\cdots\text{A})$	$\angle\text{D–H}\cdots\text{A}$
O(9)–H(9A) \cdots O(8) [Intramolecular]	1.00(7)	1.60(7)	2.583(5)	169.3(6)
O(9)–H(9B) \cdots O(6) [Intramolecular]	1.05(6)	1.52(6)	2.545(5)	163.4(6)
O(10)–H(10A) \cdots O(2) [$x, 1/2-y, 1/2+z$]	0.82	1.92	2.721(8)	164.9
C(36)–H(36) \cdots O(8) [$-1+x, y, z$]	0.93	2.49	3.342(5)	152.3

Solid state FT-IR spectra of the complex **2.1** shows a broad absorption around 3449 cm^{-1} due to O–H stretching and it is an indication of the presence of strong hydrogen bonding interactions involving the bridging aqua ligand. Two absorption bands at 1568 cm^{-1} and 1487 cm^{-1} appear due to the asymmetric and symmetric stretching of bridging carboxylate groups respectively. Due to the presence of monodentate carboxylate groups, two bands appear at 1614 cm^{-1} and 1403 cm^{-1} owing to C=O and C–O stretching respectively. The effective magnetic moment of the complex **2.1** (per dimer) at room temperature is found to be 6.54 BM. The calculated spin only magnetic moment value of this type of high spin cobalt (II) dimer is 7.76 BM. In our case the magnetic moment value is slightly lower than the expected value due to the antiferromagnetic coupling between the cobalt (II) centers³⁵⁴. In methanol, the UV–Vis spectrum of **2.1** shows a weak absorption band at 519 nm ($\epsilon = 40.10 \text{ M}^{-1} \text{ dm}^3 \text{ cm}^{-1}$) which is assigned as ${}^4\text{T}_1(\text{F}) \rightarrow {}^4\text{A}_2(\text{F})$ transition for distorted octahedral cobalt(II) complexes²⁶².

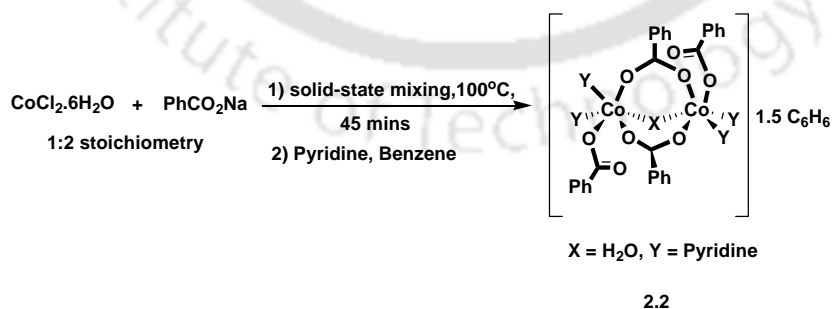
Figure 2.2 Thermogram of the complex **2.1** (heating rate 5°C/minute)

In the thermogram of the cobalt complex (**2.1**), it is observed that the complex loses weights in three steps (Figure 2.2). In the first step weight loss occurs at 75-155°C, which corresponds to 35.26% of the total weight. This loss of weight can be accounted for loss of four pyridines, one benzene and a water molecule. Theoretically, loss of four pyridines, one benzene and a water molecule amounts to 36.18% weight loss.



Scheme 2.2

After removal of these ligands from complex **2.1**, it gets converted to $[\text{Co}_2(\text{C}_6\text{H}_5\text{COO})_4] \cdot \text{C}_6\text{H}_5\text{COOH}$. At 180-240°C the complex loses the uncoordinated benzoic acid which corresponds to 45.35% of total weight loss. For the loss of four pyridines, one benzene, one water and one benzoic acid molecule the calculated loss is 46.83%. After losing pyridine, water, benzene and benzoic acid the complex **2.1** gets converted to anhydrous cobalt benzoate (Scheme 2.2). The third weight loss at 250-480°C corresponds to the loss of 86.59% of the total weight which suggests the transformation of the complex to cobalt oxide. The calculated weight loss for this transformation is 86.6%.



Scheme 2.3

Addition of pyridine to a preheated mixture of cobalt(II) chloride hexahydrate and sodium benzoate in the solid state gave a pink solid. On crystallisation from benzene, it was found to be an aqua-bridged binuclear complex of composition $[\text{Co}_2(\mu\text{-H}_2\text{O})(\mu\text{-OOC-C}_6\text{H}_5)_2(\text{OOC-}$

$\text{C}_6\text{H}_5)_2(\text{Pyridine})_4] \cdot 1.5 \text{ C}_6\text{H}_6$ (**2.2**) (Scheme 2.3). The complex crystallises in $P2_1/c$ space group. The coordination environment of **2.2** is similar to that of complex **2.1**. Each cobalt center in the complex **2.2** has octahedral geometry (Figure 2.3A). The bridging aqua group in **2.2** is hydrogen bonded to the carboxyl group of the monodentate benzoate ligand through intramolecular $\text{O9-H}\cdots\text{O2}$ [$d_{\text{O9}\cdots\text{O2}}$ 2.575 Å, $\angle\text{D-H}\cdots\text{A}$ 163.6°] and $\text{O9-H}\cdots\text{O8}$ [$d_{\text{O9}\cdots\text{O8}}$ 2.581 Å, $\angle\text{D-H}\cdots\text{A}$ 163.8°] interactions as shown in Table 2.2. The $\text{Co1-O9}_{\text{aqua}}$ and $\text{Co2-O9}_{\text{aqua}}$ bond distances are 2.139(2) and 2.143(2) Å and $\text{Co1-O9}_{\text{aqua}}\text{-Co2}$ bond angle is 111.9(11)°. The $\text{Co1-O9}_{\text{aqua}}$ and $\text{Co2-O9}_{\text{aqua}}$ bond distances in **2.2** are only slightly longer than in **2.1**, (~ 0.05 Å) and the $\text{Co1-O9}_{\text{aqua}}\text{-Co2}$ bond angle is smaller by $\sim 4^\circ$.

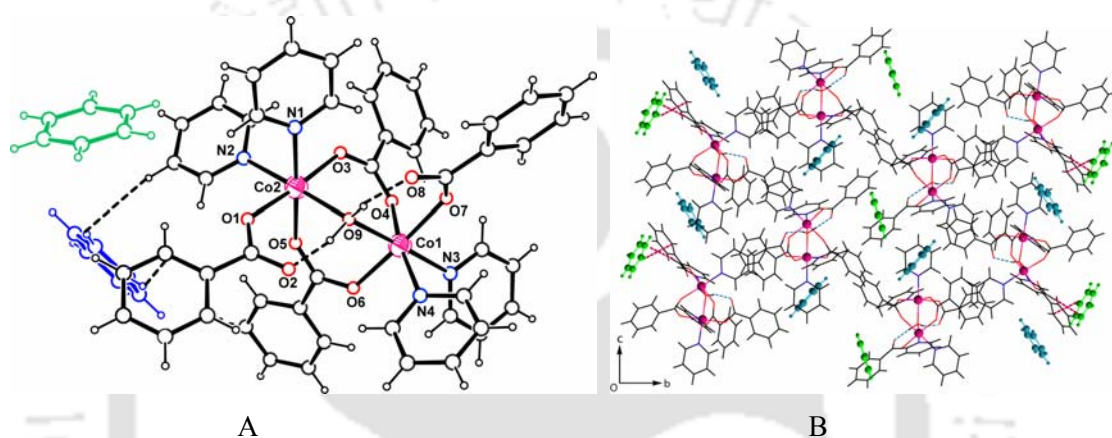


Figure 2.3 A) Crystal structure of complex **2.2**, B) Inclusion of benzene molecules in crystal lattice of complex **2.2**

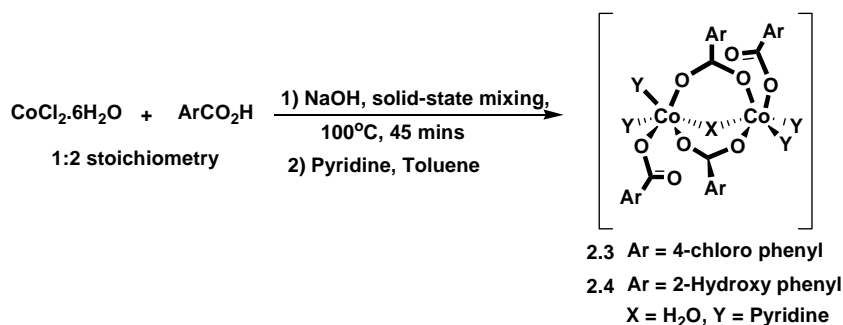
In the crystal structure of complex **2.2**, pyridine molecules are involved in $\pi\cdots\pi$ interactions ($d_{\text{C40}\cdots\text{C9}}$ 3.380 Å) with each other. Besides that, a weak $\text{C37-H}\cdots\text{O8}$ [$d_{\text{C37}\cdots\text{O8}}$ 3.442 Å, $\angle\text{D-H}\cdots\text{A}$ 162.1°] interaction is present between the aromatic hydrogen of benzoate and the free carboxyl oxygen which contributes towards the formation of molecular assembly. The aromatic hydrogens are involved in weak $\text{C-H}\cdots\pi$ [$d_{\text{C28}\cdots\pi}$ 3.789 Å, $d_{\text{C41}\cdots\pi}$ 3.640 Å] interactions. It is noteworthy that the solid state self-assembly of the binuclear complex **2.1** leads to the inclusion of both benzoic acid and benzene molecules in the lattice, while in **2.2** inclusion of only benzene is observed (Figure 2.3B). The absence of benzoic acid in the lattice of **2.2** may be rationalised by the fact that sodium benzoate has only a poor solubility in benzene. The self-assembly of dinuclear cobalt(II) benzoate complex in **2.2** led to the inclusion of two benzene molecules in the crystal lattice, which are linked by weak intermolecular $\text{C9-H}\cdots\pi$ [$d_{\text{C9}\cdots\pi}$ 3.743 Å] and $\text{C55-H}\cdots\pi$ [$d_{\text{C55}\cdots\pi}$ 3.600 Å] interactions.

Table 2.2: Hydrogen bond geometry(Å, °) in **2.2**

D–H···A	d(D–H)	d(H···A)	d(D···A)	<D–H···A
O(9)–H(9A)···O(2) [Intramolecular]	1.02(4)	1.58(4)	2.575(4)	163.6(3)
O(9)–H(9B)···O(8) [Intramolecular]	0.76(3)	1.84(3)	2.581(4)	163.8(3)
C(37)–H(37)···O(8) [x, 1/2-y, -1/2+z]	0.93	2.54	3.442(4)	162.1

The magnetic moment of the complex **2.2** at room temperature is found to be 6.52 BM, so each of the cobalt center has magnetic moment around 3.26 BM, which slightly lower than the spin only value for a Co^{2+} ion²⁶⁶. Solid state FT-IR spectra of the complex **2.2** shows a broad absorption band at 3446 cm^{-1} due to the O–H stretching of hydrogen bonded aqua ligand. The C=O stretching frequency of monodentate carboxylate appears at 1627 cm^{-1} and a strong absorption band at 1393 cm^{-1} appears due to C–O stretching of monodentate carboxylate. Two absorption bands at 1573 and 1485 cm^{-1} appear due to the asymmetric and symmetric stretching of bridging carboxylate groups respectively (Figure 2.20). The UV–Vis spectra of the complex **2.2** shows a weak absorption band at 519 nm ($\epsilon = 40.32\text{ M}^{-1}\text{ dm}^3\text{ cm}^{-1}$) in methanol, which is assigned as ${}^4\text{T}_1(\text{F}) \rightarrow {}^4\text{A}_2(\text{F})$ transition²⁶². Thermogravimetric analysis of the complex **2.2** shows that there is 9.03% weight loss at $60\text{--}110^\circ\text{C}$ which corresponds to the weight loss of one and half benzene molecules (theoretical loss 10.60%). The benzene molecules are held loosely through C–H··· π interactions in the crystal lattice. The complex **2.2** loses four coordinated pyridine ligands and one coordinated aqua ligand in the temperature range of $230\text{--}310^\circ\text{C}$. This loss corresponds to 40.50% of the total weight (theoretical loss 42.35%). After the removal of all the coordinated pyridines and water molecule the anhydrous cobalt (II) benzoate is formed. In the third step, two molecules of benzoic acids are lost at $310\text{--}450^\circ\text{C}$ which corresponds to 66.14%. The calculated weight loss for this transformation is 65.15% and the probable composition of the residue is $[\text{Co}(\text{OH})_2(\text{C}_6\text{H}_5\text{COO})_2]_n$.

To understand the effect of substituent on the formation of dinuclear cobalt (II) complexes, similar reactions with p-chlorobenzoic acid and o-hydroxybenzoic acid were performed. The complex $[\text{Co}_2(\mu\text{-H}_2\text{O})(\mu\text{-p-Cl-C}_6\text{H}_5\text{COO})_2(\text{p-Cl-C}_6\text{H}_5\text{COO})_2(\text{Pyridine})_4]$ (**2.3**) was prepared by the reaction of cobalt (II) chloride hexahydrate with p-chlorobenzoic acid in the presence of sodium hydroxide in solid state and followed by treatment with pyridine (Scheme 2.4). The complex obtained was a pink solid which was crystallised from toluene. Although the complex dissolves in benzene, diffraction quality crystals were not isolated. The structure of this aqua-bridged binuclear complex, **2.3** is similar to **2.1** and **2.2** (Figure 2.4A). The crystal structure of complex **2.3** shows that this complex has no solvent of crystallisation.



Scheme 2.4

The bridging water molecule is hydrogen bonded to the carboxyl group of monodentate carboxylate through intramolecular O9–H···O2 [$d_{\text{O9}\cdots\text{O2}}$ 2.568 Å, $\angle\text{D-H}\cdots\text{A}$ 168.9°] and O9–H···O8 [$d_{\text{O9}\cdots\text{O8}}$ 2.549 Å, $\angle\text{D-H}\cdots\text{A}$ 168.2°] interactions. There is slight variation in the Co1···Co2 separation [$d_{\text{Co1}\cdots\text{Co2}}$ = 3.644Å] due to electronic effect and the different environment created by guest molecules. Some of the selected bond distances and angles of this complex are listed in Table 3 (Appendix).

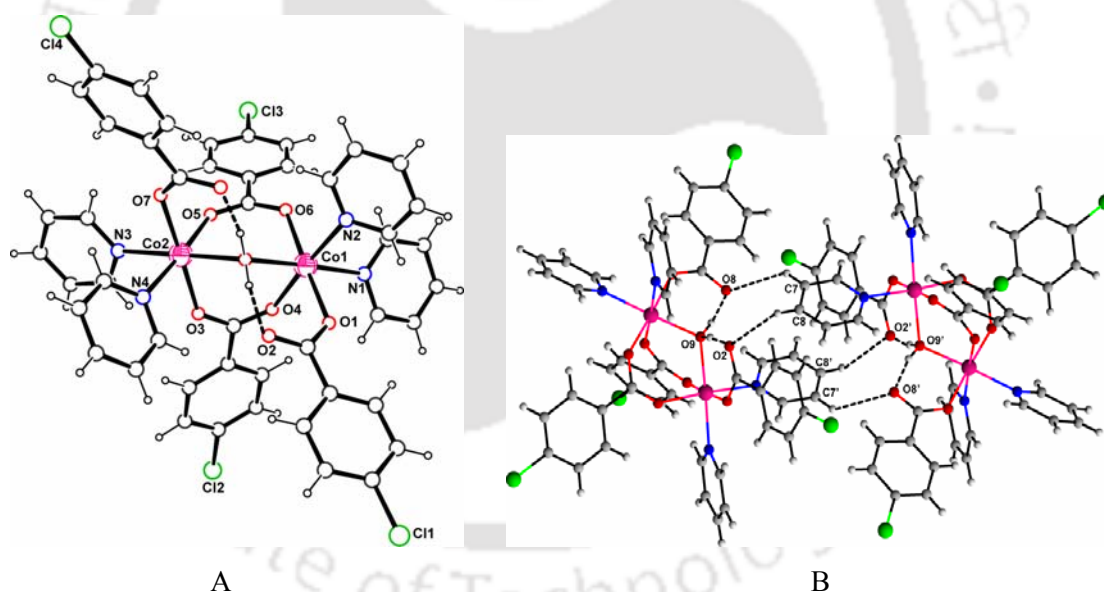


Figure 2.4 A) Crystal structure of $[\text{Co}_2(\mu\text{-H}_2\text{O})(\mu\text{-p-Cl-OBz})_2(\text{p-Cl-OBz})_2(\text{Pyridine})_4]$ (**2.3**),
 B) Hydrogen bonded dimeric assembly of complex **2.3**

Aqua-bridged Co–O_{aqua}–Co frame having pyridine as axial ligands with trifluoroacetate and stearate are reported in the literature and have similar co-ordination features to the one reported in this study²⁶⁷⁻²⁶⁸. The pyridine group attached to the cobalt center is involved in weak C–H···O hydrogen bonding with the carboxylate oxygen through C7–H···O8 [$d_{\text{C7}\cdots\text{O8}}$ 3.378Å, $\angle\text{D-H}\cdots\text{A}$ 135.1°] and C8–H···O2 [$d_{\text{C8}\cdots\text{O2}}$ 3.496 Å, $\angle\text{D-H}\cdots\text{A}$ 157.9°] interactions

(Figure 2.4B). The important hydrogen bonding parameters are listed in Table 2.3. Besides that, the pyridine groups are further involved in weak C–H $\cdots\pi$ hydrogen bonding with aromatic π -system of the carboxylic acid through C2–H $\cdots\pi$ [$d_{\text{C2}\cdots\pi}$ 3.632 Å] and C4–H $\cdots\pi$ [$d_{\text{C4}\cdots\pi}$ 3.746 Å] interactions. Crystal structure of the complex **2.3** shows that one of the pyridine has aromatic π -stacking interaction with p-chloro benzoate ligand and the distance between them is 3.40 Å.

Table 2.3: Hydrogen bond geometry(Å, °) in **2.3**

D–H \cdots A	d(D–H)	d(H \cdots A)	d(D \cdots A)	<D–H \cdots A
O(9)–H(9A) \cdots O(2) [Intramolecular]	0.94(4)	1.64(4)	2.568(4)	168.9(4)
O(9)–H(9B) \cdots O(8) [Intramolecular]	0.87(4)	1.69(4)	2.549(4)	168.2(4)
C(7)–H(7) \cdots O(8)	0.93	2.65	3.378	135.1
C(8)–H(8) \cdots O(2)	0.93	2.62	3.496	157.9

FT-IR spectra of complex **2.3** in solid state shows a strong absorption band at 1608 cm^{-1} due to C=O stretching (Figure 2.21). A band at 1403 cm^{-1} is observed for C–O stretching of monodentate carboxylate group. Two absorption bands at 1561 and 1486 cm^{-1} appear due to the asymmetric and symmetric stretching of bridging carboxylate groups respectively. A broad absorption band at 3440 cm^{-1} appears due to the hydrogen bonded O–H stretching. In methanol, the UV–Vis spectrum of **2.3** shows a weak absorption band at 518 nm ($\epsilon = 37.06 \text{ M}^{-1} \text{ dm}^3 \text{ cm}^{-1}$). The peak is assigned to be due to ${}^4\text{T}_1(\text{F}) \rightarrow {}^4\text{A}_2(\text{F})$ transition for distorted octahedral cobalt(II) complexes. The magnetic moment of the complex **2.3** at room temperature is found to be 5.93 BM.

Thermogravimetric analysis of the complex **2.3** shows a weight loss of 11.04% at the temperature range 90–160°C. This weight loss corresponds to the weight of one pyridine and one water molecule (theoretical loss 9.03%). In this complex one of the pyridine molecule does not participate to any hydrogen bonding interactions but the other pyridine molecules are involved in weak C–H $\cdots\pi$ or $\pi\cdots\pi$ interactions. So the weak interactions may be one of the reason to facilitate the loss of one pyridine molecule faster than the others. In the temperature range 160–640°C, the complex gets converted to CoO by losing 88.9% weight (theoretical 89.20%).

Similar to the earlier complexes, the dinuclear aqua bridged complex having composition $[\text{Co}_2(\mu\text{-H}_2\text{O})(\mu\text{-o-OH-OBz})_2(\text{o-OH-OBz})_2(\text{Pyridine})_4]$ (**2.4**) was prepared by using o-hydroxy benzoic acid. The complex was crystallised from toluene. In this complex, the cobalt

atoms are held in distorted octahedral environment with similar type of coordination modes that are observed in the earlier complexes (**2.1-2.3**). The solid state structure of the complex **2.4** is shown in Figure 2.5A. Two o-hydroxybenzoates are coordinated to two cobalt centers in bridging mode and the other two carboxylate groups are coordinated to each cobalt atom in monodentate fashion. The remaining coordination sites are occupied by two pyridines and a water molecule. The bridging aqua ligand is hydrogen bonded to the monodentate carboxylate group through intramolecular O6–H···O2 [$d_{O6\cdots O2}$ 2.588 Å, $\angle D-H\cdots A$ 160.7°] interaction. The hydroxy groups of carboxylic acids are intramolecularly hydrogen bonded to the carboxylate oxygen through O3–H···O2 [$d_{O3\cdots O2}$ 2.552 Å, $\angle D-H\cdots A$ 145.1°] and O5–H···O4 [$d_{O5\cdots O4}$ 2.530 Å, $\angle D-H\cdots A$ 146.8°] interactions (Table 2.4).

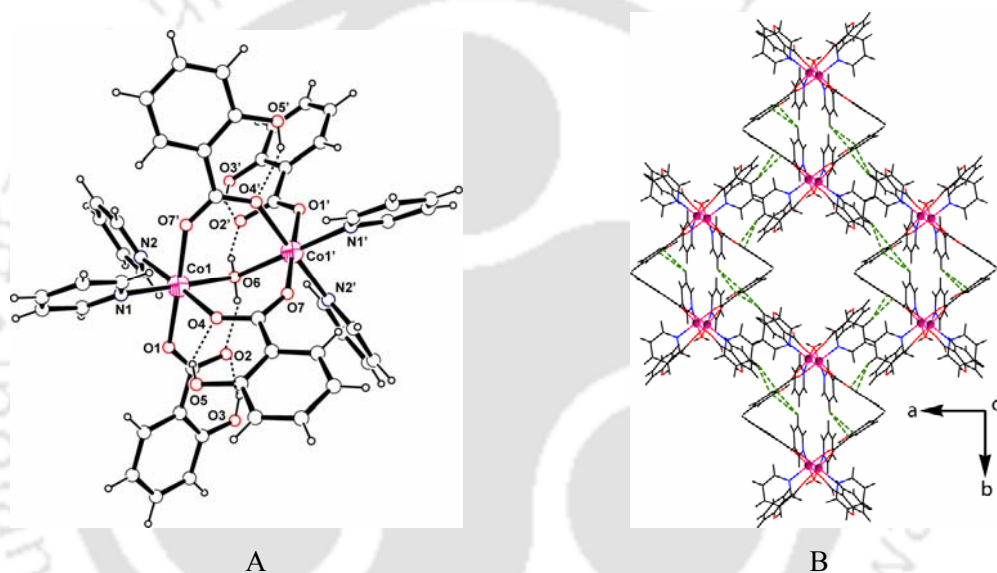


Figure 2.5 A) Intramolecular hydrogen bonded structure of complex **2.4** [$' = 1-x, y, 3/2-z$], B) Self assembled structure of complex **2.4** through weak C–H··· π interactions

Moreover, crystal structure of the complex shows that the coordinated pyridine molecules are involved in C9–H··· π [$d_{C9\cdots\pi}$ 3.511 Å] and C23–H··· π [$d_{C23\cdots\pi}$ 3.508 Å] interactions with aromatic π -system of bridging o-hydroxybenzoate groups and these weak C–H··· π interactions provide extra stability to the molecular assembly in the lattice (Figure 2.5B).

Table 2.4: Hydrogen bond geometry(Å, °) in **2.4**

D–H···A	d(D–H)	d(H···A)	d(D···A)	$\angle D-H\cdots A$
O(3)–H(3o)···O(2)[$-x, y, 1/2-z$]	0.82	1.83	2.552(10)	145.1
O(5)–H(5o)···O(4) [Intramolecular]	0.82	1.80	2.530(6)	146.8
O(6)–H(6o)···O(2) [Intramolecular]	0.76(7)	1.86(6)	2.588(5)	160.7(6)

FT-IR spectra of the complex **2.4** shows an absorption band at 3395 cm^{-1} due to O–H stretching. The C=O and C–O stretching frequencies of monodentate carboxylate appear at 1635 cm^{-1} and 1389 cm^{-1} respectively. Another two absorption bands at 1602 and 1486 cm^{-1} appear due to the asymmetric and symmetric stretching of the bridging carboxylate groups. The UV–Vis spectrum of **2.4** shows a weak absorption band at 520 nm ($\epsilon = 39.02\text{ M}^{-1}\text{ dm}^3\text{ cm}^{-1}$) in methanol, which is assigned to be the ${}^4T_1(F) \rightarrow {}^4A_2(F)$ transition for distorted octahedral cobalt(II) complexes. The room temperature magnetic moment of complex **2.4** is found to be 6.22 BM. Molar conductance values for the complexes **2.1-2.4** are measured which show that these complexes are non-ionic in nature having molar conductance value ranging from $27\text{-}40\text{ S cm}^{-1}\text{ mol}^{-1}$ in methanol at room temperature.

Thermogravimetric analysis shows that the complex **2.4** loses weight in five steps (Figure 2.6). In first step the complex loses 19.52% of its total weight in the temperature range $90\text{-}120^\circ\text{C}$. This weight loss corresponds to the weight of two pyridine molecules and the bridging water molecule (theoretical loss 17.6%). In the next step, at the temperature range $145\text{-}200^\circ\text{C}$ the complex loses 45.22% weight which refers to loss of two pyridine molecules and one o-hydroxybenzoic acid (calculated weight loss is 47.11%). This observation indicates that the four pyridine molecules present in the complex are not in equivalent environment. The third weight loss occurs at $210\text{-}330^\circ\text{C}$ which corresponds to 60.71%. This weight loss is due to the loss of another carboxylic acid. The calculated weight loss is 60.80%.

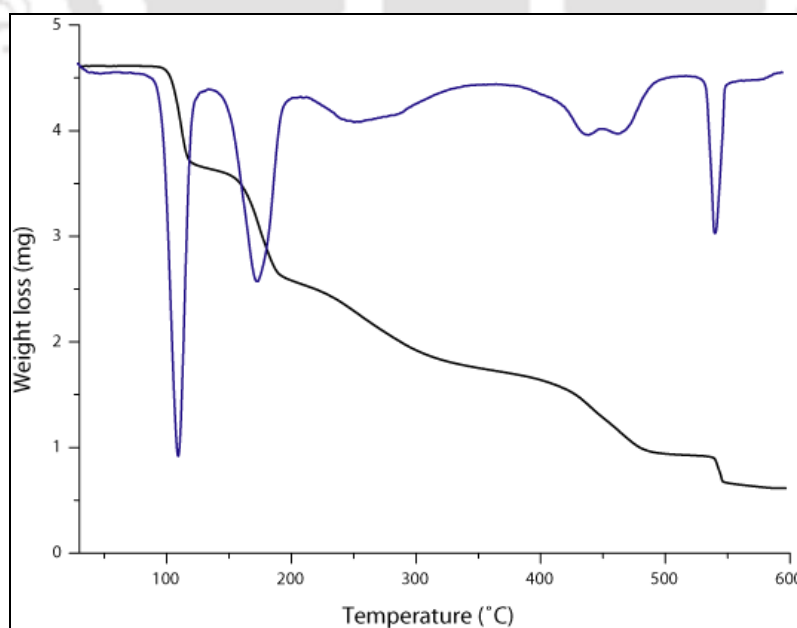


Figure 2.6 Thermogram of complex **2.4** (heating rate $5^\circ\text{C}/\text{minute}$)

In last two steps loss of two carboxylic acids take place, one at each step. At the temperature range 390-500°C the complex loses one carboxylic acid which corresponds to the weight loss of 76.13% (theoretical loss 74.50%). In the final step, at the temperature range 500-580°C, the complex loses the remaining bridging carboxylate molecule and gets converted to cobalt(II) oxide. This corresponds to a weight loss of 86.21%. Theoretically loss of four pyridine, four carboxylic acids and a water molecule amounts to 88.21% weight loss.

The presence of aromatic guest such as benzoic acid and benzene in the lattice of **2.1** and **2.2** gives rise to a strong absorption at 1537 cm^{-1} (indicated by arrows in Figure 2.7). This absorption band is absent in the solid state FT-IR spectrum of complex **2.3** and **2.4** signifying the absence of any solvent molecule in the lattice (Figure 2.7).

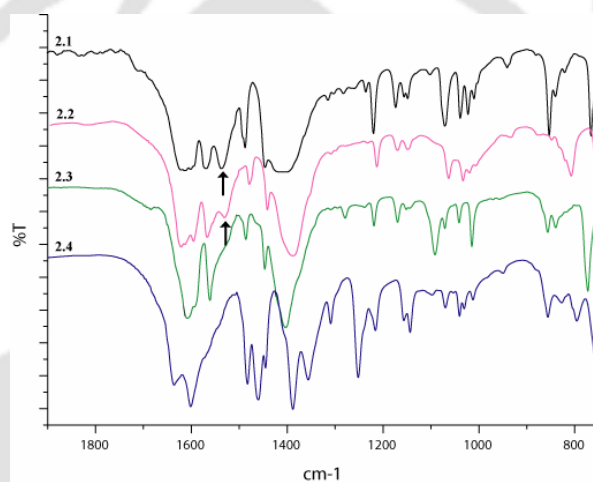


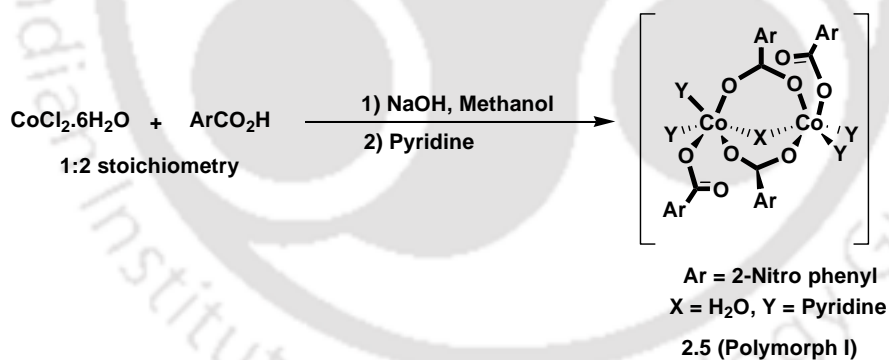
Figure 2.7 The IR spectra of complexes **2.1-2.4**

2.2 Polymorphism in an aqua bridged dinuclear cobalt(II) carboxylate

Polymorphism of a molecule (or compound) may be related to the ability to adopt different structures, which in turn lead to different crystalline phases²⁶⁹. Different polymorphs have different structures and each of them is a unique material with its own physical and chemical properties. In general, polymorphs differ dramatically with regard to their electronic properties such as electric or thermal conductivity, color, and magnetism²⁷⁰ as well as their physicochemical properties including thermal stability, solubility, and dissociation rate etc²⁷¹. Due to these unique properties, the preparation of polymorphs is important in variety of disciplines including pharmaceuticals, dyes and pigments etc. Polymorphism in organic crystals²⁷²⁻²⁷³, including crystals of pharmaceutically active compounds²⁷⁴, is an active area of research. Controlling the formation of a particular polymorph of desired properties is of

special interest in the pharmaceutical industries. The crystallisation process leading to a polymorph is generally sensitive to the variation in the conditions of temperature, pressure and/or the manner in which the crystals are obtained²⁷⁵⁻²⁷⁶. It is a most challenging aspect to understand the structural, thermodynamic, and kinetic factors associated with the crystallization of molecular compounds. The various types of supramolecular interactions such as hydrogen bonding, C–H $\cdots\pi$ and $\pi\cdots\pi$ interactions have become important implement in crystal engineering²⁷⁷. The delicate combination of hydrogen bonds and weak interactions, may efficiently contribute to the formation of different crystalline phases. The packing pattern and structural motifs of the resulting polymorphs depend remarkably on the different types of supramolecular interactions. The interconversion between polymorphs is possible through the mechanochemical processing of solid compounds²⁷⁸ or through the mixing of several components in the solid phase²⁷⁹. Consequently, aspects related to the synthesis, structure and polymorphism in metal coordination complexes are emerging as an active field of research²⁸⁰. In this subsection, we have described the synthetic and structural aspects of three polymorphs of an aqua-bridged dinuclear cobalt(II) complex.

The reaction of cobalt (II) chloride hexahydrate with 2-nitrobenzoic acid, sodium hydroxide and pyridine in methanol gives complex **2.5** (Polymorph I), which crystallises as pink rods in the triclinic space group $P\bar{1}$ (Scheme 2.5).



Scheme 2.5

In this complex each cobalt (II) centre is coordinated to a monodentate benzoate ligand and two pyridine molecules; the six-coordinate octahedral geometry is completed by two bridging 2-nitrobenzoate groups and a bridging aqua ligand. The oxygen atom of monodentate 2-nitrobenzoate is intramolecularly hydrogen bonded to the bridging aqua group through O17–H \cdots O14 [$d_{\text{O17}\cdots\text{O14}}$ 2.578 Å, $\angle\text{D-H}\cdots\text{A}$ 167.0°] and O17–H \cdots O2 [$d_{\text{O17}\cdots\text{O2}}$ 2.508 Å, $\angle\text{D-H}\cdots\text{A}$ 176.8°] interactions. The crystal structure of polymorph I is shown in Figure 2.8. The Co1–O17 and Co2–O17 bond distances in the complex are 2.126(15) and 2.128(15)Å

and the Co1–O17–Co2 bond angle is 114.5(7)°. Moreover, the nitro groups of carboxylic acid are involved in weak intramolecular C–H···O interactions namely C6–H···O3 [$d_{C6\cdots O3}$ 3.255 Å, $\angle D-H\cdots A$ 157.9°], C10–H···O12 [$d_{C10\cdots O12}$ 3.281 Å, $\angle D-H\cdots A$ 150.2°] and C14–H···O12 [$d_{C14\cdots O12}$ 3.429 Å, $\angle D-H\cdots A$ 158.4°]. The hydrogen bond parameters of the polymorph **I** are listed in Table 2.5. These interactions stabilize the *out-out* orientation of the nitro groups of 2-nitrobenzoate ligand relative to the Co1–O17–Co2 direction.

Table 2.5: Hydrogen bond geometry(Å, °) of polymorph **I**

D–H···A	d(D–H)	d(H···A)	d(D···A)	$\angle D-H\cdots A$
O(17)–H(17A)···O(14)	0.85(3)	1.74(3)	2.578(2)	167.0(3)
O(17)–H(17B)···O(2)	0.90(4)	1.62(4)	2.508(3)	176.8(4)
C(2)–H(2)···O(7) [–1+x, y, z]	0.93	2.52	3.279(5)	139.4
C(6)–H(6)···O(3)	0.93	2.37	3.255(4)	157.9
C(10)–H(10)···O(12)	0.93	2.44	3.281(5)	150.2
C(14)–H(14)···O(12) [x, 1+y, z]	0.93	2.55	3.429(4)	158.4
C(29)–H(29)···O(13)	0.93	2.65	3.572	169.4
C(40)–H(40)···O(7)	0.93	2.64	3.504	155.1
C(42)–H(42)···O(11)	0.93	2.70	3.437	136.5

The complex **2.5** (Polymorph **II**) was prepared by the reaction of cobalt (II) acetate tetrahydrate with 2-nitrobenzoic acid and pyridine in methanol. This complex crystallizes from methanol as pink plates in the monoclinic *C2/c* space group. In polymorph **II**, each cobalt (II) centre is coordinated to a monodentate 2-nitrobenzoate and two pyridine molecules; two bridged 2-nitrobenzoate groups and the bridging aqua ligand complete the six-coordinate octahedral geometry (Figure 2.8). Crystal structure of polymorph **II** shows that the Co1···Co1' distance is 3.616 Å and the complex is stabilised by intramolecular hydrogen bonding between the monodentate 2-nitrobenzoate and the bridging aqua group through O9–H···O2 [$d_{O9\cdots O2}$ 2.581 Å, $\angle D-H\cdots A$ 157.4°] interaction.

The corresponding Co1···O9 distance is 2.142(9) Å and the Co1–O9–Co1' bond angle is 115.1 (7)°. The packing structure of polymorph **II** is shown in Figure 2.10B, wherein the molecules are held in the lattice through weak intermolecular C3–H···O2 [$d_{C3\cdots O2}$ 3.229 Å, $\angle D-H\cdots A$ 155.9°], C4–H···O4 [$d_{C4\cdots O4}$ 3.293 Å, $\angle D-H\cdots A$ 127.0°], C14–H···O8 [$d_{C14\cdots O8}$ 3.367 Å, $\angle D-H\cdots A$ 135.8°] and C22–H···O4 [$d_{C22\cdots O4}$ 3.602 Å, $\angle D-H\cdots A$ 177.5°] interactions. The important hydrogen bond distances are listed in Table 2.6. In polymorph **II**,

the nitro groups of each carboxylate ligand project inwards and they therefore may be described as having *in-in* orientations.

Table 2.6: Hydrogen bond geometry(Å, °) of polymorph **II**

D–H···A	d(D–H)	d(H···A)	d(D···A)	<D–H···A
O(9)–H(9 _o)···O(2)	0.84	1.78	2.581(17)	157.4
C(3)–H(3)···O(2) [1/2+x, 1/2+y, z]	0.93	2.36	3.229(3)	155.9
C(4)–H(4)···O(4)	0.93	2.65	3.293	127.0
C(14)–H(14)···O(8)	0.93	2.64	3.367	135.8
C(22)–H(22)···O(4)	0.93	2.67	3.602	177.5

The reaction of cobalt(II) chloride hexahydrate, 2-nitrobenzoic acid and sodium hydroxide in the solid-state followed by addition of pyridine gave the dinuclear cobalt(II) complex, **2.5** (polymorph **III**). This complex is soluble in chloroform, benzene or toluene and can subsequently be crystallised from toluene as pink plates in $P2_1/n$ space group. In this complex, the cobalt centers are in distorted octahedral environment. Each cobalt center has coordinated through two bridging and one monodentate o-nitrobenzoate ligand as shown in Figure 2.8.

The remaining coordination sites are occupied by two pyridine and a water molecule. The distance between the two cobalt center is 3.651 Å and the bridging water molecule have distances 2.136 (15) Å and 2.157 (16) Å from Co1 and Co2 respectively. The bridging aqua ligand is hydrogen bonded with the monodentate carboxylate group through intramolecular O17–H···O6 [$d_{O17\cdots O6}$ 2.574 Å, <D–H···A 171.9°], O17–H···O2 [$d_{O17\cdots O2}$ 2.576 Å, <D–H···A 169.2°] interactions. Besides that the nitro groups of carboxylic acids are involved in weak C–H···O interactions with aromatic hydrogens to stabilize the molecular assembly. Some of the significant hydrogen bonds are listed in Table 2.7. In this polymorph **III** two nitro groups are in *out-out* orientation and the other two are in *in-in* orientation, so the overall orientation of nitro groups is *out-in* or *in-out*.

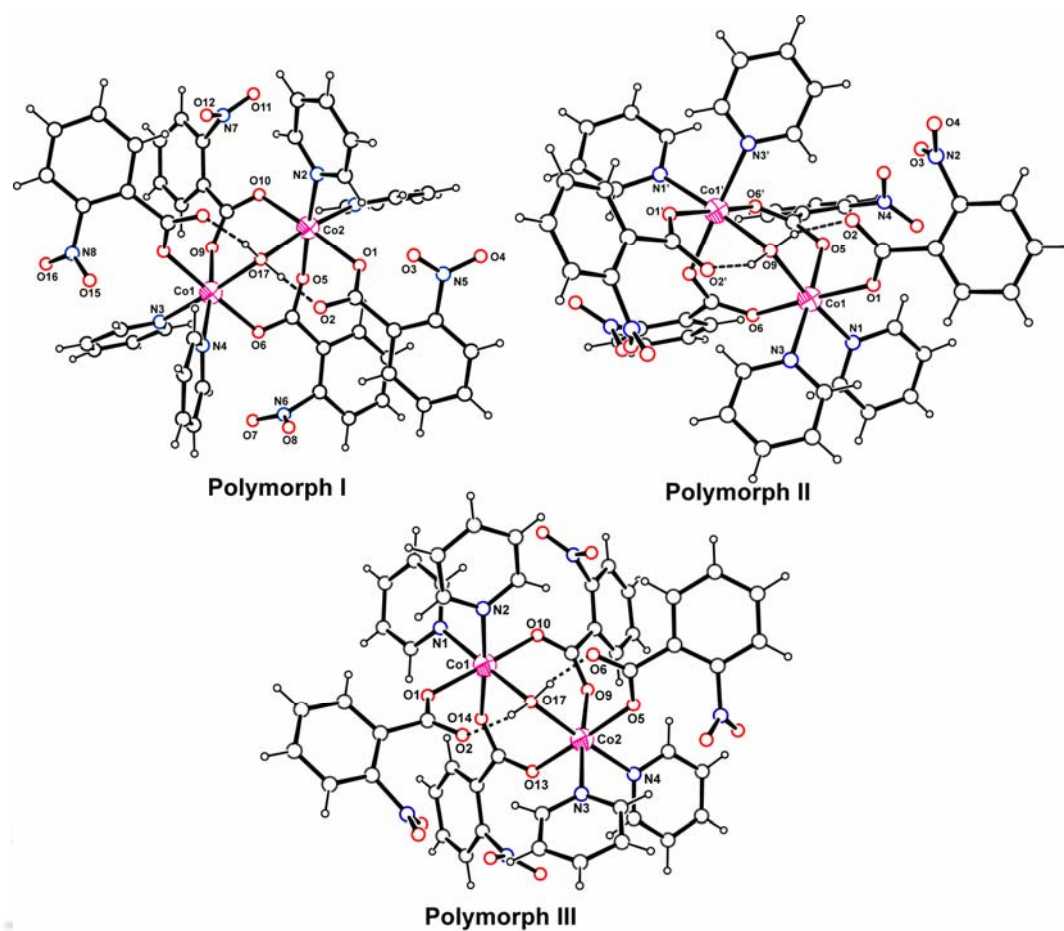


Figure 2.8 Crystal structures of three polymorphs

Table 2.7: Hydrogen bond geometry(Å, °) of polymorph III

D-H...A	d(D-H)	d(H...A)	d(D...A)	<D-H...A
O(17)-H(1A)...O(6)	0.87(3)	1.71(3)	2.574(3)	171.9(3)
O(17)-H(1B)...O(2)	0.83(3)	1.76(3)	2.576(3)	169.2(3)
C(2)-H(2)...O(1) [-x, 1-y, -z]	0.93	2.60	3.516(3)	168.7
C(8)-H(8)...O(2) [1/2-x, 1/2+y, 1/2-z]	0.93	2.52	3.313(4)	142.9
C(33)-H(33)...O(8) [3/2-x, 1/2+y, 1/2-z]	0.93	2.42	3.074(7)	127.5
C(38)-H(38)...O(3) [-x, -y, -z]	0.93	2.53	3.454(4)	170.7
C(46)-H(46)...O(14) [1-x, 1-y, -z]	0.93	2.48	3.388(4)	164.9

A close inspection of the bond distances (listed in Appendix) in the three polymorphs shows that the coordination environment around each cobalt(II) centre is similar and the coordination environment around the cobalt center is not affected due to the orientation of the nitro groups. The cobalt(II) centres are coordinated to a monodentate benzoate and two pyridine ligands and the two cobalt (II) centres are bridged by two 2-nitrobenzoate and an

aqua group, which is intramolecularly hydrogen bonded to the carboxyl group of the monodentate 2-nitrobenzoate. It is important that in polymorph **I** each of the nitro groups adopts *out-out* orientation. On the other hand, polymorph **II** can be identified by two of the 2-nitrobenzoate groups adopting *in-in* orientation, whereas the overall orientation of polymorph **III** is *out-in* or *in-out* relative to the Co–O–Co unit. The orientations of the nitro benzoate groups in the three polymorphs are pictorially presented in Figure 2.9. The 2-nitrobenzoate groups are stabilized in these orientations by the weak intermolecular interactions. The packing structures of three polymorphs are shown in Figure 2.10.

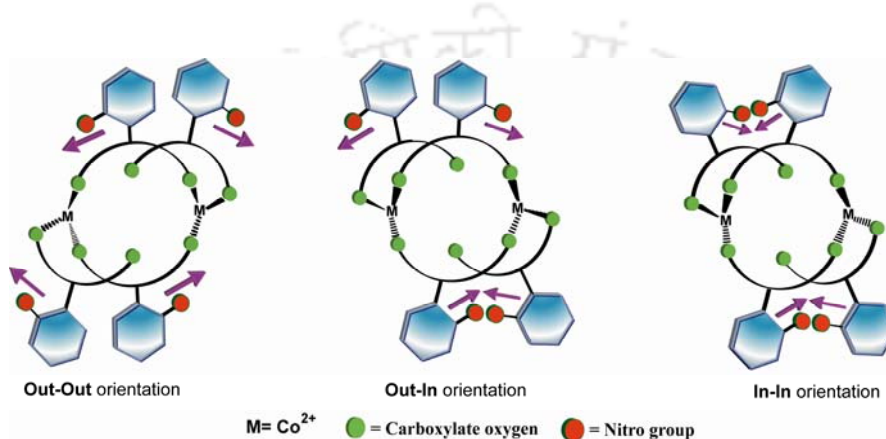


Figure 2.9 Pictorial presentations of the three polymorphs

The torsional angles (Table 2.8) are different for the different orientations of the nitrobenzoate groups in the three polymorphs. Some of the selected bond distances and angles of three polymorphs are listed in Table 5 (Appendix).

Table 2.8 : Torsional angles in polymorph **I-III**

	2.5 (Polymorph I) out-out		2.6 (Polymorph II) in-in		2.7 (Polymorph III) in-out	
Monodentate nitro benzoate groups	C18-C19-C20-N5	1.6(4)	C6-C7-C8-N2	-8.5(3)	C21-C22-C23-N8	-14.6(4)
	C32-C33-C34-N8	11.2(3)	C6'-C7'-C8'-N2'	-8.5(3)	C28-C29-C30-N7	-9.6(5)
Bridging nitro benzoate groups	C11-C12-C13-N6	-1.1(4)	C18-C19-C20-N4	-7.7(3)	C35-C36-C37-N6	7.2(4)
	C25-C26-C27-N7	-4.6(3)	C18'-C19'-C20'-N4'	-7.7(3)	C42-C43-C44-N5	13.0(4)

The polymorphism originates due to the different orientations of the nitro groups in the three polymorphs. From these observations it may be concluded that the formation of the polymorphs are controlled by three factors: (a) the synthetic route (solid or solution phase), (b) the solvent of crystallisation and (c) the stoichiometry of the auxiliary ligand.

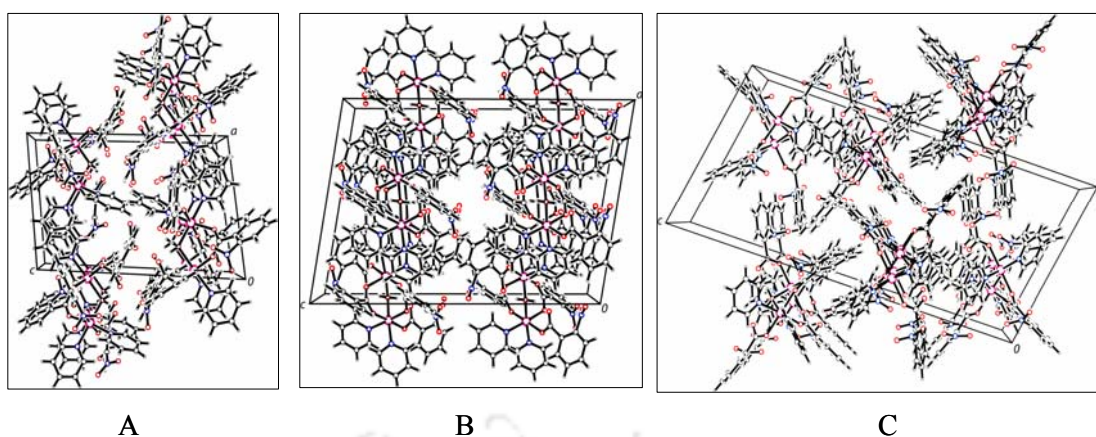
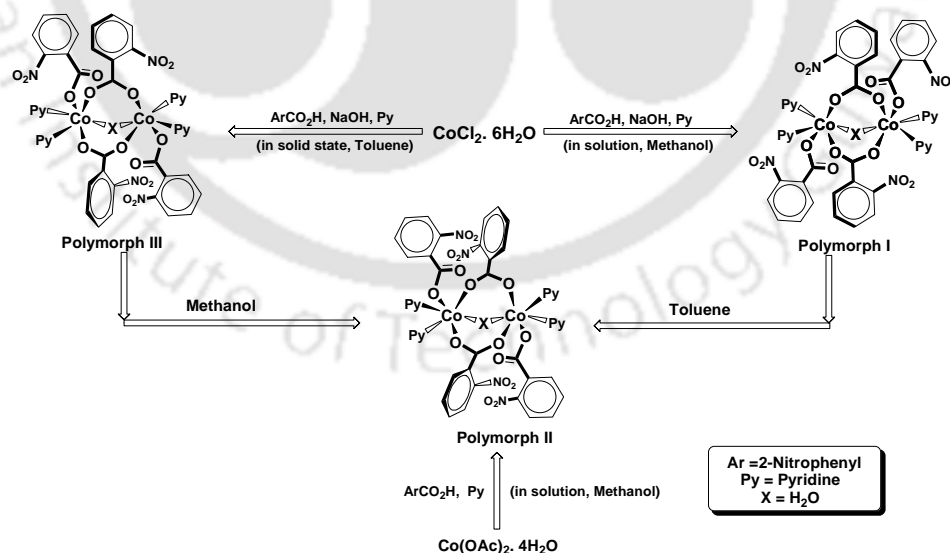


Figure 2.10 Packing structures of three polymorphs A) Polymorph I, B) Polymorph II, C) Polymorph III

The polymorph I and III, can be prepared by the reaction of cobalt(II) chloride with sodium salt of 2-nitrobenzoic acid followed by the addition of pyridine in solution and solid state respectively. These two polymorphs are easily converted to polymorph II upon dissolution in solvent like toluene and methanol. The interconversion between the polymorphs occurs when a number of possible products of a reaction have similar free energies. From an enthalpy point of view, the product which is most likely to form should have the lowest energy. However, depending upon the reaction conditions, the product that quickly crystallises has high entropy in the supersaturated system. This may then transform to the lowest energy product over time, thereby facilitating the interconversion between the polymorphs.



Scheme 2.6

The powder XRD patterns of the polymorphs substantiate our observation of the distinct crystalline phases (Figure 2.11). The powder XRD patterns of all the three polymorphs are

different, which supports the existence of the polymorphs. Subsequently, we performed powder XRD analysis of the samples after their transformation which confirm the conversion of both polymorphs **I**, and **III** into **II** as illustrated in Scheme 2.6. The PXRD patterns of three polymorphs are well in agreement with the simulated results from the single-crystal X-ray diffraction data, indicative of three distinct polymorphic forms.

Each of the polymorphs (**I–III**) shows broad signal around 3433 cm^{-1} (O–H stretching) in their solid-state FT-IR spectra. This corresponds to the presence of intramolecular hydrogen-bonding interactions involving the 2-nitrobenzoate group and the bridging aqua ligand. Solid-state FT-IR spectra of polymorphs **I**, **II** and **III** exhibit similar absorptions for monodentate carboxylate carbonyl C=O at around 1635 cm^{-1} and for the C–O group it appears at 1394 cm^{-1} . The asymmetric and symmetric band of bridging carboxylate groups appear at around 1602 and 1487 cm^{-1} respectively. The asymmetric band for nitro N–O stretching appears at the 1531 cm^{-1} and for symmetric stretching it appears at 1364 cm^{-1} . FT-IR spectra of polymorph **III** is shown in Figure 2.22. The magnetic moments of all the three polymorphs at room temperature are found to be around 6.56 BM.

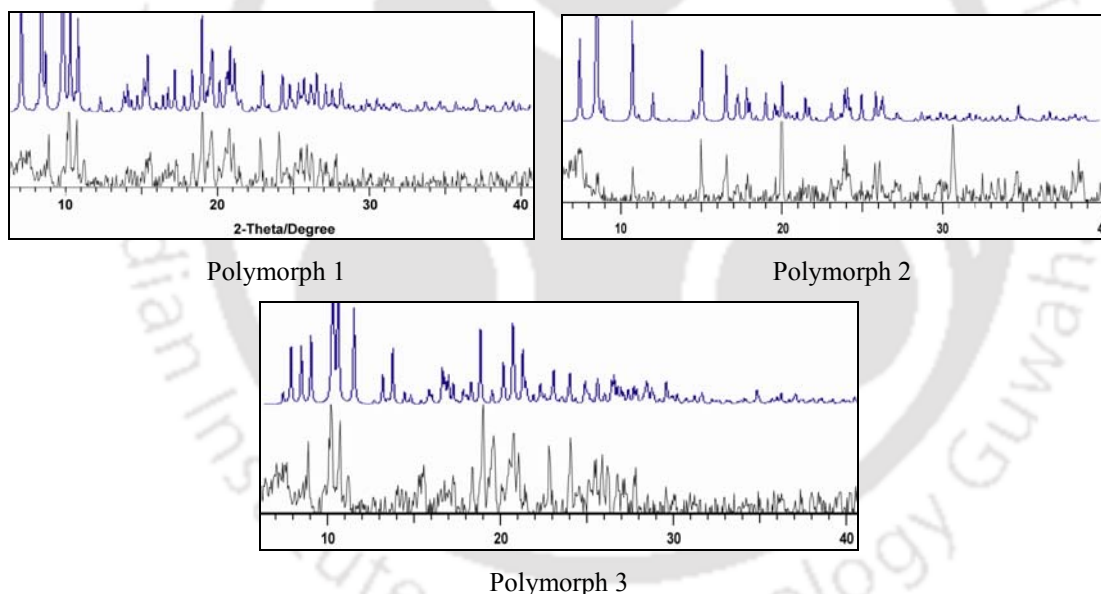


Figure 2.11 Overlay PXRD patterns of the three polymorphs (black) with their simulated ones (blue).

The UV–Vis spectrum of the three polymorphs show a weak absorption band at 521 nm ($\epsilon = 39.18\text{--}39.23\text{ M}^{-1}\text{ dm}^3\text{ cm}^{-1}$) in methanol which is assigned to be the ${}^4T_1(F) \rightarrow {}^4A_2(F)$ transition for distorted octahedral cobalt(II) complexes. At room temperature, the ESR spectrum of the polymorphs show two signals one is around 3381.0G ($g = 1.995$) and another strong signal appears at 8688.3G ($g = 0.776$) which is an identification for the distorted octahedral geometry around the Co(II) center (Figure 2.12A).

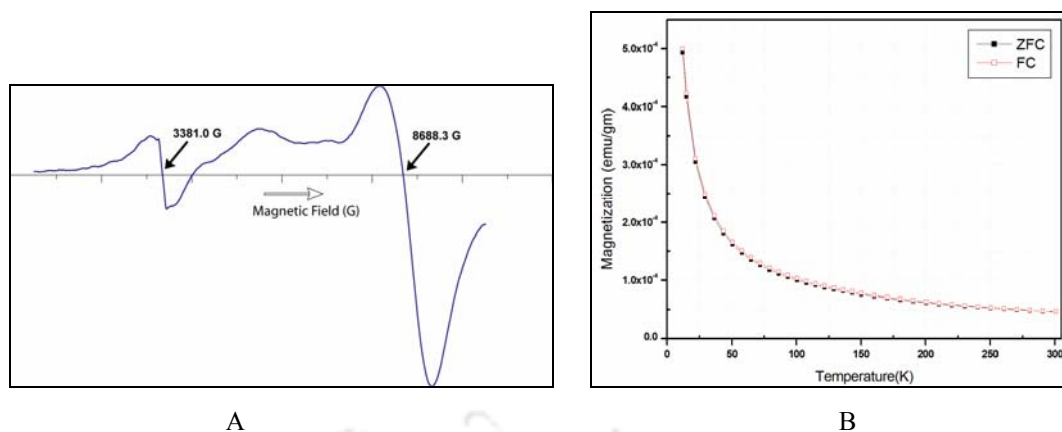


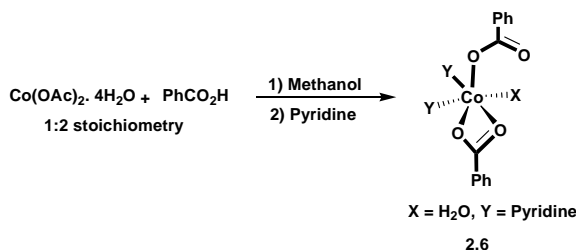
Figure 2.12 A) Solution state ESR spectra (in Methanol) of complex **2.5** (Polymorph **III**) at room temperature ($g = 1.99548$ and 0.77653 , center field= 5500.0G , Power= 0.99800 [mw], Frequency= 9442.829 [MHz], sweep time= 60 s), B) Temperature dependent magnetic susceptibility curve of polymorph **III**.

Thermogravimetric analysis of these polymorphs shows three-step decomposition to form cobalt oxide. In the temperature range $110\text{-}620^\circ\text{C}$ the polymorphs lose one water, four pyridine and four 2-nitrobenzoic acid molecules. Except for the difference of morphology, the IR, UV-Vis, thermogravimetric analyses are almost identical for the three polymorphs; hence, these techniques cannot distinguish them.

We have measured the temperature dependent magnetic susceptibility for polymorph **III** in the temperature range $12\text{-}300\text{K}$ at 100Oe . The curve shows the paramagnetic behaviour of the complex at low temperature and any antiferromagnetic coupling between the cobalt centers are not observed (Figure 2.12B). We have recorded the susceptibility under both the zero-field cooled and field-cooled condition and both the curves are almost similar to each other.

2.3 Synthesis and structure of mononuclear cobalt(II) carboxylate complexes

The reaction of cobalt(II) acetate tetrahydrate, benzoic acid and pyridine in methanolic solution gives a mononuclear cobalt complex $[\text{Co}(\text{H}_2\text{O})(\text{Pyridine})_2(\text{OBz})_2]$ (**2.6**) (Scheme 2.7).



Scheme 2.7

The crystal structure of the complex is shown in Figure 2.13. The structure of the complex **2.6** shows that the two carboxylates are coordinated to cobalt center in opposite direction. One of the carboxylates is coordinated in monodentate while the other one is coordinated in chelating fashion to the cobalt center.

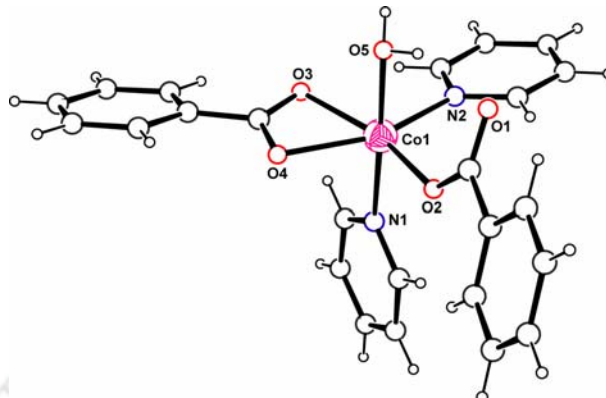


Figure 2.13 Crystal structure of complex **2.6**

The remaining coordination sites are occupied by two pyridine and a water molecule, completing the distorted octahedral geometry around the cobalt center. Two carboxylate and one pyridine ligands are occupying the equatorial position whereas the other pyridine and the water molecules are present in the axial position of the complex. The selected bond distances in the complex for Co1–O2, Co1–O3, Co1–O4, Co1–O5, Co1–N1, Co1–N2 are 2.032(10), 2.164(10), 2.179(11), 2.175(13), 2.125(13) Å respectively. The O2–Co1–N2, O2–Co1–O5, O2–Co1–O3, O2–Co1–N1, O2–Co1–O4 bond angles are 102.7(5), 89.4(5), 161.4(4), 90.1(5), 100.9(4) respectively. The C–O bond distances in the two carboxylates are C1–O1, 1.242; C1–O2, 1.275; C8–O3, 1.273; C8–O4, 1.255 Å; which clearly indicate that one carboxylate bind to cobalt center in monodentate while other in chelating coordination mode.

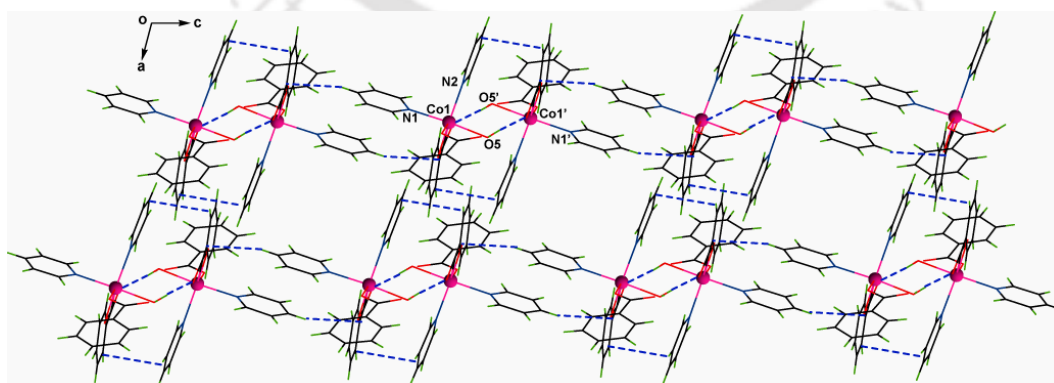


Figure 2.14 Hydrogen bonded assembly of complex **2.6**

The coordinated water molecule participate in intramolecular hydrogen bonding with the carboxylate unit through O5–H \cdots O1 [$d_{O5\cdots O1}$ 2.676 Å, \angle D–H \cdots A 151.6°] interaction. This coordinated water molecule is further involved in intermolecular hydrogen bonding through O5–H \cdots O3 [$d_{O5\cdots O3}$ 2.757 Å, \angle D–H \cdots A 171.9°] interaction to form a dimeric unit (Table 2.9).

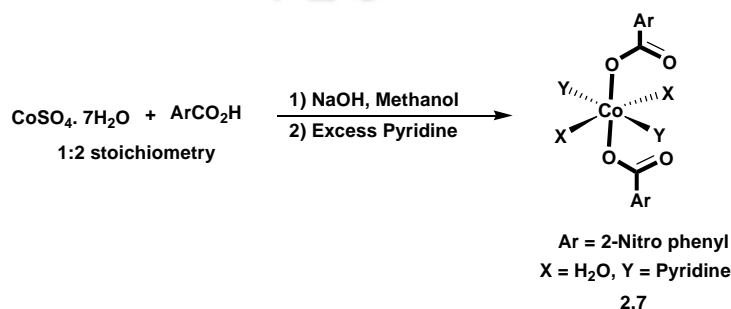
Besides that the complex is assembled through C22–H \cdots π ($d_{C22\cdots\pi}$ 3.703 Å) intermolecular interaction which leads to a hydrogen bonded assembly along *ac*-plane. Moreover, a strong aromatic π -stacking interaction ($d_{\pi\cdots\pi}$ 3.373 Å) is also present between the carboxylate and pyridine units, which stabilises the molecular assembly. These interactions support to construct the one dimensional hydrogen bonded network as shown in Figure 2.14.

Table 2.9: Hydrogen bond geometry(Å, °) in **2.6**

D–H \cdots A	d(D–H)	d(H \cdots A)	d(D \cdots A)	\angle D–H \cdots A
O(5)–H(5A) \cdots O(1)	0.78(2)	1.97(2)	2.676(19)	151.6(3)
O(5)–H(5B) \cdots O(3) [1-x, -y, 1-z]	0.84(19)	1.92(19)	2.757(19)	171.9(18)

The solid-state FT-IR of the complex shows two strong absorption bands at 1593 and 1374 cm^{-1} indicating the presence of C=O and C–O stretching of monodentate carboxylate ligand. The asymmetric and symmetric C–O stretching frequencies of chelating carboxylate appear at 1540 and 1445 cm^{-1} respectively. UV-Visible spectra of the complex **2.6** shows a weak absorbance at 517nm ($25.07 \text{ M}^{-1} \text{ dm}^3 \text{ cm}^{-1}$) in methanol. The magnetic moment of the complex is 4.04 BM at room temperature.

Analogous reaction of cobalt(II) salts with 2-nitrobenzoic acid and sodium hydroxide in the presence of excess of pyridine in methanol gave the complex (**2.7**) as orange prisms (Scheme 2.8).



Scheme 2.8

The mononuclear complex **2.7** was obtained from the reaction of cobalt(II) sulfate heptahydrate with 2-nitrobenzoic acid in the presence of sodium hydroxide and excess pyridine in methanol (Figure 2.15). Similarly, reactions of cobalt(II) chloride with 2-nitrobenzoic acid and sodium hydroxide in excess pyridine led to mononuclear complex **2.7**, which suggests that the role of anion in the synthesis through the solution route is not prominent.

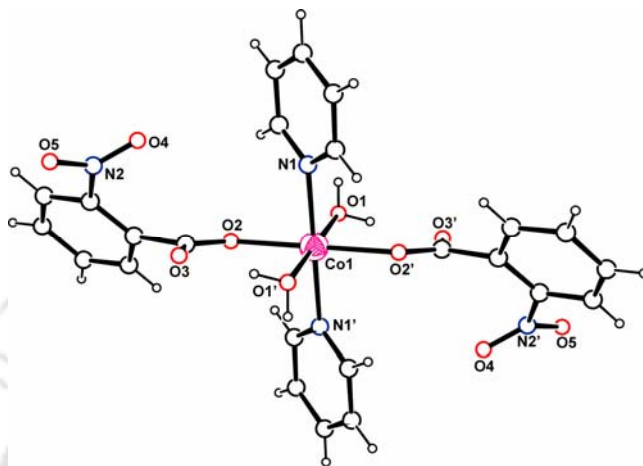


Figure 2.15 Crystal structure of complex **2.7** [$l' = 1-x, 1-y, 1-z$]

In complex **2.7**, the two nitro benzoate groups are coordinated in trans manner and that the two pyridine and two coordinated water molecules are present around the cobalt center. The 2-nitrobenzoates are coordinated to the cobalt center in monodentate fashion. The selected bond distances of Co1–O1, Co1–O2, Co1–N1 are 2.131(12), 2.088(11) and 2.138(14) respectively. Some of the important bond angles are O2–Co1–O1, 90.3(5); O2–Co1–N1, 90.7(5); O1–Co1–N1, 88.7(5); N1–Co1–N1', 180.0(1); O2–Co1–O2', 180.0, O1–Co1–O1' 180.0. These result are in accordance with an octahedral geometry around Co(II) center. The coordinated water molecules are involved in strong hydrogen bonding with the carboxyl groups of 2-nitrobenzoate through O1–H \cdots O3' [$d_{O1\cdots O3'}$ 2.812 Å, $\angle D-H\cdots A$ 150.2°] and O1–H \cdots O3 [$d_{O1\cdots O3}$ 2.669 Å, $\angle D-H\cdots A$ 164.9°] interactions. Besides that the complex has weak C–H \cdots O interactions, the aromatic protons are implicated in hydrogen bonding with the carboxylate and water oxygens (Table 2.10).

Table 2.10: Hydrogen bond geometry(Å, °) in **2.7**

D–H \cdots A	d(D–H)	d(H \cdots A)	d(D \cdots A)	$\angle D-H\cdots A$
O(1)–H(1o) \cdots O(3')	0.82(3)	2.08(3)	2.812(2)	150.2(2)
O(1)–H(2o) \cdots O(3) [2-x, 1-y, 1-z]	0.80(2)	1.89(2)	2.669(18)	164.9(2)
C(2)–H(2) \cdots O(3) [1-x, -y, 1-z]	0.93	2.59	3.439(3)	151.8
C(10)–H(10) \cdots O(1) [x, y, z-1]	0.93	2.67	3.593	170.4

In addition to that, the interplanar distance is 3.383 Å between the nitrobenzoate units situated over one another in a slightly off-set manner indicating a strong aromatic π -stacking interaction between the aromatic nitrobenzoate units of **2.7** as shown in the Figure 2.16. The O–H \cdots O, C–H \cdots O and π \cdots π interactions in the complex **2.7** are responsible in construction of a three dimensional hydrogen bonded network.

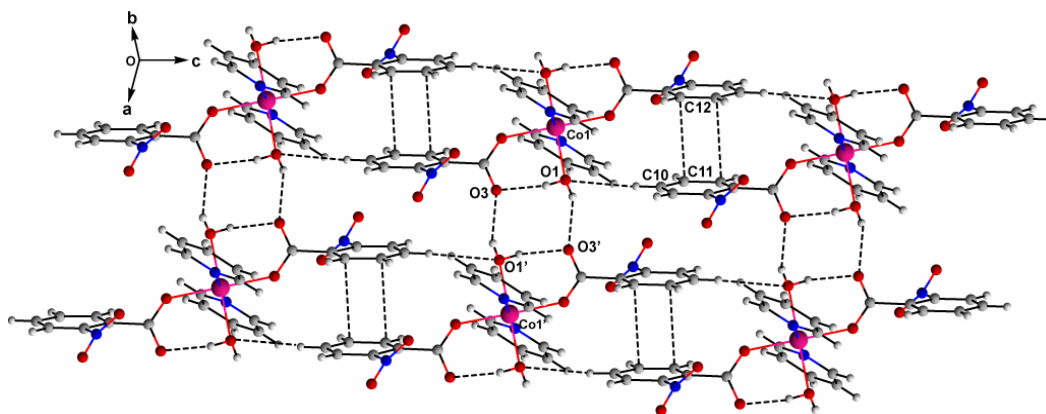


Figure 2.16 Two dimensional hydrogen bonded structure of complex **2.7**

Due to the presence of monodentate carboxylate group in the complex, two bands appear at 1604 and 1400 cm^{-1} in the solid-state FT-IR spectra. The asymmetric band for nitro N–O stretching appears at the 1526 cm^{-1} and for symmetric stretching it appears at 1356 cm^{-1} . The magnetic moment of the complex is 3.95 BM at room temperature. The complex **2.7** has molar conductance value 22.5S $\text{cm}^{-1} \text{mol}^{-1}$ in methanol at room temperature, which indicates that the complex is non-ionic in nature. In methanol, the UV–Vis spectrum of **2.7** show a band at 515 nm ($\epsilon = 6.7 \text{ M}^{-1} \text{ dm}^3 \text{ cm}^{-1}$) due to the ${}^4\text{T}_1(\text{F}) \rightarrow {}^4\text{A}_2(\text{F})$ transition.

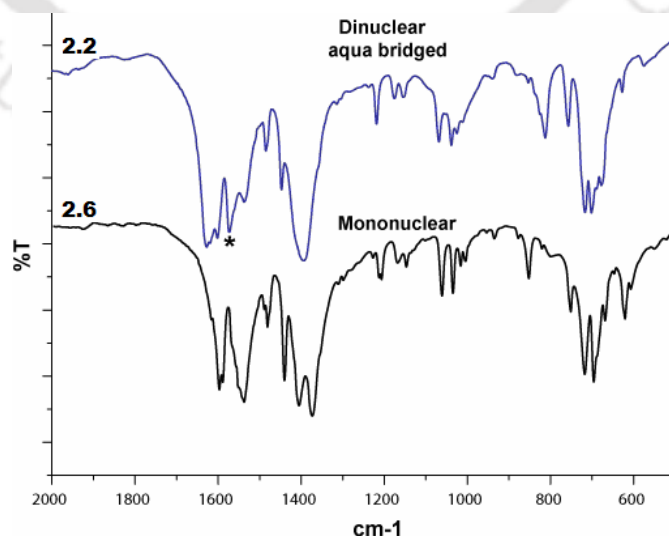
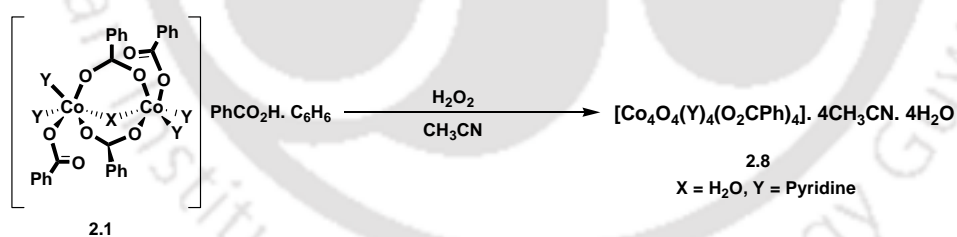


Figure 2.17 FT-IR spectra of the complexes **2.2** and **2.6**

Comparison of FT-IR spectra of dinuclear aqua bridged complex (**2.2**) and the mononuclear complex (**2.6**) in reveals distinct differences in the 1630-1500 region (Figure 2.17). In case of complex **2.2**, absorption at 1627 cm^{-1} is observed due to C=O stretching of monodentate carboxylate while the asymmetric stretching band of bridging C–O groups appears at 1573 cm^{-1} (*). For the complex **2.6**, the C=O stretching of monodentate carboxylate appears at 1593 cm^{-1} and the asymmetric C–O stretching frequency of chelating carboxylate appears at 1540 cm^{-1} . So, from the IR study we can easily distinguish the mono and dinuclear cobalt(II) carboxylates.

2.4 Synthesis and characterisation of tetranuclear cobalt(III) carboxylates

Mild oxidation of **2.1** with H_2O_2 in acetonitrile under neutral condition gave dark green complex, which was crystallised from acetonitrile (Scheme 2.9). Crystallographic study of the complex shows the composition of the complex to be $[\text{Co}_4\text{O}_4(\text{Pyridine})_4(\text{O}_2\text{CPh})_4] \cdot 4\text{CH}_3\text{CN} \cdot 4\text{H}_2\text{O}$ (**2.8**). The complex has a core comprising of Co_4O_4 cluster in which the $\text{Co}\cdots\text{Co}$ distances are 2.709(5), 2.711(5) and 2.819(5) Å. The corresponding Co–O bond distances are found to be 1.954(14), 1.960(14) and 1.866(13) Å, which indicate that the Co_4O_4 core has a distorted cubic geometry. Important bond distances and angles of the complex **2.8** are listed in Table 6 (Appendix). Each of the cobalt centres is attached to one pyridine ligand and μ -benzoate groups are bridged between two alternate cobalt centres (Figure 2.18A).



Scheme 2.9

Other coordination sites of the cobalt centers are satisfied by oxo groups. Each oxo group is bridged to three cobalt centers and fulfil the octahedral geometry around the cobalt(III) centers. Tetrameric cobalt(III) complexes can be constructed by using 2,2'-bipyridine and acetate; pyridine and acetate or 4-cyanopyridine and benzoate, which are reported in the literature²⁸¹⁻²⁸² and these complexes shows interesting catalytic oxidative properties²⁸³. The tetranuclear cobalt(III)–benzoate complex **2.8** is held in the lattice through intermolecular $\text{O}_4\text{--H}\cdots\text{O}_3$ [$d_{\text{O}_4\cdots\text{O}_3}$ 2.756 Å, $\angle\text{D--H}\cdots\text{A}$ 175.1°] hydrogen bonding interaction involving the included water molecule and the bridging oxo-groups of the Co_4O_4 units. This results in the

formation of three-dimensional network in which the acetonitrile molecules are included as guests in the lattice.

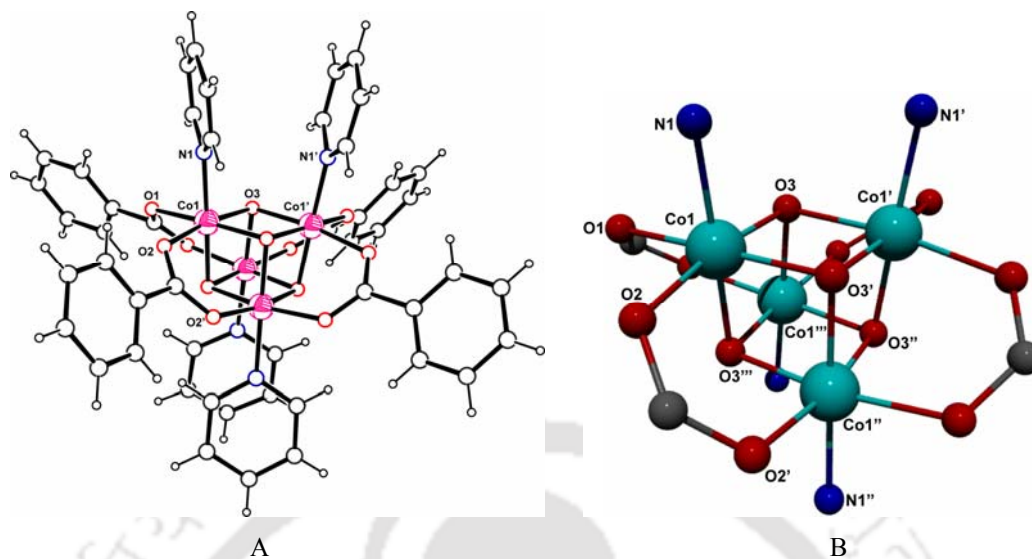


Figure 2.18 A) Crystal structure of **2.8** (Solvent molecules are not shown for clarity), B) The Co_4O_4 core, Symmetry transformations used to generate equivalent atoms: ' = $1/4-x, y, 1/4-z$; " = $x, 1/4-y, 1/4-z$; "' = $1/4-x, 1/4-y, z$

The complex is diamagnetic and shows broad absorptions at 639 nm in the visible spectrum, which is assigned to be ${}^1\text{A}_1 \rightarrow {}^1\text{T}_1$ transition for low spin Co(III) complex. The diamagnetic nature of the complex **2.8** is evident from its ${}^1\text{H}$ NMR spectrum where the aromatic protons belonging to the benzoate and pyridine ligands appear at expected positions. The ${}^1\text{H}$ NMR of the complex shows signals at 8.73, 8.02, 7.46, 7.32, 7.22, 6.97 ppm for to the benzoate and pyridine protons. The cyclic voltametry analysis of the complex **2.8** in acetonitrile solution shows a nearly reversible reduction with $E_{1/2} = 0.814$ versus saturated calomel electrode.

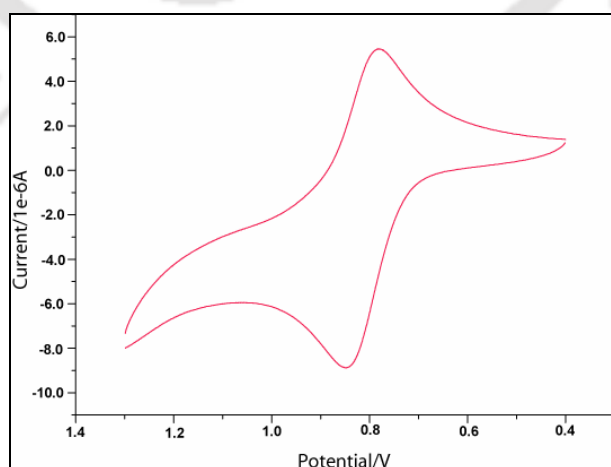


Figure 2.19 Cyclic voltammogram of complex **2.8**

(Figure 2.19). It is imperative that the tetrameric $[\text{Co}^{\text{III}}_4(\mu_3\text{-O})_4]$ core undergoes a one-electron reduction to form a species containing the reduced $[\text{Co}^{\text{III}}_3\text{Co}^{\text{II}}(\mu_3\text{-O})_4]$ core, which is also stable.

In conclusion, we have described a solid-state synthetic route for the synthesis of aqua bridged dinuclear cobalt(II) carboxylate complexes. Depending on the substituent and method of synthetic procedure inclusion of some guest molecules are observed. The aqua bridge in the dinuclear structures is stabilised by intramolecular $\text{O-H}\cdots\text{O}$ hydrogen bonding interactions between the bridging aqua group and the monodentate benzoate/substituted benzoate ligands. We have also shown that depending on the method of synthesis and crystallisation, three distinct polymorphs (**I–III**) of an aqua-bridged dinuclear 2-nitrobenzoate cobalt(II) complexes are obtained. In this case, the formation of polymorphs originates from the different orientations of the nitro groups in the complexes. The solution state reactions lead to the formation of mononuclear cobalt(II) carboxylate complex and the reaction is highly depends on substituent on aromatic ring. The aqua bridged cobalt(II) benzoate complex prone towards oxidation and such oxidation provides a method to prepare tetranuclear cobalt(III) carboxylate complex.

2.5 Experimental section

2.5.1 Materials

All chemicals are obtained from commercial sources and used without further purification. Solvents (HPLC grade) are purchased from commercial sources and used without further purification or dried according to standard procedures²⁸⁴.

2.5.2 Physical Measurement

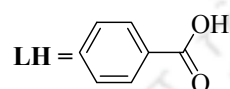
X-ray diffraction data were collected on Bruker 3-circle diffractometers with CCD area detectors ProteumM APEX or SMART 6000 or Bruker Nonius Apex 2. The diffraction data for all the crystals were collected using Bruker SMART software. This software was also used for indexing and determination of the unit cell parameters. The structures were solved by direct methods and refined by full-matrix least squares against F^2 of all data, using SHELXTL software²⁸⁵⁻²⁸⁷. The IR spectra were recorded on Perkin-Elmer spectrum one spectrometer using KBr pellets. UV-vis adsorption spectra were recorded using Perkin-Elmer Lambda 25 spectrophotometer equipped with double cell compartments. The thermogravimetric studies

were performed using a Mettler Toledo TGA/ STDA 851^e and Mettler Toledo DSC^e thermal analyser. Elemental analyses were done on a Perkin-Elmer PE 2400 II CHN analyzer 2400 (Other details of the instruments are given in Appendix).

2.5.3 Synthesis of aqua bridged dinuclear cobalt(II) carboxylate complex

Detailed synthetic methodologies are given below. Analytical data as well as spectroscopic data are also listed along with the each complex.

Complex 2.1: $[\text{Co}_2(\mu\text{-H}_2\text{O})(\mu\text{-L})_2(\text{L})_2(\text{Pyridine})_4].(\text{C}_6\text{H}_6)(\text{LH})$



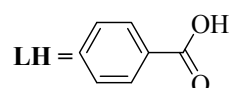
Benzoic acid (0.24 g, 2 mmol), sodium hydroxide (0.08 g, 2 mmol) and cobalt (II) chloride hexahydrate (0.24 g, 1 mmol) were finely ground in mortar and heated at 100°C for 45 min, the pink colour of reaction mixture turned blue. The solid mixture was cooled to room temperature, transferred into a round bottom flask and benzene (20 ml) was added to it and the heterogeneous mixture was stirred at room temperature for 5 min followed by the addition of pyridine (0.16 g, 2 mmol). The blue supernatant liquid turned pink in colour. The residue was filtered off and the pink filtrate was left undisturbed. Pink crystals were collected after 3 days and dried in air. Yield: 34% (Based on Co).

Elemental analysis for $\text{C}_{61}\text{H}_{54}\text{Co}_2\text{N}_4\text{O}_{11}$: calculated C, 64.37; H, 4.74; N, 4.93; found C, 64.58; H, 4.82; N, 4.84.

IR (KBr, cm^{-1}): 3449(b), 3063(s), 1614(s), 1568(s), 1537(s), 1487(m), 1403(s), 1219(m), 1070(m), 853(s), 766(s), 717(s), 701(s).

Magnetic moment: 6.54BM at 25°C. λ_{max} (MeOH): 519 nm, $\epsilon = 40.10 \text{ M}^{-1} \text{ dm}^3 \text{ cm}^{-1}$.

Complex 2.2: $[\text{Co}_2(\mu\text{-H}_2\text{O})(\mu\text{-L})_2(\text{L})_2(\text{Pyridine})_4].1.5(\text{C}_6\text{H}_6)$



A mixture of sodium benzoate (0.29g, 2 mmol) and cobalt (II) chloride hexahydrate (0.24 g, 1 mmol) was heated at 100°C for 45 min in a mortar pastel, while doing this pink colour of the

reaction mixture turned blue. Then the reaction mixture was transferred into a round bottom flask and 20ml of benzene was added to it. The mixture was stirred at room temperature for 5 min followed by the addition of pyridine (0.16g, 2 mmol). The blue supernatant liquid turned pink in colour. The residue was filtered off and the pink filtrate was left undisturbed. Pink crystals were obtained after 3 days that were collected and dried in air. Yield: 23% (Based on Co).

Elemental analysis for $C_{57}H_{51}Co_2N_4O_9$: calculated C, 64.90; H, 4.83; N, 5.32; found C, 64.98, H, 4.94; N, 5.40.

IR (KBr, cm^{-1}): 3446(b), 3066(bs), 2361(b), 1627(s), 1601(s), 1573(s), 1537(m), 1485(m), 1393(s), 1068(m), 1038(m), 812(ms), 757(ms), 716(s), 701(s), 677(m).

Magnetic moment: 6.52 BM at 25°C. λ_{max} (MeOH): 519 nm, $\epsilon = 40.32 M^{-1} dm^3 cm^{-1}$.

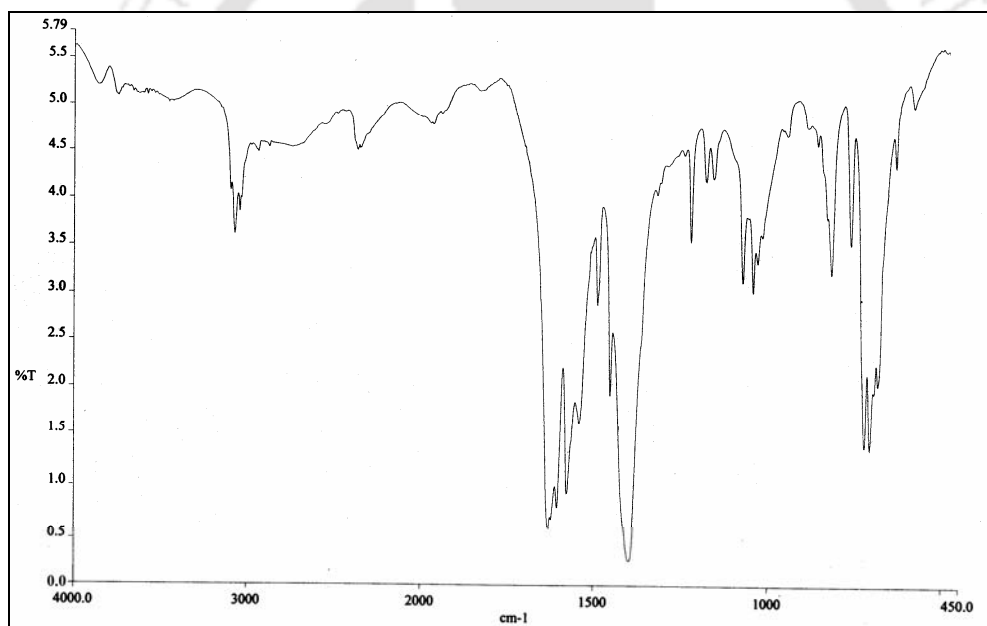
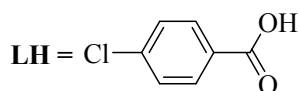


Figure 2.20 FT-IR spectra of complex 2.2

Complex 2.3: $[Co_2(\mu-H_2O)(\mu-L)_2(L)_2(Pyridine)_4]$



4-chloro benzoic acid (0.31 g, 2mmol), sodium hydroxide (0.08 g, 2mmol) and cobalt (II) chloride hexahydrate (0.24g, 1mmol) were mixed in a mortar and heated at 100°C for 45 min. The heated mixture was dissolved in 20ml of toluene and pyridine (0.16g, 2mmol) was added

to it. The blue supernatant liquid turned pink in colour. The residue was filtered off and the pink filtrate was left undisturbed for crystallisation. Pink crystals were collected after 4 days and dried in air. Yield: 39% (Based on Co).

Elemental analysis for $C_{48}H_{38}Cl_4Co_2N_4O_9$: calculated C, 53.58; H, 3.53; N, 5.22; found C, 54.52; H, 3.50; N, 5.01.

IR (KBr, cm^{-1}): 3440(b), 3069(bs), 1608(s), 1561(s), 1486(ms), 1446(ms), 1403(s), 1219(m), 1169(m), 1091(ms), 1014(ms), 856(m), 772(s), 699(s), 537(s).

Magnetic moment: 5.93 BM at 25°C. λ_{max} (MeOH): 518 nm, $\epsilon = 37.06 M^{-1} dm^3 cm^{-1}$.

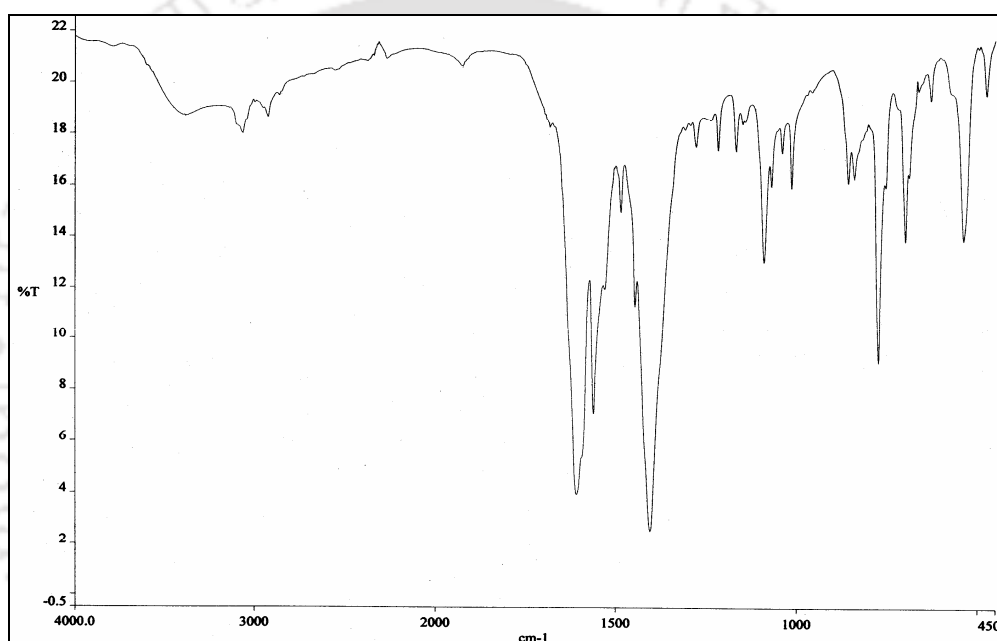
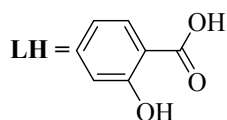


Figure 2.21 FT-IR spectra of complex 2.3

Complex 2.4: $[Co_2(\mu-H_2O)(\mu-L)_2(L)_2(Pyridine)_4]$



2-Hydroxy benzoic acid (0.28 g, 2mmol) and sodium hydroxide (0.08g, 2mmol) was finely ground in mortar pastel to prepare the sodium salt of 2-hydroxybenzoic acid. To the sodium salt of 2-hydroxybenzoic acid, cobalt(II) chloride hexahydrate (0.24g, 1mmol) was added and mixed them together. The reaction mixture was heated at 100°C for 45 min. The solid mixture was cooled to room temperature, transferred into a round bottom flask and toluene (20ml) was

added to it and the heterogeneous mixture was stirred at room temperature for 5 min followed by the addition of pyridine (0.16 g, 2 mmol). The residue was filtered off and the pink filtrate was left undisturbed for crystallization. Pink crystals were collected after 5 days and dried in air. Yield: 35% (Based on Co).

Elemental analysis for $C_{48}H_{42}Co_2N_4O_{13}$: calculated C, 57.55; H, 4.19; N, 5.60; found C, 57.31; H, 4.34; N, 5.32.

IR (KBr, cm^{-1}): 3395(bs), 3065(bs), 1635(s), 1602(s), 1486(ms), 1461(s), 1389(s), 1355(m), 1252(s), 1141(m), 1042(w), 856(m), 755(s), 699(s), 661(m).

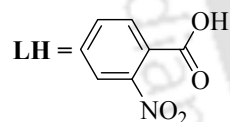
Magnetic moment: 6.22 BM at 25°C. λ_{max} (MeOH): 520 nm, $\epsilon = 39.02 M^{-1} dm^3 cm^{-1}$.

2.5.4 Synthesis of polymorphs of aqua bridged dinuclear cobalt(II) carboxylate complex of 2-nitro benzoic acid

Synthetic procedures of three polymorphs of aqua bridged dinuclear 2-nitro benzoate complex of cobalt(II) are described below.

Complex 2.5:

Polymorph I [$Co_2(\mu-H_2O)(\mu-L)_2(L)_2(Pyridine)_4$]



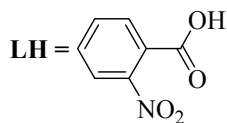
2-Nitrobenzoic acid (0.34g, 2mmol) was dissolved in methanol (10mL) and sodium hydroxide (0.08g, 2mmol) was added to it. The mixture was stirred vigorously for 5 min, and cobalt(II) chloride hexahydrate (0.24g, 1mmol) was added to it. The reaction mixture became pink, and subsequently pyridine (0.16g, 2mmol) was added. The solution was filtered, and the pink filtrate was kept at room temperature. Pink, rod like crystals were obtained after 3 days, which were then collected and dried in air. Yield: 44% (Based on Co).

Elemental analysis for $C_{48}H_{38}Co_2N_8O_{17}$: calculated C, 51.61; H, 3.40; N, 10.03; found C, 51.38; H, 3.54; N, 10.11.

IR (KBr, cm^{-1}): 3433(wb), 3072(w), 1633(s), 1602(s), 1573(m), 1529(s), 1488(s), 1446(m), 1391(s), 1360(s), 1217(w), 1153(w), 1040(m), 859(m), 817(m), 777(m), 757(m), 736(m), 695(s), 647(m).

Magnetic moment: 6.52 BM at 25°C. λ_{max} (MeOH): 521 nm, $\epsilon = 39.29 \text{ M}^{-1} \text{ dm}^3 \text{ cm}^{-1}$.

Polymorph II [$\text{Co}_2(\mu\text{-H}_2\text{O})(\mu\text{-L})_2(\text{L})_2(\text{Pyridine})_4$]



2-Nitrobenzoic acid (0.34 g, 2 mmol) was added to a solution of cobalt acetate tetrahydrate (0.25g, 1 mmol) in methanol (20 mL), and the mixture was stirred overnight. To this solution, pyridine (0.16 g, 2 mmol) was added, and the mixture was stirred for another 10 mins. On standing for 2 days, square shaped, pink crystals were obtained from the reaction mixture. Yield: 41% (Based on Co).

Elemental analysis for $\text{C}_{48}\text{H}_{38}\text{Co}_2\text{N}_8\text{O}_{17}$: calculated C, 51.61; H, 3.40; N, 10.03; found C, 51.81; H, 3.21; N, 9.95.

IR (KBr, cm^{-1}): 3429(wb), 3076(w), 1635(s), 1602(s), 1574(m), 1531(s), 1487(w), 1447(m), 1396(s), 1364(s), 1218(w), 1154(w), 1040(m), 859(w), 821(m), 781(w), 763(w), 751(w), 735(m), 701(s), 646(m).

Magnetic moment: 6.60 BM at 25°C. λ_{max} (MeOH): 521 nm, $\epsilon = 39.18 \text{ M}^{-1} \text{ dm}^3 \text{ cm}^{-1}$.

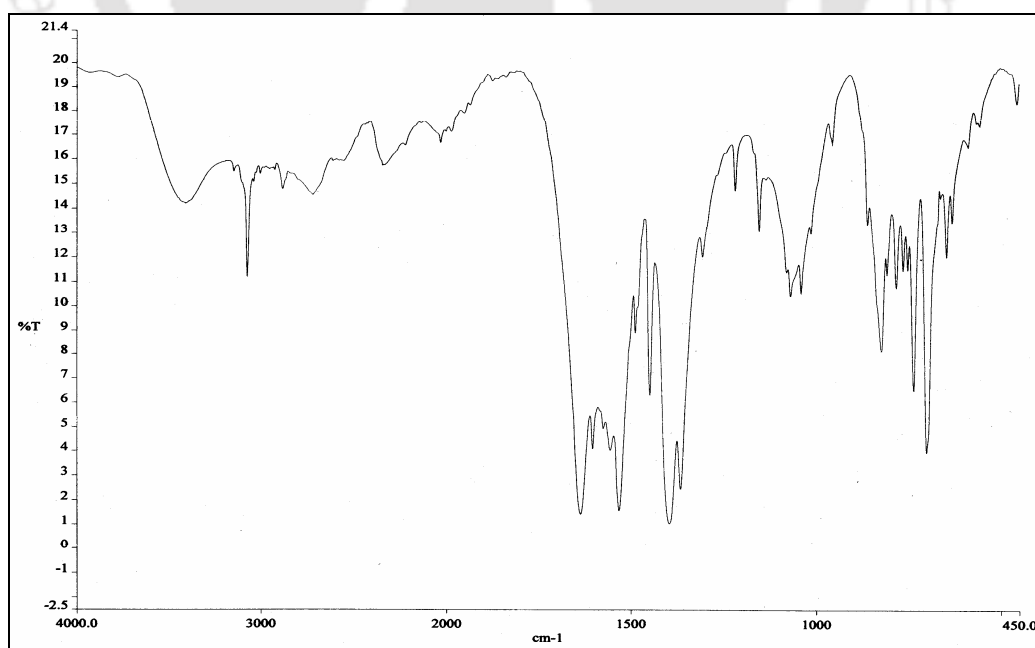
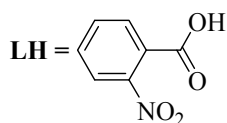


Figure 2.22 FT-IR spectra of Polymorph III

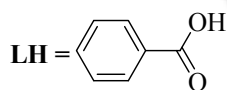
Polymorph III $[\text{Co}_2(\mu\text{-H}_2\text{O})(\mu\text{-L})_2(\text{L})_2(\text{Pyridine})_4]$ 

2-Nitrobenzoic acid (0.34 g, 2 mmol), sodium hydroxide (0.08 g, 2 mmol) and $\text{CoCl}_2 \cdot 6\text{H}_2\text{O}$ (0.24 g, 1 mmol) were mixed in a mortar and pestle and heated at $100\text{ }^\circ\text{C}$ for 45 min, the pink colour turns blue. The reaction mixture was cooled to room temperature and transferred into a round-bottomed flask, and toluene (20 mL) was added to it. The heterogeneous mixture was then stirred at room temperature for 5 min followed by the addition of pyridine (0.16 g, 2 mmol). The residue was filtered off and the pink filtrate was left undisturbed for crystallization. Pink crystals were collected after 3 days and dried in air. Yield: 34% (Based on Co).

IR (KBr, cm^{-1}): 3434 (b), 3076 (ms), 1635 (s), 1603 (ms), 1531 (s), 1487(s), 1447 (ms), 1395 (s), 1364(m), 1218 (ms), 1154 (ms), 1040 (ms), 821 (s), 735 (s), 701 (s).

Elemental analysis for $\text{C}_{48}\text{H}_{38}\text{Co}_2\text{N}_8\text{O}_{17}$: calculated C, 51.61; H, 3.40; N, 10.03; found C, 51.41; H, 3.25; N, 10.25.

Magnetic moment: 6.56 BM at $25\text{ }^\circ\text{C}$. λ_{max} (MeOH): 521 nm, $\epsilon = 39.23\text{ M}^{-1}\text{ dm}^3\text{ cm}^{-1}$.

2.5.5 Synthesis of mononuclear cobalt(II) carboxylate complex**Complex 2.6:** $[\text{Co}(\text{H}_2\text{O})(\text{Pyridine})_2(\text{L})_2]$ 

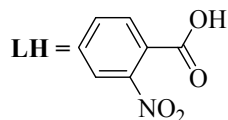
To a well-stirred solution of benzoic acid (0.24g, 2mmol) in methanol (20ml) cobalt (II) acetate tetrahydrate (0.25g, 1mmol) was added and stirred for 12 h at room temperature. After that pyridine (0.16g, 2mmol) was added and stirred at room temperature for another half an hour. On standing pink crystals were appeared after 6 days. The crystals were dried in air. Yield: 42% (Based on Co).

Elemental analysis for $\text{C}_{24}\text{H}_{22}\text{N}_2\text{O}_5\text{Co}$: calculated C, 60.37; H, 4.61; N, 4.87; found C, 60.29; H, 4.62; N, 4.98.

IR (KBr, cm^{-1}): 3265(wb), 3058(w), 1593(s), 1572(m), 1540(s), 1485(w), 1445(m), 1408(s), 1374(s), 1065(m), 1039(m), 856(m), 756(w), 722(s), 701(s), 625(m).

Magnetic moment: 4.04 BM at 25°C. λ_{max} (MeOH): 517 nm, $\epsilon = 25.07 \text{ M}^{-1} \text{ dm}^3 \text{ cm}^{-1}$.

Complex 2.7: $[\text{Co}(\text{H}_2\text{O})_2(\text{L})_2(\text{Pyridine})_2]$



2-Nitrobenzoic acid (0.34 g, 2 mmol) was dissolved in methanol (20 mL) and to this solution sodium hydroxide (0.08 g, 2 mmol) was added. After 10 min of stirring cobalt (II) sulphate heptahydrate (0.28 g, 1 mmol) was added to the solution and the heterogeneous mixture was stirred for another 30 min. To this heterogeneous mass pyridine (0.15 g, 2 mmol) was added. The residue was filtered off (if any) and discarded. Orange crystals were collected after 2 days from the filtrate. The crystals were collected and dried. Yield: 51%.

IR (KBr, cm^{-1}): 3414(wb), 3064(w), 1604(s), 1582(s), 1555(s), 1526(s), 1484(m), 1448(s), 1400(s), 1356(s), 1303(w), 1069(w), 1041(w), 911(wb), 818(s), 759(w), 738(s), 695(s).

Elemental analysis for $\text{C}_{24}\text{H}_{22}\text{CoN}_4\text{O}_{10}$: calculated C, 49.20; H, 3.76; N, 9.57; found C, 49.45; H, 3.43; N, 9.31.

Magnetic moment: 3.95 BM at 25 °C. λ_{max} (MeOH): 515 nm, $\epsilon = 6.7 \text{ M}^{-1} \text{ dm}^3 \text{ cm}^{-1}$.

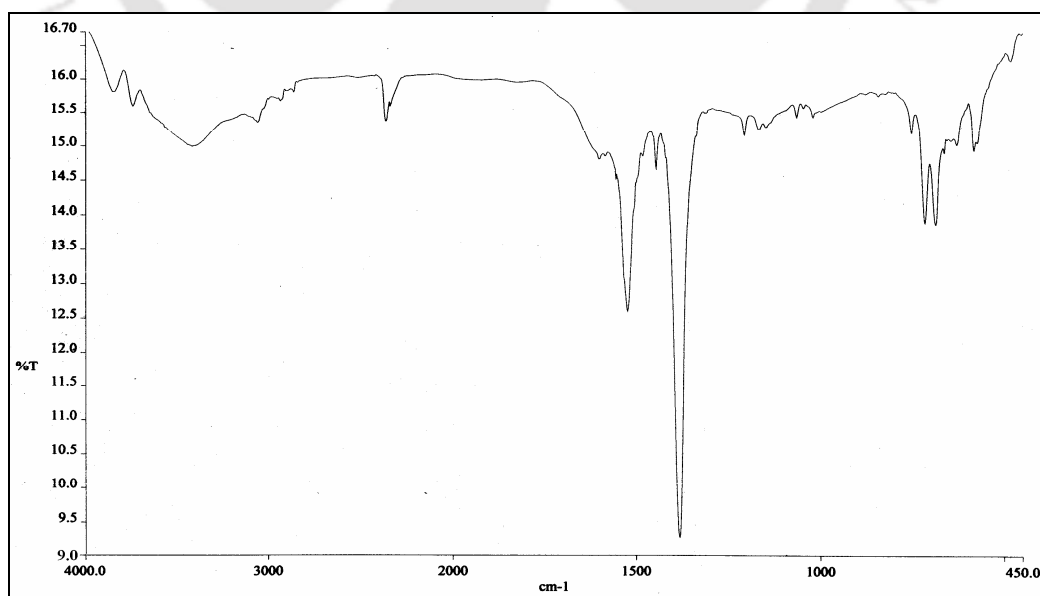
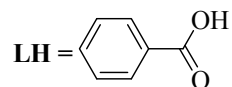


Figure 2.23 FT-IR spectra of complex 2.8

2.5.6 Synthesis of tetranuclear cobalt(III) carboxylate complex

Complex 2.8: $[\text{Co}_4\text{O}_4(\text{Pyridine})_4(\text{L})_4] \cdot (4\text{CH}_3\text{CN}) \cdot (4\text{H}_2\text{O})$



Complex **2.1** (0.15g, 0.1mmol) was dissolved in acetonitrile (10ml) and H_2O_2 (0.4 ml; 30% v/v) was added dropwise. On addition of hydrogen peroxide the pink solution became dark green. The solution was filtered to remove undissolved material (if any) and the filtrate was left undisturbed for 2 days. Dark green crystals were obtained after 2 days, which were found suitable for single crystal X-ray diffraction studies. Yield: 52% (Based on Co).

IR (KBr, cm^{-1}): 3412(b), 3060(b), 2368(ms), 1602(bs), 1527(s), 1448(ms), 1384(s), 1212(ms), 1070(ms), 1026(ms), 757(ms), 718(s), 691(s).

^1H NMR (CDCl_3 , 400 MHz): 8.73 (8H, d, $J= 6.0$ Hz), 8.02 (8H, d, $J= 8.0$ Hz), 7.46 (4H, t, $J= 7.2$ Hz), 7.32 (4H, t, $J= 7.2$ Hz), 7.22 (8H, m), 6.97 (8H, t, $J= 7.2$ Hz).

Chapter 3

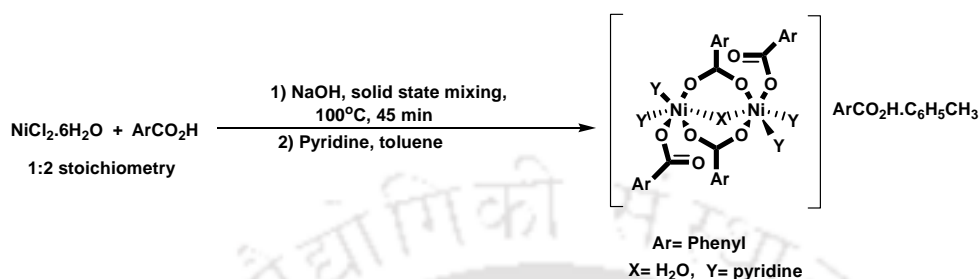
Synthesis and structures of dinuclear nickel carboxylate complexes

Carboxylate complexes of nickel are common in literature²⁸⁸ and some of them act as catalyst for different organic reactions²⁸⁹. Dimeric nickel(II) complexes are studied as model compound of urease²⁹⁰. The crystal structures of the active sites of dinuclear nickel(II) metallo-enzymes reveals that the metal centres are bridged by carboxylates as well as water or hydroxide ion²⁹¹. The dinuclear metal active site of the urease, isolated from *Klebsiella aerogenes*, has aqua-bridged dinuclear nickel(II) centres with pseudo-octahedral and square pyramidal geometry around the nickel ions¹⁹⁴. So the design of dinuclear aqua-bridged nickel(II) complexes is important in biological modelling²⁹². Study of the structure and properties of dinuclear transition-metal complexes containing bridging groups such as aqua groups is expected to increase our understanding of the crucial factors that determine the catalytic activity of metalloenzymes²⁹³. It is necessary to understand how different types of motifs can be developed from the complexes that have close structural resemblance to biological active sites. The stability of such complexes in the presence of various neutral molecules in the lattice needs attention. With these objectives in mind we have investigated multiple component solid-state synthesis of dinuclear nickel(II) carboxylate complexes and the structural aspects of aqua-bridged nickel complexes in the presence of different neutral ligands.

3.1 Synthesis and characterisation of aqua bridged dinuclear nickel(II) benzoate complex

The solid state reaction between benzoic acid, potassium hydroxide and nickel chloride followed by treatment with pyridine leads to a dimeric nickel complex of composition $[(\text{Ni}_2(\mu\text{-H}_2\text{O})(\mu\text{-C}_6\text{H}_5\text{CO}_2)_2(\text{C}_6\text{H}_5\text{-CO}_2)_2(\text{C}_5\text{H}_5\text{N})_4]. (\text{C}_7\text{H}_8). (\text{C}_6\text{H}_5\text{COOH})$ (**3.1**) as shown in scheme 3.1. The complex **3.1** has close structural similarities to urease in terms of the nickel centers bridged by carboxylate ligands and also having two nitrogen donor ligands attached to

the nickel. The complex has a free benzoic acid and a toluene molecule in the lattice (Figure 3.1A). The nickel ions are hexa-coordinated where two positions are occupied by pyridine molecules that are cis to each other. Other two cis coordination sites are occupied by two oxygen atoms, one each from the two bridged benzoates. The rest of the co-ordination sites are occupied by oxygen atoms of the bridging water and of mono-dentate benzoate ligand.



Scheme 3.1

The mono-dentate benzoates are hydrogen bonded to the bridging water molecule. The donor–acceptor bond distances are O1···O7, 2.540Å; O1···O3, 2.574Å and <D–H···A bond angles are, <O1–H···O7, 165.4°; <O1–H···O3, 160.5°. The dimeric units self assemble through C8–H···O3 [*d*_{C8···O3} 3.350Å, <D–H···A 151.2°] interaction between the uncoordinated oxygen atom of the mono-dentate carboxyl group and the C–H bond para to the nitrogen of the pyridine rings (Table 3.1). The π ··· π interaction among two pyridine rings that are coordinated to two independent metal centers contributes to this assembly. The π ··· π separation between the two pyridine rings is 3.389Å. The uncoordinated benzoic acid is held in the assembly through hydrogen bonding to one of the oxygen of the bridging benzoate group (Figure 3.1B). The toluene molecule is positioned horizontally between a cone like space, formed by the aromatic rings of two assembled dimeric units. The C–H meta to the methyl group of toluene is involved in a C–H··· π [*d*_{H··· π} 2.883Å] interaction with a coordinated pyridine molecule. The nickel complex **3.1**, is unique in a sense that it has a novel dimeric structure as well as being an acid inclusion complex. Some of the selected bond distances and angles of this complex are listed in Table 7 (Appendix).

Table 3.1: Hydrogen bond geometry(Å, °) in **3.1**

D–H···A	d(D–H)	d(H···A)	d(D···A)	<D–H···A
O(1)–H(1s)···O(3) [Intramolecular]	0.92(5)	1.69(4)	2.574(4)	160.5(4)
O(1)–H(2s)···O(7) [Intramolecular]	0.85(4)	1.71(4)	2.540(3)	165.4(4)
O(10)–H(10A)···O(8) [<i>x</i> ,3/2– <i>y</i> ,1/2+ <i>z</i>]	0.82	2.08	2.898(10)	172.5
C(8)–H(8)···O(3) [1+ <i>x</i> , <i>y</i> , <i>z</i>]	0.93	2.50	3.350(4)	151.2

FT-IR spectra of the complex **3.1** show a broad absorption at 3432 cm^{-1} due to O–H stretching of bridging aqua ligand. Two absorption bands at 1567 cm^{-1} appear due to the asymmetric stretching of bridging carboxylate groups. The monodentate carboxylate stretching appears at 1613 cm^{-1} owing to C=O stretching and 1398 cm^{-1} due to C–O stretching. Due to the presence of free benzoic acid a medium absorption band appears at 1711 cm^{-1} for C=O stretching of carboxylate group. The magnetic moment of the complex is 5.12 BM at room temperature. In methanol, the UV–Vis spectrum of **3.1** shows a weak absorption band at 653 nm ($\epsilon = 14.05\text{ M}^{-1}\text{ dm}^3\text{ cm}^{-1}$) which is assigned as 3A_2 to 3T_1 transition for distorted octahedral nickel(II) complexes.

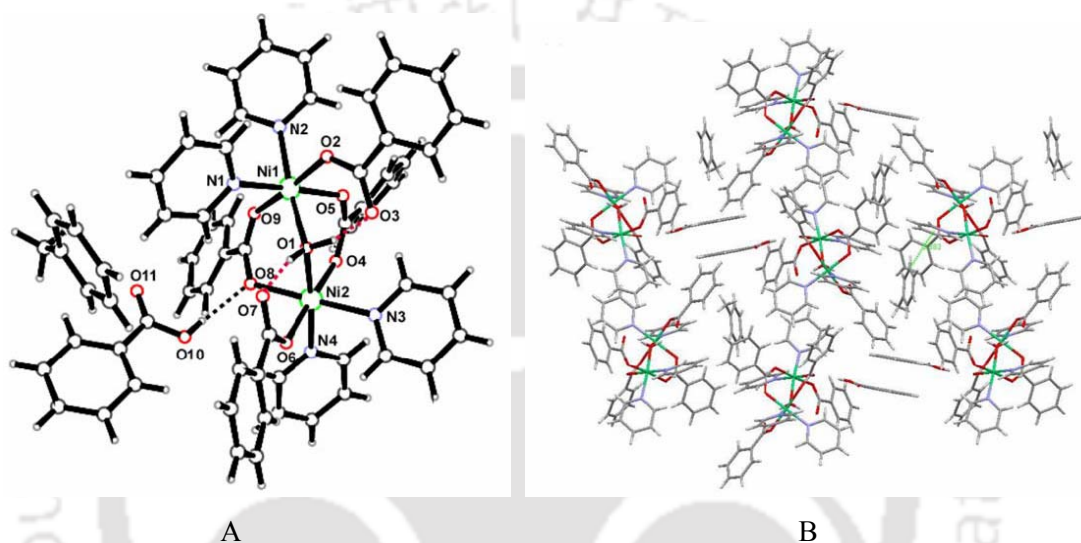


Figure 3.1 A) Structure of complex **3.1** showing the weak intra-molecular and intermolecular hydrogen bonding interactions, B) packing diagram of complex **3.1** viewed normal to [1 0 0] plane

Thermogravimetric analysis shows that the complex **3.1** loses its weight in five steps (Figure 3.2). In step one the complex loss 21.08% of its total weight in the temperature range $80\text{--}130^\circ\text{C}$, which corresponds to the loss of two pyridines, one toluene and the bridging water molecule (theoretical loss 17.6%). In the next step at the temperature range $160\text{--}250^\circ\text{C}$ the complex loses 39.07% weight which reflects the loss of remaining two pyridine molecules (calculated weight loss is 37.04%). The third weight loss occurs at $250\text{--}300^\circ\text{C}$ which corresponds to 50.01% and this is due to the loss of the free benzoic acid. The calculated weight loss is 47.56%. In the final two steps four benzoic acids are lost from the residue at the temperature range $320\text{--}520^\circ\text{C}$ and gets converted to nickel(II) oxide. The loss of these four benzoic acids corresponds to 91.60% of its total weight (theoretical loss 89.65%).

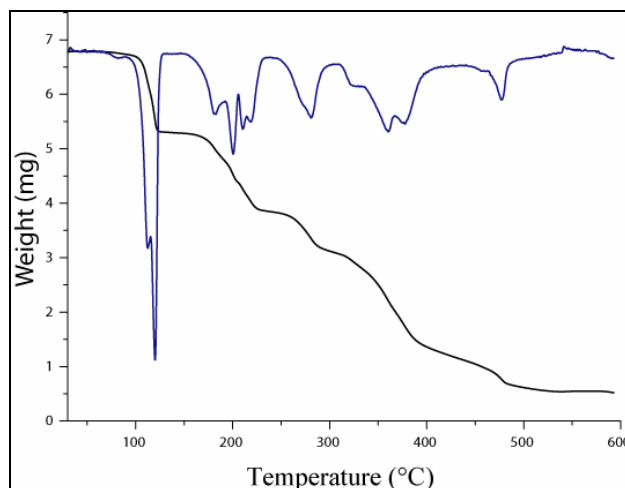
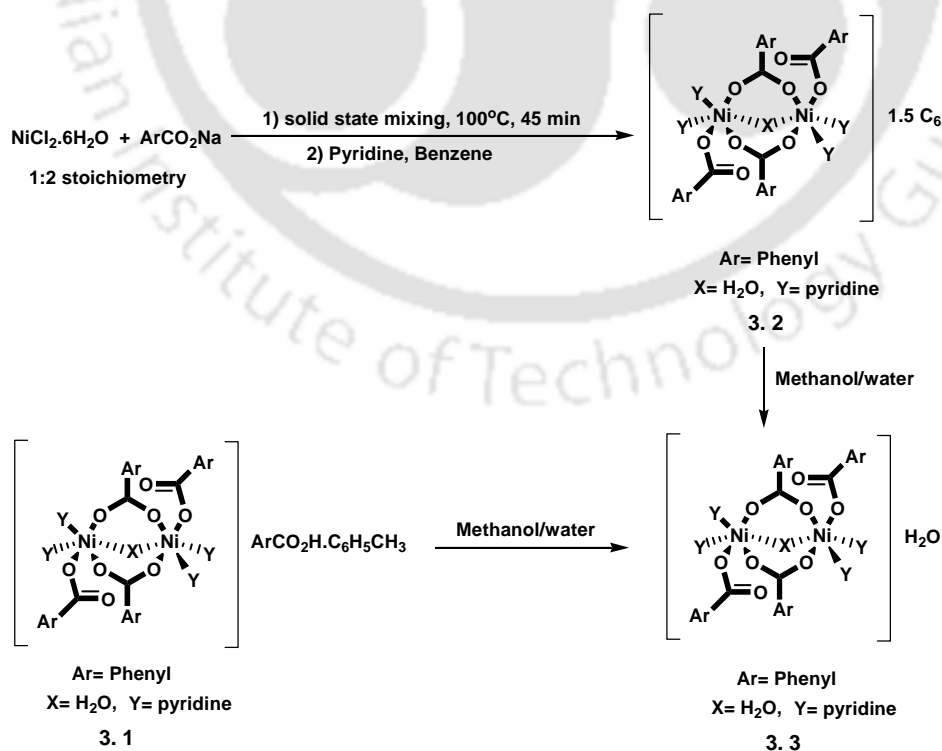


Figure 3.2: Thermogram of the complex **3.1** (heating rate 5°C/minute)

3.2 Pseudo-polymorphism in an aqua bridged dinuclear nickel(II) benzoate complex

We have synthesized two different pseudo polymorphs of aqua bridged dinuclear nickel(II) benzoate complex by using different reaction procedures. It is observed that the reaction of nickel(II) chloride hexahydrate, and sodium benzoate in the solid-state followed by addition of pyridine gave the nickel(II) benzoate complex, **3.2** (Scheme 3.2). The complex **3.2** is crystallised from benzene in $P2_1/c$ space group as light blue blocks.



Scheme 3.2

The crystal structure of **3.2** shows that each of the nickel centres have octahedral geometry involving two bridging benzoate groups (Figure 3.3A), two coordinated pyridine molecules and a monodentate benzoate apart from a bridging aqua group; the Ni1...Ni2 distance in this complex is 3.506 Å. The monodentate benzoate groups are intramolecularly hydrogen-bonded to the bridging aqua group through O9–H...O2 [$d_{O9...O2}$ 2.565 Å, $\angle D-H...A$ 166.5°] and O9–H...O8 [$d_{O9...O8}$ 2.572 Å, $\angle D-H...A$ 170.2°] interactions as shown in Table 3.2. The Ni1–O9 and Ni2–O9 bond lengths in this complex are 2.094(17) and 2.094(17) Å while the corresponding Ni1–O9–Ni2 bond angle is 113.7(8)°. Each of the nickel centres has a distorted octahedral geometry. The self-assembly of the dinuclear nickel(II) benzoate complex leads to inclusion of two benzene molecules in the crystal lattice that are stabilised by weak intermolecular C55–H... π interactions [$d_{C55... \pi}$ 3.589 Å]. Other than this the coordinated pyridine ligands are also involved in weak C2–H... π [$d_{C2... \pi}$ 3.745 Å] and $\pi... \pi$ [$d_{\pi... \pi}$ 3.379 Å] interactions.

Table 3.2: Hydrogen bond geometry(Å, °) in **3.2**

D–H...A	d(D–H)	d(H...A)	d(D...A)	$\angle D-H...A$
O(9)–H(9A)...O(2) [Intramolecular]	0.95(4)	1.63(4)	2.565(3)	166.5(3)
O(9)–H(9B)...O(8) [Intramolecular]	0.79(3)	1.79(3)	2.572(3)	170.2(3)
C(45)–H(45)...O(8) [$x, 1/2-y, -1/2+z$]	0.93	2.54	3.434(3)	161.3

When the complex **3.1** or **3.2** was dissolved in ethanol and layered over water the complex $[Ni_2(H_2O)(O_2CPh)_4(Pyridine)_4].H_2O$ (**3.3**) was formed. The complex **3.3** crystallises in the orthorhombic *Pbcn* space group. The structure of this complex is shown in Figure 3.3B.

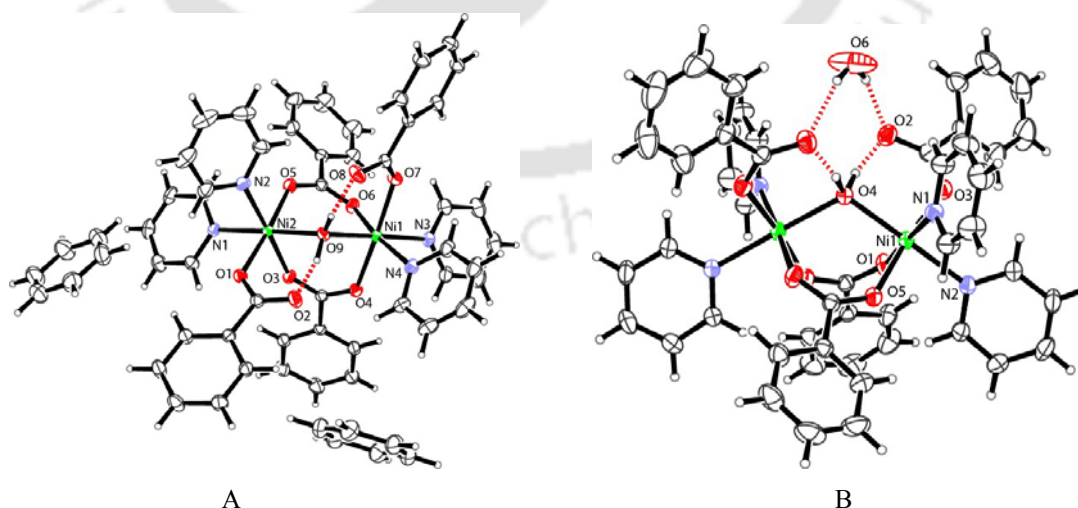


Figure 3.3 A) Crystal structure of **3.2** with included benzene molecules, B) The structure of **3.3** containing a hydrogen-bonded water molecule (In both the cases thermal ellipsoids are drawn with 30% probability)

From the crystal structure of **3.3** it is revealed that the complex has similar type of aqua bridged dinuclear core with a water of crystallisation. Intra-molecular O4–H···O2 [$d_{O4\cdots O2}$ 2.573 Å, $\angle D-H\cdots A$ 165.9°] hydrogen bonding interactions are also observed between the bridging aqua group and the monodentate benzoate group. It is observed that the Ni1–O4 bond length in **3.3** is 2.104(9) Å, which is slightly longer than that in **3.1** or **3.2**, while the Ni1–O4–Ni1' bond angle is 115.3(8)° (Table 9 in Appendix). A lattice water molecule is intermolecularly hydrogen bonded to the monodentate benzoate group through O6–H···O2 [$d_{O6\cdots O2}$ 2.910 Å, $\angle D-H\cdots A$ 163.9°] interactions. The complex self assembles in the lattice through weak C22–H···O2 [$d_{C22\cdots O2}$ 3.462 Å, $\angle D-H\cdots A$ 147.0°] interaction (Table 3.3). FT-IR spectroscopy of these complexes shows broad signals at 3412 cm^{-1} and 3478 cm^{-1} arising from O–H stretching vibrations. The asymmetric and symmetric bands of bridging carboxylate group appeared at 1572 and 1394 cm^{-1} respectively (Figure 3.6). In methanol, the UV/Visible spectrum of **3.2** and **3.3** shows an absorption band at 645 nm and 648 nm respectively, due to the 3A_2 to 3T_1 transition arising from d^8 -electronic configuration in a weak field.

Table 3.3: Hydrogen bond geometry(Å, °) in **3.3**

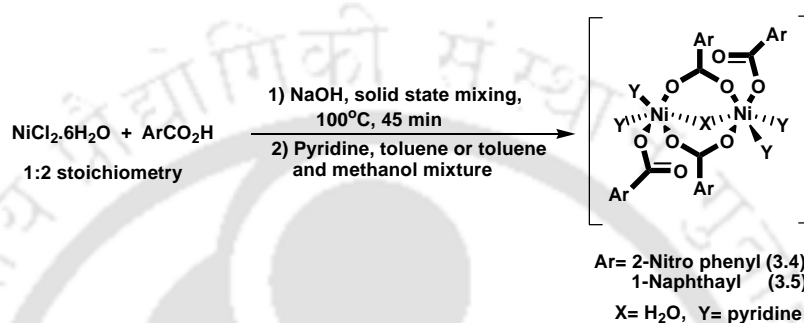
D–H···A	d(D–H)	d(H···A)	d(D···A)	$\angle D-H\cdots A$
O(4)–H(4A)···O(2) [–x,y,1/2–z]	0.91(2)	1.68(2)	2.573(17)	165.9(3)
O(6)–H(6o)···O(2) [1/2+x,1/2+y,1/2–z]	0.83(3)	2.10(3)	2.910(2)	163.9(3)

Thermogravimetric analysis of the complex **3.2** shows the loss of benzene and bridging water molecule in the temperature range 90–170°C. Similarly the complex **3.3** loses the two water molecules at the temperature range 85–125°C which corresponds to 5.10% of the total weight (theoretical weight loss 3.77%). In the temperature range 140–290°C the complex **3.3** loses four coordinated pyridine molecules, which corresponds to 34.25% of the total weight (theoretical weight loss 36.89%).

3.3 Synthesis of aqua bridged dinuclear nickel(II) benzoate complexes with substituted aromatic acids

We have performed similar type of solid state reactions with substituted aromatic acids namely 1-naphthoic acid and 2-nitrobenzoic acid (Scheme 3.3). Addition of pyridine to a mixture of nickel(II) chloride hexahydrate, 1-naphthoic acid and potassium hydroxide in toluene/methanol (1:1 v/v) gave a blue solution, from which aqua-bridged dinuclear complex, $[\text{Ni}_2(\text{H}_2\text{O})(\text{O}_2\text{CNp})_4(\text{C}_5\text{H}_5\text{N})_4]$ (**3.4**), was obtained (where Np is naphthyl) as shown in Figure

3.4A. The crystal structure of the complex shows similar type of aqua-bridged dinuclear nickel(II) core. The structure of the complex shows that the nickel(II) centres are bridged by a water molecule and by two naphthoate groups, such that the Ni1–O9–Ni2 bond angle is $117.8(9)^\circ$, with a Ni1⋯Ni2 distance of 3.593Å . Some of the selected bond distances and angles of this complex are listed in Table 10 (Appendix). The bridging aqua group is hydrogen bonded to the monodentate naphthoate group through O9–H⋯O8 [$d_{\text{O9}\cdots\text{O8}} 2.566\text{Å}$, $\angle\text{D–H}\cdots\text{A} 168.6^\circ$] and O9–H⋯O2 [$d_{\text{O9}\cdots\text{O2}} 2.533\text{Å}$, $\angle\text{D–H}\cdots\text{A} 165.9^\circ$] interactions (Table 3.4).



Scheme 3.3

The hydrogens of coordinated pyridine ligands are involved in C–H⋯O interaction with monodentate carboxylate oxygen. On the other hand an aromatic $\pi\cdots\pi$ [$d_{\pi\cdots\pi} 3.377\text{Å}$] interaction is also present between the naphthyl ring and pyridine ring. There exists some other weak interactions such as C62–H⋯ π [$d_{\text{C}\cdots\pi} 3.626\text{Å}$] interaction which stabilize the molecular assembly. The FT-IR spectra of complex 3.4 is shown in Figure 3.7.

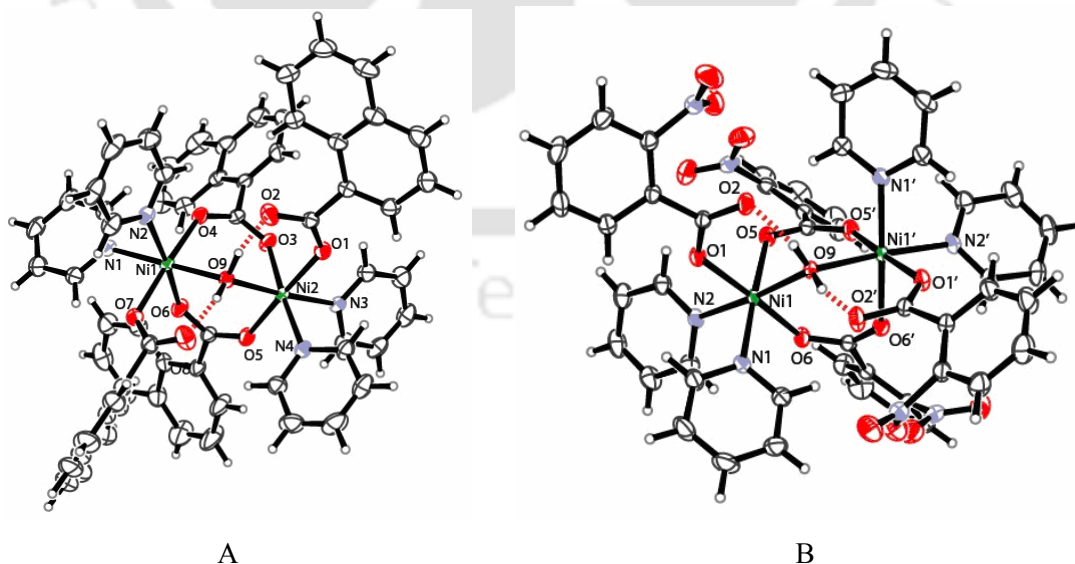


Figure 3.4 Crystal structures of (A) 3.4 and (B) 3.5 showing the intramolecular hydrogen bonding interactions between the bridging aqua molecule and the monodentate carboxylate groups (In both the cases thermal ellipsoids are drawn with 30% probability)

Similar to the one discussed above, an aqua bridged dinuclear nickel(II) complex of 2-nitrobenzoic acid (**3.5**) was also prepared and crystallised from toluene as blue-green plates in the C2/c space group.

Table 3.4: Hydrogen bond geometry(Å, °) in **3.4**

D–H···A	d(D–H)	d(H···A)	d(D···A)	<D–H···A
O(9)–H(9A)···O(8) [Intramolecular]	0.90(5)	1.68(5)	2.566(4)	168.6(5)
O(9)–H(9B)···O(2) [Intramolecular]	0.97(7)	1.59(7)	2.533(4)	165.9(6)
C(46)–H(46)···O(8) [-x, 1/2+y, 1/2-z]	0.93	2.55	3.383(5)	149.2
C(57)–H(57)···O(2) [1+x, y, z]	0.93	2.47	3.268(5)	143.9

Crystal structure analysis shows that the complex **3.5** is structurally similar to **3.4** (Figure 3.4B). It is observed that solvent molecules are not included in the crystal lattice of this complex apparently due to the steric crowding caused by the nitro substituent on the aromatic carboxylic acid molecules. Each nickel(II) centre in the complex **3.5** is coordinated to monodentate 2-nitrobenzoate group and two pyridine molecules, apart from the two bridging 2-nitrobenzoate and bridging aqua group, which gives a six-coordinate octahedral geometry. The aqua molecule in this complex is intramolecularly hydrogen bonded to the monodentate 2-nitrobenzoate through O9–H···O2 [$d_{O9\cdots O2}$ 2.571 Å, <D–H···A 167.3°] interaction (Table 3.5). In this case the Ni1–O9 bond length is 2.089(9) Å with the Ni1–O9–Ni2 bond angle being 117.1(8)°. We were unable to observe any polymorphic property in this aqua bridged dinuclear nickel carboxylate complex by varying the reaction conditions.

Table 3.5: Hydrogen bond geometry(Å, °) in **3.5**

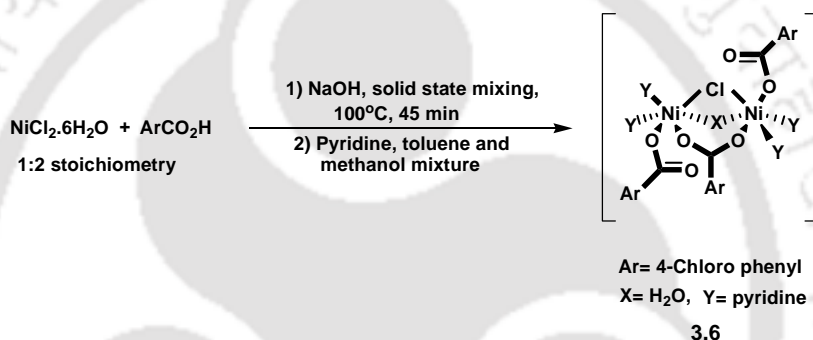
D–H···A	d(D–H)	d(H···A)	d(D···A)	<D–H···A
O(9)–H(9A)···O(2) [1-x, y, 1/2-z]	0.84(2)	1.74(2)	2.571(16)	167.3(2)
C(15)–H(15)···O(2) [-1/2+x, -1/2+y, z]	0.93	2.36	3.232(2)	156.4

FT-IR spectra of the complex **3.5** shows absorptions for monodentate carboxylate C=O at around 1637 cm⁻¹ and for the C–O group at 1396 cm⁻¹. The asymmetric and symmetric band of bridging carboxylate groups appear at around 1604 and 1486 cm⁻¹ respectively. The asymmetric band for nitro N–O stretching appears at 1520 cm⁻¹ and for symmetric stretching it appears at 1363 cm⁻¹. The magnetic moments of this complex at room temperature is 5.04 BM. Thermogravimetric analysis of the complex **3.5** shows that there is 13.85% weight loss at 140-220°C due to the lose of two pyridines and a bridging water molecule (theoretical loss 15.77%). In the temperature range of 230-290°C it loses the remaining two coordinated

pyridine ligands and two nitro benzoic acids. This loss corresponds to 57.61% of the total weight (theoretical loss 59.80%). After removal of all the coordinated pyridine and water molecule the anhydrous nickel benzoate is formed.

3.4 Synthesis and characterisation of mixed chloro and aqua bridged nickel(II) carboxylate complex

So far we have obtained systematically aqua-bridged complexes, starting from nickel(II) chloride as the inorganic salt. However, in the reaction of 4-chlorobenzoic acid under analogous conditions a chloro as well as aqua bridged complex $[\text{Ni}_2(\text{H}_2\text{O})(\text{Cl})(\text{O}_2\text{CAr})_3(\text{C}_5\text{H}_5\text{N})_4]$ (**3.6**) was formed, where Ar is p-chloro phenyl (Scheme 3.4).



Scheme 3.4

The crystal structure of the complex **3.6** revealed the presence of an aqua, chloro and benzoate bridges between the two nickel centres (Figure 3.5). Other than that a monodentate carboxylate group is also present in each nickel center. It is observed that in complex **3.6**, the bridging aqua molecule is intramolecularly hydrogen bonded to the carboxylate units of the monodentate 4-chlorobenzoate groups via O7–H···O2 [$d_{\text{O7}\cdots\text{O2}}$ 2.593 Å, $\angle\text{D-H}\cdots\text{A}$ 165.2°] and O7–H···O6 [$d_{\text{O7}\cdots\text{O6}}$ 2.562 Å, $\angle\text{D-H}\cdots\text{A}$ 164.6°] interactions (Table 3.6). The corresponding Ni1–O7 and Ni2–O7 bond lengths are 2.126(2) Å and 2.121(2) Å respectively while the Ni1–O7–Ni2 bond angle is found to be 101.2(9)°. The Ni1···Ni2 distance (3.281Å) is substantially shorter than the earlier described complexes (Table 3.7). The reported values for Ni···Ni distance of separation in aqua-bridged complexes ranges from 3.497–3.676 Å²⁹⁴. Some selected bond distances and angles of the complex **3.6** are listed in Table 12 (Appendix). The complex self assembles in the lattice through weak C–H···O interactions between the hydrogens of coordinated pyridine ligand and monodentate carboxylate oxygen.

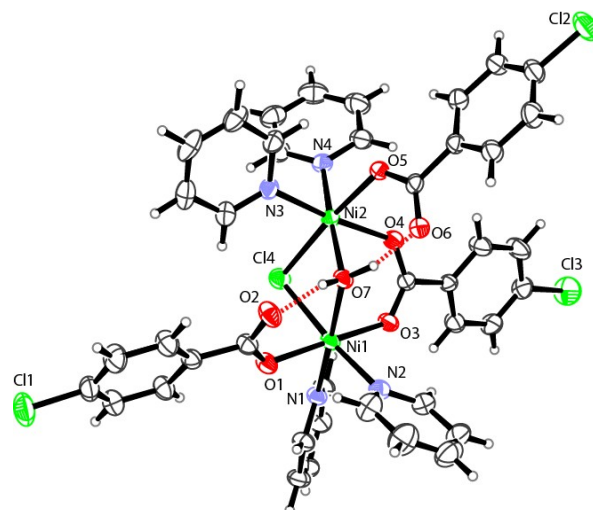


Figure 3.5 Crystal structure of **3.6** (thermal ellipsoids drawn to 30% probability)

The complex **3.6** has a distorted octahedral geometry around the nickel centres and has an electronic absorption at 633 nm due to the 3A_2 to 3T_1 transition. The FT-IR spectrum of complex **3.6** is shown in Figure 3.8. Thermogravimetric analysis of complex **3.6** shows the loss of two pyridines and a bridging water molecule in the temperature range 120-200°C, which corresponds to 16.73% of the total weight. The theoretical weight loss is 18.46%. The remaining two pyridines are removed in the temperature range 205-280°C and the weight loss is 34.16% (Theoretical weight loss is 35.05%).

Table 3.6: Hydrogen bond geometry (Å, °) in **3.6**

D–H···A	d(D–H)	d(H···A)	d(D···A)	<D–H···A
O(7)–H(7A)···O(2) [Intramolecular]	0.75(3)	1.86(3)	2.593(3)	165.2(3)
O(7)–H(7B)···O(6) [Intramolecular]	0.92(4)	1.66(4)	2.562(3)	164.6(4)
C(34)–H(34)···O(6) [1-x,1-y,1-z]	0.93	2.60	3.522(5)	171.3
C(35)–H(35)···O(2) [1-x,1-y,1-z]	0.93	2.41	3.304(4)	162.6

The Ni–O_{aqua}–Ni angles in **3.2** are smaller than that in **3.3**. This happens because the hydrogen bonding interactions of the bridging water molecules in each case are different. In the case of the complex **3.3**, the hydrogen bonding interaction involving the interstitial water molecules draws the carboxyl of the monodentate benzoate groups slightly, thereby making the Ni–O_{aqua}–Ni bond angle bigger than in **3.2**. In the case of complex **3.6** the bond angle is the smallest in comparison to **3.1–3.5** because of the presences of both chloro and aqua bridge (Table 3.7).

Table 3.7. Bond lengths (in Å) and angles (in °)

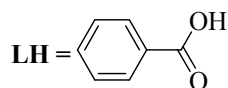
	3.1	3.2	3.3	3.4	3.5	3.6
Ni(1)–Oaqua	2.075(3)	2.094(17)	2.104(9)	2.088(19)	2.089(9)	2.126(2)
Ni(2)–Oaqua	2.086(3)	2.094 (17)	2.104(9)	2.108(2)	2.089(9)	2.121(2)
Ni(1)–Oaqua–Ni(2)	116.8(10)	113.7(8)	115.5(8)	117.8(9)	117.1(8)	101.2(9)
Ni(1)···Ni(2)	3.597	3.506	3.554	3.593	3.563	3.281

In conclusion, we have described the synthetic and structural aspects of a few dinuclear nickel(II) complexes, having bridging carboxylate groups and aqua groups. Intramolecular O–H···O hydrogen bonding interactions between the bridging aqua group and the monodentate benzoate groups are observed in these complexes which add to the stability of the bridging structure. From this structural study on aqua-bridged structures we can show the structural implications of solvent molecules in different types of pseudo-polymorphs. A mixed chloro, aqua and 4-chloro benzoato bridged nickel(II) dinuclear complex is formed from the reaction of 4-chlorobenzoate with nickel(II) chloride in the presence of pyridine. This suggests that a substituent on the aromatic ring has a role in deciding the mechanochemical process during the solid state synthesis. From this trend it can be concluded that mechanochemical synthesis prefers to yield aqua bridged dinuclear carboxylate complexes. Some of these aqua bridged complexes include free carboxylic acid.

3.5 Experimental section

Detailed synthetic methodologies are given below. Analytical data as well as spectroscopic data are also listed along with the each complex. Details of the instruments are given in Appendix.

Complex 3.1: $[\text{Ni}_2(\mu\text{-H}_2\text{O})(\mu\text{-L})_2(\text{L})_2(\text{Pyridine})_4]\cdot(\text{C}_7\text{H}_8)(\text{LH})$



A mixture of benzoic acid (0.73 g, 6 mmol), sodium hydroxide (0.34 g, 6 mmol) and anhydrous nickel(II) chloride (0.39 g, 3 mmol) were mixed together in a mortar pastel and the mixture was heated to 100°C for 45 min. The mixture was transferred into a round bottom flask and toluene (20 ml) was added to this mixture. To the heterogeneous mixture pyridine (0.47 g, 6 mmol) was added. The green solution turned blue and the residue was filtered off

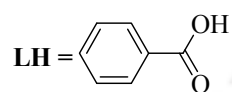
and discarded. The solution on standing gave greenish blue crystals of **3.1**. Yield: 20% (Based on Ni).

IR (KBr, cm^{-1}): 3432(wb), 3062(ms), 1711(m), 1613(s), 1567(s), 1537(s), 1398(s), 1224(w), 1160(w), 1070(w), 824(m).

Elemental analysis for $\text{C}_{62}\text{H}_{56}\text{N}_4\text{Ni}_2\text{O}_{11}$: calculated C, 64.67; H, 4.87; N, 4.87; found C, 64.37; H, 5.03; N, 4.62.

Magnetic moment: 5.12 BM at 25 °C. λ_{max} (MeOH): 653 nm, $\epsilon = 14.05 \text{ M}^{-1} \text{ dm}^3 \text{ cm}^{-1}$.

Complex 3.2: $[\text{Ni}_2(\mu\text{-H}_2\text{O})(\mu\text{-L})_2(\text{L})_2(\text{Pyridine})_4] \cdot 1.5(\text{C}_6\text{H}_6)$



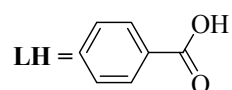
Nickel (II) chloride hexahydrate (0.24 g, 1 mmol) and sodium benzoate (0.28 g, 2 mmol) were finely ground in a mortar and heated at 100 °C for 45 min. The solid mixture was cooled to room temperature and transferred into a round-bottomed flask and benzene (20 mL) was added. The heterogeneous mixture was stirred at room temperature for 5 min followed by the addition of pyridine (0.16 g, 2 mmol). The blue supernatant liquid was filtered off and was left undisturbed for crystallisation. Blue crystals were collected after 3 days and dried in air. Yield: 0.371 g, 34% (Based on Ni).

Elemental analysis for $\text{C}_{57}\text{H}_{51}\text{Co}_2\text{N}_4\text{O}_9$: calculated C, 64.90; H, 4.84; N, 5.31; found C, 65.11; H, 4.64; N, 5.03.

IR (KBr, cm^{-1}): 3412(b), 3065(w), 3032(w), 1630(s), 1602(m), 1572(m), 1530(w), 1481(w), 1445(m), 1394(s), 1215(m), 1067(m), 1037(m), 814(m), 757(m), 716(s), 696(s), 676(s).

Magnetic moment: 5.08 BM at 25 °C. λ_{max} (MeOH): 645 nm, $\epsilon = 18.91 \text{ M}^{-1} \text{ dm}^3 \text{ cm}^{-1}$; 383 nm, $\epsilon = 65.6 \text{ M}^{-1} \text{ dm}^3 \text{ cm}^{-1}$.

Complex 3.3: $[\text{Ni}_2(\mu\text{-H}_2\text{O})(\mu\text{-L})_2(\text{L})_2(\text{Pyridine})_4] \cdot \text{H}_2\text{O}$



Complex **3.1** (0.12g, 0.1mmol) was dissolved in a mixture of methanol and water (9:1) and the resultant blue solution was left undisturbed. From this solution greenish-blue crystals were obtained after 3 days and dried in air. Yield: 0.553 g, 58% (based on Ni).

Elemental analysis for $C_{48}H_{44}N_4Ni_2O_{10}$: calculated C, 60.36; H, 4.61; N, 5.86; found C, 60.09; H, 4.39; N, 5.62.

FT-IR (KBr, cm^{-1}): 3537(w), 3478(w), 3060(w), 2065(w), 1630(s), 1602(m), 1572(s), 1528(m), 1484(m), 1447(s), 1397(s), 1215(m), 1152(w), 1070(m), 1039(m), 825(s), 760(m), 720(s), 697(s), 674(s).

Magnetic moment: 4.96 BM at 25 °C. λ_{max} (MeOH): 648 nm, $\epsilon = 16.55 M^{-1} dm^3 cm^{-1}$; 389 nm, $\epsilon = 36.63 M^{-1} dm^3 cm^{-1}$.

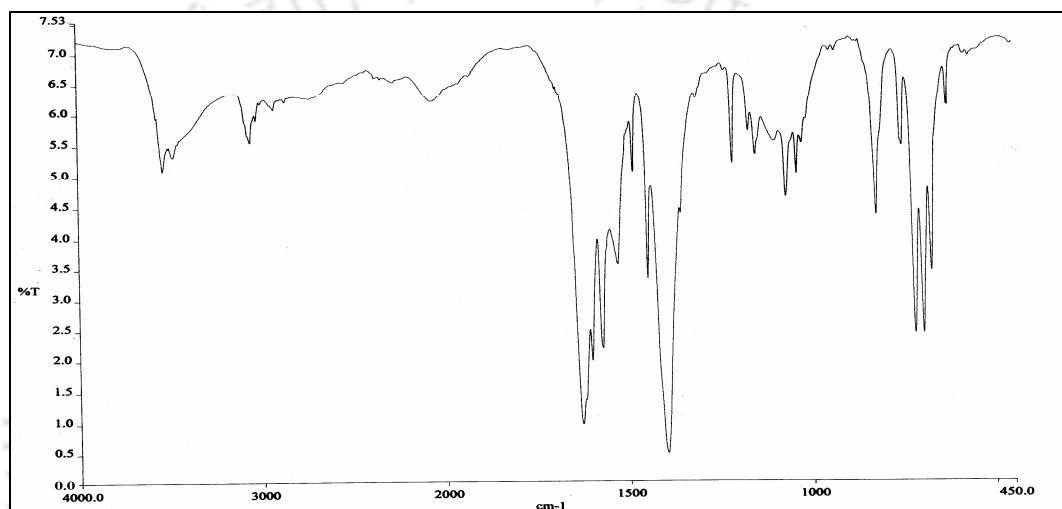
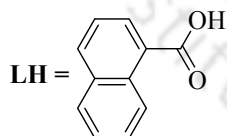


Figure 3.6 FT-IR spectra of complex 3.3

Complex 3.4: $[Ni_2(\mu-H_2O)(\mu-L)_2(L)_2(Pyridine)_4]$



The reaction mixture of 1-Naphthoic acid (0.34 g, 2 mmol), sodium hydroxide (0.08 g, 2 mmol) and $NiCl_2 \cdot 6H_2O$ (0.24 g, 1 mmol) was finely ground in a mortar and heated at 100 °C for 45 min. The heated mixture was cooled to room temperature and transferred into a round-bottomed flask, then toluene and methanol mixture (1:1, 20 mL) was added to it. The heterogeneous mixture was stirred at room temperature for 5 to 10 min followed by the addition of pyridine (0.16 g, 2 mmol). The residue was filtered off (if any) and the pink filtrate was left undisturbed. Blue block type crystals were collected after 4 days and dried in air. Yield: 0.296 g, 26% (based on Ni).

Elemental analysis for $C_{64}H_{50}N_4Ni_2O_9$: calculated C, 67.60; H, 4.40; N, 4.93; found C, 67.31; H, 4.61; N, 4.71.

IR (KBr, cm^{-1}): 3423(w), 3043(m), 2071(w), 1626(s), 1614(s), 1588(w), 1525(w), 1484(w), 1445(m), 1410(s), 1374(s), 1256(w), 1215(m), 1152(w), 1070(w), 1039(w), 891(w), 861(m), 787(s), 697(s), 655(m), 628(w).

Magnetic moment: 5.21 BM at 25 °C. λ_{max} (MeOH): 649 nm, $\epsilon = 19.53 M^{-1} dm^3 cm^{-1}$; 388 nm, $\epsilon = 55.45 M^{-1} dm^3 cm^{-1}$.

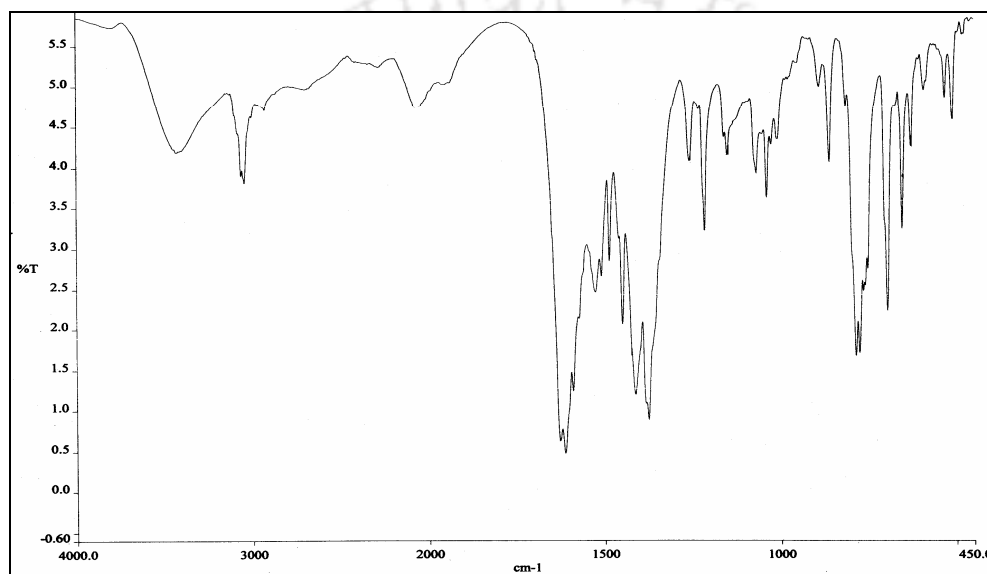
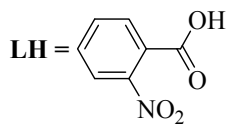


Figure 3.7 FT-IR spectra of complex 3.4

Complex 3.5: $[Ni_2(\mu-H_2O)(\mu-L)_2(L)_2(Pyridine)_4]$



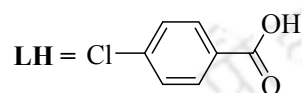
A mixture of 2-nitrobenzoic acid (0.34 g, 2 mmol), sodium hydroxide (0.08 g, 2 mmol) and nickel(II) chloride hexahydrate (0.24 g, 1 mmol) was heated to 100°C for 45 min in oven. The mixture was transferred into a round bottom flask and toluene (15 ml) was added to this mixture. To the heterogeneous mixture pyridine (0.16 g, 2 mmol) was added. The green solution turned blue and the residue was filtered off and discarded. The solution on standing gave blue crystals of complex 3.5. Yield: 0.235 g, 21% (based on Ni).

IR (KBr, cm^{-1}): 3445 (m), 3071 (m), 2071 (w), 1637 (s), 1604 (m), 1555 (w), 1520 (s), 1486 (m), 1448 (s), 1396 (s), 1363 (s), 1303 (w), 1218 (w), 1155 (w), 1071 (w), 858 (w), 824 (m), 781 (m), 736 (s), 701 (s).

Elemental analysis for $\text{C}_{48}\text{H}_{38}\text{N}_8\text{Ni}_2\text{O}_{17}$: calculated C, 51.61; H, 3.40; N, 10.03; found C, 51.83; H, 3.34; N, 10.31.

Magnetic moment: 5.04 BM at 25 °C. λ_{max} (CH_3CN): 638 nm, $\epsilon = 12.09 \text{ M}^{-1} \text{ dm}^3 \text{ cm}^{-1}$.

Complex 3.6: $[\text{Ni}_2(\mu\text{-H}_2\text{O})(\mu\text{-Cl})(\mu\text{-L})_2(\text{L})_2(\text{Pyridine})_4]$



A finely ground mixture of 4-chloro benzoic acid (0.31 g, 2mmol), sodium hydroxide (0.08 g, 2mmol) and nickel (II) chloride hexahydrate (0.24g, 1mmol) was heated at 100°C in the solid state. The mixture was cooled and transferred into a round bottom flask and a toluene: methanol mixture (2:1, 20ml) was added in to it. The heterogeneous mixture was stirred at room temp for 5 min followed by the addition of pyridine (0.16g, 2mmol). The residue was filtered off and the light blue filtrate was left undisturbed for crystallization. Blue crystals were collected after 4 days. Yield: 0.134 g, 14% (based on Ni).

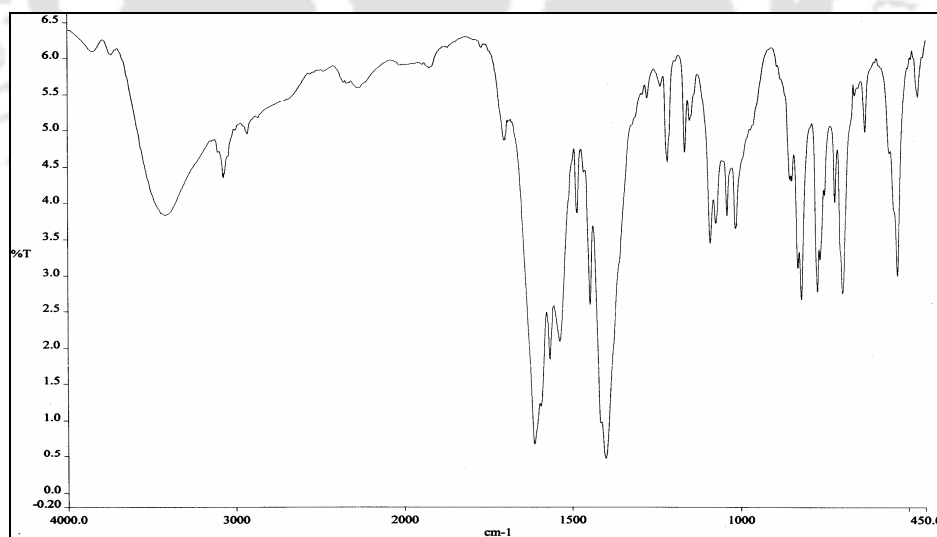


Figure 3.8 FT-IR spectra of complex 3.6

IR (KBr, cm^{-1}): 3420 (w), 3065 (w), 1703 (w), 1614 (s), 1566 (w), 1533 (w), 1484 (w), 1445 (m), 1400 (s), 1218(m), 1166 (m), 1091 (m), 1039 (w), 1012 (w), 850 (w), 820 (m), 772(m), 697 (m), 631 (w), 532 (s).

Elemental analysis for $\text{C}_{41}\text{H}_{34}\text{Cl}_4\text{N}_4\text{Ni}_2\text{O}_7$: calculated C, 51.58; H, 3.56; N, 5.87; found C, 51.32; H, 3.31; N, 5.98.

Magnetic moment: 5.24 BM at 25 °C. λ_{max} (methanol): 633 nm, $\epsilon = 24.42 \text{ M}^{-1} \text{ dm}^3 \text{ cm}^{-1}$; 389 nm, $\epsilon = 40.92 \text{ M}^{-1} \text{ dm}^3 \text{ cm}^{-1}$.



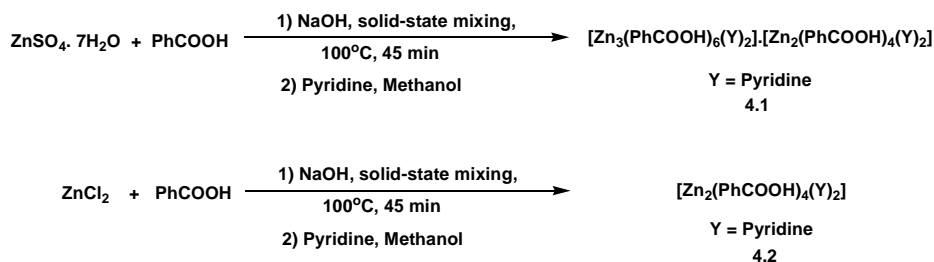
Chapter 4

Synthesis and characterisation of zinc carboxylate complexes through solid state reactions

Zinc carboxylate complexes are important for their relevance in biological systems²⁹⁵. Mono or dinuclear zinc carboxylate complexes are studied as biological model complexes²⁹⁶. The versatility of the spherical d^{10} configuration of the zinc(II) ion allows the formation of coordination environments with diverse geometries. Besides this, zinc(II) ion is able to form carboxylate clusters, which exhibit potential applications in the field of crystal engineering and also in construction of porous frameworks²⁹⁷. Multinuclear zinc carboxylate complexes are also effective catalysts for epoxide copolymerization reactions²⁹⁸. The reactivity of the zinc carboxylate complexes are greatly influenced by substituents²⁹⁹. It is very important to understand how subtle effects from the substituent and reaction conditions can change the structures of zinc complexes. Thus, there is scope to understand the formation of different zinc carboxylate complexes with different substituted carboxylic acids and under different reaction conditions. In this chapter we have described the substituent, solvent and salt effect on the solid state synthesis of mono, di and multinuclear zinc carboxylate complexes.

4.1 Study on the effect of different salts on solid state synthesis of zinc carboxylate

We have performed solid state reactions with two different salts of zinc and aromatic carboxylic acids under different reaction conditions. It is found that the solid state reaction of zinc(II) sulphate heptahydrate and benzoic acid with sodium hydroxide followed by addition of pyridine resulted in a self-assembly of two neutral zinc benzoate complexes having composition $[Zn_3(\mu\text{-OOC}_6\text{H}_5)_6(\text{pyridine})_2] \cdot [Zn_2(\text{OOC}_6\text{H}_5)_4(\text{pyridine})_2]$ (**4.1**) (Scheme 4.1). The complex is unusual as it is a self-assembly of di and trinuclear zinc(II) carboxylate complexes, of which, dinuclear complex $[Zn_2(\text{C}_5\text{H}_5\text{N})_2(\text{OOC}_6\text{H}_5)_4]$ (**4.2**) can also be independently prepared. The dinuclear complex **4.2** can be prepared by a similar solid state reaction of anhydrous zinc(II) chloride, benzoic acid and sodium hydroxide followed by reaction with pyridine.



Scheme 4.1

The crystal structure of the complex **4.1** is shown in Figure 4.1A. The crystal structure of the complex **4.1** shows that the trinuclear unit is constructed by six bridging benzoate group and two terminal pyridine ligands. Out of the three zinc centers, the central zinc is attached to six benzoate groups resulting in a hexa-coordinated metal centre. The other two zinc centers are symmetric to each other and coordinated through three carboxylate oxygen atoms and one terminal pyridine ligand. Thus, the later two zinc centers each has NO4 co-ordination environment with distorted trigonal bipyramidal geometry.

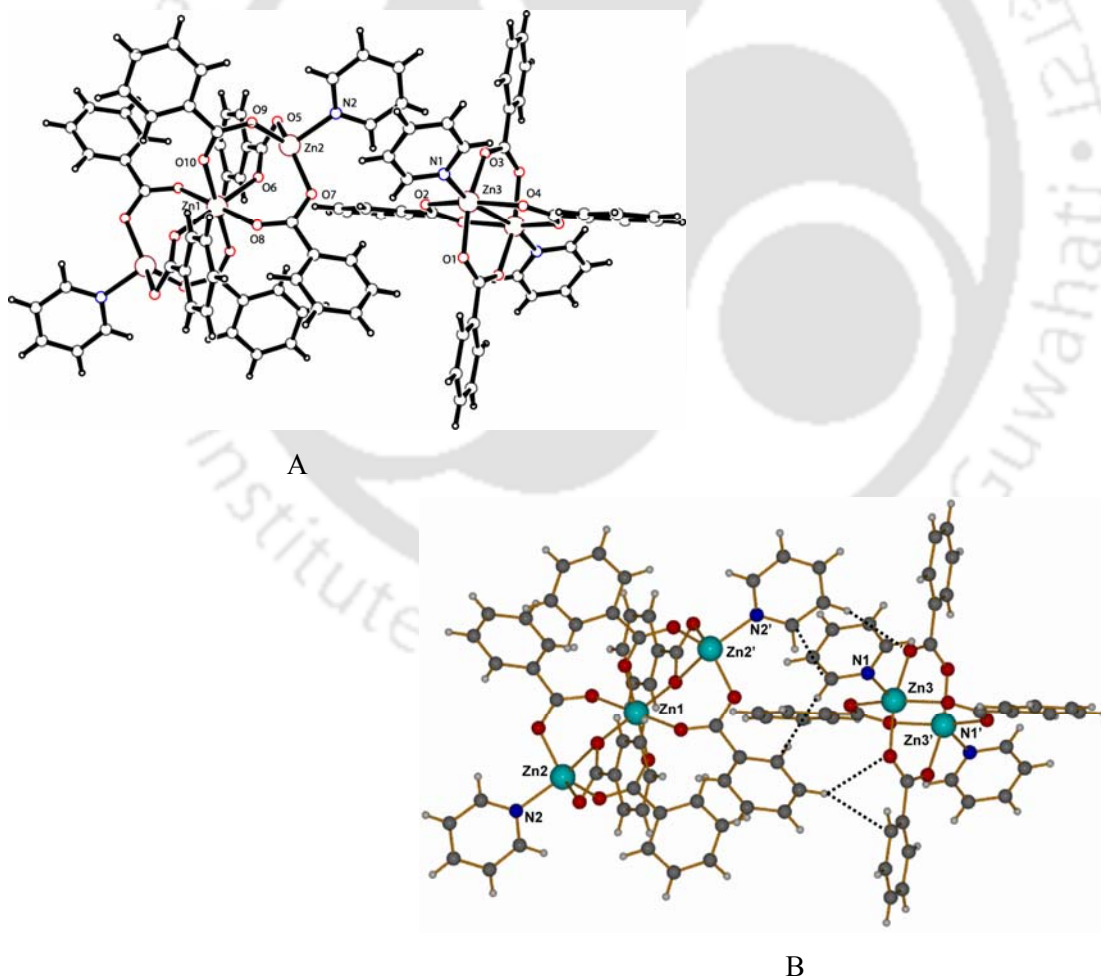


Figure 4.1 A) The crystal structure of **4.1**, B) The self assembled structure of **4.1** through C-H... π and C-H...O interactions

The central zinc has a distorted octahedral geometry. In the dinuclear part both the zinc centers are bridged by four benzoate and the axial positions are occupied by two pyridine ligands making a paddle-wheel type arrangement. Each zinc centre has a distorted square pyramidal geometry. From Figure 4.1B, it is clear that the two neutral molecules are held by C15–H $\cdots\pi$ [$d_{\text{C15}\cdots\pi}$ 3.695 Å, $d_{\text{C37}\cdots\pi}$ 3.536Å] and C–H \cdots O [$d_{\text{C28}\cdots\text{O3}}$ 3.514 Å, $\angle\text{D-H}\cdots\text{A}$ 160.7°, $d_{\text{C41}\cdots\text{O5}}$ 3.411 Å, $\angle\text{D-H}\cdots\text{A}$ 144.2°] interactions. The pyridine rings of the dinuclear and trinuclear units are assembled through aromatic $\pi\cdots\pi$ [$d_{\pi\cdots\pi}$ 3.343 Å] interactions in the lattice. Some important bond distances and angles are presented in Table 13 (Appendix).

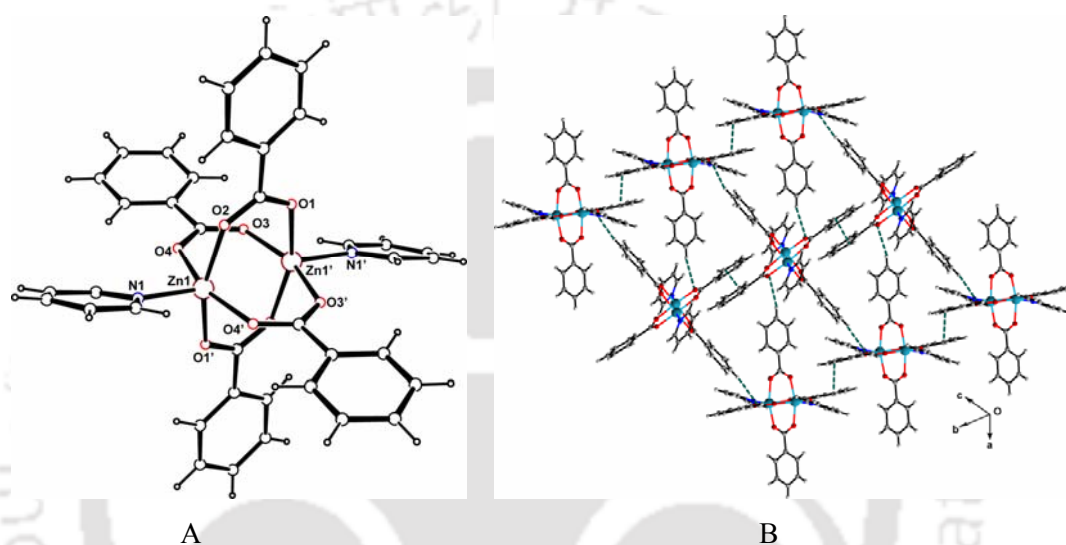


Figure 4.2 A) Paddle-wheel structure of complex **4.2**, B) Self assembly of complex **4.2** through weak C–H \cdots O and $\pi\cdots\pi$ interactions

We have also determined the crystal structure of the dinuclear complex **4.2**. The complex has a paddle-wheel type structure with a square pyramidal geometry around the zinc centre. Four carboxylate oxygens are present in the equatorial plane and the pyridine ligand is coordinated from axial direction (Figure 4.2A). The paddle-wheel type of structure of dinuclear zinc benzoate complexes is reported in literature³⁰⁰. The complex **4.2** self assembles in the lattice through weak C5–H \cdots O4 [$d_{\text{C5}\cdots\text{O4}}$ 3.627 Å, $\angle\text{D-H}\cdots\text{A}$ 166.5°] interaction. On the other hand, the benzoate groups are present in slight off set manner to each other and assembled through $\pi\cdots\pi$ [$d_{\pi\cdots\pi}$ 3.319Å] interactions as shown in Figure 4.2B. We have recorded the X-ray powder pattern of both the complexes **4.1** and **4.2** and observed that both have different powder X-ray diffraction pattern as shown in Figure 4.3A.

The solid state FT-IR spectra of the complexes **4.1** and **4.2** have close similarities for the obvious reason of composition. Both the complexes have characteristic peaks that are present

in the backbone of benzoic acid. A clear demarcation for identifying the complexes from their respective IR absorptions could not be made. The FT-IR spectra of both the complexes shows strong absorption band around 1567 cm^{-1} and 1403 cm^{-1} due to asymmetric and symmetric C=O stretching frequencies of carboxylate groups respectively.

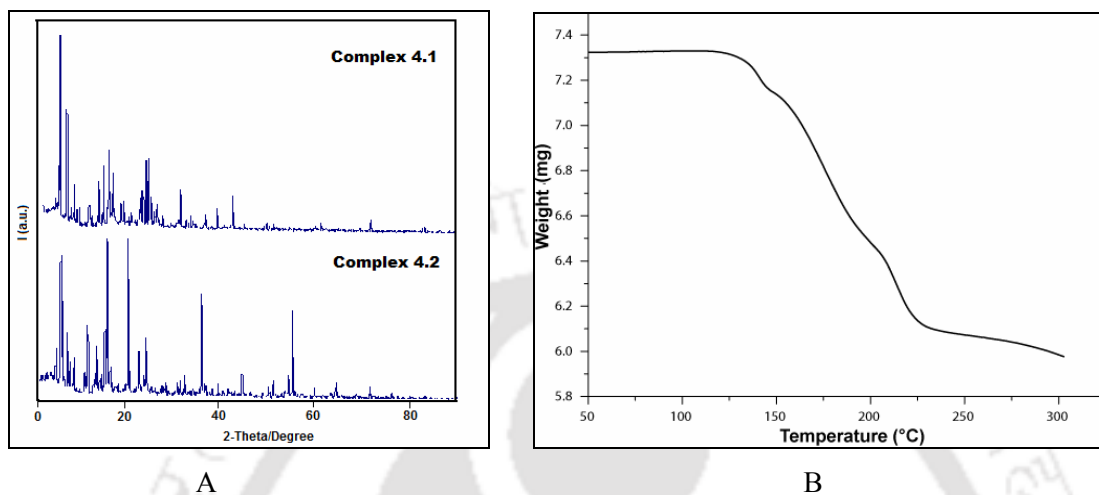
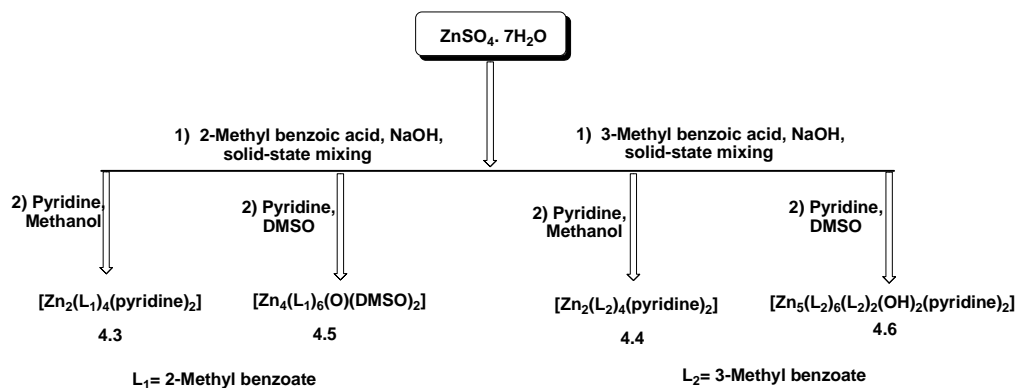


Figure 4.3 A) Powder XRD of complex **4.1** and complex **4.2**, B) Thermogravimetric curve for the complex **4.2**

Thermogravimetric analysis of the complex **4.1** shows that it loses four pyridine molecules in the temperature range $120\text{--}200^\circ\text{C}$ which corresponds to 17.22% of the total weight (theoretical weight loss 17.04%). In the temperature range $125\text{--}225^\circ\text{C}$ the complex **4.2** also loses two pyridine molecules which correspond to 18.65% of the total weight. The calculated weight loss is 20.41% due to the loss of two pyridine molecules in the complex **4.2**. Thermogravimetric curve of the complex **4.2** is shown in Figure 4.3B.

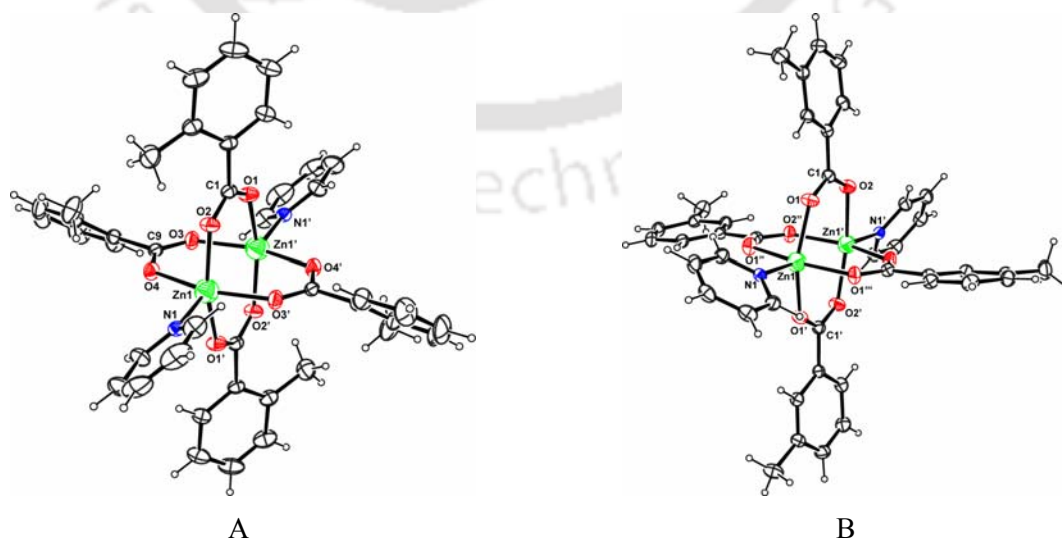
4.2 Study the substituent and solvent effect on solid state synthesis

To study the substituent and solvent effect on solid state reaction, we have done the reaction of zinc(II) sulphate with sodium salts of 3-methylbenzoic acid or 2-methylbenzoic acids, followed by dissolution of the reaction mixture in methanol or dimethylsulfoxide in the presence or absence of pyridine. A variety of complexes, as listed in Scheme 4.2, are obtained and each of the complexes is characterized by X-ray crystallography.



Scheme 4.2

The reaction of zinc(II) sulphate heptahydrate with sodium salts of 3-methylbenzoic acid or 2-methylbenzoic acids in a methanolic solution containing pyridine gave dinuclear zinc complexes **4.3** and **4.4** having a paddle-wheel type structure, with two pyridine ligands at axial positions (Figure 4.4A and 4.4B). In each case there are four carboxylate ligands bridged between two zinc centers. On a careful look at the geometry of the complexes, it is observed that in the case of complex **4.3** the two pyridine rings lies in one plane, whereas in the case of **4.4** the two rings are perpendicular to each other. The orientation of the rings is attributed to the steric effect of the methyl groups on crystal packing. The complex **4.3** assembles in the lattice through C19–H···O2 [$d_{\text{C19}\cdots\text{O2}}$ 3.480 Å, $\angle\text{D-H}\cdots\text{A}$ 166.5°] and C–H···π [$d_{\text{C18}\cdots\pi}$ 3.680 Å, and $d_{\text{C20}\cdots\pi}$ 3.603 Å] interactions and construct a herringbone type hydrogen bonded network (Figure 4.5A). The packing pattern of **4.4** is shown in Figure 4.5B, which has a grid-like structure through C6–H···π [$d_{\text{C6}\cdots\pi}$ 3.669 Å] interaction. It is also reported that non-symmetric carboxylato bridged complexes of zinc can be prepared with pyridine as an ancillary ligand⁸⁸.

Figure 4.4 A) The crystal structure of complex **4.3**, B) Structure of complex **4.4**

The FT-IR spectra of the complexes **4.3** and **4.4** show absorption band at 1568 and 1583 cm^{-1} due to asymmetric C=O stretching of bridging carboxylate groups. The symmetric C=O stretching band appears at 1403 cm^{-1} in both the complexes. $^1\text{H-NMR}$ spectra of the complex **4.3** shows that the protons of pyridine and benzoate groups appear in the range 8.62 to 7.18 ppm (Figure 4.9). The methyl protons appear at 2.45 ppm. In case of the complex **4.4** also, the methyl protons appear at 2.45 ppm and the protons of pyridine and benzoate group appear in the region 8.84-7.46 ppm (Figure 4.10).

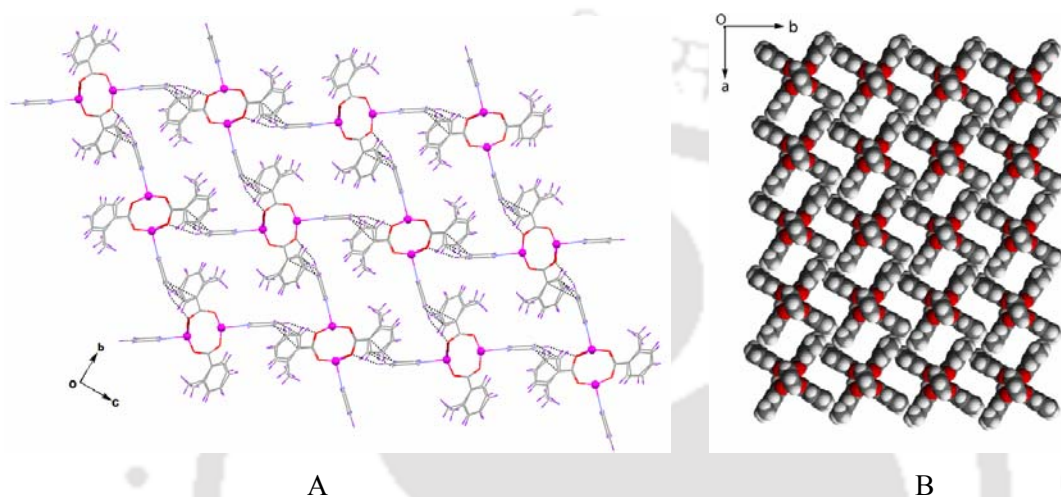


Figure 4.5 A) Solid state assembly of the complex **4.3** through weak C–H \cdots O and C–H \cdots π interaction, B) Grid like packing structure of the complex **4.4**

The reaction of zinc(II) sulphate heptahydrate with sodium salts of 3-methylbenzoic acid and 2-methylbenzoic acid in dimethylsulfoxide gave tetranuclear and pentanuclear zinc complexes **4.5** and **4.6**, respectively. It should be noted here that, in methanol paddle-wheel type structures are formed, whereas, similar reactions in DMSO lead to high nuclearity carboxylate clusters. It is clear that methanol has no role in the formation of these dinuclear structures while DMSO being a coordinating solvent leads to an expansion of the nuclearity.

Complex **4.5** is a tetranuclear complex having one oxy-ligand shared by four zinc centers (Figure 4.6A). The oxy anion acts as a central point in a tetrahedral geometry formed by four zinc ions and one oxide anion. Among the four zinc centers three zinc centers are equivalent with tetrahedral geometry as shown in Figure 4.6B. These three zinc centers are anchored by three carboxylate bridges and are attached to the central oxygen. The remaining zinc centers fulfil the octahedral geometry by three bridging carboxylate, one oxy ligand and two dimethylsulfoxide ligands. The complex **4.5** has two symmetry non-equivalent molecules per

unit cell. This is a rare example of a polynuclear complex having symmetry non-equivalent molecules in the unit cell.

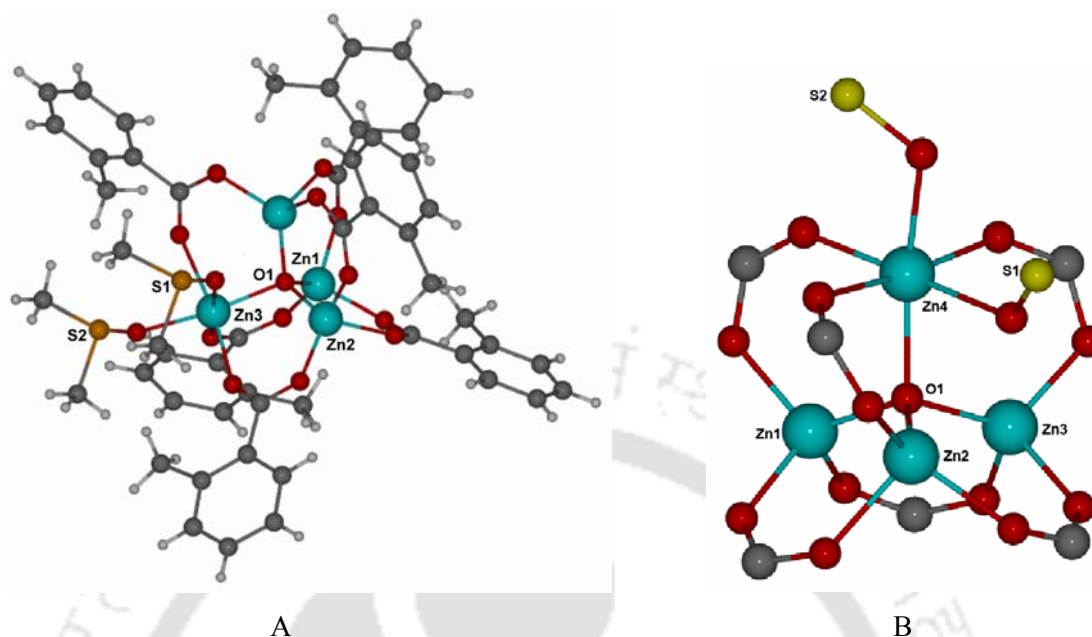


Figure 4.6 A) Crystal structure of complex **4.5**, B) Structure of oxo centered tetranuclear zinc core

The two symmetry non equivalent units are assembled through weak C29–H···O4 [$d_{C29\cdots O4}$ 3.569 Å, $\langle D-H\cdots A$ 154.9°], C65–H···O25 [$d_{C65\cdots O25}$ 3.295 Å, $\langle D-H\cdots A$ 142.3°], C89–H···O6 [$d_{C89\cdots O6}$ 3.427 Å, $\langle D-H\cdots A$ 156.4°] and C103–H···O26 [$d_{C103\cdots O26}$ 3.642 Å, $\langle D-H\cdots A$ 165.8°] interactions (Table 4.1). Apart from this, the hydrogens of benzoate groups and dimethylsulphoxide ligands are involved in weak C50–H··· π [$d_{C50\cdots \pi}$ 3.597 Å] and C44–H··· π [$d_{C44\cdots \pi}$ 3.440 Å] interactions with benzoate rings. The important bond distances and angles of this complex are listed in Table 17 (Appendix).

Table 4.1: Hydrogen bond geometry(Å, °) in **4.5**

D–H···A	d(D–H)	d(H···A)	d(D···A)	$\langle D-H\cdots A$
C(29)–H(29)···O(4)	0.93	2.71	3.569	154.9
C(65)–H(65)···O(25)	0.93	2.51	3.295	142.3
C(89)–H(89)···O(6)	0.93	2.55	3.427	156.4
C(103)–H(103)···O(26)	0.96	2.70	3.642	165.8

The complex **4.5** is similar to the tetranuclear symmetric zinc core reported³⁰¹ by Straughan et al., but with the difference that, in our case, one of the zinc centers is coordinated to solvent molecule making the complex less symmetric. Thus, our cluster possesses a new motif

containing four coordinated zinc centers along with six coordinated zinc centers. Recently, a tetranuclear oxo-cluster of zinc has been reported and it is observed that molecular oxygen is responsible for the formation of such clusters from organo-zinc reactions³⁰². In our reactions the oxo or hydroxo species are generated from water molecules in the solvent and hydrated salts. Dimethylsulphoxide being an aprotic coordinating solvent allows the deprotonation of water in basic medium whereas in methanol the labile hydrogen is in a large excess, thus facilitates the formation of neutral dinuclear species.

The crystal structure of the complex **4.6** shows that, it is a pentanuclear zinc carboxylate complex in which the zinc centers are interconnected by six bridging benzoate groups and two hydroxo ligands. The Complex **4.6** has a symmetric structure and a mirror plane bisects the two halves containing two tetrahedral units anchored by hexa-coordinated zinc center. The crystal structure is shown in Figure 4.7A.

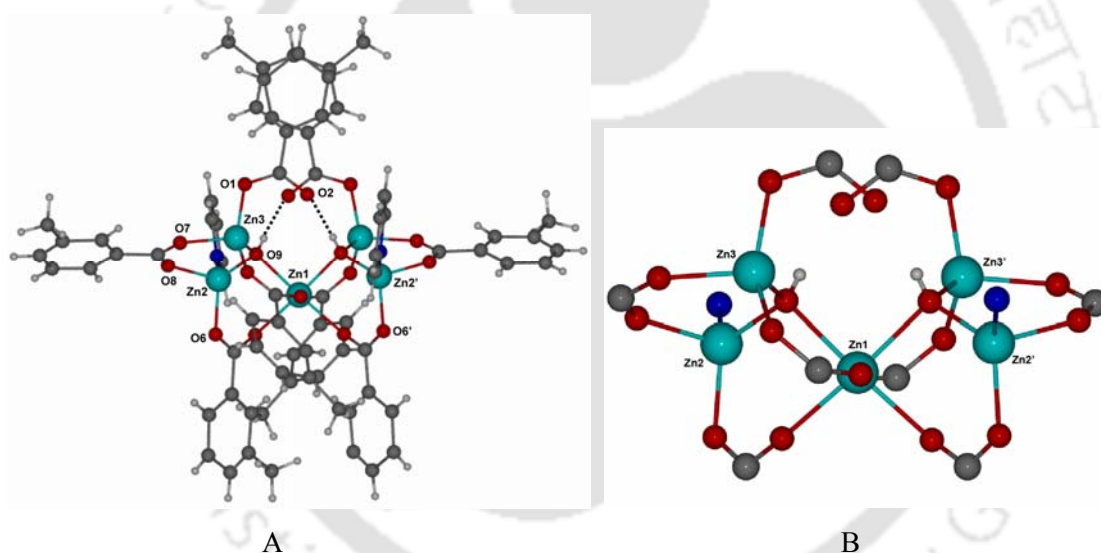


Figure 4.7 A) Crystal structure of pentanuclear zinc complex **4.6**, B) Structure of pentanuclear zinc core

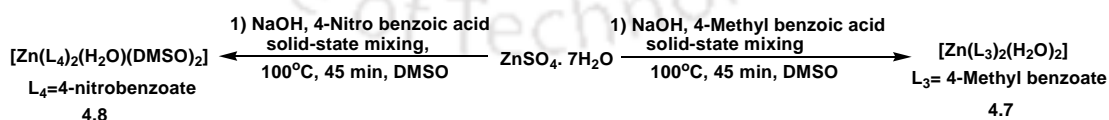
The complex has two hydroxyl ligands which are bridged between the three zinc centers. The hydroxyl groups are intramolecularly hydrogen bonded with two free carboxyl groups of the monodentate carboxylate through $O9-H\cdots O2$ [$d_{O9\cdots O2}$ 2.740 Å, $\angle D-H\cdots A$ 171.5°] interaction. The peripheral four zinc centers have tetrahedral geometry and the central zinc center have an octahedral geometry (Figure 4.7B). For the central zinc four of the coordination sites are occupied by four carboxylate oxygen and the other two sites are occupied by two hydroxyl groups. Among the four peripheral zinc centers two of them are coordinated by two carboxylate oxygens, one hydroxyl group and a pyridine molecule. Other

two zinc centers have fulfilled its coordination sites by three carboxylate oxygens and a hydroxyl group. The complex **4.6** self-assembles in the solid state through weak C12–H $\cdots\pi$ [$d_{\text{C12}\cdots\pi}$ 3.727 Å], C24–H $\cdots\pi$ [$d_{\text{C24}\cdots\pi}$ 3.730 Å] and C36–H $\cdots\pi$ [$d_{\text{C36}\cdots\pi}$ 3.666 Å] interactions. Some important bond distances and angles of complex **4.6** are listed in Table 18 (Appendix). Similar type of pentanuclear zinc(II) benzoate complex with 2,6-dimethyl pyrazine is reported by Kim and coworkers which is an effective catalyst for transesterification reactions³⁰³.

The monodentate carboxylate of **4.6** shows IR absorption at 1623cm⁻¹ whereas the bridging carboxylate of the complex has $\nu_{\text{a COO}}$ at 1578cm⁻¹ and $\nu_{\text{s COO}}$ stretching appears at 1428cm⁻¹. The C-O stretching of monodentate carboxylate group appears at 1404 cm⁻¹. On the other hand, the complex **4.5** has all bridging carboxylate ligands and IR absorptions at 1566 cm⁻¹ ($\nu_{\text{s COO}}$) and 1437cm⁻¹ ($\nu_{\text{a COO}}$) are observed. The S=O stretching of coordinated DMSO appears at 1004cm⁻¹ (Figure 4.11). The ¹H-NMR spectra of the complex **4.5** shows the benzoate protons in the region 7.15 to 7.75 ppm and the methyl protons appears at 2.52 ppm.

4.3 Synthesis and structure of mononuclear zinc carboxylate complexes

It is found that the solid phase reactions of the para-substituted benzoic acids such as 4-methylbenzoic acid and 4-nitrobenzoic acid with zinc(II) sulphate heptahydrate invariably lead to the formation of mononuclear complexes (Scheme 4.3). For example, when we use 4-methylbenzoic acid we get the mononuclear complex **4.7** with a composition [Zn(ptol)₂(H₂O)₂], where ptol is 4-methylbenzoate. Also, by the use of 4-nitrobenzoic acid we have obtained another mononuclear complex with the composition [Zn(pnitroben)₂(H₂O)(DMSO)₂] (**4.8**), where pnitroben is 4-nitrobenzoate. The structures of each of these complexes are shown in Figure 4.8A and 4.8B. The complexes are further characterized by ¹H-NMR and FT-IR spectroscopy.



Scheme 4.3

The complex **4.7** have a distorted octahedral structure with two symmetric halves and have two axially elongated Zn–O bonds [Zn1–O1, 2.505 Å] in comparison to the other Zn–O bonds [Zn1–O2, 2.009(17) Å and Zn1–O3, 1.990(17) Å]. Some of the selected bond angles are O3–Zn1–O1, 83.2°; O3–Zn1–O2, 136.6° and O1–Zn1–O2, 56.8°. The coordinated water

molecules are hydrogen bonded, in the solid state, with monodentate carboxylate oxygen through O3–H \cdots O2 [$d_{O3\cdots O2}$ 2.778 Å, \angle D–H \cdots A 169.1°] and O3–H \cdots O1 [$d_{O3\cdots O1}$ 2.724 Å, \angle D–H \cdots A 165.1°] interactions (Table 4.2).

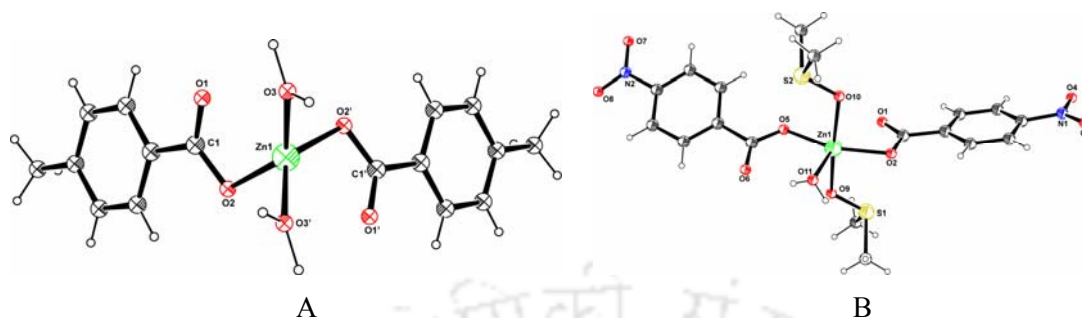


Figure 4.8 A) Crystal structure of complex **4.7**, B) Structure of penta coordinated complex (**4.8**) of zinc

The complex **4.7** has IR absorption at 3430cm^{-1} and has two closely spaced carboxylate stretching frequencies at 1621cm^{-1} and 1398cm^{-1} . In $^1\text{H-NMR}$ spectra of the complex **4.7**, two doublets appear at 7.82 and 7.20 ppm due to benzoate protons while the methyl peak appears at 2.34 ppm.

The complex **4.8** has a penta-coordinated structure with a near square pyramidal geometry. Two DMSO and two carboxylate ligands lie in the basal plane whereas a water molecule occupies the axial position. The monodentate binding of the carboxylate group is reflected in the Zn1–O2 (2.045 Å) and Zn1–O5 (2.011 Å) distances in the crystal structure; the distances between the two carboxyl oxygen and zinc that are not participating in the metal ligand bond, namely Zn1–O6 and Zn1–O1 are 3.166 and 2.584 Å respectively.

Table 4.2: Hydrogen bond geometry(Å, °) in **4.7**

D–H \cdots A	d(D–H)	d(H \cdots A)	d(D \cdots A)	\angle D–H \cdots A
O(3)–H(3A) \cdots O(2) [$-x, 1+y, 3/2-z$]	0.81	1.98	2.778(2)	169.1
O(3)–H(3B) \cdots O(1) [$-x, 3-y, 2-z$]	1.05	1.70	2.724(2)	165.1

Some of the selected metal ligand bond distances viz. Zn1–O2, Zn1–O5, Zn1–O9, Zn1–O10, Zn1–O11 are 2.045(2), 2.011(19), 2.120(2), 2.109(2), 2.044(2) Å respectively. The lone pairs of electrons on the sulphur atom of the dimethylsulfoxide ligands in the complex, project in two opposite directions and it becomes a decisive factor for formation of the five coordination geometry around the zinc centre. These lone pairs of electrons in this complex also

push the two carboxyl oxygens of the carboxylate away from each other and thereby provide space for a aquo ligand to coordinate to the metal center.

Table 4.3: Hydrogen bond geometry(Å, °) in **4.8**

D–H···A	d(D–H)	d(H···A)	d(D···A)	<D–H···A
O(11)–H(11A)···O(1) [1+x, y, z]	0.82	1.96	2.756(4)	164.3
O(11)–H(11B)···O(6)	0.71(4)	1.98(3)	2.641(4)	155.1(4)
C(16)–H(16A)···O(1) [1+x, y, z]	0.96	2.60	3.540(5)	167.4
C(16)–H(16C)···O(10) [1+x, -1+y, z]	0.96	2.55	3.493(4)	168.4

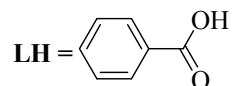
The carboxylate oxygens are hydrogen bonded with the coordinated water molecule through O11–H···O1 [$d_{\text{O11}\cdots\text{O1}}$ 2.756 Å, <D–H···A 164.3°] and O11–H···O6 [$d_{\text{O11}\cdots\text{O6}}$ 2.641 Å, <D–H···A 155.1(4)°] interactions. Besides that the complex **4.8** self assembles through weak C–H···O interactions which are listed in Table 4.3. The FT-IR spectra of the complex have signals at 3368 cm^{-1} arising from the aqua ligand and at 1010 cm^{-1} arising from DMSO. The monodentate carboxylate stretching appears at 1617 cm^{-1} (sym) while the asymmetric stretching appears at 1345 cm^{-1} .

In conclusion, we have described self-assembly formation of a new class of compounds formed by a dinuclear and trinuclear zinc benzoate complex. The dinuclear and trinuclear units are independently present in the crystal lattice and are held together by weak C–H··· π and C–H···O interactions. Polar and protic solvent like methanol leads to paddle-wheel dinuclear zinc(II) carboxylate complexes. Tetra and pentanuclear zinc carboxylates are also synthesized in polar and aprotic solvent. Para substituted benzoic acids in the solid state reactions lead to mononuclear complexes. Formation of the mononuclear aqua complex in the case of para substituted benzoic acid suggests that not only the reaction conditions but also the substituent controls the formation of different zinc complexes. The solid-state reaction of zinc with different aromatic carboxylate depends on salt, substituent on aromatic ring and solvent of crystallization. Paddle-wheel structures are generally constructed through solid state reaction which can be easily converted to zinc carboxylate clusters by changing the polarity of solvent and coordinating solvent like dimethylsulfoxide helps in formation of multinuclear clusters.

4.4 Experimental section

Detailed synthetic methodologies are given below. Analytical data as well as spectroscopic data are also listed along with the each complex. The instrumentals details are given in Appendix.

Complex 4.1: $[\text{Zn}_3(\mu\text{-L})_6(\text{Py})_2][\text{Zn}_2(\mu\text{-L})_4(\text{pyridine})_2]$

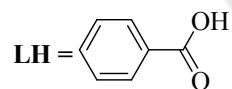


A mixture of benzoic acid (0.24 g, 2 mmol), sodium hydroxide (0.11 g, 2 mmol) and zinc(II) sulphate heptahydrate (0.29 g, 1 mmol) was finely ground in a pastel mortar and heated at 100°C for 45 min. The mixture was cooled to room temperature transferred into a round bottom flask and methanol (20 ml) was added to it and the heterogeneous mixture was stirred at room temp for 5 min followed by the addition of pyridine (0.16 g, 2 mmol). The white residue was filtered off and the colorless filtrate was left undisturbed. Colorless crystals were collected after 3 days and dried in air. Yield: 27% (based on zinc).

IR (KBr, cm^{-1}): 3059(bs), 1643(s), 1606(s), 1567(s), 1492(m), 1449(m), 1400(s), 1220(w), 1174(w), 1153(w), 1072(m), 1047(w), 839(w), 724(s), 693(m), 678(m).

^1H NMR(CDCl_3): 8.86(bs, 1H), 8.12(d, $J=7.6\text{Hz}$, 3H), 7.86(t, $J=6.8\text{Hz}$, 1H), 7.44(t, $J=7.6\text{Hz}$, 3H), 7.33(t, $J=7.2\text{Hz}$, 3H).

Complex 4.2: $[\text{Zn}_2(\mu\text{-L})_4(\text{pyridine})_2]$



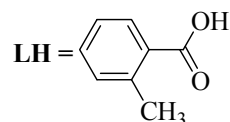
A finely ground mixture of benzoic acid (0.24 g, 2 mmol), sodium hydroxide (0.11 g, 2 mmol) and anhydrous zinc(II) chloride (0.14 g, 1 mmol) was heated in pastel-mortar. The heated mixture was cooled to room temperature transferred into a round bottom flask and methanol (20 ml) was added to it. The heterogeneous mixture was stirred at room temp followed by the addition of pyridine (0.16 g, 2 mmol). The white residue was filtered off and the colourless filtrate was left undisturbed for crystallisation. Colourless crystals were collected after 5 days and dried in air. Yield: 35% (based on zinc).

IR (KBr, cm^{-1}): 3059(bs), 1644(s), 1604(s), 1567(s), 1492(m), 1449(m), 1403(s), 1220(w), 1174(w), 1072(m), 1048(w), 840(w), 724(s), 693(m), 678(m).

Elemental analysis for $C_{38}H_{30}N_2O_8Zn_2$: calculated C, 58.97; H, 3.88; N, 3.62; found C, 59.24; H, 3.53; N, 3.94.

1H NMR($CDCl_3$): 8.86(s, 1H), 8.11(s, 3H), 7.87(t, $J=6.8$ Hz, 1H), 7.42(d, $J=14.4$ Hz, 3H), 7.32(s, 3H).

Complex 4.3: $[Zn_2(\mu-L)_4(pyridine)_2]$



2-Methylbenzoic acid (0.27 gm, 2 mmol), $ZnSO_4 \cdot 7H_2O$ (0.29 gm, 1mmol) and NaOH (0.08gm, 2mmol) were finely ground in the mortar. The mixture was heated at $100^\circ C$ for 45 min. After the dissolution of the preheated mixture in 10 ml methanol, pyridine (0.08gm, 1mmol) was added. The resultant mixture was stirred at room temperature for half an hour and was filtered. Colourless crystals were obtained after 8 days and dried in air. Yield: 41% (based on Zn).

IR (KBr, cm^{-1}): 3420(bs), 3064(w), 3021(w), 2929(w), 1634(s), 1609(s), 1568(s), 1435(s), 1403(bs), 1219(m), 1157(m), 1103(m), 1071(m), 1048(m), 852(m), 741(s), 700(s), 665(s), 550(m).

Elemental analysis for $C_{42}H_{38}N_2O_8Zn_2$: calculated C, 60.76; H, 4.58; N, 3.37; found C, 60.81; H, 5.01; N, 2.95.

1H NMR ($DMSO-d_6$): 8.62 (bs, 2H), 7.87 (t, $J=6.8$ Hz, 1H), 7.75 (d, $J = 7.2$ Hz, 2H), 7.47 (t, $J=6.8$ Hz, 2H), 7.27 (t, $J = 8.0$ Hz, 2H), 7.18 (d, $J = 7.6$ Hz, 4H), 2.45 (s, 6H).

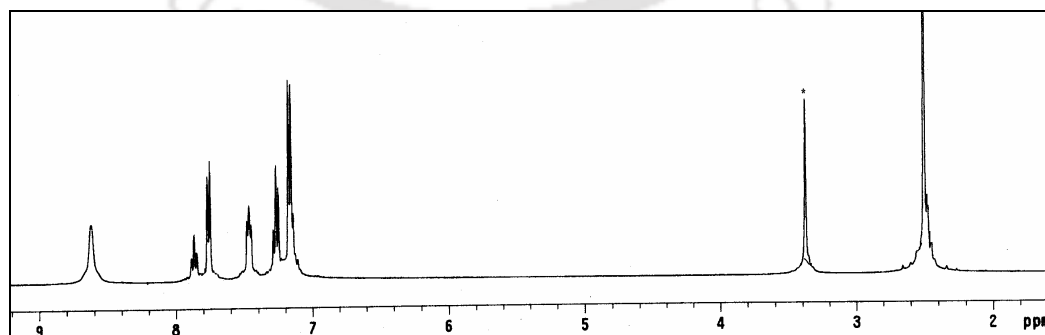
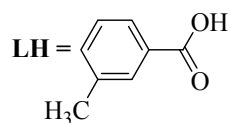


Figure 4.9 1H -NMR spectra of complex 4.3

Complex 4.4: $[\text{Zn}_2(\mu\text{-L})_4(\text{pyridine})_2]$ 

3-Methylbenzoic acid (0.27 g, 2 mmol), $\text{ZnSO}_4 \cdot 7\text{H}_2\text{O}$ (0.29 g, 1 mmol) and NaOH (0.08 g, 2mmol) was mixed thoroughly in a mortar pastel and heated for 45 min at 100°C . The mixture was cooled to room temperature and methanol (10ml) was added to it. To this solution pyridine (0.08 g, 1mmol) was added and stirred at room temperature for 5 min. Colourless crystals were obtained after 5days and dried in air. Yield: 48% (based on Zn).

Elemental analysis for $\text{C}_{42}\text{H}_{38}\text{N}_2\text{O}_8\text{Zn}_2$: calculated C, 60.76; H, 4.58; N, 3.37; found C, 60.79; H, 5.01; N, 3.86.

IR (KBr, cm^{-1}): 3431(bs), 3064(w), 3030(w), 2912(w), 1823(w), 1644(s), 1602(s), 1583(s), 1403(bs), 1214(m), 1082(m), 1069(m), 1046(m), 788(s), 755(s), 747(s), 693(m), 674(w), 642(w), 493(m), 458(m).

^1H NMR (DMSO-d_6): 8.84 (bs, 2H), 8.07 (t, $J=6.8\text{Hz}$, 1H), 7.95 (s, 2H), 7.92 (t, $J=4\text{Hz}$, 2H), 7.67 (t, $J=6.8\text{Hz}$, 2H), 7.46 (d, $J=5.2\text{Hz}$, 4H), 2.45 (s, 6H).

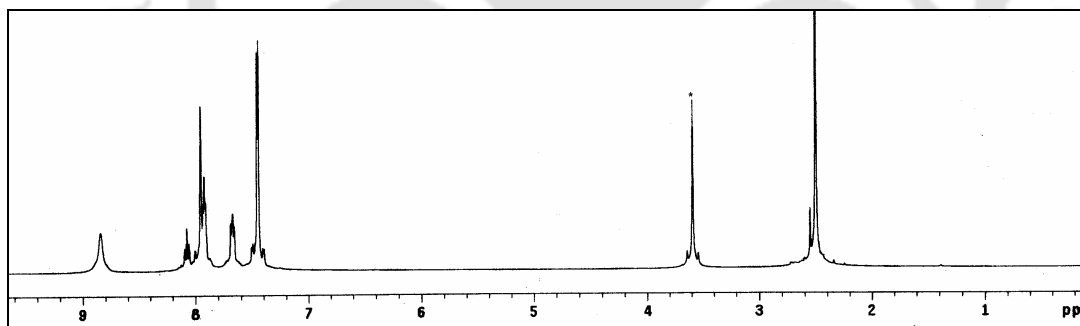
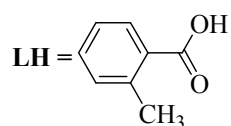


Figure 4.10 ^1H -NMR spectra of complex 4.4

Complex 4.5: $[\text{Zn}_4(\mu\text{-L})_6(\mu\text{-O})(\text{DMSO})_2]$ 

A preheated mixture of 2-Methylbenzoic acid (0.27 g, 2mmol), $\text{ZnSO}_4 \cdot 7\text{H}_2\text{O}$ (0.29 g, 1 mmol) and NaOH (0.08 g, 2mmol) was transferred into a round bottom flask and to it dimethyl sulphoxide: water (4:1) was added. The reaction mixture was stirred at room temperature and filtered to remove solid precipitate. The colourless filtrate was left

undisturbed. Block type colourless crystals were obtained after 10 days and dried in air. Yield: 24% (based on Zn).

Elemental analysis for $C_{52}H_{54}O_{15}S_2Zn_4$: calculated C, 50.14, H, 4.34; found C, 50.19; H, 4.38.

FT-IR (KBr, cm^{-1}): 3422(bs), 2968(m), 2929(m), 1611(s), 1591(s), 1566(s), 1437(s), 1399(s), 1286(w), 1196(w), 1160(m), 1103(m), 1004(s), 953(w), 785(m), 749(s), 666(m), 535(w).

1H NMR (DMSO- d_6): 7.75 (d, $J=9.2$ Hz, 2H), 7.27 (t, $J=7.2$ Hz, 2H), 7.18 (d, $J=7.2$ Hz, 3H), 7.15 (s, 1H), 2.52 (m, 6H).

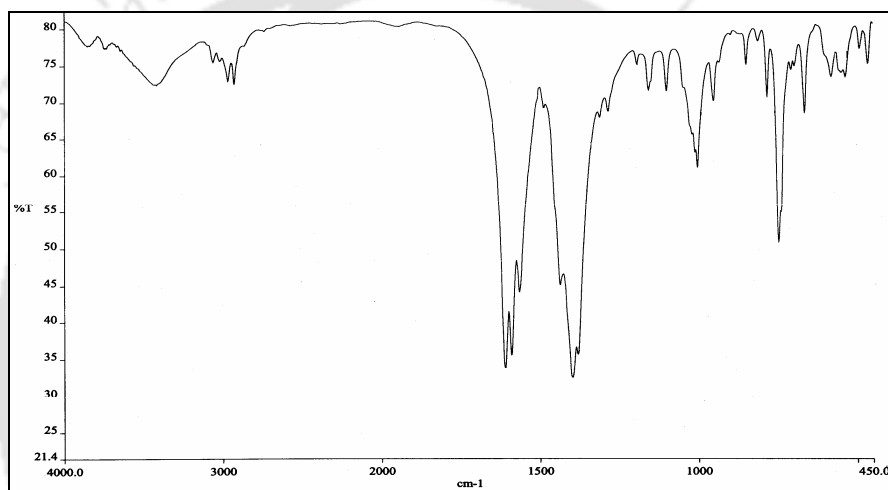
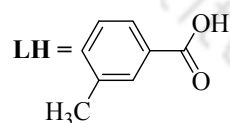


Figure 4.11 FT-IR spectra of complex 4.5

Complex 4.6: $[Zn_5(\mu-L)_6(L)_2(\mu-OH)_2(pyridine)_2]$

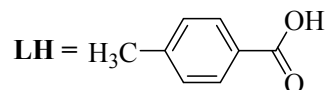


After mixing of 3-methylbenzoic acid (0.27 g, 2mmol), $ZnSO_4 \cdot 7H_2O$ (0.29 g, 1 mmol) and NaOH (0.08 g, 2 mmol) in mortar pastel, the mixture was heated at $100^\circ C$ for 45min. The mixture was cooled to room temperature, transferred into a round bottom flask and dimethyl sulphoxide: water (4:1) was added to it. The mixture was stirred at room temperature for 5min followed by addition of pyridine (0.08 g, 1 mmol). The colourless liquid was filtered off and was left undisturbed. Colourless crystals were collected after 15 days and dried in air. Yield: 34 % (based on Zn).

Elemental analysis for $C_{74}H_{68}N_2O_{18}Zn_5$: calculated C, 55.49, H, 4.25; N, 1.75; found C, 55.52; H, 4.28; N, 2.15.

IR (KBr, cm^{-1}): 3432(bs), 2919(m), 1623(s), 1601(s), 1578(s), 1531(s), 1428(s), 1404(s), 1289(w), 1229(w), 1088(m), 787(s), 764(s), 673(m), 589(m), 492(s).

Complex 4.7: $[Zn(L)_2(H_2O)_2]$



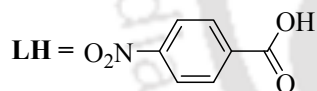
4-Methylbenzoic acid (0.27 g, 2 mmol), $ZnSO_4 \cdot 7H_2O$ (0.29 g, 1 mmol) and NaOH (0.08 g, 2 mmol) were mixed in a mortar and 45 min at $100^\circ C$. Dimethyl sulphoxide: water (4:1) was added to the mixture and stirred at room temperature. The colourless solution was left undisturbed to obtain crystals after 14 days. Yield: 38% (based on Zn).

Elemental analysis for $C_{16}H_{18}O_6Zn$: calculated C, 51.66, H, 4.84; found C, 52.16; H, 4.82.

IR (KBr, cm^{-1}): 3430(bs), 3036(w), 1621(s), 1608(s), 1566(s), 1450(m), 1398(s), 1374(s), 1354(s), 1218(w), 1164(w), 1085(m), 1014(s), 846(s), 771(s), 694(s), 572(m), 521(m).

1H NMR (DMSO- d_6): 7.84 (2H, d, $J=8Hz$), 7.20 (2H, d, $J=8Hz$), 2.34 (3H, s).

Complex 4.8: $[Zn(L)_2(H_2O)(DMSO)_2]$



4-Nitrobenzoic acid (0.33 g, 2 mmol), $ZnSO_4 \cdot 7H_2O$ (0.29 g, 1 mmol) and NaOH (0.08 g, 2 mmol) were finely ground in mortar and heated at $100^\circ C$ for 45 min. Dimethyl sulphoxide: water (4:1) was added to the mixture and stirred at room temperature. The colourless solution was left undisturbed to obtain colourless plate type crystals after 18 days. Yield: 34% (based on Zn).

Elemental analysis for $C_{18}H_{22}N_2O_{11}S_2Zn$: calculated C, 37.78, H, 3.85; found C, 37.80; H, 3.89.

IR (KBr, cm^{-1}): 3368(bs), 1617(m), 1578(s), 1516(s), 1407(s), 1388(s), 1345(s), 1319(m), 1010(s), 955(m), 874(w), 835(m), 797(m), 723(s), 604(w).

1H NMR (DMSO- d_6): 8.27 (2H, d, $J=8.8Hz$), 8.16 (2H, d, $J=8.8Hz$), 2.54 (6H, s).

Chapter 5

Structural studies and metal complexation behaviour of flexible carboxylic acids and its derivatives

The design of metal-organic hybrid materials with definite pores are investigated in depth due to their fascinating structural diversity and potential functions as microporous solids for molecular adsorption, ion exchange, and heterogeneous catalysis³⁰⁴⁻³⁰⁶. The combination of metal ions and bridging ligands containing different flexible carboxylates can allow the formation of coordination networks possessing permanent porosity and high thermal stability, which are useful for the ion exchange³⁰⁷, separation³⁰⁸, chemisorption³⁰⁹, gas storage²³⁹, catalysis³¹⁰, magnetism³¹¹, optoelectronic³¹², and luminescence properties³¹³. The carboxylate containing metallo-organic frameworks are of special interest as they can be easily synthesised with diverse structures³¹⁴. Multiple options for several binding modes in metal carboxylate complexes make them versatile³¹⁵. Metal carboxylates with flexible ligands are studied to enhance selectivity in molecular recognition and much work in this direction is required to have control over construction of voids in a predictable manner³¹⁶. Amino acids and its derivatives with flexible coordination modes have been explored in the generation of different coordination frameworks with potential application in material science and biology³¹⁷. Moreover, amino acids are good supramolecular synthons and hence chiral building blocks for supramolecular chemistry can be constructed from them.

In this chapter we have described the synthesis, structure and complexation behaviour of different types of flexible carboxylic acids which have intervening groups connected to another group/s which provide the binding sites for metal ions.

5.1 Metal complexation and structural study of flexible mono-carboxylic acid

Urea derivatives are very useful for selective guest³¹⁸ and anion recognition³¹⁹. A symmetrically disubstituted urea derivative may have different conformers³²⁰ (Figure 5.1). The conformers other than syn-syn conformer are rare³²¹. The R-N-C=O dihedral angle in a syn-syn form can be varied by substituents³²². In this study, we have synthesized 3-phenyl-2-

(3-phenyl-ureido) propionic acid with an objective to prepare a series of carboxylate complexes and also to understand the effect of complexation to stabilize conformers of the urea derivative.

The ligand 3-phenyl-2-(3-phenyl-ureido) propionic acid (**5.1**) was prepared by two step procedure (Scheme 5.1). In the first step phenylalanine ethyl ester was reacted with phenyl isocyanate to form the corresponding ethyl ester.

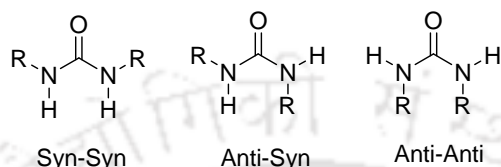
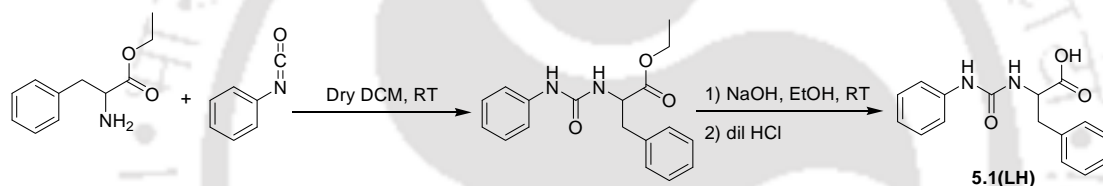


Figure 5.1

The hydrolysis of this ester by sodium hydroxide leads to the acid **5.1** in racemate form. The acid was crystallized from ethanol to get good diffraction quality crystals.



Scheme 5.1

In the crystal structure of the 3-phenyl-2-(3-phenyl-ureido) propionic acid (**5.1**), the carbonyl group of the carboxylic acid is involved in hydrogen bonding with N–H of the urea part through N1–H \cdots O2 [$d_{\text{N1}\cdots\text{O2}}$ 3.009 Å, $\angle\text{D-H}\cdots\text{A}$ 159.7°], N2–H \cdots O2 [$d_{\text{N2}\cdots\text{O2}}$ 3.261 Å, $\angle\text{D-H}\cdots\text{A}$ 145.4°], N3–H \cdots O6 [$d_{\text{N3}\cdots\text{O6}}$ 2.988 Å, $\angle\text{D-H}\cdots\text{A}$ 160.8°] and N4–H \cdots O6 [$d_{\text{N4}\cdots\text{O6}}$ 3.182 Å, $\angle\text{D-H}\cdots\text{A}$ 145.3°] interactions. It is also observed that the carbonyl group of the urea part is participating in O3–H \cdots O4 [$d_{\text{O3}\cdots\text{O4}}$ 2.579 Å, $\angle\text{D-H}\cdots\text{A}$ 159.9°] and O5–H \cdots O1 [$d_{\text{O5}\cdots\text{O1}}$ 2.562 Å, $\angle\text{D-H}\cdots\text{A}$ 160.1°] hydrogen bonding with the hydrogen of carboxylic acid group (Table 5.1). Thus, the hydrogen bonding pattern found in the structure of **5.1** is not usual as compared to the generally observed hydrogen bonding in urea derivatives. The carboxylic acid group of compound **5.1** also participates in intermolecular C24–H \cdots O2 [$d_{\text{C24}\cdots\text{O2}}$ 3.371 Å, $\angle\text{D-H}\cdots\text{A}$ 141.1°] interactions to make a self-assembled structure as illustrated in Figure 5.2B. The solid state structure is composed of two symmetrically non-equivalent molecules per unit cell (Figure 5.2A).

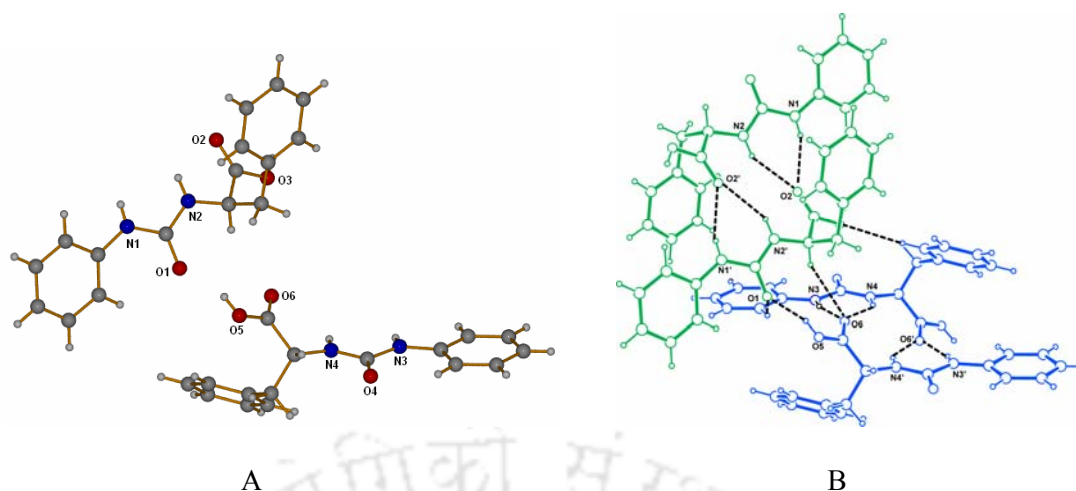


Figure 5.2 A) Structure of 3-phenyl-2-(3-phenyl-ureido)-propionic acid (**5.1**), B) Hydrogen bonding interactions among the molecules of **5.1**.

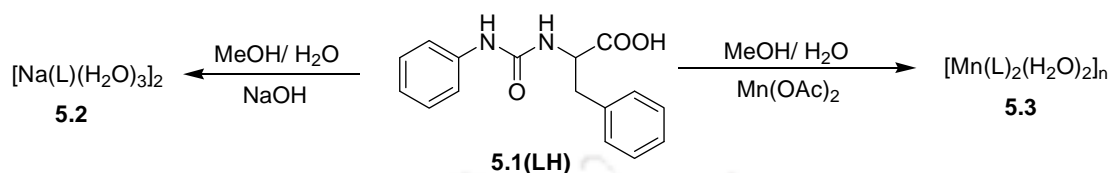
The symmetry non-equivalence arises due to the self-assembling of the two molecules in such a way that they need two sets of symmetry elements for defining their positions in the unit cell. The compound **5.1** has syn-syn orientation around the carbonyl group of the urea part, which is the most common conformation of urea group. The carbonyl groups of the two symmetry non equivalent molecules are so oriented that they are unable to form the usual urea tape motif generally seen in urea derivatives.

Table 5.1: Hydrogen bond geometry(Å, °) for **5.1**

D-H...A	d(D-H)	d(H...A)	d(D...A)	<D-H...A
N1-H1...O2 [-x, 1-y, 1-z]	0.78(6)	2.27(6)	3.009(6)	159.7(5)
N2-H2...O2 [-x, 1-y, 1-z]	0.86	2.52	3.261(5)	145.4
N3-H3...O6 [1-x, -y, 1-z]	0.91(6)	2.11(6)	2.988(5)	160.8(5)
O3-H3...O4 [-1+x, y, z]	0.82	1.79	2.579(5)	159.9
N4-H4...O6 [1-x, -y, 1-z]	0.82(5)	2.47(5)	3.182(5)	145.3
O5-H5...O1	0.82	1.78	2.562(5)	160.1
C24-H24...O2 [1+x, y, z]	0.98	2.55	3.371(5)	141.1

In the infra-red spectra of the compound there are two strong bands at 3403 cm^{-1} and 3375 cm^{-1} arising from N-H symmetrical stretching of amide. The carbonyl group of amide shows absorption at 1648 cm^{-1} . The C=O and C-O bands of the carboxylic acid appear at 1694 cm^{-1} and 1447 cm^{-1} respectively. $^1\text{H-NMR}$ spectra of the complex **5.1** shows that the amide protons appear at 8.51 and 6.23 ppm as a singlet and doublet respectively. The -CH and -CH₂ protons appeared at 5.55 ppm and 3.05 ppm, respectively (Figure 5.22).

When we have done the reaction of sodium hydroxide with the ligand **5.1(LH)** we got the sodium complex having composition $[\text{Na}(\text{L})(\text{H}_2\text{O})_3]_2$ (**5.2**) (Scheme 5.2). The complex **5.2** is dinuclear and the two sodium ions are in distorted octahedron geometry (Figure 5.3A). There are two bridging water molecules that hold the two sodium ions and the carboxylate groups attached to sodium ions in monodentate fashion.



Scheme 5.2

A chelate like structure is formed due to the coordination of both the carboxylate oxygen and the amide carbonyl oxygen to the sodium center. Two aqua ligands are coordinated to each sodium in trans orientation. The chelation makes the hydrogen bond pattern and the conformation of the ligand totally different from the parent **LH**. The urea part of the ligand in the sodium complex takes an anti-syn conformation.

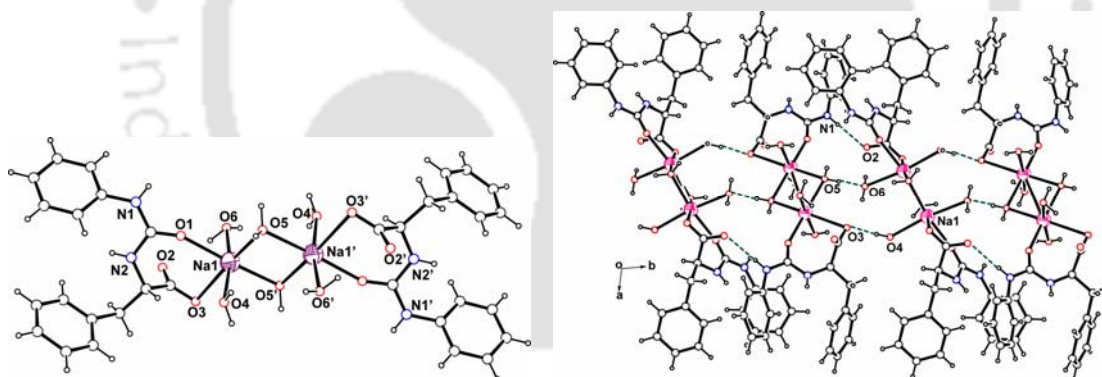


Figure 5.3 A) crystal structure of complex **5.2**, B) The hydrogen bonded self-assembly of dinuclear $[\text{NaL}(\text{H}_2\text{O})_3]_2$

Such anti-syn conformation occurs due to the puckering of the ligand on co-ordination to metal centers. The sodium complex in the solid state are self-assembled mainly through the $\text{O4-H}\cdots\text{O3}$ [$d_{\text{O4}\cdots\text{O3}}$ 2.907 Å, $\langle\text{D-H}\cdots\text{A}$ 174.0°], $\text{O4-H}\cdots\text{O2}$ [$d_{\text{O4}\cdots\text{O2}}$ 3.074 Å, $\langle\text{D-H}\cdots\text{A}$ 165.1°], $\text{O5-H}\cdots\text{O6}$ [$d_{\text{O5}\cdots\text{O6}}$ 2.853 Å, $\langle\text{D-H}\cdots\text{A}$ 176.3°], $\text{O5-H}\cdots\text{O2}$ [$d_{\text{O5}\cdots\text{O2}}$ 2.846 Å, $\langle\text{D-H}\cdots\text{A}$ 175.8°], $\text{O6-H}\cdots\text{O3}$ [$d_{\text{O6}\cdots\text{O3}}$ 2.754 Å, $\langle\text{D-H}\cdots\text{A}$ 177.2°] and $\text{O6-H}\cdots\text{O2}$ [$d_{\text{O6}\cdots\text{O2}}$ 3.236 Å, $\langle\text{D-H}\cdots\text{A}$ 166.1°] interactions. There also exists $\text{N1-H}\cdots\text{O2}$ [$d_{\text{N1}\cdots\text{O2}}$ 3.013 Å, $\langle\text{D-H}\cdots\text{A}$ 177.1°] interaction of the carboxylate group with N-H of urea part (Figure 5.3B). Some important hydrogen bonding parameters are listed in Table 5.2. Similar type of anti-syn

conformer is observed in cadmium complex of *N,N'*-bis-4-methylpyridyl oxalamide³²³. There are many examples of sodium complexes that are bridged by water³²⁴, hydroxide³²⁵ or sulphide³²⁶. However, the observation of a very stable $[\text{Na}_2(\text{H}_2\text{O})_2]$ core is exceptional. The Na1–Na1 distance in the dinuclear core is 3.470 Å. Few selected bond distances and angles of this complex are listed in Table 20 (Appendix). The stability of such $[\text{Na}_2(\text{H}_2\text{O})_2]$ core is attributed to the hydrophobic confinement provided by the ligand. The carboxylate group of the complex **5.2** has IR-absorptions at 1694 cm^{-1} and 1589 cm^{-1} . In UV it has two absorptions that appear at 242 nm and 206 nm due to $n \rightarrow \pi^*$ and $\pi \rightarrow \pi^*$ transitions respectively.

Table 5.2: Hydrogen bond geometry(Å, °) for complex **5.2**

D–H···A	d(D–H)	d(H···A)	d(D···A)	<D–H···A
N1–H1···O2 [x, –y, 1/2+z]	0.82(2)	2.20(2)	3.013(2)	177.1(3)
O4–H4A···O3[x, 1–y, 1/2+z]	0.88(4)	2.03(4)	2.907(3)	174.0(4)
O4–H4B···O2 [x, y, 1+z]	0.80(5)	2.29(5)	3.074(3)	165.1(5)
O5–H5A···O6 [x, –y, 1/2+z]	0.96(3)	1.90(3)	2.853(2)	176.3(3)
O5–H5B···O2 [x, y, 1+z]	0.86(4)	1.99(4)	2.846(2)	175.8(3)
O6–H6A···O3[1/2–x, 1/2–y, –z]	0.88(4)	1.87(4)	2.754(3)	177.2(3)
O6–H6B···O2	0.92(4)	2.33(4)	3.236(3)	166.1(4)

Reaction of **LH** with manganese(II) acetate lead to an one dimensional co-ordination polymer having composition $[\text{Mn}(\text{L})_2(\text{H}_2\text{O})_2]_n$ (**5.3**). In this complex each of the manganese centers have distorted octahedral geometry and the carboxylate groups coordinate in bridging

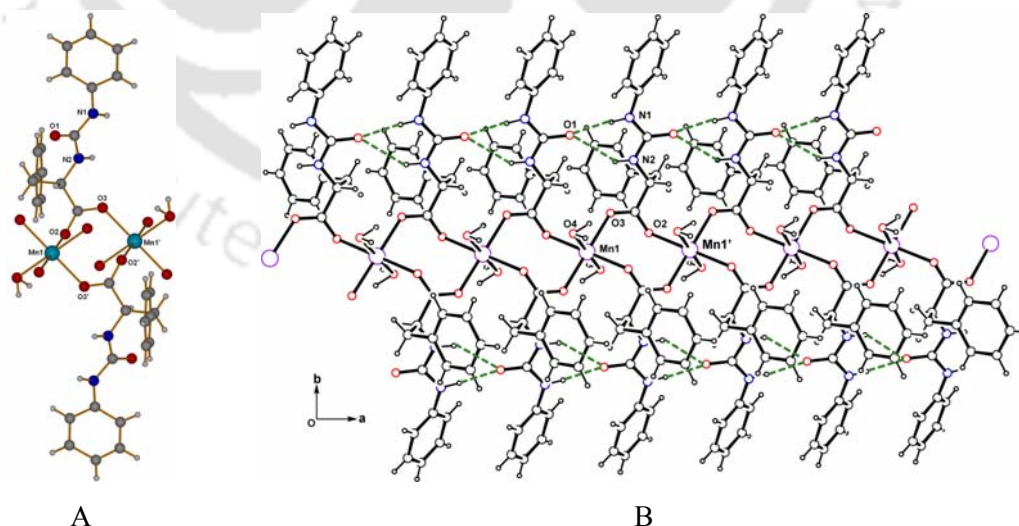


Figure 5.4 A) Structure of the asymmetric unit of complex **5.3**, B) The hydrogen bonded one-dimensional co-ordination polymer $[\text{MnL}_2(\text{H}_2\text{O})_2]_n$ (**5.3**)

bidentate mode. Structure of the asymmetric unit of complex **5.3** is shown in Figure 5.4A. The organic part attached to the carboxylate group of the ligand are positioned parallel to each other and makes a sheet like structure through $R_1^2(6)$ type hydrogen bond among the carbonyl and the N–H of urea functionality as shown in Figure 5.4B. Urea part of the ligand are hydrogen bonded through N1–H \cdots O1 [$d_{N1\cdots O1}$ 2.859 Å, $\angle D-H\cdots A$ 175.6°] and N2–H \cdots O1 [$d_{N2\cdots O1}$ 3.398 Å, $\angle D-H\cdots A$ 138.0°] interactions (Table 5.3). The polymeric chains are self-assembled through weak C–H \cdots π interactions ($d_{C13\cdots\pi}$ 3.780 Å, $d_{C5\cdots\pi}$ 3.627Å).

Table 5.3: Hydrogen bond geometry(Å, °) for complex **5.3**

D–H \cdots A	d(D–H)	d(H \cdots A)	d(D \cdots A)	$\angle D-H\cdots A$
N1–H1 \cdots O1 [–1+x, y, z]	0.86	2.00	2.859	175.6
N2–H2 \cdots O1	0.86	2.70	3.398	138.0

The complex shows IR absorptions at 1640 cm^{-1} and 1545 cm^{-1} due to the bridging carboxylate groups. It has two UV absorptions due to the $n \rightarrow \pi^*$ transition of carbonyl group at 241 nm and the $\pi \rightarrow \pi^*$ transition at 206 nm (Figure 5.6A).

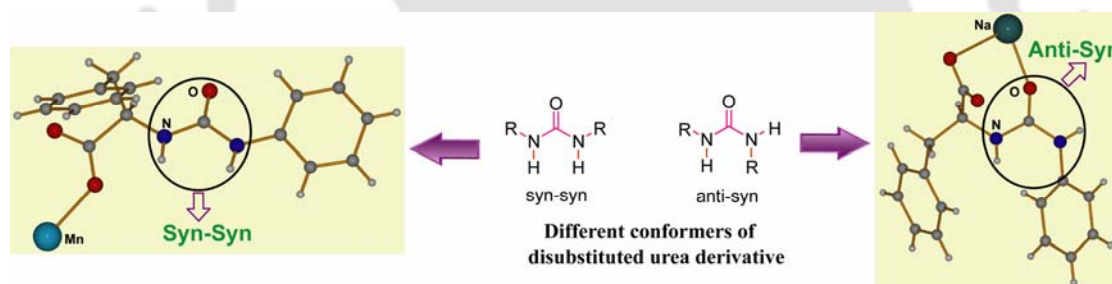


Figure 5.5 Syn-syn and anti-syn geometry of sodium and manganese complexes

The sodium complex of the 3-phenyl-2-(3-phenyl-ureido)-propionic acid has anti-syn conformation around the urea moiety; whereas, in the manganese complex the urea part adopts the conventional syn-syn conformation. The study suggests that the complexation of metal to an urea derivative allows the ligand to stabilize a particular conformer (Figure 5.5).

The ESR spectra of complex **5.3** in dimethylsulfoxide has six hyperfine lines, these are observed due to a distorted octahedral manganese(II) center having d^5 configuration in weak field (Figure 5.6B). Spectral analysis shows that the signals are uniformly spaced with a hyperfine coupling constant (a^H) of 91.127G. The room temperature magnetic moment of the complex is found to be 5.12 BM corresponding to five unpaired electrons.

We have compared the UV-visible spectra of the complexes **5.2** and **5.3** with that of the parent ligand **5.1**. In the UV-visible spectra of the complexes, each has absorptions of the

parent ligand but they are shifted from the original positions on complexation as shown in Figure 5.6A. The conformation change of the ligand occurring on complex formation is also reflected in the ^1H NMR spectra of the complex **5.2** as illustrated in Figure 5.7.

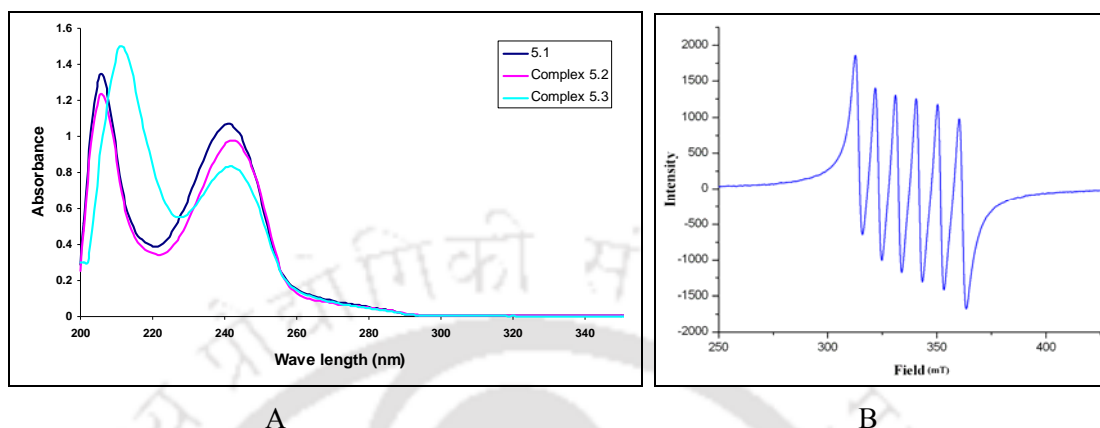


Figure 5.6 A) UV-Vis spectra of ligand **5.1** and complex **5.2-5.3**, B) Solution state ESR spectra (in DMSO) of compound **5.3** at room temperature ($g = 2.00116$, center field= 3370.0G, Power= 0.99800 [mw], Frequency= 9449.994 [MHz], sweep time= 30 s)

The ^1H NMR spectra of the complex **5.2** shows that the $-\text{CH}_2$ group is drastically shifted as compared to in the parent ligand (**5.1**) due to puckering of the ligand on complexation through the urea carbonyl. The amide protons in the sodium complex dose not appear in the spectra due to strong hydrogen bonding with solvent molecules. The proton attached to the chiral center is not affected by complex formation.

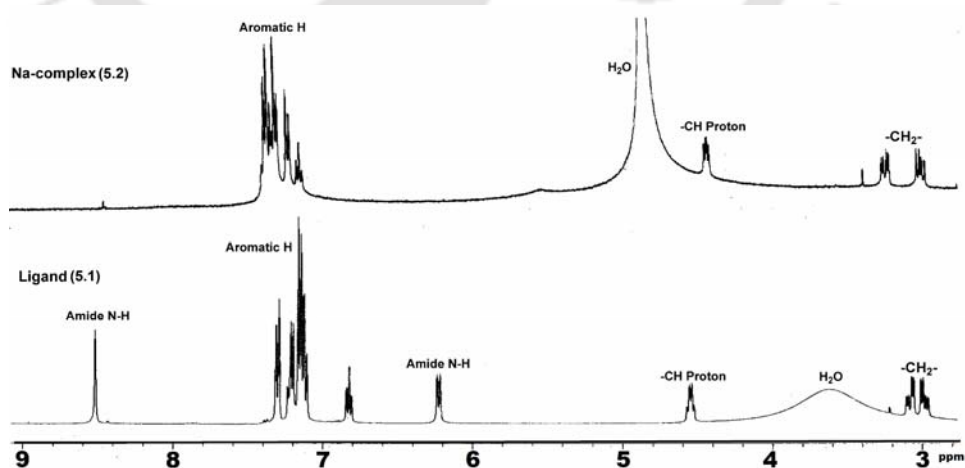
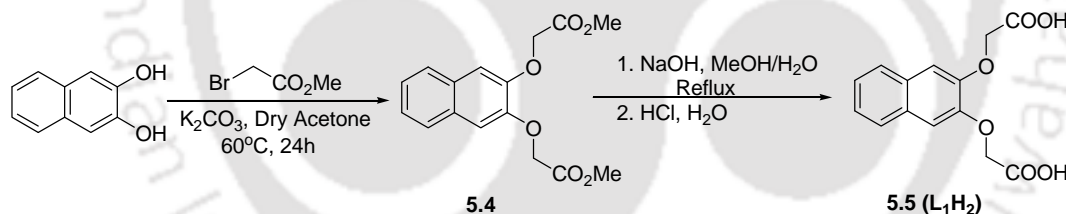


Figure 5.7 ^1H NMR spectra (400MHz) of **5.1** (in DMSO-d_6) and complex **5.2** (in D_2O)

5.2 Polymorphism and symmetry non-equivalence in (3-carboxymethoxy-naphthalen-2-yloxy) acetic acid and its derivative

Weak interactions provide elegant means in biological molecules to build assemblies of molecules³²⁷. It is a well known fact that carboxylic acids commonly assemble through carboxylic groups in $R_2^2(8)$ type of geometry³²⁸. Polycarboxylic acids with flexible groups are self assembled in the lattice through weak interactions. These weak interactions play a major role in polymorphic properties of such compounds³²⁹. We have chosen two compounds namely (3-methoxycarbonylmethoxy-naphthalen-2-yloxy) acetic acid methyl ester (**5.4**) and (3-carboxymethoxynaphthalen-2-yloxy) acetic acid (**5.5**) to study their structural aspects and to find out the role of weak interactions in polymorphism.

We have synthesized (3-carboxymethoxynaphthalen-2-yloxy) acetic acid and its methyl ester using two-step synthetic procedure³⁵⁵(Scheme 5.3). In the first step, the reaction of naphthalene-2,3-diol with bromomethylacetate leads to (3-methoxycarbonylmethoxy-naphthalen-2-yloxy) acetic acid methyl ester (**5.4**). Base hydrolysis of the ester leads to the product (3-methoxycarbonylmethoxy-naphthalen-2-yloxy) acetic acid (**5.5**) in the second step.



Scheme 5.3

On crystallization, (3-carboxymethoxynaphthalen-2-yloxy) acetic acid methyl ester from two different solvents namely methanol and THF, two different polymorphs of the ester were obtained. The two polymorphs are designated as **5.4A** and **5.4B**. The polymorphism arises due to the projection of the attached OCH_2COOCH_3 units across the rings. In the case of **5.4B** both the OCH_2COOCH_3 units are placed in opposite direction (Figure 5.8B), whereas in **5.4A** one OCH_2COOCH_3 unit is above and the other unit lies almost in the same plane of the aromatic ring as shown in Figure 5.8A.

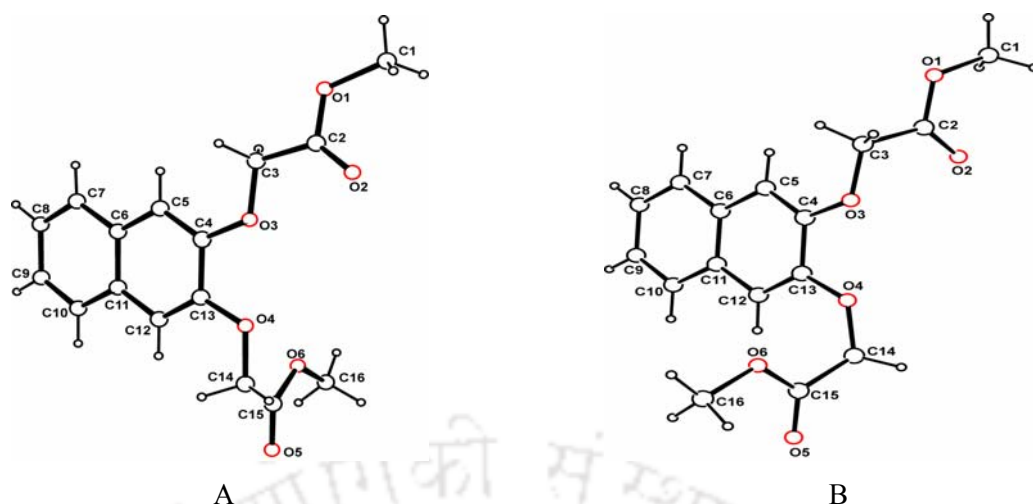


Figure 5.8 Crystal structures of two polymorphs of (3-methoxycarbonylmethoxy-naphthalen-2-yloxy) acetic acid methyl ester A) Structure of **5.4A**, B) Structure of **5.4B**.

The torsion angles C4–O3–C3–C2 and C13–O4–C14–C15 in the two polymorphs are -172.4° , 77.5° (**5.4A**) and -91.0° , -83.9° (**5.4B**) respectively. Here, the difference in the torsion angles refers to existence of two orientations of the methyl ester groups in the lattice of the two polymorphs. Both the polymorphs crystallize in the orthorhombic *Pbca* space group. Although the two polymorphs crystallize in the same space group they differ in their packing patterns. The packing diagrams of the two polymorphs of (3-methoxycarbonylmethoxy-naphthalen-2-yloxy) acetic acid methyl ester are shown in Figure 5.9. The prominent hydrogen bonding parameters of **5.4A** and **5.4B** are listed in Table 5.4 and 5.5 respectively.

Table 5.4: Hydrogen bond geometry(Å, °) in **5.4A**

D–H···A	d(D–H)	d(H···A)	d(D···A)	<D–H···A
C(1)–H(1A)···O(4) $[-1/2+x, 1/2-y, -z]$	0.96	2.57	3.374(6)	141.5
C(1)–H(1B)···O(2) $[-1/2+x, 1/2-y, -z]$	0.96	2.47	3.297(6)	144.6
C(14)–H(14A)···O(5) $[3/2-x, -1/2+y, z]$	0.97	2.53	3.496(5)	171.2
C(14)–H(14B)···O(2) $[1/2+x, 1/2-y, -z]$	0.97	2.45	3.411(4)	169.1
C(16)–H(16A)···O(5)	0.96	2.63	3.548	159.5

In the two polymorphs the hydrogen bond patterns are different, in case of **5.4A** the methyl protons are involved in C1–H···O4 [$d_{C1\cdots O4}$ 3.374 Å, <D–H···A 141.5°], C1–H···O2 [$d_{C1\cdots O2}$ 3.297 Å, <D–H···A 144.6°] and C16–H···O5 [$d_{C16\cdots O5}$ 3.548 Å, <D–H···A 159.5°] hydrogen bonding interactions with carboxylate oxygen and the $-CH_2-$ hydrogens are also involved in C14–H···O5 [$d_{C14\cdots O5}$ 3.496 Å, <D–H···A 171.2°] and C14–H···O2 [$d_{C14\cdots O2}$ 3.411 Å, <D–H···A 169.1°] interactions (Table 5.4). Apart from the C–H···O interactions, the

polymorph **5.4A** exhibits weak C16–H $\cdots\pi$ ($d_{\text{C16}\cdots\pi}$ 3.367 Å) interaction leading to the self-assembly formation.

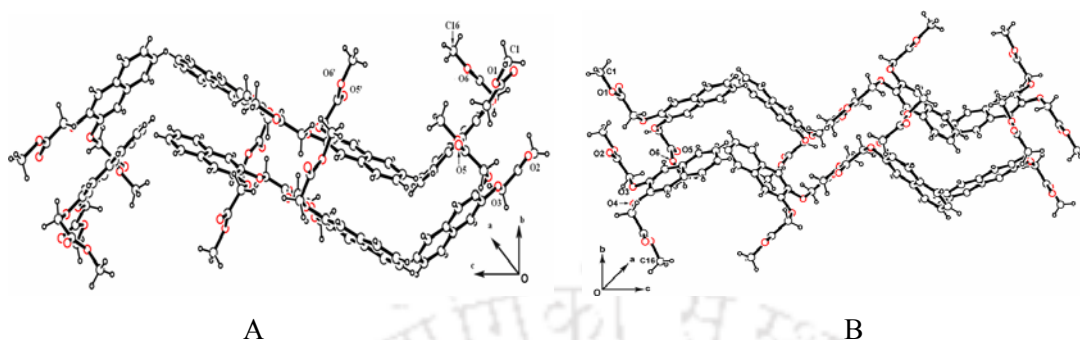


Figure 5.9 A) Packing diagram of compound **5.4A**, B) Packing diagram of compound **5.4B**.

In the polymorph **5.4B** some of the observed hydrogen bonding interactions are C14–H \cdots O2 [$d_{\text{C14}\cdots\text{O2}}$ 3.271 Å, $\langle\text{D-H}\cdots\text{A}\rangle$ 168.8°], C14–H \cdots O5 [$d_{\text{C14}\cdots\text{O5}}$ 3.665 Å, $\langle\text{D-H}\cdots\text{A}\rangle$ 176.2°] and C3–H \cdots O6 [$d_{\text{C3}\cdots\text{O6}}$ 3.587 Å, $\langle\text{D-H}\cdots\text{A}\rangle$ 170.8°] (Table 5.5). The methyl hydrogens are also involved in weak C16–H $\cdots\pi$ ($d_{\text{C16}\cdots\pi}$ 3.425 Å) interactions with aromatic naphthalene rings. Since the weak interactions are directional in nature a small change in the packing, drastically changes the overall possibility/distribution of weak interactions in the lattice.

In the FT-IR spectra of the polymorphs, a strong band appears at 1763 cm^{-1} due to the ester C=O stretching. A medium absorption at 2953 cm^{-1} due to presence of –CH₂– group and two strong absorption bands at 1248 cm^{-1} and 1048 cm^{-1} for C–O stretching of ether groups are also observed. In the ¹H NMR, the three sets of aromatic protons are appeared at 7.66, 7.35 and 7.11 ppm. The methoxy and the methylene protons appear at 3.82 and 4.84 ppm, respectively (Figure 5.23).

Table 5.5: Hydrogen bond geometry(Å, °) in **5.4B**

D–H \cdots A	d(D–H)	d(H \cdots A)	d(D \cdots A)	$\langle\text{D-H}\cdots\text{A}\rangle$
C(1)–H(1B) \cdots O(2) [1/2+x, 1/2-y, -z]	0.96	2.58	3.410(19)	145.5
C(14)–H(14A) \cdots O(2) [-x, -y, -z]	0.97	2.31	3.271(15)	168.8
C(3)–H(3B) \cdots O(6) [1/2-x, -1/2+y, z]	0.97	2.63	3.587	170.8
C(5)–H(5) \cdots O(6) [1/2-x, -1/2+y, z]	0.93	2.64	3.459	148.0
C(14)–H(14B) \cdots O(5) [3/2-x, -1/2+y, z]	0.97	2.69	3.665	176.2

We have also determined the structures of (3-carboxymethoxy-naphthalen-2-yloxy) acetic acid (**5.5**). When we crystallize the (3-carboxymethoxy-naphthalen-2-yloxy) acetic acid from dimethylsulfoxide it crystallizes in the monoclinic P2₁/c space group with Z' =1 (abbreviated

as **5.5A**), but crystallization from methanol results in the compound **5.5B** with $Z' = 2$ which crystallizes in the triclinic P-1 space group.

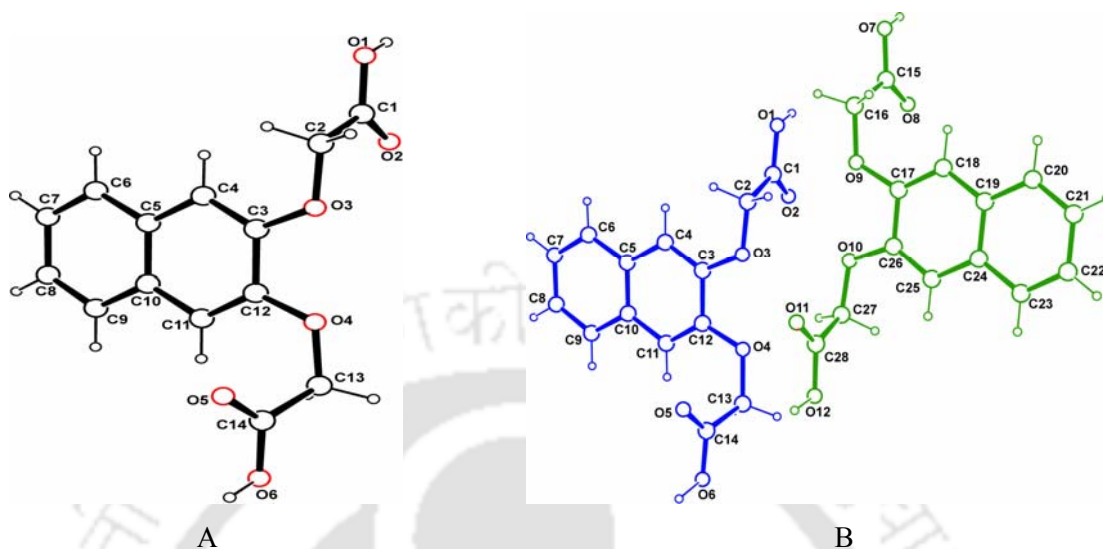


Figure 5.10 A) Crystal structure of compound **5.5A**, B) Symmetry non equivalent structure of compound **5.5B**

The two structures have the same conformation but differ in their hydrogen bonded layered structures. The two structures of acid are shown in Figure 5.10. The hydrogen bonded structure of both the compounds shows that both have same type of layered structures constructed through O–H \cdots O and C–H \cdots O interactions. In compound **5.5A**, the primary layer is constructed by $R_2^2(8)$ type O1–H \cdots O5 [$d_{O1\cdots O5}$ 2.671 Å, $\angle D-H\cdots A$ 172.8°] and O6–H \cdots O2 [$d_{O6\cdots O2}$ 2.679 Å, $\angle D-H\cdots A$ 172.4°] interactions between the carboxylic acid groups. This layer is interconnected with the second layer through weak C2–H \cdots O2 [$d_{C2\cdots O2}$ 3.398 Å, $\angle D-H\cdots A$ 131.9°] and C13–H \cdots O3 [$d_{C13\cdots O3}$ 3.272 Å, $\angle D-H\cdots A$ 149.0°] interactions (Table 5.6). In the compound **5.5A** the O–H \cdots O interactions contribute to longitudinal growth of chains whereas the other two C–H \cdots O interactions contribute to the lateral growth of the secondary structures (Figure 5.12A). The naphthalene rings in compound **5.5A** are present in parallel arrangement and the $\pi\cdots\pi$ separation between the rings is 3.358 Å which helps the formation of tertiary layered structure. For better understanding we have pictorially presented the concept of primary, secondary and tertiary layered structures in Figure 5.11.

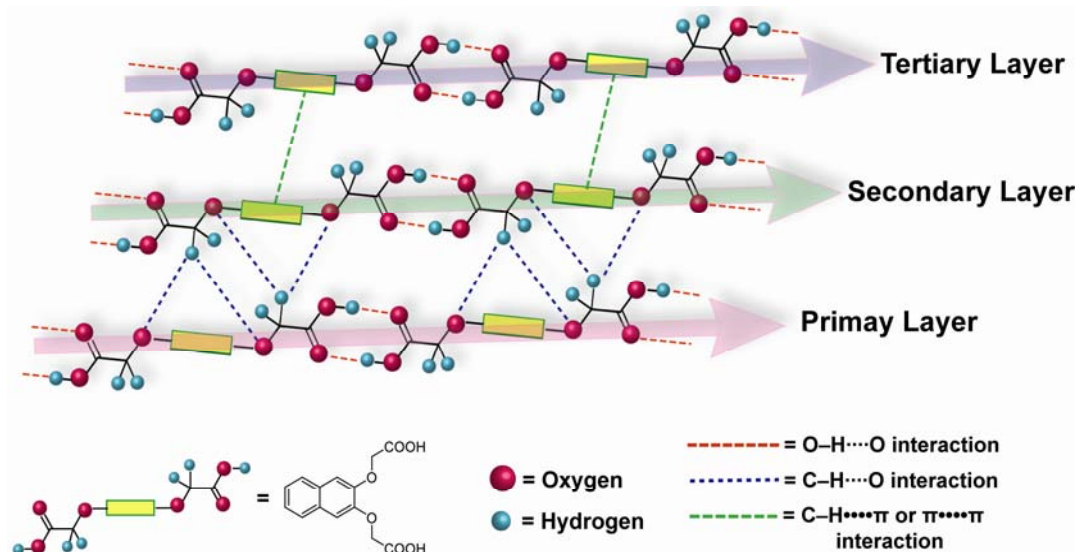


Figure 5.11 Pictorial presentation of hydrogen bonded layered structure

In the two symmetry non equivalent units of compound **5.5B** the primary layers are constructed through O6–H \cdots O2 [$d_{O6\cdots O2}$ 2.769 Å, $\angle D-H\cdots A$ 174.1°], O1–H \cdots O5 [$d_{O1\cdots O5}$ 2.681 Å, $\angle D-H\cdots A$ 171.0°], O7–H \cdots O11 [$d_{O7\cdots O11}$ 2.647 Å, $\angle D-H\cdots A$ 163.6°], and O12–H \cdots O8 [$d_{O12\cdots O8}$ 2.699 Å, $\angle D-H\cdots A$ 175.1°] interactions. The two primary layers of symmetry non equivalent units are interconnected to each other through C13–H \cdots O10 [$d_{C13\cdots O10}$ 3.351 Å, $\angle D-H\cdots A$ 143.4°] and C16–H \cdots O3 [$d_{C16\cdots O3}$ 3.244 Å, $\angle D-H\cdots A$ 148.6°] interactions which construct the secondary layer structure (Figure 5.12B). Finally, the two layered structures assemble through the C23–H \cdots π ($d_{C23\cdots \pi}$ 3.774Å) interaction between naphthalene rings resulting in a tertiary structure. The hydrogen bond parameters of the compound **5.5B** are listed in Table 5.7.

Table 5.6: Hydrogen bond geometry(Å, °) in **5.5A**

D–H \cdots A	d(D–H)	d(H \cdots A)	d(D \cdots A)	$\angle D-H\cdots A$
O1–H1o \cdots O5 [x, y-1, z]	0.82	1.86	2.671(15)	172.8
O6–H6o \cdots O2 [x, y+1, z]	0.82	1.86	2.679(15)	172.4
C13–H13A \cdots O3	0.97	2.41	3.272(17)	149.0
C2–H2A \cdots O2	0.97	2.67	3.398	131.9

From the hydrogen bonding shown in Figure 5.12, it is clear that these compounds are the result of two different packing pattern having different types of weak interactions in their layered structures. The difference in the pattern of weak interaction makes two symmetrically non-equivalent molecules in the unit cell.

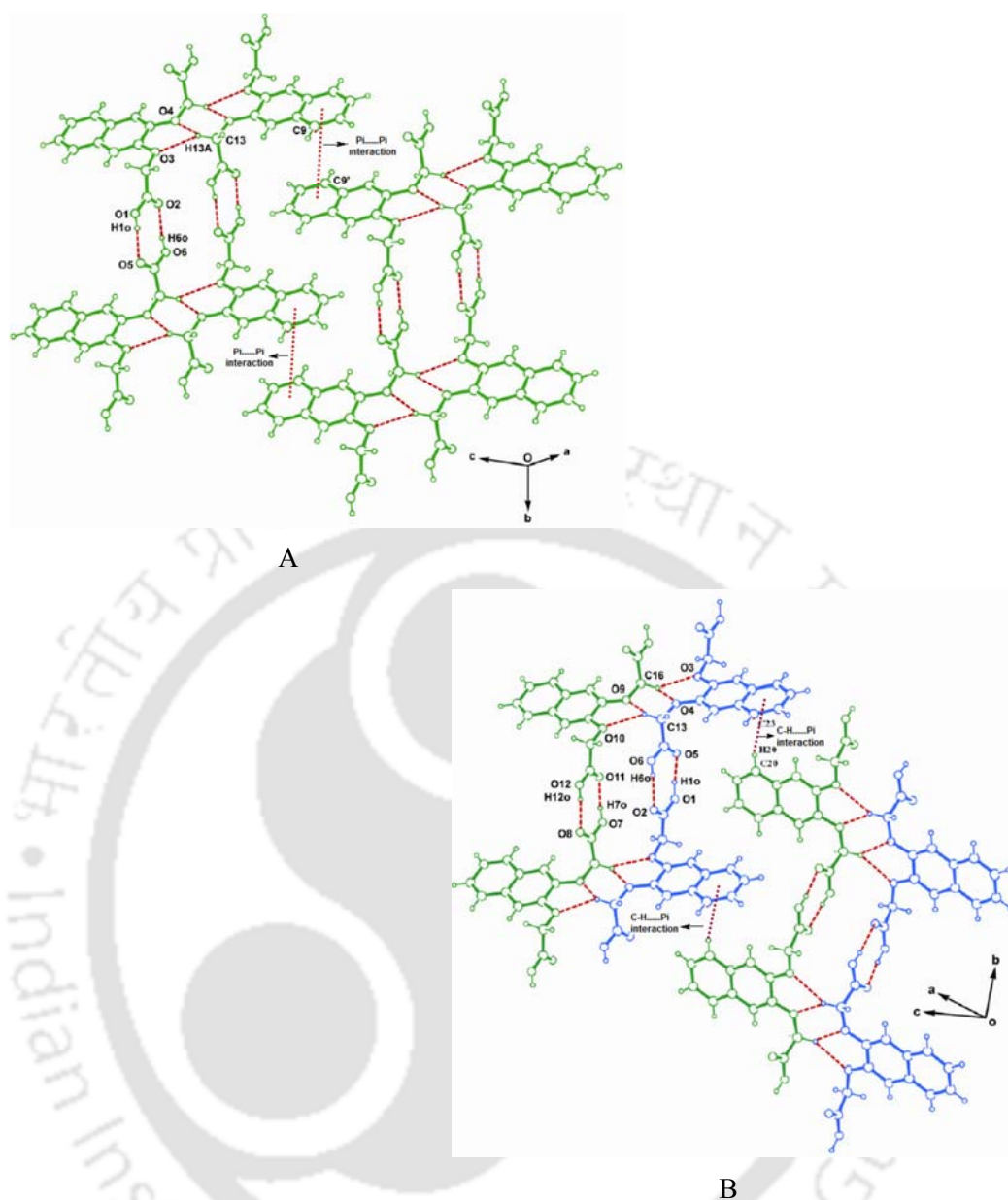


Figure 5.12 A) Hydrogen bonded structure of **5.5A**, B) Hydrogen bonded network between two symmetry non equivalent acids in compound **5.5B**.

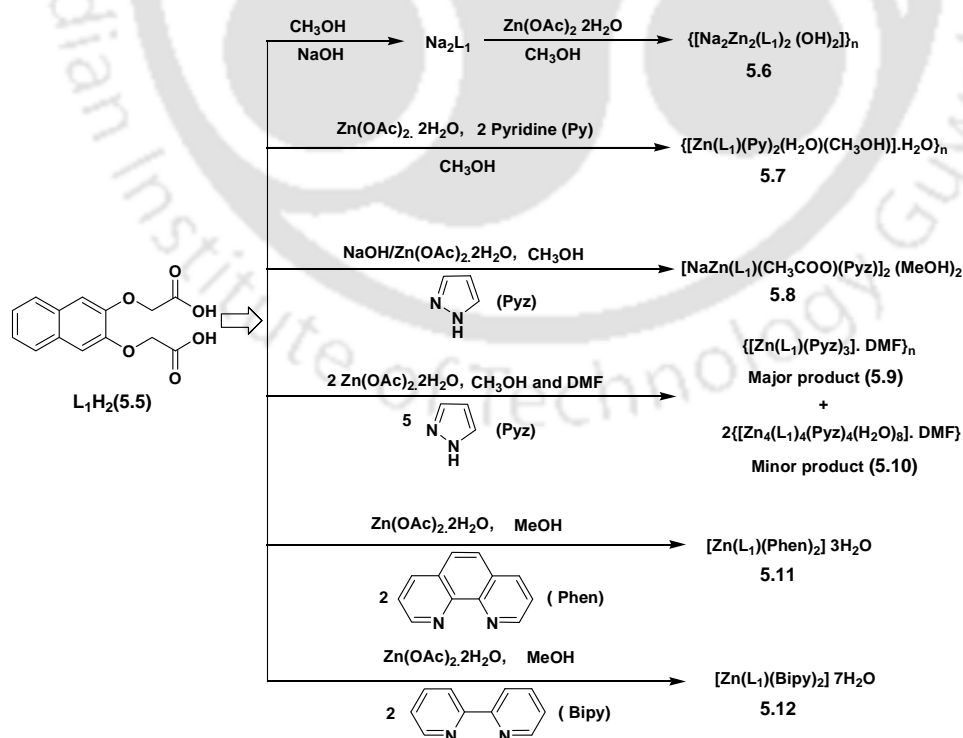
Some of the factors contributing to nucleation process as well as to make symmetry non-equivalence in the crystal lattice are addressed recently; however, our system clearly suggests that such symmetry non-equivalence may arise from differences in packing pattern to achieve particular tertiary structures. In FT-IR spectra the asymmetric stretching frequency for C=O group of carboxylate appears at 1718cm^{-1} and two strong band around 1235 and 1048cm^{-1} appear due to the C-O stretching of ether groups. The aromatic and $-\text{CH}_2-$ protons appear at 7.70, 7.31, 7.24 and 4.80 ppm respectively in the ^1H NMR spectra. ^{13}C NMR spectrum of compound **5.5** is shown in Figure 5.24.

Table 5.7: Hydrogen bond geometry(Å, °) in **5.5B**

D–H···A	d(D–H)	d(H···A)	d(D···A)	<D–H···A
O6–H6o···O2 [x, y-1, z]	0.82	1.95	2.769(2)	174.1
O12–H12o···O8 [x, y-1, z]	0.82	1.88	2.699(2)	175.1
O1–H1o···O5 [x, y+1, z]	1.02	1.66	2.681(2)	171.0(3)
O7–H7o···O11 [x, y+1, z]	0.95	1.73	2.647(2)	163.6(3)
C11–H11···O8	0.93	2.49	3.357(3)	154.5
C13–H13A···O10 [1-x, -y, -z]	0.97	2.52	3.351(3)	143.4
C16–H16B···O3 [1-x, -y, -z]	0.97	2.38	3.244(3)	148.6

5.3 Metal complexation of flexible dicarboxylic acid

In this subsection we have described the metal complexation behaviour of flexible dicarboxylic acid. In this context we have chosen (3-carboxymethoxy-naphthalen-2-yloxy)-acetic acid which is a flexible dicarboxylic acid and studied its metal complexation property. The (3-carboxymethoxy-naphthalen-2-yloxy)-acetic acid (**5.5**), abbreviated as L_1H_2 , has two carboxylic acid groups with flexible arms. So, it is suitable for synthesis of cyclic or open chain polymeric structures with metal ions. The two ether oxygen atoms of L_1H_2 , would provide supramolecular features like a podand. Moreover, the naphthalene ring of the ligand L_1H_2 might contribute to π -interactions.



Scheme 5.4

In this study several zinc (II) complexes of L_1H_2 are prepared as illustrated in Scheme 5.4. Stoichiometric amount of zinc(II) acetate dihydrate, (3-carboxymethoxy-naphthalen-2-yloxy)-acetic acid (L_1H_2) and sodium hydroxide in methanol react to form an one dimensional coordination polymer **5.6** having a composition $\{[Na_2Zn_2(L_1)_2(OH)_2]\}_n$. The complex is unusual as it binds to sodium ions due to formation of a macrocycle like structure. Metal carboxylates having cryptand type of structure are studied in literature³³⁰. The self-assembly via metal coordination also forms macrocyclic and cage-like hosts; these exhibit potential applications in molecular encapsulation, chemosensing, catalysis and in organic synthesis^{9, 331-334}.

The crystal structure of the complex **5.6** shows that it is a network of metallacycles formed by the ligand L_1 with zinc ions. Each zinc ion in the complex **5.6** has a distorted tetrahedral coordination environment (Figure 5.13). The zinc ions are co-ordinated to four independent oxygen atoms of four carboxylate groups. The lone pairs of the oxygen on the rings project in inward direction, having resemblance to structure of crown ether. Each metallacycle holds a sodium ion through co-ordination of oxygen atoms (similar to the one generally observed in crown ethers). In complex **5.6**, two carboxylates of each L_1 are attached to two independent zinc ions and construct repeated units of cyclic networks. The cyclic units of the complex bind two sodium ions. The sodium ions are held by oxygen atoms with distances Na1–O1, 2.423(15)Å; Na1–O1', 2.446(16)Å; Na1–O7, 2.372(3)Å; Na1–O5, 2.379(14); Na1–O4, 2.453(14) and Na1–O3, 2.480(15) (Table 22 in Appendix). There is also side on π -cation interaction between sodium and the C8-C9 double bond with a distance of separation 3.182Å. All these contribute to the formation of spirane type of structure around each zinc centers.

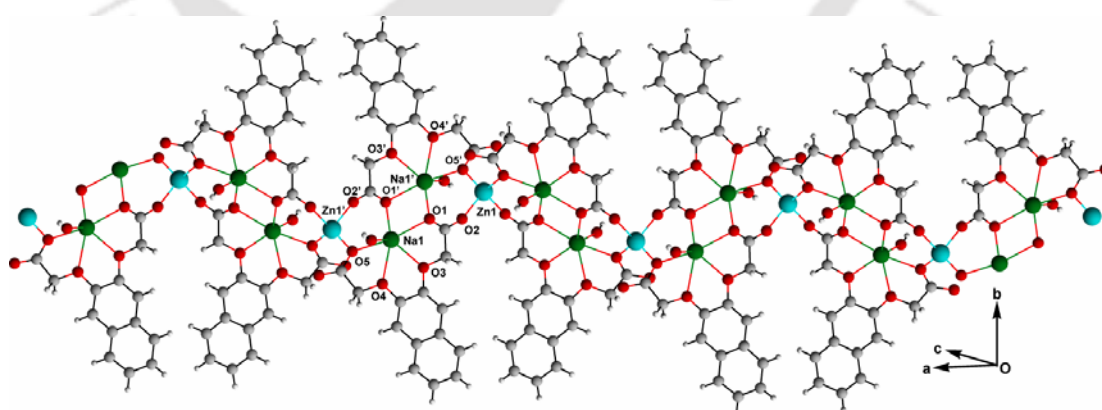


Figure 5.13 Crystal packing of complex **5.6** [$z = 1/2 - x, 1/2 - y, 1 - z$].

The hydrogens of hydroxide ions are involved in O7–H \cdots O6 [$d_{O7\cdots O6}$ 3.005 Å, $\angle D-H\cdots A$ 159.6°] hydrogen bonding interaction with the carboxylate oxygen. The complexes are also assembled in the lattice through weak C11–H \cdots O6 [$d_{C11\cdots O6}$ 3.331 Å, $\angle D-H\cdots A$ 166.8°]

interaction. The hydrogen bond parameters are given in Table 5.8. The distance between two zinc atoms in the polymeric structure is 9.021 Å. The solid state FT-IR spectra of the complex **5.6**, shows a strong absorption at 1643 cm⁻¹ due to C=O stretching frequency. A medium absorption at 2902 cm⁻¹ due to the presence of -CH₂- group and two strong absorption bands at 1259 cm⁻¹ and 1054 cm⁻¹ for C-O stretching of ether groups are observed (Figure 5.25). The hydroxyl group of the complex shows a strong IR absorption at 3550 cm⁻¹. The dicarboxylic acid **L₁H₂** has ¹H NMR signals at 7.70, 7.31, 7.24 ppm due to the three equivalent sets of aromatic protons but in the complex (**5.6**) the aromatic protons appear as four broad peaks at 7.74, 7.61, 7.49, 7.33 ppm.

Table 5.8: Hydrogen bond geometry(Å, °) for complex **5.6**

D-H...A	d(D-H)	d(H...A)	d(D...A)	<D-H...A
O(7)-H(7O)···O(6) [1-x, y, 1/2-z]	0.82	2.22	3.005(3)	159.6
C(11)-H(11)···O(6) [1-x, -y, 1-z]	0.93	2.42	3.331(2)	166.8

This happens due to asymmetry imposed on the naphthalene ring through the complexation of the ligand. The -CH₂- protons of the ligand (**5.5**) appear as sharp singlet at 4.80 ppm, shifts to 4.65 ppm as broad singlet in the complex **5.6**. The -OH signal of the complex appears as singlet at 7.95 ppm. The complex has a molar conductance value 94.86 S cm⁻¹ mol⁻¹ in dimethylsulfoxide, which suggests it to be ionic.

A similar reaction of zinc(II) acetate dihydrate with **L₁H₂** and subsequent treatment with pyridine in methanol (Scheme 5.4) results in polymeric complexes having composition {[Zn(L₁)(Pyridine)₂(H₂O)(CH₃OH)].H₂O}_n (**5.7**). The crystal structure of the polymer **5.7** is shown in Figure 5.14. In the complex **5.7**, each zinc(II) ion has a distorted octahedral geometry, where two pyridine molecules are in cis orientation to each other. The two monodentate carboxylate groups are trans to each other in the complex. The rest of the coordination sites are occupied by solvent molecules namely water and methanol. One encapsulated water molecule is also present in the lattice and forms hydrogen bond with polymeric chains. One carboxylate group is hydrogen-bonded (intra-molecular) to the hydrogen atom of the coordinated methanol molecule by O8-H...O2 [d_{O8...O2} 2.699 Å, <D-H...A 170.4°] interaction and another carboxylate is involved in intramolecular hydrogen-bonding with the coordinated water molecule through O7-H...O5 [d_{O7...O5} 2.637 Å, <D-H...A 155.8°] interaction.

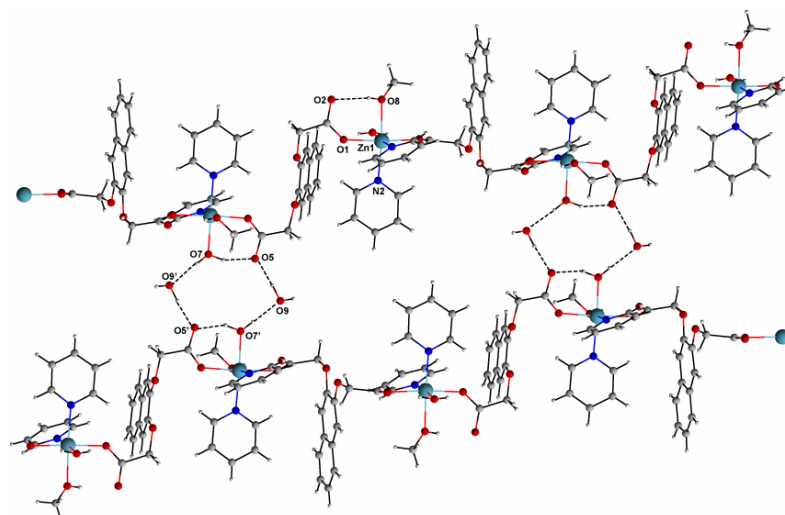


Figure 5.14 Formation of layered structures through hydrogen bonding with interstitial water molecules in the complex **5.7** [$x, 1/2-y, 1/2+z$]

In the crystal lattice, the polymeric chains are held together via inter-molecular hydrogen bonding through water molecules and form a layered structure. The water molecules between the layers are inter-molecularly hydrogen-bonded with oxygen atom of carboxylates via O9–H \cdots O2 [$d_{O9\cdots O2}$ 2.835 Å, \angle D–H \cdots A 177.2°] and O9–H \cdots O5 [$d_{O9\cdots O5}$ 2.725 Å, \angle D–H \cdots A 151.8°] interactions.

Table 5.9: Hydrogen bond geometry(Å, °) for complex **5.7**

D–H \cdots A	d(D–H)	d(H \cdots A)	d(D \cdots A)	\angle D–H \cdots A
O(7)–H(7A) \cdots O(9) [$x, -1+y, -1+z$]	0.80(4)	1.87(4)	2.672(4)	178.5(6)
O(7)–H(7B) \cdots O(5) [$1+x, 1/2-y, 1/2+z$]	0.95(8)	1.74(8)	2.637(6)	155.8(5)
O(8)–H(8O) \cdots O(2)	0.68(5)	2.02(5)	2.699(5)	170.4(4)
O(9)–H(9A) \cdots O(2) [$1-x, 1-y, 1-z$]	1.00(9)	1.83(9)	2.835(6)	177.2(8)
O(9)–H(9B) \cdots O(5) [$1-x, 1/2+y, 1/2-z$]	0.94(6)	1.86(7)	2.725(6)	151.8(5)
C(2)–H(2A) \cdots O(2) [$1-x, -y, -z$]	0.97	2.57	3.506(5)	162.8
C(22)–H(22) \cdots O(8) [$x, 1/2-y, -1/2+z$]	0.93	2.54	3.355(7)	147.2

Besides this, the polymeric chains are also interconnected by weak C22–H \cdots O8 [$d_{C22\cdots O8}$ 3.355 Å, \angle D–H \cdots A 147.2°] and C2–H \cdots O2 [$d_{C2\cdots O2}$ 3.506 Å, \angle D–H \cdots A 162.8°] interactions. The hydrogen bond parameters are included in Table 5.9. The solid state FT-IR spectra of the complex **5.7** shows strong absorptions at 1606 and 1595 cm^{-1} due to C=O stretching frequency and it also shows weak absorptions at 2927 and 2922 cm^{-1} due to the presence of –CH₂– group (Figure 5.26). Thermogravimetric analysis of the complex **5.7** shows the loss of

two water and a coordinated methanol molecules in the temperature range 40-100°C which corresponds to 14.27% of the total weight. The calculated weight loss is 12.02%. In the temperature range 210-290°C the complex loses the remaining two coordinated pyridine molecules with a weight loss of 38.06% (calculated weight loss is 40.00%).

The reaction of zinc(II) acetate with L_1Na_2 in the presence of pyrazole lead to the formation of a dinuclear zinc(II) complex, $\{[NaZn(L_1)(CH_3COO)(Pyz)]_2 \cdot 2MeOH\}$ (**5.8**) (where pyz is pyrazole). The zinc atoms in the complex have a distorted square pyramidal geometry.

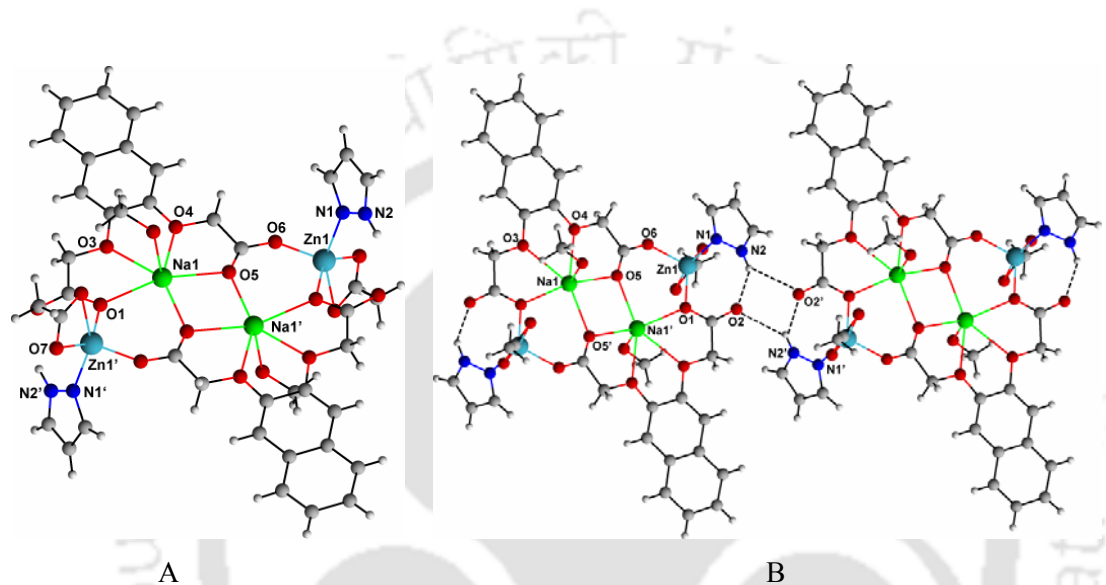


Figure 5.15 A) Crystal structure of complex **5.8** [$' = -x, 1-y, 2-z$] and B) one dimensional molecular assembly of complex **5.8**

Each zinc(II) ion is coordinated through one pyrazole molecule, two carboxylates from two independent ligands as well as a chelating acetate ligand (Figure 5.15A). The dicarboxylate ligand L_1 acts as bridging ligand and results in formation of a structure having resemblance to macrocycle, which anchored the sodium ions. Besides this, one molecule of methanol is coordinated to sodium. The sodium ions have coordination number six with Na–O bond distances Na1–O1, 2.391(19)Å, Na1–O3, 2.557(19)Å; Na1–O4, 2.519(19)Å; Na1–O5, 2.420(2)Å; Na1–O5', 2.431(2)Å and Na1–O9, 2.313(3)Å (Table 24 in Appendix). The complex has a highly symmetric structure, with a center of inversion located at the central point of the rectangle formed by the Na_2O_2 units. The complex **5.8** self-assembles through intra and intermolecular $N2-H \cdots O2$ [$d_{N2 \cdots O2}$ 2.946 Å, $\angle D-H \cdots A$ 138.4°] and $N2-H \cdots O2'$ [$d_{N2 \cdots O2'}$ 3.052 Å, $\angle D-H \cdots A$ 134.7°] interactions respectively (Figure 5.15B). The hydrogen atoms of naphthalene ring are involved in weak $C7-H \cdots O8$ [$d_{C7 \cdots O8}$ 3.597 Å, $\angle D-H \cdots A$ 161.4°] and $C11-H \cdots O7$ [$d_{C11 \cdots O7}$ 3.519 Å, $\angle D-H \cdots A$ 154.9°] interactions with the acetate

oxygen. The hydrogen bond parameters are given in Table 5.10. Besides that the sodium ions are involved in cation- π interaction with C6 and C7 atoms of the naphthalene ring with a separation of 3.957 Å. The C=O stretching frequency of the complex appears at 1620 cm^{-1} and strong C–O stretching frequencies are observed at 1256 cm^{-1} and 1061 cm^{-1} in the FT-IR spectra.

Table 5.10: Hydrogen bond geometry(Å, °) for complex **5.8**

D–H \cdots A	d(D–H)	d(H \cdots A)	d(D \cdots A)	\angle D–H \cdots A
N(2)–H(2N) \cdots O(2) [Intra]	0.86(5)	2.25(5)	2.946(3)	138.4(4)
N(2)–H(2N) \cdots O(2') [-x, -y, 1-z]	0.86(5)	2.38(5)	3.052(3)	134.7(4)
C(7)–H(7) \cdots O(8)	0.93	2.70	3.597	161.4
C(11)–H(11) \cdots O(7)	0.93	2.65	3.519	154.9
C(13)–H(13B) \cdots O(7)	0.97	2.62	3.486	147.9

When we carried out the reaction of L_1H_2 with zinc(II) acetate dihydrate and pyrazole in the absence of sodium hydroxide in a mixed solvent of methanol and dimethylformamide (DMF) it results in the formation of an one dimensional co-ordination polymer $\{[Zn(L_1)(Pyz)_3].DMF\}_n$ (**5.9**) as the major product. In this reaction a cyclic tetranuclear zinc complex $[Zn_4(L_1)_4(Pyz)_4(H_2O)_8].DMF$ (**5.10**) is also formed (Scheme 5.4).

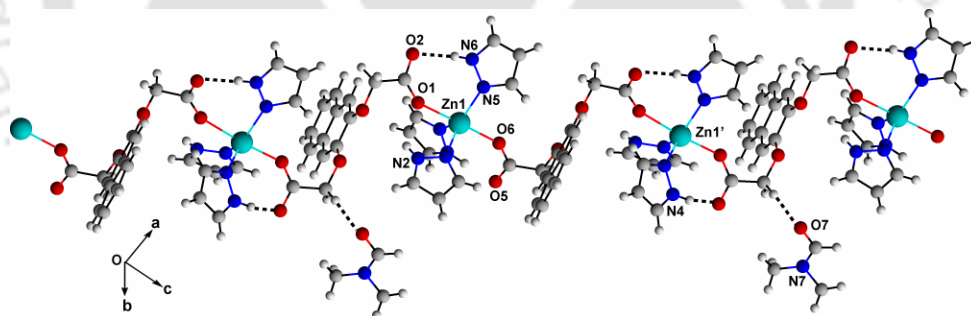


Fig. 5.16 The crystal structure of complex **5.9** showing the hydrogen bonding interactions [$= 1+x, 1/2-y, 1/2+z$]

The complex **5.9** has a zig-zag chain like structure (Figure 5.16). The zinc ions are in trigonal bipyramidal geometry formed by three coordinating pyrazoles and two monodentate carboxylates. Three nitrogen atoms form the triangular plane of the trigonal bipyramidal geometry. The bond angles $\angle N1-Zn1-N5$ and $\angle N3-Zn1-N5$ are 128.2(11)° and 124.8(11)° respectively whereas the angle $\angle N1-Zn1-N3$ is 106.7(12)°. The bond distances around the zinc centers are Zn1–N1, 2.057(3)Å; Zn1–N3, 2.023(3)Å; Zn1–N5, 2.035(3)Å; Zn1–O1, 2.196(2)Å and Zn1–O6, 2.072(2)Å (Table 25 in Appendix). The N–H hydrogen of pyrazole

molecules form intramolecular hydrogen bond with the oxygen atom of carboxylic acids through N6–H \cdots O2 [$d_{\text{N6}\cdots\text{O2}}$ 2.713 Å, $\angle\text{D–H}\cdots\text{A}$ 173.9°] and N2–H \cdots O3 [$d_{\text{N2}\cdots\text{O3}}$ 3.330 Å, $\angle\text{D–H}\cdots\text{A}$ 170.2°] interactions (Table 5.11). Dimethylformamide (DMF) molecules are held in the lattice through intermolecular C13–H \cdots O7 [$d_{\text{C13}\cdots\text{O7}}$ 3.380 Å, $\angle\text{D–H}\cdots\text{A}$ 170.8°] hydrogen bonding interactions with the –CH₂– groups of dicarboxylic acid. The polymeric chains are self-assembled via intermolecular C2–H \cdots O5 [$d_{\text{C2}\cdots\text{O5}}$ 3.407 Å, $\angle\text{D–H}\cdots\text{A}$ 157.5°] and C11–H \cdots O2 [$d_{\text{C11}\cdots\text{O2}}$ 3.205 Å, $\angle\text{D–H}\cdots\text{A}$ 153.0°] hydrogen bonding interactions.

Table 5.11: Hydrogen bond geometry(Å, °) for complex **5.9**

D–H \cdots A	d(D–H)	d(H \cdots A)	d(D \cdots A)	$\angle\text{D–H}\cdots\text{A}$
N(2)–H(2N) \cdots O(3)	0.86	2.48	3.330(4)	170.2
N(4)–H(4N) \cdots O(5) [1+x, 1/2-y, 1/2+z]	0.95(5)	1.78(5)	2.724(4)	167.6(3)
N(6)–H(6N) \cdots O(2)	0.82(5)	1.90(5)	2.713(4)	173.9(5)
C(2)–H(2A) \cdots O(5) [1+x, y, z]	0.97	2.49	3.407(5)	157.5
C(11)–H(11) \cdots O(2) [-1+x, y, z]	0.93	2.35	3.205(5)	153.0
C(13)–H(13A) \cdots O(7)	0.97	2.42	3.380(6)	170.8

The complex in the solid state has C=O stretching of DMF at 1652 cm⁻¹, whereas a strong absorption at 1600 cm⁻¹ for C=O stretching of carboxylate is also observed. The thermogravimetric analysis of the complex **5.9** shows the loss of three pyrazole molecules at the temperature range 170-270°C which corresponds to 42.17% of the total weight. The calculated weight loss is 44.89%.

The minor product in the above reaction is the tetranuclear zinc complex **5.10**. It may be considered to be a co-crystal of two tetra-nuclear cyclic zinc complexes; one of them has a DMF within the cyclic part and other does not (Figure 5.17). The structure also contains a water molecule, hydrogen atom of which could not be located and some residual electron density could not be assigned. Nevertheless structural information is good enough to describe the symmetry non-equivalence. In the cyclic units, two of the zinc atoms have octahedral geometry and the other two zinc atoms have trigonal-bipyramidal geometry. Zinc atoms having octahedral geometry are co-ordinated to three water molecules, one pyrazole and two carboxylate groups. Other zinc atoms have coordination through a water molecule, one pyrazole, and three oxygen atoms of carboxylate. The crystal structure has two tetranuclear asymmetric molecules per unit cell. A slight difference in the tetranuclear units is revealed on careful analysis of the bond distances between the zinc atoms. In one metallacycle the

distances are Zn1–Zn1', 11.561 Å and Zn2–Zn2', 12.642 Å whereas in the other metallacycle these distances are Zn4–Zn4', 11.559 Å and Zn3–Zn3', 13.095 Å. From the bond distances between the zinc centers it is quite clear that the two void sizes are almost similar in the two asymmetric molecules. The important bond distances and angles of this complex are listed in Table 26 (Appendix).

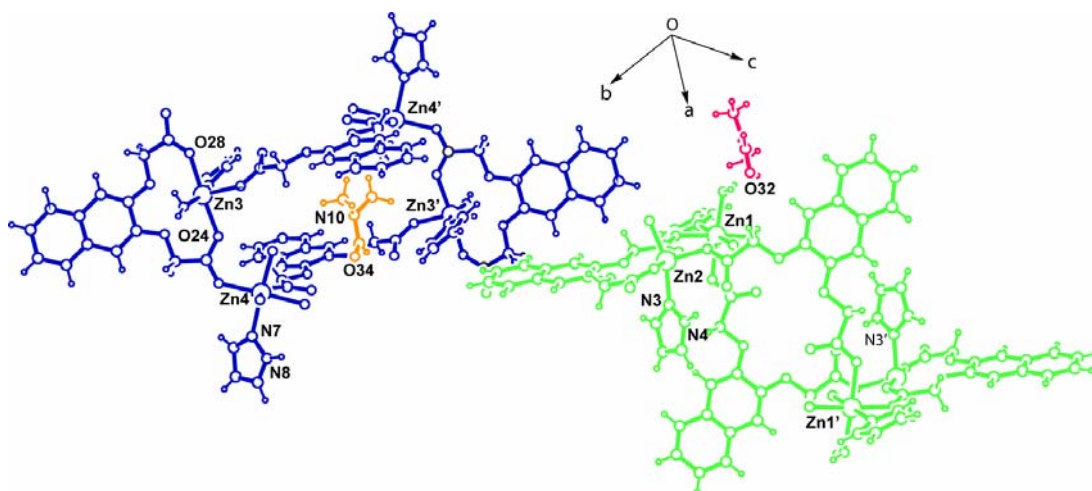


Fig. 5.17 Two symmetry non-equivalent metallacycles in the unit cell of complex **5.10** (drawn to 30 % probability) [$' = 2-x, -y, 1-z$; $'' = 1-x, 2-y, -z$]

It may be noted here that multiple voids with different sizes, in metal complex with one ligand, are not generally observed³¹⁶. The structural study on such molecules may provide important information regarding understanding of high Z' values³³⁵. In structure of the complex **5.10**, two solvent molecules are in two different environments, this makes the two rings non symmetric with respect to crystallographic axis. The crystal structure of complex

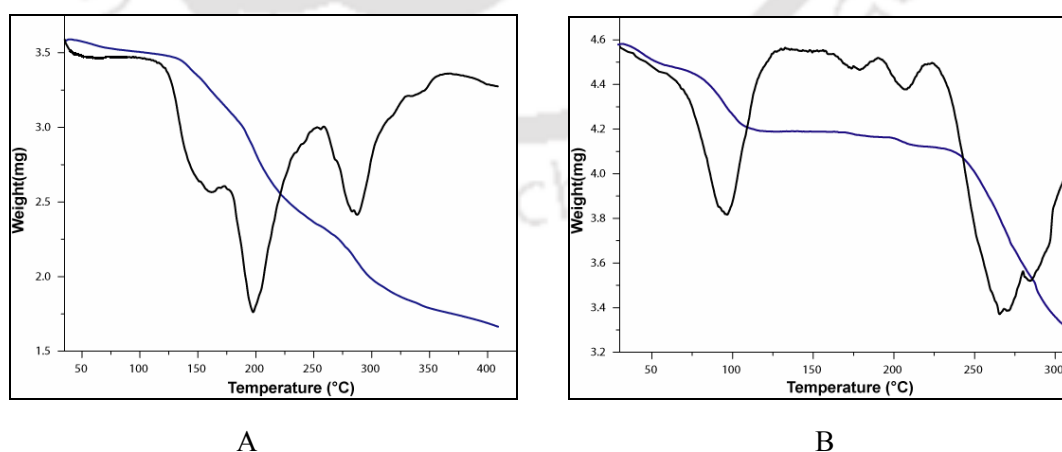


Figure 5.18 A) Thermogram of complex **5.10**, B) Thermogravimetric curve of complex **5.11**
5.10 shows that the dimethylformamide molecules are held in the lattice through N2–H···O34 [$d_{N2\cdots O34}$ 2.919 Å, $\langle D-H\cdots A \rangle$ 140.0°] and N8–H···O33 [$d_{N8\cdots O33}$ 2.763 Å, $\langle D-H\cdots A \rangle$ 143.0°]

interaction with pyrazole hydrogens. Remaining pyrazole molecules are hydrogen bonded with carboxylate oxygen through N4–H \cdots O6 [$d_{\text{N4}\cdots\text{O6}}$ 2.753 Å, $\angle\text{D–H}\cdots\text{A}$ 146.2°] and N6–H \cdots O21 [$d_{\text{N6}\cdots\text{O21}}$ 2.721 Å, $\angle\text{D–H}\cdots\text{A}$ 156.8°]. Besides that the coordinated water molecules are participate in O–H \cdots O hydrogen bonding interactions with carboxylate oxygen. The hydrogen bonds contributing to the packing is listed in Table 5.12.

Thermogravimetric analysis of the complex **5.10** shows that the complex loses eight coordinated water molecules, one dimethylformamide and four pyrazole molecules in the temperature range 100-240°C, which corresponds to 31.58% of the total weight (calculated weight loss 30.77%). In next step the complex loses 49.37% of its total weight which corresponds to the loss of one dicarboxylic acid molecule. The thermogravimetric curve of the complex **5.10** is shown in Figure 5.18A. The complex has IR absorptions at 1646 cm^{-1} and 1591 cm^{-1} due to the C=O stretching frequency of dimethylformamide and carboxylate ligand respectively (Figure 5.27).

Table 5.12: Hydrogen bond geometry (Å, °) for complex **5.10**

D–H \cdots A	d(D–H)	d(H \cdots A)	d(D \cdots A)	$\angle\text{D–H}\cdots\text{A}$
N(2)–H(2) \cdots O(34)	0.86	2.21	2.919(9)	140.0
N(4)–H(4A) \cdots O(6) [2-x, -y, 1-z]	0.86	2.00	2.753(9)	146.2
N(6)–H(6A) \cdots O(21) [1-x, 2-y, -z]	0.86	1.91	2.721(9)	156.8
N(8)–H(8A) \cdots O(33) [-1+x, y, z]	0.86	2.03	2.763(12)	143.0
O(14)–H(7A) \cdots O(27) [x, -1+y, z]	0.82	2.06	2.825(7)	155.6
O(14)–H(7B) \cdots O(34)	0.69(8)	2.02(8)	2.713(8)	174.0(10)
O(16)–H(16O) \cdots O(21) [1-x, 1-y, -z]	0.60(8)	2.15(8)	2.740(8)	166.9(7)
O(16)–H(17O) \cdots O(18) [1-x, 1-y, -z]	0.93(9)	1.88(9)	2.743(8)	153.8(8)
O(31)–H(31A) \cdots O(33) [-1+x, y, z]	1.04(12)	1.79(12)	2.801(10)	161.4(10)
O(31)–H(31B) \cdots O(11) [-1+x, 1+y, z]	0.81(10)	2.03(10)	2.789(8)	155.5(9)

The co-ordination chemistry of (3-carboxymethoxy-naphthalen-2-yloxy)-acetic acid (**L₁H₂**) with zinc is extended to nitrogen containing bidentate ligands, such as 1,10-phenanthroline (Phen) and 2,2'-bipyridine (Bpy). In both the cases, mononuclear complexes **5.11** and **5.12** are obtained. In these complexes one of the carboxylate groups of the ligand co-ordinates and other remains free in deprotonated form. Unfortunately, in both the complexes we are unable to locate few hydrogen atoms of water molecules in the difference fourier maps. The complex **5.11** has a composition [Zn(L₁)(Phen)₂].3H₂O (where Phen is 1,10-phenanthroline) and has a

distorted octahedral geometry around zinc ion (Figure 5.19A) where two phenanthroline rings are cis to each other.

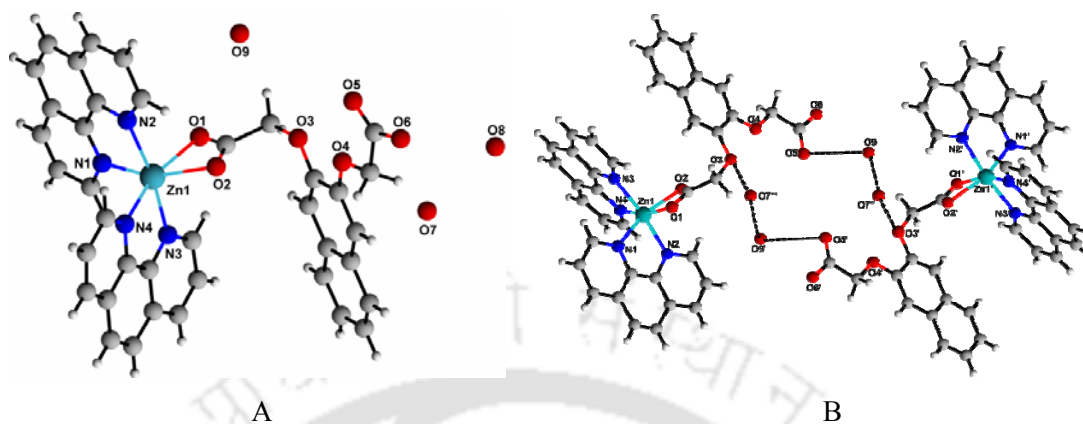


Figure 5.19 A) Crystal structure of complex **5.11**, B) Hydrogen bonded dimeric assembly of complex **5.11** (the hydrogen atom in oxygens could not be located) [$' = 1-x, -y, -z$; $'' = x, 1/2-y, -1/2+z$; $''' = 1-x, -1/2+y, 1/2-z$]

The bidentate nature of 1,10-phenanthroline and the stabilization of free carboxylic acid group through hydrogen bonding prevent polymerization process. It is already reported that bulky bidentate ligands inhibits the co-ordination polymerization of dicarboxylates³³⁶. The water molecules are hydrogen bonded with the complex through O5 \cdots O9 [d_{O5 \cdots O9} 2.995Å], O9 \cdots O7 [d_{O9 \cdots O7} 2.900Å], O7 \cdots O3 [d_{O7 \cdots O3} 2.989Å], O6 \cdots O8 [d_{O6 \cdots O8} 2.795Å] and O8 \cdots O1 [d_{O8 \cdots O1} 2.863Å] interactions to form a hydrogen bonded dimeric assembly (Figure 5.19B). The complex is self assembled in the lattice through weak C28–H \cdots O9 [d_{C28 \cdots O9} 3.295 Å, <D–H \cdots A 169.5°] and C29–H \cdots O1 [d_{C29 \cdots O1} 3.458 Å, <D–H \cdots A 159.5°] interactions. Some important hydrogen bond parameters are listed in Table 5.13. In the crystal structure of this molecule one of the phenanthroline rings is disordered and it is resolved by sharing the occupancy of the N1, N2, C15–C24 atoms with 50% occupancy (Table 65).

The FT-IR spectra of the complex **5.11** shows strong absorption at 1606 and 1420cm⁻¹ due to asymmetric and symmetric C=O stretching of carboxylate. Thermogravimetric analysis shows that it loses three water molecules in the temperature range 50-120°C which corresponds to 6.31% of the total weight. The calculated loss is 7.16%. In the temperature range 210-290°C the complex loss one phenanthroline molecule (Figure 5.18B). Due to the loss of three water molecules and a 1,10-phenanthroline total weight loss is 28.82% (calculated weight loss is 31.03%). In the ¹H NMR spectra the aromatic protons appear at 8.84, 8.69, 8.14, 7.83, 7.47, 7.24, 6.99ppm and the -CH₂- protons appear at 4.35 ppm.

Table 5.13: Hydrogen bond geometry(Å, °)for complex **5.11**

D–H···A	d(D–H)	d(H···A)	d(D···A)	<D–H···A
C(28)–H(28)···O(9) [x, 1/2- y, 1/2+z]	0.93	2.38	3.295(15)	169.5
C(29)–H(29)···O(1) [x, 1/2- y, 1/2+z]	0.93	2.57	3.458(10)	159.5
C(36)–H(36)···O(8) [1+x,-1+y, z]	0.93	2.55	3.391(11)	150.4

The complex $[\text{Zn}(\text{L}_1)(\text{Bipy})_2] \cdot 7\text{H}_2\text{O}$ (**5.12**) (where Bipy is 2,2'-bipyridine) is a mononuclear complex with similar co-ordination feature as that of complex **5.11** (Figure 5.20A). The water molecules present in the lattice are assembled through O–H···O interactions. Two mononuclear complexes are self assembled in lattice through $\text{O5} \cdots \text{O11}$ [$d_{\text{O5} \cdots \text{O11}}$ 3.027Å], $\text{O11} \cdots \text{O10}$ [$d_{\text{O11} \cdots \text{O10}}$ 2.805Å], $\text{O5}' \cdots \text{O10}$ [$d_{\text{O5}' \cdots \text{O10}}$ 2.711Å] and $\text{O3} \cdots \text{O11}$ [$d_{\text{O3} \cdots \text{O11}}$ 2.927Å] interactions which construct a hydrogen bonded hexameric unit as shown in Figure 5.20B.

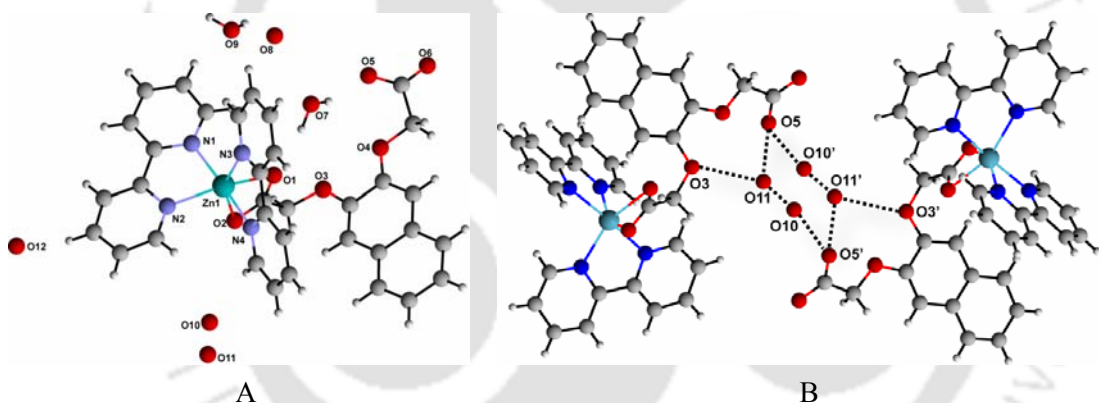


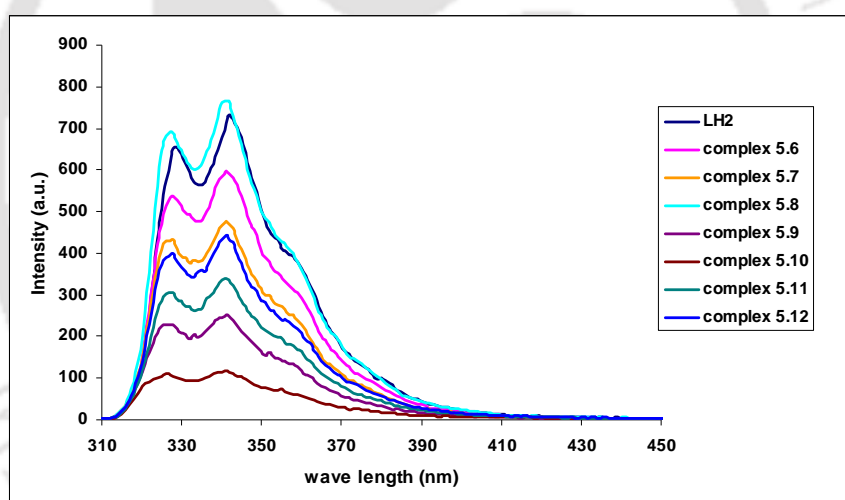
Figure 5.20 A) Crystal structure of complex **5.12** (the hydrogen atom in oxygens O8, O10, O11 and O12 could not be located); B) Hydrogen bonded hexameric structure of **5.12**

Besides that the water molecules are assembled to make a tetrameric hydrogen bonded structure through $\text{O5} \cdots \text{O10}$ [$d_{\text{O5} \cdots \text{O10}}$ 2.711Å], $\text{O8} \cdots \text{O10}$ [$d_{\text{O8} \cdots \text{O10}}$ 2.843Å], $\text{O8} \cdots \text{O7}$ [$d_{\text{O8} \cdots \text{O7}}$ 2.763Å], and $\text{O7} \cdots \text{O5}$ [$d_{\text{O7} \cdots \text{O5}}$ 2.847 Å, $\angle \text{D–H} \cdots \text{A}$ 168.9°] interactions. The aromatic hydrogens are involved in weak $\text{C28–H} \cdots \text{O7}$ [$d_{\text{C28} \cdots \text{O7}}$ 3.275 Å, $\angle \text{D–H} \cdots \text{A}$ 157.3°] and $\text{C34–H} \cdots \text{O10}$ [$d_{\text{C34} \cdots \text{O10}}$ 3.300 Å, $\angle \text{D–H} \cdots \text{A}$ 148.2°] interactions with carboxylate oxygen atoms.. The hydrogen bond parameters for the complex are listed in Table 5.14. The C=O stretching frequency of the complex appears at 1632 cm^{-1} . The zinc complexes of L_1H_2 with 2,2'-bipyridine is mononuclear, whereas various dicarboxylic acids with bipyridine forms polymeric structures³³⁰.

Table 5.14: Hydrogen bond geometry(Å, °) for complex **5.12**

D–H···A	d(D–H)	d(H···A)	d(D···A)	<D–H···A
O(7)–H(7A)···O(5)	0.73(7)	2.13(6)	2.847(6)	168.9(7)
O(9)–H(9A)···O(6) [1+x, y, z]	0.75(7)	2.17(7)	2.877(6)	156.1(6)
O(9)–H(9B)···O(8)	1.05(8)	2.13(8)	2.899(7)	128.4(5)
C(28)–H(28)···O(7) [-x, 1-y, -z]	0.93	2.40	3.275(5)	157.3
C(34)–H(34)···O(10)	0.93	2.47	3.300(6)	148.2

The ligand L_1H_2 contains naphthalene ring, it has an electronic absorbance at 280 nm ($\epsilon = 1.1 \times 10^5 \text{ mol}^{-1} \text{ dm}^3 \text{ cm}^{-1}$); the fluorescence emission spectra of all the complexes were recorded by exciting at 290 nm in dimethylsulfoxide. In each case, we found emission at 327 nm and 342 nm (Figure 5.21). The emission intensity of the complexes is slightly lower than that of the parent acid. Although the changes are very nominal, the changes reflect the complexation of the ligand to the metal.

Figure 5.21 Fluorescence emission spectra of L_1H_2 and complexes **5.6-5.12**

In conclusion the sodium complex of the 3-phenyl-2-(3-phenyl-ureido)-propionic acid (**5.1**) has anti-syn conformation around the urea moiety; whereas, in the manganese complex urea part adopts the conventional syn-syn conformation. It is also clear that polymorphism and symmetry non equivalence arise in (3-carboxymethoxy-naphthalen-2-yloxy) acetic acid (**5.5**) and its derivative due to the differences in the layered structures or in the conformers. These differences arise from the favourable closed packed structures and stable packing geometry which admits the different directional weak interactions. Depending on the type of ancillary ligands and reaction conditions (3-carboxymethoxy-naphthalen-2-yloxy)-acetic acid (**5.5**) forms varieties of zinc(II) complexes including coordination polymers. When cyclic zinc

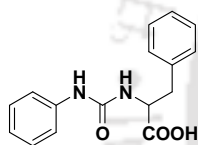
complexes are formed, the template effect of the cyclic structures anchors sodium ions. The bidentate ligands such as 1,10-phenanthroline, 2,2'-bipyridine favors formation mononuclear zinc complexes with **L**. The flexible carboxylic acid L_1H_2 generally binds to zinc in a monodentate fashion. We have also shown example on occurrence of symmetry non-equivalent metallacycles in the unit cell. The symmetry non-equivalence in the complex arises from the location of the solvent molecules in the crystal lattice.

5.4 Experimental Section

5.4.1 Synthesis of flexible mono-carboxylic acid and its metal complex

Detailed synthetic methodologies are given below. Analytical data as well as spectroscopic data are also listed. Details of the instruments are given in Appendix.

Synthesis of 3-phenyl-2-(3-phenyl-ureido) propionic acid (5.1)



Phenylalanine ethyl ester (1.92 g, 10 mmol) was dissolved in dry dichloromethane (20 ml) and the solution was stirred at 0°C for 10 mins. To this solution phenyl isocyanate (1.20 g, 10 mmol) was added dropwise over a period of 30 mins. The reaction mixture was then stirred overnight at room temperature. The reaction mixture was washed with water (10 ml), dried over sodium sulphate and solvent was removed under reduced pressure. The ethyl ester of 3-phenyl-2-(3-phenyl-ureido) propionic acid was obtained as a white solid, was further purified by recrystallisation from dichloromethane. The isolated ester (3.11 g, 10 mmol) was then treated with sodium hydroxide (0.48 g, 12 mmol) in 20 ml of MeOH : water (4:1). The reaction mixture was stirred overnight at room temperature. The solvent was removed under reduced pressure, and 10ml of water was added to it. The solution was acidified with dilute hydrochloric acid (1M, 10ml) solution. A white solid was obtained which was washed with water (25 ml) and dried. The product 3-phenyl-2-(3-phenyl-ureido) propionic acid (**LH**) was purified by recrystallisation from methanol. Isolated yield: 72%.

Elemental analysis for $C_{16}H_{16}N_2O_3$: calculated C, 67.53; H, 5.63; found C, 67.61, H, 5.60. FT-IR (KBr, cm^{-1}): 3403 (s), 3375 (m), 1694 (s), 1648 (s), 1596 (s), 1558 (s), 1500 (s), 1447 (s), 1329 (m), 1218 (s), 1058 (w), 887 (w), 754 (s), 695 (s), 578 (w), 509 (w).

^1H NMR (DMSO- d_6): 8.51 (1H, s), 7.31 (2H, d, $J = 8.4$ Hz), 7.19 (7H, m), 6.82 (1H, t, $J = 7.2$ Hz), 6.23 (1H, d, $J = 8$ Hz), 5.55 (1H, q, $J = 13.6, 7.2$ Hz), 3.05 (2H, m).

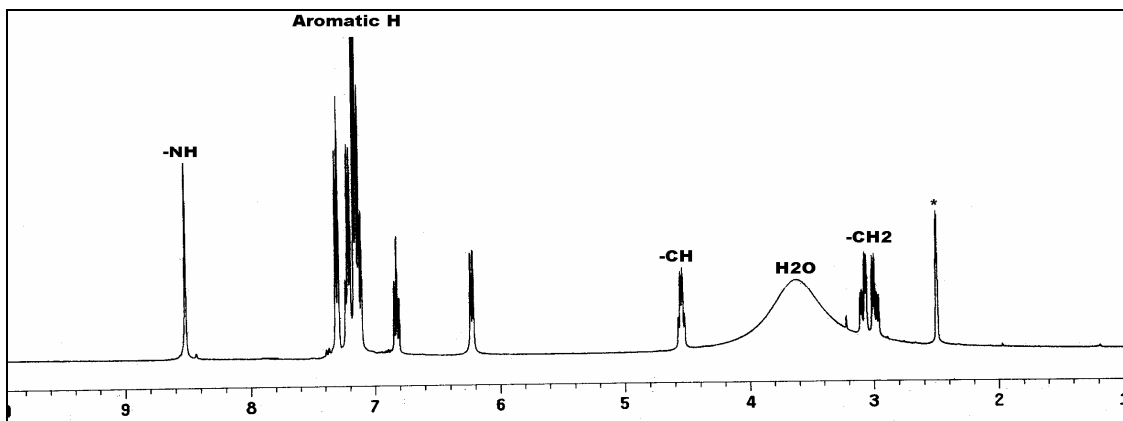
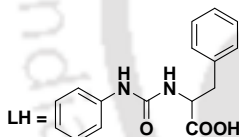


Figure 5.22 ^1H -NMR spectra of compound 5.1

Complex 5.2: $[\text{Na}(\text{L})(\text{H}_2\text{O})_3]_2$



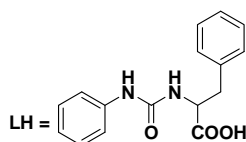
The complex **5.2** was prepared by mixing **LH** with NaOH (1:1 molar ratio) in methanol at room temperature. It was then kept for crystallization. After 2 days colourless plate type crystals of complex **5.2** was appeared. Isolated yield: 69% (Based on Na);

Elemental analysis for $\text{C}_{32}\text{H}_{42}\text{N}_4\text{Na}_2\text{O}_{12}$: calculated C, 53.28, H 5.83. found C, 53.26, H, 5.88.

FT-IR (KBr, cm^{-1}): 3446 (bs), 1694 (s), 1640 (w), 1589 (s), 1515 (s), 1395 (s), 1288 (s), 1245 (w), 1174 (w), 1135 (w), 1028 (w), 916 (w), 848 (s), 784 (m), 755 (s), 702 (s), 601 (bm).

^1H NMR (D_2O): 7.31 (5H, m), 7.20 (3H, d, $J = 7.6$ Hz), 7.12 (2H, t, $J = 7.6$ Hz), 5.39 (1H, m), 3.19 (1H, m), 2.95 (1H, m).

Complex 5.3: $[\text{Mn}(\text{L})_2(\text{H}_2\text{O})_2]_n$



The complex **5.3** was prepared by mixing **LH** with $\text{Mn}(\text{OAc})_2 \cdot 4\text{H}_2\text{O}$ (2:1 molar ratio) in methanol at room temperature and kept for crystallization. After 2 days colourless thin plate type crystals of complex **5.3** was appeared. Isolated yield: 43% (Based on Mn).;

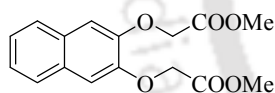
FT-IR (KBr, cm^{-1}): 3382(bs), 1640(s), 1545(s), 1495(w), 1412(s), 1343(w), 1305(w), 1240(w), 1022(w), 749(w), 693(m), 655(w).

UV-VIS: $\lambda_{\text{max}}(\text{MeOH}) = 241\text{nm}$ and 206nm , $\epsilon = 1.249 \times 10^4 \text{ M}^{-1}\text{cm}^{-1}$ and $2.248 \times 10^4 \text{ M}^{-1}\text{cm}^{-1}$.
Magnetic Moment: 5.12 BM at 25°C .

5.4.2 Synthesis of flexible di-carboxylic acid and its metal complex

Detailed synthetic methodologies are given below. Analytical data as well as spectroscopic data are also listed along with the each complex.

Synthesis of (3-Methoxycarbonylmethoxy-naphthalen-2-yloxy)-acetic acid methyl ester (5.4)



Naphthalene-2,3-diol (0.8 g, 5 mmol), bromomethylacetate (1.82 g, 12 mmol) and anhydrous K_2CO_3 (1.65 g, 12 mmol) was taken in a round bottom flask and then dry acetone (20 ml) was added into it under nitrogen atmosphere. The reaction mixture was stirred for 24h at 60°C (The reaction progress was monitored at regular intervals using TLC). After completion of the reaction, the reaction mixture was filtered off (to remove unreacted K_2CO_3). The solvent was removed under reduced pressure and a white solid was obtained. The isolated product was washed with NaOH (5%) solution and water and then the product was extracted with dichloromethane. The organic extracts were collected over anhydrous sodium sulphate; subsequent removal of the solvent gave the product **5.4**. Yield: 84%.

IR (KBr, cm^{-1}): 3448(bs), 3055(m), 2953(s), 2850(w), 2128(w), 1763(s), 1737(s), 1629(m), 1601(m), 1513(s), 1487(s), 1435(s), 1362(w), 1292(s), 1248(s), 1215(s), 1168(s), 1122(m), 1086(m), 1048(m), 1001(m), 850(s), 764(w), 737(m), 661(w), 619(w), 479(s).

Elemental analysis for $\text{C}_{16}\text{H}_{16}\text{O}_6$: calculated C, 63.10, H, 5.25; found C, 63.48; H, 5.44.

^1H NMR (CDCl_3): 7.66(d, $J=8.4$ Hz, 2H), 7.35(d, $J=8.4\text{Hz}$, 2H), 7.11(s, 2H), 4.84(s, 4H), 3.82(s, 6H).

^{13}C NMR(CDCl_3): 169.3, 147.8, 129.6, 126.7, 125.0, 109.7, 66.3, 52.5.

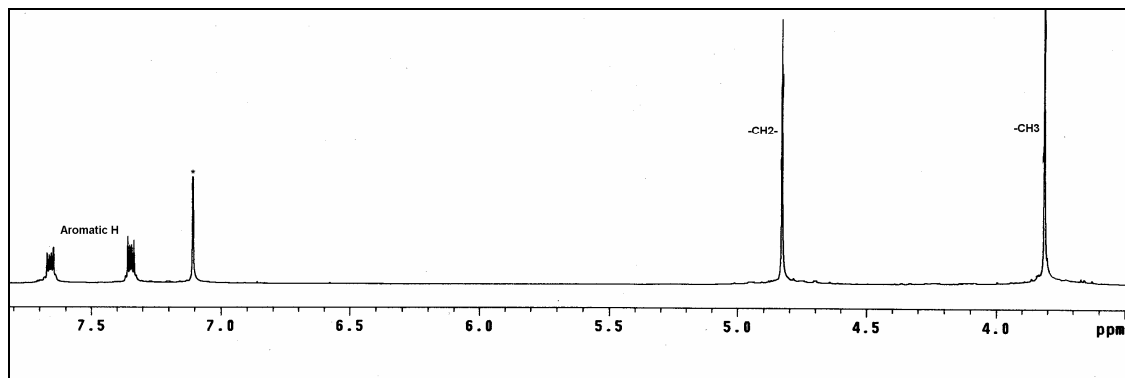


Figure 5.23 ^1H -NMR spectra of compound **5.4**

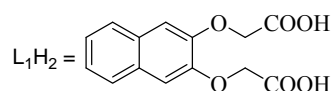
Compound 5.4A

(3-Methoxycarbonylmethoxy-naphthalen-2-yloxy)-acetic acid methyl ester (0.34 g, 1 mmol) was dissolved in methanol (10 ml) and kept for crystallisation. Colourless plate like crystals of **5.4A** were collected after 5 days and dried in air.

Compound 5.4B

Compound **5.1B** was obtained by dissolving (3-Methoxycarbonylmethoxy-naphthalen-2-yloxy)-acetic acid methyl ester (0.34 g, 1 mmol) in tetrahydrofuran (10 ml) and block type colourless crystals were collected after 3 days.

Synthesis of (3-Carboxymethoxy-naphthalen-2-yloxy)-acetic acid (5.5**)**



The isolated ester **5.4** (1.52g, 5mmol) and NaOH (0.48g, 12mmol) was dissolved in 20ml of MeOH: water (4:1). The reaction mixture was refluxed for 8h at 60°C. After completion of reaction the solvent was removed under reduced pressure, 10ml of water was added into it and the solution was acidified with dilute HCl solution. On complete acidification white solid was obtained. The product was filtered and washed properly with water until free from acid.

The product **5.5** was isolated as white solid that was purified by recrystallisation from methanol. Yield: 62%.

IR (KBr, cm^{-1}): 3503(bs), 3268(w), 2914(m), 1936(b), 1726(s), 1603(s), 1414(s), 1245(s), 1168(m), 1035(s), 856(s), 758(s).

Elemental analysis for $\text{C}_{14}\text{H}_{12}\text{O}_6$: calculated C, 60.82, H, 4.34; found C, 60.42; H, 4.83.

^1H NMR (DMSO-d_6): 7.70(d, $J=8\text{Hz}$, 2H), 7.31(d, $J=8\text{Hz}$, 2H), 7.24(s, 2H), 4.80(s, 4H).

^{13}C NMR (DMSO-d_6): 170.1, 147.5, 128.8, 126.3, 124.2, 108.1, 65.1.

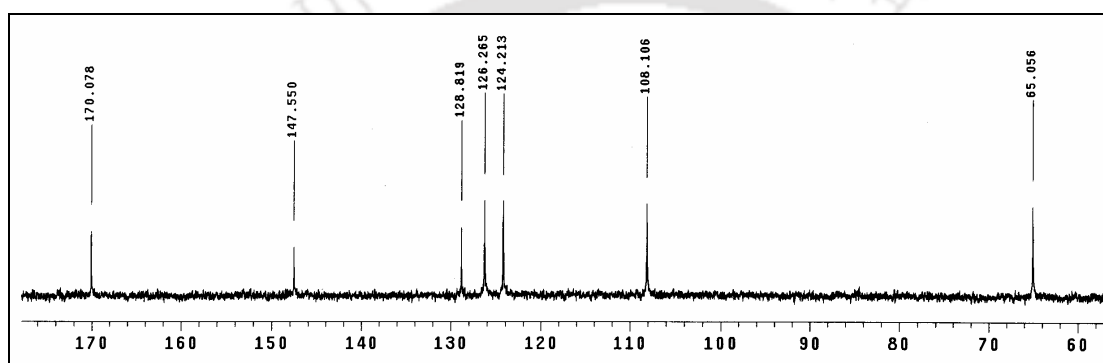


Figure 5.24 ^{13}C NMR spectra of compound **5.5**

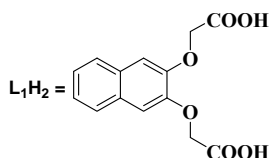
Compound 5.5A

(3-Carboxymethoxy-naphthalen-2-yloxy)-acetic acid (0.28 g, 1 mmol) was dissolved in dimethyl sulphoxide (5 ml) and kept for crystallisation. Colourless plate type crystals were appeared after 15 days.

Compound 5.5B

(3-Carboxymethoxy-naphthalen-2-yloxy)-acetic acid (0.28 g, 1 mmol) was dissolved in methanol (10 ml) by warming and kept for crystallisation. Colourless plate type crystals were appeared after 5 days.

Complex 5.6: $\{[\text{Na}_2\text{Zn}_2(\text{L}_1)_2(\text{OH})_2]\}_n$



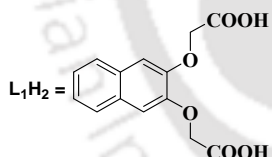
To a homogeneous solution of (3-Carboxymethoxy-naphthalen-2-yloxy)-acetic acid (0.276 g, 1 mmol) in methanol (20 ml) sodium hydroxide (0.080 g, 2 mmol) was added and heated. The solution was cooled to room temperature and zinc(II) acetate dihydrate (0.219 g, 1 mmol) was added to it. The resulting solution was stirred for 20 minutes. After this, the solution was kept for crystallization and after 10 days colourless crystals were appeared. Crystalline yield: 49 %;

Elemental analysis for $C_{28}H_{22}Na_2O_{14}Zn$: calculated C, 48.43; H, 3.17; found C, 49.01; H, 3.21. Molar conductance $94.86 \text{ S cm}^{-1}\text{mol}^{-1}$.

$^1\text{H NMR}$ (400MHz, DMSO- d_6 , ppm) 7.95 (s, 0.5H, OH signal), 7.74 (bs, 2H, aromatic), 7.61 (bs, 2H, aromatic), 7.49 (bs, 1H, aromatic), 7.33 (bs, 1H, aromatic), 4.65 (bs, 2H, $-\text{CH}_2-$).

FT-IR (KBr, cm^{-1}): 3550 (bs), 3505 (bs), 3064 (w), 3043 (w), 2943 (w), 2902 (m), 1643 (s), 1515 (s), 1486 (s), 1404 (s), 1325 (s), 1259 (s), 1171 (s), 1118 (s), 1076 (m), 1054 (s), 948 (m), 899 (m), 885 (s), 857 (m), 820 (m), 777 (m), 755 (m), 706 (s), 678 (w), 614 (m), 548 (w).

Complex 5.7: $\{[\text{Zn}(L_1)(\text{Pyridine})_2(\text{H}_2\text{O})(\text{CH}_3\text{OH})].\text{H}_2\text{O}\}_n$



The ligand L_1H_2 (0.276g, 1 mmol) was dissolved in methanol (20 ml) by heating. The solution was allowed to cool to room temperature and zinc(II) acetate dihydrate (0.438 g, 2 mmol) was added. The resulting solution was stirred for 15 mins at room temperature followed by addition of pyridine (0.395g, 5 mmol). The solution was stirred for another 15 mins. On standing for 5 days, colourless blocks appeared. Crystalline yield: 42%.

Elemental analysis for $C_{25}H_{28}N_2O_9Zn$: calculated C, 53.02; H, 4.99; N, 4.95; found C, 53.10; H, 5.01; N, 4.32.

FT-IR (KBr, cm^{-1}): 3394 (bs), 2927 (bw), 1666 (w), 1606 (s), 1510 (m), 1485 (s), 1449 (s), 1403 (s), 1333 (s), 1259 (s), 1217 (w), 1167 (s), 1118 (m), 1068 (m), 1037 (s), 883 (w), 851 (s), 750 (bs), 696 (s), 639 (w).

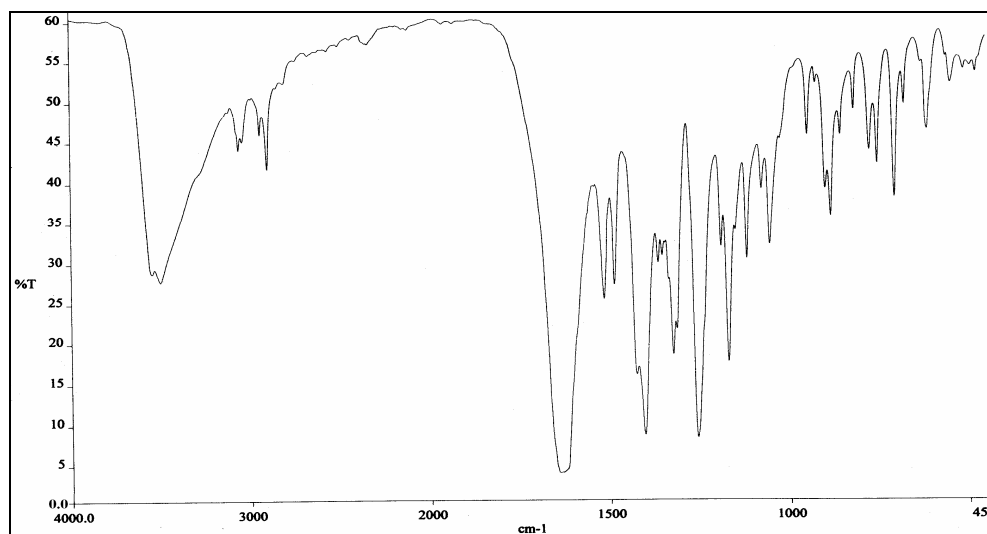


Figure 5.25 FT-IR spectra of complex 5.6

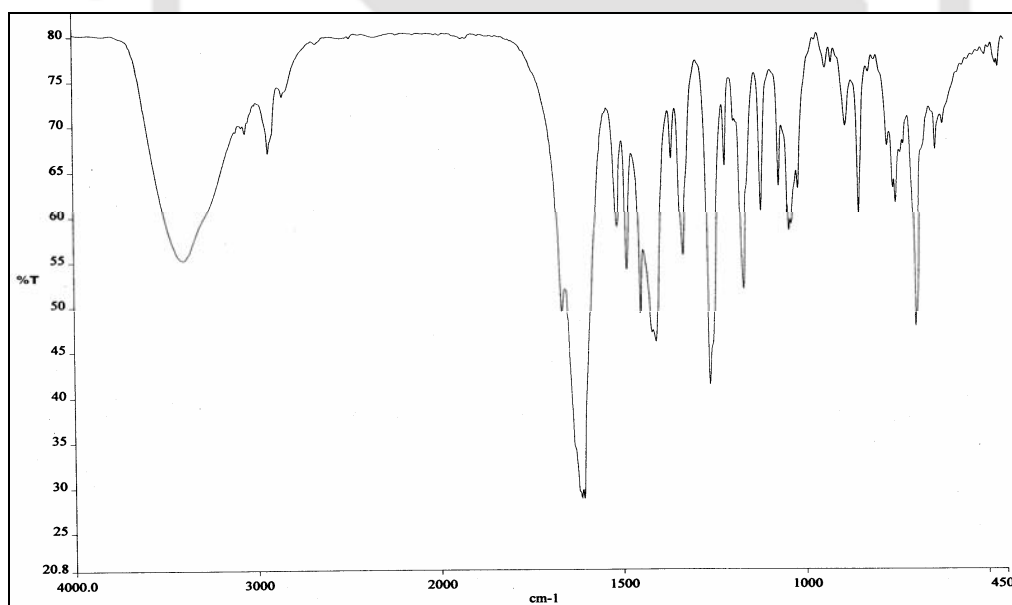
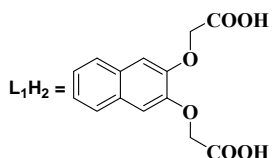


Figure 5.26 FT-IR spectra of complex 5.7

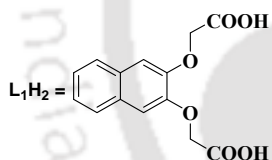
Complex 5.8: $[\text{NaZn}(\text{L}_1)(\text{CH}_3\text{COO})(\text{Pyrazole})(\text{MeOH})_2]$



The ligand L_1H_2 (0.273g, 1 mmol) was dissolved in methanol (20 ml) along with sodium hydroxide (0.080 g, 2 mmol) by heating. To this solution zinc(II) acetate dihydrate (0.219 g, 1 mmol) was added and stirred for 20 minutes. The solution was brought to room temperature. Pyrazole (0.10 g, 1.5 mmol) was added to the reaction mixture and stirred for further 20 minutes. The resulting solution was filtered off and kept for crystallization. After 6 days colourless crystals of the complex **5.8** were formed. Crystalline yield: 34%.

FT-IR (KBr, cm^{-1}): 3573 (bs), 3382 (bs), 3237 (bs), 3139 (w), 2910 (bw), 1620 (s), 1576 (s), 1514 (s), 1487 (m), 1425 (s), 1407 (s), 1340 (s), 1256 (s), 1176 (s), 1121 (s), 1061 (s), 948 (m), 904 (m), 888 (s), 858 (s), 797 (s), 775 (s), 706 (m), 682 (s), 615 (s).

Complex 5.9: $\{[Zn(L_1)(Pyrazole)_3].DMF\}_n$ and **Complex 5.10:** $[Zn_4(L_1)_4(Pyrazole)_4(H_2O)_8].DMF$



Dicarboxylic acid L_1H_2 (0.273 g, 1 mmol) was dissolved in a mixed solvent of methanol and dimethylformamide (3:1; 20 ml) by warming. To this solution zinc(II) acetate dihydrate (0.438 g, 2 mmol) was added. After stirring at room temperature for 20 minutes, pyrazole (0.34 g, 5 mmol) was added to this solution. The resulting solution was filtered to discard any insoluble material if any, and the filtrate was kept for crystallization. After 12 days flower like colourless crystals of complex **5.10** were appeared. The crystals for **5.9** were obtained after 20 days. Both these crystals were collected separately and characterised.

Complex 5.9: Yield: 63 %,

Elemental analysis $C_{26}H_{29}N_7O_7Zn$: calculated C, 50.57; H, 4.74; found C, 50.58; H, 4.70.

FT-IR (KBr, cm^{-1}): 3272 (ms), 3135 (mb), 3060 (wb), 2936 (wb), 2856 (wb), 2794 (wb), 2677 (wb), 1652 (m), 1600 (s), 1510 (m), 1485 (s), 1406 (s), 1363 (m), 1326 (m), 1258 (s), 1170

(s), 1120 (s), 1066 (s), 1048 (m), 942 (s), 911 (s), 892 (m), 872 (m), 850 (m), 771(s), 645 (m), 613 (m).

Complex 5.10: Yield: 6 %,

FT-IR (KBr, cm^{-1}): 3213 (bs), 3146 (m), 3119 (m), 2925 (wb), 1646 (m), 1591 (s), 1523 (m), 1468 (s), 1405 (s), 1380 (s), 1349 (s), 1274 (m), 1255 (m), 1164 (s), 1126 (s), 1056 (s), 952 (w), 908 (w), 880 (m), 803 (s), 770 (s), 682 (s), 628 (s).

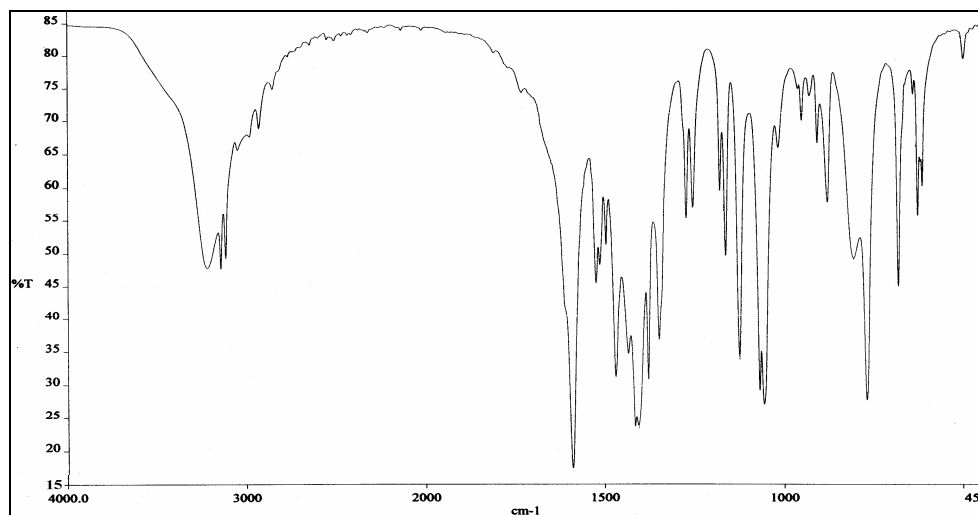
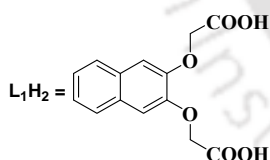


Figure 5.27 FT-IR spectra of complex **5.10**

Complex 5.11: $[\text{Zn}(\text{L}_1)(1,10\text{-Phenanthroline})_2] \cdot 3\text{H}_2\text{O}$

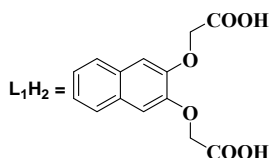


The ligand L_1H_2 (0.273 gm, 1 mmol) was dissolved in methanol (20 ml) by warming at 80°C and after dissolution the solution was allowed to attain room temperature, then zinc(II) acetate dihydrate (0.438 g, 2 mmol) was added to it and the resulting solution was stirred for 15 minutes at room temperature. To this solution 1,10-phenanthroline (0.360 g, 2mmol) was added and stirred for 10 minutes. The colourless crystalline complex **5.11** was obtained after 10 days. Yield: 53%,

FT-IR (KBr, cm^{-1}): 3453 (bs), 3066 (w), 1606 (s), 1513 (w), 1420 (s), 1328 (m), 1254 (s), 1168 (w), 1112 (w), 1039 (s), 855 (s), 728 (m);

$^1\text{H-NMR}$ (DMSO- d_6): 8.84 (4H, bs), 8.69 (4H, bs), 8.14 (4H, bs), 7.83 (4H, s), 7.47 (2H, bs), 7.24 (2H, bs), 6.99 (2H, bs), 4.35 (4H, s).

Complex 5.12: $[\text{Zn}(\text{L}_1)(2,2'\text{-bipyridine})_2]\cdot 7\text{H}_2\text{O}$



The dicarboxylic acid L_1H_2 (0.273 g, 1 mmol) was dissolved in 20ml of methanol by warming, to this solution zinc(II) acetate dihydrate (0.438 g, 2 mmol) was added and stirred for 15 minutes at room temperature. To this reaction mixture 2,2'-bipyridine (0.312 g, 2mmol) was added and stirred for further 10 minutes. The solution was filtered off and the filtrate on standing for 10 days gave colourless crystals of the complex **5.12**. Yield: 43%.

FT-IR (KBr, cm^{-1}): 3444 (bs), 1632 (s), 1483 (w), 1409 (s), 1322(s), 1252 (s), 1168 (s), 1114 (w), 1024 (m), 861 (m), 770 (m).

$^1\text{H-NMR}$ (DMSO- d_6): 8.67 (4H, bs), 8.49 (4H, bs), 8.09 (4H, bs), 7.55 (6H, bs), 7.27 (2H, bs), 7.11(2H, bs), 4.43 (4H, s).



Chapter 6

Structural aspects and acid/anion recognition properties of carboxylic acid derivatives

Development of simple receptors capable of recognizing biologically relevant anions such as fluoride, chloride, phosphate, and carboxylate has achieved considerable interest in the recent past³³⁷. Acid or anion recognition is an important process in nature, being involved in the catalytic activity of enzymes, in the transfer of genetic information, and in ion transport through membrane channels etc³³⁸. Host-guest chemistry of receptors having fluorescence properties is important for design of sensors³³⁹ and material chemistry³⁴⁰. Binding ability of receptors for selective purpose needs careful attention. Moreover in solution they may exist in different forms and identification of each form becomes difficult. However, one of the ways to understand properties of different forms that may exist in solution is by screening different co-crystals with different guests³⁴¹. Selective complexation of carboxylate anions by natural and synthetic hosts is a topic of interest in bioorganic and supramolecular chemistry³⁴²⁻³⁴³, because these species are involved in several molecular recognition phenomena in biology. In this chapter the synthesis and characterization of some 8-hydroxyquinoline derived amides and study of their structural and acid recognition properties in solid and solution state are described.

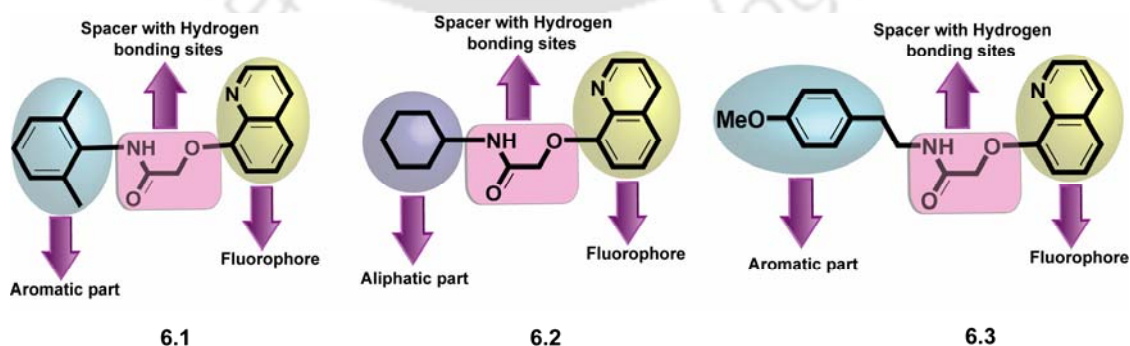


Figure 6.1

In order to understand the effect of pre-organization of binding sites and size-shape complementarities of the host molecules towards anion recognition, we have synthesized

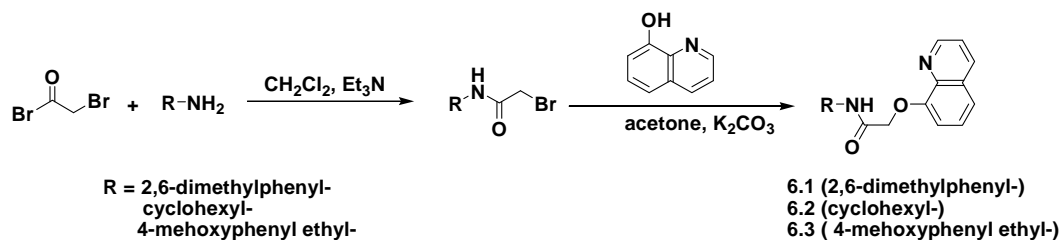
three amides namely N-(2,6-dimethylphenyl)-2-(quinolin-8-yloxy) acetamide (**6.1**), N-cyclohexyl-2-(quinolin-8-yloxy) acetamide (**6.2**), N-[2-(4-methoxy-phenyl)-ethyl]-2-(quinolin-8-yloxy) acetamide (**6.3**) and studied their acid binding properties. We have chosen such type of molecules as receptor due to the following reasons.

- 1) These types of receptors contain one 8-hydroxyquinoline group which may act as fluorophore. So, one can easily monitor the acid/anion recognition process by both fluorescence and NMR spectroscopy.
- 2) The aromatic or aliphatic part in these molecules is connected to 8-hydroxyquinoline part through a spacer having hydrogen bonding sites. Due to the spacer these receptors may bind different types of anions through hydrogen bonding. Three receptors are pictorially represented in Figure 6.1.

The design and synthesis of soft supramolecular materials such as hydrogels, through cation or anion coordination, is an emerging field of research³⁴⁴. This is because hydrogelators have potential applications in tissue engineering³⁴⁵, drug delivery³⁴⁶, and sensors³⁴⁷. An important issue in this context is the elucidation of the structure of the gelator molecule itself, which could help in identifying the interactions that induce hydrogel formation³⁴⁸. In this regard the formation of gel by small molecules attracts attention due to their simple structural features and they can also be used as model for macromolecular compounds³⁴⁹. In the context of gels the photo-luminescent gels are of prime concern, thus gels with fluorophores are of great interest³⁵⁰. On a broad perspective, such studies will enable us to gain insight and may control the process of hydrogel (or organogel) formation by tuning the intermolecular interactions. With this background, we have synthesized the compounds **6.1** and **6.2** to study their acid recognition property in solid as well as in solution phase. In the solutions phase, intermolecular interactions between the molecules result in perceptible changes in the luminescence of the 8-hydroxyquinolyl groups corresponding to aqueous environment and presence of aqueous acids.

6.1 Structural study of receptors

Compounds **6.1** and **6.2** were prepared in two steps starting from bromoacetyl bromide as illustrated in Scheme 6.1. In the first step the reaction of bromoacetyl bromide with amine lead to the corresponding amide, which is further reacted with 8-hydroxyquinoline to synthesize the corresponding receptors (**6.1** or **6.2**)³⁵⁶.



Scheme 6.1

Compound **6.1** (host) crystallizes from dichloromethane as a monohydrate (**6.1A**). The crystal structure of **6.1A** shows that two symmetry non equivalent molecules are present in the lattice and the water molecule is held inside a self-assembled cavity formed by two molecules of the host (Figure 6.2). The N–H proton of the host molecule interacts with the water molecule through intermolecular N2–H···O5 [$d_{\text{N2}\cdots\text{O5}}$ 2.835 Å, $\angle\text{D-H}\cdots\text{A}$ 162.1°] and N4–H···O5 [$d_{\text{N4}\cdots\text{O5}}$ 2.845 Å, $\angle\text{D-H}\cdots\text{A}$ 158.9°] interactions. The water molecule is also hydrogen bonded with nitrogen of 8-hydroxyquinoline ring through O5–H···N1 [$d_{\text{O5}\cdots\text{N1}}$ 2.852 Å, $\angle\text{D-H}\cdots\text{A}$ 177.8°] and O5–H···N3 [$d_{\text{O5}\cdots\text{N3}}$ 2.829 Å, $\angle\text{D-H}\cdots\text{A}$ 176.5°] hydrogen bonds (Table 6.1). It may be noted that, the molecules are assembled in lattice via head-to-head arrangement.

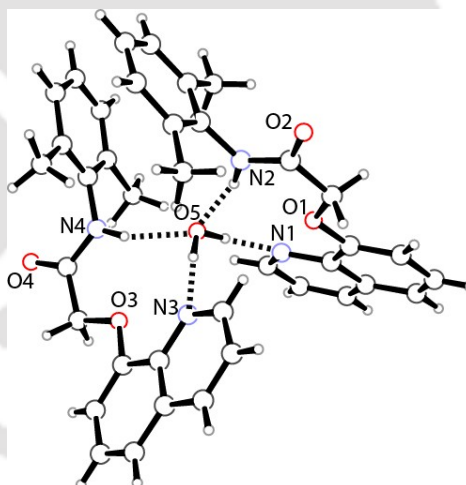


Figure 6.2 Structure of the dimeric capsules of **6.1A** assembled by an encapsulated water molecule

The self-assembly in the lattice is stabilised by weak C29–H···O4 [$d_{\text{C29}\cdots\text{O4}}$ 3.601 Å, 169.3°] interactions leading to hydrogen bonded dimeric assembly, wherein C29–H serves as a donor and O4 serves as an acceptor. The aromatic hydrogen of hydroxyquinoline is involved in weak C8–H··· π [$d_{\text{C8}\cdots\pi}$ 3.699 Å] interaction with aromatic π -system of 2,6-dimethylaniline ring, which provides the extra stability in the lattice.

Table 6.1: Hydrogen bond geometry(Å, °) in **6.1A**

D–H⋯A	d(D–H)	d(H⋯A)	d(D⋯A)	<D–H⋯A
N(2)–H(2N)⋯O(5)	0.90	1.96	2.835	162.1
N(4)–H(4N)⋯O(5)	0.88	2.01	2.845	158.9
O(5)–H(1S)⋯N(1)	0.91	1.94	2.852	177.8
O(5)–H(2S)⋯N(3)	0.92	1.92	2.829	176.5
C(29)–H(29B)⋯O(4)	0.97	2.64	3.601	169.3

The compound **6.1**, when crystallised from benzene-water mixture another pseudo-polymorphic form was obtained which crystallizes in orthorhombic $P2_12_12_1$ space group (**6.1B**). The crystal structure shows that the host molecule crystallizes along with a water molecule (Figure 6.3A). In this structure the host molecule does not form dimeric assembly, but it assembles in the lattice through extended hydrogen bonded structure as illustrated in Figure 6.3B. One of the amide hydrogens of N-(2,6-dimethylphenyl)-2-(quinolin-8-yloxy) acetamide involves in hydrogen bonding with oxygen of water through N2–H⋯O3 [$d_{N2\cdots O3}$ 2.825 Å, $\angle D-H\cdots A$ 157.1°] interaction.

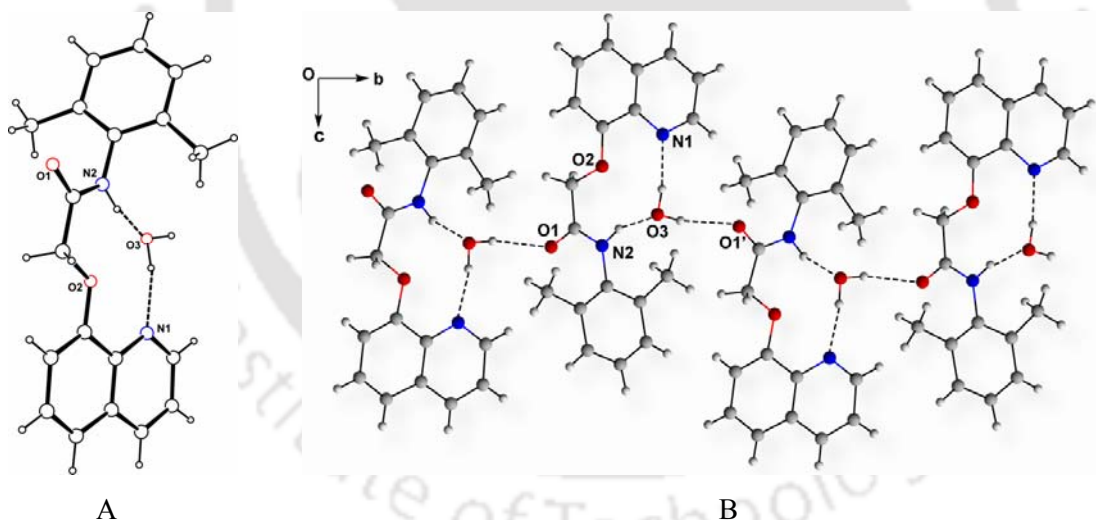


Figure 6.3 A) Crystal structure of **6.1B**, B) One dimensional hydrogen bonded assembly of **6.1B**.

The water molecule further involves in hydrogen bonding with amide oxygen and nitrogen of 8-hydroxyquinoline group through O3–H⋯O1 [$d_{O3\cdots O1}$ 2.829 Å, $\angle D-H\cdots A$ 168.2°] and O3–H⋯N1 [$d_{O3\cdots N1}$ 2.785 Å, $\angle D-H\cdots A$ 165.7°] interactions, respectively (Table 6.2). By the help of intermolecular hydrogen bonding interactions, the host molecules along with a water molecule assemble leading to extended hydrogen bonded zig-zag assembly along [100] plane.

Besides this the aromatic protons are further involved in C10–H $\cdots\pi$ [$d_{\text{C10}\cdots\pi}$ 3.666Å] and C19–H $\cdots\pi$ [$d_{\text{C19}\cdots\pi}$ 3.545Å] interaction, which stabilizes the one dimensional hydrogen bonded assembly.

In FT-IR spectra a broad band appeared at 3454 cm^{-1} , due to N–H stretching of the amide group and the C=O stretching frequency appears at 1657 cm^{-1} . A strong absorption band at 1257 cm^{-1} for C–O stretching of ether group is observed. The amide proton shows a broad singlet peak at 9.37 ppm in the ^1H -NMR spectra. The aromatic protons appear in between 6.93-8.73 ppm. The methyl and methylene protons show two singlet peaks at 2.08 and 4.89 ppm, respectively.

Table 6.2: Hydrogen bond geometry(Å, °) in **6.1B**

D–H \cdots A	d(D–H)	d(H \cdots A)	d(D \cdots A)	<D–H \cdots A
O(3)–H(3A) \cdots N(1) [x-1, y, z]	0.92	1.88	2.785	165.7
O(3)–H(3B) \cdots O(1) [-x+1,y+1/2,-z+3/2]	0.82	2.02	2.829	168.2
N(2)–H(2N) \cdots O(3) [x+1, y, z]	0.92	1.96	2.825	157.1
C(13)–H(13) \cdots O(3)	0.93	2.58	3.432	151.8

Similarly compound **6.2** is found to crystallize as a pentahydrate in triclinic P-1 space group from wet toluene. Self-assembled dimeric capsule formed by the host molecule encapsulates one of the water molecules (Figure 6.4A). The encapsulated water molecule is stabilized by intermolecular N2–H \cdots O5 [$d_{\text{N2}\cdots\text{O5}}$ 2.905 Å, <D–H \cdots A 164.7°] and N4–H \cdots O5 [$d_{\text{N4}\cdots\text{O5}}$ 2.883 Å, <D–H \cdots A 157.6°] interactions where amide proton act as donor and water oxygen behave as acceptor atom. Other than this, the encapsulated water molecule is also involved in intermolecular hydrogen bonding with the nitrogen atom of hydroxyquinoline through O–H \cdots N [$d_{\text{O5}\cdots\text{N3}}$ 2.786 Å, <D–H \cdots A 164.2°, $d_{\text{O5}\cdots\text{N1}}$ 2.800 Å, <D–H \cdots A 168.5°] interactions. Intermolecular O–H \cdots O interactions between the water molecules O6, O7, O8, O9 and O4 of the host (as bifurcated acceptor) result in 5-membered cyclic hydrogen bonded ring structure. Moreover, O6–H \cdots O9 [$d_{\text{O6}\cdots\text{O9}}$ 2.849 Å, <D–H \cdots A 172.4°] and O9–H \cdots O6 [$d_{\text{O9}\cdots\text{O6}}$ 2.870 Å, <D–H \cdots A 160.0°] hydrogen-bonding interactions between the crystallographically independent water molecules, O6 and O9 leads to the formation of distinct four membered cyclic water clusters which are flanked by 5-membered cyclic structures (Figure 6.4B)

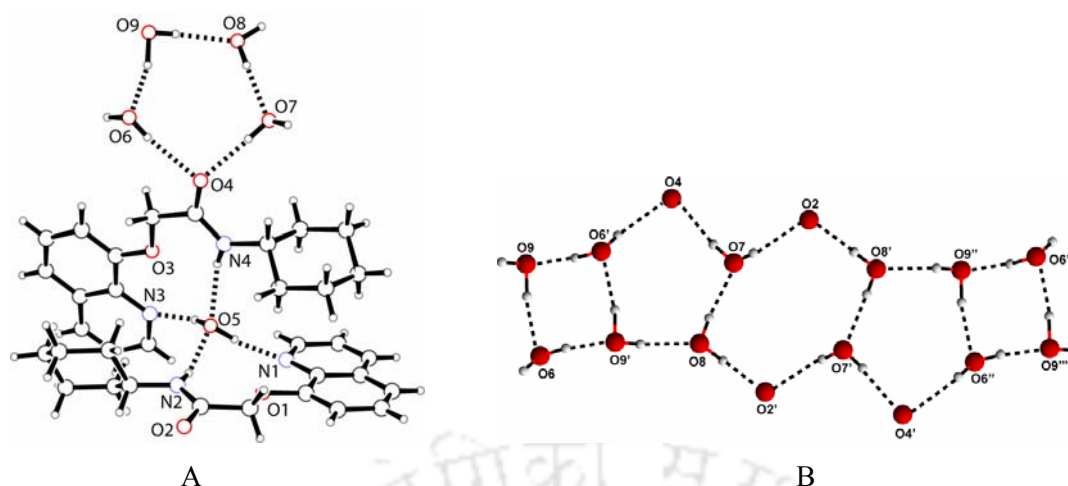


Figure 6.4 A) Structure of the hydrate of **6.2**, B) Hydrogen bonded one dimensional network of water

It is also observed that intermolecular hydrogen-bonding interactions viz. $O7-H\cdots O2$ [$d_{O7\cdots O2}$ 2.856 Å, $\angle D-H\cdots A$ 171.7°] and $O8-H\cdots O2$ [$d_{O8\cdots O2}$ 2.818 Å, $\angle D-H\cdots A$ 171.9°] between the two water molecules, O7 and O8 and O2 of the host molecule (as bifurcated acceptor) result in the formation hexameric hydrogen bonded networks. Some of the important hydrogen bonding parameters are listed in Table 6.3. The water molecules are assembled through hydrogen bonding interaction and result in the formation of infinite 2D hydrogen bonded networks parallel to [110]. FT-IR spectrum of compound **6.2** is shown in Figure 6.33.

Table 6.3: Hydrogen bond geometry (Å, °) for compound **6.2**

D-H \cdots A	d (D-H)	d (H \cdots A)	d (D \cdots A)	$\angle D-H\cdots A$
N(2)-H(2N) \cdots O(5)	0.75	2.18	2.905	164.7
N(4)-H(4N) \cdots O(5)	0.85	2.08	2.883	157.6
O(5)-H(2O) \cdots N(1)	0.95	1.86	2.800	168.5
O(5)-H(1O) \cdots N(3)	0.88	1.93	2.786	164.2
O(6)-H(4O) \cdots O(4)	0.82	2.12	2.935	172.1
O(7)-H(5O) \cdots O(4)	0.84	1.96	2.804	178.3
O(6)-H(3O) \cdots O(9) [x, y, z-1]	1.02	1.84	2.849	172.4
O(7)-H(6O) \cdots O(2) [1-x, -y, 1-z]	0.80	2.06	2.856	171.7
O(8)-H(7O) \cdots O(7) [x+1, y, z]	0.86	1.89	2.748	173.0
O(8)-H(8O) \cdots O(2) [x, 1+y, z]	0.88	1.94	2.818	171.9
O(9)-H(9O) \cdots O(8) [-x+1, -y+1, -z+1]	0.83	1.94	2.762	174.0
O(9)-H(10O) \cdots O(6) [-x, -y+1, -z+1]	1.00	1.91	2.870	160.0

The water is ubiquitous in biology and in chemistry, has motivated researchers to investigate the structural impacts of water molecules in the crystal lattice of molecular crystals as well as in crystal hydrates³⁵¹. The understanding gained from the structural study of such water clusters in crystal lattice has rarely been followed up, except in the design of porous materials. In this regard it is envisaged that the formation of water clusters through self-assembly of molecules and subsequent elucidation of the structural aspects may provide clues that may enable correlating the intermolecular interactions in the molecular assemblies with mesoscopic properties such as hydrogelation. It may be noted that the dimeric capsule formed by **6.1** involves head-to-head self-assembly of the host molecule whereas the corresponding capsule of **6.2** involves head-to-tail assembly as shown in Figure 6.5. The self-assembled capsules in **6.1** are stabilized by C–H···O interactions whereas in **6.2** self-assembly is observed due to the templating effect of the encapsulated water molecule.

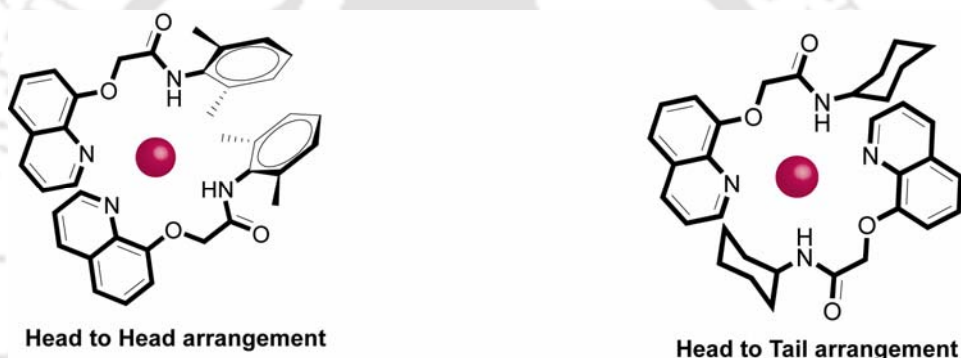
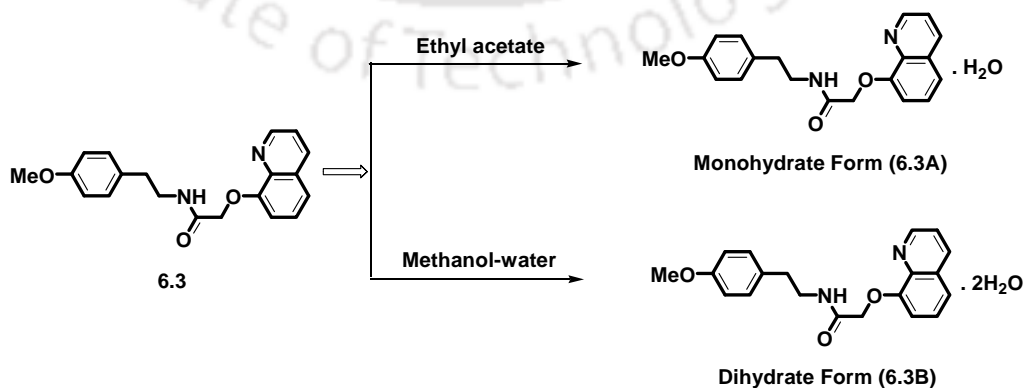


Figure 6.5 Head to head and head to tail arrangement of receptors.

Two pseudo-polymorphs of N-[2-(4-methoxy-phenyl)-ethyl]-2-(quinolin-8-yloxy)acetamide (**6.3**) can be easily prepared by varying the solvent of crystallization as shown in scheme 6.2.



Scheme 6.2

When we crystallized the compound **6.3** from dichloromethane we obtained the anhydrous form i.e. the compound **6.3** was crystallized without any solvent molecule. If we crystallize this compound from ethyl acetate or methanol-water it crystallizes as monohydrate and dihydrate respectively. We have studied the structure of N-[3-(4-methoxyphenyl)propyl]-2-(quinolin-8-yloxy)acetamide (**6.3**) to understand the type of hydrogen bonding.

The compound **6.3** crystallizes in orthorhombic $P2_12_12_1$ space group. The crystal structure of **6.3** shows that it has a parallel sheet type arrangement having intermolecular $N2-H\cdots O2$ [$d_{N2\cdots O2}$ 2.904(3) Å, $\angle D-H\cdots A$ 140.9(2)°] interaction, in which the N–H proton act as donor and the amide oxygen as acceptor atom (Figure 6.6B). This compound prefers to remain as self-assembly and does not prefer to form hydrated compound. The ring proton of quinoline participates in hydrogen bonding with amide oxygen through $C3-H\cdots O2$ [$d_{C3\cdots O2}$ 3.566 Å, $\angle D-H\cdots A$ 154.7°] interaction. Other than this the compound self-assembles via $C8-H\cdots\pi$ [$d_{C8\cdots\pi}$ 3.794 Å] and $C10-H\cdots\pi$ [$d_{C10\cdots\pi}$ 3.612 Å] interactions.

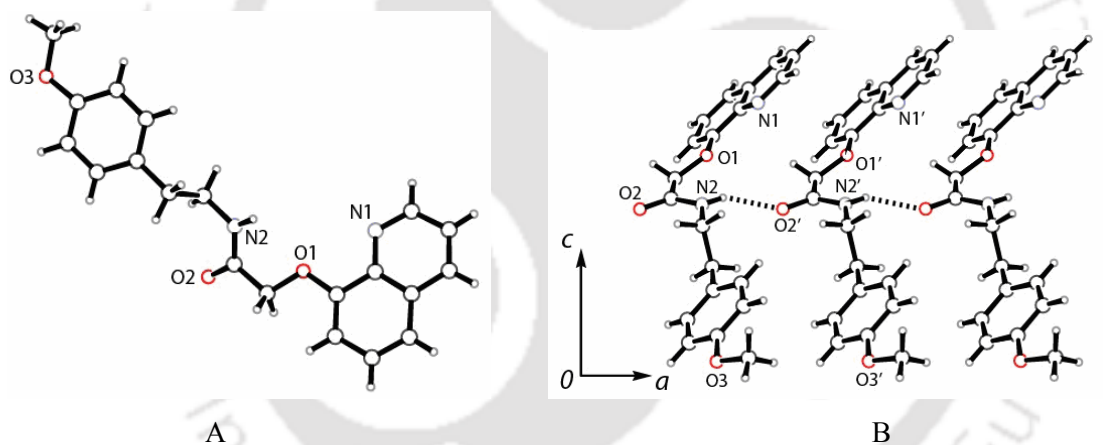


Figure 6.6 A) Structure of N-[3-(4-methoxy-phenyl)propyl]-2-(quinolin-8-yloxy)acetamide (**6.3**), B) 1D hydrogen bonded assembly of the molecules in the solid-state showing the formation of sheet-like structure

The crystal structures of monohydrate (**6.3A**) and dihydrate (**6.3B**) are determined by X-ray crystallography. The monohydrate of the compound **6.3** has self assembled dimeric structure. Two N-[2-(4-methoxy-phenyl)-ethyl]-2-(quinolin-8-yloxy) acetamide molecule are assembled with two water molecules through hydrogen bonding interactions leading to a dimer like structure. In the dimeric structure two amide molecules are arranged in a head to tail orientation (Figure 6.7B). In this arrangement the oxygen atom of the methoxy group forms hydrogen bond with the water molecule through intermolecular $O4-H\cdots O1$ [$d_{O4\cdots O1}$ 3.007 Å, $\angle D-H\cdots A$ 166.2°] interaction. Another hydrogen atom of water molecule is also hydrogen

bonded to quinoline nitrogen with O4–H \cdots N2 [$d_{O4\cdots N2}$ 2.762 Å, \angle D–H \cdots A 174.1°] interaction.

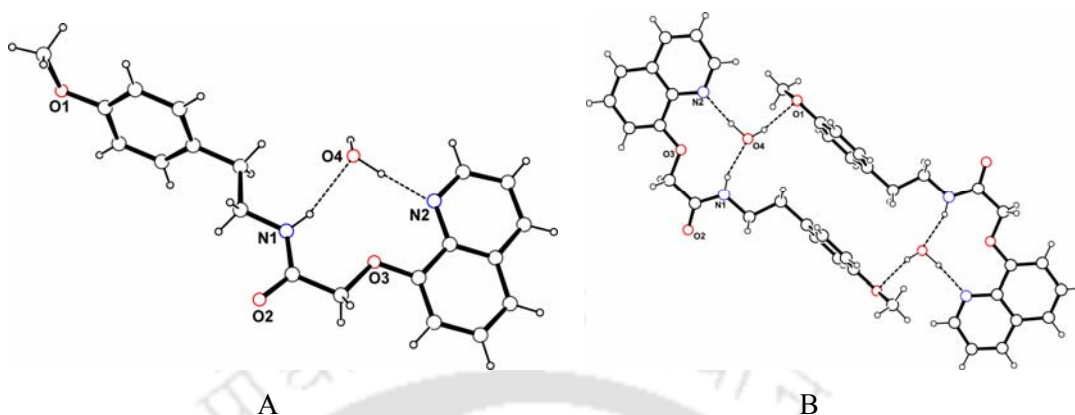


Figure 6.7 A) Crystal structure of monohydrate form (**6.3A**), B) Hydrogen bonded dimeric assembly of **6.3A**.

In N1–H \cdots O4 [$d_{N1\cdots O4}$ 2.932 Å, \angle D–H \cdots A 162.3°] interaction the amide hydrogen behave as donor and the oxygen of water as an acceptor (Table 6.4). Some of the aromatic ring protons also participate in C6–H6 \cdots O2 [$d_{C6\cdots O2}$ 3.424 Å, \angle D–H \cdots A 169.6°] and C14–H14 \cdots O2 [$d_{C14\cdots O2}$ 3.309 Å, \angle D–H \cdots A 146.0°] hydrogen binding interactions with amide oxygen. Besides these the aromatic protons are further involved in C7–H $\cdots\pi$ [$d_{C7\cdots\pi}$ 3.686Å] and C19–H $\cdots\pi$ [$d_{C19\cdots\pi}$ 3.774Å] interaction, which stabilize the hydrogen bonded assembly.

Table 6.4: Hydrogen bond geometry(Å, °) in **6.3A**

D–H \cdots A	d(D–H)	d(H \cdots A)	d(D \cdots A)	\angle D–H \cdots A
N(1)–H(1N) \cdots O(4)	0.84(19)	2.12(17)	2.932(2)	162.3(16)
O(4)–H(4A) \cdots N(2)	0.98(2)	1.79(3)	2.762(2)	174.1(2)
O(4)–H(4B) \cdots O(1) [-x, 1-y, 1-z]	0.84(2)	2.18(2)	3.007(19)	166.2(2)
C(6)–H(6) \cdots O(2) [-1+x, y, z]	0.93	2.50	3.424(2)	169.6
C(14)–H(14) \cdots O(2) [2-x, -y, 2-z]	0.93	2.50	3.309(2)	146.0

The dihydrate form (**6.3B**) is obtained upon the crystallization of compound **6.3** from methanol-water. The compound **6.3B** is crystallizes in Monoclinic Cc space group and it has an extended hydrogen bonded structure (Figure 6.8A). One of the water molecules is hydrogen bonded with receptor through N1–H \cdots O3 [$d_{N1\cdots O3}$ 2.945 Å, \angle D–H \cdots A 153.3°] and O3–H \cdots N2 [$d_{O3\cdots N2}$ 2.810 Å, \angle D–H \cdots A 171.7°] interactions (Table 6.5). The extended structure in the dihydrate is formed by the interaction of this hydrogen bonded water molecule

with an additional intervening water molecule through intermolecular O3–H···O4 [$d_{O3\cdots O4}$ 2.820 Å, $\angle D-H\cdots A$ 178.0°] interaction (Figure 6.8B).

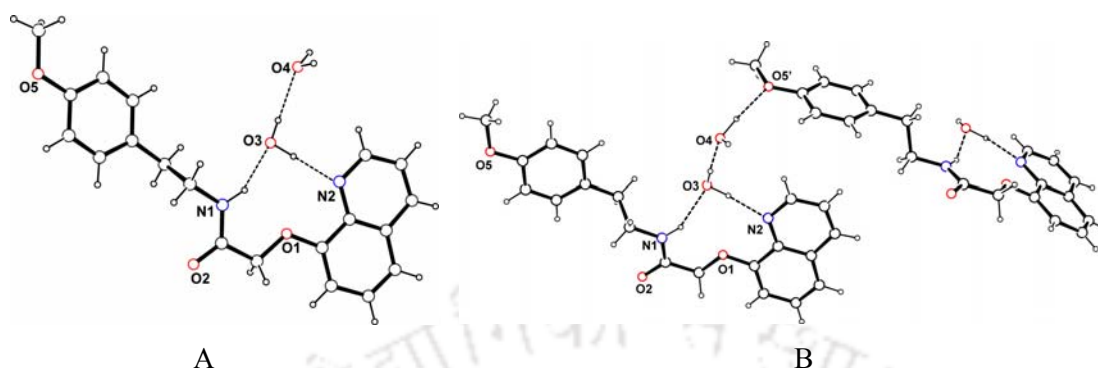


Figure 6.8 A) Structure of **6.3B**, B) Hydrogen bonded assembly of **6.3B**.

The methoxy groups attached to the aromatic ring is also intermolecularly hydrogen bonded to a water molecule through O4–H···O5 [$d_{O4\cdots O5}$ 2.907 Å, $\angle D-H\cdots A$ 167.6°] interaction leading to a zig-zag extended hydrogen bonding network. The two water molecules are hydrogen bonded in such a manner that an one dimensional zig-zag chain type of structure is formed. Aromatic π -stacking interactions ($d_{\pi\cdots\pi}$ 3.386 Å) between the quinoline rings provide the extra stability to the lattice. The ability to form different pseudo-polymorph of **6.3** suggested that the molecule would interact with varieties of molecules for formation of co-crystals through hydrogen bond.

Table 6.5: Hydrogen bond geometry(Å, °) in **6.3B**

D–H···A	d(D–H)	d(H···A)	d(D···A)	$\angle D-H\cdots A$
N(1)–H(1N)···O(3)	0.95(4)	2.07(5)	2.945(5)	153.3(3)
O(3)–H(3A)···N(2)	0.96(7)	1.86(7)	2.810(5)	171.7(8)
O(3)–H(3B)···O(4) [$1/2+x, 1/2+y, z$]	0.85(4)	1.98(4)	2.820(5)	178.0(4)
O(4)–H(4A)···O(3) [$-1/2+x, 1/2+y, z$]	0.73(5)	2.08(5)	2.793(5)	163.4(7)
O(4)–H(4B)···O(5) [$x, 1-y, 1/2+z$]	0.99(7)	1.93(7)	2.907(5)	167.6(4)

Each of these forms namely anhydrous, monohydrate and dihydrate can be distinguished by solid state IR spectra. The anhydrous form has sharp N–H absorption at 3328cm^{-1} this absorption occurs at 3572cm^{-1} and 3545cm^{-1} in monohydrate and dihydrate respectively as shown in Figure 6.9.

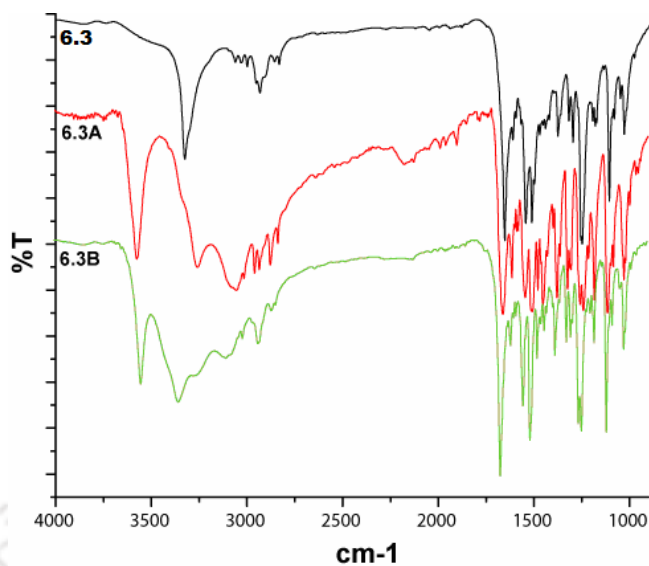
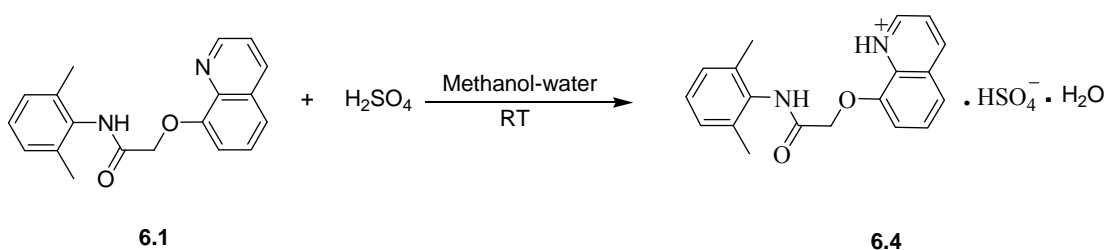


Figure 6.9 FT-IR spectra of three pseudo polymorphs

By $^1\text{H-NMR}$ spectra in solution the three co-crystals can not be distinguished. The amide proton appears at 7.99 ppm as broad singlet. The aromatic protons appear at 8.79, 8.15, 7.45, 7.08, 6.95, 6.61 ppm and two quartet peaks appear at 3.53 and 2.72 ppm due to the methylene protons. ^{13}C NMR spectrum of compound **6.3** is shown in Figure 6.34.

6.2 Salt and gel formation study of receptors

In order to establish the structure of the protonated state, compound **6.1** was crystallised from aqueous solution of hydrochloric acid, sulfuric acid, nitric acid, phosphoric acid and perchloric acid. These salts show strong tendency to give flaky crystals. Only the bisulfate and nitrate salts were found to be suitable for single crystal structure determination. N-(2,6-dimethylphenyl)-2-(quinolin-8-yloxy) acetamide (**6.1**) forms 1:1 molecular salt (**6.4**) with sulphuric acid (Scheme 6.3) which is isolated as colorless crystals and characterized by spectroscopic techniques.



Scheme 6.3

IR spectra of **6.4** in solid state shows two sharp absorption at 1305 and 1136 cm^{-1} arising from the S=O stretching vibrations of the sulphate groups and another sharp absorption at 1674 cm^{-1} is attributed to the amide group of **6.3**. The -NH protons are not present in $^1\text{H-NMR}$ spectra of **6.4** in D_2O at room temperature (Figure 6.10). If we compare the $^1\text{H-NMR}$ spectra of **6.1** and **6.4**, it is observed that after protonation the aromatic protons are shifted towards the downfield.

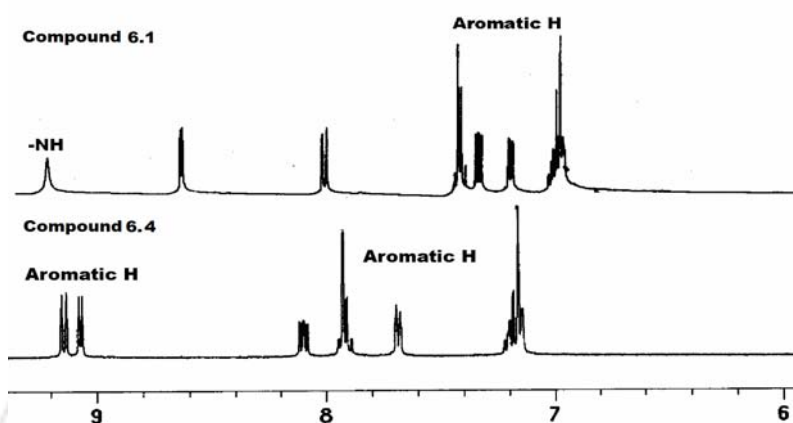


Figure 6.10 $^1\text{H-NMR}$ spectra of receptor (**6.1**) and its sulphate salt (**6.4**)

Crystal structure of **6.4** shows that it is co-crystal of two protonated cations of **6.1** along with two HSO_4^- anions and a molecule of water. It is observed that two protonated molecules of **6.1** self-assemble into hydrogen-bonded dimeric cavity-like structures, which are stabilised by the templating effect of the hydrogen sulphate anions (Figure 6.11). One of the sulphate anion is bound to the cavity formed by two symmetry non equivalent protonated host molecules through N1-H \cdots O6 [$d_{\text{N1}\cdots\text{O6}}$ 2.706 Å, $\langle\text{D-H}\cdots\text{A}$ 161.5°], N2-H \cdots O6 [$d_{\text{N2}\cdots\text{O6}}$ 2.947 Å, $\langle\text{D-H}\cdots\text{A}$ 165.5°], N3-H \cdots O7 [$d_{\text{N3}\cdots\text{O7}}$ 2.737 Å, $\langle\text{D-H}\cdots\text{A}$ 167.2°] and N4-H \cdots O7 [$d_{\text{N4}\cdots\text{O7}}$ 2.879 Å, $\langle\text{D-H}\cdots\text{A}$ 162.4°] intermolecular hydrogen bonding interactions (Table 6.6).

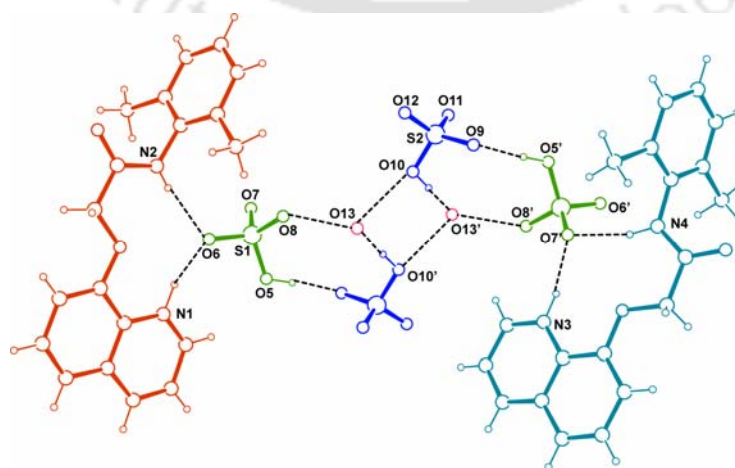


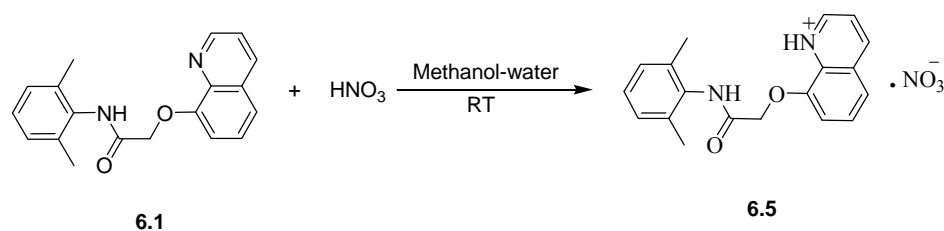
Figure 6.11 Hydrogen bonding interactions in the sulphate template assembly of **6.4**

The other crystallographically independent sulphate molecule is involved in hydrogen bonding with water and sulphate molecules through O10–H···O13 [$d_{\text{O10}\cdots\text{O13}}$ 2.700 Å, $\angle\text{D–H}\cdots\text{A}$ 158.7°] and O5–H···O9 [$d_{\text{O5}\cdots\text{O9}}$ 2.576 Å, $\angle\text{D–H}\cdots\text{A}$ 169.3°] interactions. The water molecule itself is hydrogen bonded to hydrogen sulphate anion through O13–H···O8 [$d_{\text{O13}\cdots\text{O8}}$ 2.487Å] and O13–H···O10 [$d_{\text{O13}\cdots\text{O10}}$ 2.665Å] interactions, where O8 and O10 serve as the acceptor and O13 act as donor. The H-atoms of water molecule (O13) could not be located in the Fourier maps. Moreover, weak aromatic π -stacking interactions are also observed between the quinoline rings [$d_{\pi\cdots\pi}$ 3.396 Å] of the protonated species of **6.1**, wherein the protonated host molecules adopt a head-to-tail orientation. Other than that the protonated quinoline ring is also involved in aromatic $\pi\cdots\pi$ interactions with 2,6-dimethylphenyl ring and the distance of separation is 3.325 Å.

Table 6.6: Hydrogen bond geometry (Å, °) for compound **6.4**

D–H···A	d(D–H)	d(H···A)	d(D···A)	$\angle\text{D–H}\cdots\text{A}$
N(1)–H(1N)···O(6)	0.96	1.78	2.706	161.5
N(2)–H(2N)···O(6)	0.77	2.20	2.947	165.5
N(3)–H(3N)···O(7) [x-1, y, z]	0.92	1.83	2.737	167.2
N(4)–H(4N)···O(7) [x-1, y, z]	0.88	2.03	2.879	162.4
O(5)–H(5O)···O(9) [x, y+1, z]	0.91	1.67	2.576	169.3
O(10)–H(10O)···O(13) [x, y-1, z]	0.82	1.92	2.700	158.7

The quinoline ring protons also participate in weak C8–H··· π [$d_{\text{C8}\cdots\pi}$ 3.575 Å] interaction with aromatic π -system of the 2,6-dimethylphenyl ring. Two symmetry non equivalent molecules are assembled in the lattice by weak C10–H···O4 [$d_{\text{C10}\cdots\text{O4}}$ 3.465 Å, $\angle\text{D–H}\cdots\text{A}$ 148.5°] and C18–H···O2 [$d_{\text{C18}\cdots\text{O2}}$ 3.521 Å, $\angle\text{D–H}\cdots\text{A}$ 175.7°] interactions. The oxygen atoms of hydrogen sulphate anion act as hydrogen bond acceptor in the weak C26–H···O12 [$d_{\text{C26}\cdots\text{O12}}$ 3.311 Å, $\angle\text{D–H}\cdots\text{A}$ 144.1°], C18–H···O8 [$d_{\text{C18}\cdots\text{O8}}$ 3.445 Å, $\angle\text{D–H}\cdots\text{A}$ 150.4°], and C3–H···O11 [$d_{\text{C3}\cdots\text{O11}}$ 3.541 Å, $\angle\text{D–H}\cdots\text{A}$ 161.8°] interactions.



Scheme 6.4

Similarly, compound **6.1** can be crystallised from dilute aqueous nitric acid as 1:1 molecular salt of protonated cation of **6.1** and nitrate anion as shown in Scheme 6.4. The structure of this nitrate salt (**6.5**) thus obtained was elucidated by crystallography (Figure 6.12A). In this case the asymmetric unit contains two molecules of the protonated host and two nitrate anions. Each nitrate anion is hydrogen bonded to a protonated host molecule through intermolecular N1–H···O5 [$d_{\text{N1}\cdots\text{O5}}$ 2.710 Å, $\angle\text{D-H}\cdots\text{A}$ 161.2°], N2–H···O5 [$d_{\text{N2}\cdots\text{O5}}$ 2.873 Å, $\angle\text{D-H}\cdots\text{A}$ 174.0°], N3–H···O8 [$d_{\text{N3}\cdots\text{O8}}$ 2.710 Å, $\angle\text{D-H}\cdots\text{A}$ 155.6°], and N4–H···O8 [$d_{\text{N4}\cdots\text{O8}}$ 2.992 Å, $\angle\text{D-H}\cdots\text{A}$ 154.9°] hydrogen bonding interactions. It may be noted that the hydrogen bonding interactions involving the two nitrate anions in the lattice are quite different, one of the anions is co-planar with the host molecule, while the other is almost normal to the plane of the protonated host. The quinoline ring protons are involved in intermolecular hydrogen bonding interactions with amide or nitrate oxygen through weak C4–H···O4 [$d_{\text{C4}\cdots\text{O4}}$ 3.501 Å, $\angle\text{D-H}\cdots\text{A}$ 162.1°], and C23–H···O7 [$d_{\text{C23}\cdots\text{O7}}$ 3.333 Å, $\angle\text{D-H}\cdots\text{A}$ 143.4°] interactions. Some of the hydrogen bond parameters are listed in Table 6.7.

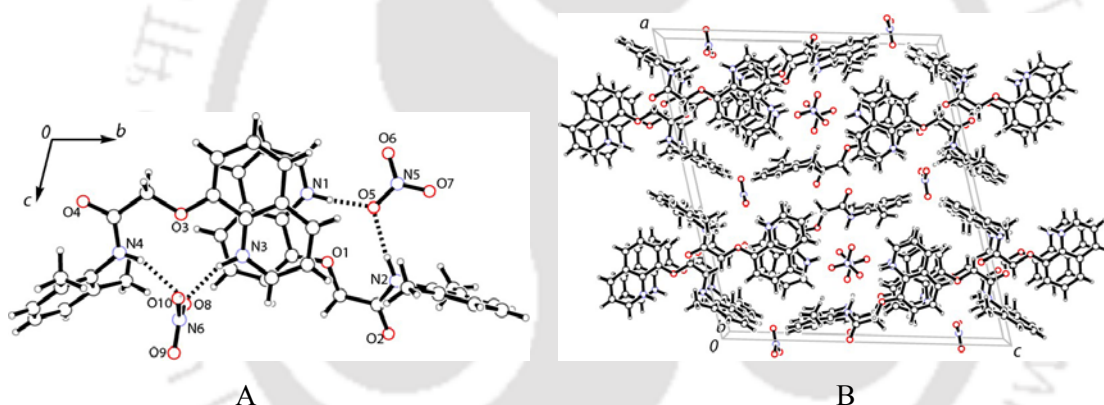


Figure 6.12 A) Structure of **6.5** showing the hydrogen bonding interaction of the nitrate anion with protonated form of the parent compound, B) crystal packing of **6.5** showing a part of the lattice displaying a channel-like structure

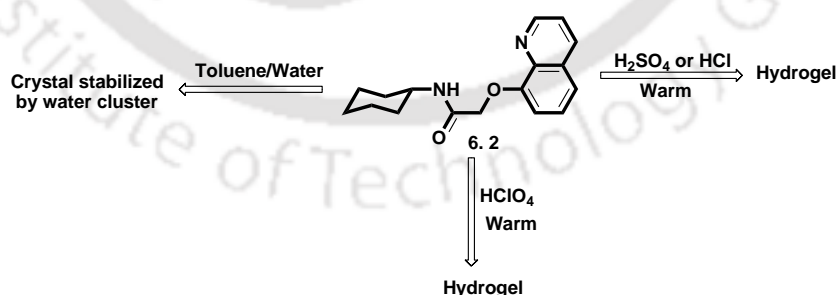
Methyl and methylene protons also participate in hydrogen bonding interactions C29–H···O4 [$d_{\text{C29}\cdots\text{O4}}$ 3.529 Å, $\angle\text{D-H}\cdots\text{A}$ 175.2°] and C38–H···O4 [$d_{\text{C38}\cdots\text{O4}}$ 3.590 Å, $\angle\text{D-H}\cdots\text{A}$ 159.1°] which provide the extra stability to the molecular assembly. Two 2,6-dimethyl phenyl rings are entailed in aromatic $\pi\cdots\pi$ interactions with each other. These rings are present in slight off-set manner and the distance between two rings is 3.373 Å. FT-IR spectra of compound **6.4** is shown in Figure 6.35. The solid-state FT-IR spectra of protonated salt shows that a strong band appeared at 1662 cm^{-1} due to C=O stretching of amide group. Two strong bands at 1384 and 1114 cm^{-1} arise for the nitrate anions present in the lattice. In $^1\text{H-NMR}$ the peaks are getting shifted towards downfield after protonation as similar to the earlier observation.

Table 6.7: Hydrogen bond geometry (\AA , $^\circ$) for compound **6.5**

D–H \cdots A	d(D–H)	d(H \cdots A)	d(D \cdots A)	\angle D–H \cdots A
N1–H1N \cdots O5	0.88	1.86	2.710	161.2
N2–H2N \cdots O5	0.94	1.94	2.873	174.0
N3–H3N \cdots O8	2.87	1.87	2.710	155.6
N4–H4N \cdots O8	0.79	2.25	2.992	154.9
C4–H4 \cdots O4	0.93	2.60	3.501	162.1
C23–H23 \cdots O7	0.93	2.54	3.333	143.4
C29–H29 \cdots O4	0.97	2.56	3.529	175.2
C38–H38A \cdots O4	0.96	2.68	3.590	159.1

From the structural investigations of the hydrogen-bonded assemblies of **6.1** and **6.2** and subsequent formation of anion template self-assemblies, it is possible that the host molecules are self-complementary and this leads to the formation of self-assembled dimeric capsules/cavities in the presence of a suitable guest molecule or anion. In each case it is found that intermolecular hydrogen bonding interactions involving the host and the guest molecule (e.g. water, or sulphate anion) provide the driving force for the self-assembly process.

Based on these observations, we attempted crystallized **6.2** from dilute acid solutions, with the expectation that the hydrophobic effect imparted by the cyclohexyl group may be enhanced due to the formation of quinolinium ions. Accordingly compound **6.2** was dissolved in dilute sulphuric acid, with slight warming. However, upon cooling, the solution became cloudy and finally transformed into a gel. Similar hydrogels were obtained from **6.2** in dilute hydrochloric acids and perchloric acids (Scheme 6.5).



Scheme 6.5

The morphology of the dehydrated hydrogels was analysed by SEM (Figure 6.13B and 6.13C) in order to get further insight into the self-assembling process. SEM analysis of the dehydrated hydrogels from **6.2** in aqueous sulfuric acid solution shows the formation of distinct aggregates of fibres that have dimensions of 5–10 μm (thickness) and approx. 100–

150 μm (length). A representative SEM image of the hydrogel formed from **6.2** in aqueous sulfuric acid is shown in Figure 6.13B.

Table 6.8

Acid	Critical gelation concentration(w/v)	Transition temperature/ $^{\circ}\text{C}$
Hydrochloric acid	0.3 M with 2.0% gelator	38
Sulfuric acid	0.3 M with 1.3% gelator	34
Perchloric acid	0.3 M with 0.8% gelator	43
Nitric acid	No gel formed	

On the other hand, the SEM images obtained from the dehydrated hydrogels from **6.2** in aqueous perchloric acid solution show that the compound self-assembles into interwoven fibre-like networks. These network structures are attributed to arise from hydrogen-bonded assemblies of the protonated amide **6.2** and the perchlorate, which subsequently assembles through aromatic π -stacking interactions.

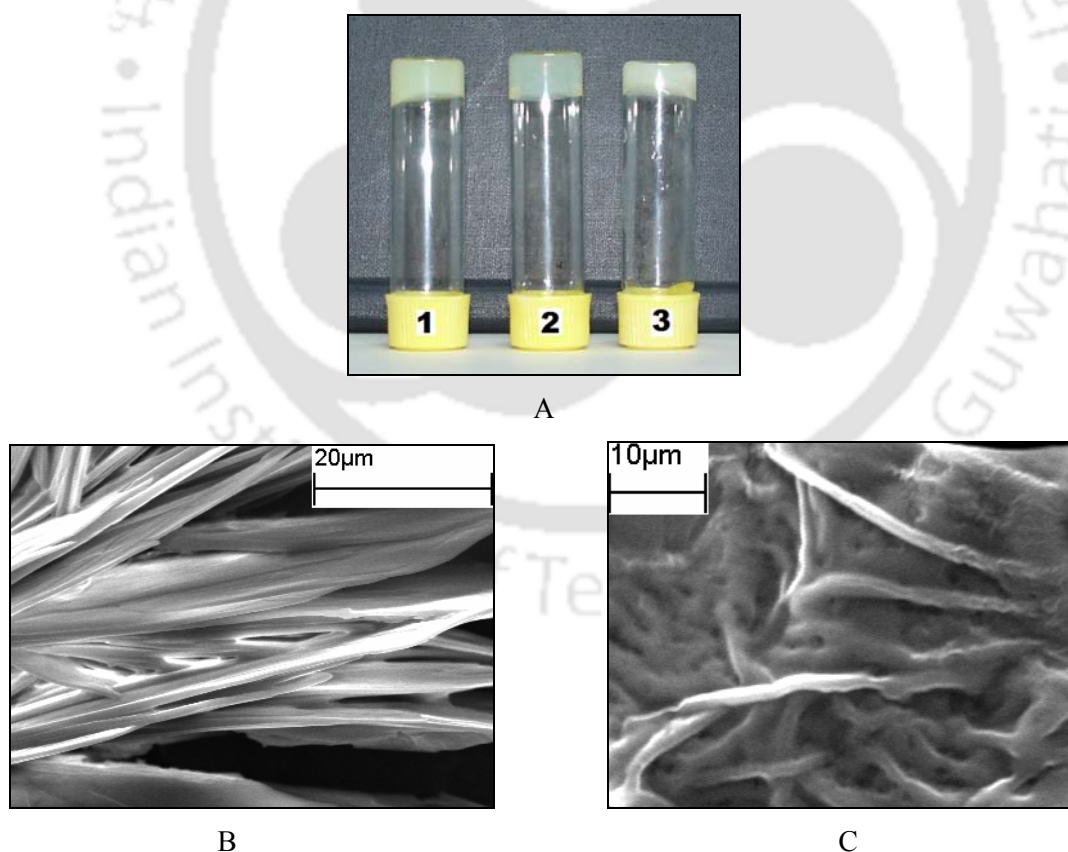


Figure 6.13 A) From left to right: gel obtained from **6.2** by addition of hydrochloric acid, sulfuric acid and perchloric acid, respectively, B) and C) are SEM images of the dehydrated hydrogels of **6.2** obtained from treatment with sulfuric acid and perchloric acid, respectively

The limiting condition for gel formation is listed in Table 6.8. The critical gelation concentrations for the aqueous sulfuric, hydrochloric and perchloric acids were found to be 1.3, 2 and 0.8% (w/v) respectively, which gives an indication of the effective hydrogelation ability of **6.2**. The translucent hydrogels thus obtained were found to be thermo-reversible with gel to sol transition temperatures (T_{gel}) being 38, 34 and 43°C, corresponding to aqueous hydrochloric, sulfuric and perchloric acids respectively. Apparently, the formation of hydrogels from **6.2** in aqueous acid solutions is driven by intermolecular hydrogen bonding. To our surprise, hydrogel formation was not observed when **6.2** was dissolved in dilute nitric acid. We feel that planar cations are not good for gel stabilisation in the case of **6.2**. Moreover, each of the acids has a critical concentration for gel formation, which was determined independently from heating and cooling solutions of **6.2** in different acid at different concentration. We could obtain crystalline salt of nitrate but the crystals were not suitable for crystallography.

Since both the compounds (**6.1** and **6.2**) possess the 8-hydroxyquinoline group (a fluorophore) we reasoned that their hydrogen bonded self-assembly in aqueous environment may be affected by protonation of the quinoline nitrogen atom, and this may be reflected in the fluorescence emission of these compounds. The effect of added acid to these compounds **6.1** and **6.2** is reflected in their UV-vis absorption as well as emission spectra.

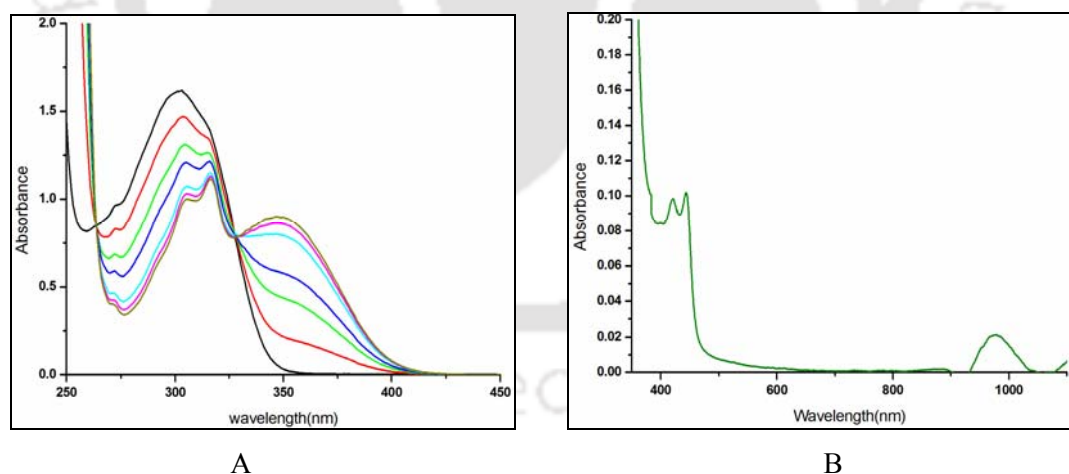


Figure 6.14 A) UV-vis spectra of **6.1** (0.5 mM) upon addition of dilute hydrochloric acid (0.1 M), B) The absorption spectra of **6.1** at higher concentration

For example, the absorption spectra of compound **6.1** has absorption at 301 nm which upon addition of dilute acid in methanol–water (9:1 v/v) solution shifts to 341 nm (Figure 6.14A).

Similar features are present in the absorption spectra of compound **6.2** in dilute solution, both in the neutral and protonated form.

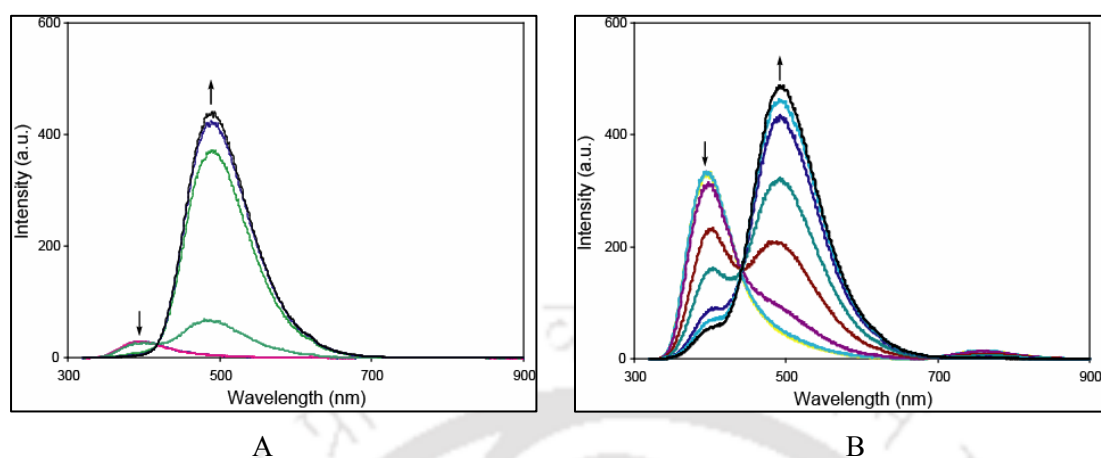


Figure 6.15 Fluorescence emission spectra of **6.1** (A) and **6.2** (B) upon addition of hydrochloric acid (1 M, 20 ml in each aliquot) in methanol–water [9 : 1 v/v, concentration 0.3 mM]

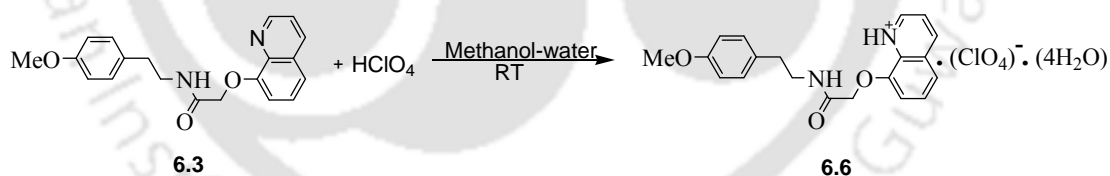
It was also observed that at higher concentrations (10mM), the absorption spectrum of **6.1** shows two weak bands at 419 and 441nm ($\epsilon \sim 9.5 \text{ M}^{-1}\text{cm}^{-1}$) that corresponds to intermolecular charge-transfer transitions along with an additional absorption band observed at 968nm ($\epsilon \sim 3.6 \text{ M}^{-1}\text{cm}^{-1}$) (Figure 6.14B). This is confirmed by the fact that similar absorptions were not observed in case of **6.2**. These results motivated us to study the fluorescence emission spectra of the two compounds upon protonation.

We have observed that **6.1** (in 9:1 methanol-water) is very weakly emissive at 396 nm when excited at 310 nm. This may be caused by fluorescence deactivation of the excited molecule due to intermolecular charge transfer in **6.1**, as evident in the absorption spectra of the compound. Subsequently addition of dilute hydrochloric acid to the solution of **6.1** leads to an increase in fluorescence with emission maximum shifted to 496 nm as shown in Figure 6.15A. On the other hand, the compound **6.2** (in 9:1 methanol-water) exhibits strong emission band at 396 nm (excitation 310 nm), and this band originates from the 8-hydroxyquinoline groups. Since intermolecular charge transfer bands were absent in the absorption spectra of **6.2**, the observed fluorescence in this case is quite reasonable. In this case, addition of dilute hydrochloric acid to the solution of **6.2** in methanol-water (9:1v/v) leads to a new emission band at 496 nm. With increase in the acid concentration the fluorescence emission at 496 nm increases along with concomitant decrease in the intensity at 396 nm, and this results in an iso-emissive point at 441nm (Figure 6.15B).

From the crystallographic study discussed in the earlier section it is clear that the anion on the protonated form of **6.1** controls the orientation of the assemblies. The bisulfate anion gives rise to an assembly that is much different from the one that is resulted from the nitrate assisted assembly and the π -interaction among the protonated quinoline rings is facilitated by a non-planar anion. Thus, the assembly formation in the bisulfate assisted assembly is more ordered than the nitrate assisted assembly. This orderliness along with the π -interaction among the protonated quinoline rings in **6.2** lead to gelation. The reason for nitric acid not resulting in gel in the case of **6.2** is attributed to the planarity of the anion, which does not facilitate the π -interaction among the protonated quinoline rings. From the available crystal structures it is proposed that the head-to-tail arrangement in this class of compounds prefer gel formation.

6.3 Acid recognition behaviour of N-[2-(4-methoxy-phenyl)-ethyl]-2-(quinolin-8-yloxy) acetamide

To comprehend the acid recognition behaviour of N-[2-(4-methoxy-phenyl)-ethyl]-2-(quinolin-8-yloxy)acetamide, we have studied binding pattern with perchloric, acetic and L(+) α -hydroxy-phenylacetic acid. The salt of **6.3** with perchloric acid (**6.6**) is synthesized by mixing stoichiometric amounts of the components in methanol-water (Scheme 6.6).



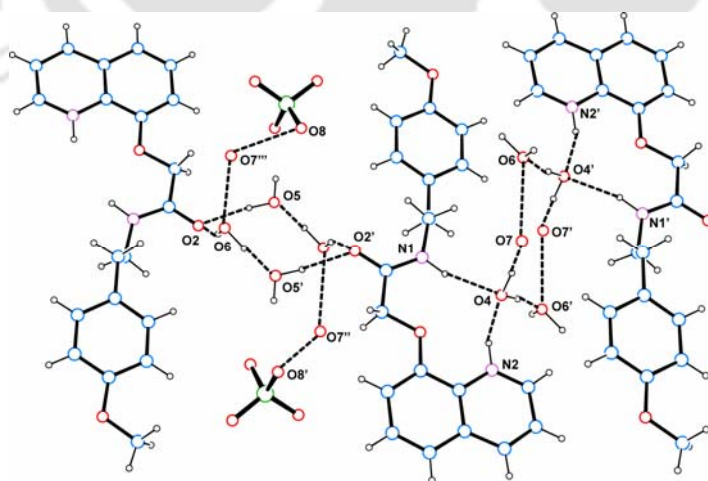
Scheme 6.6

To investigate the structural aspect of the protonated species we determined the crystal structure of the perchlorate salt of **6.3**. The salt was obtained in the hydrated form having four hydrogen bonded water molecules and a perchlorate anion present in the crystal lattice. The H-atoms of water molecule (O7) could not be located in the Fourier maps. In the salt the protonated N-atom of quinoline ring forms H-bond with water molecules. The water molecules with the aid of this interactions forms hexameric ring system.

Table 6.9: Hydrogen bond geometry (Å, °) for compound **6.6**

D–H···A	d(D–H)	d(H···A)	d(D···A)	<D–H···A
N(1)–H(1N)···O(4) [1-x,-y,1-z]	0.91(3)	2.08(4)	2.948(4)	162.6(3)
N(2)–H(2N)···O(4) [1-x,-y,1-z]	0.95(3)	1.80(3)	2.714(3)	159.1(2)
O(4)–H(4A)···O(6) [1-x,1-y,1-z]	0.83(4)	1.95(4)	2.761(4)	164.3(3)
O(4)–H(4B)···O(7) [1-x,-y,1-z]	0.93(3)	1.78(4)	2.696(4)	164.8(3)
O(5)–H(5A)···O(2) [1+x,y,z]	0.98(5)	1.84(5)	2.811(4)	172.5(3)
O(5)–H(5B)···O(8)	0.89(5)	2.37(5)	3.210(5)	163.2(4)
O(6)–H(6A)···O(5)	1.05(5)	1.65(5)	2.677(4)	164.6(4)
O(6)–H(6B)···O(2) [-x,1-y,1-z]	0.83(4)	2.06(4)	2.846(4)	157.6(3)
C(9)–H(9B)···O(2) [-x,1-y,1-z]	0.97	2.59	3.449(3)	148.0
C(13)–H(13)···O(11) [-1+x,y,z]	0.93	2.57	3.453(4)	158.2
C(17)–H(17)···O(9) [1-x,-y,-z]	0.93	2.47	3.380(4)	167.2
C(19)–H(19)···O(5) [x,-1+y,z]	0.93	2.55	3.412(4)	153.7

There are two types of hexameric hydrogen bonded water clusters present in the lattice and they are interconnected to each other. Both the rings are present in a perpendicular fashion to each other and they construct a one dimensional hydrogen bonded network as shown in Figure 6.16. The hexameric units are held by two layers of the parent compounds. Intermolecular O–H···O interactions between the water molecules O6, O7 and O4 result in 6-membered cyclic hydrogen bonded ring structure.

Figure 6.16 Hydrogen bonded assembly of compound **6.6**

The O4–H···O6 [$d_{O4\cdots O6}$ 2.761 Å, \angle D–H···A 164.3°], O4–H···O7 [$d_{O4\cdots O7}$ 2.696 Å, \angle D–H···A 164.8°], O7···O6 [$d_{O7\cdots O6}$ 2.771 Å] and O7···O4 [$d_{O7\cdots O4}$ 2.699 Å] hydrogen bonding

interactions are responsible for formation of such hexameric unit. This hexameric ring is held by the receptors through intermolecular N1–H···O4 [$d_{\text{N1}\cdots\text{O4}}$ 2.948 Å, $\angle\text{D-H}\cdots\text{A}$ 162.6°] and N2–H···O4 [$d_{\text{N2}\cdots\text{O4}}$ 2.714 Å, $\angle\text{D-H}\cdots\text{A}$ 159.1°] interactions (Table 6.9). Another hexameric hydrogen bonded ring is constructed by the two water molecules O6, O5 and the carbonyl groups of the receptor molecule as bifurcated acceptor. The carbonyl groups of the receptor participate in intermolecular hydrogen bonding with water molecules through O5–H···O2 [$d_{\text{O5}\cdots\text{O2}}$ 2.811 Å, $\angle\text{D-H}\cdots\text{A}$ 172.5°] and O6–H···O2 [$d_{\text{O6}\cdots\text{O2}}$ 2.846 Å, $\angle\text{D-H}\cdots\text{A}$ 157.6°] interactions. The water molecules are also assembled via O6–H···O5 [$d_{\text{O6}\cdots\text{O5}}$ 2.677 Å, $\angle\text{D-H}\cdots\text{A}$ 164.6°] hydrogen bonded interaction and these intermolecular O–H···O interactions are responsible for the hexameric structure³⁵⁷⁻³⁵⁸. The hydrogen bonded hexameric assembly of water molecules is shown in Figure 6.17. The perchlorate anions are held in the lattice through O7···O8 [$d_{\text{O7}\cdots\text{O8}}$ 2.973Å] and O5–H···O8 [$d_{\text{O5}\cdots\text{O8}}$ 3.210(5)Å, $\angle\text{D-H}\cdots\text{A}$ 163.2(4)°] hydrogen bonding interactions with water molecule. Besides that weak C–H···O interactions [C13–H···O11 ($d_{\text{C13}\cdots\text{O11}}$ 3.453 Å, $\angle\text{D-H}\cdots\text{A}$ 158.2°), C17–H···O9 ($d_{\text{C17}\cdots\text{O9}}$ 3.380 Å, $\angle\text{D-H}\cdots\text{A}$ 167.2°)] are also present between the hydrogens of quinoline ring and oxygen of perchlorate molecules. The protonated receptor molecules are stacked in head to tail fashion through $\pi\cdots\pi$ [$d_{\pi\cdots\pi}$ 3.390Å] interaction. The solid state FT-IR spectra of the salt (**6.6**) has a strong absorption peak at 1668 cm^{-1} , due to C=O group of amide. There is also a strong absorption peak at 1114 cm^{-1} due to perchlorate group.

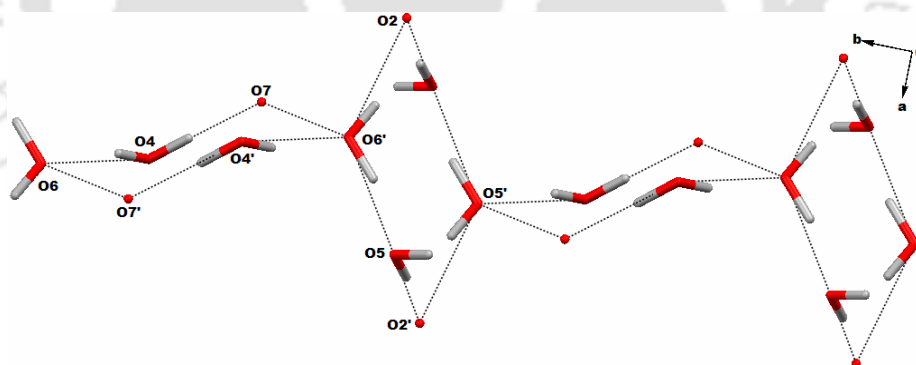


Figure 6.17 Hydrogen bonded hexameric assembly of water molecules

The $^1\text{H-NMR}$ spectra of the compound **6.3**, in benzene- d^6 and methanol- d^4 (Figure 6.18A and 6.19A) showed that aromatic region in the spectrum recorded in deuterated methanol is well resolved whereas in the case of benzene it is less resolved. The intermolecular self association is possible in the case of the compound (**6.3**) in benzene which probably makes the aromatic region of the spectra less resolved. The N–H signal appearing at 8.6 ppm in deuterated

benzene gets shifted to more downfield in deuterated methanol, suggesting its participation in strong intermolecular hydrogen bonding.

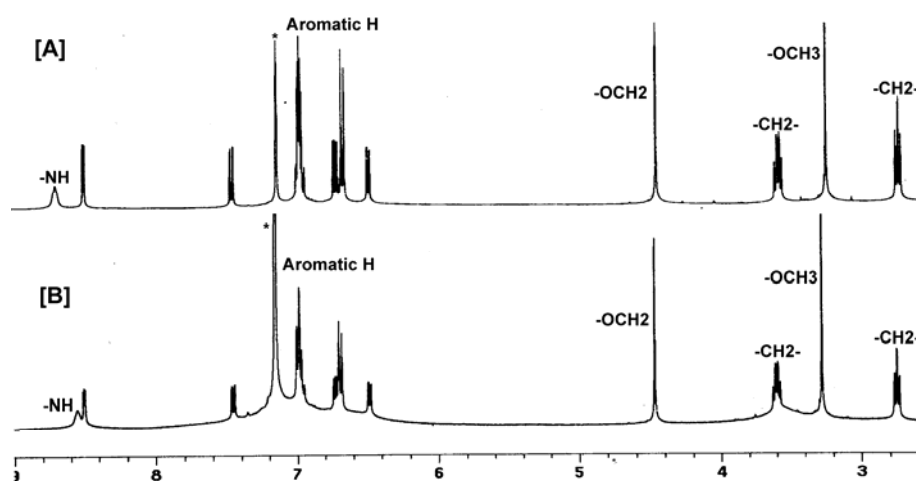


Figure 6.18 $^1\text{H-NMR}$ spectra of **6.3** A) in benzene- d^6 and B) in benzene- d^6 after the addition of perchloric acid [The solvent peaks are marked as *]

We have also recorded the $^1\text{H-NMR}$ spectra after the addition of perchloric acid in benzene- d^6 and methanol- d^4 as shown in Figure 6.18B and 6.19B respectively. In benzene, perchloric acid ionizes less relative to in methanol; so, in benzene perchloric acid is involved in hydrogen bonding without protonating the compound **6.3**. But in the protic solvent methanol the protonation of ring nitrogen leads to a new state, which significantly affects the chemical shifts of the ring protons.

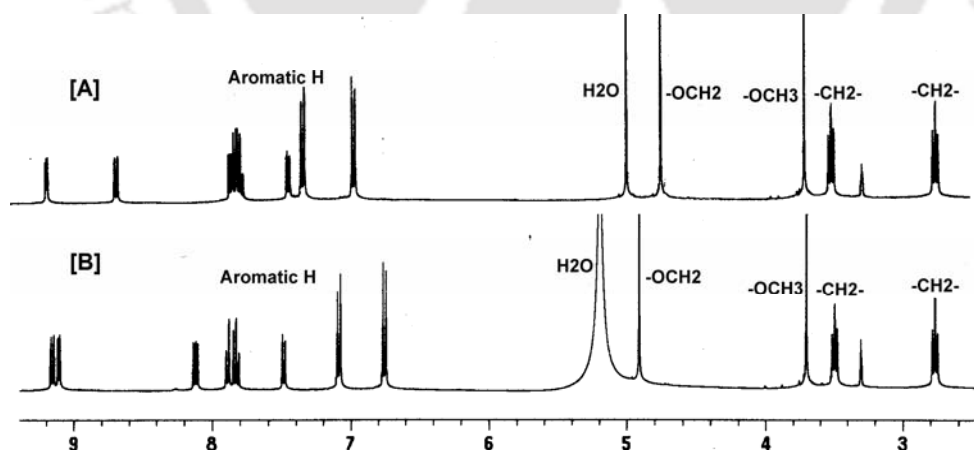


Figure 6.19 $^1\text{H-NMR}$ spectra of **6.3** in (A) CD_3OD , (B) CD_3OD after the addition of HClO_4

The effect is reflected in the fluorescence emission of the compound **6.3**. The compound **6.3** on excitation at 310 nm shows emission at 383 nm ($\phi=0.36$) in benzene whereas it shows emission at 395 nm ($\phi=0.07$) in methanol. There is an intensity difference in the emission, the

compound in benzene emits with approximately six times higher the intensity in methanol. This is attributed to the formation of intermolecular hydrogen bond in protic solvent, which affects the fluorescence emission.

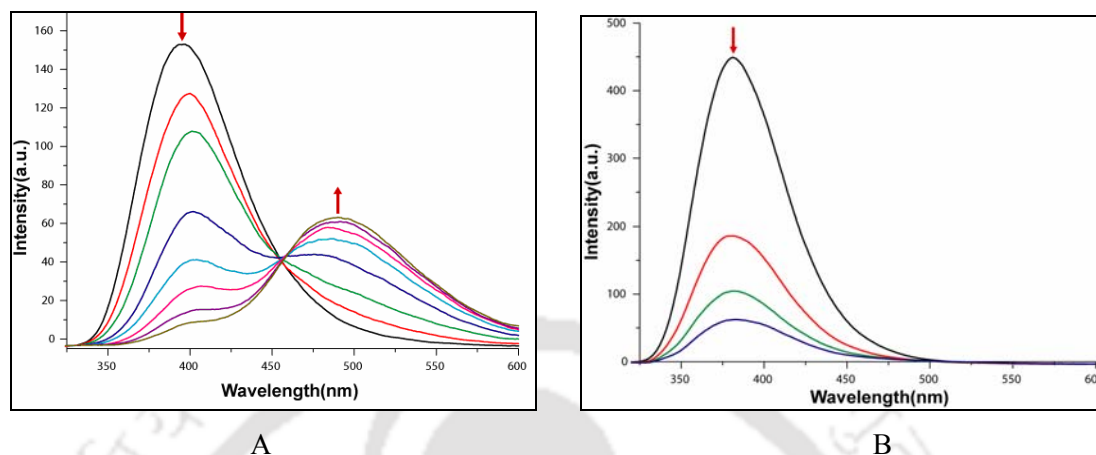
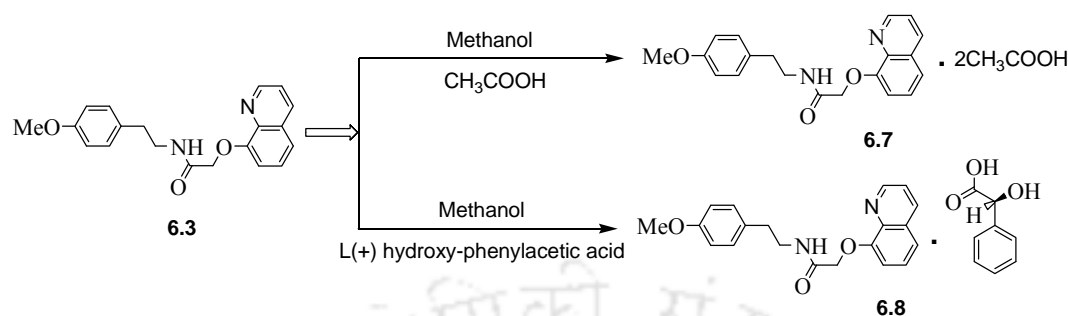


Figure 6.20 Fluorescence emission (λ_{ex} 310nm) of amide **6.3** in A) methanol (6.6×10^{-4} M) on addition of HClO₄ (10^{-1} M, 5 μ l in each aliquot), B) benzene (3.3×10^{-5} M) on addition of HClO₄ solution (2×10^{-2} M, 5 μ l in each aliquot)

It has been observed that if a solution of **6.3** is treated with perchloric acid in benzene fluorescence quenching occurs (Figure 6.20B). Whereas, a methanolic solution of **6.3** on treatment with perchloric acid, fluorescence quenching at 395nm is observed, but a new fluorescence emission state is generated at 493 nm (Figure 6.20A). This process passes through an isoemissive point at 456 nm, suggesting a direct conversion of one species to another. The observation is attributed to the protonation of ring nitrogen in methanol. It is clear that protonated and the hydrogen bonded state of **6.3** are distinguishable. The process may be attributed to the fact that benzene being an aprotic solvent allows formation of ion-pair, whereas in the case of methanol the proton transfer takes place leading to a new state. Further support to this statement comes from the fact that the ¹H-NMR spectra of the compound **6.3** in methanol-d⁴ and in benzene-d⁶ with perchloric acid are different confirming the two different states in two different solvents.

Accordingly, co-crystals of N-[2-(4-methoxy-phenyl)-ethyl]-2-(quinolin-8-yloxy)acetamide (**6.3**) with some weak acid namely acetic acid and L(+) α -hydroxy-phenylacetic acid are also prepared. N-[2-(4-methoxy-phenyl)-ethyl]-2-(quinolin-8-yloxy)acetamide forms 1:2 co crystal (**6.7**) with acetic acid which is isolated as colorless crystals (Scheme 6.7) and characterized by various spectroscopic techniques. The structure of **6.7** is determined by X-ray crystallography. In this co-crystal (**6.7**) the acetic acid binds with the host molecule by the

O–H group of carboxylic acid. From the crystal structure of the co-crystal **6.7** it is observed that two molecules of acetic acid are hydrogen bonded with the receptor (Figure 6.21A).



Scheme 6.7

In between them the -OH group of one acetic acid molecule forms hydrogen bond with the nitrogen atom of the quinoline ring through $\text{O4-H}\cdots\text{N2}$ [$d_{\text{O4}\cdots\text{N2}}$ 2.665 Å, $\langle\text{D-H}\cdots\text{A}$, 170.9°] interaction, where the -OH group behave as hydrogen bond donor and the nitrogen as acceptor. The N–H proton of the amide group participate in $\text{N1-H}\cdots\text{O4}$ [$d_{\text{N1}\cdots\text{O4}}$ 2.947 Å, $\langle\text{D-H}\cdots\text{A}$, 158.5°] hydrogen bonding interaction with -OH group of acetic acid (Table 6.10).

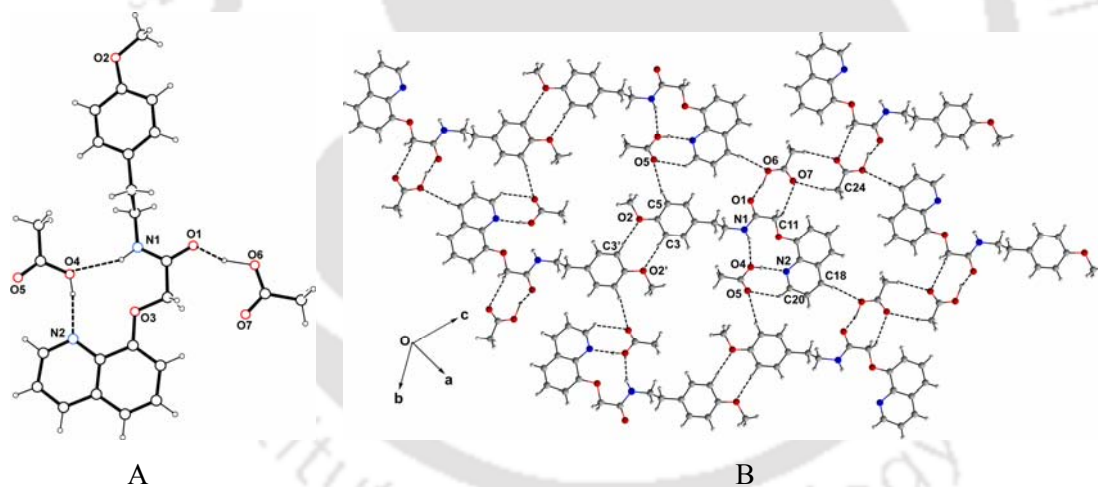


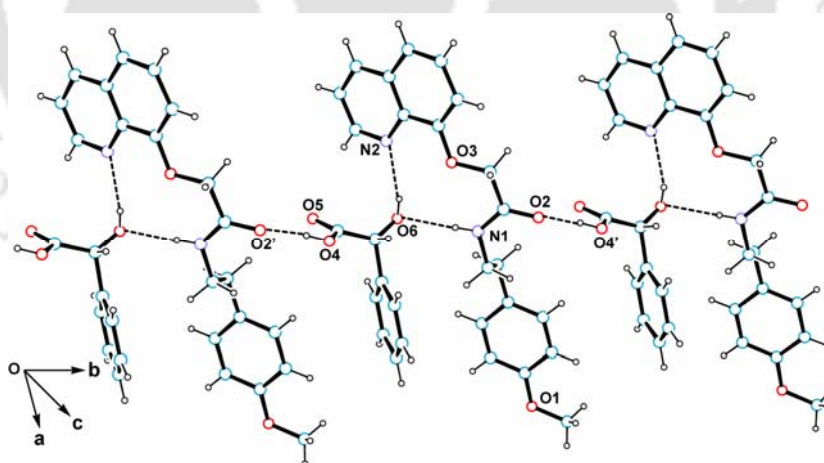
Figure 6.21 A) Crystal structure of **6.7**, B) Two dimensional hydrogen bonded assembly in compound **6.7**

The amide carbonyl also involved in $\text{O6-H}\cdots\text{O1}$ [$d_{\text{O6}\cdots\text{O1}}$ 2.591 Å, $\langle\text{D-H}\cdots\text{A}$, 161.2°] interaction with acetic acid. Two acetic acid molecules are self-assembled in the lattice through weak $\text{C24-H}\cdots\text{O8}$ [$d_{\text{C24}\cdots\text{O8}}$ 3.414 Å, $\langle\text{D-H}\cdots\text{A}$, 160.9°] interaction. These hydrogen bonded units are further held together in the lattice through weak $\text{C3-H}\cdots\text{O2}$ [$d_{\text{C3}\cdots\text{O2}}$ 3.500 Å, $\langle\text{C2-H}\cdots\text{O1}$ 152.0°] and $\text{C5-H}\cdots\text{O5}$ [$d_{\text{C5}\cdots\text{O5}}$ 3.527 Å, $\langle\text{C2-H}\cdots\text{O1}$ 166.0°] intermolecular interaction leading to two dimensional extended hydrogen bonded zig-zag assembly as shown in Figure 6.21B.

Table 6.10: Hydrogen bond geometry (Å, °) for compound **6.7**

D–H···A	d(D–H)	d(H···A)	d(D···A)	<D–H···A
N(1)–H(1N)···O(4)	0.83(3)	2.16(3)	2.947(3)	158.5(3)
O(4)–H(4O)···N(2)	0.85(3)	1.82(3)	2.665(3)	170.9(3)
O(6)–H(6O)···O(1)	1.24(5)	1.38(5)	2.591(3)	161.2(5)
C(3)–H(3)···O(2)	0.93	2.65	3.500	152.0
C(5)–H(5)···O(5)	0.93	2.62	3.527	166.0
C(18)–H(18)···O(6) [2+x,1+y,z]	0.93	2.41	3.330(5)	172.6
C(24)–H(24A)···O(8) [1-x,1-y,1-z]	0.96	2.49	3.414(6)	160.9

Similarly the co-crystal **6.8** was synthesized by mixing equimolar amount of **6.3** and L(+)- α -hydroxy phenylacetic acid in methanol (Scheme 6.7). Slow evaporation of solvent affords the co-crystal as colourless plate like crystals in good yield. ¹H-NMR spectra in CDCl₃ of the co-crystal **6.8** shows that the peaks correspond to the parent compounds and the integration of the proton signals shows it to have a 1:1 molecular composition. IR-spectra of the co-crystal shows a strong absorption at 1742 cm⁻¹, this absorption is attributed to the C=O stretching of carboxylic acid. Another strong absorption band appears at 1628 cm⁻¹ due to the carbonyl of amide group.

Figure 6.22 One dimensional hydrogen bonded assembly in co-crystal **6.8**.

Crystal structure of co-crystal **6.8** shows that hydroxy-carboxylic acid forms extended chain type structure through hydrogen bonding interactions with the host molecules. The carboxylic acid group of the hydroxy phenylacetic acid is hydrogen bonded with the carbonyl of the amide group through O4–H···O2 [*d*_{O4···O2} 2.615 Å, <D–H···A 158.4°] interaction. The hydroxyl group of hydroxy-carboxylic acid is also involved in hydrogen bonding interactions

(O6–H···N2 [$d_{O6\cdots N2}$ 2.738 Å, \angle D–H···A 137.8°] and N1–H···O6 [$d_{N1\cdots O6}$ 2.914 Å, \angle D–H···A, 150.6°]) where the hydroxyl group can behaves as donor as well as acceptor (Figure 6.22).

Table 6.11: Hydrogen bond geometry (Å, °) for compound **6.8**

D–H···A	d(D–H)	d(H···A)	d(D···A)	\angle D–H···A
N(1)–H(1N)···O(6) [1-x,-y,1-z]	0.82(6)	2.18(6)	2.914(9)	150.6(7)
O(4)–H(4A)···O(2) [1-x,1-y,1-z]	0.82	1.83	2.615(11)	158.4
O(6)–H(6A)···N(2) [1-x,-y,1-z]	0.82	2.07	2.738(11)	137.8
C(15)–H(15)···O(5)	0.93	2.61	3.486	157.2
C(27)–H(27)···O(2) [-x,1-y,1-z]	0.93	2.51	3.391(10)	158.1

The hydrogen-bonded network involving the C=O groups and aromatic protons are further stabilized by intermolecular C–H···O interactions [$d_{C15\cdots O5}$ 3.486 Å, \angle D–H···A 157.2°, $d_{C27\cdots O2}$ 3.391 Å, \angle D–H···A 158.1°] in which the aromatic hydrogens serve as donor while the oxygen atom of C=O group serves as acceptor (Table 6.11). The quinoline rings of N-[2-(4-methoxy-phenyl)-ethyl]-2-(quinolin-8-yloxy)acetamide are stacked to each other in slight offset manner and the resulting structure has an interplanar π – π distance, between the planes of the aromatic units, of 3.392 Å. This suggests that there may be considerable amount of π -interactions as it is well within the permissible limit of separation for such interactions. Besides that a considerable amount of C11–H··· π [$d_{C11\cdots \pi}$ 3.629 Å] interaction is also present which stabilizes the molecular assembly. These results clearly show that the packing patterns are different in each case and these patterns of **6.3** are decided by the guest molecules.

Table 6.12

	L(+)-Mandelic acid	Acetic acid	HClO ₄ (in methanol)	HClO ₄ (in benzene)
Binding constant (M ⁻¹)	4.25x10 ⁵	3.33x10 ⁵	9.15 x 10 ⁵	6.84 x 10 ⁷

The effect of hydrogen bonding was studied by fluorescence emission spectra of **6.3**. Addition of acetic acid to a benzene solution of **6.3** fluorescence quenching was observed as shown in Figure 6.23A. This result also is in agreement with the result on the observation of strong hydrogen bonding in the crystal structure of co-crystal of **6.3** with acetic acid.

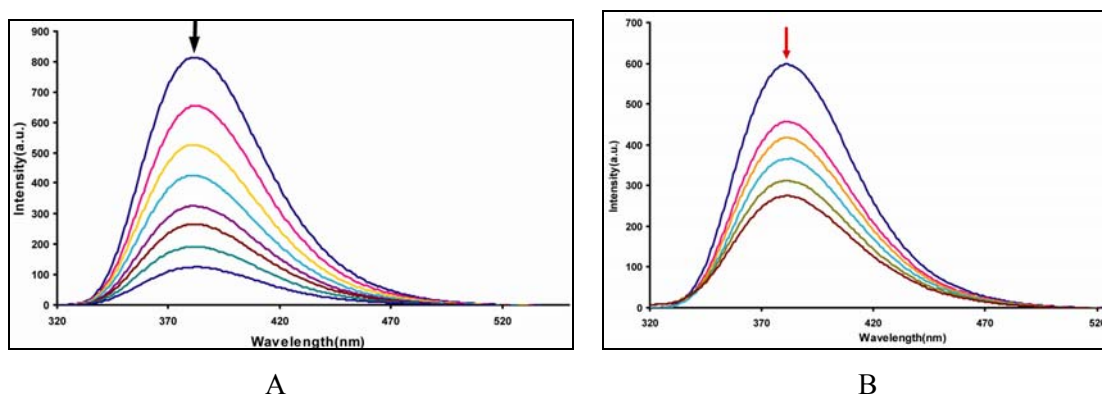
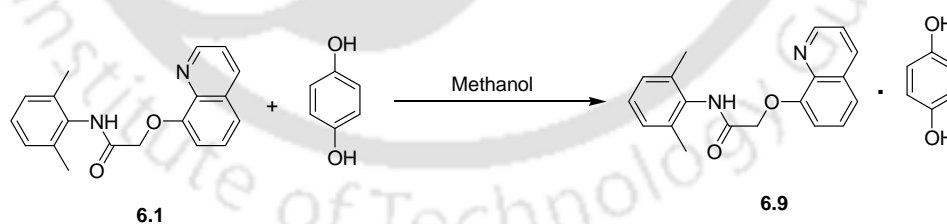


Figure 6.23 Fluorescence emission of amide **6.3** in (A) methanol on addition of acetic acid, (B) methanol on addition of L(+)- α -hydroxy-phenylacetic acid.

We have investigated the effect of addition of L(+)- α -hydroxy-phenylacetic acid to a solution of **6.3** in benzene. It is observed that in benzene the emission at 395nm gets quenched on addition of hydroxy acid (Figure 6.23B). The relative trend is decrease in intensity with increase in concentration of either of the acid. We have also determined the binding constants of **6.3** with mandelic, acetic and perchloric acid and the values of binding constants are listed in Table 6.12.

6.4 Host-guest chemistry of receptors with dihydroxy compounds

We have studied the structural and supramolecular aspect of different co-crystals of N-(2,6-dimethylphenyl)-2-(quinolin-8-yloxy) acetamide and N-[2-(4-methoxy-phenyl)-ethyl]-2-(quinolin-8-yloxy) acetamide with dihydroxy compounds.



Scheme 6.8

The co-crystal (**6.9**) of N-(2,6-dimethylphenyl)-2-(quinolin-8-yloxy) acetamide with 1,4-dihydroxybenzene was obtained by mixing stoichiometric amount of the compounds from methanol (Scheme 6.8) as colourless crystals. Elemental analysis and $^1\text{H-NMR}$ data shows 1:1 host guest composition in co-crystal **6.9**.

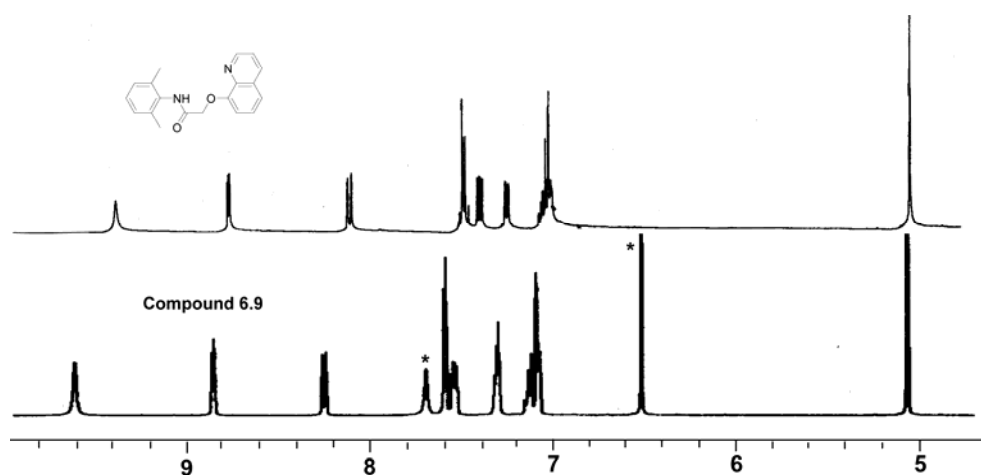


Figure 6.24 $^1\text{H-NMR}$ spectra of compound **6.1** and the co-crystal **6.9** (The peak due to guest molecule indicated by *)

The $^1\text{H-NMR}$ spectra of the co-crystal **6.9** shows that all the signals of the parent components with the desired proton integration without significant shift in the chemical shift position as compared to the parent compound except some noticeable change in the N-H signals. For example, the N-H of amide group at 9.37 ppm shifted to 9.64 ppm after co-crystallization. The hydroxyl protons of the 1,4-dihydroxybenzene appears at 7.67 ppm as shown in Figure 6.24. The aromatic protons of 1,4-dihydroxybenzene appear as a singlet at 6.46 ppm. The crystal structure of the co-crystal is determined by X-ray crystallography. It shows the formation of a self-assembled hydrogen-bonded structure. In this case two molecules of parent amide act as a host for one dihydroxy aromatic molecule as a guest. Crystal structure shows the formation of self-assembled capsules formed by two molecules of the host which held the 1,4-dihydroxy molecule through intermolecular $\text{N2-H}\cdots\text{O3}$ [$d_{\text{N2}\cdots\text{O3}}$ 2.915 Å, $\langle\text{D-H}\cdots\text{A}$ 153.3°] and $\text{O3-H}\cdots\text{N1}$ [$d_{\text{O3}\cdots\text{N1}}$ 2.723 Å, $\langle\text{D-H}\cdots\text{A}$ 171.9°] interactions (Figure 6.25A).

Table 6.13: Hydrogen bond geometry (Å, °) for compound **6.9**

D-H \cdots A	d(D-H)	d(H \cdots A)	d(D \cdots A)	$\langle\text{D-H}\cdots\text{A}$
N(2)-H(2N) \cdots O(3)	0.87(2)	2.11(2)	2.915(2)	153.3(19)
O(3)-H(3O) \cdots N(1)	0.90(3)	1.83(3)	2.723(19)	171.9(3)
C(18)-H(18B) \cdots O(2) [1-x,1-y,-z]	0.96	2.55	3.505(3)	175.5

It may be noted that in this assembly the host molecules orient in a head-to-head direction. Moreover, the host and guest molecules are assembled in the lattice through weak

C18–H···O2 [$d_{\text{C18}\cdots\text{O2}}$ 3.505 Å, $\angle\text{D–H}\cdots\text{A}$ 175.5°] interaction where the methyl protons serve as donor atom and the oxygen of amide group as acceptor (Table 6.13).

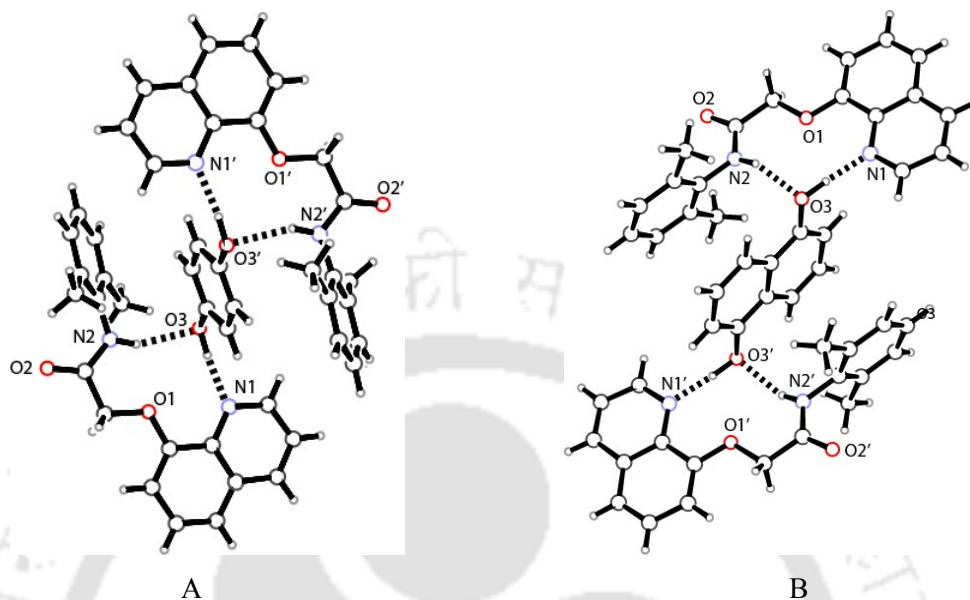
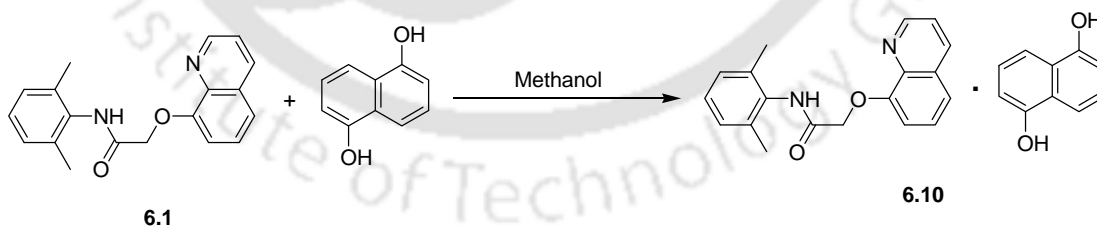


Figure 6.25 Structure of the co-crystals of **6.1** with (A) 1,4-dihydroxybenzene (**6.9**), (b) 1,5-dihydroxynaphthalene (**6.10**)

Similarly, the compound **6.3** forms inclusion complex with 1,5-dihydroxynaphthalene (Scheme 6.9). Spectroscopic characterization shows that the two components are present in the co-crystal **6.10** in 1:1 host guest ratio. The IR spectra of co-crystal **6.10**, shows strong and relatively broad absorption at 3281cm^{-1} which indicates the presence of N-H of the amide group.



Scheme 6.9

A sharp absorption appeared at 1677cm^{-1} due to carbonyl stretching of amide group. The $^1\text{H-NMR}$ spectra of the co-crystal **6.10** shows that the N-H protons appear as broad singlet at δ 9.48 ppm which is slightly shifted after the formation of the co-crystal. The aromatic protons of 1,5-dihydroxynaphthalene appears at 7.10, 7.04 and 6.75 ppm. Moreover, no appreciable changes in the chemical shift positions of the protons of the parent compounds are observed

upon co-crystal formation. A ^1H HOMO-COSY spectrum of the co-crystal **6.10** (aromatic part) is shown in Figure 6.26.

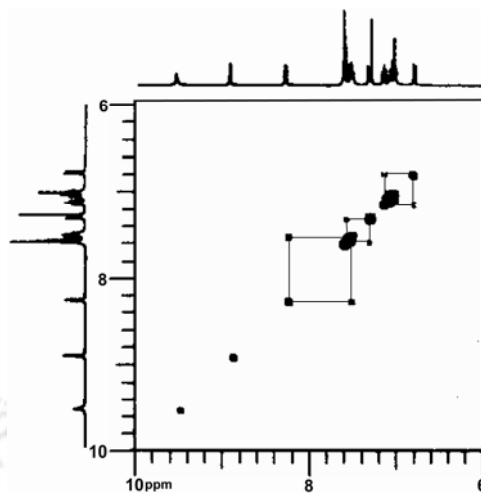


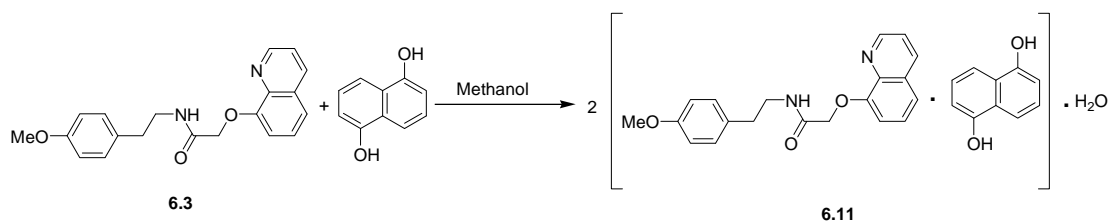
Figure 6.26 ^1H HOMO-COSY spectrum of the co-crystal **6.10** (aromatic part)

Self-assembled dimeric capsule formed by the host molecule **6.3** encapsulate 1,5-dihydroxynaphthalene molecule and is stabilized by intermolecular $\text{N2-H}\cdots\text{O3}$ [$d_{\text{N2}\cdots\text{O3}}$ 2.990 Å, $\langle\text{D-H}\cdots\text{A}$ 159.7°] and $\text{O3-H}\cdots\text{N1}$ [$d_{\text{O3}\cdots\text{N1}}$ 2.690 Å, $\langle\text{D-H}\cdots\text{A}$ 173.5°] hydrogen bonding interactions (Figure 6.25B). The self-assembled capsule in the lattice is stabilized by $\text{C18-H}\cdots\text{O2}$ [$d_{\text{C18}\cdots\text{O2}}$ 3.589 Å, $\langle\text{D-H}\cdots\text{A}$ 175.8°] interactions (Table 6.14). The formation of guest template self-assemblies of **6.1** with the inclusion of dihydroxy compounds indicates that the host molecules are self-complementary and this may lead to the formation of self-assembled dimeric capsules/cavities in the presence of a suitable guest molecule. In each case it is found that intermolecular hydrogen bonding interactions involving the host and the guest molecule provide the driving force for the self-assembly process.

Table 6.14: Hydrogen bond geometry (Å, °) for compound **6.10**

D-H \cdots A	d(D-H)	d(H \cdots A)	d(D \cdots A)	$\langle\text{D-H}\cdots\text{A}$
N(2)-H(2N) \cdots O(3)	0.85(2)	2.18(2)	2.990(2)	159.7(17)
O(3)-H(3O) \cdots N(1)	0.98(3)	1.72(3)	2.690(2)	173.5(3)
C(18)-H(18B) \cdots O(2)	0.96	2.63	3.589	175.8

N-[2-(4-methoxy-phenyl)-ethyl]-2-(quinolin-8-yloxy) acetamide forms 1:1 co-crystal (**6.11**) with 1,5-dihydroxynaphthalene which is isolated as colorless crystals and characterized by spectroscopic techniques (Scheme 6.10). A relatively strong absorption in 3472 cm^{-1} in the IR spectra of co-crystal **6.11** is observed and it is attributed to the hydrogen bonded phenolic-OH groups of 1,5-dihydroxynaphthalene.



Scheme 6.10

The carbonyl stretching of amide is appears at 1629 cm^{-1} . $^1\text{H-NMR}$ spectrum of the **6.3** shows that the N-H proton appears as broad singlet at δ 8.0 ppm in CDCl_3 . After formation of co-crystals with 1,5-naphthalenediol the N-H peak is getting shifted to 8.3 ppm, which indicates that the N-H proton participate in a strong hydrogen bonding interaction (Figure 6.27).

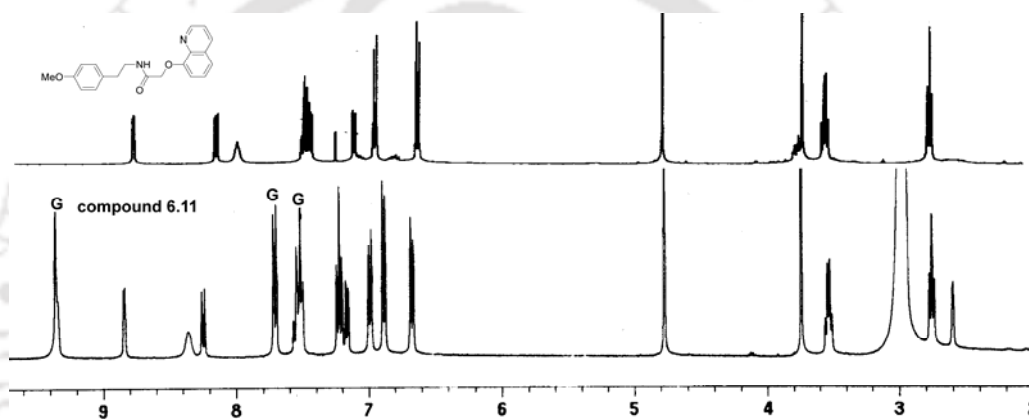
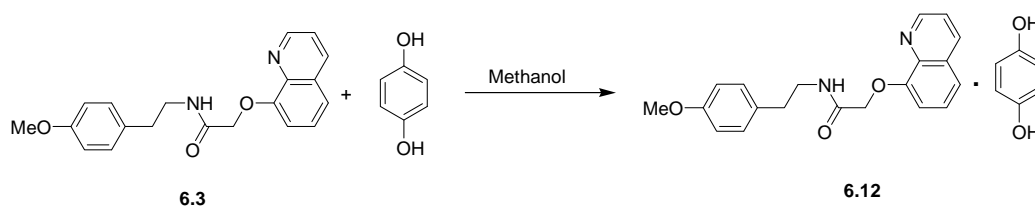


Figure 6.27 $^1\text{H-NMR}$ spectra of compound **6.3** and the co-crystal **6.11** (The peak due to guest molecule indicated by G)

The phenolic -OH proton is not observed in the $^1\text{H-NMR}$ spectra of the co-crystal **6.11** in CDCl_3 at room temperature. This probably occurs due to proton exchange with water present in the solvent. Moreover, no appreciable changes in the chemical shift positions of the protons of the host compound are observed upon co-crystal formation.

The co-crystal **6.12** is isolated by mixing **6.3** and 1,4-dihydroxybenzene in stoichiometric amounts in methanol as colorless plates (Scheme 6.11). Elemental analysis shows that **6.12** comprises of the two components in 1:1 ratio.



Scheme 6.11

In the co-crystal **6.12**, the O–H stretching appears as broad absorption at 3309 cm^{-1} and the amide carbonyl stretching frequency appears at 1651 cm^{-1} . A broad singlet appears at 2930 cm^{-1} due to the N–H stretching frequency (Figure 6.36). Apart from this a significant change in the chemical shift position of the N–H proton of the host component is observed in ^1H -NMR spectra of **6.12** in CDCl_3 . The N–H proton is shifted from 8.0 ppm to 8.3 ppm after the formation of co-crystal. A singlet is appeared at 6.7 ppm due to the aromatic protons of 1,4-dihydroxybenzene. Besides that the other aromatic protons are not affected that much after the formation of co-crystal. A ^1H HOMO-COSY spectrum of the co-crystal **6.12** (aromatic part) is shown in Figure 6.28.

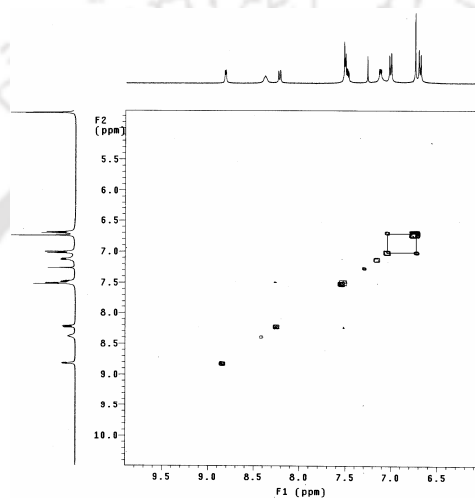


Figure 6.28 ^1H HOMO-COSY spectrum of the co-crystal **6.12** (aromatic part)

The structural aspects of **6.11** and **6.12** are studied by single crystal X-ray diffraction at room temperature. The N-[2-(4-methoxy-phenyl)-ethyl]-2-(quinolin-8-yloxy) acetamide forms 1:1 co-crystal (**6.11**) with 1,5-dihydroxynaphthalene and it crystallizes in the triclinic P-1 space group.

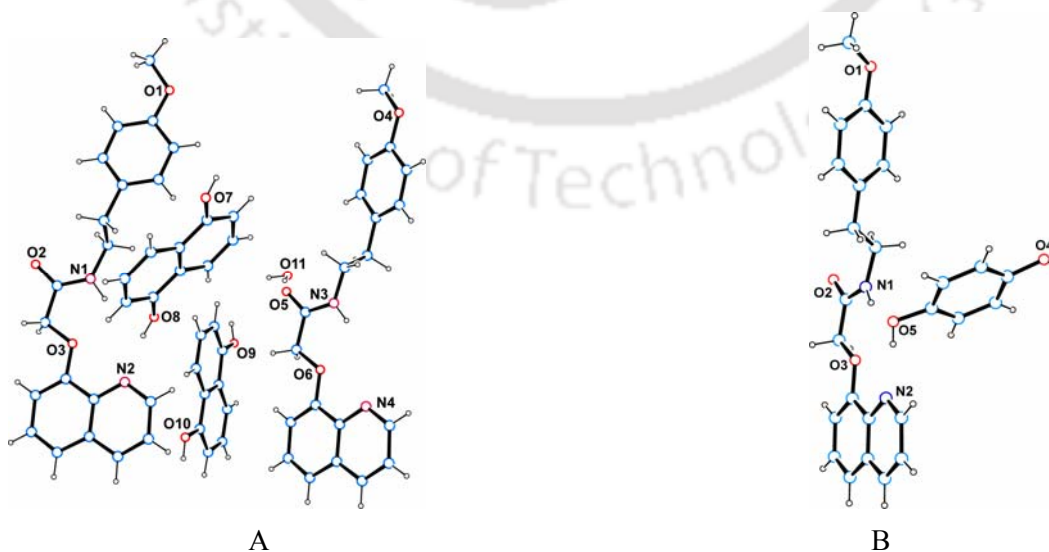


Figure 6.29 A) Crystal structure of co-crystal **6.11**, B) Structure of compound **6.12**

From the crystal structure of co-crystal **6.11** it is observed that two N-[2-(4-methoxy-phenyl)-ethyl]-2-(quinolin-8-yloxy) acetamide molecules co-crystallize with two 1,5-dihydroxynaphthalene molecule along with a water of crystallization (Figure 6.29A). So, the symmetry non equivalence ($Z'=2$) arises due to the presence of water molecule in the lattice. The dihydroxy molecules are held by the receptor through N1–H···O8 [$d_{N1\cdots O8}$ 3.049 Å, $\angle D-H\cdots A$ 147.3°], N3–H···O7 [$d_{N3\cdots O7}$ 2.962 Å, $\angle D-H\cdots A$ 151.5°], O7–H···N4 [$d_{O7\cdots N4}$ 2.674 Å, $\angle D-H\cdots A$ 173.2°] and O8–H···N2 [$d_{O8\cdots N2}$ 2.699 Å, $\angle D-H\cdots A$ 171.2°] hydrogen bonding interactions, where the N-H protons of amide behave as hydrogen bond donor but the phenolic -OH group serve as donor as well as acceptor atom.

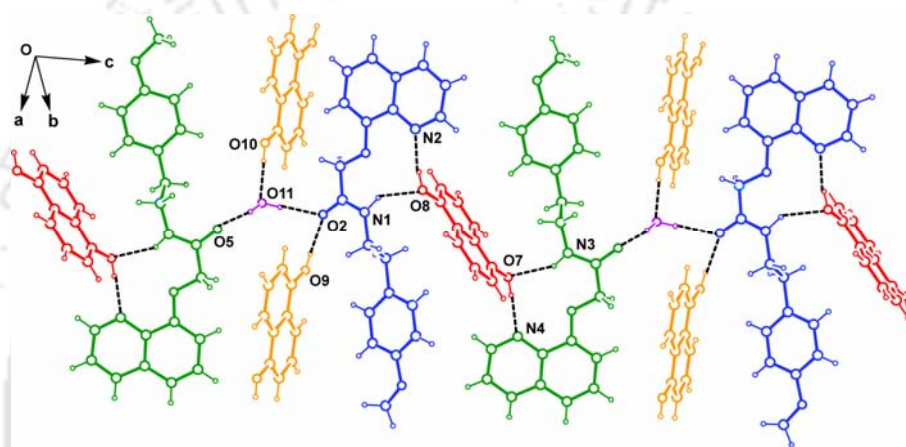


Figure 6.30 Hydrogen bonded one dimensional assembly in co-crystal **6.11**

The water molecule is hydrogen bonded with the host molecule in a bridging fashion. It is held by the oxygen atoms of two symmetry non equivalent receptors through O11–H···O2 [$d_{O11\cdots O2}$ 2.891 Å, $\angle D-H\cdots A$ 175.9°] and O11–H···O5 [$d_{O11\cdots O5}$ 2.806 Å, $\angle D-H\cdots A$ 170.0°] intermolecular hydrogen bonding interactions (Figure 6.30).

Table 6.15: Hydrogen bond geometry (Å, °) for compound **6.11**

D–H···A	d(D–H)	d(H···A)	d(D···A)	$\angle D-H\cdots A$
N(1)–H(1N)···O(8)	0.98(3)	2.18(3)	3.049(3)	147.3(2)
N(3)–H(2N)···O(7) [1-x,1-y,1-z]	0.89(3)	2.15(3)	2.962(3)	151.5(2)
O(7)–H(7A)···N(4) [1-x,1-y,1-z]	0.82	1.86	2.674(2)	173.2
O(8)–H(8)···N(2)	0.82	1.89	2.699(2)	171.2
O(9)–H(9)···O(2) [1-x,1-y,-z]	0.82	1.92	2.744(2)	178.8
O(11)–H(11O)···O(2) [1-x,1-y,-z]	0.86(5)	2.04(5)	2.891(3)	175.9(18)
O(11)–H(12O)···O(5)	0.87(4)	1.94(4)	2.806(3)	170.0(3)
O(10)–H(10)···O(11) [-1+x,y,z]	0.82	1.87	2.690(3)	174.2

These hydrogen bonding interactions between the host and guest molecules lead to a two dimensional hydrogen bonded molecular assembly. The water molecule is also hydrogen bonded with 1,5-naphthalenediol by intermolecular O10–H···O11 [$d_{O10\cdots O11}$ 2.690 Å, $\angle D-H\cdots A$ 174.2°] interaction, where the oxygen atom of water acts as acceptor and the -OH group as donor. One of the dihydroxy molecules is held by the receptor through O9–H···O2 [$d_{O9\cdots O2}$ 2.744 Å, $\angle D-H\cdots A$ 178.8°] interaction and the amide carbonyl behave as a bifurcated acceptor (Table 6.15).

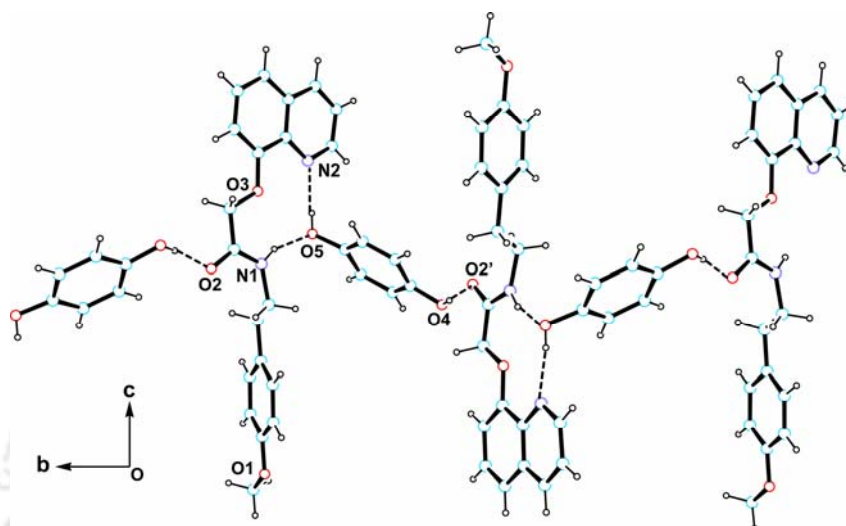


Figure 6.31 One dimensional hydrogen bonded assembly of host and guest in co-crystal **6.12**

The compound **6.3** and 1,4-dihydroxybenzene form a 1:1 co-crystal (**6.12**) of host and guest. Crystal structure of the co-crystal reveals that it crystallizes in the orthorhombic $P2_12_12_1$ space group. The crystal structure of the co-crystal is shown in Figure 6.29B. The N-H proton of the host molecule binds the guest molecule through N1–H···O5 [$d_{N1\cdots O5}$ 2.987 Å, $\angle D-H\cdots A$ 159.1°] hydrogen bonding (Figure 6.31). The phenolic -OH group of 1,4-dihydroxybenzene molecule is also hydrogen bonded with quinolinic nitrogen through O5–H···N2 [$d_{O5\cdots N2}$ 2.715 Å, $\angle D-H\cdots A$ 166.8°] interaction. The carbonyl of amide group is involved in O4–H···O2 [$d_{O4\cdots O2}$ 2.708 Å, $\angle D-H\cdots A$ 169.8°] hydrogen bonding interaction with the hydroxyl group of 1,4-dihydroxybenzene (Table 6.16). The aromatic ring protons participate in weak C13–H··· π [$d_{C13\cdots \pi}$ 3.773Å] and C18–H··· π [$d_{C18\cdots \pi}$ 3.702Å] hydrogen bonding interactions with quinoline ring system.

Table 6.16: Hydrogen bond geometry (Å, °) for compound **6.12**

D–H···A	d(D–H)	d(H···A)	d(D···A)	$\angle D-H\cdots A$
N(1)–H(1N)···O(5) [1-x, -1/2+y, 1/2-z]	0.92(3)	2.12(3)	2.987(3)	159.1(2)
O(4)–H(4A)···O(2) [1+x, y, z]	0.82	1.90	2.708(3)	169.8
O(5)–H(5)···N(2) [1-x, 1/2+y, 1/2-z]	0.82	1.91	2.715(2)	166.8

6.5 Effect of fluorescence emission of receptors on interaction with dihydroxy aromatics

The compounds having guest binding ability may have an important role in biology if they possess a fluorophore³⁴⁴ and we have in our system a hydroxy-quinoline unit having the ability to act as a fluorophore. Moreover, the heterocyclic aromatic systems are known to interact with hydroxyl aromatics³⁵² and can affect the fluorescence emission spectra³⁵³. Thus, to ascertain the difference in protonation and hydrogen bonded assembly formation in these compounds the emission spectra of the parent compounds were recorded with the addition of 1,4-dihydroxybenzene. We have studied the interaction of hydroxy-aromatics with host molecule **6.2** by recording the fluorescence emission with varying concentration of substrates. A methanolic solution of compound **6.2** on excitation at 310 nm shows emission at 396 nm and this peak gets quenched on addition of 1,4-dihydroxybenzene to show a new emission at 343 nm. This process passes through an isoemissive point at 363 nm as shown in Figure 6.32A. Thus, the process can be attributed to the formation of an assembled structure. Similar observations are obtained for compound **6.1**, in which initial weak emission at 396 nm shifts to a strong emission at 342 nm, through an iso-emissive point, showing conversion to another compound, i.e., the inclusion compound. Addition of 1,5-dihydroxynaphthalene to either **6.1** or **6.2** also shows an isoemissive point and the process occurs with the reduction of intensity of the peak for the parent compound. Similar phenomenon is observed in case of the compound **6.3** also; after the gradual addition of 1,4-dihydroxybenzene in a methanolic solution of **6.3** the emission spectra is getting shifted from 396 nm to 342 nm with gradual decrease in a fluorescence intensity of the parent compound as shown in Figure 6.32B.

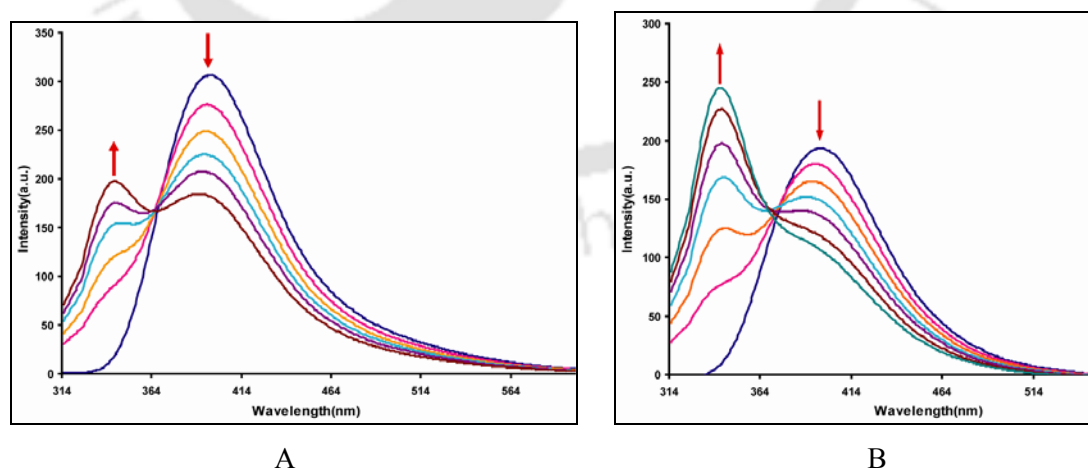


Figure 6.32 A) Fluorescence emission of amide **6.2** in methanol on addition of 1,4-dihydroxybenzene, (B) Emission spectra of amide **6.3** in methanol on addition of 1,4-dihydroxybenzene

In conclusion, it is shown that the host molecules **6.1** and **6.2** lead to the formation of self-assembled dimers (assemblies) in the presence of suitable guest molecules. These compounds have two symmetry non-equivalent molecules in pairs in the unit cells. It is found that head-to-tail, and head-to-head orientations of the host molecules can describe the structure of these assemblies. The head-to-head arrangement in the hydrated form of **6.1** can be transformed to a head-to-tail arrangement by a bisulfate anion. We have also shown that the gel formation from compound **6.2** is selective to acid and analogous compounds **6.1** and **6.3** self-assemble to give hydrogen bonded assembly in the presence of water or a suitable guest anion such as sulphate or perchlorate but does not lead to gels. The gel formation is facilitated by non-planar anions only. The planar anions such as nitrate and carboxylate are not suitable for gelation in these cases. We have also synthesized and characterized various pseudo-polymorphs of N-[2-(4-methoxy-phenyl)-ethyl]-2-(quinolin-8-yloxy)acetamide. We have isolated the co-crystal of **6.3** with acid namely L(+) α -hydroxy-phenylacetic acid and acetic acid. Finally, a clear distinction between the protonated and hydrogen bonded state of **6.3** is made by fluorescence spectroscopy. Both **6.2** and **6.3** show distinct proton responsive luminescence characteristics and significant changes in luminescence spectra are also observed upon the addition of dihydroxy aromatic compounds.

6.6 Experimental Section

Detailed synthetic methodologies are given below. Analytical data as well as spectroscopic data are also listed. Details of the instruments are given in Appendix.

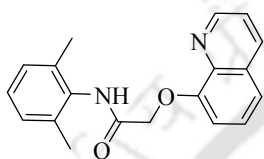
Preparation procedure for compound 6.1

2,6-Dimethylaniline (1.21 g, 10 mmol) was dissolved in dry dichloromethane (20 ml) and triethylamine (1.01 g, 10 mmol) was added to it. The solution was stirred at 0°C for 15 min after which bromoacetyl bromide (2.42 g, 12 mmol) was added dropwise to the stirred solution over a period of 30 min. The reaction mixture was then stirred overnight. It is then filtered to remove the hydrobromide salts, and the filtrate was collected and then the solvent was removed under reduced pressure. The product was obtained as a brown solid that was purified by recrystallisation from dichloromethane.

In the next step the amide (2.43 g, 10 mmol), 8-hydroxyquinoline (1.44 g, 10 mmol) and K₂CO₃ (2.07 g, 15 mmol) were added to dry acetone (20 ml) in nitrogen atmosphere and the

reaction mixture was stirred at 60°C for 9 h. (progress of the reaction was monitored at regular intervals using TLC). After completion of the reaction the solvent was removed under reduced pressure, a brown solid was obtained. The solids were partitioned between water and dichloromethane, washed with dilute sodium hydroxide solution (5%) and water, and then the organic extracts were collected over anhydrous sodium sulphate. Subsequent removal of the solvent gave the crude product, which was purified by column chromatography (silica gel; hexane/ethyl acetate 3 : 2).

Compound 6.1



Yield: 32%.

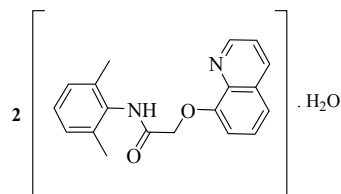
IR (KBr, cm^{-1}): 3454 (bs), 3169(b), 1657(s), 1529(m), 1504(s), 1474(m), 1437(m), 1379(m), 1321(m), 1257(s), 1115(s), 789(m), 770(m), 731(m).

Elemental analysis for $\text{C}_{19}\text{H}_{18}\text{N}_2\text{O}_2$: calculated C, 74.46; H, 5.89; N, 9.13; found C, 74.83; H, 5.41; N, 9.00.

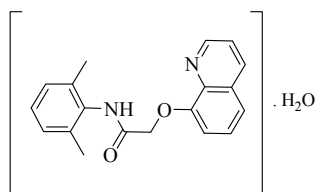
$^1\text{H-NMR}$ (CDCl_3): 9.37 (bs, 1H), 8.73 (m, 1H), 8.05 (dd, $J=8.0, 1.6$ Hz, 1H), 7.41 (m, 2H), 7.34 (t, $J=6.4$ Hz, 1H), 7.16 (t, $J=6.4$ Hz, 1H), 6.93 (m, 3H), 4.89 (s, 2H), 2.08 (s, 6H).

$^{13}\text{C NMR}$ (CDCl_3): 167.4, 154.0, 149.6, 140.4, 136.7, 135.7, 135.5, 133.5, 129.8, 128.3, 127.5, 127.0, 122.2, 122.0, 112.5, 70.3, 18.5.

Compound 6.1A

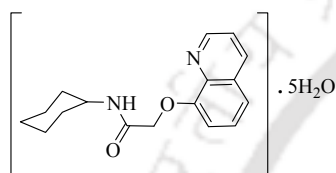


Compound **6.1** (0.31 g, 1mmol) was dissolved in 5ml of dichloromethane and kept for crystallisation. After 3 days colourless block type crystals of **6.1A** were obtained.

Compound 6.1B

Compound **6.1B** was obtained by the crystallisation of compound **6.1** from a benzene-water mixture.

The other compounds **6.2** and **6.3** were synthesized by analogous procedure.

Compound 6.2

Yield: 45%.

IR (KBr, cm^{-1}): 3408(bs), 3216(bs), 3069(m), 2929(s), 2853(s), 1623(s), 1571(m), 1505(m), 1441(m), 1376(m), 1316(s), 1260(s), 1185(m), 1117(s), 826(m), 754(s).

Elemental analysis for $\text{C}_{17}\text{H}_{20}\text{N}_2\text{O}_2$: calculated C, 71.74; H, 7.03; N, 9.85; found C, 71.33; H, 7.31; N, 9.71.

$^1\text{H-NMR}$ (CDCl_3): 8.87(d, $J=8.0$ Hz, 1H), 8.38(bs, 1H), 8.15(d, $J=8.0$ Hz, 1H), 7.46(m, 3H), 7.12(d, 6.4 Hz, 1H), 4.74(s, 2H), 3.85(m, 1H), 1.89(m, 2H), 1.68(m, 2H), 1.55–1.22(m, 6H).

$^{13}\text{C NMR}$ (CDCl_3): 167.7, 154.2, 149.5, 140.5, 136.6, 129.7, 127.1, 122.1, 121.8, 112.6, 70.5, 48.2, 32.9, 25.7, 25.0.

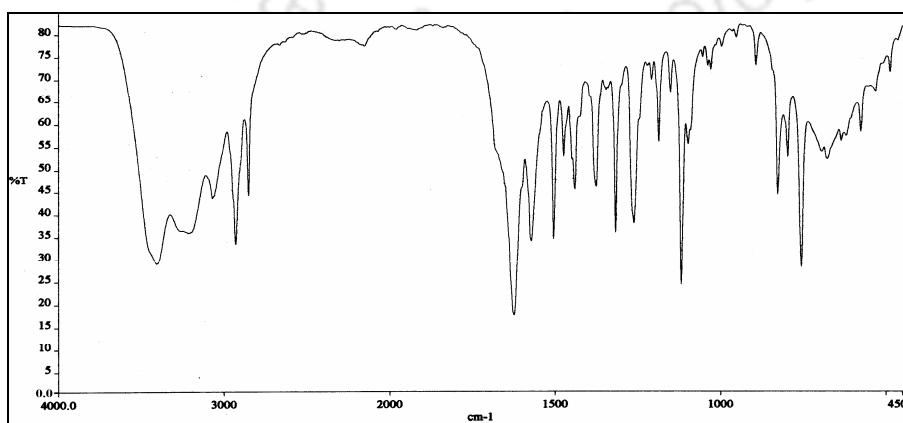
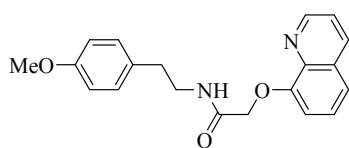


Figure 6.33 FT-IR spectra of compound **6.2**

Compound 6.3

Yield 49%.

IR (KBr, cm^{-1}): 3328(m), 2935(m), 1655(s), 1545(s), 1514(s), 1377(s), 1298(s), 1250(s), 1182(s), 1109(s), 1031(s), 819(s), 785(s), 614(s).

Elemental analysis for $\text{C}_{20}\text{H}_{20}\text{N}_2\text{O}_3$: calculated C, 71.35; H, 5.95; N, 8.32; found C, 71.51; H, 5.39; N, 8.73.

$^1\text{H-NMR}$ (CDCl_3): 8.79(dd, $J=4$ Hz, 1.2 Hz, 1H), 8.15(dd, $J=8.4, 1.6$ Hz, 1H), 7.99(bs, 1H), 7.45(m, 3H), 7.08(dd, $J=6.8, 1.6$ Hz, 1H), 6.95(d, $J=8.4$ Hz, 2H), 6.61(d, $J=8.8$ Hz, 2H), 4.76(s, 2H), 3.73(s, 3H), 3.53(q, $J=13.2$ Hz, 2H), 2.72(q, $J=13.2$ Hz, 2H).

$^{13}\text{C NMR}$ (CDCl_3): 168.6, 158.2, 153.8, 149.3, 140.0, 136.6, 131.1, 129.7, 127.0, 122.1, 121.5, 113.9, 111.6, 69.60, 55.3, 40.7, 34.8.

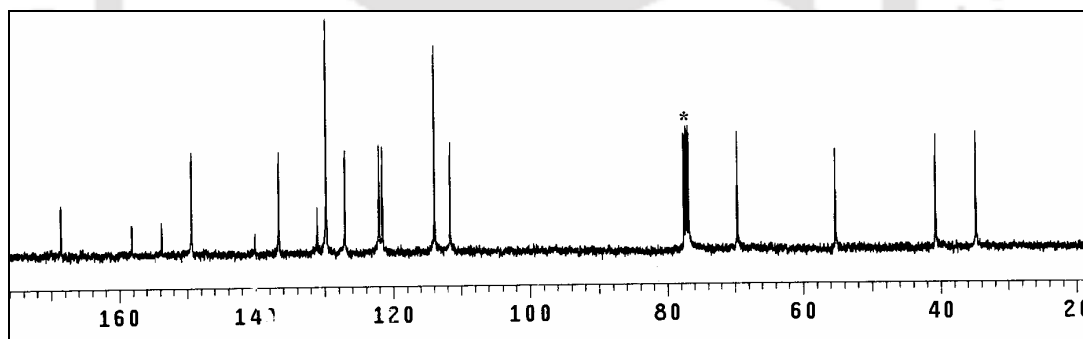
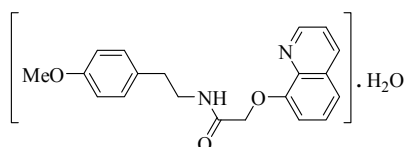


Figure 6.34 $^{13}\text{C NMR}$ spectra of compound **6.3**

Compound 6.3A

Crystallization of **6.3** from ethyl acetate gave block type crystals of **6.3A** after 3 days. The crystals were collected and dried in air.

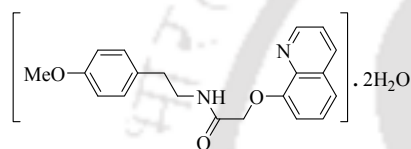
IR (KBr, cm^{-1}): 3572(s), 3254(bs), 3053(bs), 2956(m), 2932(m), 2874(m), 1657(s), 1611(m), 1540(m), 1506(s), 1449(s), 1375(s), 1320(s), 1302(m), 1254(s), 1238(s), 1180(s), 1111(s), 1025(s), 826(s), 798(s), 750(s), 600(s), 553(m), 517(m).

Elemental analysis for $\text{C}_{20}\text{H}_{22}\text{N}_2\text{O}_4$: calculated C, 67.72; H, 6.21; N, 7.90; found C, 67.94; H, 6.01; N, 7.61.

$^1\text{H-NMR}(\text{CDCl}_3)$: 8.80(dd, $J=4.4, 1.6$ Hz, 1H), 8.34(s, 1H), 8.19 (dd, $J=8.4, 1.6$ Hz, 1H), 7.48 (m, 3H), 7.12 (dd, $J=6.4, 2.4$ Hz, 1H), 7.01 (d, $J=8.8$ Hz, 2H), 6.67 (d, $J=8.8$ Hz, 2H), 4.76 (s, 2H), 3.73 (s, 3H), 3.57 (q, $J=13.2$ Hz, 2H), 2.89 (s, 2H), 2.78 (t, $J=7.2$ Hz, 2H).

$^{13}\text{C NMR}(\text{CDCl}_3)$: 168.6, 158.2, 153.8, 149.3, 136.6, 131.1, 129.7, 127.0, 122.1, 121.5, 113.9, 111.6, 69.6, 55.3, 40.7, 34.8.

Compound 6.3B



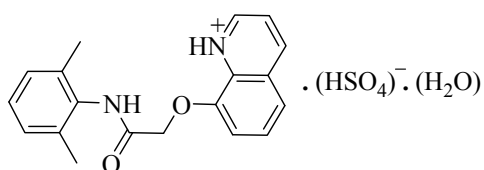
The compound **6.3** was dissolved in methanol: water (1:1), and kept for crystallisation. After 10 days needle like crystals were appeared. The compound was collected and dried in air.

IR (KBr, cm^{-1}): 3545(s), 3350(bs), 2932(m), 1666(s), 1612(m), 1547(s), 1511(s), 1473(m), 1380(m), 1320(m), 1298(m), 1258(s), 1241(s), 1175(m), 1111(s), 1020(m), 822(m), 788(m), 761(m), 747(m), 588(w), 521(w), 487(m).

Elemental analysis for $\text{C}_{20}\text{H}_{24}\text{N}_2\text{O}_5$: calculated C, 64.45; H, 6.44; N, 7.52; found C, 64.86; H, 6.73; N, 7.37.

$^1\text{H-NMR}(\text{CDCl}_3)$: 8.80(dd, $J=4.4, 1.6$ Hz, 1H), 8.34(s, 1H), 8.19 (dd, $J=8.4, 1.6$ Hz, 1H), 7.48 (m, 3H), 7.12(dd, $J=6.4, 2.4$ Hz, 1H), 7.01(d, $J=8.8$ Hz, 2H), 6.67(d, $J=8.8$ Hz, 2H), 4.76(s, 2H), 3.73(s, 3H), 3.57(q, $J=13.2$ Hz, 2H), 2.89(s, 2H), 2.78(t, $J=7.2$ Hz, 2H).

$^{13}\text{C NMR}(\text{CDCl}_3)$: 168.6, 158.2, 153.8, 149.3, 136.6, 131.1, 129.7, 127.0, 122.1, 121.5, 113.9, 111.6, 69.6, 55.3, 40.7, 34.8.

Compound 6.4

Compound **6.1** (0.031 g, 0.1mmol) was dissolved in 5ml of 0.3(M) H_2SO_4 solution by warming and kept for crystallisation. After 10 days colourless plate type crystals of **6.4** were appeared. Yield: 81%.

IR (KBr, cm^{-1}): 3444 (bs), 3276(b), 3101(w), 1674(s), 1634(w), 1598(s), 1560(m), 1519(m), 1474(m), 1415(m), 1305(m), 1276(s), 1136(s), 1111(s), 1035(m), 834(s), 760(s), 581(m).

^1H NMR (CDCl_3): 9.14 (d, $J=8.8\text{Hz}$, 1H), 9.07(d, $J=5.2\text{Hz}$, 1H), 8.10 (dd, $J=6.8, 10\text{Hz}$, 1H), 7.93 (m, 2H), 7.68 (d, $J=6.8\text{Hz}$, 1H), 7.18 (m, 3H), 5.29 (s, 2H), 2.15 (s, 6H).

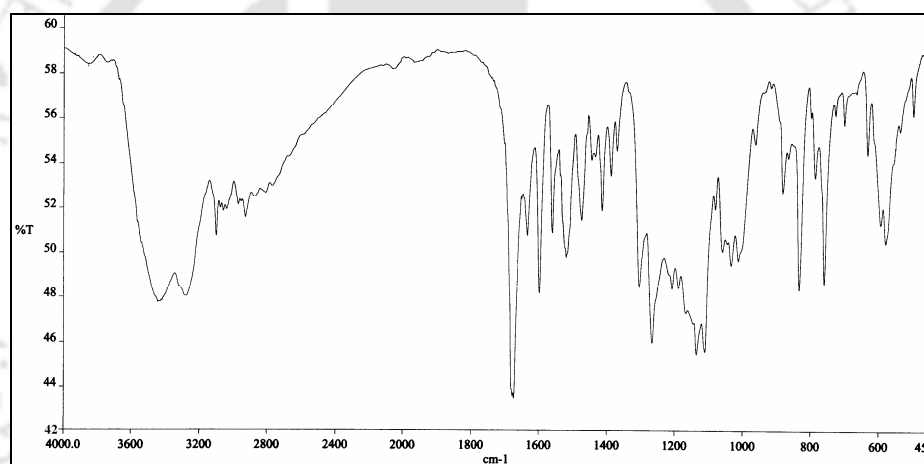
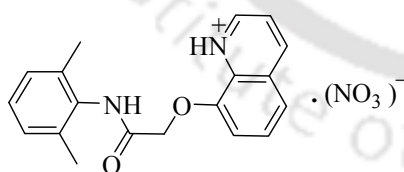


Figure 6.35 FT-IR spectra of compound **6.4**

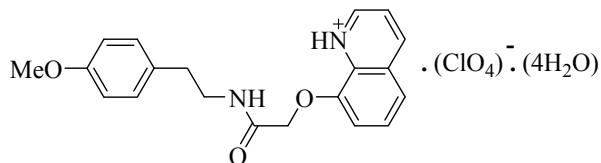
Compound 6.5

Compound **6.1** (0.031 g, 0.1mmol) was dissolved in 5ml of 0.3(M) HNO_3 solution by warming and kept for crystallisation. After 15 days colourless block type crystals of **6.5** were appeared. Yield: 73%.

IR (KBr, cm^{-1}): 3227 (bw), 2920(w), 1662(s), 1598(s), 1547(m), 1522(m), 1474(m), 1416(m), 1384(s), 1320(m), 1300(m), 1114(s), 1034(w), 1016(w), 882(w), 825(m), 792(w), 759(m).

$^1\text{H-NMR}$ (CDCl_3): 9.11 (d, $J=10\text{Hz}$, 1H), 9.07(d, $J=7.2\text{Hz}$, 1H), 8.08 (dd, $J=5.6$, 8.4Hz, 1H), 7.92 (m, 2H), 7.67 (dd, $J=2.4$, 7.2Hz, 1H), 7.18 (m, 3H), 5.29 (s, 2H), 2.17 (s, 6H).

Compound 6.6

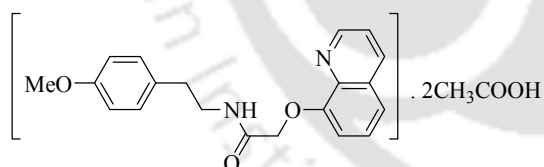


N-[2-(4-methoxy-phenyl)-ethyl]-2-(quinolin-8-yloxy) acetamide (0.1gm) (**6.3**) was taken in a round bottom flask, water (3 ml) and HClO_4 (60%, 40 μl) was added to it, warmed it for 5-10 mins until the amide got dissolved. The resultant solution was kept for crystallization. After 15 days needle like yellow crystals were appeared. Yield: 48%.

IR(KBr, cm^{-1}): 3296(bs), 3093(bs), 2935(m), 1668 (s), 1600(s), 1550(s), 1546(s), 1512(s), 1440 (m), 1392(m), 1299(s), 1244(s), 1179(m), 1144(s), 1114(s), 1083(s), 881(m), 749(s), 636(s), 625(s), 564(w), 524(w), 487(m).

$^1\text{H-NMR}$ (CDCl_3): 9.12(d, $J=8.8\text{Hz}$, 1H), 9.0(d, $J=2.4\text{Hz}$, 1H), 8.08(dd, $J=8.4, 5.2\text{Hz}$, 1H), 7.89(d, $J=8.4\text{Hz}$, 1H), 7.77(t, $J=8\text{Hz}$, 1H), 7.29(d, $J=8\text{Hz}$, 1H), 7.02(d, $J=8.4\text{Hz}$, 2H), 6.66(d, $J=8.4\text{Hz}$, 2H), 4.88(s, 2H), 3.69(s, 3H), 3.55(t, $J=6.4\text{Hz}$, 2H), 2.75(t, $J=6.4\text{Hz}$, 2H).

Compound 6.7



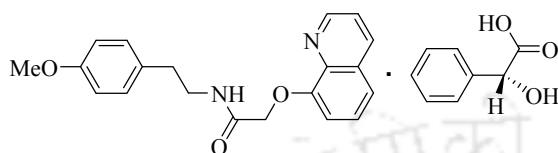
Amide **6.3** (0.1 g) was taken in a round bottom flask, 3 ml of water and 25 μl acetic acid was added it, and then the mixture was warmed for 5-10 minutes, until the amide was dissolved. The resultant solution was kept for crystallization. After 20 days, colourless crystals were appeared. Yield: 56%.

IR(KBr, cm^{-1}): 3311(bs), 3054(m), 1655(s), 1613(m), 1556(m), 1513(s), 1476(m), 1436(m), 1380(m), 1320(m), 1268(m), 1251(s), 1187(m), 1178(m), 1117(s), 1086(m), 1027(m), 818(s), 793(m), 751(s), 599(w), 519(w), 489(w).

Elemental analysis for $\text{C}_{24}\text{H}_{28}\text{N}_2\text{O}_7$: calculated C, 63.09; H, 6.13; N, 6.13; found C, 63.42; H, 6.02; N, 5.98.

$^1\text{H-NMR}(\text{CDCl}_3)$: 9.07 (d, $J=8.8\text{Hz}$, 1H), 8.98 (d, $J=2.4\text{Hz}$, 1H), 8.04 (t, $J=5.2\text{Hz}$, 1H), 7.86 (d, $J=8.4\text{Hz}$, 1H), 7.75 (t, $J=8.4\text{Hz}$, 1H), 7.27(d, $J=7.6\text{Hz}$, 1H), 7.0 (d, $J=6.4\text{Hz}$, 2H), 6.65 (d, $J=8.8\text{Hz}$, 2H), 4.89(s, 2H), 3.68 (s, 3H), 3.53 (t, $J=5.2\text{Hz}$, 2H), 2.74 (t, $J=5.2\text{Hz}$, 2H), 2.18(s, 3H).

Compound 6.8



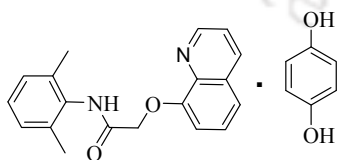
N-[2-(4-methoxy-phenyl)-ethyl]-2-(quinolin-8-yloxy) acetamide (**6.3**) (0.1 g, 0.3mmol) and L(+) α -hydroxy-phenylacetic acid (0.05 g, 0.3 mmol) were dissolved in ethylacetate (5ml). The resultant solution was kept for crystallization. After 4 days colourless crystals were appeared. Yield: 67%.

IR (KBr, cm^{-1}): 3257(bs), 3063(bs), 3033(bs), 3007(bs), 2932(m), 2832(m), 1742(s), 1722(m), 1628(s), 1510(s), 1472(w), 1455(w), 1437(w), 1376(m), 1311(m), 1263(m), 1247(s), 1180(s), 1116(s), 1043(m), 823(m), 785(m), 749(m), 721(m), 701(m), 679(w), 616(w), 489(w).

Elemental analysis for $\text{C}_{28}\text{H}_{28}\text{N}_2\text{O}_6$: calculated C, 68.79; H, 5.74; N, 5.73; found C, 68.48; H, 6.03; N, 5.41.

$^1\text{H-NMR}(\text{CDCl}_3)$: 8.93(s, 1H), 8.30(d, $J=8.4\text{Hz}$, 1H), 8.0(s, 1H), 7.53(m, 3H), 7.47(d, $J=8.4\text{Hz}$, 2H), 7.32(m, 3H), 7.10(d, $J=5.6\text{Hz}$, 1H), 6.97(d, $J=8.4\text{Hz}$, 2H), 6.65(d, $J=8.4\text{Hz}$, 2H), 5.17(s, 1H), 4.66(s, 2H), 3.73(s, 3H), 3.48(m, 2H), 2.71(t, $J=7.2\text{Hz}$, 2H), 2.17(s, 1H).

Compound 6.9



Compound **6.1** (0.15 g, 0.5 mmol) and 1,4-dihydroxybenzene (0.06 g, 0.5 mmol) were dissolved in 10 ml of methanol and kept for crystallisation. Colourless block type crystals were appeared after 5 days. Yield: 52%.

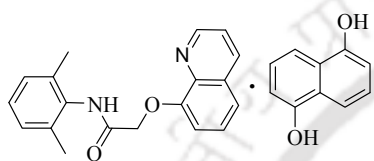
IR (KBr, cm^{-1}): 3266(bs), 2963(w), 1682(s), 1530(m), 1507(s), 1470(s), 1437(m), 1381(m), 1317(s), 1253(s), 1218(s), 1181(s), 1111(s), 1049(w), 824(s), 764(s), 733(s).

Elemental analysis for $C_{44}H_{42}N_4O_6$: calculated C, 73.05; H, 5.81; N, 7.75; found C, 73.43; H, 5.61; N, 7.91.

1H -NMR ($CDCl_3$): 9.64(bs, 1H), 8.88(d, $J=6$ Hz, 1H), 8.26(d, $J=8.4$ Hz, 1H), 7.67(bs, 1H), 7.57(d, $J=4.4$ Hz, 2H), 7.50(m, 1H), 7.26(d, $J=5.2$ Hz, 1H), 7.09(m, 3H), 6.46 (s, 2H), 4.96 (s, 2H), 2.11 (s, 6H).

^{13}C NMR ($CDCl_3$): 167.6, 154.2, 150.1, 149.9, 137.6, 136.2, 133.8, 130.3, 128.6, 127.9, 127.6, 122.6, 122.3, 116.6, 112.5, 70.3, 18.8.

Compound 6.10



Compound **6.1** (0.15 g, 0.5 mmol) and 1,5-Naphthalenediol (0.08 g, 0.5 mmol) were dissolved in 10 ml of methanol and kept for crystallisation. Brown block type crystals were appeared after 6 days. Yield: 47%.

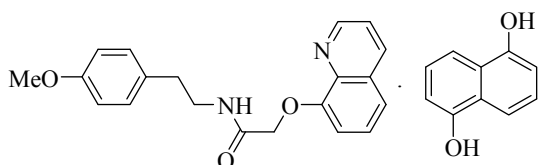
IR (KBr, cm^{-1}): 3281(bs), 3018(w), 2919(w), 1677(s), 1594(m), 1507(s), 1471(m), 1393(s), 1319(m), 1294(w), 1262(m), 1157(w), 1113(s), 939(w), 827(w), 770(m), 761(m), 561(w).

Elemental analysis for $C_{24}H_{22}N_2O_3$: calculated C, 74.53; H, 5.69; N, 7.24; found C, 73.11; H, 5.01; N, 7.18.

1H -NMR ($CDCl_3$): 9.48(s, 1H), 8.86(dd, $J=4, 1.6$ Hz, 1H), 8.23(dd, $J=8.4, 1.6$ Hz, 1H), 7.54 (m, 3H), 7.48 (m, 2H), 7.27 (q, $J=6$ Hz, 1H), 7.10 (t, $J=8.4$ Hz, 1H), 7.04 (m, 1H), 6.98 (d, $J=6.8$ Hz, 2H), 6.75 (d, $J=7.6$ Hz, 1H), 4.97 (s, 2H), 2.05 (s, 6H).

^{13}C NMR ($CDCl_3$): 167.6, 153.2, 148.9, 139.4, 137.4, 135.8, 133.8, 129.9, 128.3, 127.6, 127.4, 126.2, 125.0, 122.2, 122.0, 121.5, 113.6, 110.8, 108.7, 68.6, 18.3.

Compound 6.11



Amide **6.3** (0.1 g, 0.3 mmol) and 1,5-Naphthalenediol (0.05 g, 0.3 mmol) were dissolved in 10ml of methanol. The resultant solution was then kept for crystallization. After 9 days reddish block type crystals were appeared. Yield: 61%.

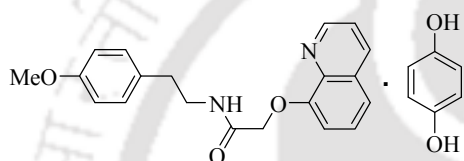
IR (KBr, cm^{-1}): 3472(bs), 3297(w), 2983(w), 1629(s), 1590(w), 1509(s), 1381(s), 1262(s), 1244(s), 1181(m), 1119(s), 937(w), 823(w), 780(s), 751(m).

Elemental analysis for $\text{C}_{60}\text{H}_{58}\text{N}_4\text{O}_{11}$: calculated C, 71.21; H, 5.74; N, 5.54; found C, 71.56; H, 5.31; N, 5.36.

$^1\text{H-NMR}$ (CDCl_3): 9.36(s, 2H), 8.84(d, $J=4.4\text{Hz}$, 1H), 8.36(bs, 1H), 8.24(d, $J=8.4\text{Hz}$, 1H), 7.71(d, $J=8.4\text{Hz}$, 2H) 7.54(m, 3H), 7.21(m, 3H), 6.98(d, $J=7.2\text{Hz}$, 2H), 6.88(d, $J=7.2\text{Hz}$, 2H), 6.67(d, $J=8.4\text{Hz}$, 2H), 4.78(s, 2H), 3.74(s, 3H), 3.53(q, $J=14\text{Hz}$, 2H), 2.76(t, $J=7.2\text{Hz}$, 2H).

$^{13}\text{C NMR}$ (CDCl_3): 168.5, 158.1, 152.7, 148.9, 136.1, 134.2, 130.4, 129.2, 126.5, 126.1, 124.4, 121.6, 121.3, 113.4, 112.9, 111.8, 108.3, 69.6, 54.8, 40.2, 34.3.

Compound 6.12



N-[2-(4-methoxyphenyl)ethyl]-2-(quinolin-8-yloxy) acetamide [6.3] (0.1 g, 0.3 mmol) and 1,4-Dihydroxy benzene (0.03 g, 0.3 mmol) were dissolved in methanol (5ml). The resultant solution was kept for crystallization. After 5 days colourless block type crystals were appeared. Yield: 54%.

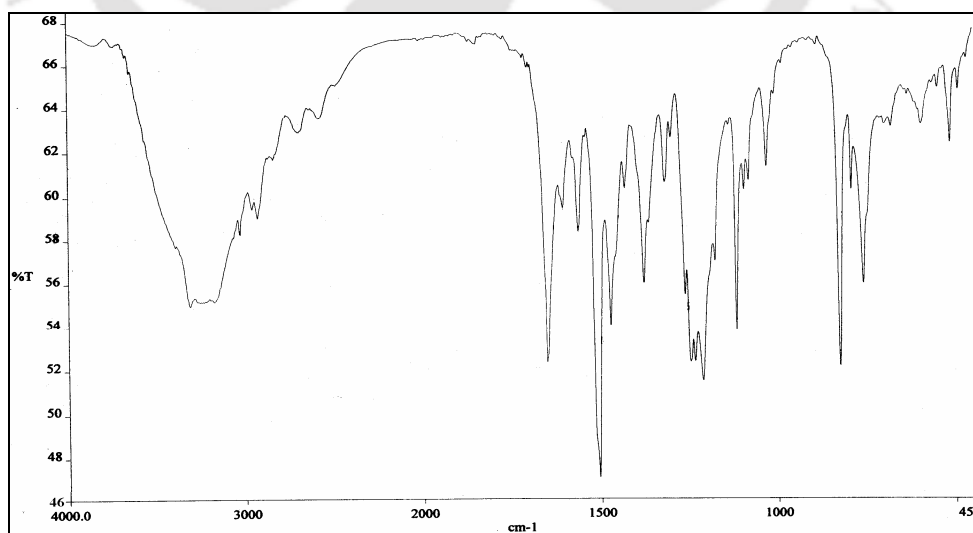


Figure 6.36 FT-IR spectra of co-crystal 6.12

IR (KBr, cm^{-1}): 3309(bs), 2930(w), 1651(s), 1563(m), 1506(s), 1472(m), 1377(m), 1317(m), 1246(s), 1212(s), 1118(s), 1032(m), 824(s), 759(s), 515(w).

Elemental analysis for $\text{C}_{26}\text{H}_{26}\text{N}_2\text{O}_5$: calculated C, 69.88; H, 5.82; N, 6.27; found C, 69.61; H, 5.61; N, 5.93.

$^1\text{H-NMR}$ (CDCl_3): 8.79(d, $J=4.4\text{Hz}$, 1H), 8.33(bs, 1H), 8.20(d, $J=9.6\text{Hz}$, 1H), 7.48(m, 3H), 7.10(dd, $J=3.2, 5.6\text{Hz}$, 1H), 6.98(d, $J=8.8\text{Hz}$, 2H), 6.72(s, 1H), 6.67(d, $J=8.4\text{Hz}$, 2H), 4.73(s, 2H), 3.72(s, 3H), 3.51(q, $J=14\text{Hz}$, 2H), 2.73(t, $J=7.6\text{Hz}$, 2H).

$^{13}\text{C NMR}$ (CDCl_3): 167.8, 159.0, 153.8, 149.7, 148.4, 135.8, 132.2, 129.5, 127.0, 122.4, 121.5, 113.5, 116.7, 110.5, 68.8, 54.8, 40.3, 35.1.



Appendix

Details of the analytical instruments

X-Ray Crystallography

X-ray diffraction data were collected on Bruker 3-circle diffractometers with CCD area detectors ProteumM APEX or SMART 6000 or Bruker Nonius Apex 2, using graphite-monochromated Mo- $K\alpha$ radiation ($\lambda = 0.71073 \text{ \AA}$) from a 60W microfocus Bede Microsource® with glass polycapillary optics or a sealed tube. In case of the structures that were determined at 120K, the low temperature of the crystals was maintained using Cryostream (Oxford Cryosystems) open-flow N₂ cryostats.

X-ray diffraction data for all crystals were collected using Bruker SMART software. This software was also used for indexing and determination of the unit cell parameters. The structures were solved by direct methods and refined by full-matrix least squares against F^2 of all data, using SHELXTL software²¹⁵⁻²¹⁷.

All non-H atom were refined by full-matrix least squares in anisotropic, all H atoms in isotropic approximation, against F^2 of all reflections. All non-H atoms were refined by full-matrix least squares in the anisotropic approximation and the hydrogen atoms attached to these atoms were treated as 'riding' in calculated positions and in some of the cases the hydrogen atoms have been located on the difference Fourier maps. In all cases the hydrogen atoms attached to polar atoms such as O and N were located on the difference Fourier maps and refined in the final structure in isotropic approximation. The crystallographic tables for all the compounds are given at the end of this section, which includes the crystal parameters and the refinement factors. Refine positions and thermal parameters of all the crystal structures along with the CIF are provided in CD.

UV-visible Spectroscopy, emission and IR Spectroscopy

UV-vis adsorption spectra were recorded using Perkin-Elmer Lambda 25 spectrophotometer equipped with double cell compartments. All the chemicals and solvents used were as obtained from the standard suppliers such as E.Merck Germany, Sigma Aldrich USA, Ranbaxy India. The solvents for spectroscopic were of HPLC grade (Aldrich or Merck) and used as obtained. The fluorescence spectra were recorded in Cary Eclipse fluorescence spectrometer. The IR spectra were recorded on Perkin-Elmer spectrum one spectrometer.

NMR Spectroscopy

The NMR spectra, ^1H , ^{13}C as well as the HOMO COSY were recorded in a Varian 400MHz spectrometer. The chemical shifts in the NMR spectra are all given in ppm and tetramethylsilane as the internal standard. The concentration dependent NMR spectra of compounds were recorded by dissolving calculated amounts of the sample in a fixed amount of appropriate solvent.

Thermogravimetric Studies and Elemental analysis

The thermogravimetric studies were performed using a Mettler Toledo TGA/ STDA 851[°] and Mettler Toledo DSC[°] thermal analyser. Typically about 8-10mg of the samples were mounted on platinum crucibles and the TG/DSC profiles recorded at the heating rate of 5°C/min and under nitrogen atmosphere. Elemental analyses were done on a Perkin-Elmer PE 2400 II CHN analyzer 2400.

Cyclic Voltammetry and Electron Paramagnetic Resonance Spectroscopy

Cyclic voltammograms are recorded using a Model 263 potentiostat from Princeton Applied Research (USA). All cyclic voltammetric experiments have been performed in dry degassed solvents, under nitrogen atmosphere.

Cyclic voltammograms were measured for 0.01mM solutions of the tetra-nuclear cobalt (III) complex (**2.8**) in dry degassed acetonitrile at 298K. Tetrabutylammonium perchlorate (TBAP) was used as supporting electrolyte and the experimental solution was purged with dry argon before each measurement. The glassy-carbon working electrode, which was used for performing the experiment, was cleaned with electrode polishing materials available from BAS, washed with deionised water and acetone. The non-aqueous Ag/AgCl electrode was used as reference in all the measurements while a Pt-foil (1cm²) was used as counter electrode.

The ESR experiments were performed using a Bruker X-band spectrometer calibrated with internal teslameter. Simulations of the ESR data were done using standard WinEPR software available from Bruker. The ESR spectrometer magnetic field is calibrated with respect to diphenyl picryl hydrazyl radical as the standard and the spectra were recorded at room temperature.

Selected inter-nuclear distances (in Å) and angles (in °) of metal complexes

Bond distances		Bond angles		Bond angles	
Co(1)–O(1)	2.075(3)	O(1)–Co(1)–O(7)	175.65(12)	O(4)–Co(2)–O(2)	88.64(12)
Co(1)–O(7)	2.082(3)	O(1)–Co(1)–O(3)	88.11(13)	O(5)–Co(2)–O(2)	91.29(12)
Co(1)–O(3)	2.093(3)	O(7)–Co(1)–O(3)	90.65(13)	O(4)–Co(2)–O(9)	94.19(12)
Co(1)–O(9)	2.135(3)	O(1)–Co(1)–O(9)	95.88(12)	O(5)–Co(2)–O(9)	88.03(12)
Co(1)–N(1)	2.136(4)	O(7)–Co(1)–O(9)	88.18(12)	O(2)–Co(2)–O(9)	88.74(13)
Co(1)–N(2)	2.148(4)	O(3)–Co(1)–O(9)	85.79(13)	O(4)–Co(2)–N(4)	91.95(14)
Co(2)–O(4)	2.086(3)	O(1)–Co(1)–N(1)	90.65(14)	O(5)–Co(2)–N(4)	85.84(14)
Co(2)–O(5)	2.088(3)	O(7)–Co(1)–N(1)	90.78(14)	O(2)–Co(2)–N(4)	89.57(14)
Co(2)–O(2)	2.127(3)	O(3)–Co(1)–N(1)	177.09(15)	O(9)–Co(2)–N(4)	173.60(14)
Co(2)–O(9)	2.129(3)	O(9)–Co(1)–N(1)	91.73(14)	O(4)–Co(2)–N(3)	90.82(13)
Co(2)–N(3)	2.168(4)	O(1)–Co(1)–N(2)	89.47(13)	O(5)–Co(2)–N(3)	89.28(13)
Co(2)–N(4)	2.148(4)	O(7)–Co(1)–N(2)	86.40(12)	O(2)–Co(2)–N(3)	178.88(15)
Co(1) ... Co(2)	3.597(3)	O(3)–Co(1)–N(2)	91.55(14)	O(9)–Co(2)–N(3)	90.31(14)
		O(9)–Co(1)–N(2)	173.94(14)	N(4)–Co(2)–N(3)	91.44(15)
		N(1)–Co(1)–N(2)	91.07(15)	Co1–O9–Co2	115.03(12)

Bond distances		Bond angles		Bond angles	
Co(1)–O(4)	2.070(2)	Co1–O9–Co2	111.87(11)	O(1)–Co(2)–O(3)	175.58(10)
Co(1)–O(6)	2.065(2)	O(6)–Co(1)–O(7)	177.19(9)	O(1)–Co(2)–O(5)	89.09(9)
Co(1)–O(7)	2.107(2)	O(4)–Co(1)–O(6)	91.55(8)	O(3)–Co(2)–O(5)	94.46(9)
Co(1)–O(9)	2.139(2)	O(4)–Co(1)–O(7)	87.20(9)	O(1)–Co(2)–O(9)	89.88(9)
Co(1)–N(3)	2.146(3)	O(6)–Co(1)–O(9)	88.81(10)	O(5)–Co(2)–O(9)	89.80(9)
Co(1)–N(4)	2.164(3)	O(4)–Co(1)–O(9)	98.72(9)	O(3)–Co(2)–O(9)	92.75(1)
Co(2)–O(1)	2.066(2)	O(7)–Co(1)–O(9)	88.89(10)	O(1)–Co(2)–N(2)	88.71(9)
Co(2)–O(3)	2.050(2)	O(4)–Co(1)–N(3)	84.40(10)	O(3)–Co(2)–N(2)	88.69(10)
Co(2)–O(5)	2.099(2)	O(6)–Co(1)–N(3)	91.19(10)	O(5)–Co(2)–N(2)	89.49(9)
Co(2)–O(9)	2.143(2)	O(7)–Co(1)–N(3)	91.20(10)	O(9)–Co(2)–N(2)	178.44(11)
Co(2)–N(1)	2.174(3)	O(9)–Co(1)–N(3)	176.88(10)	O(1)–Co(2)–N(1)	89.98(11)
Co(2)–N(2)	2.165(3)	O(4)–Co(1)–N(4)	170.32(10)	O(3)–Co(2)–N(1)	86.40(11)
Co(1) ... Co(2)	3.547(2)	O(6)–Co(1)–N(4)	91.79(10)	O(5)–Co(2)–N(1)	178.13(11)
		O(7)–Co(1)–N(4)	89.84(10)	O(9)–Co(2)–N(1)	91.81(11)
		O(9)–Co(1)–N(4)	90.43(10)	N(1)–Co(2)–N(2)	88.87(11)
		N(3)–Co(1)–N(4)	86.45(10)		

Table 3:- Complex 2.3

Bond distances		Bond angles		Bond angles	
Co(1)–O(1)	2.099(2)	Co(1)–O(9)–Co(2)	115.2(10)	O(3)–Co(2)–O(5)	91.89(10)
Co(1)–O(4)	2.064(2)	O(1)–Co(1)–O(6)	176.31(10)	O(3)–Co(2)–O(7)	177.87(9)
Co(1)–O(6)	2.044(2)	O(1)–Co(1)–O(4)	90.50(10)	O(5)–Co(2)–O(7)	88.73(11)
Co(1)–O(9)	2.156(2)	O(4)–Co(1)–O(6)	93.13(10)	O(3)–Co(2)–O(9)	92.07(9)
Co(1)–N(1)	2.193(3)	O(6)–Co(1)–O(9)	88.42(10)	O(5)–Co(2)–O(9)	92.02(9)
Co(1)–N(2)	2.183(3)	O(4)–Co(1)–O(9)	91.77(9)	O(7)–Co(2)–O(9)	89.94(9)
Co(2)–O(3)	2.062(2)	O(1)–Co(1)–O(9)	90.84(9)	O(3)–Co(2)–N(3)	90.77(10)
Co(2)–O(5)	2.080(2)	O(1)–Co(1)–N(1)	90.27(9)	O(5)–Co(2)–N(3)	87.36(10)
Co(2)–O(7)	2.095(2)	O(4)–Co(1)–N(1)	87.42(10)	O(7)–Co(2)–N(3)	87.23(10)
Co(2)–O(9)	2.160(2)	O(6)–Co(1)–N(1)	90.52(10)	O(9)–Co(2)–N(3)	177.11(10)
Co(2)–N(3)	2.155(3)	O(9)–Co(1)–N(1)	178.63(10)	O(3)–Co(2)–N(4)	90.37(10)
Co(2)–N(4)	2.180(3)	O(1)–Co(1)–N(2)	87.87(10)	O(5)–Co(2)–N(4)	176.23(10)
Co(1)···Co(2)	3.644(2)	O(4)–Co(1)–N(2)	176.08(11)	O(7)–Co(2)–N(4)	88.90(11)
		O(6)–Co(1)–N(2)	88.54(10)	O(9)–Co(2)–N(4)	90.91(10)
		O(9)–Co(1)–N(2)	91.82(10)	N(4)–Co(2)–N(3)	89.60(11)
		N(1)–Co(1)–N(2)	89.02(11)		

Table 4:- Complex 2.4

Bond distances		Bond angles		Bond angles	
Co(1)–O(1)	2.072(3)	Co(1)–O(6)–Co(1) ⁷	116.3(2)	O(4)–Co(1)–N(1)	87.83(12)
Co(1)–O(4)	2.094(3)	O(1)–Co(1)–O(4)	86.38(13)	O(4)–Co(1)–N(2)	178.04(15)
Co(1)–O(6)	2.141(2)	O(1)–Co(1)–O(6)	90.78(11)	O(6)–Co(1)–O(7)	92.51(11)
Co(1)–O(7)	2.068(3)	O(1)–Co(1)–O(7)	176.34(12)	O(6)–Co(1)–N(1)	178.22(13)
Co(1)–N(1)	2.140(3)	O(1)–Co(1)–N(1)	90.56(12)	O(6)–Co(1)–N(2)	88.94(13)
Co(1)–N(2)	2.144(4)	O(1)–Co(1)–N(2)	91.65(16)	O(7)–Co(1)–N(1)	86.12(11)
Co(1)···Co(1) ⁷	3.639	O(4)–Co(1)–O(6)	91.10(11)	O(7)–Co(1)–N(2)	90.01(15)
		O(4)–Co(1)–O(7)	91.96(12)	N(1)–Co(1)–N(2)	92.19(14)

Table 5:- Polymorph I-III

Bond distances (Polymorph I)		Bond distances (Polymorph II)		Bond distances (Polymorph III)	
Co(1)–O(6)	2.1144(13)	Co(1)–O(1)	2.0910(12)	Co(1)–O(1)	2.1273(15)
Co(1)–O(9)	2.0779(15)	Co(1)–O(5)	2.1078(12)	Co(1)–O(10)	2.0857(15)
Co(1)–O(13)	2.1198(13)	Co(1)–O(6)	2.0751(12)	Co(1)–O(14)	2.1053(14)
Co(2)–O(1)	2.1478(14)	Co(1')–O(1')	2.0910(12)	Co(2)–O(5)	2.1218(17)
Co(2)–O(5)	2.0959(14)	Co(1')–O(5')	2.1078(12)	Co(2)–O(9)	2.0627(16)
Co(2)–O(10)	2.1016(13)	Co(1')–O(6')	2.0751(12)	Co(2)–O(13)	2.0759(16)
Co(1)–N(3)	2.1464(18)	Co(1)–N(1)	2.1389(14)	Co(1)–N(1)	2.1643(17)
Co(1)–N(4)	2.1575(18)	Co(1)–N(3)	2.1471(15)	Co(1)–N(2)	2.1561(18)
Co(2)–N(1)	2.1511(18)	Co(1')–N(1')	2.1389(14)	Co(2)–N(3)	2.1402(19)

Co(2)–N(2)	2.1464(18)	Co(1')–N(3')	2.1471(15)	Co(2)–N(4)	2.162(2)
Co(1)–O _{aqua} (17)	2.1255(15)	Co(1)–O _{aqua} (9)	2.1425(8)	Co(1)–O _{aqua} (17)	2.1364(15)
Co(2)–O _{aqua} (17)	2.1278(15)	Co(1')–O _{aqua} (9')	2.1425(8)	Co(2)–O _{aqua} (17)	2.1572(16)
Co(1)⋯Co(2)	3.578	Co(1)⋯Co(2)	3.616	Co(1)⋯Co(2)	3.651
' = -x, y, -z+1/2					

Table 6:- Complex 2.8

Bond distances		Bond angles		Bond angles	
Co(1)–O(1)	1.9539(14)	O(3)–Co(1)–O(3')	81.86(6)	O(1)–Co(1)–N(1)	90.72(6)
Co(1)–O(2)	1.9600(14)	O(3)–Co(1)–O(3'')	86.41(6)	O(3)–Co(1)–O(2)	170.89(6)
Co(1)–O(3)	1.8658(12)	O(3')–Co(1)–O(3'')	86.36(6)	O(3')–Co(1)–O(2)	90.42(6)
Co(1)–O(3')	1.8661(13)	O(3)–Co(1)–O(1)	90.68(6)	O(3'')–Co(1)–O(2)	88.29(6)
Co(1)–O(3'')	1.8692(13)	O(3')–Co(1)–O(1)	171.04(6)	O(1)–Co(1)–O(2)	96.55(6)
Co(1)–N(1)	1.9561(17)	O(3'')–Co(1)–O(1)	88.22(6)	N(1)–Co(1)–O(2)	90.86(6)
Co(1)⋯Co(1')	2.7093(5)	O(3)–Co(1)–N(1)	94.57(6)		
Co(1)⋯Co(1'')	2.7111(5)	O(3')–Co(1)–N(1)	94.82(6)		
Co(1)⋯Co(1''')	2.8191(5)	O(3'')–Co(1)–N(1)	178.56(7)		

Table 7:- Complex 3.1

Bond distances		Bond angles		Bond angles	
Ni(1)–O(1)	2.075(3)	O(9)–Ni(1)–O(4)	88.14(9)	O(6)–Ni(2)–O(5)	176.32(9)
Ni(1)–O(2)	2.082(3)	O(9)–Ni(1)–O(2)	174.56(9)	O(6)–Ni(2)–O(1)	89.43(9)
Ni(1)–O(4)	2.093(3)	O(4)–Ni(1)–O(2)	90.45(9)	O(5)–Ni(2)–O(1)	94.23(9)
Ni(1)–O(9)	2.135(3)	O(9)–Ni(1)–N(1)	91.32(10)	O(6)–Ni(2)–O(8)	91.12(9)
Ni(1)–N(1)	2.136(4)	O(4)–Ni(1)–N(1)	177.61(10)	O(5)–Ni(2)–O(8)	88.60(9)
Ni(1)–N(2)	2.148(4)	O(2)–Ni(1)–N(1)	90.30(10)	O(1)–Ni(2)–O(8)	88.70(9)
Ni(2)–O(1)	2.086(3)	O(9)–Ni(1)–O(1)	95.87(9)	O(6)–Ni(2)–N(4)	86.08(10)
Ni(2)–O(5)	2.088(3)	O(4)–Ni(1)–O(1)	85.87(10)	O(5)–Ni(2)–N(4)	90.25(10)
Ni(2)–O(6)	2.127(3)	O(2)–Ni(1)–O(1)	89.26(9)	O(1)–Ni(2)–N(4)	174.87(11)
Ni(2)–O(8)	2.129(3)	N(1)–Ni(1)–O(1)	91.86(10)	O(8)–Ni(2)–N(4)	88.91(10)
Ni(2)–N(3)	2.168(4)	O(9)–Ni(1)–N(2)	88.28(9)	O(6)–Ni(2)–N(3)	89.39(10)
Ni(2)–N(4)	2.148(4)	O(4)–Ni(1)–N(2)	90.53(10)	O(5)–Ni(2)–N(3)	90.93(10)
Ni(1)⋯Ni(2)	3.597	O(2)–Ni(1)–N(2)	86.48(9)	O(1)–Ni(2)–N(3)	90.84(10)
		N(1)–Ni(1)–N(2)	91.78(11)	O(8)–Ni(2)–N(3)	179.31(10)
		O(1)–Ni(1)–N(2)	174.41(11)	Ni(2)–O(1)–Ni(1)	116.78(10)

Table 8:- Complex 3.2

Bond distances		Bond angles		Bond angles	
Ni(1)–O(4)	2.0370(15)	O(4)–Ni(1)–O(6)	91.00(7)	O(5)–Ni(2)–O(3)	93.88(7)
Ni(1)–O(6)	2.0466(16)	O(4)–Ni(1)–O(7)	177.41(6)	O(1)–Ni(2)–O(3)	88.67(7)
Ni(1)–O(7)	2.0834(15)	O(6)–Ni(1)–O(7)	86.93(7)	O(5)–Ni(2)–O(9)	92.81(7)

Ni(1)–O(9)	2.0938(17)	O(4)–Ni(1)–O(9)	88.99(7)	O(1)–Ni(2)–O(9)	90.84(6)
Ni(1)–N(3)	2.109(2)	O(6)–Ni(1)–O(9)	98.22(6)	O(3)–Ni(2)–O(9)	89.82(7)
Ni(1)–N(4)	2.113(2)	O(7)–Ni(1)–O(9)	89.77(7)	O(5)–Ni(2)–N(2)	87.24(8)
Ni(2)–O(5)	2.0300(16)	O(4)–Ni(1)–N(3)	90.48(7)	O(1)–Ni(2)–N(2)	90.09(8)
Ni(2)–O(1)	2.0536(15)	O(6)–Ni(1)–N(3)	83.91(7)	O(3)–Ni(2)–N(2)	177.82(7)
Ni(2)–O(3)	2.0684(15)	O(7)–Ni(1)–N(3)	90.85(7)	O(9)–Ni(2)–N(2)	91.99(8)
Ni(2)–O(9)	2.0944(17)	O(9)–Ni(1)–N(3)	177.80(7)	O(5)–Ni(2)–N(1)	88.07(7)
Ni(2)–N(2)	2.114(2)	O(4)–Ni(1)–N(4)	91.87(7)	O(1)–Ni(2)–N(1)	88.35(7)
Ni(2)–N(1)	2.118(2)	O(6)–Ni(1)–N(4)	170.50(7)	O(3)–Ni(2)–N(1)	88.45(7)
Ni(1) ... Ni(2)	3.506	O(7)–Ni(1)–N(4)	90.41(7)	O(9)–Ni(2)–N(1)	178.11(7)
		O(9)–Ni(1)–N(4)	90.88(7)	N(2)–Ni(2)–N(1)	89.73(8)
		N(3)–Ni(1)–N(4)	87.01(8)	Ni(1)–O(9)–Ni(2)	113.70(8)
		O(5)–Ni(2)–O(1)	175.55(7)		

Table 9:- Complex 3.3

Bond distances		Bond angles		Bond angles	
Ni(1)–N(1)	2.1097(14)	O(1)–Ni(1)–O(5)	92.07(5)	O(3)–Ni(1)–N(2)	88.28(5)
Ni(1)–N(2)	2.1088(14)	O(1)–Ni(1)–O(3)	86.89(5)	O(4)–Ni(1)–N(2)	176.59(4)
Ni(1)–O(1)	2.0323(12)	O(5)–Ni(1)–O(3)	175.10(5)	O(1)–Ni(1)–N(1)	177.32(5)
Ni(1)–O(5)	2.0437(12)	O(1)–Ni(1)–O(4)	88.72(4)	O(5)–Ni(1)–N(1)	89.84(5)
Ni(1)–O(3)	2.0551(12)	O(5)–Ni(1)–O(4)	94.30(5)	O(3)–Ni(1)–N(1)	91.05(5)
Ni(1)–O(4)	2.1040(9)	O(3)–Ni(1)–O(4)	90.46(5)	O(4)–Ni(1)–N(1)	93.00(5)
Ni(1) ... Ni(1')	3.554	O(1)–Ni(1)–N(2)	88.04(6)	N(2)–Ni(1)–N(1)	90.19(6)
		O(5)–Ni(1)–N(2)	86.89(5)	Ni(1)–O(4)–Ni(1')	115.25(8)

Table 10:- Complex 3.4

Bond distances		Bond angles		Bond angles	
Ni(1)–O(4)	2.0470(19)	O(4)–Ni(1)–O(6)	90.18(8)	O(3)–Ni(2)–O(1)	87.72(8)
Ni(1)–O(6)	2.067(2)	O(4)–Ni(1)–O(7)	176.31(8)	O(5)–Ni(2)–O(1)	177.09(7)
Ni(1)–O(7)	2.072(2)	O(6)–Ni(1)–O(7)	86.33(9)	O(3)–Ni(2)–N(4)	175.65(8)
Ni(1)–O(9)	2.0885(19)	O(4)–Ni(1)–O(9)	89.38(8)	O(5)–Ni(2)–N(4)	89.65(9)
Ni(1)–N(1)	2.133(2)	O(6)–Ni(1)–O(9)	93.19(8)	O(1)–Ni(2)–N(4)	90.18(9)
Ni(1)–N(2)	2.145(2)	O(7)–Ni(1)–O(9)	89.60(8)	O(3)–Ni(2)–O(9)	90.63(8)
Ni(2)–O(5)	2.059(2)	O(4)–Ni(1)–N(1)	90.17(8)	O(5)–Ni(2)–O(9)	92.91(8)
Ni(2)–O(1)	2.090(2)	O(6)–Ni(1)–N(1)	86.78(8)	O(1)–Ni(2)–O(9)	90.00(8)
Ni(2)–O(3)	2.0459(19)	O(7)–Ni(1)–N(1)	90.85(8)	N(4)–Ni(2)–O(9)	93.19(8)
Ni(2)–O(9)	2.108(2)	O(9)–Ni(1)–N(1)	179.55(10)	O(3)–Ni(2)–N(3)	86.77(8)
Ni(2)–N(3)	2.121(2)	O(4)–Ni(1)–N(2)	90.68(9)	O(5)–Ni(2)–N(3)	89.92(9)
Ni(2)–N(4)	2.106(2)	O(6)–Ni(1)–N(2)	174.22(8)	O(1)–Ni(2)–N(3)	87.18(8)
Ni(1) ... Ni(2)	3.593	O(7)–Ni(1)–N(2)	92.91(9)	N(4)–Ni(2)–N(3)	89.32(8)
		O(9)–Ni(1)–N(2)	92.53(8)	O(9)–Ni(2)–N(3)	176.23(9)
		N(1)–Ni(1)–N(2)	87.51(8)	Ni(1)–O(9)–Ni(2)	117.78(9)

Table 11:- Complex 3.5					
Bond distances		Bond angles		Bond angles	
Ni(1)–N(1)	2.0903(14)	O(5)–Ni(1)–O(1)	174.01(5)	O(6)–Ni(1)–O(9)	89.07(4)
Ni(1)–N(2)	2.0825(13)	O(5)–Ni(1)–O(6)	86.90(5)	N(2)–Ni(1)–O(9)	175.23(4)
Ni(1)–O(1)	2.0674(11)	O(1)–Ni(1)–O(6)	91.21(5)	O(5)–Ni(1)–N(1)	89.31(5)
Ni(1)–O(5)	2.0502(11)	O(5)–Ni(1)–N(2)	88.57(5)	O(1)–Ni(1)–N(1)	92.51(5)
Ni(1)–O(6)	2.0768(11)	O(1)–Ni(1)–N(2)	85.69(5)	O(6)–Ni(1)–N(1)	176.18(5)
Ni(1)–O(9)	2.0890(9)	O(6)–Ni(1)–N(2)	88.16(5)	N(2)–Ni(1)–N(1)	91.26(6)
Ni(1) ⋯ Ni(1')	3.563	O(5)–Ni(1)–O(9)	95.16(5)	O(9)–Ni(1)–N(1)	91.76(4)
		O(1)–Ni(1)–O(9)	90.50(4)	Ni(1)–O(9)–Ni(1')	117.05(8)

Table 12:- Complex 3.6					
Bond distances		Bond angles		Bond angles	
Ni(1)–O(3)	2.0062(19)	O(3)–Ni(1)–O(1)	175.07(8)	O(7)–Ni(2)–Cl(4)	83.61(7)
Ni(1)–O(1)	2.0437(19)	O(3)–Ni(1)–N(1)	86.35(9)	O(5)–Ni(2)–N(4)	87.78(9)
Ni(1)–N(1)	2.086(2)	O(1)–Ni(1)–N(1)	89.14(9)	O(4)–Ni(2)–N(4)	88.10(9)
Ni(1)–O(7)	2.126(2)	O(3)–Ni(1)–O(7)	92.37(9)	O(5)–Ni(2)–N(3)	89.73(9)
Ni(1)–N(2)	2.128(3)	O(1)–Ni(1)–O(7)	92.00(9)	O(4)–Ni(2)–N(3)	173.65(9)
Ni(1)–Cl(4)	2.4860(9)	N(1)–Ni(1)–O(7)	176.20(10)	N(4)–Ni(2)–N(3)	90.95(10)
Ni(2)–O(5)	2.0518(19)	O(3)–Ni(1)–N(2)	88.60(10)	O(5)–Ni(2)–O(7)	92.70(9)
Ni(2)–O(4)	2.057(2)	O(1)–Ni(1)–N(2)	93.50(10)	O(4)–Ni(2)–O(7)	87.93(9)
Ni(2)–N(4)	2.073(3)	N(1)–Ni(1)–N(2)	91.35(10)	N(4)–Ni(2)–O(7)	175.93(10)
Ni(2)–N(3)	2.106(2)	O(7)–Ni(1)–N(2)	92.20(9)	N(3)–Ni(2)–O(7)	93.09(10)
Ni(2)–O(7)	2.121(2)	O(3)–Ni(1)–Cl(4)	89.14(7)	O(5)–Ni(2)–Cl(4)	174.73(6)
Ni(2)–Cl(4)	2.4470(9)	O(1)–Ni(1)–Cl(4)	89.17(7)	N(4)–Ni(2)–Cl(4)	95.64(7)
Ni(1)⋯Ni(2)	3.281	N(1)–Ni(1)–Cl(4)	93.84(7)	O(4)–Ni(2)–Cl(4)	92.13(6)
		O(7)–Ni(1)–Cl(4)	82.55(7)	N(3)–Ni(2)–Cl(4)	94.21(7)
		N(2)–Ni(1)–Cl(4)	174.20(7)	Ni(2)–Cl(4)–Ni(1)	83.39(3)
		O(5)–Ni(2)–O(4)	83.96(8)	Ni(2)–O(7)–Ni(1)	101.18(9)

Table 13:- Complex 4.1					
Bond distances		Bond angles		Bond angles	
Zn(1)–O(10)	2.056(2)	O(10)–Zn(1)–O(10')	180.0	O(7)–Zn(2)–O(6)	87.30(9)
Zn(1)–O(8)	2.062(2)	O(10)–Zn(1)–O(8)	86.68(10)	N(2)–Zn(2)–O(6)	144.55(9)
Zn(1)–O(6)	2.141(2)	O(10')–Zn(1)–O(8)	93.32(10)	O(5)–Zn(2)–O(6)	57.62(9)
Zn(2)–O(9)	1.949(2)	O(8)–Zn(1)–O(8')	180.0	N(2)–Zn(2)–O(5)	96.72(10)
Zn(2)–O(7)	1.9558(19)	O(10)–Zn(1)–O(6)	87.37(11)	O(1)–Zn(3)–N(1)	105.11(10)
Zn(2)–N(2)	2.039(2)	O(10')–Zn(1)–O(6)	92.63(11)	O(1)–Zn(3)–O(2)	90.88(10)
Zn(2)–O(5)	2.120(3)	O(8)–Zn(1)–O(6)	90.46(8)	N(1)–Zn(3)–O(2)	101.73(10)
Zn(2)–O(6)	2.329(3)	O(8')–Zn(1)–O(6)	89.54(8)	O(1)–Zn(3)–O(4)	86.54(10)

Zn(3)–O(1)	2.027(2)	O(6)–Zn(1)–O(6')	179.998(1)	N(1)–Zn(3)–O(4)	98.01(10)
Zn(3)–N(1)	2.028(2)	O(9)–Zn(2)–O(7)	117.78(9)	O(2)–Zn(3)–O(4)	160.07(9)
Zn(3)–O(2)	2.039(2)	O(9)–Zn(2)–N(2)	101.99(9)	O(1v)–Zn(3)–O(3)	160.34(9)
Zn(3)–O(4)	2.054(2)	O(7)–Zn(2)–N(2)	96.82(9)	N(1)–Zn(3)–O(3)	94.28(9)
Zn(3)–O(3)	2.062(2)	O(9)–Zn(2)–O(5)	102.69(10)	O(2)–Zn(3)–O(3)	88.30(10)
Zn(3)–Zn(3')	2.9269	O(7)–Zn(2)–O(5)	133.22(10)	O(4)–Zn(3)–O(3)	87.57(10)
Zn(1)–Zn(2)	3.444	O(9)–Zn(2)–O(6)	107.08(9)		

Table 14:- Complex 4.2

Bond distances		Bond angles		Bond angles	
N(1)–Zn(1)	2.0338(16)	O(1)–Zn(1)–N(1)	103.26(7)	O(1)–Zn(1)–O(2)	159.36(7)
O(1)–Zn(1)	2.0258(14)	O(1)–Zn(1)–O(4)	89.51(7)	N(1)–Zn(1)–O(2)	97.37(7)
O(2)–Zn(1)	2.0574(14)	N(1)–Zn(1)–O(4)	102.79(7)	O(4)–Zn(1)–O(2)	86.47(7)
O(3)–Zn(1)	2.0445(14)	O(1)–Zn(1)–O(3)	88.63(7)	O(3)–Zn(1)–O(2)	88.04(7)
O(4)–Zn(1)	2.0341(14)	N(1)–Zn(1)–O(3)	97.73(7)		
Zn(1)–Zn(1')	2.9582(4)	O(4)–Zn(1)–O(3)	159.27(6)		

Table 15:- Complex 4.3

Bond distances		Bond angles	
Zn(1)–O(1)	2.0346(19)	O(1)–Zn(1)–O(1')	152.25(10)
Zn(1)–N(1)	2.0361(19)	O(1)–Zn(1)–N(1)	103.87(5)
Zn(1)–O(2)	2.0557(19)	O(1)–Zn(1)–O(2)	88.32(8)
Zn(1)–Zn(1')	2.9799(5)	N(1)–Zn(1)–O(2)	97.45(5)
		O(1)–Zn(1)–O(2')	88.12(7)
		O(2)–Zn(1)–O(2')	165.10(10)

Table 16:- Complex 4.4

Bond distances		Bond angles	
Zn(1)–O(1)	2.0340(12)	N(1)–Zn(1)–O(3)	101.81(5)
Zn(1)–O(2)	2.0544(12)	O(1)–Zn(1)–O(3)	89.23(6)
Zn(1)–O(3)	2.0340(12)	N(1)–Zn(1)–O(4)	98.27(5)
Zn(1)–O(4)	2.0465(12)	O(1)–Zn(1)–O(4)	88.97(6)
Zn(1)–N(1)	2.0287(13)	O(3)–Zn(1)–O(4)	159.72(5)
Zn(1)–Zn(1')	2.9341(4)	N(1)–Zn(1)–O(2)	96.92(6)
		O(1)–Zn(1)–O(2)	159.88(5)
		O(3)–Zn(1)–O(2)	87.41(6)
		O(4)–Zn(1)–O(2)	87.36(6)

Table 17:- Complex 4.5

Bond distances		Bond angles		Bond angles	
Zn(1)–O(1)	1.909(3)	O(1)–Zn(1)–O(13)	118.10(15)	O(16)–Zn(5)–O(27)	111.51(16)

Zn(1)–O(8)	1.956(4)	O(1)–Zn(1)–O(10)	112.00(16)	O(24)–Zn(5)–O(27)	104.48(18)
Zn(1)–O(10)	1.944(4)	O(13)–Zn(1)–O(10)	107.05(19)	O(25)–Zn(5)–O(27)	102.60(19)
Zn(1)–O(13)	1.930(4)	O(1)–Zn(1)–O(8)	111.60(15)	O(21)–Zn(6)–O(16)	121.73(14)
Zn(2)–O(1)	1.924(3)	O(13)–Zn(1)–O(8)	104.38(18)	O(21)–Zn(6)–O(20)	105.38(18)
Zn(2)–O(3)	1.912(4)	O(10)–Zn(1)–O(8)	102.3(2)	O(16)–Zn(6)–O(20)	110.93(16)
Zn(2)–O(4)	1.966(4)	O(3)–Zn(2)–O(1)	120.01(14)	O(21)–Zn(6)–O(28)	106.45(17)
Zn(2)–O(9)	1.983(4)	O(3)–Zn(2)–O(4)	106.50(17)	O(16)–Zn(6)–O(28)	110.71(15)
Zn(3)–O(1)	1.935(3)	O(1)–Zn(2)–O(4)	112.91(15)	O(20)–Zn(6)–O(28)	99.16(17)
Zn(3)–O(5)	1.958(4)	O(3)–Zn(2)–O(9)	106.89(17)	O(16)–Zn(7)–O(17)	123.03(15)
Zn(3)–O(6)	1.928(4)	O(1)–Zn(2)–O(9)	110.36(15)	O(16)–Zn(7)–O(19)	115.12(15)
Zn(3)–O(11)	2.046(4)	O(4)–Zn(2)–O(9)	97.73(17)	O(17)–Zn(7)–O(19)	112.66(18)
Zn(4)–O(1)	2.007(3)	O(6)–Zn(3)–O(1)	121.81(14)	O(16)–Zn(7)–O(26)	104.59(15)
Zn(4)–O(2)	2.104(4)	O(6)–Zn(3)–O(5)	112.24(17)	O(17)–Zn(7)–O(26)	98.54(17)
Zn(4)–O(7)	2.257(4)	O(1)–Zn(3)–O(5)	117.11(16)	O(19)–Zn(7)–O(26)	96.94(16)
Zn(4)–O(12)	2.104(3)	O(6)–Zn(3)–O(11)	97.16(16)	O(16)–Zn(8)–O(30)	167.77(14)
Zn(4)–O(14)	2.195(3)	O(1)–Zn(3)–O(11)	105.70(15)	O(16)–Zn(8)–O(23)	100.61(13)
Zn(4)–O(15)	2.077(3)	O(5)–Zn(3)–O(11)	96.53(17)	O(30)–Zn(8)–O(23)	90.80(14)
Zn(5)–O(16)	1.912(3)	O(1)–Zn(4)–O(15)	170.65(14)	O(16)–Zn(8)–O(22)	96.77(14)
Zn(5)–O(24)	1.936(4)	O(1)–Zn(4)–O(2)	96.22(14)	O(30)–Zn(8)–O(22)	86.66(15)
Zn(5)–O(25)	1.946(4)	O(15)–Zn(4)–O(2)	87.90(14)	O(23)–Zn(8)–O(22)	94.31(16)
Zn(5)–O(27)	1.968(4)	O(1)–Zn(4)–O(12)	99.72(13)	O(16)–Zn(8)–O(29)	80.32(13)
Zn(6)–O(16)	1.919(3)	O(15)–Zn(4)–O(12)	88.36(13)	O(30)–Zn(8)–O(29)	88.00(14)
Zn(6)–O(20)	1.949(4)	O(2)–Zn(4)–O(12)	93.54(15)	O(23)–Zn(8)–O(29)	175.93(15)
Zn(6)–O(21)	1.912(4)	O(1)–Zn(4)–O(14)	79.68(12)	O(22)–Zn(8)–O(29)	89.51(15)
Zn(6)–O(28)	1.982(4)	O(15)–Zn(4)–O(14)	92.02(13)	O(16)–Zn(8)–O(18)	90.48(15)
Zn(7)–O(16)	1.936(3)	O(2)–Zn(4)–O(14)	89.15(14)	O(30)–Zn(8)–O(18)	85.28(15)
Zn(7)–O(17)	1.946(4)	O(12)–Zn(4)–O(14)	177.29(15)	O(23)–Zn(8)–O(18)	89.01(16)
Zn(7)–O(19)	1.979(4)	O(1)–Zn(4)–O(7)	92.12(14)	O(22)–Zn(8)–O(18)	171.32(16)
Zn(7)–O(26)	2.036(4)	O(15)–Zn(4)–O(7)	83.06(14)	O(29)–Zn(8)–O(18)	87.01(15)
Zn(8)–O(16)	2.004(3)	O(2)–Zn(4)–O(7)	170.02(15)		
Zn(8)–O(18)	2.224(4)	O(12)–Zn(4)–O(7)	90.45(14)		
Zn(8)–O(22)	2.096(4)	O(14)–Zn(4)–O(7)	86.94(14)		
Zn(8)–O(23)	2.082(4)	O(16)–Zn(5)–O(24)	117.06(15)		
Zn(8)–O(29)	2.216(4)	O(16)–Zn(5)–O(25)	112.12(16)		
Zn(8)–O(30)	2.068(3)	O(24)–Zn(5)–O(25)	107.84(18)		

Table 18:- Complex 4.6

Bond distances		Bond angles		Bond angles	
Zn(1)–O(4)	2.061(5)	O(4)–Zn(1)–O(4')	175.2(3)	O(9)–Zn(2)–O(8)	105.59(18)
Zn(1)–O(5)	2.080(5)	O(4)–Zn(1)–O(5)	85.9(2)	O(6)–Zn(2)–N(1)	108.7(2)
Zn(1)–O(9)	2.096(4)	O(4')–Zn(1)–O(5)	91.0(3)	O(8)–Zn(2)–N(1)	111.3(2)
Zn(2)–N(1)	2.016(6)	O(5)–Zn(1)–O(5')	96.8(4)	O(21)–Zn(2)–N(1)	102.8(2)

Zn(2)–O(6)	1.938(5)	O(4)–Zn(1)–O(9)	98.7(2)	O(1)–Zn(3)–O(3)	117.3(2)
Zn(2)–O(9)	1.954(4)	O(4')–Zn(1)–O(9)	84.64(18)	O(1)–Zn(3)–O(9)	112.0(2)
Zn(2)–O(8)	1.974(5)	O(5)–Zn(1)–O(9)	86.8(2)	O(3)–Zn(3)–O(9)	114.8(2)
Zn(2)–O(1)	1.920(5)	O(5')–Zn(1)–O(9)	169.9(2)	O(1)–Zn(3)–O(7)	104.3(2)
Zn(3)–O(3)	1.936(6)	O(9)–Zn(1)–O(9')	91.2(2)	O(3)–Zn(3)–O(7)	101.2(3)
Zn(3)–O(9)	1.956(4)	O(6)–Zn(2)–O(9)	122.9(2)	O(9)–Zn(3)–O(7)	105.02(19)
Zn(3)–O(7)	1.978(5)	O(6)–Zn(2)–O(8)	103.3(2)		

Table 19:- Complex 4.8

Bond distances		Bond angles		Bond angles	
Zn(1)–O(5)	2.0111(19)	O(5)–Zn(1)–O(11)	99.06(10)	O(2)–Zn(1)–O(10)	85.58(8)
Zn(1)–O(11)	2.044(2)	O(5)–Zn(1)–O(2)	159.44(9)	O(5)–Zn(1)–O(9)	90.31(8)
Zn(1)–O(2)	2.045(2)	O(11)–Zn(1)–O(2)	101.14(10)	O(11)–Zn(1)–O(9)	94.00(10)
Zn(1)–O(10)	2.109(2)	O(5)–Zn(1)–O(10)	88.64(8)	O(2)–Zn(1)–O(9)	92.08(8)
Zn(1)–O(9)	2.120(2)	O(11)–Zn(1)–O(10)	95.71(10)	O(10)–Zn(1)–O(9)	170.28(9)

Table 20:- Complex 5.2

Bond distances		Bond angles		Bond angles	
Na(1)–O(1)	2.2761(15)	O(1)–Na(1)–O(5)	168.06(8)	O(1)–Na(1)–O(3)	83.75(5)
Na(1)–O(3)	2.782(2)	O(1)–Na(1)–O(4)	97.71(8)	O(5)–Na(1)–O(3)	90.88(6)
Na(1)–O(6)	2.515(2)	O(5)–Na(1)–O(4)	93.17(8)	O(4)–Na(1)–O(3)	92.62(8)
Na(1)–O(4)	2.447(2)	O(1)–Na(1)–O(6)	76.74(6)	O(6)–Na(1)–O(3)	77.90(6)
Na(1)–O(5)	2.3682(17)	O(5)–Na(1)–O(6)	91.74(7)		
Na(1)–Na(1)	3.4702(16)	O(4)–Na(1)–O(6)	169.40(9)		

Table 21:- Complex 5.3

Bond distances		Bond angles		Bond angles	
Mn(1)–O(2)	2.187(4)	O(3)–Mn(1)–O(3')	180.0 (1)	O(3)–Mn(1)–O(4)	85.8(2)
Mn(1)–O(3)	2.176(3)	O(3)–Mn(1)–O(2)	91.88(14)	O(2)–Mn(1)–O(4')	91.9(3)
Mn(1)–O(4)	2.216(9)	O(3)–Mn(1)–O(2')	88.12(14)	O(2)–Mn(1)–O(4)	88.1(3)
		O(2)–Mn(1)–O(2')	180.0(11)	O(3)–Mn(1)–O(4')	94.2(2)
		O(3)–Mn(1)–O(4')	94.2(2)	O(4)–Mn(1)–O(4')	180.0(5)

Table 22:- Complex 5.6

Bond distances		Bond angles		Bond angles	
Zn(1)–O(5)	1.9475(13)	O(5)–Zn(1)–O(5')	114.34(8)	O(7)–Na(1)–O(4)	83.17(7)
Zn(1)–O(2)	1.9690(15)	O(5)–Zn(1)–O(2)	109.08(6)	O(5)–Na(1)–O(4)	65.71(5)
Na(1)–O(7)	2.373(3)	O(5)–Zn(1)–O(2')	113.50(6)	O(1)–Na(1)–O(4)	127.94(6)
Na(1)–O(5)	2.3790(15)	O(2)–Zn(1)–O(2')	96.00(10)	O(1')–Na(1)–O(4)	144.08(6)
Na(1)–O(1)	2.4233(16)	O(7)–Na(1)–O(5)	85.27(9)	O(7)–Na(1)–O(3)	89.70(9)
Na(1)–O(1')	2.4463(16)	O(7)–Na(1)–O(1)	98.95(8)	O(5)–Na(1)–O(3)	127.60(5)
Na(1)–O(4)	2.4538(15)	O(5)–Na(1)–O(1)	165.95(6)	O(1)–Na(1)–O(3)	66.08(5)

Na(1)–O(3)	2.4800(15)	O(7)–Na(1)–O(1')	115.61(8)	O(1')–Na(1)–O(3)	141.83(6)
Na(1)–Na(1')	3.6926(16)	O(5)–Na(1)–O(1')	84.72(5)	O(4)–Na(1)–O(3)	61.91(4)
Table 23:- Complex 5.7					
Bond distances		Bond angles		Bond angles	
Zn(1)–O(1)	2.063(3)	O(1)–Zn(1)–O(6)	175.72(10)	O(7)–Zn(1)–N(2)	95.25(13)
Zn(1)–O(6)	2.067(2)	O(1)–Zn(1)–O(7)	88.12(12)	N(1)–Zn(1)–N(2)	88.52(12)
Zn(1)–O(7)	2.091(3)	O(6)–Zn(1)–O(7)	88.31(12)	O(1)–Zn(1)–O(8)	87.02(11)
Zn(1)–O(8)	2.214(3)	O(1)–Zn(1)–N(1)	93.18(11)	O(6)–Zn(1)–O(8)	90.40(11)
Zn(1)–N(1)	2.150(3)	O(6)–Zn(1)–N(1)	90.23(11)	O(7)–Zn(1)–O(8)	86.21(13)
Zn(1)–N(2)	2.159(3)	O(7)–Zn(1)–N(1)	176.04(13)	N(1)–Zn(1)–O(8)	90.12(11)
Zn(1)–O(6)	2.067(2)	O(1)–Zn(1)–N(2)	88.85(11)	N(2)–Zn(1)–O(8)	175.57(12)
		O(6)–Zn(1)–N(2)	93.82(11)		

Table 24:- Complex 5.8					
Bond distances		Bond angles		Bond angles	
Zn(1)–O(6)	1.9447(18)	O(6)–Zn(1)–O(1)	108.55(7)	O(1)–Na(1)–O(5)	86.90(7)
Zn(1)–O(1)	1.9822(17)	O(6)–Zn(1)–O(7)	105.08(10)	O(9)–Na(1)–O(5)	104.22(11)
Zn(1)–O(7)	2.015(3)	O(1)–Zn(1)–O(7)	135.01(10)	O(1)–Na(1)–O(5')	160.55(9)
Zn(1)–N(1)	2.052(2)	O(6)–Zn(1)–N(1)	99.46(10)	O(5)–Na(1)–O(5')	81.15(7)
Zn(1)–O(8)	2.407(3)	O(1)–Zn(1)–N(1)	105.17(8)	O(9)–Na(1)–O(4)	90.06(11)
Na(1)–O(9)	2.313(3)	O(7)–Zn(1)–N(1)	97.73(9)	O(1)–Na(1)–O(4)	123.42(7)
Na(1)–O(1)	2.3908(19)	O(6)–Zn(1)–O(8)	99.30(11)	O(5)–Na(1)–O(4)	146.37(7)
Na(1)–O(5)	2.420(2)	O(1)–Zn(1)–O(8)	89.27(9)	O(5')–Na(1)–O(4)	65.60(6)
Na(1)–O(5')	2.431(2)	O(7)–Zn(1)–O(8)	56.15(10)	O(9)–Na(1)–O(3)	87.11(10)
Na(1)–O(4)	2.5188(19)	N(1)–Zn(1)–O(8)	151.17(10)	O(1)–Na(1)–O(3)	63.70(6)
Na(1)–O(3)	2.5571(19)	O(9)–Na(1)–O(1)	93.41(11)	O(5)–Na(1)–O(3)	149.51(7)
Na(1)–Na(1')	3.685(2)	O(9)–Na(1)–O(5)	103.40(12)	O(5')–Na(1)–O(3)	124.45(7)

Table 25:- Complex 5.9					
Bond distances		Bond angles		Bond angles	
Zn(1)–N(3)	2.023(3)	N(3)–Zn(1)–N(5)	124.79(11)	N(1)–Zn(1)–O(6)	91.06(11)
Zn(1)–N(5)	2.035(3)	N(3)–Zn(1)–N(1)	106.64(12)	N(3)–Zn(1)–O(1)	89.76(11)
Zn(1)–N(1)	2.057(3)	N(5)–Zn(1)–N(1)	128.23(11)	N(5)–Zn(1)–O(1)	91.95(10)
Zn(1)–O(6)	2.072(2)	N(3)–Zn(1)–O(6)	99.80(10)	N(1)–Zn(1)–O(1)	82.03(10)
Zn(1)–O(1)	2.196(2)	N(5)–Zn(1)–O(6)	86.13(10)	O(6)–Zn(1)–O(1)	169.52(10)

Table 26:- Complex 5.10					
Bond distances		Bond angles		Bond angles	
Zn(1)–O(7)	2.039(4)	O(7)–Zn(1)–O(15)	92.96(18)	O(22)–Zn(3)–O(32)	95.3(2)
Zn(1)–O(15)	2.092(5)	O(7)–Zn(1)–O(13)	174.4(2)	O(22)–Zn(3)–N(5)	104.0(2)

Zn(1)–O(13)	2.114(5)	O(15)–Zn(1)–O(13)	90.86(19)	O(32)–Zn(3)–N(5)	160.6(2)
Zn(1)–O(14)	2.123(5)	O(7)–Zn(1)–O(14)	95.1(2)	O(22)–Zn(3)–O(27)	89.86(18)
Zn(1)–O(1)	2.163(4)	O(15)–Zn(1)–O(14)	89.14(19)	O(32)–Zn(3)–O(27)	88.98(18)
Zn(1)–N(1)	2.163(6)	O(13)–Zn(1)–O(14)	89.0(2)	N(5)–Zn(3)–O(27)	89.4(2)
Zn(2)–O(16)	1.994(6)	O(7)–Zn(1)–O(1)	88.32(19)	O(22)–Zn(3)–O(24)	86.60(19)
Zn(2)–O(5)	2.030(5)	O(15)–Zn(1)–O(1)	91.72(18)	O(32)–Zn(3)–O(24)	90.53(19)
Zn(2)–N(3)	2.060(6)	O(13)–Zn(1)–O(1)	87.54(18)	N(5)–Zn(3)–O(24)	92.3(2)
Zn(2)–O(11)	2.130(4)	O(14)–Zn(1)–O(1)	176.4(2)	O(27)–Zn(3)–O(24)	176.37(18)
Zn(2)–O(8)	2.144(4)	O(7)–Zn(1)–N(1)	86.2(2)	O(23)–Zn(4)–O(29)	93.23(19)
Zn(3)–O(22)	2.023(5)	O(15)–Zn(1)–N(1)	179.1(2)	O(23)–Zn(4)–N(7)	90.4(2)
Zn(3)–O(32)	2.027(5)	O(13)–Zn(1)–N(1)	90.0(2)	O(29)–Zn(4)–N(7)	175.8(2)
Zn(3)–O(27)	2.106(4)	O(14)–Zn(1)–N(1)	90.6(2)	O(23)–Zn(4)–O(17)	90.7(2)
Zn(3)–O(24)	2.121(4)	O(1)–Zn(1)–N(1)	88.6(2)	O(29)–Zn(4)–O(17)	91.9(2)
Zn(4)–O(23)	2.077(5)	O(16)–Zn(2)–O(5)	95.8(2)	N(7)–Zn(4)–O(17)	90.1(2)
Zn(4)–O(29)	2.080(5)	O(16)–Zn(2)–N(3)	160.5(3)	O(23)–Zn(4)–O(30)	177.1(2)
Zn(4)–N(7)	2.138(6)	O(5)–Zn(2)–N(3)	103.6(2)	O(29)–Zn(4)–O(30)	89.3(2)
Zn(4)–O(17)	2.139(5)	O(16)–Zn(2)–O(11)	89.0(2)	N(7)–Zn(4)–O(30)	87.1(2)
Zn(4)–O(30)	2.142(5)	O(5)–Zn(2)–O(11)	91.11(18)	O(17)–Zn(4)–O(30)	87.8(2)
Zn(4)–O(31)	2.158(5)	N(3)–Zn(2)–O(11)	89.2(2)	O(23)–Zn(4)–O(31)	94.0(2)
		O(16)–Zn(2)–O(8)	90.0(2)	O(29)–Zn(4)–O(31)	89.7(2)
		O(5)–Zn(2)–O(8)	87.85(18)	N(7)–Zn(4)–O(31)	88.0(2)
		N(3)–Zn(2)–O(8)	92.1(2)	O(17)–Zn(4)–O(31)	175.0(2)

Table 27:- Complex **5.11**

Bond distances		Bond angles		Bond angles	
Zn(1)–N(4)	2.097(5)	N(4)–Zn(1)–N(2)	101.1(3)	N(2)–Zn(1)–N(1)	78.5(5)
Zn(1)–O(2)	2.128(4)	N(4)–Zn(1)–O(2)	107.20(17)	O(2)–Zn(1)–N(1)	150.8(3)
Zn(1)–N(3)	2.138(5)	N(2)–Zn(1)–O(2)	95.4(3)	N(3)–Zn(1)–N(1)	90.9(4)
Zn(1)–O(1)	2.297(5)	N(4)–Zn(1)–N(3)	78.8(2)	N(4)–Zn(1)–O(1)	164.03(17)
Zn(1)–N(1)	2.140(9)	N(2)–Zn(1)–N(3)	169.1(4)	N(2)–Zn(1)–O(1)	89.7(3)
Zn(1)–N(2)	2.119(9)	O(2)–Zn(1)–N(3)	95.0(2)	O(2)–Zn(1)–O(1)	59.55(17)
		N(4)–Zn(1)–N(1)	102.0(3)	N(3)–Zn(1)–O(1)	92.90(19)

Table 28:- Complex **5.12**

Bond distances		Bond angles		Bond angles	
Zn(1)–N(2)	2.114(3)	N(2)–Zn(1)–N(3)	113.74(10)	N(4)–Zn(1)–O(1)	93.75(11)
Zn(1)–N(3)	2.114(3)	N(2)–Zn(1)–N(4)	99.23(11)	N(1)–Zn(1)–O(1)	91.39(10)
Zn(1)–N(4)	2.117(3)	N(3)–Zn(1)–N(4)	77.17(10)	N(2)–Zn(1)–O(2)	94.38(10)
Zn(1)–N(1)	2.127(3)	N(2)–Zn(1)–N(1)	77.79(10)	N(3)–Zn(1)–O(2)	151.03(9)
Zn(1)–O(1)	2.208(3)	N(3)–Zn(1)–N(1)	98.94(10)	N(4)–Zn(1)–O(2)	92.13(11)
Zn(1)–O(2)	2.274(3)	N(4)–Zn(1)–N(1)	173.80(11)	N(1)–Zn(1)–O(2)	93.51(10)
		N(2)–Zn(1)–O(1)	150.32(10)	O(1)–Zn(1)–O(2)	58.37(9)

Crystallographic data and refinement parameters for the compounds

Compound code	2.1	2.2	2.3
Empirical formula	C ₆₁ H ₅₄ Co ₂ N ₄ O ₁₁	C ₅₇ H ₅₁ Co ₂ N ₄ O ₉	C ₄₈ H ₃₈ Cl ₄ Co ₂ N ₄ O ₉
Formula weight	1136.94	1053.88	1074.48
Temperature	296(2)	296(2)	296(2)
Wavelength(Å)	0.71073	0.71073	0.71073
Crystal system	Monoclinic	Monoclinic	Monoclinic
Space group	P2 ₁ /c	P2 ₁ /c	P2 ₁ /c
Unit cell dimensions	a=10.5613(3)Å, α=90.00° b=26.0992(7)Å, β=95.750(2)° c=21.1667(6)Å, γ=90.00°	a=10.8300(4)Å, α=90.00° b=38.4304(15)Å, β=91.559(3)° c=12.6302(6)Å, γ=90.00°	a=21.8994(10)Å, α=90.00° b=20.5157(10)Å, β=92.144(10)° c=12.0381(6)Å, γ=90.00°
Volume	5805.1(3) Å ³	5254.8(4) Å ³	5404.7(5) Å ³
Z	4	4	4
Density (calculated)	1.301 mg/m ³	1.332 mg/m ³	1.320 mg/m ³
Absorption coefficient	0.633 mm ⁻¹	0.691 mm ⁻¹	0.864 mm ⁻¹
F(000)	2360	2188	2192
Crystal size	0.16 x 0.21 x 0.25 mm ³	0.12 x 0.23 x 0.46 mm ³	0.23 x 0.39 x 0.46 mm ³
Theta range for data collection	1.84 to 28.29	1.70 to 29.16	1.96 to 28.34
Index ranges	-13 ≤ h ≤ 14 -29 ≤ k ≤ 34 -28 ≤ l ≤ 27	-14 ≤ h ≤ 13 -44 ≤ k ≤ 52 -15 ≤ l ≤ 17	-28 ≤ h ≤ 29 -27 ≤ k ≤ 27 -16 ≤ l ≤ 16
Reflections collected	52884	37792	55233
Independent reflections	14382	13907	13454
Completeness to theta	99.8%	98.1%	99.8%
Absorption correction	None	None	None
Refinement method	Full-matrix least-squares on F ²	Full-matrix least-squares on F ²	Full-matrix least-squares on F ²
Data / restraints / parameters	14382 / 0 / 669	13907 / 0 / 657	13454 / 0 / 612
Goodness-of-fit on F ²	1.021	1.104	1.048
Final R indices [I > 2σ(I)]	0.0704	0.0616	0.0551
R indices (all data)	0.1574	0.1835	0.0828

Compound code	2.4	2.5 (Polymorph I)	2.5 (Polymorph II)
Empirical formula	C ₄₈ H ₄₂ Co ₂ N ₄ O ₁₃	C ₄₈ H ₃₈ Co ₂ N ₈ O ₁₇	C ₄₈ H ₃₈ Co ₂ N ₈ O ₁₇
Formula weight	1000.72	1116.72	1116.72
Temperature	296(2)	296(2)	296(2)
Wavelength(Å)	0.71073	0.71073	0.71073
Crystal system	Monoclinic	Triclinic	Monoclinic
Space group	C2/c	P-1	C2/c
Unit cell dimensions	a=21.6032(3)Å, α=90.00° b=24.005(3)Å, β=116.536(10)° c=11.9388(2)Å, γ=90.00°	a=11.8668(2)Å, α=68.727(10)° b=13.8387(2)Å, β=75.229(10)° c=17.8115(3)Å, γ=66.628(10)°	a=16.0312(3)Å, α=90.00° b=13.5441(3)Å, β=99.850(10)° c=23.7144(5)Å, γ=90.00°
Volume	5539.05(14) Å ³	2480.91(7) Å ³	5073.16(18) Å ³
Z	4	2	4
Density (calculated)	1.200 mg/m ³	1.495 mg/m ³	1.462 mg/m ³
Absorption coefficient	0.657 mm ⁻¹	0.750 mm ⁻¹	0.734 mm ⁻¹
F(000)	2064	1144	2288
Crystal size	0.19 x 0.25 x 0.34 mm ³	0.11 x 0.21 x 0.33 mm ³	0.14 x 0.23 x 0.50 mm ³
Theta range for data collection	1.35 to 28.75	1.24 to 28.28	1.74 to 25.50
Index ranges	-26 ≤ h ≤ 29 -32 ≤ k ≤ 30 -16 ≤ l ≤ 16	-15 ≤ h ≤ 15 -18 ≤ k ≤ 18 -23 ≤ l ≤ 21	-19 ≤ h ≤ 19 -16 ≤ k ≤ 12 -28 ≤ l ≤ 28
Reflections collected	28547	29432	21391
Independent reflections	7120	11705	4696
Completeness to theta	99.0%	95.0%	99.2%
Absorption correction	None	None	None
Refinement method	Full-matrix least-squares on F ²	Full-matrix least-squares on F ²	Full-matrix least-squares on F ²
Data / restraints / parameters	7120 / 0 / 307	11705 / 0 / 684	4696 / 0 / 339
Goodness-of-fit on F ²	1.028	1.019	1.023
Final R indices [I > 2σ(I)]	0.0698	0.0384	0.0276
R indices (all data)	0.1265	0.0591	0.0364

Compound code	2.5 (Polymorph III)	2.6	2.7
Empirical formula	C ₄₈ H ₃₈ Co ₂ N ₈ O ₁₇	C ₂₄ H ₂₂ Co N ₂ O ₅	C ₂₄ H ₂₂ Co N ₄ O ₁₀
Formula weight	1116.72	477.37	585.39
Temperature	296(2)	296(2)	296(2)
Wavelength(Å)	0.71073	0.71073	0.71073
Crystal system	Monoclinic	Monoclinic	Triclinic
Space group	P2(1)/n	P2 ₁ /c	P-1
Unit cell dimensions	a=13.6133(4)Å, α=90.00° b=13.3201(4)Å, β=101.746(2)° c=28.6728(9)Å, γ=90.00°	a=9.3345(2)Å, α=90.00° b=20.6701(3)Å, β=116.784(10)° c=13.0538(2)Å, γ=90.00°	a=7.2206(5)Å, α=97.169(10)° b=8.5518(6)Å, β=98.233(10)° c=11.0026(7)Å, γ=108.126(10)°
Volume	5090.4(3) Å ³	2248.44(7) Å ³	628.59(7) Å ³
Z	4	4	1
Density (calculated)	1.457 mg/m ³	1.410 mg/m ³	1.546 mg/m ³
Absorption coefficient	0.731 mm ⁻¹	0.801 mm ⁻¹	0.748 mm ⁻¹
F(000)	2288	988	301
Crystal size	0.24 x 0.27 x 0.32 mm ³	0.21 x 0.24 x 0.33 mm ³	0.16 x 0.24 x 0.27 mm ³
Theta range for data collection	1.55 to 28.21	1.97 to 28.28	2.55 to 25.99
Index ranges	-17 ≤ h ≤ 17 -17 ≤ k ≤ 17 -38 ≤ l ≤ 35	-12 ≤ h ≤ 12 -25 ≤ k ≤ 26 -16 ≤ l ≤ 16	-8 ≤ h ≤ 8 -10 ≤ k ≤ 10 -12 ≤ l ≤ 13
Reflections collected	60000	17289	4750
Independent reflections	12446	5147	2221
Completeness to theta	99.1%	92.0%	89.8%
Absorption correction	None	None	None
Refinement method	Full-matrix least-squares on F ²	Full-matrix least-squares on F ²	Full-matrix least-squares on F ²
Data / restraints / parameters	12446 / 0 / 684	5147 / 0 / 298	2221 / 0 / 187
Goodness-of-fit on F ²	1.006	0.884	1.048
Final R indices [I > 2σ(I)]	0.0417	0.0293	0.0254
R indices (all data)	0.0787	0.0470	0.0271

Compound code	2.8	3.1	3.2
Empirical formula	C ₅₆ H ₅₆ Co ₄ N ₈ O ₁₆	C ₆₂ H ₅₆ N ₄ Ni ₂ O ₁₁	C ₅₇ H ₅₁ N ₄ Ni ₂ O ₉
Formula weight	1332.81	1150.53	1053.40
Temperature	296(2)	296(2)	296(2)
Wavelength(Å)	0.71073	0.71073	0.71073
Crystal system	Orthorhombic	Monoclinic	Monoclinic
Space group	F (d d d)	P2(1)/c	P2(1)/c
Unit cell dimensions	a=21.1772(6)Å, α=90.00° b=25.7730(12)Å, β=90.00° c=22.5183(6)Å, γ=90.00°	a=10.50220(10)Å, α=90.00° b=26.0953(4)Å, β=95.601(10)° c=21.1012(3)Å, γ=90.00°	a=10.7917(2)Å, α=90.00° b=38.3193(7)Å, β=91.375(10)° c=12.5877(2)Å, γ=90.00°
Volume	12290.5(7) Å ³	5755.34(13) Å ³	5203.90(16) Å ³
Z	8	4	4
Density (calculated)	1.441 mg/m ³	1.328 mg/m ³	1.345 mg/m ³
Absorption coefficient	1.132 mm ⁻¹	0.718 mm ⁻¹	0.784 mm ⁻¹
F(000)	5472	2400	2196
Crystal size	0.19 x 0.24 x 0.28 mm ³	0.24 x 0.32 x 0.41 mm ³	0.23 x 0.31 x 0.44 mm ³
Theta range for data collection	2.71 to 28.34	1.24 to 25.93	1.06 to 28.33
Index ranges	-28 ≤ h ≤ 28 -34 ≤ k ≤ 33 -30 ≤ l ≤ 30	-12 ≤ h ≤ 12 -31 ≤ k ≤ 31 -25 ≤ l ≤ 25	-11 ≤ h ≤ 14 -51 ≤ k ≤ 45 -16 ≤ l ≤ 16
Reflections collected	30772	70360	50748
Independent reflections	3841	11173	12870
Completeness to theta	99.7%	99.6%	99.1%
Absorption correction	None	None	None
Refinement method	Full-matrix least-squares on F ²	Full-matrix least-squares on F ²	Full-matrix least-squares on F ²
Data / restraints / parameters	3841 / 0 / 197	11173 / 0 / 691	12870 / 0 / 657
Goodness-of-fit on F ²	0.952	1.032	1.016
Final R indices [I > 2σ(I)]	0.0323	0.0480	0.0417
R indices (all data)	0.0502	0.0716	0.0761

Compound code	3.3	3.4	3.5
Empirical formula	C ₄₈ H ₄₄ N ₄ Ni ₂ O ₁₀	C ₆₄ H ₅₀ N ₄ Ni ₂ O ₉	C ₄₈ H ₃₈ N ₈ Ni ₂ O ₁₇
Formula weight	954.29	1136.50	1116.28
Temperature	296(2)	296(2)	296(2)
Wavelength(Å)	0.71073	0.71073	0.71073
Crystal system	Orthorhombic	Monoclinic	Monoclinic
Space group	Pbcn	P2(1)/c	C2/c
Unit cell dimensions	a=14.2706(6)Å, α=90.00° b=21.2846(8)Å, β=90.00° c=15.2229(6)Å, γ=90.00°	a=10.490(4)Å, α=90.00° b=20.917(9)Å, β=96.16(3)° c=25.180(11)Å, γ=90.00°	a=15.9027(5)Å, α=90.00° b=13.5204(5)Å, β=99.906(2)° c=23.6140(10)Å, γ=90.00°
Volume	4623.9(3) Å ³	5493(4) Å ³	5001.6(3) Å ³
Z	4	4	4
Density (calculated)	1.371 mg/m ³	1.374 mg/m ³	1.482 mg/m ³
Absorption coefficient	0.876 mm ⁻¹	0.748 mm ⁻¹	0.834 mm ⁻¹
F(000)	1984	2360	2296
Crystal size	0.15 x 0.24 x 0.32 mm ³	0.09 x 0.17 x 0.33 mm ³	0.11 x 0.29 x 0.35 mm ³
Theta range for data collection	1.72 to 28.32	6.60 to 28.28	3.11 to 28.33
Index ranges	-13 ≤ h ≤ 19 -28 ≤ k ≤ 28 -16 ≤ l ≤ 20	-13 ≤ h ≤ 13 -27 ≤ k ≤ 27 -27 ≤ l ≤ 33	-16 ≤ h ≤ 21 -17 ≤ k ≤ 16 -31 ≤ l ≤ 31
Reflections collected	34247	39758	21611
Independent reflections	5768	12863	6153
Completeness to theta	99.9%	94.4%	98.9%
Absorption correction	None	None	None
Refinement method	Full-matrix least-squares on F ²	Full-matrix least-squares on F ²	Full-matrix least-squares on F ²
Data / restraints / parameters	5768 / 0 / 298	12863 / 0 / 720	6153 / 0 / 343
Goodness-of-fit on F ²	1.021	0.948	0.993
Final R indices [I > 2σ(I)]	0.0332	0.0472	0.0319
R indices (all data)	0.0556	0.1025	0.0452

Compound code	3.6	4.1	4.2
Empirical formula	C ₄₁ H ₃₄ Cl ₄ N ₄ Ni ₂ O ₇	C ₉₀ H ₇₀ N ₄ O ₂₀ Zn ₅	C ₃₈ H ₃₀ N ₂ O ₈ Zn ₂
Formula weight	953.94	1854.35	773.38
Temperature	296(2)	296(2)	296(2)
Wavelength(Å)	0.71073	0.71073	0.71073
Crystal system	Monoclinic	Triclinic	Monoclinic
Space group	P2(1)/c	P-1	P2(1)/n
Unit cell dimensions	a=12.9935(5)Å, α=90.00° b=14.3654(5)Å, β=97.762(3)° c=22.6612(8)Å, γ=90.00°	a=10.7105(4)Å, α=101.771(2)° b=10.9616(4)Å, β=101.908(2)° c=18.8659(8)Å, γ=97.202(2)°	a=10.05170(10)Å, α=90.00° b=10.5364(10)Å, β=99.266(10)° c=17.3429(2)Å, γ=90.00°
Volume	4191.1(3) Å ³	2089.02(14) Å ³	1812.80(3) Å ³
Z	4	1	2
Density (calculated)	1.512 mg/m ³	1.474 mg/m ³	1.417 mg/m ³
Absorption coefficient	1.207 mm ⁻¹	1.489 mm ⁻¹	1.376 mm ⁻¹
F(000)	1952	948	792
Crystal size	0.16 x 0.21 x 0.32 mm ³	0.11 x 0.18 x 0.28 mm ³	0.18 x 0.22 x 0.41 mm ³
Theta range for data collection	1.68 to 28.32	1.14 to 25.00	2.20 to 28.66
Index ranges	-16 ≤ h ≤ 17 -19 ≤ k ≤ 19 -30 ≤ l ≤ 30	-12 ≤ h ≤ 12 -12 ≤ k ≤ 12 -22 ≤ l ≤ 22	-13 ≤ h ≤ 12 -14 ≤ k ≤ 10 -22 ≤ l ≤ 23
Reflections collected	41439	14402	16775
Independent reflections	10403	6986	4542
Completeness to theta	99.7%	95.2%	97.2%
Absorption correction	None	None	None
Refinement method	Full-matrix least-squares on F ²	Full-matrix least-squares on F ²	Full-matrix least-squares on F ²
Data / restraints / parameters	10403/ 0 / 531	6986/ 0 / 538	4542/ 0 / 227
Goodness-of-fit on F ²	0.974	1.037	1.036
Final R indices [I > 2σ(I)]	0.0451	0.0343	0.0307
R indices (all data)	0.1146	0.0476	0.0412

Compound code	4.3	4.4	4.5
Empirical formula	C ₄₂ H ₃₈ N ₂ O ₈ Zn ₂	C ₄₂ H ₃₈ N ₂ O ₈ Zn ₂	C ₅₂ H ₅₄ O ₁₅ S ₂ Zn ₄
Formula weight	829.48	829.48	1244.55
Temperature	296(2)	296(2)	296(2)
Wavelength(Å)	0.71073	0.71073	0.71073
Crystal system	Monoclinic	Tetragonal	Orthorhombic
Space group	P2(1)/c	I-42d	Pca2(1)
Unit cell dimensions	a=10.7319(10)Å, α=90.00° b=10.9111(10)Å, β=114.387(5)° c=18.7835(15)Å, γ=90.00°	a=12.4107(2)Å, α=90.00° b=12.4107(2)Å, β=90.00° c=24.7015(5)Å, γ=90.00°	a=23.7229(8)Å, α=90.00° b=11.3117(4)Å, β=90.00° c=41.1802(14)Å, γ=90.00°
Volume	2003.2(3) Å ³	3804.66(12) Å ³	11050.6(7) Å ³
Z	2	4	8
Density (calculated)	1.375 mg/m ³	1.448 mg/m ³	1.496 mg/m ³
Absorption coefficient	1.251 mm ⁻¹	1.317 mm ⁻¹	1.855 mm ⁻¹
F(000)	856	1712	5104
Crystal size	0.21 x 0.27 x 0.38 mm ³	0.19 x 0.24 x 0.31 mm ³	0.16 x 0.21 x 0.28 mm ³
Theta range for data collection	2.08 to 28.23	1.84 to 28.29	0.99 to 28.30
Index ranges	-14 ≤ h ≤ 14 -14 ≤ k ≤ 14 -24 ≤ l ≤ 21	-16 ≤ h ≤ 16 -16 ≤ k ≤ 15 -32 ≤ l ≤ 32	-31 ≤ h ≤ 31 -15 ≤ k ≤ 12 -54 ≤ l ≤ 52
Reflections collected	26347	23239	125528
Independent reflections	4860	2361	26306
Completeness to theta	98.0%	99.7%	99.7%
Absorption correction	None	None	None
Refinement method	Full-matrix least-squares on F ²	Full-matrix least-squares on F ²	Full-matrix least-squares on F ²
Data / restraints / parameters	4860 / 0 / 246	2361 / 0 / 124	26306 / 902 / 1335
Goodness-of-fit on F ²	1.062	1.038	0.975
Final R indices [I > 2σ(I)]	0.0272	0.0248	0.0422
R indices (all data)	0.0356	0.0365	0.1005

Compound code	4.6	4.7	4.8
Empirical formula	C ₇₄ H ₆₈ N ₂ O ₁₈ Zn ₅	C ₁₆ H ₁₈ O ₆ Zn	C ₁₈ H ₂₂ N ₂ O ₁₁ S ₂ Zn
Formula weight	1600.15	371.67	571.87
Temperature	296(2)	296(2)	296(2)
Wavelength(Å)	0.71073	0.71073	0.71073
Crystal system	Monoclinic	Monoclinic	Triclinic
Space group	C2/c	C2/c	P-1
Unit cell dimensions	a=15.9469(8)Å, α=90.00° b=22.1141(8)Å, β=107.563(4)° c=21.6548(13)Å, γ=90.00°	a=26.8543(12)Å, α=90.00° b=5.0620(2)Å, β=106.837(5)° c=12.0699(6)Å, γ=90.00°	a=6.0159(5)Å, α=84.584(5)° b=7.7149(5)Å, β=84.464(4)° c=26.7675(17)Å, γ=70.371(3)°
Volume	7280.6(6) Å ³	1570.40(12) Å ³	1162.13(14) Å ³
Z	4	4	2
Density (calculated)	1.460 mg/m ³	1.572 mg/m ³	1.634 mg/m ³
Absorption coefficient	1.693 mm ⁻¹	1.592 mm ⁻¹	1.298 mm ⁻¹
F(000)	3280	768	588
Crystal size	0.11 x 0.16 x 0.25 mm ³	0.21 x 0.24 x 0.44 mm ³	0.16 x 0.22 x 0.35 mm ³
Theta range for data collection	1.63 to 28.46	1.58 to 28.28	0.77 to 28.20
Index ranges	-21 ≤ h ≤ 19 -28 ≤ k ≤ 29 -15 ≤ l ≤ 28	-35 ≤ h ≤ 35 -6 ≤ k ≤ 6 -15 ≤ l ≤ 16	-7 ≤ h ≤ 7 -9 ≤ k ≤ 10 -35 ≤ l ≤ 35
Reflections collected	39072	9890	14736
Independent reflections	8910	1937	5405
Completeness to theta	96.8%	99.2%	94.8%
Absorption correction	None	None	None
Refinement method	Full-matrix least-squares on F ²	Full-matrix least-squares on F ²	Full-matrix least-squares on F ²
Data / restraints / parameters	8910 / 529 / 455	1937 / 0 / 106	5405 / 0 / 316
Goodness-of-fit on F ²	1.136	1.086	1.030
Final R indices [I > 2σ(I)]	0.0813	0.0356	0.0500
R indices (all data)	0.2085	0.0495	0.0628

Compound code	5.1	5.2	5.3
Empirical formula	C ₁₆ H ₁₆ N ₂ O ₃	C ₃₂ H ₄₂ N ₄ Na ₂ O ₁₂	C ₃₂ H ₃₄ MnN ₄ O ₈
Formula weight	284.31	720.68	657.57
Temperature	Triclinic	Monoclinic	Triclinic
Wavelength(Å)	P-1	C2/c	P-1
Crystal system	296(2)	296(2)	296(2)
Space group	0.71073	0.71073	0.71073
Unit cell dimensions	a=9.835(2)Å, α=71.04(6)° b=12.268(3)Å, β=80.37(8)° c=13.548(3)Å, γ=89.39(8)°	a= 41.683(2)Å, α= 90.00° b= 11.0892(5)Å, β= 94.873(5)° c= 7.6453(4)Å, γ= 90.00°	a= 4.8260(5)Å, α=106.631(11)° b= 13.7417(16)Å, β=95.693(8)° c= 14.7777(18)Å, γ=94.310(8)°
Volume	1522.4(6) Å ³	3521.1(3)	928.86(18)
Z	4	4	1
Density (calculated)	1.240 mg/m ³	1.359 mg/m ³	1.176 mg/m ³
Absorption coefficient	0.087 mm ⁻¹	0.124	0.403
F(000)	600	1520	343
Crystal size	0.21 x 0.27 x 0.35 mm ³	0.21 x 0.28 x 0.41 mm ³	0.19 x 0.25 x 0.31 mm ³
Theta range for data collection	1.61 to 25.50	0.98 to 25.50	1.45 to 28.19
Index ranges	-11 ≤ h ≤ 11 -14 ≤ k ≤ 14 -16 ≤ l ≤ 15	-46 ≤ h ≤ 50 -13 ≤ k ≤ 13 -9 ≤ l ≤ 9	-6 ≤ h ≤ 6 -18 ≤ k ≤ 18 -19 ≤ l ≤ 19
Reflections collected	12913	17758	12588
Independent reflections	5358	3202	4367
Completeness to theta	94.6	97.4	95.2
Absorption correction	None	None	None
Refinement method	Full-matrix least-squares on F ²	Full-matrix least-squares on F ²	Full-matrix least-squares on F ²
Data / restraints / parameters	5358/ 0 / 393	3202 / 0 / 258	4367 / 0 / 209
Goodness-of-fit on F ²	1.057	1.071	0.948
Final R indices [I > 2σ(I)]	0.1034	0.0461	0.1270
R indices (all data)	0.1544	0.0625	0.2534

Compound code	5.4A	5.4B	5.5A
Empirical formula	C ₁₆ H ₁₆ O ₆	C ₁₆ H ₁₆ O ₆	C ₁₄ H ₁₂ O ₆
Formula weight	304.29	304.29	276.24
Temperature	296(2)	296(2)	296(2)
Wavelength(Å)	0.71073	0.71073	0.71073
Crystal system	Orthorhombic	Orthorhombic	Triclinic
Space group	Pbca	Pbca	P-1
Unit cell dimensions	a=11.2656(3)Å, α=90.00° b=8.7582(2)Å, β=90.00° c=30.4390(7)Å, γ=90.00°	a=11.6404(3)Å, α=90.00° b=8.1726(3)Å, β=90.00° c=31.7753(9)Å, γ=90.00°	a=4.81350(10)Å, α=101.05(2)° b=10.3319(2)Å, β=95.545(2)° c=12.9176(3)Å, γ=92.127(2)°
Volume	3003.31(13) Å ³	3022.86(16) Å ³	626.56(2) Å ³
Z	8	8	2
Density (calculated)	1.346 mg/m ³	1.337 mg/m ³	1.464 mg/m ³
Absorption coefficient	0.104 mm ⁻¹	0.103 mm ⁻¹	0.116 mm ⁻¹
F(000)	1280	1280	288
Crystal size	0.21 x 0.35 x 0.40 mm ³	0.15 x 0.24 x 0.35 mm ³	0.17 x 0.32 x 0.41 mm ³
Theta range for data collection	2.25 to 28.22	1.28 to 28.35	1.62 to 25.50
Index ranges	-14 ≤ h ≤ 14 -11 ≤ k ≤ 11 -40 ≤ l ≤ 40	-15 ≤ h ≤ 9 -10 ≤ k ≤ 10 -42 ≤ l ≤ 33	-5 ≤ h ≤ 5 -11 ≤ k ≤ 12 -15 ≤ l ≤ 15
Reflections collected	39559	24325	6492
Independent reflections	3683	3746	2236
Completeness to theta	99.6%	99.5%	95.9%
Absorption correction	None	None	None
Refinement method	Full-matrix least-squares on F ²	Full-matrix least-squares on F ²	Full-matrix least-squares on F ²
Data / restraints / parameters	3683 / 0 / 201	3746 / 0 / 201	2236 / 0 / 183
Goodness-of-fit on F ²	1.036	1.093	1.039
Final R indices [I > 2σ(I)]	0.0386	0.0766	0.0341
R indices (all data)	0.0528	0.1615	0.0418

Compound code	5.5B	5.6	5.7
Empirical formula	C ₁₄ H ₁₂ O ₆	C ₂₈ H ₂₂ Na ₂ O ₁₄ Zn	C ₂₅ H ₂₈ N ₂ O ₉ Zn
Formula weight	276.24	693.81	565.86
Temperature	296(2)	296(2)	296(2)
Wavelength(Å)	0.71073	0.71073	0.71073
Crystal system	Monoclinic	Monoclinic	Monoclinic
Space group	P2(1)/c	C2/c	P2(1)/c
Unit cell dimensions	a=9.4630(8)Å, α=90.00° b=10.2791(8)Å, β=91.532(6)° c=26.299(3)Å, γ=90.00°	a= 16.3719(6)Å, α=90.00° b= 22.7018(6)Å, β= 94.705(2)° c= 7.4514(2)Å, γ=90.00°	a=10.727(2)Å, α=90.00° b=17.456(4)Å, β=120.721(12)° c=16.435(3)Å, γ=90.00°
Volume	2557.2(4) Å ³	2760.14(15) Å ³	2645.6(9) Å ³
Z	8	4	4
Density (calculated)	1.435 mg/m ³	1.670 mg/m ³	1.421 mg/m ³
Absorption coefficient	0.114 mm ⁻¹	0.997 mm ⁻¹	0.982 mm ⁻¹
F(000)	1152	1416	1176
Crystal size	0.18 x 0.32 x 0.44 mm ³	0.18 x 0.21 x 0.38 mm ³	0.36 x 0.38 x 0.44 mm ³
Theta range for data collection	1.55 to 28.35	1.54 to 28.35	1.85 to 28.37
Index ranges	-12 ≤ h ≤ 12 -13 ≤ k ≤ 12 -34 ≤ l ≤ 34	-21 ≤ h ≤ 21 -30 ≤ k ≤ 30 -9 ≤ l ≤ 9	-14 ≤ h ≤ 14 -23 ≤ k ≤ 23 -21 ≤ l ≤ 20
Reflections collected	27322	20978	32182
Independent reflections	6355	3376	6531
Completeness to theta	99.3%	97.9%	98.7%
Absorption correction	None	None	None
Refinement method	Full-matrix least-squares on F ²	Full-matrix least-squares on F ²	Full-matrix least-squares on F ²
Data / restraints / parameters	6355 / 0 / 371	3376 / 0 / 204	6531 / 0 / 355
Goodness-of-fit on F ²	1.021	1.028	1.059
Final R indices [I > 2σ(I)]	0.0592	0.0328	0.0501
R indices (all data)	0.1289	0.0438	0.1037

Compound code	5.8	5.9	5.10
Empirical formula	C ₄₀ H ₄₂ N ₄ Na ₂ O ₁₈ Zn ₂	C ₂₆ H ₂₉ N ₇ O ₇ Zn	C ₁₄₈ H ₁₇₆ N ₂₀ O ₇₀ Zn ₈
Formula weight	1043.50	616.93	3878.05
Temperature	296(2)	296(2)	296(2)
Wavelength(Å)	0.71073	0.71073	0.71073
Crystal system	Triclinic	Monoclinic	Triclinic
Space group	P-1	P2(1)/c	P-1
Unit cell dimensions	a=8.6774(7)Å, α=108.070(3)° b=11.7824(9)Å, β=94.205(3)° c=12.3236(15)Å, γ=109.158(2)°	a=9.3548(3)Å, α=90.00° b=18.3574(6)Å, β=115.724(2)° c=18.7369(6)Å, γ=90.00°	a=11.3948(5)Å, α=98.390(2)° b=17.2622(7)Å, β=90.784(2)° c=22.0932(9)Å, γ=98.487(2)°
Volume	1109.77(18) Å ³	2898.80(16) Å ³	4249.4(3) Å ³
Z	1	4	1
Density (calculated)	1.561 mg/m ³	1.414 mg/m ³	1.515 mg/m ³
Absorption coefficient	1.181 mm ⁻¹	0.903 mm ⁻¹	1.209 mm ⁻¹
F(000)	536	1280	2004
Crystal size	0.14 x 0.22 x 0.35 mm ³	0.19 x 0.24 x 0.38 mm ³	0.24 x 0.31 x 0.44 mm ³
Theta range for data collection	2.53 to 28.36	1.64 to 25.00	0.93 to 26.00
Index ranges	-11 ≤ h ≤ 11 -15 ≤ k ≤ 15 -16 ≤ l ≤ 16	-10 ≤ h ≤ 10 -21 ≤ k ≤ 21 -20 ≤ l ≤ 21	-13 ≤ h ≤ 14 -20 ≤ k ≤ 21 -27 ≤ l ≤ 26
Reflections collected	12883	24225	42586
Independent reflections	5282	4849	16377
Completeness to theta	94.9%	95.0%	98.1%
Absorption correction	None	None	None
Refinement method	Full-matrix least-squares on F ²	Full-matrix least-squares on F ²	Full-matrix least-squares on F ²
Data / restraints / parameters	5282 / 0 / 304	4849 / 0 / 380	16377 / 0 / 1133
Goodness-of-fit on F ²	1.038	1.036	1.054
Final R indices [I > 2σ(I)]	0.0397	0.0442	0.0692
R indices (all data)	0.0576	0.0600	0.1093

Compound code	5.11	5.12	6.1A
Empirical formula	C ₃₈ H ₃₂ N ₄ O ₉ Zn	C ₃₄ H ₃₈ N ₄ O ₁₂ Zn	C ₃₈ H ₃₈ N ₄ O ₅
Formula weight	754.05	760.05	630.72
Temperature	296(2)	296(2)	296(2)
Wavelength(Å)	0.71073	0.71073	0.71073
Crystal system	Monoclinic	Triclinic	Triclinic
Space group	P2(1)/c	P-1	P-1
Unit cell dimensions	a= 11.4686(7)Å, α= 90.00° b= 18.0561(11)Å, β=103.013(3)° c= 17.4989(10)Å, γ= 90.00°	a=10.8004(1)Å, α=102.683(1)° b=11.7121(2)Å, β=106.283(1)° c= 15.6378(2)Å, γ=101.937(1)°	a=11.4032(5)Å, α=80.782(3)° b=11.4631(5)Å, β=72.286(3)° c=15.0226(7)Å, γ=68.221(3)°
Volume	3530.6(4) Å ³	1774.72(4) Å ³	1734.59(13)Å ³
Z	4	2	2
Density (calculated)	1.419 mg/m ³	1.422 mg/m ³	1.208 mg/m ³
Absorption coefficient	0.758 mm ⁻¹	0.760 mm ⁻¹	0.081 mm ⁻¹
F(000)	1560	792	668
Crystal size	0.12 x 0.22 x 0.31 mm ³	0.18 x 0.33 x 0.42 mm ³	0.15 x 0.23 x 0.49 mm ³
Theta range for data collection	1.64 to 25.00	1.86 to 28.33	5.37 to 30.55
Index ranges	-13 ≤ h ≤ 13 -21 ≤ k ≤ 21 -20 ≤ l ≤ 20	-14 ≤ h ≤ 14 -15 ≤ k ≤ 15 -19 ≤ l ≤ 20	-13 ≤ h ≤ 16 -16 ≤ k ≤ 15 -21 ≤ l ≤ 21
Reflections collected	32573	26316	19198
Independent reflections	6187	8670	9486
Completeness to theta	99.3 %	97.9 %	89.1%
Absorption correction	None	None	None
Refinement method	Full-matrix least-squares on F ²	Full-matrix least-squares on F ²	Full-matrix least-squares on F ²
Data / restraints / parameters	6187 / 0 / 423	8670 / 0 / 476	9486 / 0 / 445
Goodness-of-fit on F ²	1.155	1.025	0.984
Final R indices [I > 2σ(I)]	0.0911	0.0570	0.0688
R indices (all data)	0.1300	0.0919	0.1814

Compound code	6.1B	6.2	6.3
Empirical formula	C ₁₉ H ₂₀ N ₂ O ₃	C ₃₄ H ₅₀ N ₄ O ₉	C ₂₀ H ₂₀ N ₂ O ₃
Formula weight	324.37	658.78	336.38
Temperature	296(2)	296(2)	296(2)
Wavelength(Å)	0.71073	0.71073	0.71073
Crystal system	Orthorhombic	Triclinic	Orthorhombic
Space group	P2(1)2(1)2(1)	P-1	P2(1)2(1)2(1)
Unit cell dimensions	a=9.4877(15)Å, α=90.00° b=12.6863(19)Å, β=90.00° c=14.832(2)Å, γ=90.00°	a=12.2204(2)Å, α=69.946(10)° b=12.5113(2)Å, β=87.210(10)° c=13.5098(2)Å, γ=68.896(10)°	a=5.11390(10)Å, α=90.00° b=13.4807(3)Å, β=90.00° c=24.8362(5)Å, γ=90.00°
Volume	1785.2(5)Å ³	1803.58(5) Å ³	1712.18(6)Å ³
Z	4	2	4
Density (calculated)	1.207 mg/m ³	1.213 mg/m ³	1.305 mg/m ³
Absorption coefficient	0.082 mm ⁻¹	0.088 mm ⁻¹	0.089 mm ⁻¹
F(000)	688	708	712
Crystal size	0.21 x 0.25 x 0.46 mm ³	0.24 x 0.27 x 0.41 mm ³	0.05 x 0.15 x 0.48 mm ³
Theta range for data collection	2.11 to 28.33	1.61 to 28.32	1.64 to 28.34
Index ranges	-11 ≤ h ≤ 12 -16 ≤ k ≤ 16 -18 ≤ l ≤ 18	-16 ≤ h ≤ 15 -16 ≤ k ≤ 16 -17 ≤ l ≤ 17	-6 ≤ h ≤ 6 -17 ≤ k ≤ 17 -33 ≤ l ≤ 33
Reflections collected	13050	21315	18583
Independent reflections	3962	8106	4201
Completeness to theta	92.5%	90.3%	98.9
Absorption correction	None	None	None
Refinement method	Full-matrix least-squares on F ²	Full-matrix least-squares on F ²	Full-matrix least-squares on F ²
Data / restraints / parameters	3962 / 0 / 231	8106 / 0 / 472	4201 / 0 / 232
Goodness-of-fit on F ²	0.931	1.064	0.989
Final R indices [I > 2σ(I)]	0.0481	0.0690	0.0501
R indices (all data)	0.1017	0.1046	0.1171

Compound code	6.3A	6.3B	6.4
Empirical formula	C ₂₀ H ₂₂ N ₂ O ₄	C ₂₀ H ₂₄ N ₂ O ₅	C ₃₈ H ₄₀ N ₄ O ₁₃ S ₂
Formula weight	354.40	372.41	824.86
Temperature	296(2)	296(2)	296(2)
Wavelength(Å)	0.71073	0.71073	0.71073
Crystal system	Triclinic	Monoclinic	Triclinic
Space group	P-1	Cc	P-1
Unit cell dimensions	a=7.1037(15)Å, α=62.431(6)° b=11.806(3)Å, β=87.595(7)° c=12.231(3)Å, γ=88.176(6)°	a=21.9919(4)Å, α=90.00° b=4.80880(10)Å, β=119.546(3)° c=20.9465(4)Å, γ=90.00°	a=11.1900(2)Å, α=80.895(10)° b=11.3769(2)Å, β=76.141(10)° c=17.1563(4)Å, γ=65.615(10)°
Volume	908.4(3) Å ³	1927.13(6)	1927.02(7) Å ³
Z	2	4	2
Density (calculated)	1.296 mg/m ³	1.284 mg/m ³	1.422 mg/m ³
Absorption coefficient	0.091 mm ⁻¹	0.093 mm ⁻¹	0.210 mm ⁻¹
F(000)	376	792	864
Crystal size	0.31 x 0.36 x 0.41 mm ³	0.12 x 0.21 x 0.33 mm ³	0.11 x 0.19 x 0.26 mm ³
Theta range for data collection	1.95 to 28.21	2.13 to 28.30	1.23 to 25.00
Index ranges	-9 ≤ h ≤ 9 -15 ≤ k ≤ 15 -16 ≤ l ≤ 15	-26 ≤ h ≤ 28 -6 ≤ k ≤ 6 -27 ≤ l ≤ 24	-13 ≤ h ≤ 12 -13 ≤ k ≤ 13 -19 ≤ l ≤ 18
Reflections collected	9706	8211	12342
Independent reflections	4392	3569	6109
Completeness to theta	97.8%	97.9%	89.7%
Absorption correction	None	None	None
Refinement method	Full-matrix least-squares on F ²	Full-matrix least-squares on F ²	Full-matrix least-squares on F ²
Data / restraints / parameters	4392 / 0 / 248	3569 / 0 / 265	6109 / 0 / 542
Goodness-of-fit on F ²	1.046	1.021	1.042
Final R indices [I > 2σ(I)]	0.0422	0.0469	0.0634
R indices (all data)	0.0594	0.0823	0.0812

Compound code	6.5	6.6	6.7
Empirical formula	C ₃₈ H ₃₈ N ₆ O ₁₀	C ₂₀ H ₂₇ ClN ₂ O ₁₁	C ₂₄ H ₂₈ N ₂ O ₇
Formula weight	738.74	506.89	456.48
Temperature	296(2)	296(2)	296(2)
Wavelength(Å)	0.71073	0.71073	0.71073
Crystal system	Monoclinic	Triclinic	Triclinic
Space group	P2(1)/c	P-1	P-1
Unit cell dimensions	a=20.7294(19)Å, α=90.00° b=7.8139(7)Å, β=104.081(2)° c=22.774(2)Å, γ=90.00°	a=8.3309(8)Å, α=87.815(7)° b=9.2665(9)Å, β=76.962(7)° c=16.4365(15)Å, γ=79.988(7)°	a=5.06960(10)Å, α=91.913(2)° b=9.0991(2)Å, β=91.993(2)° c=26.4899(6)Å, γ=100.875(2)°
Volume	3578.0(6) Å ³	1217.3(2) Å ³	1198.28(4) Å ³
Z	4	2	2
Density (calculated)	1.371 mg/m ³	1.383 mg/m ³	1.265 mg/m ³
Absorption coefficient	0.101 mm ⁻¹	0.217 mm ⁻¹	0.093 mm ⁻¹
F(000)	1552	532	484
Crystal size	0.17 x 0.22 x 0.41 mm ³	0.14 x 0.26 x 0.34 mm ³	0.11 x 0.21 x 0.36 mm ³
Theta range for data collection	2.03 to 28.25	2.23 to 28.40	3.85 to 28.30
Index ranges	-26 ≤ h ≤ 24 -10 ≤ k ≤ 10 -29 ≤ l ≤ 25	-11 ≤ h ≤ 11 -12 ≤ k ≤ 11 -21 ≤ l ≤ 21	-6 ≤ h ≤ 6 -12 ≤ k ≤ 12 -35 ≤ l ≤ 35
Reflections collected	25241	17295	11741
Independent reflections	8478	5698	5697
Completeness to theta	95.6%	93.2%	95.5%
Absorption correction	None	None	None
Refinement method	Full-matrix least-squares on F ²	Full-matrix least-squares on F ²	Full-matrix least-squares on F ²
Data / restraints / parameters	8478 / 0 / 507	5698 / 0 / 340	5697 / 0 / 313
Goodness-of-fit on F ²	1.041	0.985	1.023
Final R indices [I > 2σ(I)]	0.0958	0.0625	0.0618
R indices (all data)	0.1887	0.1298	0.1396

Compound code	6.8	6.9	6.10
Empirical formula	C ₂₈ H ₂₈ N ₂ O ₆	C ₄₄ H ₄₂ N ₄ O ₆	C ₂₄ H ₂₂ N ₂ O ₃
Formula weight	488.52	722.82	386.44
Temperature	296(2)	296(2)	296(2)
Wavelength(Å)	0.71073	0.71073	0.71073
Crystal system	Triclinic	Triclinic	Triclinic
Space group	P-1	P-1	P-1
Unit cell dimensions	a=9.3056(3)Å, α=77.184(2)° b=9.6907(4)Å, β=74.467(2)° c=16.2492(6)Å, γ=64.461(2)°	a=7.528(2)Å, α=114.290(4)° b=11.516(3)Å, β=99.137(4)° c=12.334(3)Å, γ=96.136(4)°	a=8.1869(2)Å, α=111.239(2)° b=10.4020(2)Å, β=93.668(2)° c=13.6322(3)Å, γ=105.441(2)°
Volume	1264.28(8) Å ³	944.4(4) Å ³	1026.25(4) Å ³
Z	2	1	2
Density (calculated)	1.283 mg/m ³	1.271 mg/m ³	1.251 mg/m ³
Absorption coefficient	0.091 mm ⁻¹	0.085 mm ⁻¹	0.083 mm ⁻¹
F(000)	516	382	408
Crystal size	0.26 x 0.28 x 0.46 mm ³	0.16 x 0.20 x 0.31 mm ³	0.10 x 0.32 x 0.42 mm ³
Theta range for data collection	2.35 to 28.20	7.61 to 28.25	3.08 to 26.00
Index ranges	-12 ≤ h ≤ 12 -12 ≤ k ≤ 12 -20 ≤ l ≤ 21	-9 ≤ h ≤ 9 -15 ≤ k ≤ 15 -16 ≤ l ≤ 13	-10 ≤ h ≤ 10 -12 ≤ k ≤ 11 -10 ≤ l ≤ 16
Reflections collected	18094	8512	5472
Independent reflections	6032	4332	3430
Completeness to theta	96.7%	92.9	85.3%
Absorption correction	None	None	None
Refinement method	Full-matrix least-squares on F ²	Full-matrix least-squares on F ²	Full-matrix least-squares on F ²
Data / restraints / parameters	6032 / 0 / 332	4332 / 0 / 254	3430 / 0 / 272
Goodness-of-fit on F ²	1.071	0.990	1.021
Final R indices [I > 2σ(I)]	0.1613	0.0456	0.0437
R indices (all data)	0.1821	0.0768	0.0581

Compound code	6.11	6.12
Empirical formula	C ₆₀ H ₅₈ N ₄ O ₁₁	C ₂₆ H ₂₆ N ₂ O ₅
Formula weight	1011.10	446.49
Temperature	296(2)	296(2)
Wavelength(Å)	0.71073	0.71073
Crystal system	Triclinic	Orthorhombic
Space group	P-1	P2(1)2(1)2(1)
Unit cell dimensions	a=10.8194(5)Å, α=79.482(4)° b=14.2801(7)Å, β=88.028(3)° c=17.6702(9)Å, γ=74.127(3)°	a= 5.6277(2)Å, α= 90.00° b= 18.3147(6)Å, β= 90.00° c= 22.0626(7)Å, γ= 90.00°
Volume	2581.5(2) Å ³	2273.98(13) Å ³
Z	2	4
Density (calculated)	1.301 mg/m ³	1.304 mg/m ³
Absorption coefficient	0.090 mm ⁻¹	0.091 mm ⁻¹
F(000)	1068	944
Crystal size	0.12 x 0.24 x 0.48 mm ³	0.16 x 0.21 x 0.28 mm ³
Theta range for data collection	1.73 to 25.00	1.45 to 28.33
Index ranges	-12 ≤ h ≤ 12 -16 ≤ k ≤ 15 -21 ≤ l ≤ 21	-7 ≤ h ≤ 7 -23 ≤ k ≤ 24 -29 ≤ l ≤ 24
Reflections collected	23784	25648
Independent reflections	8740	5630
Completeness to theta	96.2%	99.3%
Absorption correction	None	None
Refinement method	Full-matrix least-squares on F ²	Full-matrix least-squares on F ²
Data / restraints / parameters	8740 / 0 / 698	5630 / 0 / 305
Goodness-of-fit on F ²	1.030	1.040
FinalRindices[I>2sigma(I)]	0.0471	0.0487
R indices (all data)	0.0836	0.0713

Refine positions and thermal parameters of all the compounds

Table 29:- 2.1

Atom label	X	Y	Z	Uiso	Uaniso-U11	Uaniso-U22	Uaniso-U33
Co1	0.47795(5)	0.69050(2)	0.37837(3)	0.04067(18)	0.0349(3)	0.0459(4)	0.0417(3)
Co2	0.25641(5)	0.71247(2)	0.49396(3)	0.04098(18)	0.0364(3)	0.0450(4)	0.0421(3)
C1	0.5178(4)	0.75729(17)	0.4992(2)	0.0442(11)	0.045(2)	0.042(3)	0.046(3)
C2	0.6105(4)	0.77359(18)	0.5536(2)	0.0459(11)	0.041(2)	0.054(3)	0.044(2)
C3	0.5828(5)	0.8089(2)	0.5971(2)	0.0606(13)	0.057(3)	0.068(4)	0.057(3)
C4	0.6703(6)	0.8236(3)	0.6464(3)	0.0812(19)	0.076(4)	0.100(5)	0.068(4)
C5	0.7873(6)	0.8016(3)	0.6522(3)	0.095(2)	0.065(4)	0.158(7)	0.060(4)
C6	0.8164(6)	0.7649(3)	0.6110(3)	0.110(3)	0.061(4)	0.172(8)	0.090(5)
C7	0.7287(5)	0.7516(3)	0.5600(3)	0.083(2)	0.058(3)	0.110(5)	0.078(4)
C8	0.4660(4)	0.62969(18)	0.4972(2)	0.0463(11)	0.042(2)	0.045(3)	0.052(3)
C9	0.5524(4)	0.5952(2)	0.5383(2)	0.0524(12)	0.045(2)	0.055(3)	0.059(3)
C10	0.5907(8)	0.6071(4)	0.5998(3)	0.121(3)	0.137(6)	0.167(8)	0.059(4)
C11	0.6706(9)	0.5749(5)	0.6369(4)	0.162(5)	0.173(9)	0.243(13)	0.069(5)
C12	0.7047(7)	0.5284(4)	0.6123(4)	0.126(4)	0.097(5)	0.180(9)	0.105(6)
C13	0.6733(6)	0.5182(3)	0.5527(4)	0.094(2)	0.077(4)	0.071(5)	0.133(7)
C14	0.5977(5)	0.5511(2)	0.5142(3)	0.0701(16)	0.055(3)	0.054(3)	0.099(4)
C15	0.0886(4)	0.78699(17)	0.4123(2)	0.0449(11)	0.040(2)	0.042(3)	0.053(3)
C16	-0.0288(4)	0.82050(19)	0.4052(3)	0.0537(12)	0.044(2)	0.048(3)	0.069(3)
C17	-0.0704(6)	0.8411(3)	0.3480(3)	0.087(2)	0.084(4)	0.094(5)	0.086(4)
C18	-0.1825(8)	0.8694(4)	0.3409(5)	0.127(3)	0.101(6)	0.152(8)	0.124(7)
C19	-0.2498(7)	0.8781(3)	0.3907(5)	0.107(3)	0.065(4)	0.092(6)	0.165(8)
C20	-0.2093(6)	0.8562(3)	0.4480(4)	0.100(2)	0.072(4)	0.104(6)	0.131(7)
C21	-0.0991(5)	0.8287(2)	0.4558(3)	0.0738(16)	0.060(3)	0.072(4)	0.092(4)
C22	0.3060(4)	0.62183(18)	0.2914(2)	0.0470(11)	0.041(2)	0.052(3)	0.048(3)
C23	0.2920(4)	0.58575(18)	0.2358(2)	0.0500(12)	0.053(3)	0.052(3)	0.044(2)
C24	0.1935(6)	0.5517(2)	0.2290(3)	0.0807(19)	0.091(4)	0.086(5)	0.065(4)
C25	0.1812(9)	0.5195(3)	0.1770(4)	0.114(3)	0.150(7)	0.102(6)	0.091(5)
C26	0.2629(10)	0.5224(3)	0.1306(4)	0.118(3)	0.165(8)	0.110(7)	0.077(5)
C27	0.3611(9)	0.5571(3)	0.1375(3)	0.111(3)	0.142(7)	0.121(7)	0.074(5)
C28	0.3729(5)	0.5880(3)	0.1894(3)	0.0756(17)	0.071(3)	0.088(5)	0.070(4)
C29	0.5077(5)	0.7539(2)	0.2603(3)	0.0672(15)	0.077(4)	0.072(4)	0.055(3)
C30	0.5067(7)	0.7949(3)	0.2194(3)	0.094(2)	0.132(6)	0.087(5)	0.070(4)
C31	0.4696(7)	0.8414(3)	0.2427(4)	0.096(2)	0.121(6)	0.086(5)	0.084(5)
C32	0.4391(6)	0.8457(2)	0.3028(3)	0.0804(18)	0.093(4)	0.065(4)	0.084(4)
C33	0.4430(5)	0.8026(2)	0.3401(2)	0.0581(13)	0.070(3)	0.053(3)	0.052(3)
C34	0.6880(4)	0.6230(2)	0.3349(3)	0.0583(13)	0.042(2)	0.056(3)	0.077(3)
C35	0.8026(5)	0.6083(2)	0.3160(3)	0.0666(15)	0.053(3)	0.059(3)	0.088(4)
C36	0.9005(4)	0.6436(2)	0.3184(3)	0.0666(15)	0.039(2)	0.093(5)	0.070(3)
C37	0.8793(4)	0.6911(2)	0.3396(3)	0.0619(14)	0.038(2)	0.072(4)	0.076(4)
C38	0.7609(4)	0.7037(2)	0.3578(2)	0.0561(13)	0.046(3)	0.062(3)	0.061(3)
C39	0.1321(4)	0.60819(19)	0.4610(2)	0.0515(12)	0.043(2)	0.051(3)	0.061(3)
C40	0.0417(5)	0.5700(2)	0.4526(3)	0.0697(15)	0.061(3)	0.056(3)	0.092(4)
C41	-0.0773(5)	0.5797(2)	0.4704(3)	0.0758(17)	0.060(3)	0.063(4)	0.105(5)
C42	-0.1026(5)	0.6265(3)	0.4956(3)	0.0750(17)	0.044(3)	0.090(5)	0.095(4)
C43	-0.0055(4)	0.6624(2)	0.5019(3)	0.0598(13)	0.047(3)	0.062(3)	0.073(3)
C44	0.2046(5)	0.6933(3)	0.6331(3)	0.0718(16)	0.079(4)	0.080(4)	0.057(3)
C45	0.1734(7)	0.7034(4)	0.6934(3)	0.093(2)	0.095(5)	0.133(7)	0.052(4)
C46	0.1553(6)	0.7530(4)	0.7102(3)	0.095(2)	0.080(4)	0.161(8)	0.047(4)

C47	0.1675(6)	0.7913(3)	0.6673(3)	0.084(2)	0.076(4)	0.110(6)	0.064(4)
C48	0.1993(5)	0.7779(2)	0.6071(3)	0.0630(14)	0.062(3)	0.070(4)	0.057(3)
C49	0.3593(8)	0.9018(3)	0.4660(4)	0.093(2)	0.096(5)	0.092(6)	0.093(5)
C50	0.2865(11)	0.9468(4)	0.4532(4)	0.128(3)	0.163(9)	0.138(9)	0.080(5)
C51	0.1595(8)	0.9474(5)	0.4522(4)	0.132(3)	0.088(6)	0.166(10)	0.134(8)
C52	0.0997(15)	0.9935(7)	0.4393(7)	0.193(6)	0.175(13)	0.185(15)	0.213(15)
C53	0.1578(17)	1.0385(7)	0.4258(9)	0.203(7)	0.195(15)	0.156(14)	0.247(18)
C54	0.2833(18)	1.0350(6)	0.4266(7)	0.193(6)	0.242(17)	0.140(12)	0.195(13)
C55	0.3508(11)	0.9913(4)	0.4417(4)	0.128(3)	0.170(9)	0.076(6)	0.142(8)
C59	0.6667(7)	0.4769(3)	0.2775(5)	0.208(6)	0.175(13)	0.185(15)	0.213(15)
C60	0.7642(10)	0.4657(3)	0.2402(3)	0.174(4)	0.163(9)	0.138(9)	0.080(5)
C61	0.8815(8)	0.4490(4)	0.2685(5)	0.263(8)	0.043(2)	0.051(3)	0.061(3)
C62	0.9013(7)	0.4436(3)	0.3341(5)	0.239(7)	0.053(3)	0.059(3)	0.088(4)
C63	0.8038(10)	0.4549(3)	0.3714(3)	0.172(4)	0.060(3)	0.063(4)	0.105(5)
C64	0.6865(8)	0.4715(3)	0.3431(4)	0.180(5)	0.132(6)	0.087(5)	0.070(4)
N1	0.4769(3)	0.75684(16)	0.31922(18)	0.0490(9)	0.047(2)	0.052(3)	0.049(2)
N2	0.6651(3)	0.67019(15)	0.35549(17)	0.0455(9)	0.0370(18)	0.048(2)	0.051(2)
N3	0.1106(3)	0.65372(15)	0.48512(18)	0.0472(9)	0.0388(19)	0.047(2)	0.057(2)
N4	0.2167(3)	0.72966(17)	0.58923(18)	0.0512(10)	0.049(2)	0.060(3)	0.045(2)
O1	0.5590(3)	0.73236(13)	0.45541(15)	0.0486(8)	0.0415(15)	0.060(2)	0.0455(17)
O2	0.4013(3)	0.76934(12)	0.50128(15)	0.0501(8)	0.0405(16)	0.0454(19)	0.064(2)
O3	0.4724(3)	0.62739(12)	0.43901(16)	0.0543(8)	0.0634(19)	0.047(2)	0.053(2)
O4	0.3937(3)	0.65842(13)	0.52567(15)	0.0515(8)	0.0472(16)	0.056(2)	0.0532(18)
O5	0.1178(3)	0.76717(12)	0.46586(15)	0.0507(8)	0.0481(17)	0.056(2)	0.0475(18)
O6	0.1464(3)	0.78055(15)	0.36455(17)	0.0643(10)	0.061(2)	0.080(3)	0.054(2)
O7	0.4098(3)	0.64564(13)	0.30097(14)	0.0509(8)	0.0401(16)	0.064(2)	0.0495(18)
O8	0.2151(3)	0.62653(15)	0.32416(17)	0.0652(10)	0.0418(17)	0.088(3)	0.068(2)
O9	0.2852(3)	0.70324(13)	0.39648(14)	0.0443(7)	0.0372(15)	0.053(2)	0.0436(17)
O10	0.2903(6)	0.8630(3)	0.4836(3)	0.141(2)	0.112(4)	0.138(6)	0.177(6)
O11	0.4706(7)	0.8974(3)	0.4638(4)	0.172(3)	0.106(5)	0.185(7)	0.232(9)

Table 30:- 2.2

Atom label	X	Y	Z	Uiso	Uaniso-U11	Uaniso-U22	Uaniso-U33
Co1	0.52528(3)	0.135546(12)	0.11843(3)	0.04574(13)	0.0414(2)	0.0435(3)	0.0525(3)
Co2	0.31924(4)	0.134706(12)	0.33202(3)	0.04664(13)	0.0477(2)	0.0417(3)	0.0508(3)
C1	0.3186(4)	0.17476(12)	0.5409(4)	0.0820(12)	0.100(3)	0.080(3)	0.066(3)
C2	0.3280(5)	0.20213(19)	0.6133(4)	0.1126(18)	0.117(4)	0.131(5)	0.089(4)
C3	0.3617(5)	0.23342(18)	0.5768(6)	0.125(2)	0.101(4)	0.091(5)	0.181(7)
C4	0.3834(5)	0.23795(14)	0.4751(6)	0.1106(19)	0.089(3)	0.061(4)	0.181(6)
C5	0.3717(3)	0.20981(12)	0.4063(4)	0.0834(13)	0.075(3)	0.056(3)	0.118(4)
C6	0.0482(3)	0.15450(10)	0.3640(3)	0.0642(10)	0.063(2)	0.055(2)	0.075(3)
C7	-0.0761(3)	0.15135(12)	0.3860(3)	0.0745(12)	0.054(2)	0.087(3)	0.084(3)
C8	-0.1169(4)	0.12134(15)	0.4282(3)	0.0807(13)	0.048(2)	0.116(4)	0.079(3)
C9	-0.0334(4)	0.09482(12)	0.4468(3)	0.0806(12)	0.060(2)	0.085(3)	0.096(3)
C10	0.0874(3)	0.10001(10)	0.4213(3)	0.0608(10)	0.053(2)	0.061(3)	0.068(3)
C11	0.4724(3)	0.08469(9)	0.4676(3)	0.0493(8)	0.051(2)	0.044(2)	0.053(2)
C12	0.4752(3)	0.05807(8)	0.5534(2)	0.0441(8)	0.0459(18)	0.040(2)	0.046(2)
C13	0.3792(3)	0.05440(9)	0.6209(3)	0.0583(9)	0.0503(19)	0.058(2)	0.067(3)
C14	0.3824(3)	0.02971(12)	0.6999(3)	0.0748(12)	0.062(2)	0.094(3)	0.069(3)
C15	0.4815(4)	0.00740(11)	0.7096(3)	0.0756(12)	0.078(3)	0.075(3)	0.074(3)
C16	0.5772(3)	0.01073(11)	0.6438(3)	0.0724(11)	0.069(2)	0.074(3)	0.074(3)

C17	0.5755(3)	0.03614(10)	0.5663(3)	0.0615(10)	0.060(2)	0.066(3)	0.059(2)
C18	0.3541(3)	0.07623(9)	0.1617(3)	0.0456(8)	0.0404(19)	0.048(2)	0.049(2)
C19	0.2988(3)	0.04334(8)	0.1173(2)	0.0426(8)	0.0411(18)	0.038(2)	0.048(2)
C20	0.3485(3)	0.02699(9)	0.0311(3)	0.0578(9)	0.063(2)	0.048(2)	0.062(3)
C21	0.2942(4)	-0.00269(11)	-0.0109(3)	0.0740(11)	0.098(3)	0.065(3)	0.059(3)
C22	0.1903(4)	-0.01589(11)	0.0325(3)	0.0796(12)	0.101(3)	0.066(3)	0.072(3)
C23	0.1404(3)	-0.00001(11)	0.1188(3)	0.0722(11)	0.072(2)	0.065(3)	0.080(3)
C24	0.1959(3)	0.02925(9)	0.1607(3)	0.0544(9)	0.054(2)	0.049(2)	0.060(2)
C25	0.2735(3)	0.17082(9)	0.1229(3)	0.0486(9)	0.050(2)	0.041(2)	0.055(3)
C26	0.1829(3)	0.19286(9)	0.0593(3)	0.0511(9)	0.0411(19)	0.048(2)	0.064(3)
C27	0.1053(3)	0.21533(10)	0.1096(3)	0.0699(11)	0.056(2)	0.069(3)	0.085(3)
C28	0.0263(4)	0.23684(12)	0.0515(4)	0.0960(15)	0.076(3)	0.096(4)	0.116(4)
C29	0.0255(4)	0.23568(14)	-0.0568(5)	0.1100(18)	0.093(3)	0.110(4)	0.125(5)
C30	0.1004(4)	0.21231(15)	-0.1071(4)	0.1055(16)	0.102(3)	0.129(5)	0.083(4)
C31	0.1793(3)	0.19153(11)	-0.0490(3)	0.0718(11)	0.069(2)	0.079(3)	0.067(3)
C32	0.6379(3)	0.20412(9)	0.1949(3)	0.0477(8)	0.0428(19)	0.047(2)	0.053(3)
C33	0.6916(3)	0.23920(9)	0.1693(3)	0.0442(8)	0.0428(18)	0.048(2)	0.042(2)
C34	0.7480(3)	0.25913(10)	0.2483(3)	0.0596(10)	0.071(2)	0.057(3)	0.051(2)
C35	0.7965(3)	0.29103(10)	0.2251(3)	0.0702(11)	0.087(3)	0.055(3)	0.068(3)
C36	0.7873(3)	0.30409(10)	0.1243(3)	0.0675(10)	0.082(3)	0.048(2)	0.072(3)
C37	0.7297(3)	0.28511(10)	0.0453(3)	0.0626(10)	0.073(2)	0.062(3)	0.054(2)
C38	0.6834(3)	0.25262(9)	0.0687(3)	0.0531(9)	0.054(2)	0.052(2)	0.054(2)
C39	0.7429(3)	0.08790(11)	0.1889(3)	0.0679(11)	0.074(3)	0.061(3)	0.068(3)
C40	0.8646(4)	0.07603(12)	0.1980(3)	0.0850(13)	0.085(3)	0.072(3)	0.096(3)
C41	0.9558(4)	0.09556(15)	0.1552(4)	0.0945(16)	0.063(3)	0.096(4)	0.123(4)
C42	0.9261(3)	0.12512(15)	0.1048(4)	0.0910(14)	0.048(2)	0.106(4)	0.120(4)
C43	0.8050(3)	0.13517(11)	0.0969(3)	0.0711(11)	0.050(2)	0.077(3)	0.087(3)
C44	0.5846(3)	0.10119(11)	-0.0938(3)	0.0701(11)	0.061(2)	0.072(3)	0.077(3)
C45	0.6008(4)	0.09726(15)	-0.2010(4)	0.0949(15)	0.101(3)	0.107(4)	0.078(4)
C46	0.5849(5)	0.1255(2)	-0.2649(4)	0.1065(19)	0.108(4)	0.149(6)	0.062(3)
C47	0.5531(4)	0.15610(16)	-0.2212(4)	0.0935(15)	0.097(3)	0.119(5)	0.064(4)
C48	0.5376(3)	0.15779(12)	-0.1140(3)	0.0730(11)	0.071(2)	0.085(3)	0.062(3)
C49	0.0857(6)	0.12554(14)	0.7149(4)	0.1110(17)	0.128(4)	0.106(4)	0.099(4)
C50	-0.0213(5)	0.11219(15)	0.7491(4)	0.1094(17)	0.102(4)	0.106(4)	0.119(4)
C51	-0.0221(5)	0.09102(15)	0.8330(5)	0.1186(18)	0.101(4)	0.116(5)	0.141(5)
C52	0.0855(6)	0.08280(15)	0.8844(4)	0.1141(17)	0.136(4)	0.108(4)	0.100(4)
C53	0.1927(5)	0.09652(15)	0.8518(4)	0.1037(15)	0.105(4)	0.105(4)	0.102(4)
C54	0.1934(5)	0.11773(15)	0.7660(5)	0.1069(16)	0.101(4)	0.108(4)	0.113(5)
C55	0.1233(4)	0.00589(12)	0.5084(4)	0.0861(13)	0.058(2)	0.085(3)	0.116(4)
C56	0.0506(4)	0.01466(12)	0.5896(4)	0.0856(13)	0.068(3)	0.093(4)	0.095(4)
C57	-0.0742(4)	0.00893(12)	0.5811(4)	0.0831(13)	0.076(3)	0.084(3)	0.090(4)
N1	0.3393(2)	0.17855(8)	0.4400(3)	0.0616(8)	0.0627(18)	0.050(2)	0.072(2)
N2	0.1298(2)	0.12917(8)	0.3799(2)	0.0504(7)	0.0491(15)	0.0472(19)	0.0552(18)
N3	0.5527(2)	0.13118(9)	-0.0486(2)	0.0547(7)	0.0465(15)	0.061(2)	0.0572(19)
N4	0.7131(2)	0.11702(8)	0.1391(2)	0.0558(7)	0.0511(17)	0.0489(19)	0.067(2)
O1	0.37200(18)	0.10116(6)	0.45281(16)	0.0538(6)	0.0493(13)	0.0530(15)	0.0592(15)
O2	0.5677(2)	0.08998(7)	0.4177(2)	0.0744(8)	0.0521(14)	0.082(2)	0.0898(19)
O3	0.2603(2)	0.17028(6)	0.2207(2)	0.0657(7)	0.0730(15)	0.0625(17)	0.0620(17)
O4	0.35411(19)	0.15531(6)	0.07290(17)	0.0572(6)	0.0505(13)	0.0595(16)	0.0615(16)
O5	0.29554(18)	0.09171(6)	0.23107(17)	0.0561(6)	0.0545(13)	0.0522(15)	0.0620(16)
O6	0.45597(18)	0.08555(6)	0.12396(17)	0.0556(6)	0.0459(12)	0.0461(14)	0.0752(16)
O7	0.59023(19)	0.18723(6)	0.11883(17)	0.0550(6)	0.0652(14)	0.0464(15)	0.0530(15)
O8	0.6429(2)	0.19416(6)	0.28880(19)	0.0666(7)	0.0885(16)	0.0628(17)	0.0481(16)

O9	0.5079(2)	0.13882(8)	0.28643(19)	0.0489(6)	0.0467(13)	0.0431(15)	0.0571(16)
----	-----------	------------	-------------	-----------	------------	------------	------------

Table 31:- 2.3

Atom label	X	Y	Z	Uiso	Uaniso-U11	Uaniso-U22	Uaniso-U33
Co1	0.179826(17)	0.439777(19)	0.68108(3)	0.04268(13)	0.0364(2)	0.0445(2)	0.0475(2)
Co2	0.287677(18)	0.453081(19)	0.45891(3)	0.04356(13)	0.0407(2)	0.0462(2)	0.0442(2)
C8	-0.0162(3)	0.5565(3)	0.6196(5)	0.108(2)	0.070(3)	0.136(5)	0.116(4)
C6	0.04129(16)	0.4675(2)	0.6940(4)	0.0769(11)	0.0402(18)	0.084(3)	0.108(3)
C3	0.1464(3)	0.4499(3)	1.0852(4)	0.1073(19)	0.119(4)	0.151(6)	0.052(2)
C7	-0.01450(19)	0.4988(3)	0.6753(6)	0.1059(19)	0.037(2)	0.136(5)	0.145(5)
C10	0.0909(2)	0.5490(2)	0.6058(3)	0.0688(10)	0.065(2)	0.073(2)	0.069(2)
C4	0.1760(4)	0.4969(3)	1.0331(4)	0.115(2)	0.204(7)	0.077(3)	0.063(3)
C1	0.1404(3)	0.3931(3)	0.9160(4)	0.0960(17)	0.122(4)	0.111(4)	0.055(2)
C5	0.1848(3)	0.4901(2)	0.9205(4)	0.0880(14)	0.142(4)	0.062(2)	0.060(2)
C2	0.1289(3)	0.3955(4)	1.0261(4)	0.126(2)	0.150(5)	0.171(6)	0.057(3)
C9	0.0366(3)	0.5819(3)	0.5859(4)	0.0945(16)	0.093(4)	0.101(4)	0.089(3)
C11	0.11111(14)	0.32488(14)	0.5783(2)	0.0463(6)	0.0515(16)	0.0433(15)	0.0443(15)
C12	0.06207(14)	0.27392(15)	0.5881(2)	0.0465(6)	0.0525(16)	0.0453(15)	0.0420(14)
C13	0.0336(2)	0.24870(19)	0.4942(3)	0.0693(10)	0.086(3)	0.072(2)	0.0495(18)
C14	-0.0110(2)	0.2021(2)	0.5000(4)	0.0846(13)	0.097(3)	0.089(3)	0.066(2)
C16	-0.0014(3)	0.2062(3)	0.6967(4)	0.1015(18)	0.127(4)	0.112(4)	0.067(3)
C15	-0.0292(2)	0.1818(2)	0.6015(4)	0.0781(11)	0.075(3)	0.075(3)	0.084(3)
C17	0.0436(2)	0.2525(2)	0.6888(3)	0.0884(15)	0.122(4)	0.099(3)	0.0457(19)
C25	0.27280(14)	0.54835(15)	0.6555(3)	0.0483(7)	0.0417(15)	0.0450(16)	0.0583(18)
C26	0.29793(14)	0.60960(15)	0.7097(3)	0.0486(7)	0.0422(15)	0.0453(15)	0.0586(17)
C27	0.26342(16)	0.64513(17)	0.7812(3)	0.0581(8)	0.0564(19)	0.0549(18)	0.064(2)
C19	0.35559(14)	0.33890(16)	0.7364(3)	0.0496(7)	0.0431(15)	0.0582(18)	0.0476(16)
C18	0.30668(14)	0.37190(15)	0.6647(2)	0.0466(6)	0.0457(15)	0.0475(15)	0.0465(16)
C29	0.34458(18)	0.72034(18)	0.8093(4)	0.0709(10)	0.068(2)	0.0495(19)	0.094(3)
C24	0.41061(16)	0.3219(2)	0.6943(3)	0.0657(9)	0.0549(19)	0.086(3)	0.0571(19)
C22	0.44408(17)	0.2807(2)	0.8711(3)	0.0677(10)	0.056(2)	0.083(3)	0.064(2)
C31	0.35596(17)	0.6311(2)	0.6873(4)	0.0808(13)	0.049(2)	0.074(2)	0.121(4)
C28	0.28647(19)	0.70128(17)	0.8301(3)	0.0650(9)	0.077(2)	0.0523(19)	0.066(2)
C23	0.45569(18)	0.2934(2)	0.7629(3)	0.0765(12)	0.053(2)	0.102(3)	0.075(2)
C30	0.3799(2)	0.6863(2)	0.7402(5)	0.0951(16)	0.055(2)	0.081(3)	0.150(5)
C20	0.34436(18)	0.3237(3)	0.8467(3)	0.0807(13)	0.058(2)	0.133(4)	0.051(2)
C21	0.3891(2)	0.2944(3)	0.9131(3)	0.0923(16)	0.073(3)	0.155(5)	0.049(2)
C32	0.20948(15)	0.55596(15)	0.3396(3)	0.0500(7)	0.0449(16)	0.0538(17)	0.0511(17)
C33	0.20497(14)	0.61504(15)	0.2664(2)	0.0484(7)	0.0495(16)	0.0505(16)	0.0445(15)
C34	0.25206(17)	0.63286(17)	0.1996(3)	0.0594(8)	0.066(2)	0.0570(19)	0.0548(18)
C36	0.1935(2)	0.72220(18)	0.1281(3)	0.0695(10)	0.096(3)	0.055(2)	0.056(2)
C38	0.15280(18)	0.6533(2)	0.2665(3)	0.0672(9)	0.064(2)	0.072(2)	0.065(2)
C35	0.2464(2)	0.6865(2)	0.1293(3)	0.0721(10)	0.089(3)	0.069(2)	0.059(2)
C37	0.1474(2)	0.7073(2)	0.1969(4)	0.0770(11)	0.076(3)	0.074(3)	0.079(3)
O1	0.13015(10)	0.35250(11)	0.66631(17)	0.0529(5)	0.0610(13)	0.0520(12)	0.0457(11)
O7	0.26040(10)	0.52759(12)	0.3488(2)	0.0577(6)	0.0472(12)	0.0599(13)	0.0665(14)
N1	0.16757(13)	0.44018(14)	0.8610(2)	0.0530(6)	0.0475(14)	0.0605(16)	0.0510(15)
O3	0.31748(10)	0.37942(11)	0.56409(17)	0.0539(5)	0.0582(13)	0.0585(13)	0.0454(11)
O5	0.30331(10)	0.52331(12)	0.5813(2)	0.0604(6)	0.0516(13)	0.0616(14)	0.0692(15)
O4	0.25945(10)	0.38807(12)	0.71245(19)	0.0595(6)	0.0459(12)	0.0758(16)	0.0572(13)

O6	0.22330(10)	0.52786(11)	0.6917(2)	0.0584(6)	0.0475(12)	0.0517(12)	0.0773(15)
N4	0.27495(13)	0.38330(15)	0.3235(2)	0.0570(7)	0.0605(16)	0.0634(17)	0.0476(14)
O8	0.16237(12)	0.53803(16)	0.3851(3)	0.0815(9)	0.0465(14)	0.097(2)	0.102(2)
N3	0.37975(12)	0.47024(14)	0.4088(2)	0.0563(6)	0.0470(15)	0.0596(16)	0.0631(17)
O2	0.12902(14)	0.33661(14)	0.4833(2)	0.0755(8)	0.096(2)	0.0818(18)	0.0500(13)
N2	0.09334(12)	0.49191(14)	0.6586(3)	0.0574(7)	0.0440(14)	0.0586(16)	0.0696(18)
O9	0.19403(10)	0.44036(12)	0.50481(19)	0.0473(5)	0.0424(11)	0.0499(12)	0.0498(12)
Cl2	0.50069(5)	0.24491(8)	0.95692(10)	0.1001(4)	0.0739(7)	0.1376(11)	0.0875(7)
Cl4	0.18579(8)	0.78934(6)	0.04019(11)	0.1081(5)	0.1638(14)	0.0762(7)	0.0830(8)
Cl3	0.37371(7)	0.79157(6)	0.87117(16)	0.1215(6)	0.1075(10)	0.0700(7)	0.1822(15)
Cl1	-0.08608(8)	0.12360(10)	0.61081(16)	0.1435(7)	0.1308(13)	0.1485(14)	0.1506(14)
C44	0.2480(2)	0.32614(19)	0.3362(4)	0.0733(10)	0.078(3)	0.061(2)	0.082(3)
C43	0.39907(19)	0.5307(2)	0.3916(4)	0.0794(12)	0.055(2)	0.068(2)	0.116(4)
C48	0.2910(2)	0.3990(2)	0.2212(3)	0.0836(12)	0.108(3)	0.090(3)	0.053(2)
C39	0.41894(19)	0.4222(2)	0.3936(4)	0.0805(12)	0.060(2)	0.072(2)	0.111(3)
C45	0.2364(3)	0.2830(3)	0.2497(6)	0.1067(18)	0.100(4)	0.083(3)	0.136(5)
C42	0.4566(2)	0.5449(3)	0.3578(7)	0.127(3)	0.068(3)	0.094(4)	0.222(8)
C40	0.4774(3)	0.4327(3)	0.3594(7)	0.132(3)	0.069(3)	0.122(5)	0.209(8)
C46	0.2544(4)	0.2999(4)	0.1457(5)	0.133(3)	0.166(6)	0.148(6)	0.082(4)
C47	0.2813(4)	0.3585(4)	0.1322(4)	0.130(3)	0.198(7)	0.132(5)	0.059(3)
C41	0.4966(3)	0.4946(4)	0.3426(8)	0.149(3)	0.071(3)	0.139(6)	0.240(9)

Table 32:- 2.4

Atom label	X	Y	Z	Uiso	Uaniso-U11	Uaniso-U22	Uaniso-U33
Co1	0.47568(2)	0.18430(2)	0.58313(4)	0.0517(2)	0.0563(4)	0.0568(4)	0.0424(3)
O2	0.5885(2)	0.28907(18)	0.7076(4)	0.1012(13)	0.111(3)	0.116(3)	0.103(3)
C1	0.5824(3)	0.2722(2)	0.6040(5)	0.0746(12)	0.084(3)	0.072(3)	0.080(3)
C2	0.6283(3)	0.2966(2)	0.5554(5)	0.0818(14)	0.095(4)	0.065(3)	0.100(4)
C5	0.7161(5)	0.3404(4)	0.4627(10)	0.148(3)	0.155(7)	0.148(7)	0.187(9)
C4	0.7172(4)	0.3617(3)	0.5673(10)	0.137(3)	0.137(6)	0.100(5)	0.207(9)
C6	0.6276(4)	0.2752(3)	0.4461(7)	0.121(2)	0.161(6)	0.127(5)	0.122(5)
C3	0.6724(4)	0.3398(3)	0.6162(8)	0.111(2)	0.123(5)	0.088(4)	0.160(6)
C12	0.4319(2)	0.1577(2)	0.3068(4)	0.0684(11)	0.083(3)	0.077(3)	0.052(2)
C8	0.4498(3)	0.07916(19)	0.4247(4)	0.0700(11)	0.093(3)	0.061(3)	0.059(2)
C10	0.4084(3)	0.0702(3)	0.2060(5)	0.0877(15)	0.097(4)	0.104(5)	0.063(3)
C11	0.4098(3)	0.1251(3)	0.1988(4)	0.0853(15)	0.098(4)	0.112(5)	0.049(3)
C9	0.4288(3)	0.0466(2)	0.3207(6)	0.0895(15)	0.111(4)	0.070(3)	0.097(4)
C13	0.5993(19)	0.11783(16)	0.7905(4)	0.0532(9)	0.055(2)	0.058(2)	0.049(2)
C14	0.6597(2)	0.08232(17)	0.8130(4)	0.0562(9)	0.061(2)	0.057(2)	0.059(2)
C19	0.6781(3)	0.06929(19)	0.7183(5)	0.0688(11)	0.079(3)	0.064(3)	0.079(3)
C15	0.7018(3)	0.0624(2)	0.9324(5)	0.0815(14)	0.082(3)	0.095(4)	0.081(3)
C18	0.7363(3)	0.0370(3)	0.7440(6)	0.0936(16)	0.096(4)	0.100(4)	0.111(4)
C17	0.7758(3)	0.0183(3)	0.8618(8)	0.109(2)	0.103(4)	0.097(4)	0.160(6)
C16	0.7602(3)	0.0318(3)	0.9593(7)	0.110(2)	0.100(4)	0.120(5)	0.126(5)
O1	0.5404(17)	0.23410(13)	0.5402(3)	0.0736(8)	0.093(2)	0.0712(19)	0.0680(19)
O4	0.5618(15)	0.13292(13)	0.6778(2)	0.0667(8)	0.0657(16)	0.087(2)	0.0449(15)
O5	0.6409(2)	0.08686(19)	0.6004(3)	0.0996(12)	0.105(3)	0.145(4)	0.062(2)
O3	0.6761(4)	0.3630(2)	0.7195(7)	0.181(3)	0.202(6)	0.155(5)	0.250(7)
N1	0.4515(17)	0.13496(14)	0.4195(3)	0.0573(8)	0.0639(19)	0.065(2)	0.0464(17)
N2	0.3896(2)	0.23873(19)	0.4846(4)	0.0788(11)	0.092(3)	0.084(3)	0.061(2)
C21	0.3982(5)	0.2936(3)	0.4874(7)	0.124(3)	0.169(7)	0.105(5)	0.107(5)

C20	0.3257(3)	0.2194(3)	0.4263(5)	0.0997(19)	0.072(3)	0.154(6)	0.066(3)
C24	0.2704(4)	0.2544(5)	0.3708(7)	0.158(4)	0.108(5)	0.261(12)	0.101(5)
C23	0.2792(9)	0.3091(8)	0.3742(13)	0.220(9)	0.221(13)	0.301(19)	0.149(10)
C22	0.3457(9)	0.3310(5)	0.4338(11)	0.194(6)	0.296(16)	0.148(9)	0.173(11)
C26	0.6725(6)	0.2973(5)	0.4004(10)	0.181(5)	0.242(11)	0.207(9)	0.176(9)
O6	0.5	0.23134(18)	0.75	0.0580(10)	0.063(3)	0.059(3)	0.059(2)
O7	0.5879(15)	0.13057(13)	0.8806(3)	0.0683(8)	0.0751(18)	0.085(2)	0.0499(16)

Table 33:- 2.5 I

Atom label	X	Y	Z	Uiso	Uaniso-U11	Uaniso-U22	Uaniso-U33
Co1	0.37816(2)	0.71284(2)	0.2354(16)	0.03339(8)	0.0317(14)	0.0331(13)	0.0362(16)
Co2	0.05809(2)	0.75613(2)	0.2426(17)	0.03389(8)	0.0307(14)	0.0348(13)	0.0386(16)
C1	-0.2103(2)	0.8764(2)	0.2089(17)	0.0560(6)	0.0400(13)	0.0704(15)	0.0572(16)
C2	-0.3077(3)	0.9539(2)	0.1691(2)	0.0705(8)	0.0446(15)	0.0829(19)	0.082(2)
C3	-0.2851(3)	1.0021(2)	0.0873(2)	0.0787(9)	0.069(2)	0.0685(17)	0.097(3)
C4	-0.1669(3)	0.9693(3)	0.0480(19)	0.0725(8)	0.084(2)	0.0821(19)	0.0554(18)
C5	-0.0746(2)	0.8896(2)	0.0927(16)	0.0550(6)	0.0512(14)	0.0718(15)	0.0479(15)
C6	-0.0788(3)	0.6259(2)	0.3896(19)	0.0813(10)	0.112(3)	0.0625(16)	0.0660(19)
C7	-0.1221(3)	0.5418(3)	0.4398(2)	0.0885(10)	0.106(3)	0.082(2)	0.066(2)
C8	-0.0948(4)	0.4528(3)	0.4162(2)	0.0972(12)	0.130(3)	0.093(2)	0.091(3)
C9	-0.0261(6)	0.4506(4)	0.3440(3)	0.163(3)	0.279(7)	0.136(4)	0.132(4)
C10	0.0112(4)	0.5393(3)	0.2963(2)	0.1154(17)	0.189(4)	0.111(3)	0.089(3)
C11	0.1845(19)	0.9331(15)	0.1842(12)	0.0356(4)	0.0401(11)	0.0322(9)	0.0327(11)
C12	0.1279(19)	1.0572(15)	0.1679(13)	0.0394(5)	0.0395(11)	0.0326(9)	0.0430(12)
C13	0.1807(2)	1.1217(17)	0.1808(15)	0.0466(5)	0.0439(12)	0.0408(10)	0.0544(14)
C14	0.1252(3)	1.2345(19)	0.1666(18)	0.0634(7)	0.0672(17)	0.0394(11)	0.084(2)
C15	0.0136(3)	1.2854(19)	0.1372(2)	0.0717(9)	0.0594(17)	0.0350(11)	0.098(2)
C16	-0.0431(2)	1.2246(2)	0.1242(19)	0.0675(8)	0.0440(14)	0.0451(13)	0.093(2)
C17	0.0134(2)	1.1118(18)	0.1400(16)	0.0526(6)	0.0403(12)	0.0446(11)	0.0681(17)
C18	0.0020(2)	0.8637(18)	0.3766(14)	0.0449(5)	0.0419(12)	0.0491(11)	0.0408(13)
C19	-0.0690(2)	0.9608(17)	0.4095(13)	0.0434(5)	0.0474(13)	0.0423(10)	0.0406(12)
C20	-0.1821(2)	0.9752(2)	0.4573(15)	0.0533(6)	0.0523(14)	0.0556(13)	0.0498(15)
C21	-0.2443(3)	1.0652(3)	0.4858(18)	0.0747(9)	0.0703(19)	0.0777(19)	0.0666(19)
C22	-0.1924(4)	1.1431(2)	0.4677(2)	0.0839(11)	0.104(3)	0.0609(17)	0.087(2)
C23	-0.0807(4)	1.1333(2)	0.4205(2)	0.0779(10)	0.109(3)	0.0489(14)	0.093(2)
C24	-0.0182(3)	1.0426(2)	0.3912(17)	0.0608(7)	0.0647(17)	0.0574(14)	0.0641(17)
C25	0.2624(18)	0.6712(15)	0.1175(12)	0.0348(4)	0.0369(11)	0.0315(9)	0.0347(11)
C26	0.3030(18)	0.6297(15)	0.0438(13)	0.0373(4)	0.0358(11)	0.0368(9)	0.0365(11)
C27	0.2632(2)	0.5546(17)	0.0338(14)	0.0437(5)	0.0418(12)	0.0428(10)	0.0480(13)
C28	0.3033(2)	0.5163(2)	-0.0333(16)	0.0576(7)	0.0612(16)	0.0569(13)	0.0612(17)
C29	0.3883(3)	0.5535(2)	-0.0934(16)	0.0624(7)	0.0671(17)	0.0668(15)	0.0430(15)
C30	0.4294(2)	0.6291(2)	-0.0865(15)	0.0605(7)	0.0594(16)	0.0684(16)	0.0375(14)
C31	0.3876(2)	0.6663(19)	-0.0185(14)	0.0481(5)	0.0486(13)	0.0515(12)	0.0402(13)
C32	0.4189(2)	0.4652(16)	0.3170(13)	0.0397(5)	0.0426(12)	0.0347(9)	0.0397(12)
C33	0.4938(2)	0.3482(16)	0.3153(13)	0.0445(5)	0.0589(14)	0.0339(9)	0.0389(12)
C34	0.6214(2)	0.3081(17)	0.3014(14)	0.0494(6)	0.0601(15)	0.0391(10)	0.0428(13)
C35	0.6877(3)	0.2048(2)	0.2910(17)	0.0695(8)	0.084(2)	0.0487(13)	0.0630(18)
C36	0.6244(4)	0.1385(2)	0.2969(2)	0.0846(11)	0.123(3)	0.0417(13)	0.086(2)
C37	0.4976(4)	0.1739(2)	0.3119(2)	0.0846(10)	0.132(3)	0.0480(14)	0.092(2)
C38	0.4318(3)	0.2787(2)	0.3211(17)	0.0645(7)	0.085(2)	0.0480(13)	0.0679(18)
C39	0.5488(3)	0.7985(2)	0.0882(16)	0.0665(7)	0.078(2)	0.0814(18)	0.0465(16)

C40	0.6558(4)	0.8018(4)	0.0367(2)	0.0961(12)	0.123(3)	0.132(3)	0.054(2)
C41	0.7662(4)	0.7314(4)	0.0610(3)	0.0974(13)	0.080(3)	0.139(3)	0.108(3)
C42	0.7682(3)	0.6578(3)	0.1368(3)	0.0814(10)	0.0450(16)	0.097(2)	0.117(3)
C43	0.6573(2)	0.6585(2)	0.1857(18)	0.0577(6)	0.0419(13)	0.0650(15)	0.0700(18)
C44	0.4828(2)	0.8051(2)	0.3227(16)	0.0555(6)	0.0679(17)	0.0541(13)	0.0515(15)
C45	0.5349(3)	0.8134(2)	0.3796(17)	0.0599(7)	0.0660(17)	0.0703(16)	0.0589(17)
C46	0.5484(3)	0.7330(2)	0.4520(17)	0.0665(7)	0.0758(19)	0.0856(19)	0.0518(17)
C47	0.5039(4)	0.6500(2)	0.4660(18)	0.0822(10)	0.135(3)	0.0699(17)	0.0444(17)
C48	0.4521(3)	0.6478(2)	0.4058(16)	0.0625(7)	0.096(2)	0.0531(13)	0.0446(15)
N1	-0.094(16)	0.8446(14)	0.1724(11)	0.0408(4)	0.0345(9)	0.0476(9)	0.0448(11)
N2	-0.012(17)	0.6262(14)	0.3181(12)	0.0441(4)	0.0438(10)	0.0466(9)	0.0462(11)
N3	0.5487(17)	0.7272(15)	0.1621(12)	0.0454(4)	0.0425(11)	0.0548(10)	0.0461(11)
N4	0.4431(16)	0.7226(13)	0.3342(11)	0.0404(4)	0.0415(10)	0.0409(9)	0.0385(10)
N5	-0.2391(3)	0.8895(3)	0.4808(17)	0.0818(8)	0.0669(18)	0.093(2)	0.0780(19)
N6	0.2993(2)	1.0745(17)	0.2137(19)	0.0666(6)	0.0702(17)	0.0490(11)	0.092(2)
N7	0.1814(2)	0.5029(19)	0.0994(16)	0.0611(6)	0.0607(14)	0.0620(13)	0.0793(17)
N8	0.6943(19)	0.3725(17)	0.3017(14)	0.0575(5)	0.0449(12)	0.0548(11)	0.0635(14)
O1	-0.040(14)	0.8529(12)	0.3248(10)	0.0485(4)	0.0428(9)	0.0525(8)	0.0573(10)
O2	0.1018(2)	0.8035(18)	0.4025(14)	0.0945(8)	0.0792(14)	0.1069(16)	0.0977(16)
O3	-0.1776(3)	0.7962(2)	0.4978(19)	0.1218(11)	0.138(2)	0.0850(17)	0.134(2)
O4	-0.3504(3)	0.9186(3)	0.4829(3)	0.1754(17)	0.105(3)	0.174(3)	0.240(5)
O5	0.1186(14)	0.8893(11)	0.1727(10)	0.0456(4)	0.0457(9)	0.0364(7)	0.0592(10)
O6	0.2898(13)	0.8855(10)	0.2059(10)	0.0437(4)	0.0437(8)	0.0336(7)	0.0574(10)
O7	0.3919(2)	1.0663(2)	0.1673(18)	0.1097(10)	0.0481(13)	0.0987(17)	0.144(2)
O8	0.2957(3)	1.0493(2)	0.2870(18)	0.1064(9)	0.132(2)	0.1031(18)	0.105(2)
O9	0.3374(14)	0.7020(13)	0.13266(9)	0.0456(4)	0.0431(9)	0.0627(9)	0.0418(9)
O10	0.1574(13)	0.6722(11)	0.15585(9)	0.0407(3)	0.0396(8)	0.0441(7)	0.0462(9)
O11	0.0774(2)	0.5244(2)	0.0869(18)	0.1057(8)	0.0742(16)	0.145(2)	0.137(2)
O12	0.2253(2)	0.4385(16)	0.1604(14)	0.0821(6)	0.1092(18)	0.0572(11)	0.0732(15)
O13	0.4612(13)	0.5389(11)	0.26819(9)	0.0438(4)	0.0401(8)	0.0335(7)	0.0513(9)
O14	0.3211(15)	0.4794(12)	0.3645(10)	0.0566(4)	0.0505(10)	0.0418(8)	0.0584(11)
O15	0.6675(18)	0.4128(16)	0.3567(12)	0.0681(5)	0.0680(12)	0.0739(12)	0.0734(13)
O16	0.7794(2)	0.3804(2)	0.2473(16)	0.0961(7)	0.0636(14)	0.1136(18)	0.1116(19)
O17	0.2135(13)	0.6886(12)	0.30746(9)	0.0366(3)	0.0327(7)	0.0362(7)	0.0366(8)

Table 34:- 2.5 II

Atom label	X	Y	Z	Uiso	Uaniso-U11	Uaniso-U22	Uaniso-U33
Co1	0.114198(13)	0.46427(16)	0.26841(10)	0.02975(8)	0.0245(12)	0.0306(13)	0.0333(15)
C1	0.27386(13)	0.58244(15)	0.25694(10)	0.0512(5)	0.0466(11)	0.0445(12)	0.0622(14)
C2	0.35196(14)	0.62697(16)	0.27374(13)	0.0644(7)	0.0497(13)	0.0505(13)	0.095(2)
C3	0.38544(13)	0.63063(16)	0.33055(13)	0.0655(7)	0.0374(11)	0.0474(13)	0.105(2)
C4	0.34088(13)	0.59085(17)	0.36909(11)	0.0599(6)	0.0482(12)	0.0548(14)	0.0701(16)
C5	0.26403(12)	0.54745(14)	0.34968(9)	0.0455(5)	0.0408(10)	0.0443(11)	0.0492(13)
C6	0.12766(11)	0.29104(13)	0.35107(8)	0.0331(4)	0.0319(9)	0.0341(9)	0.0326(10)
C7	0.18175(11)	0.22926(13)	0.39628(8)	0.0348(4)	0.0326(9)	0.0345(9)	0.0353(10)
C8	0.15131(11)	0.18271(14)	0.44080(8)	0.0396(4)	0.0372(10)	0.0433(10)	0.0360(11)
C9	0.20026(14)	0.11925(17)	0.47836(10)	0.0563(6)	0.0602(14)	0.0568(13)	0.0488(13)
C10	0.28230(15)	0.10161(18)	0.47211(11)	0.0652(7)	0.0590(14)	0.0598(15)	0.0696(17)
C11	0.31469(14)	0.14616(18)	0.42869(11)	0.0617(6)	0.0411(11)	0.0677(15)	0.0730(17)
C12	0.26517(12)	0.20936(15)	0.39132(9)	0.0472(5)	0.0369(10)	0.0545(12)	0.0497(13)
C13	0.12287(12)	0.39671(15)	0.14684(8)	0.0443(5)	0.0433(10)	0.0475(11)	0.0422(12)

C14	0.15672(15)	0.36489(18)	0.10089(10)	0.0604(6)	0.0663(14)	0.0751(16)	0.0418(13)
C15	0.23667(17)	0.3257(2)	0.11024(12)	0.0745(8)	0.0712(17)	0.095(2)	0.0659(18)
C16	0.27960(15)	0.3183(2)	0.16540(12)	0.0687(7)	0.0458(12)	0.0843(18)	0.0805(19)
C17	0.24182(12)	0.35231(16)	0.20933(10)	0.0494(5)	0.0380(10)	0.0558(13)	0.0546(13)
C18	-0.00375(11)	0.59658(13)	0.32089(7)	0.0332(4)	0.0340(9)	0.0351(9)	0.0315(10)
C19	-0.00048(11)	0.69540(13)	0.35035(8)	0.0357(4)	0.0336(9)	0.0356(10)	0.0396(11)
C20	0.04537(12)	0.71330(15)	0.40443(8)	0.0418(5)	0.0436(10)	0.0473(11)	0.0370(11)
C21	0.05223(15)	0.80578(19)	0.42888(11)	0.0635(7)	0.0660(15)	0.0690(16)	0.0575(15)
C22	0.01188(19)	0.88413(19)	0.39806(14)	0.0804(8)	0.0916(19)	0.0461(14)	0.106(2)
C23	-0.03384(18)	0.86882(18)	0.34458(14)	0.0776(8)	0.0915(19)	0.0424(14)	0.097(2)
C24	-0.04057(14)	0.77524(15)	0.32105(10)	0.0531(5)	0.0558(12)	0.0438(12)	0.0582(14)
N1	0.23056(9)	0.54206(11)	0.29428(7)	0.0393(4)	0.0316(8)	0.0354(8)	0.0495(10)
N2	0.06541(11)	0.20186(15)	0.45127(7)	0.0496(4)	0.0433(9)	0.0689(13)	0.0359(10)
N3	0.16450(9)	0.39251(11)	0.20078(7)	0.0377(4)	0.0332(8)	0.0404(9)	0.0401(9)
N4	0.08574(12)	0.63161(15)	0.43927(7)	0.0533(5)	0.0598(12)	0.0698(13)	0.0305(10)
O1	0.16474(7)	0.35910(9)	0.32933(5)	0.0387(3)	0.0310(6)	0.0376(7)	0.0456(8)
O2	0.05190(8)	0.26746(10)	0.33709(6)	0.0496(4)	0.0319(7)	0.0591(9)	0.0528(9)
O3	0.04387(10)	0.28644(14)	0.45608(8)	0.0706(5)	0.0530(9)	0.0825(13)	0.0764(12)
O4	0.02048(11)	0.12989(14)	0.45672(8)	0.0767(5)	0.0634(10)	0.0931(13)	0.0783(12)
O5	0.06176(8)	0.54481(9)	0.32991(5)	0.0416(3)	0.0385(7)	0.0447(7)	0.0395(8)
O6	0.07203(7)	0.57729(9)	0.21155(6)	0.0415(3)	0.0345(7)	0.0404(7)	0.0474(8)
O7	0.04230(12)	0.56175(13)	0.44760(7)	0.0710(5)	0.0841(12)	0.0706(11)	0.0602(11)
O8	0.16113(11)	0.63996(15)	0.45949(7)	0.0817(6)	0.0611(11)	0.1151(16)	0.0615(11)
O9	0	0.37940(12)	0.25	0.0304(4)	0.0278(8)	0.0341(9)	0.0276(9)

Table 35:- 2.5 III

Atom label	X	Y	Z	Uiso	Uaniso-U11	Uaniso-U22	Uaniso-U33
Co1	0.22998(2)	0.43482(2)	0.106586(9)	0.03174(8)	0.0332(16)	0.0296(14)	0.0323(15)
Co2	0.36516(2)	0.19645(2)	0.11877(11)	0.03876(9)	0.0383(18)	0.0332(16)	0.0459(18)
C1	0.1156(18)	0.56460(18)	0.02525(8)	0.0457(6)	0.0411(13)	0.0427(12)	0.0511(14)
C2	0.0843(2)	0.6470(2)	-0.0031(10)	0.0621(7)	0.0564(17)	0.0631(17)	0.0595(17)
C3	0.1258(2)	0.7386(2)	0.01064(12)	0.0729(9)	0.079(2)	0.0507(16)	0.084(2)
C4	0.1968(2)	0.74468(19)	0.05142(11)	0.0688(8)	0.087(2)	0.0379(14)	0.077(2)
C5	0.2254(2)	0.65922(17)	0.07743(9)	0.0518(6)	0.0604(17)	0.0393(12)	0.0515(15)
C6	0.1737(2)	0.57281(19)	0.18197(9)	0.0595(7)	0.0652(18)	0.0560(15)	0.0604(17)
C7	0.1840(3)	0.6445(2)	0.21705(12)	0.0796(10)	0.111(3)	0.0615(18)	0.075(2)
C8	0.2767(3)	0.6701(2)	0.24031(10)	0.0815(11)	0.144(4)	0.0547(17)	0.0454(17)
C9	0.3583(3)	0.6234(2)	0.22922(10)	0.0737(9)	0.095(3)	0.0661(18)	0.0486(16)
C10	0.3425(2)	0.55073(19)	0.19384(9)	0.0544(6)	0.0631(18)	0.0532(15)	0.0424(13)
C11	0.1995(2)	0.06472(17)	0.14385(9)	0.0502(6)	0.0550(16)	0.0416(12)	0.0542(15)
C12	0.1541(2)	-0.0075(2)	0.16674(10)	0.0647(8)	0.0625(19)	0.0544(16)	0.080(2)
C13	0.2136(3)	-0.0735(2)	0.19611(12)	0.0822(10)	0.103(3)	0.0547(18)	0.095(2)
C14	0.3157(3)	-0.0664(2)	0.20178(12)	0.0813(10)	0.088(3)	0.0555(17)	0.098(2)
C15	0.3554(2)	0.00822(19)	0.17795(10)	0.0634(7)	0.0641(19)	0.0474(15)	0.0779(19)
C16	0.4268(3)	0.0045(2)	0.07189(11)	0.0741(9)	0.087(2)	0.0557(17)	0.083(2)
C17	0.4897(4)	-0.0650(3)	0.05720(15)	0.1068(14)	0.147(4)	0.061(2)	0.123(3)
C18	0.5875(4)	-0.0431(4)	0.06058(17)	0.1179(16)	0.127(4)	0.101(3)	0.139(4)
C19	0.6230(3)	0.0465(4)	0.07933(16)	0.1075(13)	0.074(2)	0.125(3)	0.132(3)
C20	0.5574(2)	0.1119(2)	0.09450(12)	0.0742(9)	0.060(2)	0.076(2)	0.089(2)
C21	0.0463(17)	0.34488(16)	0.13706(8)	0.0389(5)	0.0358(12)	0.0382(11)	0.0425(12)
C22	-0.0632(17)	0.35086(17)	0.13994(8)	0.0411(5)	0.0341(12)	0.0496(14)	0.0388(12)

C23	-0.1185(19)	0.2681(2)	0.14854(9)	0.0537(6)	0.0374(14)	0.0606(16)	0.0618(16)
C24	-0.2131(2)	0.2757(3)	0.15826(12)	0.0771(9)	0.0409(17)	0.105(3)	0.085(2)
C25	-0.2558(2)	0.3678(3)	0.15847(11)	0.0815(10)	0.0443(18)	0.131(3)	0.073(2)
C26	-0.2055(2)	0.4509(3)	0.14908(11)	0.0758(9)	0.0501(18)	0.096(2)	0.081(2)
C27	-0.1094(2)	0.4425(2)	0.13977(10)	0.0593(7)	0.0448(15)	0.0564(16)	0.0756(18)
C28	0.4851(18)	0.27087(18)	0.21525(9)	0.0448(6)	0.0432(14)	0.0457(13)	0.0449(14)
C29	0.5849(19)	0.2775(2)	0.24897(9)	0.0543(7)	0.0427(15)	0.0688(17)	0.0499(15)
C30	0.6527(2)	0.2000(3)	0.25710(11)	0.0719(9)	0.0509(18)	0.085(2)	0.076(2)
C31	0.7487(3)	0.2097(4)	0.28397(15)	0.1046(14)	0.050(2)	0.150(4)	0.103(3)
C32	0.7763(3)	0.2998(5)	0.30493(18)	0.130(2)	0.055(3)	0.201(6)	0.120(4)
C33	0.7098(4)	0.3778(4)	0.29913(15)	0.1159(15)	0.095(3)	0.139(4)	0.099(3)
C34	0.6154(3)	0.3680(3)	0.27073(11)	0.0792(9)	0.074(2)	0.085(2)	0.072(2)
C35	0.2038(17)	0.25657(16)	0.03319(8)	0.0370(5)	0.0372(12)	0.0346(11)	0.0412(12)
C36	0.1470(18)	0.22720(16)	-0.01591(8)	0.0408(5)	0.0441(13)	0.0365(11)	0.0425(13)
C37	0.1220(19)	0.12941(17)	-0.02989(8)	0.0476(6)	0.0580(16)	0.0394(12)	0.0458(14)
C38	0.0773(3)	0.1023(2)	-0.0752(10)	0.0702(9)	0.103(2)	0.0486(15)	0.0564(17)
C39	0.0549(3)	0.1754(2)	-0.1091(11)	0.0894(12)	0.136(3)	0.077(2)	0.0458(17)
C40	0.0762(3)	0.2747(2)	-0.0968(11)	0.0872(11)	0.133(3)	0.0627(18)	0.0529(18)
C41	0.1214(2)	0.29923(19)	-0.05099(9)	0.0599(7)	0.079(2)	0.0429(14)	0.0502(15)
C42	0.4407(17)	0.40393(17)	0.09029(8)	0.0387(5)	0.0324(12)	0.0436(12)	0.0399(12)
C43	0.5272(17)	0.44835(18)	0.07145(8)	0.0446(6)	0.0338(12)	0.0542(14)	0.0450(13)
C44	0.5612(19)	0.5452(2)	0.07949(10)	0.0556(7)	0.0398(14)	0.0607(16)	0.0653(17)
C45	0.6321(2)	0.5870(2)	0.05637(12)	0.0744(9)	0.0534(18)	0.076(2)	0.091(2)
C46	0.6705(2)	0.5286(3)	0.02516(11)	0.0808(10)	0.0530(19)	0.126(3)	0.067(2)
C47	0.6412(2)	0.4317(3)	0.01746(11)	0.0774(9)	0.0560(19)	0.116(3)	0.0659(19)
C48	0.5697 (19)	0.3920(2)	0.04025(9)	0.0572(7)	0.0446(15)	0.0737(18)	0.0573(16)
N1	0.1851(13)	0.56896(12)	0.06511(6)	0.0372(4)	0.0376(10)	0.0342(9)	0.0389(10)
N2	0.2516(15)	0.52631(13)	0.16989(6)	0.0423(4)	0.0522(12)	0.0381(10)	0.0362(10)
N3	0.2986(16)	0.07407(14)	0.14954(7)	0.0468(5)	0.0510(13)	0.0375(10)	0.0523(12)
N4	0.4604(17)	0.09227(15)	0.09078(8)	0.0537(5)	0.0537(14)	0.0488(12)	0.0606(14)
N5	0.5288(2)	0.6072(2)	0.11568(14)	0.0827(8)	0.0599(17)	0.0596(17)	0.130(3)
N6	0.1398(2)	0.04699(17)	0.00462(9)	0.0683(7)	0.090(2)	0.0399(13)	0.0664(16)
N7	0.6224(3)	0.1010(3)	0.23812(15)	0.1027(11)	0.081(2)	0.085(2)	0.128(3)
N8	-0.0790(2)	0.1654(2)	0.14395(13)	0.0797(8)	0.0499(16)	0.0591(16)	0.126(3)
O1	0.0783(11)	0.40908(11)	0.11181(5)	0.0415(4)	0.0352(9)	0.0432(8)	0.0465(9)
O2	0.0969 (12)	0.27917(13)	0.16180(7)	0.0569(5)	0.0371(9)	0.0579(10)	0.0770(12)
O3	-0.0485(2)	0.14726(18)	0.10783(12)	0.1089(9)	0.119(2)	0.0699(16)	0.131(2)
O4	-0.0823(2)	0.1073(2)	0.17600(14)	0.1422(13)	0.096(2)	0.0974(19)	0.241(4)
O5	0.4781(13)	0.20931(12)	0.18148(6)	0.0517(4)	0.0471(10)	0.0508(10)	0.0542(10)
O6	0.4173(14)	0.32708(14)	0.22282(6)	0.0574(5)	0.0510(11)	0.0648(11)	0.0541(11)
O7	0.5585(3)	0.0574(2)	0.25452(12)	0.1266(12)	0.125(3)	0.0892(19)	0.137(3)
O8	0.6647(3)	0.0670(3)	0.20786(17)	0.1723(17)	0.147(3)	0.132(3)	0.238(4)
O9	0.4396(13)	0.31100(12)	0.09213(6)	0.0539(4)	0.0518(11)	0.0415(9)	0.0756(12)
O10	0.3771(11)	0.46385(11)	0.10003(5)	0.0414(4)	0.0362(9)	0.0396(8)	0.0501(9)
O11	0.5479(19)	0.5771(2)	0.15692(10)	0.1027(9)	0.0767(17)	0.140(2)	0.0933(18)
O12	0.4883(3)	0.6865(2)	0.10316(16)	0.1514(14)	0.154(3)	0.0573(16)	0.259(4)
O13	0.2544(12)	0.18855(11)	0.05727(6)	0.0467(4)	0.0531(10)	0.0342(8)	0.0488(9)
O14	0.1969(12)	0.34645(10)	0.04448(5)	0.0408(4)	0.0511(10)	0.0322(8)	0.0380(8)
O15	0.1991(2)	-0.0182(17)	-0.0015(10)	0.1150(10)	0.148(3)	0.0487(12)	0.133(2)
O16	0.0914(2)	0.04593(19)	0.03539(8)	0.0987(9)	0.119(2)	0.1093(19)	0.0646(14)
O17	0.2769(14)	0.30432(11)	0.14854(6)	0.0375(3)	0.0346(9)	0.0378(8)	0.0408(9)

Atom label	X	Y	Z	Uiso	Uaniso-U11	Uaniso-U22	Uaniso-U33
Co1	0.47865(3)	0.088199(9)	0.65105(17)	0.03840(8)	0.0423(14)	0.0347(13)	0.0421(13)
C1	0.3513(19)	0.22275(7)	0.57070(13)	0.0421(4)	0.0454(10)	0.0362(9)	0.0443(10)
C2	0.2608(18)	0.27904(7)	0.58627(13)	0.0407(4)	0.0408(9)	0.0343(9)	0.0445(9)
C3	0.1908(2)	0.32411(8)	0.49896(16)	0.0577(5)	0.0697(13)	0.0479(11)	0.0563(11)
C4	0.1015(3)	0.37454(10)	0.5097(2)	0.0749(6)	0.0793(16)	0.0532(13)	0.0857(16)
C5	0.0843(3)	0.38136(10)	0.6075(2)	0.0746(6)	0.0690(14)	0.0548(13)	0.1002(18)
C6	0.1539(2)	0.33741(10)	0.69517(18)	0.0659(5)	0.0653(13)	0.0698(14)	0.0708(13)
C7	0.2413(2)	0.28627(8)	0.68446(15)	0.0503(4)	0.0499(11)	0.0506(11)	0.0517(10)
C8	0.3429(19)	-0.01895(7)	0.63235(12)	0.0388(3)	0.0433(10)	0.0416(9)	0.0351(8)
C9	0.2671(19)	-0.08290(7)	0.62833(12)	0.0386(3)	0.0447(9)	0.0410(9)	0.0343(8)
C10	0.1038(2)	-0.08781(8)	0.59227(13)	0.0460(4)	0.0451(10)	0.0535(10)	0.0395(9)
C11	0.0353(2)	-0.1467(10)	0.59280(16)	0.0619(5)	0.0517(12)	0.0757(14)	0.0563(11)
C12	0.1300(3)	-0.2009(10)	0.63028(18)	0.0730(6)	0.0827(16)	0.0566(13)	0.0779(14)
C13	0.2922(3)	-0.19679(9)	0.66654(18)	0.0691(6)	0.0785(16)	0.0431(12)	0.0854(15)
C14	0.3619(2)	-0.13826(8)	0.66494(15)	0.0522(4)	0.0516(11)	0.0456(11)	0.0620(11)
C15	0.8187(2)	0.05462(9)	0.69069(15)	0.0538(4)	0.0499(11)	0.0558(11)	0.0553(11)
C16	0.9698(2)	0.06303(11)	0.70003(16)	0.0648(5)	0.0507(12)	0.0862(15)	0.0575(12)
C17	1.0185(2)	0.12375(12)	0.68679(17)	0.0679(6)	0.0476(12)	0.1009(18)	0.0605(12)
C18	0.9132(3)	0.17361(10)	0.66412(18)	0.0691(6)	0.0639(14)	0.0711(14)	0.0826(15)
C19	0.7636(2)	0.16166(9)	0.65574(16)	0.0586(5)	0.0550(11)	0.0503(12)	0.0763(13)
C20	0.5451(3)	0.13296(9)	0.89494(16)	0.0639(5)	0.0827(15)	0.0586(13)	0.0497(11)
C21	0.5962(3)	0.13180(11)	1.01089(18)	0.0808(7)	0.0971(18)	0.0919(18)	0.0538(13)
C22	0.6708(3)	0.07831(12)	1.07085(18)	0.0798(7)	0.0838(16)	0.115(2)	0.0404(11)
C23	0.6913(3)	0.02653(11)	1.01298(17)	0.0744(6)	0.0842(17)	0.0819(16)	0.0500(13)
C24	0.6370(2)	0.03147(9)	0.89646(15)	0.0595(5)	0.0700(13)	0.0558(12)	0.0495(11)
N1	0.5649(17)	0.08386(6)	0.83595(11)	0.0458(3)	0.0523(9)	0.0445(9)	0.0433(8)
N2	0.7140(16)	0.10325(6)	0.66905(11)	0.0451(3)	0.0435(8)	0.0470(8)	0.0464(8)
O1	0.3728(17)	0.22065(6)	0.48358(11)	0.0631(4)	0.0976(11)	0.0487(8)	0.0627(8)
O2	0.3989(14)	0.17985(5)	0.64927(9)	0.0475(3)	0.0619(8)	0.0363(6)	0.0441(6)
O3	0.4839(13)	-0.01619(5)	0.64059(9)	0.0431(3)	0.0444(7)	0.0391(6)	0.0526(7)
O4	0.2697(14)	0.03222(5)	0.63108(10)	0.0500(3)	0.0519(7)	0.0377(7)	0.0697(8)
O5	0.3847(15)	0.09177(7)	0.46961(10)	0.0477(3)	0.0577(8)	0.0457(8)	0.0455(7)

Atom label	X	Y	Z	Uiso	Uaniso-U11	Uaniso-U22	Uaniso-U33
Co1	0.5	0.5	0.5	0.0299(11)	0.03114(18)	0.03407(19)	0.0262(17)
O1	0.7616(2)	0.45282(18)	0.57648(13)	0.0385(3)	0.0379(7)	0.0485(8)	0.0324(7)
O2	0.5820(17)	0.48984(15)	0.32557(10)	0.0385(3)	0.0402(7)	0.0522(7)	0.0299(6)
O3	0.8272(18)	0.38075(16)	0.34686(10)	0.0422(3)	0.0428(7)	0.0571(8)	0.0309(6)
O4	0.5713(3)	0.0937(2)	0.16265(17)	0.0756(5)	0.0832(13)	0.0526(10)	0.0794(12)
O5	0.8087(3)	0.0722(3)	0.0725(2)	0.0990(7)	0.1248(18)	0.0930(14)	0.1067(16)
N1	0.3483(2)	0.23593(18)	0.45622(13)	0.0381(3)	0.0381(8)	0.0358(8)	0.0420(8)
N2	0.7002(3)	0.1472(2)	0.10409(16)	0.0556(5)	0.0621(12)	0.0532(11)	0.0442(9)
C1	0.3474(3)	0.1385(2)	0.54288(19)	0.0462(4)	0.0450(11)	0.0483(11)	0.0537(11)
C2	0.2450(3)	-0.0309(3)	0.5172(2)	0.0601(6)	0.0528(13)	0.0463(11)	0.0945(17)
C3	0.1384(3)	-0.1035(3)	0.3995(3)	0.0664(7)	0.0498(13)	0.0349(10)	0.109(2)
C4	0.1378(3)	-0.0059(3)	0.3101(2)	0.0595(6)	0.0525(13)	0.0443(11)	0.0723(14)

C5	0.2439(3)	0.1619(2)	0.34171(18)	0.0482(5)	0.0517(12)	0.0437(10)	0.0455(10)
C6	0.7082(2)	0.4351(2)	0.28541(14)	0.0322(3)	0.0295(8)	0.0330(8)	0.0289(8)
C7	0.7211(2)	0.4429(2)	0.15021(14)	0.0342(4)	0.0245(8)	0.0475(10)	0.0289(8)
C8	0.7243(3)	0.3095(2)	0.06589(15)	0.0408(4)	0.0344(9)	0.0546(11)	0.0320(8)
C9	0.7409(3)	0.3209(3)	-0.05665(17)	0.0547(6)	0.0436(11)	0.0884(16)	0.0311(9)
C10	0.7571(3)	0.4705(3)	-0.09600(18)	0.0597(6)	0.0446(11)	0.109(2)	0.0317(10)
C11	0.7570(3)	0.6059(3)	-0.01436(19)	0.0537(5)	0.0401(11)	0.0780(15)	0.0476(11)
C12	0.7381(3)	0.5920(2)	0.10751(17)	0.0422(4)	0.0349(9)	0.0517(11)	0.0397(9)

Table 38:- 2.8

Atom label	X	Y	Z	Uiso	Uaniso-U11	Uaniso-U22	Uaniso-U33
Co1	0.1720(12)	0.1606(10)	0.16929(11)	0.03427(9)	0.0328(14)	0.0345(14)	0.0354(14)
C1	0.125	0.125	0.28030(12)	0.0406(6)	0.0431(15)	0.0405(15)	0.0383(14)
C2	0.125	0.125	0.34694(13)	0.0456(7)	0.0456(16)	0.0523(18)	0.0389(15)
C3	0.1528(12)	0.1654(10)	0.37784(11)	0.0597(6)	0.0680(15)	0.0652(16)	0.0457(12)
C4	0.1526(16)	0.1652(14)	0.43943(12)	0.0818(9)	0.095(2)	0.101(3)	0.0488(15)
C5	0.125	0.125	0.46944(18)	0.0908(15)	0.109(4)	0.127(4)	0.0357(19)
C6	0.2902(13)	0.125	0.125	0.0398(6)	0.0358(14)	0.0421(15)	0.0416(14)
C7	0.3612(14)	0.125	0.125	0.0454(7)	0.0345(14)	0.0566(19)	0.0449(16)
C8	0.3940(11)	0.1654(11)	0.15042(12)	0.0617(6)	0.0433(12)	0.0746(18)	0.0671(15)
C9	0.4597(13)	0.1655(15)	0.15038(15)	0.0858(10)	0.0470(15)	0.118(3)	0.092(2)
C10	0.4915(2)	0.125	0.125	0.0972(17)	0.036(2)	0.157(5)	0.099(4)
C11	0.2184(11)	0.26289(9)	0.14189(11)	0.0562(6)	0.0549(14)	0.0468(13)	0.0670(15)
C12	0.2271(14)	0.3152(11)	0.14757(15)	0.0767(9)	0.0780(19)	0.0504(15)	0.102(2)
C13	0.1957(16)	0.3414(11)	0.19130(16)	0.0790(9)	0.085(2)	0.0432(15)	0.109(2)
C14	0.15579(15)	0.3145(11)	0.22739(13)	0.0734(8)	0.090(2)	0.0518(15)	0.0784(19)
C15	0.14876(12)	0.26211(9)	0.21897(11)	0.0562(6)	0.0638(15)	0.0480(13)	0.0568(13)
C16	0.3022(2)	0.2197(3)	0.2934(2)	0.194(3)	0.091(3)	0.373(10)	0.117(4)
C17	0.3680(2)	0.2288(18)	0.29915(17)	0.1102(13)	0.118(3)	0.140(4)	0.072(2)
N1	0.17998(8)	0.23593(7)	0.17717(7)	0.0412(4)	0.0395(9)	0.0390(9)	0.0450(9)
N2	0.4212(2)	0.23460(18)	0.3036(2)	0.1403(15)	0.120(3)	0.164(4)	0.137(3)
O1	0.16646(6)	0.15318(5)	0.25548(6)	0.0417(3)	0.0427(7)	0.0460(8)	0.0366(7)
O2	0.26397(6)	0.15337(5)	0.16373(6)	0.0416(3)	0.0343(7)	0.0464(8)	0.0439(7)
O3	0.16584(6)	0.16154(5)	0.08663(5)	0.0341(3)	0.0327(6)	0.0349(7)	0.0346(6)
O4	0.25064(15)	0.1964(11)	0.00279(14)	0.1233(10)	0.133(2)	0.106(2)	0.131(2)

Table 39:- 3.1

Atom label	X	Y	Z	Uiso	Uaniso-U11	Uaniso-U22	Uaniso-U33
Ni1	0.47214(3)	0.6900(15)	0.3767(18)	0.037(12)	0.0321(2)	0.0432(2)	0.0387(2)
Ni2	0.25214(3)	0.7125(15)	0.4908(18)	0.038(12)	0.0331(2)	0.0435(2)	0.0386(2)
C1	0.5014(4)	0.7511(16)	0.2583(18)	0.060(10)	0.064(2)	0.067(3)	0.054(2)
C2	0.5020(5)	0.7918(19)	0.2183(2)	0.083(14)	0.114(4)	0.080(3)	0.062(3)
C3	0.4674(5)	0.8390(2)	0.2405(2)	0.086(14)	0.109(4)	0.073(3)	0.080(3)
C4	0.4343(4)	0.8435(16)	0.3010(2)	0.072(11)	0.087(3)	0.055(2)	0.074(3)
C5	0.4374(4)	0.8006(14)	0.3384(18)	0.0554(9)	0.061(2)	0.057(2)	0.049(2)
C6	0.7519(3)	0.7035(14)	0.3566(17)	0.0522(8)	0.040(17)	0.056(2)	0.060(2)
C7	0.8705(3)	0.6911(17)	0.3379(19)	0.061(10)	0.037(18)	0.078(3)	0.070(2)
C8	0.8920(3)	0.6427(17)	0.3176(18)	0.062(10)	0.035(17)	0.085(3)	0.067(2)

C9	0.7953(3)	0.6073(16)	0.3168(2)	0.062(10)	0.048(2)	0.061(2)	0.080(3)
C10	0.6789(3)	0.6220(14)	0.3360(18)	0.0530(8)	0.041(17)	0.051(2)	0.068(2)
C11	0.3010(3)	0.6216(13)	0.2909(15)	0.0441(7)	0.038(16)	0.049(19)	0.044(18)
C12	0.2840(3)	0.5863(14)	0.2350(16)	0.0490(8)	0.047(18)	0.054(2)	0.044(18)
C13	0.1863(5)	0.5514(18)	0.2289(2)	0.078(13)	0.091(3)	0.078(3)	0.066(3)
C14	0.1725(7)	0.5192(2)	0.1761(3)	0.116(2)	0.143(5)	0.112(5)	0.091(4)
C15	0.2531(7)	0.5224(3)	0.1298(3)	0.115(2)	0.162(6)	0.113(5)	0.070(3)
C16	0.3483(6)	0.5577(2)	0.1347(2)	0.101(17)	0.116(4)	0.120(5)	0.071(3)
C17	0.3652(4)	0.5889(18)	0.1872(2)	0.074(12)	0.075(3)	0.086(3)	0.065(3)
C18	0.4626(3)	0.6310(12)	0.495(16)	0.0429(7)	0.038(16)	0.039(18)	0.051(2)
C19	0.5513(3)	0.5972(14)	0.5371(16)	0.0497(8)	0.040(17)	0.057(2)	0.053(2)
C20	0.5955(4)	0.5521(15)	0.5141(2)	0.064(10)	0.055(2)	0.050(2)	0.086(3)
C21	0.6708(4)	0.5194(19)	0.5521(3)	0.089 (15)	0.070(3)	0.070(3)	0.129(5)
C22	0.7083(5)	0.5321(3)	0.6125(3)	0.116(2)	0.093(4)	0.156(6)	0.101(4)
C23	0.6738(6)	0.5791(3)	0.6361(3)	0.138(3)	0.138(5)	0.214(8)	0.059(3)
C24	0.5921(5)	0.6109(2)	0.5983(2)	0.097 (18)	0.102(4)	0.133(5)	0.056(3)
C25	0.5107(3)	0.7568(12)	0.4961(15)	0.0412(7)	0.041(17)	0.042(18)	0.040(17)
C26	0.6046(3)	0.7738(13)	0.5502(15)	0.0446(7)	0.042(17)	0.051(19)	0.040(17)
C27	0.7248(4)	0.7522(19)	0.5580(2)	0.075 (13)	0.048(2)	0.109(4)	0.067(3)
C28	0.8120(5)	0.7666(3)	0.6076(2)	0.102(19)	0.059(3)	0.162(5)	0.080(3)
C29	0.7812(5)	0.8040(2)	0.6491(2)	0.092 (16)	0.068(3)	0.144(5)	0.062(3)
C30	0.6625(4)	0.8256(2)	0.6424(2)	0.078 (13)	0.073(3)	0.103(4)	0.062(3)
C31	0.5738(4)	0.8103(15)	0.5931(18)	0.0591(9)	0.052(2)	0.068(3)	0.058(2)
C32	0.2027(4)	0.6928(18)	0.6277(18)	0.065 (10)	0.068(2)	0.078(3)	0.050(2)
C33	0.1703(5)	0.7029(2)	0.6880(2)	0.086 (15)	0.087(3)	0.123(5)	0.050(3)
C34	0.1523(4)	0.7523(3)	0.7055(2)	0.087 (16)	0.070(3)	0.150(5)	0.043(2)
C35	0.1665(4)	0.7906(2)	0.6624(2)	0.077 (13)	0.064(3)	0.105(4)	0.065(3)
C36	0.1978(4)	0.7775(16)	0.6023(18)	0.0593(9)	0.060(2)	0.070(3)	0.049(2)
C38	0.1327(3)	0.6087(13)	0.4600(17)	0.0503(8)	0.044(18)	0.050(2)	0.058(2)
C39	0.0419(4)	0.5705(16)	0.4526(2)	0.065 (10)	0.056(2)	0.055(2)	0.085(3)
C40	-0.0781(4)	0.5802(17)	0.4702(2)	0.072 (12)	0.058(2)	0.070(3)	0.090(3)
C41	-0.1038(4)	0.6279(17)	0.4942(2)	0.068 (11)	0.041(19)	0.080(3)	0.087(3)
C42	-0.0085(3)	0.6643(15)	0.4990(18)	0.0561(9)	0.043(18)	0.063(2)	0.064(2)
C43	0.0847(3)	0.7861(13)	0.4093(16)	0.0451(7)	0.037(16)	0.046(19)	0.051(2)
C44	-0.0327(3)	0.8197(13)	0.4017(18)	0.0514(8)	0.044(18)	0.048(2)	0.062(2)
C45	-0.0735(5)	0.8403(2)	0.3440(2)	0.087 (15)	0.080(3)	0.106(4)	0.077(3)
C46	-0.1855(6)	0.8694(3)	0.3365(3)	0.117(2)	0.108(4)	0.133(5)	0.109(4)
C47	-0.2537(5)	0.8781(2)	0.3860(3)	0.100 (18)	0.068(3)	0.091(4)	0.142(5)
C48	-0.2146(4)	0.8575(2)	0.4437(3)	0.097(16)	0.068(3)	0.092(4)	0.123(4)
C49	-0.1037(4)	0.8286(17)	0.4521(2)	0.071 (11)	0.062(2)	0.075(3)	0.080(3)
C50	0.3575(9)	0.5975(3)	0.9621(3)	0.115(2)	0.113(5)	0.122(6)	0.111(5)
C58	0.3197(7)	0.5274(18)	0.7184(16)	0.261(11)	0.37(2)	0.085(7)	0.284(16)
C59	0.3172(8)	0.5310(2)	0.6526(16)	0.199(6)	0.396(18)	0.100(6)	0.099(5)
C60	0.2056(9)	0.5459(17)	0.6164(13)	0.298(11)	0.45(3)	0.139(11)	0.275(18)
C61	0.0965(8)	0.5572(2)	0.6462(15)	0.393(18)	0.76(4)	0.133(10)	0.241(15)
C62	0.0990(6)	0.5536(2)	0.7120(15)	0.244(7)	0.315(17)	0.116(8)	0.287(17)
C63	0.2106(6)	0.5386(12)	0.7481(13)	0.171(5)	0.237(13)	0.124(8)	0.153(8)
C51	0.2902(6)	0.5544(2)	0.9505(13)	0.221(7)	0.373(19)	0.183(11)	0.095(6)
C56	0.1580(6)	0.5529(3)	0.9512(15)	0.169(4)	0.102(5)	0.259(12)	0.141(7)
C55	0.0928(6)	0.5068(3)	0.9414(17)	0.261(7)	0.191(12)	0.35(2)	0.230(14)
C54	0.1597(8)	0.4622(3)	0.9307(18)	0.273(8)	0.227(16)	0.36(2)	0.226(14)
C53	0.2919(7)	0.4636(2)	0.9300(18)	0.245(6)	0.258(15)	0.243(15)	0.238(14)
C52	0.3571(5)	0.5097(3)	0.9399(16)	0.166(4)	0.264(12)	0.095(5)	0.145(7)

N1	0.4702(2)	0.7542(11)	0.3181(13)	0.0466(6)	0.041(14)	0.052(17)	0.046(16)
N2	0.6564(2)	0.6698(11)	0.3555(12)	0.0431(6)	0.033(13)	0.048(16)	0.046(15)
N3	0.1096(2)	0.6551(10)	0.4827(12)	0.0442(6)	0.035(13)	0.049(17)	0.047(15)
N4	0.2152(2)	0.7292(12)	0.5847(13)	0.0475(6)	0.042(15)	0.057(18)	0.041(15)
O1	0.2839(2)	0.70281(0)	0.3958(10)	0.0412(5)	0.035(11)	0.047(14)	0.041(12)
O2	0.4055(19)	0.64528(9)	0.2999(10)	0.0478(5)	0.036(11)	0.060(15)	0.046(12)
O3	0.2095(2)	0.6265(11)	0.3242(12)	0.0648(7)	0.042(13)	0.087(2)	0.067(16)
O4	0.4675(2)	0.62775(9)	0.4365(11)	0.0496(5)	0.056(14)	0.045(13)	0.046(14)
O5	0.3890(2)	0.65958(9)	0.5240(10)	0.0471(5)	0.042(12)	0.049(13)	0.050(13)
O6	0.1138(2)	0.76666(9)	0.4636(10)	0.0467(5)	0.042(12)	0.054(14)	0.043(13)
O7	0.1426(2)	0.7787(10)	0.3612(12)	0.0601(7)	0.058(15)	0.075(18)	0.048(14)
O8	0.3944(19)	0.76876(8)	0.4982(11)	0.0461(5)	0.036(11)	0.044(13)	0.057(14)
O9	0.5549(19)	0.73129(9)	0.4529(10)	0.0466(5)	0.038(11)	0.056(14)	0.045(12)
O10	0.2811(7)	0.6307(4)	0.9770(4)	0.280(6)	0.182(7)	0.399(14)	0.274(9)
O11	0.4644(8)	0.6010(5)	0.9592(4)	0.271(5)	0.160(6)	0.391(14)	0.272(10)
C64	0.4028(17)	0.5139(4)	0.7526(8)	0.301(10)	0.44(2)	0.093(7)	0.34(2)

Table 40:- 3.2

Atom label	X	Y	Z	Uiso	Uaniso-U11	Uaniso-U22	Uaniso-U33
Ni1	0.52519(3)	0.13579(7)	0.11882(2)	0.03922(8)	0.0342(15)	0.0412(15)	0.0423(17)
Ni2	0.32022(3)	0.13519(7)	0.33078(2)	0.04001(8)	0.0404(16)	0.0383(14)	0.0415(17)
C1	0.0921(2)	0.09949(6)	0.4165(2)	0.0538(6)	0.0505(15)	0.0535(14)	0.0573(16)
C3	-0.1131(3)	0.12098(9)	0.4265(2)	0.0724(8)	0.0458(16)	0.110(2)	0.0625(19)
C2	-0.0299(3)	0.09460(8)	0.4420(2)	0.0688(8)	0.0568(18)	0.0770(18)	0.073(2)
C4	-0.0718(3)	0.15183(9)	0.3868(2)	0.0709(8)	0.0544(17)	0.090(2)	0.069(2)
C5	0.0520(3)	0.15516(7)	0.3639(2)	0.0598(7)	0.0587(17)	0.0572(15)	0.0641(18)
C6	0.3207(3)	0.17338(8)	0.5401(2)	0.0711(8)	0.082(2)	0.0748(18)	0.0569(18)
C10	0.3721(3)	0.20918(7)	0.4049(3)	0.0693(8)	0.0623(18)	0.0475(14)	0.098(2)
C7	0.3284(4)	0.2003(11)	0.6123(3)	0.0955(12)	0.096(3)	0.109(3)	0.081(2)
C8	0.3589(4)	0.2324(11)	0.5788(4)	0.1022(14)	0.085(3)	0.088(3)	0.132(4)
C9	0.3809(3)	0.23739(8)	0.4747(4)	0.0926(12)	0.070(2)	0.0510(17)	0.156(4)
C11	0.5367(3)	0.15839(8)	-0.1102(2)	0.0604(7)	0.0564(17)	0.0725(17)	0.0522(16)
C15	0.5838(3)	0.10105(7)	-0.0901(2)	0.0611(7)	0.0546(16)	0.0668(16)	0.0625(18)
C13	0.5842(3)	0.1253(12)	-0.2622(3)	0.0935(12)	0.092(3)	0.141(3)	0.0472(18)
C12	0.5525(3)	0.1565(10)	-0.2180(3)	0.0807(9)	0.076(2)	0.110(3)	0.0549(19)
C14	0.6007(3)	0.0969(10)	-0.1971(3)	0.0837(10)	0.083(2)	0.100(2)	0.069(2)
C36	0.1836(2)	0.19256(6)	0.0583(2)	0.0468(5)	0.0370(13)	0.0484(12)	0.0550(15)
C35	0.2734(2)	0.17060(6)	-0.1224(19)	0.0434(5)	0.0385(12)	0.0432(11)	0.0487(15)
C40	0.1019(4)	0.2120(10)	-0.1104(3)	0.0958(12)	0.096(3)	0.121(3)	0.069(2)
C37	0.1045(3)	0.21542(7)	0.1081(2)	0.0644(7)	0.0534(16)	0.0704(17)	0.0696(19)
C41	0.1814(3)	0.19107(8)	-0.0514(2)	0.0672(8)	0.0613(18)	0.0798(19)	0.0598(18)
C39	0.0261(4)	0.2352(10)	-0.0592(3)	0.1010(12)	0.081(3)	0.115(3)	0.106(3)
C21	0.4718(2)	0.08523(6)	0.4644(18)	0.0440(5)	0.0433(13)	0.0453(12)	0.0434(13)
C22	0.4762(2)	0.05833(5)	0.5518(18)	0.0424(5)	0.0436(13)	0.0438(11)	0.0398(13)
C23	0.5777(2)	0.03654(6)	0.5648(2)	0.0558(6)	0.0497(15)	0.0624(15)	0.0555(16)
C27	0.3790(2)	0.05478(6)	0.6200(2)	0.0529(6)	0.0430(14)	0.0619(15)	0.0540(15)
C24	0.5802(3)	0.01141(7)	0.6431(2)	0.0675(8)	0.0618(18)	0.0702(17)	0.0707(19)
C25	0.4826(3)	0.00798(8)	0.7099(2)	0.0675(8)	0.0666(19)	0.0739(18)	0.0617(18)
C26	0.3827(3)	0.02994(8)	0.6994(2)	0.0683(8)	0.0553(17)	0.087(2)	0.0631(18)
C42	0.6350(2)	0.20418(6)	0.1932(18)	0.0422(5)	0.0387(12)	0.0463(12)	0.0417(13)
C43	0.6897(2)	0.23943(6)	0.1679(18)	0.0414(5)	0.0383(12)	0.0459(11)	0.0402(12)

C45	0.7278(3)	0.28562(6)	0.0444(2)	0.0556(6)	0.0628(17)	0.0549(14)	0.0492(15)
C44	0.6814(2)	0.25303(6)	0.0662(19)	0.0488(6)	0.0497(14)	0.0554(13)	0.0411(13)
C46	0.7862(3)	0.30458(6)	0.1236(2)	0.0601(7)	0.0712(19)	0.0456(13)	0.0637(18)
C48	0.7472(2)	0.25892(6)	0.2470(2)	0.0528(6)	0.0668(17)	0.0523(13)	0.0394(13)
C47	0.7966(3)	0.29134(6)	0.2245(2)	0.0621(7)	0.077(2)	0.0517(14)	0.0570(17)
C29	0.2983(2)	0.04402(5)	0.1170(17)	0.0401(5)	0.0390(12)	0.0388(11)	0.0424(13)
C28	0.3549(2)	0.07726(5)	0.1614(18)	0.0403(5)	0.0406(13)	0.0365(10)	0.0437(13)
C30	0.1940(2)	0.02986(6)	0.1622(2)	0.0502(6)	0.0507(15)	0.0500(13)	0.0501(15)
C34	0.3483(2)	0.02733(6)	0.0307(2)	0.0532(6)	0.0569(16)	0.0516(13)	0.0515(15)
C31	0.1389(3)	0.00040(7)	0.1197(2)	0.0664(8)	0.0656(18)	0.0637(16)	0.0702(19)
C32	0.1887(3)	-0.0156(7)	0.0328(2)	0.0721(8)	0.093(2)	0.0572(16)	0.0659(19)
C33	0.2943(3)	-0.0022(7)	-0.0108(2)	0.0678(8)	0.092(2)	0.0571(15)	0.0554(17)
C16	0.8017(2)	0.13618(7)	0.0983(2)	0.0622(7)	0.0401(14)	0.0721(17)	0.075(2)
C17	0.9232(3)	0.12581(9)	0.1047(3)	0.0781(9)	0.0427(16)	0.099(2)	0.093(2)
C19	0.8599(3)	0.07596(9)	0.1963(3)	0.0758(9)	0.075(2)	0.0781(19)	0.074(2)
C18	0.9519(3)	0.0953(10)	0.1546(3)	0.0847(10)	0.0497(19)	0.106(3)	0.098(3)
N2	0.3417(19)	0.17754(5)	0.4372(18)	0.0533(5)	0.0503(12)	0.0467(11)	0.0630(14)
N1	0.1339 (18)	0.12948(5)	0.3772(15)	0.0455(4)	0.0449(11)	0.0489(10)	0.0428(11)
N3	0.5521(18)	0.13125(5)	-0.046(16)	0.0487(5)	0.0393(11)	0.0603(12)	0.0467(12)
N4	0.7093(18)	0.11788(5)	0.1403(16)	0.0499(5)	0.0397(11)	0.0569(12)	0.0531(13)
O1	0.3710(15)	0.10111(4)	0.4499(13)	0.0488(4)	0.0434(9)	0.0506(9)	0.0525(10)
O2	0.5673(16)	0.09008(5)	0.4125(15)	0.0669(5)	0.0466(10)	0.0787(12)	0.0762(13)
O5	0.2599(17)	0.17037(4)	0.2206(13)	0.0560(4)	0.0630(11)	0.0585(10)	0.0470(10)
O6	0.3550(15)	0.15479(4)	0.0726(13)	0.0499(4)	0.0398(9)	0.0625(10)	0.0476(10)
O7	0.5873(15)	0.18726(4)	0.1169(12)	0.0479(4)	0.0574(11)	0.0448(8)	0.0414(9)
O8	0.6399(18)	0.19432(5)	0.2876(13)	0.0621(5)	0.0803(13)	0.0654(11)	0.0402(10)
O3	0.2945 (15)	0.09290(4)	0.2305(13)	0.0487(4)	0.0463(9)	0.0466(8)	0.0536(10)
O4	0.4571(15)	0.08625(4)	-0.1232(13)	0.0488(4)	0.0410(9)	0.0444(8)	0.0615(11)
O9	0.5044 (15)	0.13910(5)	0.2834(13)	0.0429(4)	0.0418(9)	0.0420(9)	0.0451(10)
C56	0.9249(3)	0.00932(8)	0.5812(3)	0.0742(8)	0.062(2)	0.081(2)	0.080(2)
C57	1.0507(3)	0.01516(8)	0.5892(3)	0.0792(9)	0.067(2)	0.086(2)	0.084(2)
C55	0.8750(3)	-0.0057(8)	0.4929(3)	0.0748(9)	0.0505(17)	0.0755(19)	0.099(3)
C50	0.1928(4)	0.1171(10)	0.7651(3)	0.0943(11)	0.091(3)	0.102(3)	0.090(3)
C51	0.1925(4)	0.0961(10)	0.8520(3)	0.0949(11)	0.088(3)	0.103(3)	0.094(3)
C53	-0.0238(4)	0.0906(10)	0.8334(3)	0.1022(12)	0.087(3)	0.104(3)	0.116(3)
C52	0.0842(4)	0.0826(10)	0.8856(3)	0.0983(12)	0.114(3)	0.094(3)	0.087(3)
C49	0.0842(4)	0.1249(10)	0.7123(3)	0.0983(12)	0.116(4)	0.103(3)	0.077(3)
C54	-0.0236(4)	0.1117(10)	0.7472(3)	0.1014(12)	0.091(3)	0.104(3)	0.109(3)
C20	0.7382(3)	0.08809(7)	0.1894(2)	0.0583(7)	0.0597(17)	0.0564(15)	0.0584(16)
C38	0.0264(3)	0.23679(9)	0.0487(3)	0.0884(10)	0.068(2)	0.095(2)	0.102(3)

Table 41:- 3.3

Atom label	X	Y	Z	Uiso	Uaniso-U11	Uaniso-U22	Uaniso-U33
Ni1	0.0607(15)	0.2299(10)	0.1481(13)	0.037(8)	0.038(13)	0.041(12)	0.031(12)
C1	0.1143(12)	0.30529(8)	0.3068(11)	0.039(4)	0.041(10)	0.0416(9)	0.0344(9)
C2	0.1815(13)	0.35430(8)	0.3392(11)	0.043(4)	0.051(11)	0.0426(9)	0.0357(9)
C3	0.1571(17)	0.39394(9)	0.4072(15)	0.065(6)	0.075(15)	0.055(12)	0.064(14)
C4	0.2199(2)	0.4384(11)	0.4376(19)	0.088(8)	0.121(2)	0.061(14)	0.083(18)
C5	0.3064(2)	0.4436(12)	0.4000(19)	0.088(9)	0.108(2)	0.072(16)	0.086(2)
C6	0.3325(18)	0.4042(13)	0.3333(17)	0.079(7)	0.069(16)	0.094(18)	0.074(17)
C7	0.2700(14)	0.3598(10)	0.3032(13)	0.058(5)	0.056(13)	0.070(13)	0.049(11)

C8	0.1918(12)	0.12284(8)	0.1901(12)	0.043(4)	0.042(10)	0.045(10)	0.040(10)
C9	0.2854(13)	0.09349(9)	0.1756(12)	0.048(4)	0.046(10)	0.058(11)	0.039(10)
C10	0.3024(17)	0.0319(10)	0.2003(15)	0.064(6)	0.073(15)	0.061(12)	0.059(13)
C11	0.3894(2)	0.0053(14)	0.1835(19)	0.091(9)	0.102(2)	0.092(19)	0.080(18)
C12	0.4583(2)	0.0391(19)	0.1446(19)	0.11(12)	0.079(2)	0.169(3)	0.076(19)
C13	0.4429(19)	0.1002(19)	0.1220(2)	0.10(11)	0.056(16)	0.169(3)	0.099(2)
C14	0.3560(16)	0.1270(13)	0.1362(17)	0.075(7)	0.052(13)	0.093(17)	0.080(17)
C15	-0.011(15)	0.11947(9)	0.0408(13)	0.055(5)	0.064(13)	0.049(11)	0.054(12)
C16	-0.054(16)	0.0883(10)	-0.027(16)	0.069(6)	0.080(16)	0.052(12)	0.073(15)
C17	-0.102(18)	0.1212(12)	-0.088(16)	0.074(7)	0.085(17)	0.080(16)	0.057(14)
C18	-0.107(18)	0.1851(11)	-0.080(15)	0.074(7)	0.093(18)	0.074(15)	0.054(13)
C19	-0.063(15)	0.2133(10)	-0.010(14)	0.057(5)	0.069(14)	0.054(11)	0.048(11)
C20	0.1681(14)	0.26071(9)	-0.020(13)	0.053(5)	0.057(12)	0.055(11)	0.047(11)
C21	0.2088(16)	0.2973(11)	-0.084(14)	0.064(6)	0.067(14)	0.079(15)	0.047(12)
C22	0.2098(16)	0.3613(11)	-0.074(15)	0.067(6)	0.067(14)	0.077(15)	0.058(13)
C23	0.1695(16)	0.3858(10)	-0.0004(1)	0.065(6)	0.070(14)	0.050(11)	0.073(16)
C24	0.1302(14)	0.34651(9)	0.0605(13)	0.052(5)	0.056(12)	0.048(10)	0.052(11)
N1	-0.014(10)	0.18178(7)	0.04979(9)	0.043(3)	0.0462(8)	0.0467(8)	0.0378(8)
N2	0.1282(10)	0.28433(7)	0.05114(9)	0.043(3)	0.0444(8)	0.0457(8)	0.0394(8)
O1	0.13906(9)	0.27558(6)	0.23955(8)	0.049(3)	0.0417(7)	0.0652(8)	0.0419(7)
O2	0.14218(9)	0.10263(6)	0.25219(9)	0.055(3)	0.0458(8)	0.0633(8)	0.0579(8)
O3	0.16908(9)	0.16662(6)	0.13911(8)	0.048(3)	0.0487(7)	0.0535(7)	0.0429(7)
O4	0	0.17699(8)	0.25	0.040(4)	0.039(10)	0.0441(9)	0.0374(9)
O5	-0.0402(9)	0.29797(6)	0.15061(8)	0.046(3)	0.0466(7)	0.0476(7)	0.0439(7)
O6	0.5	0.5046(14)	0.25	0.158(2)	0.082(2)	0.055(16)	0.336(7)

Table 42:- 3.4

Atom label	X	Y	Z	Uiso	Uaniso-U11	Uaniso-U22	Uaniso-U33
Ni1	0.08373(3)	0.98373(14)	0.25706(13)	0.0342(10)	0.0315(18)	0.0332(17)	0.038(19)
Ni2	0.32389(3)	0.86877(14)	0.30441(13)	0.0334(10)	0.0311(17)	0.0311(16)	0.038(19)
C1	0.1797(2)	0.83515(12)	0.39890(11)	0.0384(6)	0.0313(14)	0.0450(14)	0.039(15)
C2	0.1756(2)	0.80567(12)	0.45322(11)	0.0387(6)	0.0348(14)	0.0436(14)	0.038(15)
C3	0.2481(3)	0.75122(14)	0.46439(12)	0.0500(7)	0.0541(18)	0.0488(16)	0.048(18)
C4	0.2414(4)	0.71721(15)	0.51186(14)	0.0626(9)	0.083(2)	0.0494(18)	0.056(2)
C5	0.1635(4)	0.73789(16)	0.54831(14)	0.0652(9)	0.089(3)	0.0560(19)	0.051(2)
C6	0.0886(3)	0.79399(16)	0.53964(12)	0.0547(8)	0.0530(18)	0.067(2)	0.045(18)
C7	0.0072(4)	0.8155(2)	0.57775(14)	0.0703(10)	0.069(2)	0.099(3)	0.046(2)
C8	-0.0621(4)	0.8708(3)	0.56965(17)	0.0844(12)	0.067(2)	0.129(4)	0.062(3)
C9	-0.0528(4)	0.9062(2)	0.52364(17)	0.0814(11)	0.078(3)	0.101(3)	0.067(3)
C10	0.0233(3)	0.88689(17)	0.48534(14)	0.0626(8)	0.062(2)	0.074(2)	0.053(19)
C11	0.0955(3)	0.82938(14)	0.49168(11)	0.0446(6)	0.0394(15)	0.0543(17)	0.040(16)
C12	0.3397(3)	0.95625(12)	0.20880(11)	0.0398(6)	0.0371(15)	0.0407(14)	0.042(16)
C13	0.4156(3)	0.97437(14)	0.16331(12)	0.0492(7)	0.0466(16)	0.0527(17)	0.050(18)
C14	0.4816(4)	0.9263(2)	0.14079(18)	0.0924(14)	0.114(3)	0.081(3)	0.095(3)
C15	0.5506(6)	0.9365(3)	0.0970(2)	0.135(2)	0.170(5)	0.135(4)	0.120(4)
C16	0.5560(5)	0.9945(3)	0.0752(2)	0.1168(19)	0.122(4)	0.137(4)	0.107(4)
C17	0.4931(3)	1.04773(19)	0.09692(15)	0.0703(10)	0.056(2)	0.090(3)	0.068(2)
C18	0.4994(4)	1.1101(3)	0.07437(18)	0.0864(13)	0.076(3)	0.103(3)	0.083(3)
C19	0.4363(5)	1.1590(2)	0.09330(19)	0.0864(13)	0.091(3)	0.077(3)	0.088(3)
C20	0.3630(4)	1.15008(16)	0.13594(16)	0.0742(10)	0.094(3)	0.0463(18)	0.080(3)
C21	0.3549(3)	1.09118(14)	0.15919(13)	0.0568(8)	0.0634(19)	0.0487(17)	0.058(2)

C22	0.4198(3)	1.03781(14)	0.14070(12)	0.0483(7)	0.0383(15)	0.0583(17)	0.048(17)
C23	0.2923(2)	1.00438(12)	0.34821(11)	0.0369(6)	0.0337(14)	0.0365(13)	0.041(15)
C24	0.3534(2)	1.05239(12)	0.38802(11)	0.0421(6)	0.0374(15)	0.0423(15)	0.045(17)
C25	0.3770(3)	1.03532(16)	0.44026(14)	0.0650(9)	0.077(2)	0.0597(19)	0.054(2)
C26	0.4312(4)	1.0802(2)	0.47875(16)	0.0861(13)	0.104(3)	0.092(3)	0.054(2)
C27	0.4614(4)	1.1398(2)	0.46301(19)	0.0853(13)	0.088(3)	0.077(3)	0.083(3)
C28	0.4392(3)	1.15921(16)	0.40975(16)	0.0634(9)	0.0505(18)	0.0555(19)	0.082(3)
C29	0.4676(4)	1.2224(2)	0.3922(3)	0.0896(14)	0.070(3)	0.062(2)	0.136(5)
C30	0.4422(5)	1.2394(2)	0.3407(3)	0.0981(14)	0.109(4)	0.059(2)	0.129(5)
C31	0.3908(4)	1.19579(18)	0.30273(19)	0.0818(11)	0.091(3)	0.061(2)	0.095(3)
C32	0.3637(3)	1.13513(15)	0.31697(14)	0.0568(8)	0.0505(18)	0.0547(18)	0.066(2)
C33	0.3844(2)	1.11512(13)	0.37084(13)	0.0469(7)	0.0315(14)	0.0451(16)	0.064(2)
C34	-0.0255(3)	0.88779(14)	0.17427(12)	0.0467(7)	0.0414(16)	0.0477(17)	0.048(17)
C35	-0.0665(3)	0.87354(15)	0.11641(13)	0.0544(8)	0.0513(18)	0.0541(17)	0.054(19)
C36	-0.1655(3)	0.83076(18)	0.10469(16)	0.0697(10)	0.060(2)	0.074(2)	0.071(2)
C37	-0.2109(4)	0.8168(2)	0.0516(2)	0.0916(14)	0.072(3)	0.115(3)	0.083(3)
C38	-0.1554(5)	0.8432(3)	0.0113(2)	0.0985(16)	0.086(3)	0.137(4)	0.065(3)
C39	-0.0481(4)	0.8852(2)	0.02036(16)	0.0781(12)	0.081(3)	0.097(3)	0.051(2)
C40	0.0161(7)	0.9111(3)	-0.0218(18)	0.1021(16)	0.125(4)	0.136(4)	0.044(2)
C41	0.1221(7)	0.9469(3)	-0.0117(2)	0.1056(16)	0.123(4)	0.135(4)	0.063(3)
C42	0.1691(5)	0.9606(2)	0.04027(18)	0.0880(12)	0.094(3)	0.107(3)	0.065(3)
C43	0.1094(4)	0.93908(17)	0.08261(15)	0.0684(10)	0.077(2)	0.074(2)	0.053(2)
C44	-0.0029(3)	0.90066(16)	0.07417(13)	0.0599(9)	0.064(2)	0.066(2)	0.047(19)
C45	0.0499(3)	1.12773(13)	0.26281(13)	0.0501(7)	0.0477(17)	0.0412(15)	0.060(19)
C46	0.0274(3)	1.19051(14)	0.24700(17)	0.0634(9)	0.0571(19)	0.0384(16)	0.094(3)
C47	-0.0104(4)	1.20270(16)	0.19497(17)	0.0689(10)	0.074(2)	0.0444(18)	0.092(3)
C48	-0.0254(4)	1.15248(18)	0.16027(16)	0.0816(12)	0.122(3)	0.063(2)	0.061(2)
C49	0.0011(4)	1.09128(16)	0.17846(14)	0.0652(9)	0.096(3)	0.0521(18)	0.047(19)
C50	-0.0899(3)	0.99588(16)	0.34713(14)	0.0570(8)	0.0452(18)	0.069(2)	0.059(2)
C51	-0.2004(4)	1.00224(19)	0.37187(17)	0.0731(10)	0.062(2)	0.086(3)	0.077(3)
C52	-0.3176(4)	0.99722(16)	0.3424(2)	0.0738(11)	0.053(2)	0.0515(19)	0.124(4)
C53	-0.3192(3)	0.98620(16)	0.2891(2)	0.0698(11)	0.0332(17)	0.0548(19)	0.121(4)
C54	-0.2053(3)	0.98117(14)	0.26601(16)	0.0587(8)	0.0360(17)	0.0548(18)	0.085(2)
C55	0.5632(3)	0.84887(14)	0.38113(13)	0.0505(7)	0.0382(16)	0.0598(18)	0.053(19)
C56	0.6900(3)	0.83758(17)	0.39949(15)	0.0645(9)	0.0419(18)	0.075(2)	0.072(2)
C57	0.7760(3)	0.82515(16)	0.36336(18)	0.0672(10)	0.0336(17)	0.062(2)	0.103(3)
C58	0.7329(3)	0.82404(15)	0.31016(17)	0.0630(9)	0.0407(18)	0.0559(19)	0.096(3)
C59	0.6038(3)	0.83552(13)	0.29492(13)	0.0497(7)	0.0463(17)	0.0453(16)	0.059(19)
C60	0.3366(3)	0.72529(13)	0.29676(13)	0.0516(7)	0.0527(18)	0.0375(15)	0.064(2)
C61	0.3302(3)	0.66491(15)	0.27529(18)	0.0700(10)	0.068(2)	0.0383(17)	0.103(3)
C62	0.2890(4)	0.65819(19)	0.2223(2)	0.0830(12)	0.086(3)	0.051(2)	0.110(3)
C63	0.2592(4)	0.71111(19)	0.19217(17)	0.0751(11)	0.079(3)	0.075(3)	0.070(2)
C64	0.2676(3)	0.77030(15)	0.21614(13)	0.0542(7)	0.0526(18)	0.0557(18)	0.052(19)
N1	0.0386(2)	1.07830(10)	0.22948(9)	0.0409(5)	0.0395(12)	0.0376(11)	0.046(14)
N2	-0.0899(2)	0.98585(10)	0.29498(10)	0.0431(5)	0.0354(12)	0.0393(12)	0.055(16)
N3	0.5189(2)	0.84794(9)	0.32956(9)	0.0383(5)	0.0341(12)	0.0336(11)	0.047(14)
N4	0.3051(2)	0.77826(10)	0.26775(9)	0.0405(5)	0.0371(12)	0.0345(11)	0.049(14)
O1	0.2807(17)	0.82891(9)	0.37648(7)	0.0434(4)	0.0344(10)	0.0523(11)	0.045(11)
O2	0.0800(19)	0.86290(12)	0.37797(8)	0.0644(6)	0.0393(12)	0.1068(18)	0.048(13)
O3	0.3532(17)	0.95386(8)	0.34391(8)	0.0471(5)	0.0414(10)	0.0368(10)	0.061(13)
O4	0.1846(16)	1.02003(8)	0.32444(8)	0.0417(4)	0.0317(9)	0.0417(10)	0.050(11)
O5	0.3760(18)	0.90686(9)	0.23449(8)	0.0469(5)	0.0478(11)	0.0432(10)	0.051(12)
O6	0.2449(18)	0.99029(9)	0.21690(8)	0.0495(5)	0.0471(11)	0.0495(11)	0.055(12)

O7	-0.007(19)	0.94553(8)	0.18709(7)	0.0480(5)	0.0587(12)	0.0385(10)	0.044(11)
O8	-0.0149(2)	0.84185(10)	0.20643(9)	0.0684(6)	0.0904(17)	0.0447(11)	0.063(14)
O9	0.1288(17)	0.89143(8)	0.28460(9)	0.0361(4)	0.0337(10)	0.0361(9)	0.037(11)

Atom label	X	Y	Z	Uiso	Uaniso-U11	Uaniso-U22	Uaniso-U33
Ni1	0.38649(12)	0.03440(15)	0.232131(8)	0.02791(6)	0.0215(10)	0.0300(11)	0.03144(10)
C1	0.37313(10)	0.20595(12)	0.14966(7)	0.0315(3)	0.0284(8)	0.0334(9)	0.0313(8)
C2	0.31878(10)	0.26849(12)	0.10456(7)	0.0333(3)	0.0295(8)	0.0335(9)	0.0348(8)
C3	0.34971(11)	0.31561(14)	0.06017(7)	0.0386(4)	0.0330(9)	0.0431(10)	0.0379(9)
C4	0.30087(14)	0.37954(16)	0.02254(9)	0.0543(5)	0.0550(13)	0.0573(13)	0.0475(11)
C5	0.21804(15)	0.39759(17)	0.02885(10)	0.0625(6)	0.0564(14)	0.0575(14)	0.0668(14)
C6	0.18524(13)	0.35264(17)	0.07219(10)	0.0589(6)	0.0377(11)	0.0671(15)	0.0687(14)
C7	0.23491(11)	0.28843(15)	0.10949(8)	0.0455(4)	0.0339(10)	0.0537(12)	0.0481(10)
C8	0.25941(12)	0.14671(15)	0.28872(9)	0.0470(4)	0.0351(10)	0.0537(12)	0.0520(11)
C9	0.22085(14)	0.18105(19)	0.33265(11)	0.0658(6)	0.0407(12)	0.0832(17)	0.0770(16)
C10	0.26366(16)	0.1739(2)	0.38819(11)	0.0705(7)	0.0636(15)	0.0931(19)	0.0625(14)
C11	0.34406(14)	0.13439(17)	0.39790(9)	0.0573(5)	0.0590(13)	0.0744(15)	0.0406(10)
C12	0.37831(12)	0.10165(14)	0.35200(8)	0.0423(4)	0.0395(10)	0.0462(11)	0.0415(9)
C13	0.23842(11)	-0.0477(14)	0.15143(8)	0.0433(4)	0.0364(9)	0.0420(11)	0.0495(10)
C14	0.16058(13)	-0.0913(16)	0.13227(10)	0.0561(5)	0.0424(11)	0.0523(13)	0.0669(13)
C15	0.11607(13)	-0.1309(16)	0.17153(11)	0.0626(6)	0.0353(11)	0.0469(13)	0.0995(18)
C16	0.15059(13)	-0.1269(16)	0.22847(11)	0.0596(6)	0.0446(12)	0.0477(13)	0.0881(17)
C17	0.22941(12)	-0.0827(14)	0.24490(9)	0.0479(5)	0.0415(11)	0.0436(11)	0.0582(12)
C18	0.49686(10)	-0.0966(12)	0.32048(7)	0.0322(3)	0.0324(8)	0.0339(9)	0.0309(8)
C19	0.50041(10)	-0.1954(12)	0.35046(7)	0.0345(4)	0.0305(8)	0.0365(9)	0.0380(8)
C20	0.54693(11)	-0.2131(14)	0.40477(7)	0.0405(4)	0.0396(10)	0.0470(11)	0.0373(9)
C21	0.55423(15)	-0.3057(18)	0.42949(10)	0.0605(6)	0.0608(14)	0.0657(15)	0.0570(13)
C22	0.51398(18)	-0.3838(18)	0.39913(13)	0.0778(8)	0.0878(19)	0.0451(14)	0.103(2)
C23	0.46761(17)	-0.3690(17)	0.34523(12)	0.0740(7)	0.0824(18)	0.0409(13)	0.098(2)
C24	0.46057(13)	-0.2758(14)	0.32115(9)	0.0510(5)	0.0516(12)	0.0413(11)	0.0587(12)
N1	0.33712(8)	0.1058(10)	0.29775(6)	0.0350(3)	0.0295(7)	0.0375(8)	0.0386(7)
N2	0.27275(8)	-0.0426(11)	0.20719(6)	0.0365(3)	0.0278(7)	0.0345(8)	0.0458(8)
N5	0.43640(10)	0.29595(14)	0.04940(6)	0.0477(4)	0.0412(9)	0.0665(12)	0.0343(8)
N7	0.58753(12)	-0.1308(14)	0.43965(6)	0.0513(4)	0.0561(11)	0.0675(12)	0.0306(8)
O1	0.33527(7)	0.13835(8)	0.17171(5)	0.0359(3)	0.0271(6)	0.0359(7)	0.0428(6)
O2	0.44981(7)	0.22883(10)	0.16351(5)	0.0465(3)	0.0283(6)	0.0561(8)	0.0505(7)
O3	0.45732(10)	0.21113(14)	0.04382(7)	0.0682(4)	0.0508(9)	0.0801(12)	0.0738(11)
O4	0.48176(10)	0.36768(14)	0.04465(7)	0.0749(5)	0.0585(10)	0.0929(13)	0.0771(11)
O5	0.42773(7)	-0.07866(9)	0.28789(5)	0.0384(3)	0.0294(6)	0.0386(7)	0.0451(7)
O6	0.43726(7)	-0.04465(9)	0.17055(5)	0.0380(3)	0.0320(6)	0.0419(7)	0.0384(6)
O7	0.54362(11)	-0.0608(13)	0.44767(7)	0.0687(4)	0.0825(12)	0.0689(11)	0.0566(9)
O8	0.66323(11)	-0.1392(15)	0.46017(7)	0.0796(5)	0.0600(11)	0.1115(15)	0.0601(10)
O9	0.5	0.11508(12)	0.25	0.0286(3)	0.0234(8)	0.0311(9)	0.0299(8)

Atom label	X	Y	Z	Uiso	Uaniso-U11	Uaniso-U22	Uaniso-U33
Ni1	0.1465(3)	0.5223(3)	0.2908(16)	0.045(11)	0.0464(3)	0.0428(2)	0.0443(2)

Ni2	0.3890(3)	0.4524(3)	0.3135(16)	0.044(11)	0.0427(2)	0.0402(2)	0.0471(2)
C1	0.1776(3)	0.6368(2)	0.4019(14)	0.0499(8)	0.053(2)	0.049(19)	0.047(19)
C2	0.1799(2)	0.7330(2)	0.4287(13)	0.0464(8)	0.047(2)	0.048(18)	0.044(18)
C5	0.1791(3)	0.9062(2)	0.4802(17)	0.062(10)	0.069(3)	0.048(2)	0.073(2)
C3	0.1459(3)	0.8094(2)	0.3957(14)	0.0585(9)	0.073(3)	0.052(2)	0.050(19)
C7	0.2159(3)	0.7446(2)	0.4884(15)	0.067(10)	0.084(3)	0.058(2)	0.056(2)
C4	0.1457(3)	0.8969(2)	0.4210(16)	0.064(10)	0.079(3)	0.048(2)	0.068(2)
C6	0.2152(3)	0.8318(3)	0.5142(16)	0.075(11)	0.094(3)	0.072(3)	0.055(2)
C22	0.0702(3)	0.5953(2)	0.1689(14)	0.0539(8)	0.052(2)	0.058(2)	0.050(19)
C25	-0.102(3)	0.6824(2)	0.1938(15)	0.0593(9)	0.048(2)	0.060(2)	0.069(2)
C26	-0.033(3)	0.6404(2)	0.2371(14)	0.0543(8)	0.053(2)	0.055(2)	0.054(2)
C23	0.0049(3)	0.6353(2)	0.1234(15)	0.0622(9)	0.068(3)	0.068(2)	0.047(19)
C24	-0.083(3)	0.6795(2)	0.1359(16)	0.0639(9)	0.056(2)	0.062(2)	0.068(2)
C36	0.5536(3)	0.4859(2)	0.4170(14)	0.0563(9)	0.058(2)	0.052(19)	0.056(2)
C35	0.6106(3)	0.5266(3)	0.4654(15)	0.069(10)	0.067(3)	0.082(3)	0.053(2)
C33	0.5001(4)	0.6570(3)	0.4494(18)	0.076(12)	0.094(3)	0.061(2)	0.075(3)
C32	0.4469(3)	0.6121(2)	0.4010(15)	0.0596(9)	0.069(3)	0.050(2)	0.060(2)
C34	0.5833(4)	0.6138(3)	0.4817(17)	0.081(13)	0.088(3)	0.101(3)	0.053(2)
C8	0.2275(3)	0.3713(2)	0.2190(13)	0.0448(7)	0.044(2)	0.041(17)	0.046(18)
C9	0.2034(2)	0.3070(2)	0.1667(12)	0.0414(7)	0.038(19)	0.043(17)	0.041(16)
C14	0.2595(3)	0.2277(2)	0.1619(15)	0.065(10)	0.064(2)	0.068(2)	0.060(2)
C12	0.1556(3)	0.1899(3)	0.0713(15)	0.063(10)	0.062(3)	0.070(2)	0.056(2)
C10	0.1228(3)	0.3264(2)	0.1225(14)	0.0581(9)	0.060(2)	0.053(2)	0.058(2)
C13	0.2351(3)	0.1679(3)	0.1148(17)	0.081(12)	0.083(3)	0.072(3)	0.081(3)
C11	0.0995(3)	0.2685(2)	0.0739(14)	0.0616(9)	0.058(2)	0.073(2)	0.048(19)
C15	0.3886(3)	0.2697(2)	0.3744(13)	0.0449(7)	0.046(2)	0.040(17)	0.044(17)
C18	0.4341(3)	0.0227(2)	0.4295(16)	0.068(10)	0.080(3)	0.049(2)	0.074(2)
C21	0.5278(3)	0.1517(2)	0.3651(14)	0.0547(8)	0.056(2)	0.047(19)	0.060(2)
C16	0.4379(2)	0.1756(2)	0.3873(13)	0.0452(7)	0.048(2)	0.038(17)	0.045(17)
C19	0.5227(3)	0.0004(2)	0.4056(15)	0.0612(9)	0.073(3)	0.044(2)	0.064(2)
C20	0.5700(3)	0.0638(2)	0.3738(15)	0.0591(9)	0.057(2)	0.052(2)	0.066(2)
C17	0.3912(3)	0.1108(2)	0.4201(14)	0.0578(9)	0.060(2)	0.050(2)	0.065(2)
C38	0.6589(3)	0.5284(3)	0.2327(17)	0.074(11)	0.058(3)	0.087(3)	0.078(3)
C37	0.5739(3)	0.5275(2)	0.2626(15)	0.0613(9)	0.061(2)	0.060(2)	0.061(2)
C41	0.5464(3)	0.3728(3)	0.2433(15)	0.0624(9)	0.055(2)	0.066(2)	0.066(2)
N3	0.4725(2)	0.527(17)	0.3844(11)	0.0487(6)	0.050(18)	0.044(15)	0.048(15)
N2	0.0161(2)	0.451(18)	0.3168(12)	0.0543(7)	0.049(18)	0.051(16)	0.059(17)
N4	0.5174(2)	0.451(18)	0.2681(11)	0.0501(6)	0.045(17)	0.051(16)	0.051(15)
N1	0.051(19)	0.595(16)	0.2253(10)	0.0460(6)	0.045(17)	0.046(14)	0.044(15)
C30	-0.098(4)	0.4155(3)	0.3867(2)	0.099(15)	0.101(4)	0.116(4)	0.087(3)
C29	-0.151(3)	0.3535(3)	0.3490(2)	0.092(14)	0.066(3)	0.092(3)	0.117(4)
C31	-0.015(3)	0.4634(3)	0.3696(17)	0.076(11)	0.081(3)	0.085(3)	0.063(2)
O1	0.135(17)	0.630(14)	0.34844(9)	0.0533(6)	0.062(16)	0.050(13)	0.043(12)
O2	0.216(19)	0.571(15)	0.43342(9)	0.0634(6)	0.087(19)	0.048(13)	0.050(13)
O3	0.154(16)	0.424(14)	0.22862(9)	0.0522(5)	0.048(14)	0.050(13)	0.054(13)
O4	0.315(18)	0.366(14)	0.24851(9)	0.0541(6)	0.047(15)	0.052(13)	0.057(13)
O5	0.442(15)	0.329(13)	0.35298(9)	0.0488(5)	0.041(13)	0.038(11)	0.063(13)
O6	0.297(18)	0.281(14)	0.3859(10)	0.0559(6)	0.046(15)	0.042(12)	0.078(15)
O7	0.251(17)	0.449(18)	0.3545(10)	0.0465(5)	0.049(14)	0.041(14)	0.045(13)
Cl2	0.5736(9)	-0.111(6)	0.41478(5)	0.0917(3)	0.1134(9)	0.0505(5)	0.1066(8)
Cl3	0.125(10)	0.1163(9)	0.01000(5)	0.1065(4)	0.112(10)	0.1173(9)	0.0842(7)
Cl1	0.174(10)	1.0148(7)	0.51376(5)	0.0988(4)	0.126(10)	0.0602(6)	0.1110(8)
C39	0.6874(3)	0.4472(4)	0.2075(18)	0.083(12)	0.062(3)	0.113(4)	0.078(3)

C40	0.6310(3)	0.3688(3)	0.2130(17)	0.078(11)	0.068(3)	0.085(3)	0.084(3)
C27	-0.036(3)	0.3896(3)	0.2807(17)	0.066(10)	0.055(3)	0.066(2)	0.076(2)
C28	-0.119(3)	0.3403(3)	0.2954(2)	0.078(11)	0.056(3)	0.075(3)	0.098(3)
C14	0.3096(7)	0.5915(5)	0.26439(4)	0.0565(2)	0.0577(6)	0.0524(5)	0.0573(5)

Atom label	X	Y	Z	Uiso	Uaniso-U11	Uaniso-U22	Uaniso-U33
Zn1	1	0.5	0	0.04261(13)	0.0549(3)	0.0316(3)	0.0455(3)
Zn2	0.97740(3)	0.80453(3)	0.082406(17)	0.04280(11)	0.0518(2)	0.0358(2)	0.0441(2)
Zn3	0.90077(3)	0.97903(3)	0.430512(17)	0.04724(12)	0.0529(2)	0.0508(2)	0.03635(19)
C1	0.8985(3)	0.7790(3)	0.50959(17)	0.0511(7)	0.067(2)	0.0456(18)	0.0422(17)
C2	0.8443(3)	0.6531(3)	0.51996(17)	0.0546(8)	0.076(2)	0.0454(18)	0.0436(17)
C3	0.7203(4)	0.5941(4)	0.4849(2)	0.0715(10)	0.082(3)	0.066(2)	0.064(2)
C4	0.6725(5)	0.4748(4)	0.4923(3)	0.0944(14)	0.103(4)	0.078(3)	0.097(3)
C5	0.7512(7)	0.4157(5)	0.5347(3)	0.1085(17)	0.160(5)	0.063(3)	0.118(4)
C6	0.8756(6)	0.4728(5)	0.5706(3)	0.1028(16)	0.148(5)	0.069(3)	0.113(4)
C7	0.9221(4)	0.5920(4)	0.5643(2)	0.0741(10)	0.097(3)	0.060(2)	0.074(2)
C8	1.1460(3)	0.9051(3)	0.41711(17)	0.0496(7)	0.063(2)	0.0401(17)	0.0470(18)
C9	1.2433(3)	0.8591(3)	0.37650(16)	0.0482(7)	0.059(2)	0.0386(16)	0.0502(17)
C10	1.3729(3)	0.8769(4)	0.4139(2)	0.0673(9)	0.059(2)	0.067(2)	0.071(2)
C11	1.4634(4)	0.8308(5)	0.3773(3)	0.0891(13)	0.058(3)	0.099(3)	0.118(4)
C12	1.4228(5)	0.7660(5)	0.3039(3)	0.0918(14)	0.098(4)	0.091(3)	0.112(4)
C13	1.2970(5)	0.7488(4)	0.2665(2)	0.0807(12)	0.111(4)	0.073(3)	0.071(3)
C14	1.2063(4)	0.7947(3)	0.30235(18)	0.0602(8)	0.077(2)	0.053(2)	0.0536(19)
C15	0.7348(4)	0.9083(4)	0.27638(19)	0.0705(10)	0.081(3)	0.062(2)	0.053(2)
C16	0.6504(5)	0.9244(5)	0.2148(2)	0.0977(15)	0.101(4)	0.117(4)	0.046(2)
C17	0.5953(5)	1.0290(7)	0.2209(3)	0.1122(19)	0.100(4)	0.145(5)	0.080(3)
C18	0.6216(5)	1.1132(5)	0.2871(3)	0.1026(16)	0.096(3)	0.096(4)	0.114(4)
C19	0.7067(4)	1.0924(4)	0.3462(2)	0.0705(10)	0.072(2)	0.070(3)	0.064(2)
C20	1.2000(3)	0.7609(3)	0.06306(16)	0.0508(7)	0.0523(19)	0.053(2)	0.0403(16)
C21	1.3312(3)	0.7482(3)	0.05170(15)	0.0448(7)	0.0438(17)	0.0407(16)	0.0444(16)
C22	1.3871(4)	0.6478(3)	0.06966(19)	0.0628(9)	0.071(2)	0.051(2)	0.060(2)
C23	1.5077(5)	0.6349(5)	0.0592(3)	0.0936(15)	0.073(3)	0.096(4)	0.095(3)
C24	1.5705(5)	0.7166(7)	0.0287(3)	0.110(2)	0.050(3)	0.151(6)	0.096(4)
C25	1.5187(5)	0.8164(6)	0.0102(3)	0.0986(16)	0.073(3)	0.122(4)	0.084(3)
C26	1.3972(3)	0.8338(3)	0.02285(19)	0.0663(9)	0.063(2)	0.062(2)	0.070(2)
C27	0.9861(3)	1.0148(3)	0.21261(17)	0.0520(7)	0.066(2)	0.0490(19)	0.0468(17)
C28	0.9760(3)	1.1314(3)	0.25104(17)	0.0568(8)	0.076(2)	0.051(2)	0.0432(17)
C29	0.9283(3)	1.2149(3)	0.21155(19)	0.0627(9)	0.082(3)	0.0403(18)	0.069(2)
C30	0.8929(3)	1.1772(3)	0.13446(19)	0.0620(9)	0.080(2)	0.049(2)	0.066(2)
C31	0.9065(3)	1.0591(3)	0.09983(17)	0.0507(7)	0.062(2)	0.0464(18)	0.0476(17)
C32	0.8700(3)	0.5895(3)	0.12828(15)	0.0414(6)	0.0431(16)	0.0433(17)	0.0395(15)
C33	0.8013(3)	0.5370(3)	0.17983(15)	0.0423(6)	0.0527(18)	0.0364(15)	0.0425(15)
C34	0.7015(3)	0.4347(3)	0.15229(17)	0.0525(7)	0.065(2)	0.0422(17)	0.0484(17)
C35	0.6299(4)	0.3929(4)	0.1982(2)	0.0764(11)	0.086(3)	0.061(2)	0.079(3)
C36	0.6624(5)	0.4514(4)	0.2733(2)	0.0978(16)	0.135(4)	0.085(3)	0.073(3)
C37	0.7641(5)	0.5488(4)	0.3012(2)	0.0953(16)	0.136(4)	0.090(3)	0.048(2)
C38	0.8325(4)	0.5938(3)	0.25494(17)	0.0639(9)	0.083(3)	0.055(2)	0.0453(18)
C39	0.8569(3)	0.6954(3)	-0.07142(17)	0.0476(7)	0.0512(18)	0.0453(18)	0.0506(18)
C40	0.7872(3)	0.7081(3)	-0.14669(16)	0.0499(7)	0.0461(18)	0.0546(19)	0.0476(17)
C41	0.7535(3)	0.8223(4)	-0.1558(2)	0.0602(9)	0.0463(19)	0.071(2)	0.066(2)

C42	0.6997(4)	0.8362(5)	-0.2266(3)	0.0893(14)	0.063(3)	0.120(4)	0.092(3)
C43	0.6778(5)	0.7360(7)	-0.2861(3)	0.1088(19)	0.074(3)	0.176(6)	0.070(3)
C44	0.7084(5)	0.6236(6)	-0.2783(2)	0.1061(17)	0.094(4)	0.144(5)	0.053(3)
C45	0.7654(4)	0.6083(4)	-0.2081(2)	0.0783(11)	0.083(3)	0.079(3)	0.059(2)
N1	0.7631(2)	0.9916(2)	0.34198(13)	0.0489(6)	0.0537(15)	0.0492(15)	0.0410(13)
N2	0.9528(2)	0.9768(2)	0.13766(13)	0.0440(6)	0.0539(15)	0.0376(13)	0.0441(13)
O1	0.8415(2)	0.8105(2)	0.45232(12)	0.0654(6)	0.0825(17)	0.0540(14)	0.0527(13)
O2	1.0339(2)	0.9044(2)	0.37966(12)	0.0621(6)	0.0605(15)	0.0685(16)	0.0595(14)
O3	1.0052(2)	1.1564(2)	0.44266(12)	0.0625(6)	0.0715(16)	0.0518(14)	0.0555(13)
O4	0.8177(2)	1.0589(2)	0.51348(12)	0.0672(6)	0.0767(17)	0.0824(18)	0.0449(13)
O5	1.1639(2)	0.8648(2)	0.06701(15)	0.0757(7)	0.0720(17)	0.0685(17)	0.0897(18)
O6	1.1257(2)	0.6682(2)	0.06904(13)	0.0717(7)	0.0680(16)	0.0780(18)	0.0567(14)
O7	0.9161(2)	0.7069(19)	0.14833(11)	0.0518(5)	0.0722(14)	0.0374(12)	0.0528(12)
O8	0.8739(2)	0.5168(2)	0.06919(12)	0.0624(6)	0.0692(15)	0.0598(15)	0.0532(13)
O9	0.8655(2)	0.7853(2)	-0.01618(11)	0.0549(5)	0.0621(14)	0.0545(14)	0.0454(12)
O10	0.9042(3)	0.5982(2)	-0.06948(13)	0.0786(8)	0.121(2)	0.0655(17)	0.0614(15)

Table 46:- 4.2

Atom label	X	Y	Z	Uiso	Uaniso-U11	Uaniso-U22	Uaniso-U33
Zn1	0.10734(2)	0.444172(18)	0.058528(11)	0.03572(9)	0.0431(13)	0.03507(13)	0.0286(13)
C1	0.1350(2)	0.42549(17)	-0.10630(12)	0.0443(4)	0.0559(11)	0.0369(9)	0.0440(12)
C2	0.2051(2)	0.37856(17)	-0.17121(11)	0.0429(4)	0.0539(11)	0.0387(9)	0.0390(10)
C3	0.3203(2)	0.3061(2)	-0.15568(13)	0.0534(5)	0.0601(12)	0.0611(13)	0.0407(11)
C4	0.3788(3)	0.2578(3)	-0.21624(15)	0.0650(6)	0.0671(14)	0.0741(16)	0.0574(14)
C5	0.3240(3)	0.2820(3)	-0.29223(14)	0.0692(7)	0.0782(16)	0.0871(18)	0.0475(14)
C6	0.2104(3)	0.3554(3)	-0.30831(14)	0.0728(7)	0.0805(16)	0.104(2)	0.0355(12)
C7	0.1509(2)	0.4036(2)	-0.24801(13)	0.0607(6)	0.0649(13)	0.0753(15)	0.0451(13)
C8	0.1238(2)	0.71519(17)	0.00666(11)	0.0414(4)	0.0542(11)	0.0358(9)	0.0367(10)
C9	0.1982(2)	0.83910(18)	0.01364(11)	0.0441(4)	0.0568(11)	0.0383(9)	0.0392(10)
C10	0.3241(3)	0.8482(3)	0.05952(16)	0.0750(8)	0.0854(17)	0.0600(14)	0.0711(17)
C11	0.3897(4)	0.9631(3)	0.0692(2)	0.0978(12)	0.107(2)	0.084(2)	0.089(2)
C12	0.3297(4)	1.0704(3)	0.0334(2)	0.0840(9)	0.107(2)	0.0539(15)	0.093(2)
C13	0.2084(3)	1.0617(2)	-0.01353(19)	0.0713(8)	0.0845(18)	0.0381(11)	0.097(2)
C14	0.1427(2)	0.94566(18)	-0.02416(15)	0.0544(5)	0.0567(12)	0.0407(11)	0.0685(16)
C15	0.2249(3)	0.2948(3)	0.19584(18)	0.0898(10)	0.0737(17)	0.118(3)	0.0767(19)
C16	0.3117(4)	0.2623(5)	0.2625(2)	0.1186(15)	0.121(3)	0.155(4)	0.076(2)
C17	0.4257(5)	0.3287(4)	0.2815(2)	0.1221(16)	0.134(3)	0.117(3)	0.093(3)
C18	0.4572(5)	0.4168(4)	0.2328(3)	0.148(2)	0.124(3)	0.088(3)	0.193(5)
C19	0.3660(3)	0.4441(3)	0.1659(3)	0.1033(13)	0.0741(19)	0.075(2)	0.143(3)
N1	0.25091(17)	0.38700(17)	0.14809(10)	0.0478(4)	0.0516(9)	0.0489(9)	0.0409(9)
O1	0.18784(16)	0.39817(16)	-0.03761(9)	0.0571(4)	0.0707(10)	0.0659(9)	0.0387(8)
O2	0.02765(16)	0.48553(17)	-0.12522(9)	0.0602(4)	0.0637(9)	0.0701(10)	0.0504(9)
O3	0.17485(17)	0.62567(13)	0.04907(9)	0.0575(4)	0.0748(10)	0.0391(7)	0.0542(9)
O4	-0.0153(14)	0.28992(13)	0.04003(9)	0.0524(3)	0.0541(8)	0.0437(7)	0.0577(9)

Table 47:- 4.3

Atom label	X	Y	Z	Uiso	Uaniso-U11	Uaniso-U22	Uaniso-U33
Zn1	0.0051(16)	0.39838(15)	-0.04986(9)	0.03910(7)	0.0464(11)	0.0398(11)	0.0336(11)

O1	0.149(13)	0.33198(13)	0.05206(7)	0.0608(3)	0.0628(7)	0.0683(8)	0.0417(7)
O2	0.142(14)	0.48791(12)	0.12625(8)	0.0641(3)	0.0724(8)	0.0617(8)	0.0519(7)
O3	-0.142(13)	0.32841(12)	-0.02050(8)	0.0618(3)	0.0646(7)	0.0649(8)	0.0703(8)
O4	0.1476(13)	0.51795(12)	-0.05556(8)	0.0636(3)	0.0717(8)	0.0603(8)	0.0700(8)
N1	0.0072(15)	0.27548(13)	-0.13040(8)	0.0491(3)	0.0652(8)	0.0468(7)	0.0398(7)
C1	0.1849(15)	0.38572(15)	0.11608(10)	0.0452(4)	0.0403(7)	0.0536(9)	0.0423(9)
C2	0.2898(16)	0.32536(17)	0.18773(9)	0.0509(4)	0.0439(8)	0.0650(11)	0.0420(9)
C3	0.2879(2)	0.2000(2)	0.20168(12)	0.0672(5)	0.0725(12)	0.0674(12)	0.0583(11)
C4	0.1810(4)	0.1159(2)	0.1483(2)	0.1086(11)	0.127(2)	0.0612(15)	0.111(2)
C5	0.3897(3)	0.1548(3)	0.27116(17)	0.1017(9)	0.118(2)	0.0952(19)	0.0809(18)
C6	0.4889(3)	0.2281(4)	0.32253(18)	0.1259(13)	0.113(2)	0.159(3)	0.0637(17)
C7	0.4894(3)	0.3502(4)	0.30828(17)	0.1137(11)	0.0774(17)	0.154(3)	0.0677(17)
C8	0.3890(2)	0.3998(2)	-0.24106(13)	-0.0764(6)	0.0581(11)	0.0950(17)	0.0595(13)
C9	-0.18642(16)	0.37970(15)	0.02401(10)	-0.0455(4)	0.0416(7)	0.0530(9)	0.0398(8)
C10	-0.29525(15)	0.31649(16)	0.04182(9)	0.0486(4)	0.0435(7)	0.0604(10)	0.0403(8)
C11	-0.30983(19)	0.18914(19)	0.04152(12)	0.0626(5)	0.0617(10)	0.0635(11)	0.0607(11)
C12	-0.2218(3)	0.1007(2)	0.0220(2)	0.0905(8)	0.0943(18)	0.0586(13)	0.120(2)
C13	-0.4140(3)	0.1436(3)	0.06160(17)	0.0911(8)	0.0966(18)	0.0840(16)	0.0992(18)
C14	-0.5003(3)	0.2187(3)	0.07796(19)	0.1046(10)	0.0911(17)	0.129(3)	0.122(2)
C16	-0.3836(2)	0.3907(2)	0.05967(14)	0.0671(5)	0.0586(10)	0.0782(14)	0.0732(13)
C15	-0.4873(3)	0.3427(3)	0.07629(18)	0.0935(8)	0.0773(15)	0.115(2)	0.113(2)
C17	0.1237(3)	0.2287(2)	-0.1265(15)	0.0800(6)	0.0947(15)	0.0831(15)	0.0815(15)
C18	0.1263(5)	0.1499(3)	-0.1836(2)	0.1237(13)	0.202(4)	0.097(2)	0.135(3)
C21	-0.1081(3)	0.2460(2)	-0.1903(12)	0.0814(6)	0.0973(16)	0.0817(15)	0.0535(12)
C19	0.0102(6)	0.1207(3)	-0.2447(2)	0.141(2)	0.299(6)	0.0758(19)	0.101(3)
C20	-0.1092(5)	0.1685(3)	-0.2489(15)	0.1233(13)	0.204(4)	0.101(2)	0.0532(15)

Table 48:- 4.4

Atom label	X	Y	Z	Uiso	Uaniso-U11	Uaniso-U22	Uaniso-U33
Zn1	0	0	0.06032(10)	0.03905(10)	0.0439(16)	0.0441(17)	0.0298(15)
O1	0.0997(15)	0.12401(15)	0.04057(7)	0.0581(5)	0.0666(11)	0.0599(10)	0.0477(12)
O2	0.1027(14)	0.12815(15)	-0.04953(7)	0.0585(5)	0.0693(11)	0.0591(10)	0.0472(12)
N1	0	0	0.14275(8)	0.0402(4)	0.0406(11)	0.0470(11)	0.0329(11)
C1	0.1258(14)	0.16521(15)	-0.0037(10)	0.0432(4)	0.0395(9)	0.0449(9)	0.0451(12)
C2	0.1896(15)	0.26786(14)	-0.00205(9)	0.0389(4)	0.0358(8)	0.0420(9)	0.0388(10)
C3	0.2220(16)	0.31054(17)	0.04750(9)	0.0440(5)	0.0465(11)	0.0471(11)	0.0385(12)
C4	0.2754(16)	0.40833(18)	0.05118(10)	0.0473(5)	0.0417(11)	0.0498(11)	0.0505(13)
C5	0.3106(2)	0.4519(2)	-0.10509(10)	0.0722(8)	0.0804(17)	0.0745(17)	0.0616(17)
C6	0.2942(17)	0.46415(17)	0.00348(10)	0.0561(5)	0.0548(12)	0.0455(10)	0.0680(16)
C7	0.2637(19)	0.4221(2)	-0.0457(11)	0.0574(6)	0.0566(13)	0.0605(14)	0.0552(15)
C8	0.2124(17)	0.32430(18)	-0.04888(9)	0.0478(5)	0.0458(11)	0.0596(13)	0.0379(12)
C9	0.0380(17)	-0.08402(18)	0.17082(10)	0.0497(5)	0.0536(12)	0.0484(11)	0.0471(13)
C10	0.0394(2)	-0.0865(2)	0.22646(10)	0.0610(6)	0.0618(14)	0.0759(16)	0.0452(14)
C11	0	0	0.25495(11)	0.0597(7)	0.0566(16)	0.088(2)	0.0343(14)

Table 49:- 4.5

Atom label	X	Y	Z	Uiso	Uaniso-U11	Uaniso-U22	Uaniso-U33
Zn1	0.01115(2)	0.26037(5)	0.33853(14)	0.03904(14)	0.0353(3)	0.0394(3)	0.0425(3)

Zn6	0.13306(2)	0.76155(5)	0.55068(14)	0.03988(15)	0.0376(3)	0.0380(3)	0.0439(3)
Zn8	0.16985(2)	0.52048(5)	0.58592(15)	0.04165(15)	0.0413(3)	0.0323(3)	0.0514(4)
Zn4	0.09584(2)	0.48529(5)	0.33045(15)	0.04066(14)	0.0400(3)	0.0315(3)	0.0505(4)
Zn3	0.11777(2)	0.24885(5)	0.29133(14)	0.04111(15)	0.0401(3)	0.0402(4)	0.0430(3)
Zn5	0.25483(2)	0.74539(4)	0.57945(14)	0.03831(14)	0.0333(3)	0.0390(3)	0.0426(3)
Zn2	0.13438(3)	0.24378(5)	0.36527(14)	0.04102(15)	0.0388(3)	0.0381(3)	0.0462(4)
Zn7	0.14669(3)	0.75153(5)	0.62568(15)	0.04374(15)	0.0423(4)	0.0462(4)	0.0427(3)
O2	0.12337(16)	0.5043(3)	0.37873(9)	0.0522(10)	0.060(2)	0.051(2)	0.046(2)
O3	0.16985(16)	0.3458(3)	0.39609(9)	0.0576(10)	0.065(3)	0.044(2)	0.064(3)
O12	0.01247(15)	0.5355(3)	0.34146(9)	0.0516(10)	0.039(2)	0.044(2)	0.072(3)
O6	0.12134(16)	0.3451(3)	0.25266(8)	0.0551(10)	0.080(3)	0.040(2)	0.046(2)
O5	0.18125(16)	0.1386(4)	0.29436(10)	0.0617(11)	0.053(2)	0.066(3)	0.066(3)
O13	-0.0445(16)	0.3809(3)	0.34638(10)	0.0643(11)	0.044(2)	0.045(2)	0.105(3)
O7	0.07622(17)	0.4920(3)	0.27690(9)	0.0600(11)	0.067(3)	0.065(3)	0.048(2)
O4	0.19372(17)	0.1395(3)	0.34830(10)	0.0625(11)	0.057(3)	0.064(3)	0.067(3)
C1	0.1563(2)	0.4542(5)	0.39806(13)	0.0462(12)	0.043(3)	0.052(3)	0.043(3)
C2	0.1833(2)	0.5222(5)	0.42546(13)	0.0480(11)	0.051(3)	0.053(2)	0.040(3)
C4	0.2410(3)	0.5118(7)	0.47380(16)	0.0829(17)	0.090(4)	0.096(3)	0.063(3)
C5	0.2378(3)	0.6324(7)	0.47653(18)	0.094(2)	0.101(5)	0.100(3)	0.082(4)
C3	0.2141(3)	0.4593(5)	0.44772(14)	0.0613(13)	0.065(4)	0.068(3)	0.052(3)
C7	0.1781(3)	0.6448(5)	0.42846(14)	0.0615(13)	0.075(4)	0.056(2)	0.054(3)
C8	0.1448(3)	0.7250(5)	0.40710(18)	0.085(2)	0.129(6)	0.054(3)	0.072(4)
C6	0.2071(3)	0.6976(6)	0.45473(17)	0.0833(17)	0.103(5)	0.070(3)	0.077(4)
C17	0.0982(2)	0.4462(5)	0.25277(14)	0.0482(12)	0.055(3)	0.042(3)	0.048(3)
C18	0.1012(2)	0.5118(4)	0.22087(13)	0.0504(11)	0.062(3)	0.039(3)	0.051(2)
C21	0.1189(3)	0.6294(7)	0.16255(18)	0.0915(19)	0.112(5)	0.083(4)	0.079(4)
C23	0.0621(3)	0.5962(5)	0.21102(16)	0.0679(14)	0.080(3)	0.054(3)	0.070(3)
C22	0.0731(3)	0.6558(6)	0.18090(17)	0.0848(17)	0.111(4)	0.067(4)	0.076(4)
C19	0.1472(3)	0.4842(5)	0.20068(14)	0.0632(13)	0.074(3)	0.061(3)	0.055(3)
C33	0.0409(3)	0.1023(5)	0.39257(13)	0.0468(12)	0.057(3)	0.038(3)	0.045(3)
C34	0.0220(3)	0.0111(5)	0.41666(15)	0.0598(12)	0.070(3)	0.049(3)	0.060(3)
C35	0.0604(3)	-0.0269(5)	0.43912(15)	0.0721(15)	0.095(3)	0.057(3)	0.064(4)
C36	0.0466(4)	-0.1088(7)	0.46230(19)	0.104(2)	0.131(5)	0.085(5)	0.095(4)
O8	0.00456(17)	0.1546(4)	0.37588(10)	0.0686(12)	0.054(3)	0.079(3)	0.073(3)
O9	0.09230(17)	0.1234(3)	0.39047(10)	0.0612(11)	0.052(3)	0.062(3)	0.070(3)
O11	0.05998(17)	0.1291(3)	0.27463(10)	0.0633(11)	0.046(3)	0.063(3)	0.081(3)
O10	-0.0166(17)	0.1627(4)	0.30312(10)	0.0798(14)	0.052(3)	0.117(4)	0.071(3)
C41	0.0094(3)	0.1179(5)	0.27983(14)	0.0465(12)	0.048(3)	0.042(3)	0.049(3)
C42	-0.0250(2)	0.0400(5)	0.25802(13)	0.0502(11)	0.044(3)	0.054(3)	0.052(2)
C43	-0.0497(3)	-0.0603(5)	0.27143(17)	0.0664(14)	0.065(4)	0.061(3)	0.074(3)
O15	0.11469(15)	0.6627(3)	0.32364(9)	0.0500(10)	0.046(2)	0.0332(19)	0.071(3)
C9	0.2056(2)	0.1043(5)	0.32014(15)	0.0468(13)	0.031(3)	0.042(3)	0.068(4)
C10	0.2526(2)	0.0153(5)	0.31595(15)	0.0509(11)	0.031(2)	0.037(3)	0.084(3)
O1	0.08735(13)	0.3088(3)	0.33166(8)	0.0357(8)	0.0394(19)	0.0282(16)	0.039(2)
O21	0.09629(16)	0.6628(3)	0.51957(9)	0.0541(10)	0.064(3)	0.041(2)	0.057(2)
O22	0.13925(17)	0.5018(3)	0.53850(9)	0.0561(10)	0.074(3)	0.050(2)	0.044(2)
C70	0.0804(2)	0.4828(5)	0.49173(13)	0.0477(11)	0.050(3)	0.050(2)	0.043(3)
C69	0.1080(2)	0.5528(5)	0.51893(13)	0.0443(12)	0.045(3)	0.050(3)	0.038(3)
C75	0.0836(3)	0.3616(5)	0.48928(15)	0.0625(14)	0.075(4)	0.054(2)	0.059(3)
C72	0.0253(3)	0.4927(7)	0.44308(16)	0.0811(17)	0.091(4)	0.091(3)	0.062(4)
C73	0.0267(3)	0.3741(7)	0.44086(18)	0.0916(19)	0.109(5)	0.093(3)	0.073(4)
C71	0.0517(3)	0.5473(5)	0.46851(14)	0.0607(14)	0.069(4)	0.066(3)	0.047(3)
O17	0.14384(17)	0.6541(4)	0.66454(9)	0.0591(11)	0.069(3)	0.056(3)	0.052(2)

O18	0.19389(18)	0.5176(4)	0.63815(9)	0.0651(11)	0.066(3)	0.084(3)	0.045(2)
C53	0.1714(2)	0.5566(6)	0.66322(14)	0.0510(13)	0.044(3)	0.060(3)	0.049(3)
C54	0.1757(2)	0.4836(5)	0.69387(14)	0.0549(12)	0.056(3)	0.058(3)	0.051(2)
C55	0.2089(3)	0.3844(5)	0.69212(15)	0.0646(13)	0.060(3)	0.062(3)	0.072(3)
C58	0.1573(3)	0.4332(6)	0.75004(15)	0.0744(15)	0.079(4)	0.088(4)	0.056(3)
C59	0.1492(3)	0.5102(5)	0.72308(14)	0.0640(13)	0.070(4)	0.068(3)	0.053(2)
C56	0.2164(3)	0.3091(6)	0.71883(17)	0.0774(16)	0.075(4)	0.069(3)	0.088(4)
O25	0.28115(17)	0.8429(4)	0.61533(10)	0.0718(13)	0.045(3)	0.095(3)	0.075(3)
O26	0.20219(17)	0.8759(3)	0.64170(10)	0.0638(11)	0.046(3)	0.068(3)	0.077(3)
C85	0.2533(3)	0.8894(5)	0.63753(14)	0.0462(13)	0.047(3)	0.042(3)	0.049(3)
C86	0.2847(2)	0.9733(5)	0.65958(13)	0.0493(11)	0.046(3)	0.048(2)	0.053(2)
C91	0.2919(3)	0.9452(5)	0.69240(14)	0.0621(13)	0.071(4)	0.063(3)	0.052(2)
C87	0.3066(3)	1.0752(5)	0.64658(16)	0.0661(15)	0.070(4)	0.056(3)	0.072(3)
C92	0.2701(4)	0.8350(6)	0.70715(16)	0.098(2)	0.148(7)	0.090(5)	0.056(4)
C90	0.3232(3)	1.0279(6)	0.71123(17)	0.0777(16)	0.083(4)	0.086(4)	0.065(3)
O16	0.17830(13)	0.6966(3)	0.58503(8)	0.0361(7)	0.0347(19)	0.0330(17)	0.0407(19)
O20	0.07423(18)	0.8640(4)	0.56803(11)	0.0687(12)	0.067(3)	0.076(3)	0.063(3)
O19	0.08074(15)	0.8575(3)	0.62153(10)	0.0554(10)	0.045(2)	0.055(2)	0.066(3)
O24	0.31016(15)	0.6220(3)	0.57230(10)	0.0604(11)	0.038(2)	0.049(2)	0.094(3)
O23	0.25147(17)	0.4684(3)	0.57413(10)	0.0557(11)	0.044(2)	0.045(2)	0.078(3)
O28	0.17629(17)	0.8801(3)	0.52555(10)	0.0599(11)	0.049(3)	0.060(3)	0.071(3)
O27	0.26339(17)	0.8517(4)	0.54195(10)	0.0690(12)	0.053(3)	0.080(3)	0.074(3)
C61	0.0594(2)	0.8937(5)	0.59574(17)	0.0504(13)	0.037(3)	0.038(3)	0.076(4)
C62	0.0106(2)	0.9797(5)	0.59846(16)	0.0561(12)	0.035(3)	0.039(3)	0.094(3)
C93	0.2278(3)	0.9012(5)	0.52479(13)	0.0450(12)	0.057(3)	0.042(3)	0.037(3)
C77	0.2984(2)	0.5141(5)	0.56975(13)	0.0491(13)	0.046(3)	0.055(3)	0.046(3)
O30	0.14638(15)	0.3463(3)	0.59307(9)	0.0546(10)	0.055(2)	0.038(2)	0.071(3)
C63	-0.0172(2)	0.9856(6)	0.62828(19)	0.0763(14)	0.048(3)	0.071(4)	0.110(3)
C65	-0.0819(3)	1.1220(7)	0.6061(3)	0.105(2)	0.051(4)	0.086(4)	0.179(6)
C66	-0.0548(3)	1.1205(6)	0.5776(2)	0.0928(18)	0.064(4)	0.059(4)	0.156(5)
C78	0.3467(2)	0.4312(5)	0.56275(14)	0.0548(12)	0.045(3)	0.052(3)	0.068(3)
C83	0.3898(3)	0.4598(5)	0.54055(15)	0.0638(14)	0.052(3)	0.067(3)	0.073(4)
C84	0.3916(3)	0.5739(6)	0.52091(18)	0.087(2)	0.084(5)	0.083(4)	0.095(5)
O29	0.08423(15)	0.5728(3)	0.60211(9)	0.0544(10)	0.043(2)	0.056(2)	0.064(3)
S3	0.04648(7)	0.4989(15)	0.62310(4)	0.0679(4)	0.0591(10)	0.0671(10)	0.0776(11)
O14	0.18132(15)	0.4310(3)	0.31667(9)	0.0517(10)	0.042(2)	0.046(2)	0.067(3)
S1	0.23821(6)	0.4869(14)	0.31040(4)	0.0576(4)	0.0387(8)	0.0638(9)	0.0704(10)
C16	0.2531(3)	-0.0448(6)	0.37662(19)	0.094(2)	0.099(5)	0.084(5)	0.100(3)
C15	0.2743(3)	-0.0487(5)	0.34216(18)	0.0655(13)	0.051(3)	0.043(3)	0.103(3)
C13	0.3409(3)	-0.1352(6)	0.3043(2)	0.0882(18)	0.049(4)	0.060(4)	0.156(5)
C11	0.2754(2)	0.0031(5)	0.28546(17)	0.0680(14)	0.049(3)	0.061(4)	0.094(3)
C12	0.3196(3)	-0.0726(6)	0.2794(2)	0.0855(17)	0.052(4)	0.078(4)	0.126(4)
C82	0.4331(3)	0.3765(6)	0.53597(19)	0.0862(18)	0.065(4)	0.089(4)	0.105(5)
C80	0.3930(3)	0.2460(6)	0.5747(2)	0.102(2)	0.092(5)	0.077(4)	0.138(6)
C81	0.4337(3)	0.2732(7)	0.5530(2)	0.101(2)	0.080(4)	0.087(4)	0.137(6)
C79	0.3491(3)	0.3265(5)	0.57959(19)	0.0792(17)	0.069(4)	0.062(3)	0.107(4)
C89	0.3437(3)	1.1298(6)	0.69770(18)	0.0826(17)	0.079(4)	0.077(3)	0.091(3)
C88	0.3347(3)	1.1554(6)	0.66580(18)	0.0820(17)	0.089(4)	0.060(3)	0.097(4)
C39	-0.0316(3)	-0.0372(7)	0.4157(2)	0.104(2)	0.073(3)	0.106(5)	0.133(5)
C40	-0.0773(4)	0.0028(10)	0.3921(3)	0.162(4)	0.076(5)	0.196(9)	0.213(10)
S2	0.07287(6)	0.7511(12)	0.31075(4)	0.0529(4)	0.0559(9)	0.0385(8)	0.0644(9)
C51	0.1115(3)	0.8334(6)	0.28086(19)	0.097(3)	0.093(6)	0.071(5)	0.126(7)
C49	0.2289(3)	0.5881(6)	0.27727(16)	0.0764(19)	0.063(4)	0.086(5)	0.080(5)

C50	0.2481(3)	0.5936(5)	0.34180(17)	0.082(2)	0.067(4)	0.081(4)	0.099(6)
S4	0.18502(7)	0.2526(12)	0.60716(4)	0.0586(4)	0.0722(11)	0.0383(8)	0.0654(10)
C104	0.1962(4)	0.1508(7)	0.5752(2)	0.123(4)	0.166(9)	0.091(5)	0.112(7)
C94	0.2464(3)	0.9908(5)	0.50069(15)	0.0606(13)	0.072(3)	0.051(3)	0.059(3)
C57	0.1906(3)	0.3358(6)	0.74694(17)	0.0802(16)	0.082(4)	0.083(4)	0.075(3)
C76	0.1175(4)	0.2843(6)	0.51147(18)	0.090(2)	0.126(7)	0.051(3)	0.091(5)
C74	0.0544(3)	0.3109(6)	0.46282(17)	0.0850(17)	0.105(5)	0.068(3)	0.082(4)
C31	-0.1236(2)	0.5452(5)	0.37747(15)	0.0581(12)	0.041(3)	0.069(3)	0.064(3)
C25	-0.0341(2)	0.4899(5)	0.34679(13)	0.0461(12)	0.040(3)	0.047(3)	0.052(3)
C26	-0.0834(2)	0.5705(5)	0.35401(15)	0.0525(12)	0.038(3)	0.052(3)	0.068(3)
C27	-0.0881(2)	0.6730(5)	0.33506(17)	0.0670(14)	0.052(3)	0.056(3)	0.093(4)
C32	-0.1220(3)	0.4402(6)	0.39928(17)	0.0830(19)	0.065(4)	0.103(5)	0.082(5)
C48	-0.0061(3)	0.1712(6)	0.21061(17)	0.091(2)	0.093(5)	0.101(5)	0.080(4)
C46	-0.0674(3)	-0.0096(7)	0.20726(17)	0.0902(18)	0.098(5)	0.114(5)	0.059(3)
C47	-0.0326(3)	0.0666(6)	0.22601(15)	0.0657(14)	0.056(3)	0.089(3)	0.052(2)
C20	0.1553(3)	0.5442(6)	0.17158(16)	0.0804(17)	0.088(4)	0.091(4)	0.063(3)
C96	0.2212(4)	1.1194(7)	0.4560(2)	0.106(2)	0.127(5)	0.089(5)	0.104(5)
C95	0.2076(3)	1.0359(5)	0.47928(16)	0.0754(16)	0.093(3)	0.059(4)	0.074(4)
C97	0.2736(5)	1.1573(9)	0.4543(2)	0.138(3)	0.133(5)	0.134(6)	0.148(6)
C24	0.0095(3)	0.6229(6)	0.22952(17)	0.095(2)	0.093(5)	0.098(5)	0.093(5)
C28	-0.1320(3)	0.7486(5)	0.3388(2)	0.0788(16)	0.063(4)	0.066(3)	0.107(4)
C30	-0.1681(3)	0.6255(6)	0.38054(17)	0.0726(15)	0.049(3)	0.083(4)	0.085(4)
C64	-0.0640(3)	1.0572(7)	0.6315(2)	0.0982(19)	0.053(4)	0.092(5)	0.149(5)
C60	0.1134(3)	0.6164(6)	0.72847(17)	0.098(2)	0.125(6)	0.095(5)	0.076(5)
C14	0.3194(3)	-0.1267(5)	0.3354(2)	0.0824(16)	0.053(3)	0.053(3)	0.141(4)
C45	-0.0905(3)	-0.1065(7)	0.22073(18)	0.098(2)	0.094(5)	0.120(5)	0.080(3)
C44	-0.0813(3)	-0.1374(6)	0.25347(17)	0.0851(18)	0.091(4)	0.076(4)	0.088(3)
C101	-0.0070(3)	0.5993(6)	0.6352(2)	0.111(3)	0.079(5)	0.085(5)	0.169(9)
C52	0.0656(4)	0.8578(7)	0.3423(2)	0.134(4)	0.175(9)	0.111(6)	0.116(7)
C103	0.1393(4)	0.1672(6)	0.6314(2)	0.113(3)	0.136(8)	0.071(5)	0.133(7)
C102	0.0076(3)	0.4136(7)	0.59485(19)	0.102(3)	0.087(6)	0.102(6)	0.118(7)
C37	-0.0044(4)	-0.1563(9)	0.4620(2)	0.130(3)	0.127(5)	0.120(5)	0.144(6)
C29	-0.1726(3)	0.7237(6)	0.36135(19)	0.0813(17)	0.054(3)	0.082(4)	0.108(5)
C68	0.0183(4)	1.0487(7)	0.5399(2)	0.105(2)	0.106(6)	0.094(6)	0.115(4)
C38	-0.0422(4)	-0.1271(8)	0.4387(3)	0.138(3)	0.101(5)	0.138(6)	0.176(6)
C67	-0.0074(3)	1.0484(5)	0.57233(19)	0.0712(14)	0.051(3)	0.044(3)	0.118(3)
C99	0.3014(3)	1.0325(8)	0.4990(2)	0.116(2)	0.070(3)	0.129(5)	0.149(5)
C98	0.3137(4)	1.1183(9)	0.4749(3)	0.152(3)	0.102(4)	0.163(6)	0.192(6)
C100	0.3484(4)	0.9874(11)	0.5204(3)	0.193(5)	0.074(5)	0.240(11)	0.264(12)

Table 50:- 4.6

Atom label	X	Y	Z	Uiso	Uaniso-U11	Uaniso-U22	Uaniso-U33
Zn1	0.5	0.10980(5)	0.25	0.0603(4)	0.0470(7)	0.0490(7)	0.083(10)
Zn2	0.29520(6)	0.13714(4)	0.21349(5)	0.0646(3)	0.0491(6)	0.0815(7)	0.0618(6)
Zn3	0.42615(6)	0.20116(4)	0.34427(4)	0.0663(3)	0.0657(7)	0.0801(7)	0.0548(6)
O7	0.3086(4)	0.1949(3)	0.3573(3)	0.104(2)	0.083(5)	0.173(7)	0.067(4)
O8	0.2189(4)	0.1598(3)	0.2663(3)	0.0842(18)	0.057(4)	0.129(5)	0.070(4)
O6	0.2809(4)	0.0502(3)	0.2050(3)	0.0912(19)	0.069(4)	0.094(4)	0.119(6)
O3	0.4941(5)	0.1449(3)	0.4090(3)	0.100(2)	0.101(5)	0.122(6)	0.066(4)
O4	0.5696(4)	0.1053(3)	0.3467(3)	0.100(2)	0.059(4)	0.145(6)	0.091(5)
O1	0.4549(4)	0.2858(3)	0.3568(3)	0.0849(18)	0.098(5)	0.075(4)	0.091(5)

O2	0.5712(4)	0.2687(3)	0.3235(3)	0.095(2)	0.080(4)	0.095(5)	0.110(5)
O5	0.4160(5)	0.0475(3)	0.2723(4)	0.129(3)	0.094(5)	0.081(4)	0.189(8)
O9	0.4085(3)	0.1759(2)	0.2546(3)	0.0520(13)	0.060(3)	0.052(3)	0.047(3)
N1	0.2329(4)	0.1755(4)	0.1275(3)	0.0719(19)	0.049(4)	0.101(6)	0.064(5)
C25	0.2360(6)	0.1769(4)	0.3238(5)	0.0662(18)	0.069(4)	0.060(4)	0.076(5)
C26	0.1639(6)	0.1785(4)	0.3532(5)	0.0836(19)	0.082(3)	0.090(5)	0.091(4)
C27	0.0840(7)	0.1575(6)	0.3225(6)	0.126(3)	0.078(4)	0.188(7)	0.129(6)
C28	0.0158(8)	0.1561(7)	0.3495(7)	0.138(3)	0.086(4)	0.212(8)	0.137(6)
C29	0.0263(8)	0.1764(6)	0.4061(6)	0.120(3)	0.102(5)	0.155(7)	0.126(6)
C30	0.0998(9)	0.1984(7)	0.4385(7)	0.131(3)	0.119(5)	0.185(7)	0.116(5)
C31	0.1707(8)	0.2010(6)	0.4107(6)	0.120(3)	0.112(5)	0.163(7)	0.105(5)
C18	0.3420(8)	-0.0461(5)	0.2424(7)	0.111(2)	0.119(5)	0.083(3)	0.172(7)
C19	0.2659(10)	-0.0755(5)	0.2094(7)	0.135(3)	0.163(6)	0.100(4)	0.177(8)
C20	0.2638(12)	-0.1387(6)	0.2154(8)	0.150(3)	0.195(7)	0.102(4)	0.195(8)
C21	0.3361(13)	-0.1661(7)	0.2531(9)	0.163(4)	0.220(8)	0.121(5)	0.205(9)
C22	0.4057(12)	-0.1418(7)	0.2868(9)	0.152(3)	0.184(7)	0.110(4)	0.211(8)
C23	0.4134(10)	-0.0756(6)	0.2837(8)	0.136(3)	0.143(6)	0.111(4)	0.201(8)
C37	0.2067(6)	0.1419(5)	0.0716(5)	0.094(3)	0.072(6)	0.140(6)	0.075(5)
C36	0.1659(7)	0.1702(6)	0.0141(5)	0.112(3)	0.096(6)	0.171(6)	0.067(4)
C35	0.1530(7)	0.2293(7)	0.0116(6)	0.116(3)	0.091(6)	0.171(6)	0.086(5)
C34	0.1776(7)	0.2622(6)	0.0630(6)	0.107(3)	0.082(6)	0.130(6)	0.107(5)
C33	0.2196(6)	0.2345(5)	0.1213(5)	0.091(3)	0.067(5)	0.110(7)	0.092(5)
C1	0.5225(7)	0.3027(4)	0.3406(4)	0.074(2)	0.074(5)	0.084(3)	0.068(5)
C2	0.5427(7)	0.3683(5)	0.3466(6)	0.102(2)	0.100(5)	0.091(3)	0.128(6)
C3	0.6076(8)	0.3914(5)	0.3257(7)	0.129(3)	0.129(6)	0.105(5)	0.179(7)
C7	0.4952(8)	0.4055(5)	0.3765(7)	0.132(3)	0.130(6)	0.099(4)	0.191(7)
C17	0.3453(8)	0.0225(5)	0.2377(7)	0.103(3)	0.098(6)	0.082(3)	0.161(8)
C9	0.5496(7)	0.1087(6)	0.3985(6)	0.099(3)	0.067(6)	0.120(6)	0.093(5)
C10	0.5919(7)	0.0653(6)	0.4526(6)	0.114(2)	0.080(5)	0.144(6)	0.104(4)
C15	0.6440(8)	0.0176(7)	0.4402(7)	0.139(3)	0.105(6)	0.174(7)	0.130(5)
C13	0.6659(11)	-0.0127(8)	0.5493(8)	0.176(4)	0.158(8)	0.215(8)	0.135(5)
C12	0.6157(10)	0.0275(7)	0.5591(7)	0.163(3)	0.156(8)	0.202(8)	0.113(5)
C11	0.5741(8)	0.0689(6)	0.5108(6)	0.134(3)	0.121(6)	0.166(7)	0.098(5)
C6	0.5124(11)	0.4665(6)	0.3812(9)	0.165(3)	0.167(7)	0.102(4)	0.255(8)
C5	0.5827(11)	0.4884(7)	0.3663(9)	0.179(3)	0.177(7)	0.110(6)	0.277(9)
C4	0.6329(10)	0.4515(6)	0.3368(8)	0.162(3)	0.157(7)	0.116(5)	0.244(9)
C32	0.1100(11)	0.2326(9)	0.5029(8)	0.215(6)	0.181(10)	0.358(15)	0.144(10)
C24	0.4826(12)	-0.1704(7)	0.3312(9)	0.203(5)	0.226(10)	0.158(8)	0.267(13)
C8	0.4570(12)	0.5084(6)	0.4094(10)	0.212(6)	0.229(12)	0.119(7)	0.334(15)
C16	0.7380(12)	-0.0777(8)	0.4726(8)	0.216(6)	0.205(13)	0.225(11)	0.194(10)
C14	0.6849(10)	-0.0259(8)	0.4859(8)	0.169(3)	0.139(7)	0.199(7)	0.157(6)

Table 51:- 4.7

Atom label	X	Y	Z	Uiso	Uaniso-U11	Uaniso-U22	Uaniso-U33
Zn1	0	1.42428(7)	0.75	0.0362(15)	0.0398(2)	0.0231(2)	0.0477(3)
O1	0.03757(7)	1.2474(3)	0.95075(15)	0.0430(4)	0.0509(10)	0.0402(10)	0.0381(9)
O2	0.05930(6)	1.1659(3)	0.79248(14)	0.0372(4)	0.0477(9)	0.0348(9)	0.0279(8)
O5	-0.02905(7)	1.7008(3)	0.83082(15)	0.0460(4)	0.0732(12)	0.0305(9)	0.0386(10)
C1	0.06497(9)	1.1267(4)	0.9005(2)	0.0326(5)	0.0381(11)	0.0264(11)	0.0311(11)
C2	0.10492(9)	0.9302(4)	0.96129(19)	0.0320(5)	0.0365(11)	0.0310(11)	0.0275(11)
C3	0.14233(10)	0.8408(6)	0.9107(2)	0.0422(6)	0.0470(14)	0.0511(15)	0.0319(13)

C4	0.17878(10)	0.6553(6)	0.9677(2)	0.0474(6)	0.0425(14)	0.0577(16)	0.0446(15)
C5	0.17914(10)	0.5537(5)	1.0739(2)	0.0404(6)	0.0414(12)	0.0339(13)	0.0399(13)
C6	0.14155(11)	0.6423(5)	1.1230(2)	0.0451(6)	0.0562(15)	0.0439(14)	0.0364(14)
C7	0.10471(10)	0.8270(5)	1.0670(2)	0.0425(6)	0.0509(14)	0.0447(14)	0.0372(13)
C8	0.21818(11)	0.3480(6)	1.1346(3)	0.0563(8)	0.0524(16)	0.0469(15)	0.0594(18)

Table 52:- 4.8

Atom label	X	Y	Z	Uiso	Uaniso-U11	Uaniso-U22	Uaniso-U33
Zn1	0.21729(5)	0.99596(4)	0.24581(11)	0.0315(12)	0.0356(19)	0.0302(2)	0.0272(19)
S2	-0.047(14)	1.32929(10)	0.31158(3)	0.0411(19)	0.0477(4)	0.0342(4)	0.0349(4)
S1	0.4347(14)	0.65397(10)	0.17685(3)	0.0408(19)	0.0516(4)	0.0313(4)	0.0317(4)
C2	-0.0664(5)	1.1058(4)	0.10804(11)	0.0344(6)	0.0334(13)	0.0317(14)	0.0334(14)
C5	-0.2202(6)	1.2290(5)	0.01391(12)	0.0454(7)	0.0543(18)	0.0443(19)	0.0302(15)
C1	0.0140(5)	1.0468(4)	0.16055(11)	0.0378(6)	0.0441(15)	0.0295(14)	0.0313(14)
C3	0.0467(6)	1.2058(5)	0.07525(12)	0.0443(7)	0.0477(17)	0.0509(19)	0.0382(17)
C7	-0.2568(6)	1.0659(5)	0.09244(12)	0.0454(7)	0.0489(17)	0.0516(19)	0.0405(17)
C4	-0.0294(6)	1.2671(5)	0.02793(12)	0.0496(8)	0.064(2)	0.051(2)	0.0368(17)
C6	-0.3331(6)	1.1273(5)	0.04464(13)	0.0506(8)	0.0486(18)	0.064(2)	0.0438(19)
C8	0.2596(5)	0.8747(4)	0.35136(11)	0.0361(6)	0.0422(15)	0.0309(15)	0.0303(14)
C12	-0.0257(6)	0.7551(4)	0.49733(11)	0.0436(7)	0.0622(19)	0.0416(18)	0.0271(15)
C9	0.1544(5)	0.8317(4)	0.40276(11)	0.0359(6)	0.0405(14)	0.0340(15)	0.0318(14)
C14	0.3042(6)	0.7366(5)	0.43963(12)	0.0464(7)	0.0405(16)	0.054(2)	0.0392(17)
C10	-0.0876(5)	0.8886(5)	0.41389(12)	0.0427(7)	0.0398(15)	0.0500(19)	0.0334(15)
C11	-0.1798(6)	0.8531(5)	0.46160(12)	0.0466(7)	0.0423(16)	0.053(2)	0.0400(17)
C13	0.2166(6)	0.6974(5)	0.48753(13)	0.0514(8)	0.0563(19)	0.056(2)	0.0356(17)
O5	0.1214(4)	0.9145(3)	0.31574(7)	0.0374(4)	0.0444(11)	0.0392(11)	0.0286(10)
O2	0.1963(4)	1.0785(3)	0.17103(8)	0.0429(5)	0.0541(13)	0.0391(12)	0.0351(11)
O1	-0.0999(4)	0.9707(4)	0.19098(9)	0.0541(6)	0.0560(13)	0.0587(15)	0.0377(12)
O6	0.4682(4)	0.8680(4)	0.34804(9)	0.0574(7)	0.0397(12)	0.0856(19)	0.0408(13)
O8	0.0152(6)	0.6057(5)	0.57642(10)	0.0797(9)	0.109(2)	0.089(2)	0.0366(15)
O4	-0.4832(7)	1.2706(7)	-0.0472(13)	0.1066(14)	0.089(2)	0.174(4)	0.059(2)
O3	-0.2168(9)	1.3984(6)	-0.0616(13)	0.1094(14)	0.180(4)	0.117(3)	0.054(2)
O7	-0.3346(6)	0.7696(5)	0.55728(12)	0.0900(11)	0.083(2)	0.105(3)	0.0645(19)
O9	0.3993(4)	0.7175(3)	0.22997(8)	0.0459(5)	0.0657(14)	0.0316(11)	0.0319(11)
O10	-0.0151(4)	1.2642(3)	0.25832(8)	0.0452(5)	0.0574(13)	0.0348(11)	0.0329(11)
O11	0.5169(4)	1.0455(4)	0.26057(10)	0.0446(5)	0.0429(12)	0.0478(14)	0.0439(14)
C18	-0.0497(7)	1.5618(5)	0.30306(15)	0.0567(9)	0.065(2)	0.044(2)	0.063(2)
C16	0.7452(6)	0.5903(5)	0.16135(15)	0.0569(9)	0.058(2)	0.057(2)	0.053(2)
C17	-0.3533(6)	1.3748(6)	0.32935(15)	0.0593(10)	0.057(2)	0.065(2)	0.059(2)
C15	0.4135(7)	0.4284(5)	0.18383(16)	0.0593(10)	0.066(2)	0.051(2)	0.067(2)
N2	-0.1222(7)	0.7090(5)	0.54724(12)	0.0573(8)	0.088(2)	0.0529(18)	0.0318(15)
N1	-0.3127(7)	1.3037(5)	-0.0357(12)	0.0640(9)	0.079(2)	0.068(2)	0.0363(17)

Table 53:- 5.1

Atom label	X	Y	Z	Uiso	Uaniso-U11	Uaniso-U22	Uaniso-U33
C8	0.7884(5)	0.6727(4)	0.4801(4)	0.0542(11)	0.060(3)	0.033(2)	0.066(3)
C6	0.6241(5)	0.2999(4)	0.7460(4)	0.0547(12)	0.066(3)	0.042(3)	0.057(3)
C7	0.6899(5)	0.4919(4)	0.6123(4)	0.0519(11)	0.050(3)	0.040(3)	0.066(3)
C16	0.9285(5)	0.7294(4)	0.4605(4)	0.0524(11)	0.060(3)	0.044(3)	0.056(3)

C9	0.7353(5)	0.6954(4)	0.3731(4)	0.0623(13)	0.054(3)	0.052(3)	0.080(4)
C10	0.8425(5)	0.6763(4)	0.2879(4)	0.0595(12)	0.062(3)	0.053(3)	0.072(3)
C1	0.5100(6)	0.3280(5)	0.8076(4)	0.0716(14)	0.080(4)	0.050(3)	0.076(4)
C15	0.9251(6)	0.7670(5)	0.2156(4)	0.0725(15)	0.091(4)	0.061(3)	0.061(3)
C5	0.6519(6)	0.1849(4)	0.7665(4)	0.0745(15)	0.095(4)	0.049(3)	0.071(4)
C2	0.4262(6)	0.2417(6)	0.8836(4)	0.0799(16)	0.076(4)	0.078(4)	0.068(4)
C11	0.8676(6)	0.5659(5)	0.2847(5)	0.0800(16)	0.085(4)	0.063(4)	0.093(4)
C3	0.4543(8)	0.1295(6)	0.9001(5)	0.100(2)	0.120(6)	0.083(5)	0.076(4)
C13	1.0524(7)	0.6391(7)	0.1410(5)	0.0922(19)	0.091(5)	0.102(5)	0.082(4)
C12	0.9713(8)	0.5468(6)	0.2116(6)	0.097(2)	0.119(6)	0.081(5)	0.100(5)
C14	1.0295(7)	0.7487(6)	0.1413(5)	0.0843(17)	0.099(5)	0.085(4)	0.062(4)
C4	0.5691(9)	0.1002(5)	0.8414(5)	0.098(2)	0.143(6)	0.046(3)	0.089(5)
O2	1.0346(3)	0.6788(3)	0.4633(3)	0.0605(9)	0.0511(19)	0.0476(19)	0.087(2)
O3	0.9216(3)	0.8426(2)	0.4360(3)	0.0645(9)	0.061(2)	0.0338(17)	0.099(3)
O1	0.5781(3)	0.5348(3)	0.6305(3)	0.0703(10)	0.057(2)	0.048(2)	0.088(3)
N2	0.7946(4)	0.5503(3)	0.5374(3)	0.0611(11)	0.057(2)	0.035(2)	0.080(3)
N1	0.7154(5)	0.3809(3)	0.6671(4)	0.0620(12)	0.058(3)	0.040(2)	0.077(3)
C23	0.2345(5)	1.0212(4)	0.3876(4)	0.0501(11)	0.051(3)	0.037(2)	0.066(3)
C24	0.2695(5)	0.8379(3)	0.5192(4)	0.0517(11)	0.059(3)	0.034(2)	0.069(3)
C22	0.2501(5)	1.2130(4)	0.2445(4)	0.0531(11)	0.060(3)	0.040(3)	0.058(3)
C25	0.1661(5)	0.8035(4)	0.6230(4)	0.0581(12)	0.060(3)	0.046(3)	0.072(3)
C26	0.2208(5)	0.8132(4)	0.7177(4)	0.0577(12)	0.057(3)	0.051(3)	0.070(3)
C21	0.3172(6)	1.3206(4)	0.2096(5)	0.0740(15)	0.090(4)	0.050(3)	0.080(4)
C17	0.1522(6)	1.1937(5)	0.1888(4)	0.0703(14)	0.078(4)	0.063(3)	0.067(3)
C18	0.1263(7)	1.2799(5)	0.1000(4)	0.0797(16)	0.100(5)	0.075(4)	0.064(4)
C27	0.2726(6)	0.7184(5)	0.7873(4)	0.0706(14)	0.088(4)	0.055(3)	0.064(3)
C31	0.2244(7)	0.9161(5)	0.7365(5)	0.091(2)	0.122(5)	0.062(4)	0.115(5)
C20	0.2905(8)	1.4060(5)	0.1209(5)	0.093(2)	0.121(5)	0.048(3)	0.092(5)
C28	0.3255(7)	0.7289(6)	0.8729(5)	0.0868(18)	0.095(4)	0.083(4)	0.072(4)
C30	0.2759(10)	0.9261(7)	0.8205(7)	0.129(3)	0.184(9)	0.104(6)	0.144(7)
C29	0.3268(8)	0.8317(7)	0.8888(6)	0.103(2)	0.116(6)	0.121(6)	0.090(5)
C19	0.1947(7)	1.3864(5)	0.0651(5)	0.0867(18)	0.110(5)	0.069(4)	0.069(4)
C32	0.4046(5)	0.7793(4)	0.5371(3)	0.0497(11)	0.057(3)	0.037(2)	0.057(3)
O5	0.3908(3)	0.6680(3)	0.5562(3)	0.0670(10)	0.060(2)	0.0384(19)	0.107(3)
O6	0.5097(3)	0.8300(2)	0.5376(3)	0.0589(9)	0.055(2)	0.0424(18)	0.082(2)
O4	0.1380(3)	0.9802(3)	0.3613(3)	0.0645(9)	0.064(2)	0.0446(18)	0.085(2)
N4	0.2970(5)	0.9605(3)	0.4691(3)	0.0583(11)	0.068(3)	0.036(2)	0.079(3)
N3	0.2879(4)	1.1302(3)	0.3345(3)	0.0594(11)	0.067(3)	0.040(2)	0.072(3)

Table 54:- 5.2

Atom label	X	Y	Z	Uiso	Uaniso-U11	Uaniso-U22	Uaniso-U33
Na1	0.21856(2)	0.76021(8)	0.8367(11)	0.0457(3)	0.0346(5)	0.0564(6)	0.0459(5)
C6	0.11176(5)	1.07612(17)	0.5811(2)	0.0320(5)	0.0340(11)	0.0327(10)	0.0296(10)
C5	0.08265(5)	1.01698(19)	0.5966(3)	0.0380(5)	0.0341(11)	0.0383(11)	0.0420(12)
C1	0.11182(6)	1.18534(19)	0.4929(3)	0.0432(5)	0.0602(14)	0.0341(11)	0.0373(12)
C4	0.05437(5)	1.0665(2)	0.5213(3)	0.0500(6)	0.0365(13)	0.0595(15)	0.0536(15)
C3	0.05431(6)	1.1740(2)	0.4340(3)	0.0573(7)	0.0561(16)	0.0662(17)	0.0481(15)
C2	0.08285(8)	1.2337(2)	0.4203(3)	0.0561(7)	0.093(2)	0.0407(13)	0.0347(12)
C8	0.14684(4)	0.71306(16)	0.5358(3)	0.0299(4)	0.0273(10)	0.0282(10)	0.0345(11)
C10	0.08913(4)	0.63604(16)	0.4590(2)	0.0304(5)	0.0294(10)	0.0304(10)	0.0313(11)
C16	0.17988(4)	0.71089(16)	0.4610(3)	0.0313(5)	0.0273(10)	0.0266(10)	0.0400(12)

C7	0.15200(4)	0.91469(17)	0.6586(3)	0.0306(4)	0.0243(10)	0.0343(10)	0.0343(11)
C9	0.12347(5)	0.64005(17)	0.4103(3)	0.0343(5)	0.0324(11)	0.0346(11)	0.0366(11)
C15	0.06694(5)	0.72265(18)	0.3976(3)	0.0377(5)	0.0362(12)	0.0342(11)	0.0422(12)
C14	0.03551(5)	0.71862(19)	0.4421(3)	0.0431(5)	0.0313(12)	0.0428(12)	0.0542(14)
C12	0.04710(5)	0.5404(2)	0.6079(3)	0.0431(5)	0.0417(13)	0.0479(13)	0.0403(13)
C11	0.07867(5)	0.54433(17)	0.5652(3)	0.0361(5)	0.0373(12)	0.0332(11)	0.0371(12)
C13	0.02554(5)	0.6275(2)	0.5470(3)	0.0445(6)	0.0302(11)	0.0539(14)	0.0500(14)
N1	0.14103(4)	1.02991(15)	0.6625(2)	0.0362(4)	0.0319(9)	0.0309(9)	0.0452(11)
N2	0.13489(4)	0.83460(14)	0.5540(2)	0.0307(4)	0.0264(9)	0.0310(9)	0.0346(10)
O1	0.17675(3)	0.88378(12)	0.7471(2)	0.0440(4)	0.0309(8)	0.0462(9)	0.0528(9)
O3	0.19999(4)	0.63639(14)	0.5282(2)	0.0540(5)	0.0360(9)	0.0498(10)	0.0782(12)
O2	0.18455(4)	0.78174(14)	0.3400(2)	0.0475(4)	0.0368(9)	0.0537(9)	0.0545(10)
O6	0.24143(5)	0.89065(15)	0.6086(3)	0.0515(5)	0.0368(10)	0.0514(10)	0.0683(12)
O4	0.18897(6)	0.6224(2)	1.0145(3)	0.0731(6)	0.0972(17)	0.0509(12)	0.0740(15)
O5	0.23340(4)	0.85416(16)	1.1237(2)	0.0431(4)	0.0364(9)	0.0438(10)	0.0500(10)

Table 55:- 5.3

Atom label	X	Y	Z	Uiso	Uaniso-U11	Uaniso-U22	Uaniso-U33
Mn1	0.5	0	1	0.0490(5)	0.0249(6)	0.0769(11)	0.061(11)
O1	0.3091(7)	0.2280(4)	0.7566(4)	0.0759(18)	0.026(2)	0.098(4)	0.130(5)
O2	0.1046(7)	-0.0452(3)	0.9051(3)	0.0496(13)	0.034(2)	0.071(3)	0.059(3)
O3	-0.2791(7)	0.0308(4)	0.8881(3)	0.0543(13)	0.0252(18)	0.094(4)	0.063(3)
N1	-0.1225(10)	0.2789(5)	0.7361(5)	0.0622(18)	0.031(2)	0.071(4)	0.101(5)
N2	-0.0643(9)	0.1323(4)	0.7769(4)	0.0527(16)	0.026(2)	0.068(4)	0.078(4)
C1	-0.164(2)	0.4527(8)	0.7464(9)	0.111(4)	0.099(6)	0.099(8)	0.175(12)
C2	-0.103(3)	0.5424(9)	0.7191(11)	0.138(5)	0.145(9)	0.089(9)	0.209(17)
C3	0.075(2)	0.5355(10)	0.6474(9)	0.114(4)	0.094(7)	0.113(10)	0.164(12)
C4	0.188(2)	0.4505(9)	0.6128(9)	0.110(4)	0.096(7)	0.112(9)	0.158(12)
C5	0.1318(16)	0.3643(7)	0.6396(6)	0.079(3)	0.076(5)	0.083(6)	0.096(7)
C6	-0.0450(13)	0.3659(6)	0.7087(6)	0.062(2)	0.039(3)	0.069(5)	0.088(6)
C7	0.0541(12)	0.2139(5)	0.7553(5)	0.0516(19)	0.033(3)	0.065(5)	0.066(5)
C8	0.1051(11)	0.0606(5)	0.8037(5)	0.0464(17)	0.029(3)	0.062(4)	0.059(5)
C9	0.1755(11)	-0.0224(5)	0.7164(5)	0.055(2)	0.037(3)	0.077(5)	0.066(5)
C10	-0.0660(12)	-0.0901(6)	0.6568(5)	0.054(2)	0.041(3)	0.073(5)	0.057(5)
C11	-0.1603(15)	-0.1781(6)	0.6746(6)	0.072(2)	0.063(4)	0.085(6)	0.076(7)
C12	-0.3924(19)	-0.2435(8)	0.6172(9)	0.096(3)	0.083(6)	0.082(7)	0.104(10)
C13	-0.5216(18)	-0.2198(10)	0.5414(9)	0.101(4)	0.060(5)	0.131(10)	0.084(9)
C14	-0.423(2)	-0.1303(9)	0.5229(7)	0.094(3)	0.086(6)	0.133(10)	0.068(8)
C15	-0.2000(15)	-0.0677(7)	0.5804(6)	0.071(2)	0.058(4)	0.100(7)	0.060(6)
C16	-0.0334(11)	0.0111(5)	0.8720(5)	0.0480(18)	0.030(3)	0.071(5)	0.052(5)
O4	0.3712(17)	0.1561(7)	1.0489(7)	0.151(4)	0.145(7)	0.195(10)	0.185(10)

Table 56:- 5.4A

Atom label	X	Y	Z	Uiso	Uaniso-U11	Uaniso-U22	Uaniso-U33
O3	0.7670(17)	0.0752(3)	0.42072(6)	0.0610(7)	0.0434(12)	0.0871(17)	0.0524(13)
O4	0.9836(17)	0.1269(3)	0.41560(6)	0.0574(6)	0.0426(12)	0.0813(16)	0.0482(13)
C11	0.9441(3)	-0.1144(4)	0.31759(9)	0.0489(8)	0.0526(18)	0.0470(17)	0.0471(18)
C12	0.9985(3)	-0.0223(4)	0.34945(9)	0.0509(8)	0.0389(15)	0.0601(19)	0.0538(19)

C6	0.8256(3)	-0.1493(4)	0.32179(10)	0.0505(8)	0.0508(18)	0.0483(17)	0.0525(19)
C4	0.8192(2)	0.0043(4)	0.38675(9)	0.0484(7)	0.0420(16)	0.0598(18)	0.0435(18)
C5	0.7659(3)	-0.0882(4)	0.35708(10)	0.0534(8)	0.0418(16)	0.060(2)	0.059(2)
C13	0.9389(2)	0.0361(4)	0.38313(9)	0.0468(7)	0.0456(16)	0.0525(17)	0.0423(17)
O6	1.0551(2)	0.3677(3)	0.36668(7)	0.0696(7)	0.0608(15)	0.0717(16)	0.0761(16)
C15	1.1411(3)	0.2903(4)	0.38497(12)	0.0631(9)	0.0420(19)	0.068(2)	0.079(2)
C14	1.1032(3)	0.1587(5)	0.41482(10)	0.0630(10)	0.0463(19)	0.084(2)	0.059(2)
C7	0.7714(3)	-0.2444(4)	0.29039(11)	0.0655(9)	0.063(2)	0.066(2)	0.068(2)
C10	1.0028(3)	-0.1726(4)	0.28164(11)	0.0622(9)	0.065(2)	0.062(2)	0.059(2)
O1	0.4851(2)	0.1599(5)	0.45319(9)	0.1034(11)	0.0498(16)	0.180(3)	0.0799(19)
C2	0.5975(3)	0.1610(5)	0.45635(12)	0.0689(10)	0.051(2)	0.106(3)	0.050(2)
C3	0.6457(3)	0.0613(5)	0.42142(10)	0.0666(10)	0.050(2)	0.093(3)	0.057(2)
O5	1.2397(2)	0.3211(4)	0.37944(11)	0.1097(11)	0.0477(16)	0.103(2)	0.179(3)
C8	0.8314(4)	-0.2974(5)	0.25615(12)	0.0765(11)	0.089(3)	0.076(2)	0.065(2)
C9	0.9476(4)	-0.2618(4)	0.25186(12)	0.0727(11)	0.091(3)	0.065(2)	0.061(2)
O2	0.6492(2)	0.2298(5)	0.48313(9)	0.1062(11)	0.0649(17)	0.176(3)	0.078(2)
C16	1.0851(4)	0.5020(5)	0.33924(14)	0.1019(14)	0.127(4)	0.076(3)	0.103(3)
C1	0.4187(5)	0.2603(9)	0.48506(16)	0.140(2)	0.087(3)	0.223(7)	0.109(4)

Table 57:- 5.4B

Atom label	X	Y	Z	Uiso	Uaniso-U11	Uaniso-U22	Uaniso-U33
C11	0.43653(11)	0.85886(13)	0.68125(4)	0.0375(3)	0.0401(6)	0.0325(6)	0.0401(6)
C6	0.32032(11)	0.80924(14)	0.67054(4)	0.0391(3)	0.0396(6)	0.0340(6)	0.0436(6)
C5	0.26638(11)	0.86259(15)	0.63134(4)	0.0406(3)	0.0315(6)	0.0414(7)	0.0490(7)
C12	0.49596(10)	0.96024(13)	0.65221(4)	0.0364(3)	0.0311(5)	0.0362(6)	0.0419(6)
C13	0.44130(10)	1.01200(13)	0.61519(4)	0.0345(3)	0.0335(6)	0.0339(6)	0.0360(6)
C4	0.32319(10)	0.96382(14)	0.60479(4)	0.0364(3)	0.0347(6)	0.0379(6)	0.0366(6)
C10	0.48971(13)	0.80600(15)	0.72049(4)	0.0497(3)	0.0569(8)	0.0437(7)	0.0485(7)
C7	0.26188(14)	0.70810(16)	0.69954(5)	0.0519(3)	0.0510(8)	0.0457(8)	0.0590(8)
C9	0.42981(16)	0.70927(18)	0.74786(5)	0.0603(4)	0.0813(12)	0.0520(8)	0.0476(8)
C8	0.31522(16)	0.66018(19)	0.73735(5)	0.0620(4)	0.0753(11)	0.0537(9)	0.0571(9)
C2	0.17576(10)	0.85763(15)	0.51956(4)	0.0393(3)	0.0341(6)	0.0466(7)	0.0371(6)
C14	0.61086(11)	1.14942(16)	0.58948(4)	0.0449(3)	0.0360(6)	0.0499(7)	0.0488(7)
C15	0.63604(11)	1.27814(16)	0.62072(5)	0.0450(3)	0.0348(6)	0.0446(7)	0.0555(8)
C3	0.16560(11)	0.98614(17)	0.55190(4)	0.0457(3)	0.0344(6)	0.0554(8)	0.0473(7)
O3	0.27891(8)	1.03131(11)	0.56765(3)	0.0487(2)	0.0416(5)	0.0567(6)	0.0478(5)
O4	0.48950(8)	1.10965(11)	0.58492(3)	0.0432(2)	0.0392(5)	0.0505(5)	0.0400(4)
O2	0.26715(9)	0.80280(13)	0.50707(3)	0.0547(3)	0.0384(5)	0.0702(7)	0.0556(6)
O1	0.06854(8)	0.81731(11)	0.50535(3)	0.0494(2)	0.0370(5)	0.0546(6)	0.0565(6)
O6	0.54054(9)	1.35320(12)	0.63318(3)	0.0559(3)	0.0445(5)	0.0541(6)	0.0689(7)
O5	0.73486(10)	1.31087(16)	0.63131(5)	0.0869(4)	0.0413(6)	0.0827(9)	0.1368(12)
C1	0.06580(14)	0.69034(19)	0.47486(6)	0.0646(4)	0.0535(9)	0.0676(10)	0.0726(10)
C16	0.55816(18)	1.4866(2)	0.66073(7)	0.0758(5)	0.0855(13)	0.0559(10)	0.0861(12)

Table 58:- 5.5A

Atom label	X	Y	Z	Uiso	Uaniso-U11	Uaniso-U22	Uaniso-U33
C3	0.9104(3)	0.78174(13)	0.75533(10)	0.0363(3)	0.0371(7)	0.0321(7)	0.0425(7)
C5	0.6446(3)	0.73784(14)	0.58239(11)	0.0426(3)	0.0427(8)	0.0445(8)	0.0405(7)
C12	0.7625(3)	0.89819(12)	0.78420(10)	0.0365(3)	0.0427(8)	0.0287(6)	0.0388(7)

C1	1.1145(3)	0.52435(13)	0.82741(10)	0.0368(3)	0.0346(7)	0.0352(7)	0.0419(7)
C13	0.7020(3)	1.08101(13)	0.92314(11)	0.0416(3)	0.0524(9)	0.0315(7)	0.0408(7)
C10	0.4987(3)	0.85283(14)	0.61069(11)	0.0412(3)	0.0411(8)	0.0409(8)	0.0427(8)
C4	0.8512(3)	0.70396(14)	0.65760(11)	0.0428(3)	0.0437(8)	0.0386(7)	0.0465(8)
C2	1.2662(3)	0.64895(13)	0.81290(12)	0.0416(3)	0.0368(7)	0.0379(7)	0.0521(8)
C14	0.8192(3)	1.20058(13)	0.88779(10)	0.0380(3)	0.0396(7)	0.0322(7)	0.0409(7)
C11	0.5631(3)	0.93226(14)	0.71370(11)	0.0426(3)	0.0481(8)	0.0328(7)	0.0470(8)
C9	0.2923(3)	0.88600(17)	0.53618(12)	0.0541(4)	0.0535(9)	0.056(10)	0.0510(9)
C6	0.5823(4)	0.66111(18)	0.47885(12)	0.0579(4)	0.0591(10)	0.062(10)	0.0471(9)
C8	0.2363(4)	0.80905(19)	0.43770(13)	0.0607(5)	0.0563(10)	0.076(12)	0.0475(9)
C7	0.3827(4)	0.6963(2)	0.40876(13)	0.0636(5)	0.0601(11)	0.082(13)	0.0414(9)
O3	1.1069(2)	0.76116(9)	0.83417(7)	0.0411(3)	0.0439(6)	0.0332(5)	0.0468(6)
O4	0.8384(2)	0.96470(9)	0.88618(7)	0.0447(3)	0.0590(7)	0.0305(5)	0.0422(5)
O6	0.6862(2)	1.30480(10)	0.92022(9)	0.0528(3)	0.0562(7)	0.0348(5)	0.0729(7)
O1	1.2454(2)	0.42018(10)	0.79443(10)	0.0589(3)	0.0571(7)	0.0382(6)	0.0866(8)
O5	1.0213(2)	1.19808(10)	0.83652(9)	0.0542(3)	0.0561(7)	0.0381(6)	0.0694(7)
O2	0.8953(2)	0.52482(10)	0.86821(9)	0.0518(3)	0.0440(6)	0.0400(6)	0.0775(7)

Table 59:- 5.5B

Atom label	X	Y	Z	Uiso	Uaniso-U11	Uaniso-U22	Uaniso-U33
C17	0.1913(2)	0.4205(2)	0.63433(9)	0.0474(5)	0.0575(13)	0.0317(12)	0.0529(15)
C27	0.4418(2)	0.1570(2)	0.61361(10)	0.0526(6)	0.0517(13)	0.0430(13)	0.0632(16)
C12	0.3070(2)	0.5256(2)	0.42254(9)	0.0446(5)	0.0488(12)	0.0357(12)	0.0494(15)
C11	0.3908(2)	0.4792(2)	0.38552(9)	0.0512(6)	0.0532(13)	0.0412(13)	0.0591(16)
C15	0.1949(2)	0.6947(2)	0.58368(9)	0.0481(6)	0.0524(13)	0.0421(13)	0.0500(14)
C5	0.2962(3)	0.6386(2)	0.32522(9)	0.0548(6)	0.0669(15)	0.0444(14)	0.0529(16)
C25	0.2686(2)	0.2532(2)	0.69280(9)	0.0518(6)	0.0560(13)	0.0374(13)	0.0617(17)
C16	0.1206(2)	0.5702(2)	0.56892(9)	0.0519(6)	0.0677(14)	0.0367(12)	0.0510(15)
C28	0.3666(2)	0.0281(2)	0.60749(9)	0.0490(6)	0.0559(14)	0.0431(13)	0.0481(14)
C24	0.1924(2)	0.3127(2)	0.73208(9)	0.0507(6)	0.0522(13)	0.0458(13)	0.0539(15)
C19	0.1157(2)	0.4279(2)	0.72141(9)	0.0519(6)	0.0543(13)	0.0492(14)	0.0523(16)
C3	0.2148(2)	0.6321(2)	0.41147(9)	0.0458(5)	0.0503(12)	0.0347(12)	0.0527(15)
C10	0.3893(2)	0.5347(2)	0.33627(9)	0.0495(6)	0.0533(13)	0.0424(13)	0.0529(15)
C18	0.1168(2)	0.4788(2)	0.67130(9)	0.0550(6)	0.0634(15)	0.0419(13)	0.0595(17)
C26	0.2718(2)	0.3063(2)	0.64556(9)	0.0457(5)	0.0528(12)	0.0331(12)	0.0510(15)
C4	0.2096(3)	0.6856(2)	0.36440(10)	0.0579(6)	0.0666(15)	0.0436(14)	0.0634(18)
C9	0.4788(3)	0.4906(3)	0.29767(11)	0.0640(7)	0.0664(16)	0.0597(16)	0.0663(19)
C8	0.4738(3)	0.5453(3)	0.25080(11)	0.0732(8)	0.088(2)	0.074(2)	0.0592(19)
C23	0.1925(3)	0.2629(3)	0.78192(10)	0.0666(7)	0.0736(17)	0.0672(18)	0.0588(18)
C22	0.1197(3)	0.3235(3)	0.81903(11)	0.0780(8)	0.090(2)	0.088(2)	0.0563(19)
C21	0.0423(3)	0.4362(3)	0.80836(11)	0.0771(8)	0.0844(19)	0.090(2)	0.0575(19)
C20	0.0404(3)	0.4874(3)	0.76075(11)	0.0697(7)	0.0751(18)	0.0690(18)	0.0654(19)
C6	0.2933(3)	0.6932(3)	0.27594(11)	0.0756(8)	0.103(2)	0.0659(18)	0.0575(19)
C7	0.3796(4)	0.6469(3)	0.23963(11)	0.0821(9)	0.125(3)	0.070(2)	0.0518(19)
C13	0.3860(2)	0.3731(2)	0.48669(9)	0.0499(6)	0.0532(13)	0.0400(13)	0.0563(15)
C1	0.1409(2)	0.9064(2)	0.45151(9)	0.0493(6)	0.0493(13)	0.0472(14)	0.0513(15)
C2	0.0539(2)	0.7845(2)	0.44676(10)	0.0530(6)	0.0515(13)	0.0392(13)	0.0685(17)
C14	0.3183(2)	0.2449(2)	0.47275(9)	0.0469(5)	0.0497(13)	0.0431(13)	0.0480(14)
O4	0.30232(16)	0.48150(14)	0.47175(6)	0.0531(4)	0.0653(10)	0.0400(9)	0.0543(11)
O3	0.13560(17)	0.66963(14)	0.45213(6)	0.0574(4)	0.0681(10)	0.0407(9)	0.0640(11)
O10	0.34843(16)	0.26254(14)	0.60543(6)	0.0524(4)	0.0660(10)	0.0352(8)	0.0561(11)

O9	0.19878(17)	0.45858(14)	0.58446(6)	0.0571(4)	0.0827(11)	0.0365(9)	0.0523(11)
O5	0.20058(17)	0.23774(16)	0.45290(7)	0.0655(5)	0.0577(10)	0.0526(10)	0.0854(13)
O8	0.31535(17)	0.70150(16)	0.60023(7)	0.0681(5)	0.0563(10)	0.0484(10)	0.0989(15)
O6	0.39508(17)	0.14548(16)	0.48561(7)	0.0666(5)	0.0671(11)	0.0451(10)	0.0868(14)
O12	0.45135(17)	-0.0700(16)	0.61450(7)	0.0681(5)	0.0704(11)	0.0473(10)	0.0865(14)
O7	0.11575(18)	0.79518(16)	0.57491(7)	0.0673(5)	0.0575(10)	0.0362(9)	0.1073(16)
O1	0.06847(18)	1.00860(18)	0.44108(8)	0.0764(6)	0.0648(11)	0.0428(10)	0.1203(17)
O11	0.24206(18)	0.01941(16)	0.59579(8)	0.0741(5)	0.0572(11)	0.0476(10)	0.1168(16)
O2	0.26567(17)	0.90905(16)	0.46484(8)	0.0726(5)	0.0537(10)	0.0557(11)	0.1079(16)

Table 60:- 5.6

Atom label	X	Y	Z	Uiso	Uaniso-U11	Uaniso-U22	Uaniso-U33
Zn1	0	0.301627(13)	0.25	0.0296(11)	0.02291(16)	0.0234(16)	0.0408(2)
Na1	0.30525(5)	0.18323(3)	0.4366(12)	0.0381(2)	0.0326(4)	0.0308(4)	0.0492(5)
O1	0.18022(9)	0.23621(6)	0.3451(2)	0.0397(4)	0.0390(8)	0.0289(7)	0.0491(9)
O2	0.07130(9)	0.24359(7)	0.1438(2)	0.0424(4)	0.0441(8)	0.0398(8)	0.0415(9)
O3	0.20022(8)	0.12275(6)	0.2630(2)	0.0350(3)	0.0274(7)	0.0246(6)	0.0507(9)
O4	0.33570(8)	0.07888(6)	0.3881(2)	0.0333(3)	0.0228(6)	0.0239(6)	0.0512(9)
O5	0.43469(8)	0.15186(6)	0.5716(2)	0.0376(3)	0.0279(7)	0.0295(7)	0.0529(9)
O6	0.54478(9)	0.09854(7)	0.5204(3)	0.0590(5)	0.0230(7)	0.0444(9)	0.1069(16)
O7	0.37467(19)	0.19625(9)	0.1721(3)	0.0920(9)	0.142(2)	0.0612(13)	0.0806(17)
C1	0.12948(11)	0.21565(9)	0.2322(3)	0.0311(4)	0.0283(9)	0.0306(9)	0.0341(11)
C2	0.12782(12)	0.15047(9)	0.1869(3)	0.0335(4)	0.0270(9)	0.0326(10)	0.0393(12)
C3	0.20273(11)	0.06239(8)	0.2553(3)	0.0280(4)	0.0257(9)	0.0244(8)	0.0331(10)
C4	0.14065(11)	0.02628(9)	0.1891(3)	0.0320(4)	0.0239(9)	0.0350(10)	0.0361(11)
C5	0.15048(11)	-0.03595(9)	0.1950(3)	0.0305(4)	0.0290(9)	0.0321(10)	0.0302(11)
C6	0.08643(13)	-0.07481(10)	0.1341(3)	0.0393(5)	0.0311(10)	0.0432(11)	0.0428(13)
C7	0.09677(14)	-0.13440(10)	0.1448(3)	0.0437(5)	0.0419(12)	0.0400(12)	0.0499(14)
C8	0.17154(15)	-0.15810(10)	0.2159(3)	0.0434(5)	0.0523(13)	0.0282(10)	0.0505(15)
C9	0.23521(13)	-0.12196(9)	0.2743(3)	0.0376(5)	0.0400(11)	0.0296(10)	0.0433(13)
C10	0.22600(12)	-0.06000(8)	0.2656(3)	0.0298(4)	0.0305(9)	0.0272(9)	0.0319(11)
C11	0.29034(11)	-0.02156(8)	0.3296(3)	0.0304(4)	0.0255(9)	0.0276(9)	0.0371(11)
C12	0.27880(11)	0.03777(8)	0.3259(3)	0.0277(4)	0.0234(8)	0.0263(9)	0.0328(10)
C13	0.41581(11)	0.05747(8)	0.4358(3)	0.0341(4)	0.0218(8)	0.0256(9)	0.0533(13)
C14	0.47015(11)	0.10658(9)	0.5138(3)	0.0350(5)	0.0246(9)	0.0278(9)	0.0510(13)

Table 61:- 5.7

Atom label	X	Y	Z	Uiso	Uaniso-U11	Uaniso-U22	Uaniso-U33
Zn1	0.88144(5)	0.15631(2)	0.15271(3)	0.04228(15)	0.0393(2)	0.0466(3)	0.0367(2)
C1	0.5636(4)	0.1095(2)	0.0684(2)	0.0406(8)	0.040(2)	0.039(2)	0.0417(18)
C2	0.4138(4)	0.1171(2)	-0.0188(3)	0.0497(9)	0.049(2)	0.042(2)	0.0427(19)
C3	0.3898(4)	0.2506(2)	-0.0290(3)	0.0490(9)	0.043(2)	0.046(2)	0.0436(19)
C4	0.3905(4)	0.2569(2)	0.0549(3)	0.0539(10)	0.052(2)	0.057(3)	0.046(2)
C5	0.3785(4)	0.3283(2)	0.0900(2)	0.0446(9)	0.039(2)	0.051(2)	0.0372(17)
C6	0.3824(5)	0.3334(3)	0.1770(3)	0.0578(11)	0.059(3)	0.068(3)	0.045(2)
C7	0.3741(5)	0.4027(3)	0.2120(3)	0.0652(12)	0.061(3)	0.086(3)	0.051(2)
C8	0.3601(5)	0.4698(3)	0.1613(3)	0.0660(12)	0.072(3)	0.066(3)	0.066(3)
C9	0.3546(5)	0.4668(2)	0.0761(3)	0.0597(11)	0.063(3)	0.050(2)	0.064(3)
C10	0.3655(4)	0.3956(2)	0.0393(3)	0.0475(9)	0.046(2)	0.044(2)	0.050(2)

C11	0.3655(4)	0.3891(2)	-0.0475(3)	0.0544(10)	0.057(3)	0.045(2)	0.058(2)
C12	0.3785(4)	0.3195(2)	-0.0807(3)	0.0490(9)	0.041(2)	0.053(2)	0.045(2)
C13	0.3518(4)	0.3699(2)	-0.2235(3)	0.0511(10)	0.044(2)	0.062(3)	0.045(2)
C14	0.1918(4)	0.3856(2)	-0.2873(2)	0.0458(9)	0.041(2)	0.050(2)	0.0422(19)
C15	1.0042(4)	0.2579(2)	0.3298(3)	0.0550(10)	0.047(2)	0.060(3)	0.056(2)
C16	1.0125(5)	0.3181(3)	0.3867(3)	0.0649(12)	0.055(3)	0.073(3)	0.065(3)
C17	0.9021(6)	0.3694(3)	0.3544(4)	0.0718(13)	0.074(3)	0.058(3)	0.095(4)
C18	0.7828(6)	0.3588(3)	0.2655(4)	0.0722(13)	0.066(3)	0.059(3)	0.091(4)
C19	0.7827(5)	0.2979(2)	0.2125(3)	0.0603(11)	0.055(3)	0.056(3)	0.061(2)
C20	0.9873(5)	0.2898(2)	0.0832(3)	0.0573(10)	0.056(3)	0.063(3)	0.049(2)
C21	0.9906(6)	0.3468(3)	0.0271(3)	0.0687(12)	0.069(3)	0.066(3)	0.076(3)
C22	0.8728(6)	0.3554(3)	-0.0618(4)	0.0758(14)	0.085(4)	0.080(3)	0.081(3)
C23	0.7586(5)	0.3069(3)	-0.0918(3)	0.0735(14)	0.064(3)	0.102(4)	0.052(2)
C24	0.7622(5)	0.2506(3)	-0.0315(3)	0.0608(11)	0.049(3)	0.082(3)	0.047(2)
C25	0.9532(6)	0.0040(3)	0.2798(4)	0.0820(15)	0.078(4)	0.071(3)	0.099(4)
N1	0.8903(3)	0.24753(17)	0.2434(2)	0.0457(7)	0.0456(19)	0.0442(18)	0.0481(17)
N2	0.8775(3)	0.24171(19)	0.0564(2)	0.0497(8)	0.0417(19)	0.063(2)	0.0406(16)
O1	0.6577(3)	0.15506(14)	0.07629(18)	0.0491(6)	0.0396(15)	0.0462(15)	0.0559(15)
O2	0.5808(3)	0.05619(16)	0.12475(18)	0.0560(7)	0.0449(16)	0.0576(17)	0.0551(15)
O3	0.3944(3)	0.18576(14)	-0.0706(17)	0.0503(7)	0.0576(17)	0.0414(14)	0.0395(13)
O4	0.3839(3)	0.30729(15)	-0.1605(17)	0.0504(6)	0.0502(16)	0.0580(17)	0.0387(13)
O5	0.1615(3)	0.4323(2)	-0.3522(3)	0.0928(13)	0.0473(19)	0.119(3)	0.104(3)
O6	0.1051(3)	0.35125(14)	-0.2716(16)	0.0461(6)	0.0378(14)	0.0554(16)	0.0390(12)
O7	0.8779(4)	0.0624(2)	0.0725(2)	0.0673(9)	0.049(2)	0.084(2)	0.0490(17)
O8	0.8680(4)	0.07132(17)	0.2479(2)	0.0527(7)	0.0473(19)	0.0569(18)	0.0465(16)
O9	0.6722(4)	1.0171(2)	0.9001(2)	0.0709(9)	0.058(2)	0.091(3)	0.0635(19)

Table 62:- 5.8

Atom label	X	Y	Z	Uiso	Uaniso-U11	Uaniso-U22	Uaniso-U33
Zn1	0.10884(4)	0.13614(3)	0.83947(2)	0.0439(11)	0.0666(2)	0.0394(17)	0.03809(16)
Na1	0.09306(14)	0.46351(9)	0.86999(9)	0.0485(3)	0.0692(7)	0.0414(5)	0.0463(5)
C1	0.1275(3)	0.2217(2)	0.6595(2)	0.0397(5)	0.0491(14)	0.0338(11)	0.0388(12)
C2	0.1653(3)	0.3165(2)	0.5969(2)	0.0405(5)	0.0563(15)	0.0338(11)	0.0373(11)
C3	0.1754(3)	0.5244(2)	0.6147(2)	0.0361(5)	0.0441(13)	0.0310(11)	0.0373(11)
C4	0.2308(3)	0.5180(2)	0.5135(2)	0.0413(5)	0.0544(15)	0.0354(12)	0.0392(12)
C5	0.2639(3)	0.6230(2)	0.4733(2)	0.0413(5)	0.0478(14)	0.0402(12)	0.0413(12)
C6	0.3196(4)	0.6175(3)	0.3678(2)	0.0539(7)	0.0705(19)	0.0544(16)	0.0488(15)
C7	0.3540(5)	0.7213(3)	0.3319(3)	0.0658(8)	0.089(2)	0.072(2)	0.0596(18)
C8	0.3323(5)	0.8328(3)	0.3990(3)	0.0657(9)	0.092(2)	0.0611(18)	0.072(2)
C9	0.2779(4)	0.8406(3)	0.5018(3)	0.0531(7)	0.0658(18)	0.0471(15)	0.0617(17)
C10	0.2418(3)	0.7356(2)	0.5414(2)	0.0410(5)	0.0453(14)	0.0394(12)	0.0442(12)
C11	0.1844(3)	0.7401(2)	0.6467(2)	0.0411(5)	0.0495(14)	0.0356(12)	0.0431(12)
C12	0.1501(3)	0.6374(2)	0.6829(2)	0.0364(5)	0.0431(13)	0.0353(11)	0.0356(11)
C13	0.0467(4)	0.7333(2)	0.8447(2)	0.0438(6)	0.0644(17)	0.0403(13)	0.0396(12)
C14	-0.0108(3)	0.7153(2)	0.9530(2)	0.0410(5)	0.0520(15)	0.0411(12)	0.0363(12)
C15	-0.3195(4)	-0.1579(3)	0.6198(3)	0.0642(8)	0.062(2)	0.0589(18)	0.0648(19)
C16	-0.3524(5)	-0.1786(4)	0.7194(4)	0.0742(10)	0.062(2)	0.069(2)	0.099(3)
C17	-0.2150(4)	-0.0914(3)	0.8059(3)	0.0609(8)	0.069(2)	0.069(2)	0.0663(19)
C18	0.4007(4)	0.1314(4)	0.8828(3)	0.0656(8)	0.0543(19)	0.077(2)	0.067(2)
C19	0.5593(5)	0.1099(5)	0.9034(5)	0.1150(18)	0.068(3)	0.145(4)	0.181(5)
N1	-0.1031(3)	-0.0237(2)	0.75913(19)	0.0492(5)	0.0643(15)	0.0475(12)	0.0452(12)

N2	-0.1706(3)	-0.0674(2)	0.6449(2)	0.0532(6)	0.0675(17)	0.0488(13)	0.0465(13)
O1	0.1006(2)	0.25889(16)	0.76182(14)	0.0452(4)	0.0687(12)	0.0402(9)	0.0362(8)
O2	0.1287(3)	0.11391(17)	0.60704(17)	0.0552(5)	0.0856(15)	0.0352(9)	0.0536(11)
O3	0.1375(2)	0.42895(15)	0.66112(14)	0.0424(4)	0.0650(11)	0.0349(8)	0.0399(8)
O4	0.0932(2)	0.62993(16)	0.78185(14)	0.0434(4)	0.0661(12)	0.0383(9)	0.0395(9)
O5	-0.0078(3)	0.62475(18)	0.98143(16)	0.0532(5)	0.0826(14)	0.0501(10)	0.0486(10)
O6	-0.0565(3)	0.80585(19)	1.00697(16)	0.0583(5)	0.0989(16)	0.0592(12)	0.0429(10)
O7	0.2641(3)	0.0448(2)	0.8559(3)	0.0862(8)	0.0578(15)	0.0649(15)	0.117(2)
O8	0.4071(3)	0.2398(3)	0.8896(3)	0.0898(8)	0.0757(17)	0.099(2)	0.112(2)
O9	0.3792(4)	0.5593(4)	0.9276(3)	0.1120(11)	0.0759(19)	0.144(3)	0.100(2)
C20	0.4919(7)	0.5410(6)	0.8583(5)	0.1262(19)	0.130(5)	0.130(5)	0.117(4)

Table 63:- 5.9

Atom label	X	Y	Z	Uiso	Uaniso-U11	Uaniso-U22	Uaniso-U33
Zn1	1.03195(4)	0.18696(2)	0.52226(2)	0.04327(16)	0.0389(2)	0.0481(2)	0.0470(3)
C1	0.9191(4)	0.19393(17)	0.3288(2)	0.0411(8)	0.0308(17)	0.0532(18)	0.042(2)
C2	0.7894(4)	0.22907(19)	0.2560(2)	0.0467(8)	0.0380(19)	0.061(2)	0.044(2)
C3	0.5551(4)	0.18936(17)	0.2628(2)	0.0415(8)	0.0345(17)	0.0461(17)	0.0425(19)
C4	0.5819(4)	0.11814(18)	0.2530(2)	0.0484(8)	0.0390(19)	0.053(2)	0.055(2)
C5	0.4757(4)	0.06288(17)	0.2520(19)	0.0467(8)	0.049(2)	0.0465(18)	0.043(2)
C6	0.5015(5)	-0.01208(19)	0.2438(2)	0.0590(10)	0.061(2)	0.050(2)	0.065(2)
C7	0.3978(6)	-0.0630(2)	0.2446(2)	0.0696(12)	0.092(3)	0.042(2)	0.067(3)
C8	0.2634(6)	-0.0431(2)	0.2528(3)	0.0694(12)	0.084(3)	0.053(2)	0.070(3)
C9	0.2310(5)	0.0286(2)	0.2592(2)	0.0571(9)	0.057(2)	0.064(2)	0.056(2)
C10	0.3359(4)	0.08355(17)	0.2596(19)	0.0446(8)	0.054(2)	0.0418(17)	0.0380(19)
C11	0.3093(4)	0.15836(18)	0.2679(19)	0.0439(8)	0.0406(19)	0.0513(18)	0.043(2)
C12	0.4157(4)	0.21012(16)	0.2712(19)	0.0404(7)	0.0387(18)	0.0410(16)	0.0401(19)
C13	0.2643(4)	0.31046(17)	0.2851(2)	0.0441(8)	0.048(2)	0.0434(17)	0.046(2)
C14	0.1288(4)	0.32321(16)	0.2044(2)	0.0420(8)	0.043(2)	0.0416(17)	0.048(2)
C17	0.6936(5)	0.3521(2)	0.4681(3)	0.0754(13)	0.068(3)	0.082(3)	0.075(3)
C16	0.7658(6)	0.3651(2)	0.5475(3)	0.0790(13)	0.089(3)	0.076(3)	0.082(3)
C15	0.8897(5)	0.3165(2)	0.5777(2)	0.0632(11)	0.073(3)	0.066(2)	0.053(2)
C18	0.7514(5)	0.0213(2)	0.5406(3)	0.0746(13)	0.084(3)	0.069(3)	0.072(3)
C19	0.7245(5)	0.0058(2)	0.4651(3)	0.0725(13)	0.081(3)	0.056(2)	0.065(3)
C20	0.8169(5)	0.0543(2)	0.4479(2)	0.0649(11)	0.084(3)	0.057(2)	0.046(2)
C21	1.4336(5)	0.1728(3)	0.4804(2)	0.0668(11)	0.046(2)	0.102(3)	0.059(3)
C22	1.5104(5)	0.1869(3)	0.5587(3)	0.0730(13)	0.035(2)	0.116(4)	0.062(3)
C23	1.3923(4)	0.1956(2)	0.5837(2)	0.0568(10)	0.039(2)	0.082(3)	0.046(2)
C24	0.0760(10)	0.4006(6)	0.4184(5)	0.218(5)	0.129(7)	0.297(14)	0.163(8)
C25	0.2304(16)	0.4086(7)	0.5559(5)	0.280(8)	0.407(19)	0.280(15)	0.101(7)
C26	0.3440(10)	0.4426(5)	0.4722(8)	0.186(5)	0.093(6)	0.136(7)	0.284(14)
N1	0.8948(3)	0.27507(15)	0.5207(17)	0.0495(7)	0.0486(18)	0.0537(16)	0.0495(18)
N2	0.7726(4)	0.29811(17)	0.4542(19)	0.0589(8)	0.053(2)	0.070(2)	0.051(2)
N3	0.8976(3)	0.09721(15)	0.5096(17)	0.0490(7)	0.0522(18)	0.0484(15)	0.0462(17)
N4	0.8544(4)	0.07570(17)	0.5661(2)	0.0565(8)	0.060(2)	0.0611(18)	0.051(2)
N5	1.2503(3)	0.18681(14)	0.5232(16)	0.0444(7)	0.0396(16)	0.0547(16)	0.0393(16)
N6	1.2790(4)	0.17277(17)	0.4603(2)	0.0508(8)	0.0377(18)	0.074(2)	0.0397(19)
N7	0.2188(6)	0.4214(3)	0.4749(3)	0.0996(14)	0.080(3)	0.101(3)	0.102(4)
O1	0.9140(3)	0.20377(14)	0.3935(14)	0.0510(6)	0.0426(14)	0.0748(16)	0.0388(14)
O2	1.0225(3)	0.16006(16)	0.3181(15)	0.0624(7)	0.0378(14)	0.0975(19)	0.0528(16)
O3	0.6511(2)	0.24710(11)	0.2663(14)	0.0444(5)	0.0330(12)	0.0443(12)	0.0586(15)

O4	0.4060(3)	0.28339(11)	0.2836(13)	0.0433(5)	0.0381(13)	0.0400(11)	0.0534(14)
O5	0.0060(3)	0.34896(15)	0.2040(16)	0.0639(7)	0.0531(16)	0.0874(19)	0.0619(17)
O6	0.1515(3)	0.30866(13)	0.1447(14)	0.0529(6)	0.0492(15)	0.0702(16)	0.0412(14)
O7	0.3378(8)	0.4592(3)	0.4021(3)	0.152(2)	0.202(6)	0.142(4)	0.153(5)
Table 64:- 5.10							
Atom label	X	Y	Z	Uiso	Uaniso-U11	Uaniso-U22	Uaniso-U33
Zn1	0.59182(6)	0.13363(4)	0.42929(3)	0.0350(2)	0.0317(4)	0.0381(4)	0.0354(4)
Zn2	0.90530(6)	0.11002(4)	0.24545(3)	0.0359(2)	0.0311(4)	0.0404(4)	0.0373(4)
Zn3	0.35462(6)	0.86669(5)	0.25566(3)	0.0368(2)	0.0297(4)	0.0415(5)	0.0383(4)
Zn4	0.04041(7)	0.85287(5)	0.06644(3)	0.0421(2)	0.0467(5)	0.0422(5)	0.0369(4)
C1	0.7813(5)	0.1983(4)	0.5342(3)	0.0364(14)	0.033(3)	0.034(4)	0.042(4)
C2	0.8908(5)	0.2583(4)	0.5551(3)	0.0368(14)	0.033(3)	0.035(4)	0.043(4)
C3	1.0524(5)	0.2804(4)	0.6277(3)	0.0360(14)	0.028(3)	0.040(4)	0.040(3)
C4	1.0971(6)	0.3510(4)	0.6111(3)	0.0389(15)	0.039(3)	0.034(4)	0.043(4)
C5	1.2072(6)	0.3948(4)	0.6379(3)	0.0394(15)	0.033(3)	0.034(4)	0.052(4)
C6	1.2534(7)	0.4695(4)	0.6214(4)	0.0519(19)	0.047(4)	0.033(4)	0.073(5)
C7	1.3600(7)	0.5085(5)	0.6460(4)	0.063(2)	0.055(5)	0.038(4)	0.092(6)
C8	1.4242(7)	0.4766(5)	0.6899(4)	0.062(2)	0.042(4)	0.047(5)	0.088(6)
C9	1.3804(6)	0.4045(4)	0.7052(4)	0.0509(18)	0.042(4)	0.045(4)	0.061(5)
C10	1.2703(6)	0.3623(4)	0.6802(3)	0.0403(15)	0.034(3)	0.032(4)	0.051(4)
C11	1.2224(6)	0.2869(4)	0.6959(3)	0.0418(16)	0.032(3)	0.047(4)	0.046(4)
C12	1.1170(5)	0.2470(4)	0.6713(3)	0.0339(14)	0.032(3)	0.025(3)	0.044(4)
C13	1.1296(6)	0.1327(4)	0.7187(4)	0.0437(16)	0.035(3)	0.028(3)	0.069(5)
C14	1.0621(6)	0.0510(4)	0.7210(3)	0.0363(14)	0.037(3)	0.034(4)	0.036(3)
C15	0.7226(6)	0.1956(4)	0.3244(3)	0.0354(14)	0.035(3)	0.042(4)	0.030(3)
C16	0.7472(6)	0.2682(4)	0.2936(3)	0.0399(15)	0.036(3)	0.043(4)	0.041(4)
C17	0.8796(6)	0.3180(4)	0.2210(3)	0.0383(15)	0.038(3)	0.040(4)	0.037(3)
C18	0.8334(6)	0.3862(4)	0.2210(3)	0.0399(15)	0.042(4)	0.035(4)	0.044(4)
C19	0.8786(6)	0.4409(4)	0.1818(3)	0.0404(15)	0.041(4)	0.032(4)	0.047(4)
C20	0.8326(7)	0.5122(5)	0.1799(4)	0.058(2)	0.056(5)	0.045(5)	0.076(6)
C21	0.8798(8)	0.5647(5)	0.1429(5)	0.068(2)	0.077(6)	0.038(5)	0.096(7)
C22	0.9724(9)	0.5466(5)	0.1055(5)	0.073(3)	0.080(6)	0.051(5)	0.091(7)
C23	1.0187(8)	0.4795(5)	0.1058(4)	0.062(2)	0.068(5)	0.049(5)	0.071(6)
C24	0.9710(6)	0.4235(4)	0.1434(3)	0.0430(16)	0.043(4)	0.037(4)	0.050(4)
C25	1.0161(6)	0.3518(4)	0.1430(3)	0.0437(16)	0.041(4)	0.044(4)	0.049(4)
C26	0.9711(6)	0.2989(4)	0.1808(3)	0.0384(15)	0.036(3)	0.038(4)	0.043(4)
C27	1.0893(6)	0.2014(4)	0.1432(3)	0.0436(16)	0.039(4)	0.044(4)	0.050(4)
C28	1.0947(6)	0.1147(4)	0.1451(3)	0.0387(15)	0.034(3)	0.040(4)	0.042(4)
C29	0.3519(8)	0.2800(6)	0.5159(4)	0.066(2)	0.060(5)	0.074(6)	0.062(5)
C30	0.4193(9)	0.3362(6)	0.4922(5)	0.075(3)	0.073(6)	0.055(6)	0.094(7)
C31	0.4976(8)	0.2966(5)	0.4551(4)	0.066(2)	0.062(5)	0.052(5)	0.086(6)
C32	1.2287(7)	0.1679(5)	0.3423(4)	0.055(2)	0.040(4)	0.070(6)	0.054(5)
C33	1.1997(8)	0.2411(6)	0.3557(4)	0.068(2)	0.064(5)	0.062(6)	0.068(6)
C34	1.0885(8)	0.2349(5)	0.3286(4)	0.065(2)	0.073(6)	0.049(5)	0.069(5)
C35	0.1930(6)	0.8023(4)	-0.0426(3)	0.0388(15)	0.040(4)	0.040(4)	0.036(4)
C36	0.2735(6)	0.7451(4)	-0.0696(3)	0.0418(15)	0.041(4)	0.042(4)	0.044(4)
C37	0.4231(6)	0.7330(4)	-0.1427(3)	0.0387(15)	0.032(3)	0.037(4)	0.045(4)
C38	0.4375(6)	0.6589(4)	-0.1301(3)	0.0436(16)	0.043(4)	0.043(4)	0.049(4)
C39	0.5281(6)	0.6201(4)	-0.1581(3)	0.0434(16)	0.044(4)	0.033(4)	0.050(4)
C40	0.5464(7)	0.5445(5)	-0.1444(4)	0.056(2)	0.061(5)	0.041(4)	0.066(5)
C41	0.6376(9)	0.5089(5)	-0.1689(4)	0.069(2)	0.077(6)	0.045(5)	0.086(7)

C42	0.7119(8)	0.5459(5)	-0.2105(4)	0.064(2)	0.055(5)	0.055(5)	0.082(6)
C43	0.6968(7)	0.6182(5)	-0.2253(4)	0.056(2)	0.048(4)	0.051(5)	0.064(5)
C44	0.6034(6)	0.6569(4)	-0.1988(3)	0.0433(16)	0.034(3)	0.046(4)	0.047(4)
C45	0.5879(6)	0.7338(4)	-0.2099(3)	0.0448(16)	0.037(4)	0.046(4)	0.052(4)
C46	0.5016(5)	0.7715(4)	-0.1825(3)	0.0366(14)	0.031(3)	0.033(4)	0.044(4)
C47	0.5642(6)	0.8900(4)	-0.2236(3)	0.0428(16)	0.045(4)	0.030(4)	0.053(4)
C48	0.5383(6)	0.9738(4)	-0.2193(3)	0.0417(16)	0.037(4)	0.044(4)	0.043(4)
C49	0.1352(6)	0.7831(4)	0.1729(3)	0.0390(15)	0.038(3)	0.047(4)	0.033(3)
C50	0.1175(6)	0.7164(4)	0.2106(3)	0.0445(16)	0.036(3)	0.051(4)	0.044(4)
C51	0.2208(6)	0.6686(4)	0.2882(3)	0.0369(14)	0.038(3)	0.032(4)	0.040(4)
C52	0.1356(6)	0.6055(4)	0.2928(3)	0.0397(15)	0.038(3)	0.033(4)	0.046(4)
C53	0.1476(6)	0.5556(4)	0.3376(3)	0.0413(15)	0.043(4)	0.033(4)	0.047(4)
C54	0.0596(7)	0.4913(4)	0.3453(4)	0.0518(18)	0.048(4)	0.042(4)	0.062(5)
C55	0.0714(8)	0.4449(5)	0.3896(4)	0.065(2)	0.073(6)	0.043(5)	0.075(6)
C56	0.1746(9)	0.4607(5)	0.4279(4)	0.069(2)	0.092(7)	0.046(5)	0.071(6)
C57	0.2640(8)	0.5214(5)	0.4207(4)	0.061(2)	0.073(6)	0.045(5)	0.068(5)
C58	0.2514(6)	0.5701(4)	0.3760(3)	0.0449(16)	0.047(4)	0.037(4)	0.052(4)
C59	0.3398(6)	0.6372(4)	0.3700(3)	0.0437(16)	0.039(4)	0.044(4)	0.048(4)
C60	0.3228(6)	0.6853(4)	0.3279(3)	0.0356(14)	0.036(3)	0.030(3)	0.039(3)
C61	0.4920(5)	0.7803(4)	0.3631(3)	0.0392(15)	0.032(3)	0.039(4)	0.045(4)
C62	0.5377(5)	0.8655(4)	0.3591(3)	0.0359(14)	0.031(3)	0.043(4)	0.032(3)
C63	-0.2843(9)	0.7354(8)	-0.0262(5)	0.092(3)	0.062(6)	0.114(10)	0.089(8)
C64	-0.2445(11)	0.6712(8)	-0.0109(6)	0.108(4)	0.099(9)	0.099(9)	0.102(9)
C65	-0.1409(11)	0.6995(7)	0.0217(6)	0.098(4)	0.105(9)	0.069(7)	0.117(9)
C66	0.6493(8)	0.8084(6)	0.1573(4)	0.070(3)	0.057(5)	0.093(8)	0.072(6)
C67	0.5977(10)	0.7349(7)	0.1543(5)	0.087(3)	0.091(8)	0.081(8)	0.092(8)
C68	0.4909(9)	0.7382(6)	0.1838(5)	0.076(3)	0.072(6)	0.057(6)	0.092(7)
C69	0.4429(14)	0.9156(18)	0.0573(9)	0.267(17)	0.078(11)	0.54(5)	0.152(17)
C70	0.5507(15)	0.8997(15)	-0.0384(7)	0.217(12)	0.122(13)	0.39(3)	0.090(11)
C71	0.6597(12)	0.9579(10)	0.0580(6)	0.123(5)	0.082(9)	0.171(15)	0.095(9)
C72	0.1036(9)	0.1203(7)	0.5276(5)	0.089(3)	0.066(6)	0.113(9)	0.080(7)
C73	-0.0316(8)	0.0699(7)	0.4374(5)	0.084(3)	0.046(5)	0.128(9)	0.082(7)
C74	0.1693(7)	0.0382(5)	0.4408(4)	0.059(2)	0.054(5)	0.079(6)	0.046(4)
N1	0.4772(5)	0.2204(4)	0.4583(3)	0.0449(14)	0.038(3)	0.050(4)	0.048(3)
N2	0.3863(6)	0.2117(4)	0.4958(3)	0.0565(17)	0.046(4)	0.064(4)	0.060(4)
N3	1.0497(5)	0.1622(4)	0.3017(3)	0.0450(14)	0.043(3)	0.051(4)	0.041(3)
N4	1.1389(5)	0.1215(4)	0.3099(3)	0.0461(14)	0.043(3)	0.047(4)	0.050(3)
N5	0.4783(5)	0.8114(4)	0.2038(3)	0.0459(14)	0.042(3)	0.046(4)	0.048(3)
N6	0.5784(6)	0.8541(4)	0.1874(3)	0.0586(17)	0.046(4)	0.063(4)	0.070(4)
N7	-0.1167(6)	0.7775(4)	0.0280(3)	0.0490(15)	0.053(4)	0.052(4)	0.040(3)
N8	-0.2059(7)	0.7970(5)	-0.0022(4)	0.078(2)	0.073(5)	0.079(6)	0.077(5)
N9	0.5559(10)	0.9355(14)	0.0233(7)	0.228(11)	0.063(7)	0.46(3)	0.123(11)
N10	0.0826(6)	0.0724(5)	0.4685(3)	0.0644(19)	0.041(4)	0.090(6)	0.064(4)
O1	0.7343(4)	0.2088(3)	0.4847(2)	0.0439(11)	0.046(3)	0.042(3)	0.040(3)
O2	0.7455(4)	0.1470(3)	0.5666(2)	0.0516(13)	0.046(3)	0.057(3)	0.048(3)
O3	0.9482(4)	0.2345(3)	0.6061(2)	0.0408(11)	0.031(2)	0.042(3)	0.049(3)
O4	1.0626(4)	0.1746(3)	0.6829(2)	0.0411(11)	0.035(2)	0.035(3)	0.053(3)
O5	1.1266(4)	0.0022(3)	0.7347(2)	0.0440(11)	0.035(2)	0.043(3)	0.059(3)
O6	0.9524(4)	0.0372(3)	0.7117(3)	0.0514(13)	0.032(2)	0.045(3)	0.081(4)
O7	0.6365(4)	0.1971(3)	0.3599(2)	0.0428(11)	0.042(3)	0.051(3)	0.041(3)
O8	0.7832(4)	0.1416(3)	0.3145(2)	0.0458(12)	0.047(3)	0.043(3)	0.053(3)
O9	0.8467(4)	0.2611(3)	0.2565(2)	0.0489(12)	0.050(3)	0.047(3)	0.057(3)
O10	1.0042(4)	0.2277(3)	0.1849(2)	0.0446(11)	0.048(3)	0.040(3)	0.051(3)

O11	1.0233(4)	0.0760(3)	0.1760(2)	0.0405(10)	0.038(2)	0.036(3)	0.047(3)
O12	1.1708(5)	0.0868(3)	0.1121(3)	0.0601(15)	0.056(3)	0.049(3)	0.080(4)
O13	0.5481(4)	0.0783(3)	0.5070(2)	0.0493(12)	0.049(3)	0.053(3)	0.044(3)
O14	0.4476(5)	0.0576(3)	0.3800(2)	0.0424(12)	0.035(3)	0.046(3)	0.043(3)
O15	0.7027(4)	0.0503(3)	0.3998(2)	0.0440(11)	0.032(2)	0.044(3)	0.059(3)
O16	0.7756(5)	0.0952(4)	0.1814(3)	0.0508(15)	0.033(3)	0.073(4)	0.051(3)
O17	0.1460(5)	0.7862(3)	0.0058(2)	0.0506(12)	0.060(3)	0.051(3)	0.044(3)
O18	0.1789(5)	0.8591(3)	-0.0692(2)	0.0562(14)	0.061(3)	0.066(4)	0.052(3)
O19	0.3399(4)	0.7762(3)	-0.1171(2)	0.0462(12)	0.038(3)	0.051(3)	0.055(3)
O20	0.4795(4)	0.8455(3)	-0.1896(2)	0.0457(12)	0.037(2)	0.040(3)	0.066(3)
O21	0.4373(4)	0.9885(3)	-0.2062(3)	0.0606(15)	0.039(3)	0.050(3)	0.098(4)
O22	0.6236(4)	1.0224(3)	-0.2338(2)	0.0471(12)	0.035(2)	0.049(3)	0.060(3)
O23	0.0553(4)	0.7796(3)	0.1320(2)	0.0464(12)	0.042(3)	0.051(3)	0.043(3)
O24	0.2241(4)	0.8366(3)	0.1833(2)	0.0469(12)	0.042(3)	0.050(3)	0.045(3)
O25	0.2216(4)	0.7197(3)	0.2467(2)	0.0459(12)	0.037(2)	0.048(3)	0.052(3)
O26	0.3959(4)	0.7515(3)	0.3200(2)	0.0439(11)	0.041(3)	0.043(3)	0.044(3)
O27	0.4839(4)	0.9042(3)	0.3271(2)	0.0406(10)	0.037(2)	0.038(3)	0.046(3)
O28	0.6285(4)	0.8941(3)	0.3926(3)	0.0569(14)	0.047(3)	0.043(3)	0.075(4)
O29	0.1885(4)	0.9331(3)	0.1016(2)	0.0509(12)	0.044(3)	0.045(3)	0.062(3)
O30	0.0212(6)	0.9232(3)	-0.0043(3)	0.0682(17)	0.095(4)	0.067(4)	0.056(3)
O31	-0.0723(5)	0.9236(4)	0.1207(3)	0.0531(14)	0.048(3)	0.047(4)	0.059(3)
O32	0.2272(4)	0.8851(3)	0.3170(2)	0.0465(12)	0.033(2)	0.065(3)	0.047(3)
O33	0.7491(7)	0.9480(5)	0.0403(4)	0.107(3)	0.073(5)	0.098(6)	0.146(8)
O34	0.2718(4)	0.0480(3)	0.4613(2)	0.0583(14)	0.041(3)	0.069(4)	0.064(3)
O35	0.8056(8)	0.3563(5)	0.4448(4)	0.118(3)	0.133(7)	0.112(7)	0.103(6)

Table 65:- 5.11

Atom label	X	Y	Z	Uiso	Uaniso-U11	Uaniso-U22	Uaniso-U33
Zn1	1.03025(6)	0.13414(4)	0.33441(4)	0.0586(4)	0.0626(5)	0.0608(6)	0.0530(5)
C1	0.82447(13)	0.1643(2)	0.2559(16)	0.0612(16)	0.061(4)	0.076(5)	0.051(4)
C2	0.69927(19)	0.1793(3)	0.2046(3)	0.072(2)	0.066(4)	0.091(5)	0.058(4)
C3	0.5778(5)	0.1255(4)	0.2836(4)	0.0606(16)	0.051(3)	0.076(5)	0.052(4)
C4	0.6027(5)	0.1760(4)	0.3391(4)	0.0625(16)	0.056(3)	0.064(4)	0.066(4)
C5	0.5569(5)	0.1706(4)	0.4093(4)	0.0593(16)	0.055(3)	0.059(4)	0.060(4)
C6	0.5774(7)	0.2252(4)	0.4686(4)	0.0734(19)	0.086(5)	0.058(4)	0.076(5)
C7	0.5312(7)	0.2185(5)	0.5328(5)	0.088(2)	0.090(5)	0.097(6)	0.077(5)
C8	0.4622(8)	0.1537(5)	0.5410(5)	0.090(3)	0.100(6)	0.111(7)	0.067(5)
C9	0.4391(7)	0.1026(4)	0.4868(4)	0.0727(19)	0.080(4)	0.074(5)	0.070(5)
C10	0.4855(5)	0.1071(4)	0.4177(4)	0.0618(16)	0.055(3)	0.069(4)	0.058(4)
C11	0.4608(6)	0.0551(4)	0.3568(4)	0.0663(17)	0.066(4)	0.066(4)	0.068(4)
C12	0.5040(6)	0.0610(4)	0.2908(4)	0.0665(17)	0.064(4)	0.074(4)	0.059(4)
C13	0.4017(6)	-0.0438(4)	0.2325(4)	0.0732(19)	0.078(4)	0.072(5)	0.067(5)
C14	0.3777(8)	-0.0857(5)	0.1537(5)	0.088(2)	0.093(6)	0.084(6)	0.086(6)
C27	0.9432(8)	0.2454(5)	0.4498(5)	0.090(2)	0.106(6)	0.073(5)	0.087(6)
C28	0.9355(9)	0.2737(6)	0.5225(6)	0.102(3)	0.117(7)	0.085(6)	0.111(8)
C29	0.9907(8)	0.2348(5)	0.5871(5)	0.086(2)	0.097(6)	0.092(6)	0.075(6)
C30	1.0523(6)	0.1693(4)	0.5806(4)	0.0693(19)	0.073(4)	0.078(5)	0.063(5)
C31	1.1107(8)	0.1231(5)	0.6456(4)	0.084(2)	0.110(6)	0.095(6)	0.047(4)
C32	1.1637(7)	0.0607(5)	0.6340(4)	0.082(2)	0.090(5)	0.096(6)	0.057(5)
C33	1.1641(6)	0.0326(4)	0.5583(4)	0.0669(18)	0.061(4)	0.077(5)	0.059(4)
C34	1.2138(6)	-0.0348(4)	0.5434(5)	0.0684(18)	0.067(4)	0.059(4)	0.076(5)

C35	1.2061(6)	-0.0565(4)	0.4693(5)	0.074(2)	0.066(4)	0.055(4)	0.099(6)
C36	1.1523(5)	-0.0108(4)	0.4068(4)	0.0644(17)	0.060(4)	0.060(4)	0.074(5)
C37	1.1091(5)	0.0765(3)	0.4934(4)	0.0544(15)	0.049(3)	0.058(4)	0.057(4)
C38	1.0547(6)	0.1452(4)	0.5046(4)	0.0594(16)	0.058(3)	0.066(4)	0.055(4)
N3	1.0019(5)	0.1836(3)	0.4398(3)	0.0651(14)	0.076(3)	0.054(3)	0.067(4)
N4	1.1055(4)	0.0541(3)	0.4179(3)	0.0551(12)	0.054(3)	0.055(3)	0.057(3)
O1	0.9012(4)	0.2145(3)	0.2557(3)	0.0693(12)	0.066(3)	0.066(3)	0.074(3)
O2	0.8478(4)	0.1046(3)	0.2905(3)	0.0652(12)	0.068(3)	0.065(3)	0.063(3)
O3	0.6159(4)	0.1254(3)	0.2143(3)	0.0765(14)	0.063(3)	0.106(4)	0.061(3)
O4	0.4837(4)	0.0153(3)	0.2293(3)	0.0795(14)	0.083(3)	0.093(4)	0.065(3)
O5	0.4342(8)	-0.0709(5)	0.1053(4)	0.137(3)	0.194(8)	0.141(7)	0.091(5)
O6	0.2986(7)	-0.1358(4)	0.1502(4)	0.115(2)	0.128(5)	0.095(5)	0.118(5)
O7	0.3075(9)	0.4842(5)	0.3489(6)	0.166(3)	0.197(9)	0.117(6)	0.203(9)
O8	0.1508(9)	0.8697(4)	0.2571(6)	0.157(4)	0.231(10)	0.082(5)	0.198(9)
O9	0.7602(8)	0.0858(6)	0.0402(4)	0.163(4)	0.199(8)	0.195(9)	0.090(5)
N1	1.1793(8)	0.2058(6)	0.3355(7)	0.055(3)			
N2	1.0895(9)	0.0962(6)	0.2350(5)	0.063(3)			
C15	1.2203(11)	0.2576(7)	0.3875(8)	0.069(3)			
C16	1.3150(11)	0.3043(8)	0.3736(9)	0.085(4)			
C17	1.3535(15)	0.2941(8)	0.3128(9)	0.081(4)			
C18	1.3150(12)	0.2411(8)	0.2561(8)	0.074(3)			
C19	1.3550(12)	0.2265(9)	0.1894(9)	0.085(4)			
C20	1.3065(15)	0.1626(12)	0.1319(10)	0.083(5)			
C21	1.2238(12)	0.1302(7)	0.1490(8)	0.074(3)			
C22	1.1736(13)	0.0689(9)	0.1036(10)	0.092(4)			
C23	1.0813(16)	0.0232(9)	0.1143(9)	0.098(5)			
C24	1.0406(11)	0.0458(7)	0.1862(7)	0.071(3)			
C25	1.1772(10)	0.1397(8)	0.2196(7)	0.057(3)			
C26	1.2211(9)	0.1969(6)	0.2735(7)	0.054(3)			
C19'	1.3288(16)	0.1897(12)	0.1478(12)	0.054(5)			
C20'	1.267(3)	0.118(2)	0.105(2)	0.127(10)			
N1'	1.1744(11)	0.1903(8)	0.3092(9)	0.076(6)			
C15'	1.2307(16)	0.2499(10)	0.3525(9)	0.094(7)			
C16'	1.3216(17)	0.2876(10)	0.3282(12)	0.17(2)			
C17'	1.3563(14)	0.2656(11)	0.2605(13)	0.112(9)			
C18'	1.3001(13)	0.2059(10)	0.2171(9)	0.101(7)			
C26'	1.2091(12)	0.1683(8)	0.2415(9)	0.062(5)			
N2'	1.0618(4)	0.0778(4)	0.2328(16)	0.061(5)			
C24'	1.0034(6)	0.0172(4)	0.1924(4)	0.074(5)			
C23'	1.0355(8)	-0.0077(7)	0.1248(4)	0.120(9)			
C22'	1.1258(8)	0.0279(9)	0.0977(3)	0.114(10)			
C21'	1.1842(6)	0.0884(8)	0.1383(2)	0.103(8)			
C25'	1.1521(4)	0.1134(6)	0.2058(16)	0.064(5)			

Table 66:- 5.12

Ato m label	X	Y	Z	Uiso	Uaniso- U11	Uaniso- U22	Uaniso- U33
Zn1	0.22317(3)	0.47607(3)	0.25687(2)	0.05043(16)	0.0412(2)	0.0569(3)	0.0443(2)
C1	0.0617(3)	0.5185(3)	0.3441(2)	0.0597(9)	0.0403(17)	0.074(2)	0.0508(19)
C2	-0.0298(3)	0.5495(4)	0.3974(2)	0.0584(9)	0.0504(18)	0.081(2)	0.0463(17)
C3	-0.2322(3)	0.5266(3)	0.2750(2)	0.0458(7)	0.0405(15)	0.0626(19)	0.0439(15)
C4	-0.2640(3)	0.4042(3)	0.2458(2)	0.0504(7)	0.0512(18)	0.0589(19)	0.0568(18)

C5	-0.3825(3)	0.3344(3)	0.1681(2)	0.0506(7)	0.0510(18)	0.0554(18)	0.0601(19)
C6	-0.4216(4)	0.2059(3)	0.1384(3)	0.0647(9)	0.075(2)	0.0532(19)	0.084(3)
C7	-0.5391(5)	0.1423(4)	0.0667(3)	0.0755(11)	0.082(3)	0.050(2)	0.091(3)
C8	-0.6188(4)	0.2046(4)	0.0204(3)	0.0726(11)	0.060(2)	0.060(2)	0.079(3)
C9	-0.5836(3)	0.3280(3)	0.0458(3)	0.0586(8)	0.0461(18)	0.060(2)	0.069(2)
C10	-0.4648(3)	0.3969(3)	0.1214(2)	0.0476(7)	0.0421(16)	0.0486(16)	0.0562(18)
C11	-0.4261(3)	0.5268(3)	0.1523(2)	0.0468(7)	0.0379(15)	0.0509(17)	0.0551(18)
C12	-0.3135(3)	0.5911(3)	0.2262(2)	0.0444(7)	0.0405(15)	0.0459(16)	0.0543(17)
C13	-0.3431(4)	0.7866(3)	0.2235(3)	0.0571(8)	0.0566(19)	0.0463(17)	0.066(2)
C14	-0.2591(4)	0.9185(3)	0.2556(3)	0.0629(9)	0.061(2)	0.057(2)	0.068(2)
C15	0.3674(4)	0.7528(3)	0.3541(3)	0.0636(9)	0.060(2)	0.060(2)	0.063(2)
C16	0.4735(4)	0.8540(4)	0.4075(3)	0.0719(11)	0.079(3)	0.058(2)	0.065(2)
C17	0.5946(4)	0.8368(4)	0.4519(3)	0.0779(12)	0.068(3)	0.063(2)	0.071(3)
C18	0.6061(4)	0.7205(4)	0.4429(3)	0.0698(10)	0.0486(19)	0.077(3)	0.058(2)
C19	0.4951(3)	0.6222(3)	0.3881(2)	0.0505(7)	0.0414(16)	0.065(2)	0.0392(15)
C20	0.4967(3)	0.4926(3)	0.3750(2)	0.0475(7)	0.0424(16)	0.0621(19)	0.0394(15)
C21	0.6030(3)	0.4596(4)	0.4262(2)	0.0593(9)	0.0431(17)	0.086(3)	0.0524(19)
C22	0.5970(4)	0.3382(4)	0.4097(3)	0.0707(11)	0.060(2)	0.101(3)	0.075(3)
C23	0.4853(4)	0.2514(4)	0.3423(3)	0.0722(10)	0.079(3)	0.076(3)	0.083(3)
C24	0.3835(4)	0.2901(3)	0.2948(3)	0.0633(9)	0.061(2)	0.063(2)	0.066(2)
C25	0.2673(3)	0.6090(3)	0.1120(2)	0.0522(7)	0.0408(16)	0.0599(19)	0.0544(18)
C26	0.2518(3)	0.6233(3)	0.0258(3)	0.0591(9)	0.0504(19)	0.072(2)	0.068(2)
C27	0.1703(4)	0.5274(4)	-0.0512(2)	0.0619(9)	0.060(2)	0.091(3)	0.054(2)
C28	0.1069(3)	0.4203(3)	-0.0385(2)	0.0559(8)	0.0501(18)	0.071(2)	0.0444(17)
C29	0.1277(3)	0.4122(3)	0.0515(2)	0.0461(7)	0.0367(15)	0.0547(17)	0.0443(16)
C30	0.0587(3)	0.3016(3)	0.0712(2)	0.0500(7)	0.0382(15)	0.0502(17)	0.0544(18)
C31	-0.0316(4)	0.1990(3)	0.0012(3)	0.0709(11)	0.066(2)	0.059(2)	0.064(2)
C32	-0.0975(5)	0.1051(4)	0.0260(4)	0.0925(15)	0.083(3)	0.062(3)	0.094(3)
C33	-0.0709(5)	0.1156(4)	0.1192(4)	0.0997(16)	0.089(3)	0.070(3)	0.120(4)
C34	0.0199(4)	0.2183(4)	0.1850(3)	0.0807(12)	0.076(3)	0.070(3)	0.081(3)
N1	0.3767(3)	0.6388(3)	0.34390(18)	0.0524(6)	0.0450(14)	0.0586(16)	0.0461(14)
N2	0.3862(3)	0.4085(3)	0.31032(18)	0.0514(6)	0.0463(14)	0.0584(16)	0.0446(14)
N3	0.2074(2)	0.5050(2)	0.12592(17)	0.0450(6)	0.0369(12)	0.0510(14)	0.0446(13)
N4	0.0842(3)	0.3112(3)	0.1617(2)	0.0564(7)	0.0482(15)	0.0576(16)	0.0553(16)
O1	0.0645(2)	0.5603(3)	0.27703(17)	0.0653(6)	0.0516(13)	0.0857(18)	0.0556(14)
O2	0.1350(3)	0.4554(3)	0.37058(19)	0.0766(8)	0.0570(15)	0.0922(19)	0.0764(17)
O3	-0.1253(2)	0.6033(2)	0.35143(15)	0.0565(6)	0.0524(13)	0.0687(15)	0.0508(12)
O4	-0.2639(2)	0.7147(2)	0.26092(16)	0.0552(6)	0.0468(12)	0.0491(12)	0.0640(14)
O5	-0.1350(3)	0.9397(3)	0.2816(3)	0.0956(11)	0.0590(17)	0.0585(17)	0.154(3)
O6	-0.3202(3)	0.9959(2)	0.2517(2)	0.0927(10)	0.0771(19)	0.0519(15)	0.134(3)
O7	0.0255(4)	0.7836(4)	0.2441(3)	0.0840(9)	0.070(2)	0.083(2)	0.094(3)
O8	0.2314(4)	0.9915(4)	0.2808(4)	0.1425(17)	0.095(3)	0.099(3)	0.238(5)
O9	0.3909(5)	0.9064(4)	0.1730(3)	0.1026(12)	0.091(3)	0.073(2)	0.121(3)
O10	0.0928(3)	0.1275(3)	0.3738(3)	0.1090(12)	0.078(2)	0.107(3)	0.116(3)
O11	0.0499(6)	0.1382(4)	0.5438(3)	0.1508(18)	0.179(5)	0.139(4)	0.102(3)
O12	0.8424(6)	0.2171(5)	0.3862(5)	0.221(4)	0.159(5)	0.124(4)	0.264(7)

Table 67:- 6.1A

Ato m label	X	Y	Z	Uiso	Uaniso- U11	Uaniso- U22	Uaniso- U33
C1	0.6261(2)	0.1171(2)	0.08474(14)	0.0535(5)	0.0625(14)	0.0456(13)	0.0562(12)
C2	0.7554(2)	0.0909(2)	0.03813(17)	0.0707(7)	0.0648(16)	0.0672(17)	0.0855(17)

C3	0.8314(3)	-0.0295(3)	0.0047(2)	0.0876(8)	0.0660(16)	0.085(2)	0.108(2)
C4	0.7785(3)	-0.1205(3)	0.0172(2)	0.0878(8)	0.090(2)	0.0610(18)	0.113(2)
C5	0.6461(3)	-0.0976(2)	0.06482(17)	0.0667(6)	0.0860(18)	0.0501(15)	0.0708(15)
C6	0.5683(2)	0.0217(2)	0.10074(14)	0.0548(5)	0.0735(15)	0.0498(14)	0.0510(12)
C7	0.3881(3)	-0.0393(3)	0.15871(16)	0.0732(7)	0.1004(19)	0.0714(18)	0.0693(15)
C8	0.4564(4)	-0.1580(3)	0.12280(19)	0.0827(8)	0.132(3)	0.0663(19)	0.0811(17)
C9	0.5838(3)	-0.1869(2)	0.07772(19)	0.0806(8)	0.125(3)	0.0475(16)	0.0861(18)
C10	0.5895(2)	0.3339(2)	0.09187(16)	0.0587(6)	0.0590(13)	0.0532(14)	0.0710(14)
C11	0.4842(2)	0.4571(2)	0.11785(14)	0.0544(5)	0.0671(14)	0.0495(14)	0.0550(12)
C12	0.2525(2)	0.5710(2)	0.18336(15)	0.0641(6)	0.0678(15)	0.0553(15)	0.0582(13)
C13	0.1574(3)	0.5902(3)	0.13768(18)	0.0765(7)	0.0627(16)	0.083(2)	0.0739(16)
C14	0.0528(3)	0.7028(4)	0.1492(3)	0.1065(10)	0.072(2)	0.102(3)	0.118(3)
C15	0.0442(4)	0.7918(4)	0.2040(3)	0.1247(13)	0.088(3)	0.087(3)	0.147(3)
C16	0.1361(4)	0.7700(3)	0.2513(3)	0.1116(11)	0.110(3)	0.080(2)	0.114(3)
C17	0.2421(3)	0.6570(3)	0.24376(18)	0.0809(8)	0.094(2)	0.0686(19)	0.0700(16)
C18	0.3379(3)	0.6289(3)	0.3013(2)	0.1071(10)	0.148(3)	0.111(3)	0.0756(18)
C19	0.1668(3)	0.4924(3)	0.0780(2)	0.0966(9)	0.0871(19)	0.122(3)	0.093(2)
C20	0.2916(2)	0.1341(2)	0.52737(14)	0.0596(6)	0.0545(13)	0.0734(16)	0.0523(12)
C21	0.2761(2)	0.0707(3)	0.61224(16)	0.0773(7)	0.0720(15)	0.097(2)	0.0582(14)
C22	0.3621(3)	0.0557(3)	0.66649(18)	0.0924(9)	0.093(2)	0.120(2)	0.0575(15)
C23	0.4608(3)	0.1014(3)	0.6360(2)	0.0933(9)	0.0812(19)	0.129(3)	0.0736(18)
C24	0.4812(2)	0.1656(2)	0.54820(17)	0.0706(7)	0.0635(15)	0.0876(18)	0.0655(15)
C25	0.3958(2)	0.1821(2)	0.49208(14)	0.0566(5)	0.0510(12)	0.0669(15)	0.0544(12)
C26	0.5100(3)	0.2851(3)	0.37572(19)	0.0845(8)	0.0771(17)	0.107(2)	0.0885(18)
C27	0.5984(3)	0.2739(3)	0.4260(2)	0.0972(9)	0.0823(19)	0.128(3)	0.109(2)
C28	0.5839(3)	0.2143(3)	0.5109(2)	0.0921(9)	0.0718(17)	0.126(3)	0.102(2)
C29	0.0924(2)	0.1310(3)	0.50835(18)	0.0810(8)	0.0638(15)	0.113(2)	0.0791(16)
C30	-0.0062(2)	0.1993(2)	0.45384(16)	0.0690(7)	0.0556(14)	0.0920(19)	0.0701(15)
C31	-0.0564(2)	0.3415(3)	0.3212(15)	0.0625(6)	0.0502(12)	0.0809(18)	0.0629(13)
C32	-0.1135(3)	0.4676(3)	0.3331(2)	0.1019(9)	0.110(2)	0.079(2)	0.114(2)
C33	-0.1977(4)	0.5378(4)	0.2749(4)	0.1458(15)	0.128(3)	0.099(3)	0.169(4)
C34	-0.2150(4)	0.4795(7)	0.2100(4)	0.148(2)	0.098(3)	0.211(6)	0.135(4)
C35	-0.1533(5)	0.3595(6)	0.1990(3)	0.1357(16)	0.114(3)	0.225(5)	0.105(3)
C36	-0.0760(3)	0.2855(3)	0.2542(19)	0.0883(9)	0.0821(18)	0.125(3)	0.0746(17)
C37	-0.0135(5)	0.1443(4)	0.2444(3)	0.1628(18)	0.213(5)	0.145(4)	0.153(4)
C38	-0.0874(6)	0.5269(4)	0.4045(4)	0.190(2)	0.287(6)	0.105(3)	0.205(5)
N1	0.43950(19)	0.04949(17)	0.1486(12)	0.0612(5)	0.0790(13)	0.0591(12)	0.0577(10)
N2	0.36483(18)	0.45733(19)	0.1674(12)	0.0584(5)	0.0660(13)	0.0495(12)	0.0601(11)
N3	0.41193(17)	0.24192(19)	0.4055(13)	0.0664(5)	0.0611(11)	0.0840(14)	0.0652(12)
N4	0.0304(2)	0.26527(19)	0.3755(13)	0.0645(5)	0.0473(11)	0.0849(15)	0.0676(12)
O1	0.54244(14)	0.23157(13)	0.1174(10)	0.0597(4)	0.0642(9)	0.0483(9)	0.0686(9)
O2	0.51258(16)	0.55277(14)	0.0915(11)	0.0723(5)	0.0856(11)	0.0527(10)	0.0840(11)
O3	0.21078(14)	0.15781(16)	0.4700(10)	0.0703(5)	0.0586(9)	0.1069(13)	0.0590(9)
O4	-0.11592(16)	0.1922(2)	0.4848(13)	0.0994(6)	0.0630(11)	0.1496(18)	0.0987(13)
O5	0.28616(16)	0.25482(18)	0.2666(13)	0.0631(4)	0.0609(10)	0.0782(13)	0.0560(9)

Table 68:- 6.1B

Atom label	X	Y	Z	Uiso	Uaniso-U11	Uaniso-U22	Uaniso-U33
C1	0.9778(3)	0.8507(2)	0.62564(18)	0.0760(8)	0.0660(17)	0.095(2)	0.0665(17)
C2	0.9088(4)	0.9423(3)	0.5955(3)	0.1163(13)	0.099(3)	0.129(3)	0.121(3)
C6	1.0590(4)	0.7863(4)	0.5721(2)	0.1186(15)	0.090(2)	0.170(4)	0.096(3)

C4	1.0050(12)	0.9059(9)	0.4523(5)	0.251(8)	0.283(12)	0.369(16)	0.101(4)
C7	1.1335(5)	0.6927(4)	0.6065(4)	0.178(3)	0.097(3)	0.160(4)	0.277(6)
C8	0.8218(5)	1.0065(3)	0.6589(4)	0.174(2)	0.119(3)	0.125(3)	0.278(7)
C3	0.9218(8)	0.9682(6)	0.5056(4)	0.199(4)	0.201(7)	0.247(8)	0.148(5)
C5	1.0683(8)	0.8147(7)	0.4796(4)	0.206(5)	0.196(7)	0.303(10)	0.120(5)
C16	1.0117(2)	0.88106(17)	1.03805(15)	0.0576(6)	0.0548(13)	0.0596(14)	0.0585(15)
C15	1.0151(3)	0.87735(19)	1.13262(16)	0.0666(7)	0.0611(15)	0.0786(18)	0.0599(16)
C11	0.9456(3)	0.79702(18)	0.99035(16)	0.0635(6)	0.0690(15)	0.0634(15)	0.0581(15)
C12	0.8839(3)	0.7163(2)	1.03655(18)	0.0821(8)	0.0973(19)	0.0725(17)	0.0766(18)
C19	1.1254(3)	1.0395(2)	1.03600(19)	0.0784(7)	0.0867(18)	0.0742(17)	0.0744(18)
C18	1.1355(3)	1.0430(2)	1.1292(2)	0.0872(8)	0.093(2)	0.086(2)	0.082(2)
C17	1.0814(3)	0.9616(2)	1.17700(19)	0.0804(8)	0.0807(18)	0.100(2)	0.0606(16)
C13	0.8905(4)	0.7142(2)	1.1308(2)	0.0923(9)	0.110(2)	0.081(2)	0.085(2)
C14	0.9535(3)	0.7903(2)	1.17789(18)	0.0834(8)	0.097(2)	0.091(2)	0.0628(16)
C10	0.8728(4)	0.7296(2)	0.84846(17)	0.0829(8)	0.107(2)	0.0702(17)	0.0711(17)
N1	1.0675(2)	0.96201(15)	0.99005(12)	0.0657(6)	0.0703(13)	0.0643(13)	0.0626(12)
N2	0.9650(2)	0.82583(17)	0.71917(13)	0.0680(6)	0.0753(13)	0.0678(13)	0.0609(13)
C9	0.8826(3)	0.74819(18)	0.74927(17)	0.0675(6)	0.0762(16)	0.0554(14)	0.0709(16)
O2	0.9486(2)	0.80613(13)	0.89843(11)	0.0765(5)	0.0971(13)	0.0731(12)	0.0594(11)
O1	0.8130(2)	0.69055(14)	0.69930(12)	0.0866(6)	0.1051(14)	0.0754(11)	0.0791(11)
O3	0.1433(2)	0.97019(16)	0.80877(14)	0.0781(5)	0.0985(14)	0.0691(13)	0.0667(12)

Table 69:- 6.2

Atom label	X	Y	Z	Uiso	Uaniso-U11	Uaniso-U22	Uaniso-U33
C1	0.8229(3)	0.3394(3)	0.3954(3)	0.0726(8)	0.0738(19)	0.0606(18)	0.084(2)
C2	0.8386(3)	0.3862(3)	0.4717(3)	0.0794(9)	0.079(2)	0.0652(19)	0.107(3)
C3	0.8615(3)	0.3118(3)	0.5740(3)	0.0752(9)	0.0694(19)	0.089(2)	0.095(2)
C4	0.8697(2)	0.1896(3)	0.6032(2)	0.0608(7)	0.0519(15)	0.081(2)	0.0665(16)
C5	0.8533(2)	0.1496(2)	0.52040(19)	0.0515(6)	0.0423(12)	0.0656(16)	0.0533(13)
C6	0.8921(3)	0.1076(3)	0.7082(2)	0.0745(9)	0.082(2)	0.104(3)	0.0587(17)
C7	0.8993(3)	-0.0082(4)	0.7304(2)	0.0767(9)	0.088(2)	0.102(3)	0.0449(14)
C8	0.8847(3)	-0.0508(3)	0.64963(19)	0.0617(7)	0.0702(17)	0.0717(18)	0.0447(13)
C9	0.8446(2)	-0.1252(2)	0.48741(18)	0.0498(6)	0.0564(14)	0.0507(14)	0.0438(12)
C10	0.8267(2)	-0.1510(2)	0.38957(18)	0.0493(6)	0.0508(13)	0.0524(14)	0.0458(12)
C11	0.7852(3)	-0.0771(3)	0.1968(2)	0.0699(8)	0.105(2)	0.0492(15)	0.0505(14)
C12	0.8245(5)	0.0086(6)	0.1106(3)	0.137(2)	0.163(4)	0.253(7)	0.064(2)
C13	0.8193(5)	-0.0096(7)	0.0048(3)	0.150(2)	0.148(4)	0.278(8)	0.074(3)
C14	0.7065(5)	-0.0023(4)	-0.0240(3)	0.1090(15)	0.147(4)	0.106(3)	0.0541(19)
C15	0.6676(7)	-0.0877(10)	0.0608(4)	0.224(5)	0.240(8)	0.473(14)	0.086(3)
C16	0.6724(5)	-0.0693(8)	0.1667(4)	0.181(3)	0.130(4)	0.399(11)	0.086(3)
C17	0.4352(3)	0.3700(3)	-0.0793(2)	0.0651(7)	0.0664(17)	0.0778(19)	0.0459(13)
C18	0.4674(3)	0.3922(3)	-0.1839(2)	0.0830(10)	0.101(3)	0.103(3)	0.0381(14)
C19	0.5744(4)	0.3943(3)	-0.2087(2)	0.0822(10)	0.116(3)	0.096(2)	0.0375(14)
C20	0.6578(3)	0.3759(3)	-0.1303(2)	0.0631(7)	0.090(2)	0.0535(15)	0.0458(13)
C21	0.6282(2)	0.3520(2)	-0.0235(18)	0.0515(6)	0.0677(16)	0.0441(13)	0.0428(12)
C22	0.8106(3)	0.3340(3)	0.0323(3)	0.0730(8)	0.0697(19)	0.080(2)	0.079(2)
C23	0.8473(3)	0.3582(3)	-0.0708(3)	0.0850(10)	0.087(2)	0.091(2)	0.094(2)
C24	0.7709(4)	0.3787(3)	-0.1501(3)	0.0831(10)	0.113(3)	0.083(2)	0.0682(19)
C25	0.3821(2)	0.3128(3)	0.12899(19)	0.0556(6)	0.0500(14)	0.0759(18)	0.0450(12)
C26	0.3657(2)	0.2873(2)	0.24551(19)	0.0516(6)	0.0507(14)	0.0628(15)	0.0455(12)
C27	0.4492(2)	0.2365(3)	0.42408(18)	0.0548(6)	0.0500(13)	0.0824(19)	0.0405(12)

C28	0.4425(3)	0.3449(3)	0.4526(2)	0.0675(8)	0.0777(19)	0.0752(19)	0.0520(15)
C29	0.4387(3)	0.3182(3)	0.5714(2)	0.0758(9)	0.093(2)	0.092(2)	0.0541(16)
C30	0.5408(3)	0.2041(4)	0.6337(2)	0.0796(10)	0.073(2)	0.123(3)	0.0502(15)
C31	0.5466(3)	0.0972(3)	0.6042(2)	0.0764(9)	0.075(2)	0.092(2)	0.0470(15)
C32	0.5541(3)	0.1249(3)	0.4854(2)	0.0655(7)	0.0654(17)	0.0743(19)	0.0524(15)
C33	0.8616(2)	0.0262(2)	0.54653(18)	0.0486(6)	0.0450(12)	0.0617(15)	0.0443(12)
C34	0.5145(2)	0.3486(2)	-0.0006(17)	0.0510(6)	0.0612(15)	0.0521(14)	0.0354(11)
N1	0.8291(2)	0.2256(2)	0.41731(17)	0.0582(5)	0.0499(12)	0.0844(16)	0.0424(11)
N2	0.7938(2)	-0.0600(2)	0.29799(17)	0.0587(6)	0.0646(14)	0.0624(13)	0.0512(12)
N3	0.7058(2)	0.3311(2)	0.05594(17)	0.0579(6)	0.0604(13)	0.0553(13)	0.0600(13)
N4	0.4555(2)	0.2617(2)	0.31030(16)	0.0563(6)	0.0797(16)	0.0493(14)	0.0481(12)
O1	0.84484(15)	-0.00587(15)	0.46268(12)	0.0508(4)	0.0626(10)	0.0510(9)	0.0422(8)
O2	0.84504(18)	-0.25880(17)	0.40095(14)	0.0614(5)	0.0806(13)	0.0519(11)	0.0526(10)
O3	0.49254(15)	0.32254(18)	0.10399(12)	0.0563(5)	0.0531(10)	0.0828(13)	0.0360(8)
O4	0.26615(16)	0.2908(2)	0.27313(14)	0.0668(5)	0.0483(10)	0.1040(16)	0.0533(10)
O5	0.69977(17)	0.19883(18)	0.26796(15)	0.0578(5)	0.0623(11)	0.0701(12)	0.0410(9)
O6	0.0792(3)	0.3343(3)	0.1195(3)	0.0952(8)	0.0850(18)	0.114(2)	0.0871(19)
O7	0.1258(2)	0.4298(2)	0.3887(2)	0.0792(7)	0.0960(17)	0.0637(14)	0.0630(14)
O8	0.9231(4)	0.6015(3)	0.2686(2)	0.1174(12)	0.166(3)	0.0766(17)	0.0683(15)
O9	0.1218(3)	0.4468(3)	0.9068(2)	0.0990(9)	0.0863(19)	0.127(2)	0.0945(19)

Table 70:- 6.3

Atom label	X	Y	Z	Uiso	Uaniso-U11	Uaniso-U22	Uaniso-U33
C1	0.5401(5)	0.85863(18)	0.28605(9)	0.0621(6)	0.0639(16)	0.0673(17)	0.0551(14)
C2	0.6096(5)	0.9425(2)	0.31608(10)	0.0709(7)	0.0735(18)	0.0822(18)	0.0569(16)
C3	0.4855(6)	1.02869(19)	0.30693(10)	0.0664(7)	0.0792(18)	0.0647(17)	0.0555(15)
C4	0.2875(5)	1.03323(16)	0.26772(9)	0.0518(6)	0.0631(17)	0.0444(15)	0.0478(13)
C5	0.2323(5)	0.94469(15)	0.23896(8)	0.0453(5)	0.0518(14)	0.0430(13)	0.0412(12)
C6	0.1451(6)	1.12012(18)	0.25671(10)	0.0686(8)	0.097(2)	0.0455(15)	0.0632(16)
C7	-0.0466(6)	1.11946(17)	0.21852(10)	0.0691(7)	0.092(2)	0.0394(15)	0.0756(18)
C8	-0.1027(5)	1.03313(16)	0.18870(10)	0.0600(7)	0.0668(16)	0.0526(15)	0.0607(15)
C9	0.0326(4)	0.94813(15)	0.19848(8)	0.0469(5)	0.0551(14)	0.0375(12)	0.0482(13)
C10	-0.2302(4)	0.85498(15)	0.13757(8)	0.0530(6)	0.0484(13)	0.0604(15)	0.0501(13)
C11	-0.2487(5)	0.75478(15)	0.11118(8)	0.0455(5)	0.0389(12)	0.0590(14)	0.0387(11)
C12	-0.0171(5)	0.61043(15)	0.07619(8)	0.0538(6)	0.0544(14)	0.0526(14)	0.0544(14)
C13	0.0496(5)	0.62013(15)	0.01749(8)	0.0646(7)	0.0790(18)	0.0573(14)	0.0574(15)
C14	0.0636(5)	0.52135(16)	-0.01133(8)	0.0515(6)	0.0567(14)	0.0542(15)	0.0436(13)
C15	0.2549(5)	0.45247(18)	0.00089(9)	0.0610(6)	0.0556(14)	0.0726(16)	0.0549(14)
C16	0.2747(5)	0.36265(17)	-0.02615(9)	0.0601(6)	0.0518(14)	0.0674(16)	0.0610(14)
C17	0.1006(5)	0.34019(17)	-0.06624(9)	0.0522(6)	0.0501(14)	0.0590(15)	0.0476(13)
C18	-0.0931(5)	0.40734(18)	-0.07871(9)	0.0597(7)	0.0547(16)	0.0689(16)	0.0555(15)
C19	-0.1115(5)	0.49630(17)	-0.05153(9)	0.0582(6)	0.0533(15)	0.0620(16)	0.0594(15)
C20	0.3132(6)	0.18791(19)	-0.08803(11)	0.0896(9)	0.089(2)	0.0782(18)	0.102(2)
N1	0.3587(4)	0.85782(13)	0.24842(7)	0.0524(5)	0.0572(12)	0.0500(12)	0.0501(11)
N2	-0.0273(4)	0.70594(14)	0.10364(7)	0.0508(5)	0.0421(12)	0.0538(12)	0.0563(12)
O1	-0.0063(3)	0.86000(10)	0.17140(5)	0.0549(4)	0.0550(9)	0.0512(9)	0.0584(9)
O2	-0.4625(3)	0.72432(12)	0.09652(7)	0.0659(5)	0.0380(9)	0.0831(11)	0.0766(11)
O3	0.1021(4)	0.25477(13)	-0.09607(7)	0.0754(5)	0.0748(12)	0.0742(11)	0.0773(12)

Atom label	X	Y	Z	Uiso	Uaniso-U11	Uaniso-U22	Uaniso-U33
C20	0.43054(16)	1.19156(11)	0.14154(10)	0.0435(3)	0.0417(6)	0.0473(6)	0.0412(6)
C12	0.31633(16)	1.11536(11)	0.10869(11)	0.0459(3)	0.0426(6)	0.0476(6)	0.0480(6)
C16	0.36578(17)	1.31521(11)	0.11695(11)	0.0471(3)	0.0496(7)	0.0465(6)	0.0431(6)
C10	0.36354(18)	0.78580(12)	0.15071(12)	0.0507(3)	0.0537(7)	0.0537(7)	0.0503(7)
C13	0.14911(18)	1.16365(13)	0.05294(13)	0.0567(3)	0.0462(7)	0.0634(8)	0.0621(8)
C11	0.27706(18)	0.91716(12)	0.10555(13)	0.0523(3)	0.0491(7)	0.0574(7)	0.0563(7)
C17	0.4815(2)	1.38725(12)	0.15184(13)	0.0557(3)	0.0646(8)	0.0459(7)	0.0593(8)
C15	0.19121(19)	1.36093(13)	0.06068(13)	0.0575(3)	0.0554(8)	0.0524(7)	0.0602(8)
C19	0.69945(19)	1.21448(13)	0.22624(13)	0.0569(3)	0.0522(7)	0.0568(7)	0.0655(8)
C18	0.6467(2)	1.33722(13)	0.20633(14)	0.0604(3)	0.0667(8)	0.0559(8)	0.0686(9)
C5	0.8502(2)	0.48086(13)	0.39327(14)	0.0591(3)	0.0633(8)	0.0586(8)	0.0674(9)
C9	0.6093(2)	0.63273(13)	0.25720(13)	0.0573(3)	0.0681(8)	0.0497(7)	0.0637(8)
C2	1.0118(2)	0.23803(13)	0.47465(12)	0.0567(3)	0.0643(8)	0.0558(7)	0.0503(7)
C14	0.08709(19)	1.28691(14)	0.02918(14)	0.0616(4)	0.0481(7)	0.0648(8)	0.0645(8)
C6	1.0157(2)	0.46214(14)	0.34034(14)	0.0619(4)	0.0641(9)	0.0559(8)	0.0638(8)
C7	1.0971(2)	0.34210(14)	0.37969(13)	0.0608(3)	0.0569(8)	0.0675(9)	0.0578(8)
C4	0.7679(2)	0.37426(15)	0.48879(14)	0.0665(4)	0.0651(9)	0.0749(10)	0.0672(9)
C8	0.7612(2)	0.61186(15)	0.34675(17)	0.0720(4)	0.0784(10)	0.0621(9)	0.0930(11)
C3	0.8462(2)	0.25428(15)	0.52953(13)	0.0646(4)	0.0702(9)	0.0652(9)	0.0532(8)
C1	1.2451(3)	0.0931(2)	0.4634(2)	0.1053(7)	0.1079(15)	0.0805(12)	0.1065(15)
O2	0.28233(16)	0.70864(10)	0.12880(10)	0.0724(3)	0.0801(7)	0.0628(6)	0.0841(7)
O1	1.08281(17)	0.11522(10)	0.52300(10)	0.0766(3)	0.0870(8)	0.0630(6)	0.0659(6)
O3	0.38758(12)	0.99624(8)	0.13721(9)	0.0549(2)	0.0485(5)	0.0515(5)	0.0739(6)
N2	0.59799(14)	1.14260(10)	0.19593(10)	0.0498(3)	0.0469(6)	0.0489(6)	0.0570(6)
N1	0.51998(16)	0.75789(11)	0.21372(11)	0.0533(3)	0.0585(7)	0.0472(6)	0.0639(7)
O4	0.80153(16)	0.92705(11)	0.22702(12)	0.0666(3)	0.0644(6)	0.0579(6)	0.0864(8)

Atom label	X	Y	Z	Uiso	Uaniso-U11	Uaniso-U22	Uaniso-U33
C3	0.21633(15)	0.3499(6)	-0.11922(16)	0.0586(7)	0.0517(17)	0.0667(17)	0.0519(19)
C19	0.51681(18)	0.4635(7)	0.47647(18)	0.0747(10)	0.067(2)	0.080(2)	0.050(2)
C10	0.37571(17)	0.0121(6)	0.34715(17)	0.0642(8)	0.0615(19)	0.0670(17)	0.060(2)
C8	0.30609(19)	0.2771(7)	0.15349(18)	0.0700(9)	0.072(2)	0.0712(18)	0.0504(19)
C7	0.33763(17)	0.1479(7)	0.11058(18)	0.0713(9)	0.0603(19)	0.085(2)	0.0579(19)
C9	0.33215(16)	0.0306(6)	0.26566(17)	0.0615(8)	0.0586(19)	0.0594(16)	0.0608(19)
C15	0.5560(2)	0.5188(10)	0.5524(2)	0.1054(17)	0.089(3)	0.117(3)	0.053(2)
C6	0.29603(16)	0.2124(6)	0.03012(17)	0.0616(7)	0.0564(18)	0.0666(17)	0.056(2)
C12	0.4496(2)	0.1169(9)	0.4992(2)	0.0882(12)	0.098(3)	0.107(3)	0.052(2)
C2	0.28015(19)	0.4660(9)	-0.0761(2)	0.0887(12)	0.070(2)	0.105(3)	0.065(2)
C1	0.31889(19)	0.3983(9)	-0.0025(2)	0.0909(12)	0.057(2)	0.118(3)	0.066(2)
C4	0.1930(2)	0.1610(9)	-0.0879(2)	0.0957(13)	0.077(3)	0.130(3)	0.060(2)
C14	0.5389(3)	0.3744(14)	0.6003(3)	0.133(3)	0.147(5)	0.155(5)	0.040(2)
C5	0.2328(2)	0.0967(9)	-0.0149(2)	0.0989(14)	0.090(3)	0.129(3)	0.061(2)
C18	0.5796(2)	0.7970(8)	0.4513(3)	0.1024(15)	0.061(2)	0.092(2)	0.126(4)
C16	0.6115(3)	0.7220(14)	0.5753(3)	0.140(3)	0.085(4)	0.144(5)	0.098(4)
C17	0.6209(3)	0.8567(14)	0.5245(4)	0.139(3)	0.068(3)	0.134(5)	0.151(6)
C13	0.4875(3)	0.1808(13)	0.5739(3)	0.1186(19)	0.140(5)	0.155(4)	0.053(3)

C20	0.1983(2)	0.5990(7)	-0.2266(2)	0.0785(10)	0.084(3)	0.085(2)	0.062(2)
N1	0.34768(15)	0.2288(5)	0.23184(14)	0.0626(6)	0.0608(15)	0.0647(15)	0.0456(15)
N2	0.52888(14)	0.6035(6)	0.42685(17)	0.0796(9)	0.0555(16)	0.0803(18)	0.077(2)
O1	0.42750(11)	0.2242(4)	0.37585(11)	0.0676(6)	0.0713(14)	0.0732(12)	0.0434(12)
O2	0.28234(13)	-0.1295(5)	0.23371(15)	0.0879(7)	0.0818(16)	0.0883(16)	0.0801(17)
O4	0.02259(17)	0.5652(6)	0.24610(16)	0.0863(8)	0.077(2)	0.0874(18)	0.091(2)
O3	0.47443(16)	0.5619(6)	0.27448(19)	0.0868(8)	0.0957(19)	0.0746(15)	0.084(2)
C11	0.46327(17)	0.2601(7)	0.45057(17)	0.0692(9)	0.066(2)	0.080(2)	0.0407(19)
O5	0.17327(11)	0.4084(5)	-0.19232(12)	0.0747(6)	0.0609(13)	0.0971(15)	0.0542(14)

Table 73:- 6.4

Atom label	X	Y	Z	Uiso	Uaniso-U11	Uaniso-U22	Uaniso-U33
S1	0.72348(10)	0.82891(8)	0.22196(5)	0.0418(3)	0.0489(6)	0.0396(5)	0.0360(5)
S2	0.57577(12)	0.17990(11)	0.05711(8)	0.0618(3)	0.0594(7)	0.0600(6)	0.0715(8)
C1	0.6410(3)	0.8029(3)	0.5441(2)	0.0354(8)	0.040(2)	0.0272(15)	0.041(2)
C2	0.6131(4)	0.7876(3)	0.6262(2)	0.0428(9)	0.057(2)	0.0334(17)	0.040(2)
C3	0.6050(4)	0.8811(3)	0.6739(2)	0.0489(9)	0.063(3)	0.047(2)	0.037(2)
C4	0.6258(4)	0.9890(3)	0.6403(2)	0.0470(9)	0.057(2)	0.0411(19)	0.047(2)
C5	0.6553(3)	1.0094(3)	0.5558(2)	0.0383(8)	0.037(2)	0.0310(16)	0.048(2)
C6	0.6628(3)	0.9151(3)	0.5077(2)	0.0332(7)	0.0329(19)	0.0306(15)	0.038(2)
C7	0.7112(4)	1.0384(3)	0.3896(2)	0.0445(9)	0.054(2)	0.0364(17)	0.045(2)
C8	0.7041(4)	1.1340(3)	0.4345(2)	0.0482(9)	0.054(2)	0.0329(17)	0.060(3)
C9	0.6765(4)	1.1201(3)	0.5158(2)	0.0442(9)	0.046(2)	0.0335(17)	0.059(3)
C10	0.6368(4)	0.6017(3)	0.5265(2)	0.0389(8)	0.051(2)	0.0282(15)	0.041(2)
C11	0.6995(4)	0.4725(3)	0.3243(2)	0.0436(9)	0.066(3)	0.0376(18)	0.035(2)
C12	0.8175(4)	0.3637(3)	0.3057(2)	0.0481(9)	0.065(3)	0.0425(19)	0.041(2)
C13	0.8212(5)	0.2831(4)	0.2510(2)	0.0583(11)	0.083(3)	0.043(2)	0.046(2)
C14	0.7128(5)	0.3105(4)	0.2169(2)	0.0635(12)	0.099(4)	0.066(3)	0.043(2)
C15	0.5992(5)	0.4194(4)	0.2342(2)	0.0595(11)	0.081(3)	0.072(3)	0.044(2)
C16	0.5897(4)	0.5048(4)	0.2882(2)	0.0495(10)	0.068(3)	0.049(2)	0.043(2)
C17	0.9341(5)	0.3321(4)	0.3453(3)	0.0661(12)	0.065(3)	0.062(3)	0.070(3)
C18	0.4659(5)	0.6246(4)	0.3066(3)	0.0642(12)	0.068(3)	0.061(3)	0.071(3)
C19	0.0596(4)	0.3863(3)	0.1165(2)	0.0478(9)	0.065(3)	0.0397(18)	0.040(2)
C20	0.1594(5)	0.2662(4)	0.1001(3)	0.0616(11)	0.073(3)	0.044(2)	0.061(3)
C21	0.1395(6)	0.1859(4)	0.0532(3)	0.0735(14)	0.103(4)	0.045(2)	0.064(3)
C22	0.0268(6)	0.2240(4)	0.0235(3)	0.0712(14)	0.118(4)	0.055(2)	0.050(3)
C23	-0.0769(5)	0.3461(4)	0.0392(2)	0.0560(11)	0.089(3)	0.054(2)	0.038(2)
C24	-0.0587(4)	0.4279(3)	0.0861(2)	0.0456(9)	0.067(3)	0.0458(19)	0.0308(19)
C25	-0.2719(5)	0.5878(4)	0.0752(2)	0.0580(11)	0.067(3)	0.065(2)	0.050(2)
C26	-0.2953(5)	0.5110(5)	0.0299(3)	0.0678(13)	0.086(4)	0.084(3)	0.052(3)
C27	-0.1977(6)	0.3922(5)	0.0121(3)	0.0670(13)	0.106(4)	0.077(3)	0.045(2)
C28	0.1793(4)	0.4290(3)	0.1980(2)	0.0494(9)	0.047(2)	0.0414(19)	0.057(2)
C29	0.0655(4)	0.7441(3)	0.2955(2)	0.0441(9)	0.041(2)	0.0370(17)	0.056(2)
C30	0.0960(5)	0.8442(4)	0.2501(3)	0.0583(11)	0.070(3)	0.049(2)	0.060(3)
C31	0.0959(5)	0.9403(4)	0.2915(3)	0.0695(13)	0.082(3)	0.052(2)	0.089(4)
C32	0.0653(5)	0.9371(4)	0.3737(3)	0.0715(14)	0.073(3)	0.053(2)	0.099(4)
C33	0.0338(5)	0.8378(4)	0.4172(3)	0.0633(12)	0.065(3)	0.068(3)	0.057(3)
C34	0.0323(4)	0.7396(4)	0.3791(2)	0.0487(9)	0.041(2)	0.051(2)	0.052(2)
C35	0.1286(7)	0.8487(6)	0.1600(3)	0.0967(19)	0.144(6)	0.084(4)	0.072(4)
C36	-0.0040(5)	0.6330(4)	0.4270(3)	0.0656(12)	0.065(3)	0.072(3)	0.056(3)
C39	0.1719(4)	0.5266(3)	0.2517(2)	0.0460(9)	0.044(2)	0.0404(19)	0.054(2)

C40	0.6631(4)	0.5118(3)	0.4632(2)	0.0386(8)	0.047(2)	0.0313(16)	0.042(2)
N1	0.6909(3)	0.9348(2)	0.42587(17)	0.0361(6)	0.0433(17)	0.0283(13)	0.0385(17)
N2	0.6875(3)	0.5515(3)	0.38568(18)	0.0435(8)	0.070(2)	0.0317(15)	0.0399(18)
N3	-0.1584(3)	0.5460(3)	0.10164(19)	0.0474(8)	0.061(2)	0.0475(17)	0.0384(18)
N4	0.0704(3)	0.6420(3)	0.2534(2)	0.0460(8)	0.048(2)	0.0393(16)	0.054(2)
O1	0.6505(2)	0.7199(2)	0.49148(13)	0.0395(6)	0.0597(16)	0.0304(11)	0.0367(13)
O2	0.6615(3)	0.4050(2)	0.48599(15)	0.0552(7)	0.092(2)	0.0346(13)	0.0466(15)
O3	0.0651(3)	0.4723(2)	0.16194(16)	0.0495(6)	0.0544(17)	0.0408(13)	0.0547(16)
O4	0.2600(3)	0.4939(3)	0.29035(19)	0.0646(8)	0.0564(18)	0.0514(15)	0.087(2)
O5	0.7234(3)	0.9616(3)	0.21045(19)	0.0673(9)	0.096(2)	0.0401(14)	0.0539(19)
O6	0.7150(3)	0.7913(2)	0.30703(15)	0.0610(8)	0.108(2)	0.0456(14)	0.0373(15)
O7	0.8448(3)	0.7418(2)	0.17429(16)	0.0537(7)	0.0534(17)	0.0513(15)	0.0535(17)
O8	0.6071(3)	0.8313(4)	0.1955(2)	0.0883(11)	0.058(2)	0.139(3)	0.076(2)
O9	0.7095(4)	0.0935(4)	0.0739(2)	0.0944(12)	0.071(2)	0.098(3)	0.069(2)
O10	0.5285(9)	0.1164(11)	0.0194(9)	0.340(8)	0.209(9)	0.306(12)	0.59(2)
O11	0.4858(5)	0.2273(7)	0.1243(3)	0.198(3)	0.091(4)	0.270(7)	0.091(4)
O12	0.5892(6)	0.2675(8)	-0.0007(5)	0.254(5)	0.105(4)	0.279(9)	0.246(8)
O13	0.4194(6)	0.9691(5)	0.1259(4)	0.156(2)	0.132(4)	0.125(4)	0.212(6)

Table 74:- 6.5

Atom label	X	Y	Z	Uiso	Uaniso-U11	Uaniso-U22	Uaniso-U33
C1	0.34770(18)	0.3780(5)	0.35129(17)	0.0471(9)	0.037(2)	0.058(2)	0.046(2)
C2	0.3107(2)	0.3203(6)	0.3891(2)	0.0652(12)	0.045(2)	0.096(3)	0.053(3)
C3	0.2419(2)	0.2962(6)	0.3686(2)	0.0715(13)	0.046(3)	0.103(4)	0.069(3)
C4	0.2098(2)	0.3291(6)	0.3104(2)	0.0670(12)	0.037(2)	0.091(3)	0.071(3)
C5	0.24588(18)	0.3860(5)	0.26949(18)	0.0522(10)	0.035(2)	0.062(2)	0.057(3)
C6	0.31522(17)	0.4112(5)	0.29013(17)	0.0450(9)	0.039(2)	0.051(2)	0.047(2)
C7	0.2171(2)	0.4186(6)	0.2074(2)	0.0711(13)	0.049(3)	0.090(3)	0.063(3)
C8	0.2547(2)	0.4700(7)	0.1702(2)	0.0760(14)	0.063(3)	0.106(4)	0.050(3)
C9	0.3227(2)	0.4921(6)	0.19265(19)	0.0678(12)	0.061(3)	0.092(3)	0.049(3)
C10	0.45215(18)	0.3347(5)	0.41995(18)	0.0589(11)	0.045(2)	0.068(3)	0.056(3)
C11	0.52191(18)	0.4027(5)	0.44006(18)	0.0486(9)	0.038(2)	0.057(2)	0.048(2)
C12	0.60805(17)	0.5946(5)	0.42493(16)	0.0477(9)	0.036(2)	0.062(3)	0.043(2)
C13	0.66485(19)	0.4939(5)	0.43106(18)	0.0533(10)	0.050(2)	0.061(3)	0.051(2)
C14	0.72636(19)	0.5687(6)	0.45383(18)	0.0609(12)	0.035(2)	0.091(3)	0.060(3)
C15	0.7315(2)	0.7401(6)	0.46800(18)	0.0601(11)	0.040(2)	0.080(3)	0.061(3)
C16	0.6755(2)	0.8380(6)	0.45992(19)	0.0605(11)	0.050(3)	0.064(3)	0.069(3)
C17	0.61244(18)	0.7690(5)	0.43857(18)	0.0507(10)	0.037(2)	0.056(2)	0.059(3)
C18	0.6597(2)	0.3080(6)	0.4128(2)	0.0798(14)	0.079(3)	0.072(3)	0.095(4)
C19	0.5513(2)	0.8781(5)	0.4314(2)	0.0750(14)	0.050(3)	0.063(3)	0.110(4)
C20	0.18006(17)	0.8737(5)	0.27170(17)	0.0472(9)	0.033(2)	0.065(2)	0.045(2)
C21	0.17298(19)	0.9329(6)	0.21463(18)	0.0606(11)	0.041(2)	0.091(3)	0.047(3)
C22	0.2296(2)	0.9768(6)	0.19360(19)	0.0665(12)	0.058(3)	0.095(3)	0.050(3)
C23	0.2918(2)	0.9617(5)	0.22904(19)	0.0588(11)	0.048(2)	0.076(3)	0.059(3)
C24	0.30143(18)	0.9011(5)	0.28888(18)	0.0486(9)	0.039(2)	0.054(2)	0.055(3)
C25	0.24517(17)	0.8571(4)	0.31004(16)	0.0426(9)	0.039(2)	0.048(2)	0.043(2)
C26	0.36451(18)	0.8802(5)	0.3292(2)	0.0592(11)	0.033(2)	0.073(3)	0.075(3)
C27	0.3699(2)	0.8176(6)	0.3862(2)	0.0691(13)	0.040(2)	0.090(3)	0.071(3)
C28	0.31306(19)	0.7776(5)	0.40444(19)	0.0602(11)	0.044(2)	0.077(3)	0.055(3)
C29	0.06430(18)	0.8437(6)	0.26289(19)	0.0662(13)	0.036(2)	0.103(3)	0.055(3)
C30	0.01527(19)	0.7843(6)	0.29723(19)	0.0582(11)	0.038(2)	0.077(3)	0.057(3)

C31	-0.00392(17)	0.6567(5)	0.38872(16)	0.0463(9)	0.0295(19)	0.064(3)	0.044(2)
C32	0.00229(18)	0.4830(5)	0.40193(16)	0.0470(9)	0.043(2)	0.054(2)	0.041(2)
C33	-0.0421(2)	0.4129(6)	0.43243(18)	0.0581(11)	0.055(3)	0.062(3)	0.052(3)
C34	-0.0888(2)	0.5122(7)	0.4496(2)	0.0670(12)	0.048(3)	0.095(4)	0.061(3)
C35	-0.0917(2)	0.6837(6)	0.4383(2)	0.0647(12)	0.038(2)	0.091(4)	0.067(3)
C36	-0.04909(18)	0.7614(5)	0.40837(18)	0.0546(10)	0.037(2)	0.064(3)	0.062(3)
C37	-0.0486(2)	0.9525(6)	0.4013(3)	0.0859(16)	0.069(3)	0.064(3)	0.123(5)
C38	0.0562(2)	0.3781(6)	0.3860(2)	0.0679(12)	0.062(3)	0.068(3)	0.074(3)
N1	0.35034(17)	0.4654(4)	0.25028(15)	0.0513(9)	0.0369(19)	0.064(2)	0.051(2)
N2	0.54310(15)	0.5182(4)	0.40547(15)	0.0513(8)	0.0383(18)	0.066(2)	0.046(2)
N3	0.25387(15)	0.7978(4)	0.36777(15)	0.0493(8)	0.0312(18)	0.070(2)	0.048(2)
N4	0.03809(17)	0.7309(4)	0.35387(16)	0.0527(9)	0.0301(18)	0.072(2)	0.055(2)
N5	0.5055(2)	0.6290(5)	0.2469(2)	0.0652(10)	0.053(2)	0.076(3)	0.069(3)
N6	0.16809(18)	0.8584(5)	0.4704(2)	0.0666(10)	0.070(3)	0.067(3)	0.059(3)
O1	0.41438(11)	0.4106(3)	0.36594(11)	0.0536(7)	0.0325(14)	0.0783(18)	0.0470(16)
O2	0.55530(13)	0.3496(4)	0.48856(12)	0.0631(8)	0.0464(16)	0.081(2)	0.0545(18)
O3	0.13130(12)	0.8239(4)	0.29816(11)	0.0611(8)	0.0304(14)	0.100(2)	0.0502(17)
O4	-0.04398(13)	0.7842(5)	0.27064(14)	0.0867(11)	0.0314(15)	0.151(3)	0.071(2)
O5	0.47208(15)	0.6125(5)	0.28515(14)	0.0835(10)	0.0531(19)	0.138(3)	0.060(2)
O6	0.4782(2)	0.6141(7)	0.19406(19)	0.1374(18)	0.129(4)	0.219(5)	0.064(3)
O7	0.56433(17)	0.6618(5)	0.26294(19)	0.1066(13)	0.054(2)	0.130(3)	0.142(3)
O8	0.17201(14)	0.7246(4)	0.44077(13)	0.0635(8)	0.0643(19)	0.0636(19)	0.066(2)
O9	0.1713(3)	0.8609(6)	0.5232(2)	0.1256(16)	0.185(5)	0.121(3)	0.084(3)
O10	0.1585(3)	0.9925(6)	0.4411(2)	0.152(2)	0.229(6)	0.080(3)	0.134(4)

Table 75:- 6.6

Atom label	X	Y	Z	Uiso	Uaniso-U11	Uaniso-U22	Uaniso-U33
C11	0.56946(9)	0.29935(9)	0.18753(4)	0.0655(3)	0.0684(5)	0.0696(6)	0.0579(4)
C12	0.8239(3)	0.9098(3)	0.80462(14)	0.0440(6)	0.0501(13)	0.0471(16)	0.0375(12)
C20	0.6951(3)	1.0298(3)	0.82913(14)	0.0429(6)	0.0445(13)	0.0448(16)	0.0406(12)
C11	0.9831(3)	0.7489(3)	0.69526(15)	0.0549(7)	0.0618(16)	0.0477(17)	0.0512(15)
C13	0.9120(3)	0.8480(3)	0.86139(15)	0.0554(7)	0.0612(16)	0.0572(18)	0.0488(14)
C7	1.1311(3)	0.6230(3)	0.21568(15)	0.0546(7)	0.0570(15)	0.0543(18)	0.0494(14)
C3	0.9201(3)	0.8210(3)	0.19575(16)	0.0563(7)	0.0563(16)	0.061(2)	0.0542(15)
C4	0.8990(3)	0.8663(3)	0.27711(16)	0.0565(7)	0.0546(15)	0.0546(18)	0.0585(16)
C10	0.9939(3)	0.7103(3)	0.60648(16)	0.0530(6)	0.0612(16)	0.0401(17)	0.0558(15)
C2	1.0338(3)	0.6998(3)	0.16534(15)	0.0511(6)	0.0531(14)	0.0586(18)	0.0424(13)
C19	0.4857(3)	1.2099(3)	0.79256(17)	0.0581(7)	0.0543(16)	0.0547(19)	0.0634(17)
C6	1.1090(3)	0.6704(3)	0.29707(15)	0.0570(7)	0.0611(16)	0.0617(19)	0.0504(15)
C15	0.7493(3)	1.0189(3)	0.96796(15)	0.0600(7)	0.0735(18)	0.074(2)	0.0355(13)
C16	0.6554(3)	1.0862(3)	0.91117(14)	0.0499(6)	0.0551(15)	0.0547(18)	0.0408(13)
C5	0.9955(3)	0.7917(3)	0.32921(15)	0.0523(6)	0.0572(15)	0.0545(18)	0.0477(14)
C14	0.8722(4)	0.9040(3)	0.94338(16)	0.0611(7)	0.0715(18)	0.073(2)	0.0455(14)
C17	0.5247(3)	1.2073(3)	0.93048(18)	0.0635(8)	0.0660(18)	0.065(2)	0.0543(16)
C9	0.8796(3)	0.7468(3)	0.48112(15)	0.0594(7)	0.0720(17)	0.0620(19)	0.0461(14)
C18	0.4417(4)	1.2685(3)	0.87207(18)	0.0667(8)	0.0625(17)	0.058(2)	0.0707(19)
C8	0.9753(4)	0.8416(3)	0.41824(16)	0.0644(8)	0.0789(19)	0.067(2)	0.0519(15)
C1	1.1665(4)	0.5444(4)	0.04733(18)	0.0803(9)	0.096(2)	0.083(2)	0.0583(18)
N2	0.6061(2)	1.0955(2)	0.77293(13)	0.0467(5)	0.0485(12)	0.0478(14)	0.0437(12)
N1	0.8815(3)	0.7809(3)	0.56751(13)	0.0567(6)	0.0650(14)	0.0563(16)	0.0468(12)
O3	0.8507(2)	0.86867(18)	0.72326(9)	0.0514(4)	0.0602(10)	0.0502(11)	0.0415(9)

O1	1.0447(3)	0.6642(2)	0.08335(11)	0.0711(6)	0.0887(14)	0.0796(15)	0.0443(10)
O2	1.1084(2)	0.6109(2)	0.57392(12)	0.0686(5)	0.0788(13)	0.0550(13)	0.0643(12)
O9	0.4842(3)	0.3419(4)	0.12369(16)	0.1310(11)	0.133(2)	0.174(3)	0.0887(17)
O11	0.7030(3)	0.3779(3)	0.18081(19)	0.1113(9)	0.0919(17)	0.0981(19)	0.151(2)
O10	0.6323(4)	0.1483(3)	0.1844(2)	0.1273(10)	0.142(2)	0.0625(19)	0.173(3)
O8	0.4564(3)	0.3407(4)	0.26444(15)	0.1284(11)	0.118(2)	0.176(3)	0.0668(15)
O4	0.3849(3)	0.9624(3)	0.38895(12)	0.0677(6)	0.0795(14)	0.0689(16)	0.0586(12)
O5	0.3545(4)	0.4540(3)	0.65081(17)	0.0907(8)	0.0995(18)	0.0846(19)	0.0860(16)
O6	0.3965(4)	0.6907(3)	0.46514(16)	0.0835(7)	0.0880(17)	0.0753(17)	0.0791(16)
O7	0.5867(3)	0.1580(3)	0.39568(14)	0.0951(7)	0.1115(18)	0.0965(18)	0.0849(15)

Table 76:- 6.7

Atom label	X	Y	Z	Uiso	Uaniso-U11	Uaniso-U22	Uaniso-U33
C6	-0.1921(5)	0.2920(3)	0.14228(8)	0.0630(6)	0.0745(17)	0.0628(14)	0.0541(12)
C4	-0.4072(5)	0.3250(3)	0.06333(8)	0.0604(6)	0.0593(15)	0.0633(14)	0.0559(12)
C11	0.6339(5)	0.6424(3)	0.32809(9)	0.0764(7)	0.0716(18)	0.0887(18)	0.0627(14)
C1	0.0043(5)	0.4164(2)	0.13679(8)	0.0597(6)	0.0651(15)	0.0567(13)	0.0580(13)
C3	-0.2137(5)	0.4508(3)	0.05695(9)	0.0711(7)	0.0731(18)	0.0718(16)	0.0645(14)
C9	0.1791(5)	0.5974(3)	0.20932(8)	0.0666(6)	0.0637(16)	0.0722(15)	0.0634(13)
C5	-0.3979(5)	0.2449(2)	0.10640(8)	0.0637(6)	0.0700(16)	0.0563(13)	0.0626(13)
C10	0.4018(5)	0.5855(3)	0.29129(9)	0.0679(6)	0.0628(16)	0.0719(16)	0.0640(15)
C8	0.2287(5)	0.4675(3)	0.17644(9)	0.0704(7)	0.0710(17)	0.0729(16)	0.0688(14)
C2	-0.0113(5)	0.4948(3)	0.09318(9)	0.0721(7)	0.0687(17)	0.0653(15)	0.0764(16)
C12	1.0235(5)	0.8330(3)	0.34003(9)	0.0738(7)	0.0594(16)	0.0890(18)	0.0678(15)
C13	1.0585(6)	0.7930(4)	0.38896(10)	0.0949(9)	0.077(2)	0.123(2)	0.0749(18)
C7	-0.8017(6)	0.1616(3)	0.02939(11)	0.0893(9)	0.0759(19)	0.0901(19)	0.0897(18)
C17	1.2076(5)	0.9516(3)	0.31933(11)	0.0743(7)	0.0564(16)	0.0752(16)	0.0873(19)
C16	1.4259(6)	1.0272(4)	0.35042(12)	0.0910(9)	0.070(2)	0.098(2)	0.096(2)
C20	1.3526(6)	1.0965(3)	0.25281(13)	0.0923(9)	0.080(2)	0.0698(17)	0.121(2)
C14	1.2766(8)	0.8710(5)	0.41925(12)	0.1155(12)	0.097(3)	0.153(3)	0.084(2)
C18	1.6061(7)	1.1438(4)	0.32905(17)	0.1097(11)	0.072(2)	0.103(2)	0.139(3)
C19	1.5707(7)	1.1773(4)	0.28067(17)	0.1112(11)	0.095(3)	0.087(2)	0.140(3)
C15	1.4540(7)	0.9843(5)	0.40034(14)	0.1148(12)	0.083(2)	0.138(3)	0.109(3)
O3	0.8155(3)	0.76353(19)	0.30812(6)	0.0745(5)	0.0619(11)	0.0851(11)	0.0687(10)
O2	-0.5970(4)	0.2889(2)	0.02460(6)	0.0797(5)	0.0731(12)	0.0899(12)	0.0662(10)
O1	0.2241(4)	0.4817(2)	0.30400(7)	0.0865(6)	0.0797(13)	0.0968(14)	0.0710(11)
N1	0.3954(5)	0.6469(3)	0.24710(7)	0.0658(6)	0.0614(14)	0.0719(14)	0.0607(12)
N2	1.1743(4)	0.9878(2)	0.27025(9)	0.0773(6)	0.0685(15)	0.0702(13)	0.0905(16)
O4	0.7834(4)	0.8824(2)	0.20127(8)	0.0829(6)	0.0705(13)	0.0933(14)	0.0827(14)
C22	0.6515(6)	0.8367(3)	0.11553(11)	0.0924(9)	0.094(2)	0.098(2)	0.0860(18)
O5	1.0874(4)	0.9593(3)	0.14541(8)	0.1065(7)	0.0788(15)	0.1197(17)	0.1210(16)
C21	0.8633(6)	0.8992(3)	0.15430(11)	0.0754(7)	0.079(2)	0.0648(15)	0.0901(19)
O6	0.1400(5)	0.3540(3)	0.38947(10)	0.1352(10)	0.124(2)	0.156(2)	0.0968(16)
C23	0.2657(10)	0.3876(5)	0.42947(13)	0.1287(15)	0.146(4)	0.128(3)	0.080(2)
C24	0.1718(10)	0.3107(5)	0.47524(13)	0.1552(18)	0.189(5)	0.171(4)	0.088(2)
O7	0.4656(12)	0.4740(7)	0.42885(12)	0.318(4)	0.341(6)	0.389(7)	0.108(2)

Atom label	X	Y	Z	Uiso	Uaniso-U11	Uaniso-U22	Uaniso-U33
C12	0.4625(7)	0.3510(7)	0.0962(4)	0.0521(13)	0.061(3)	0.056(3)	0.047(3)
C20	0.5414(7)	0.2376(7)	0.0379(4)	0.0528(13)	0.066(3)	0.055(3)	0.047(3)
C11	0.4918(7)	0.4650(7)	0.2024(4)	0.0549(13)	0.056(3)	0.056(3)	0.057(3)
C6	1.1070(9)	0.4158(8)	0.3531(5)	0.0708(17)	0.073(4)	0.053(3)	0.082(5)
C16	0.4575(8)	0.2457(8)	-0.0257(4)	0.0614(15)	0.082(4)	0.073(4)	0.042(3)
C5	1.1292(7)	0.3074(8)	0.3049(4)	0.0622(15)	0.055(3)	0.068(4)	0.062(4)
C13	0.3093(8)	0.4624(8)	0.0924(4)	0.0663(16)	0.068(4)	0.072(4)	0.062(4)
C9	0.8693(9)	0.2985(8)	0.3031(5)	0.0719(18)	0.085(5)	0.065(4)	0.084(5)
C15	0.2993(9)	0.3610(10)	-0.0282(5)	0.0735(19)	0.076(4)	0.103(5)	0.061(4)
C4	1.2642(8)	0.1694(8)	0.3100(5)	0.0699(17)	0.058(4)	0.071(4)	0.077(4)
C2	1.3459(7)	0.2521(9)	0.4106(5)	0.0714(18)	0.046(3)	0.094(5)	0.080(5)
C7	1.2140(9)	0.3907(8)	0.4054(5)	0.0678(17)	0.077(4)	0.063(4)	0.075(4)
C8	1.0105(9)	0.3303(10)	0.2504(5)	0.081(2)	0.072(4)	0.097(5)	0.069(4)
C18	0.6875(11)	0.0274(9)	-0.0761(5)	0.082(2)	0.112(6)	0.077(5)	0.052(4)
C19	0.7590(10)	0.0260(9)	-0.0113(4)	0.0753(19)	0.088(5)	0.074(4)	0.057(4)
C3	1.3690(8)	0.1436(9)	0.3619(5)	0.079(2)	0.053(4)	0.085(5)	0.092(5)
C14	0.2291(9)	0.4634(10)	0.0295(5)	0.078(2)	0.059(4)	0.091(5)	0.084(5)
C17	0.5383(11)	0.1362(10)	-0.0841(4)	0.077(2)	0.118(6)	0.097(5)	0.041(3)
C1	1.4360(17)	0.3324(18)	0.5086(9)	0.163(6)	0.180(13)	0.219(15)	0.168(12)
C23	0.9415(11)	0.8864(8)	0.3007(5)	0.074(2)	0.111(6)	0.069(4)	0.076(5)
C26	1.1133(10)	0.8160(9)	0.4273(5)	0.077(2)	0.089(5)	0.081(5)	0.079(5)
C24	0.8654(10)	0.9062(9)	0.3824(6)	0.084(2)	0.078(5)	0.087(5)	0.103(6)
C25	0.9517(9)	0.8714(9)	0.4458(5)	0.0735(19)	0.074(4)	0.085(5)	0.070(4)
C21	0.7981(12)	0.8144(11)	0.2199(5)	0.086(2)	0.134(7)	0.112(6)	0.055(4)
C27	1.1951(9)	0.7927(8)	0.3449(6)	0.077(2)	0.054(4)	0.068(4)	0.103(6)
C28	1.1080(12)	0.8286(9)	0.2815(5)	0.083(2)	0.127(7)	0.076(5)	0.059(4)
C22	0.853(2)	0.9317(15)	0.2259(8)	0.180(8)	0.333(19)	0.171(10)	0.179(11)
O3	0.5526(5)	0.3395(4)	0.1537(3)	0.0555(10)	0.059(2)	0.051(2)	0.063(2)
O2	0.5926(6)	0.5686(6)	0.2806(4)	0.0781(14)	0.069(3)	0.078(3)	0.106(4)
O1	1.4532(7)	0.2210(9)	0.4610(5)	0.111(2)	0.074(4)	0.151(6)	0.125(5)
O6	0.8512(11)	1.0426(7)	0.1780(5)	0.132(3)	0.232(9)	0.060(3)	0.144(6)
O4	0.6935(9)	0.7826(9)	0.2796(5)	0.115(2)	0.145(6)	0.122(5)	0.124(5)
O5	0.8708(12)	0.7357(11)	0.1622(6)	0.145(3)	0.177(8)	0.186(8)	0.127(6)
N1	0.7453(8)	0.3238(7)	0.2548(4)	0.0699(16)	0.087(4)	0.058(3)	0.086(4)
N2	0.6889(7)	0.1270(6)	0.0453(3)	0.0618(13)	0.074(3)	0.060(3)	0.052(3)
C10	0.6188(7)	0.4545(7)	0.2481(4)	0.0560(13)	0.064(3)	0.054(3)	0.061(3)

Atom label	X	Y	Z	Uiso	Uaniso-U11	Uaniso-U22	Uaniso-U33
C1	0.3093(2)	0.96285(15)	0.79988(15)	0.0578(4)	0.0642(10)	0.0504(8)	0.0606(9)
C2	0.3056(3)	1.09456(15)	0.86397(19)	0.0650(5)	0.0670(11)	0.0468(8)	0.0846(12)
C3	0.2747(2)	1.13718(14)	0.97649(18)	0.0629(5)	0.0590(10)	0.0359(7)	0.0851(12)
C4	0.2488(2)	1.05089(13)	1.02955(15)	0.0518(4)	0.0433(8)	0.0370(6)	0.0627(9)
C5	0.25724(18)	0.91926(12)	0.95874(12)	0.0438(3)	0.0397(7)	0.0355(6)	0.0493(7)
C6	0.2173(2)	1.08908(15)	1.14757(16)	0.0651(5)	0.0656(11)	0.0432(7)	0.0663(10)
C7	0.1944(3)	1.00181(18)	1.19289(16)	0.0674(5)	0.0701(11)	0.0628(10)	0.0545(9)
C8	0.2052(2)	0.87052(16)	1.12487(14)	0.0592(4)	0.0676(10)	0.0562(8)	0.0534(8)

C9	0.2367(2)	0.82983(12)	1.00999(13)	0.0466(3)	0.0493(8)	0.0383(6)	0.0477(7)
C10	0.2484(3)	0.61646(14)	0.98924(15)	0.0591(4)	0.0861(12)	0.0457(7)	0.0575(8)
C11	0.2879(3)	0.48843(14)	0.90456(15)	0.0572(4)	0.0797(11)	0.0412(7)	0.0568(8)
C12	0.3744(2)	0.36887(13)	0.71104(13)	0.0492(4)	0.0616(10)	0.0405(6)	0.0474(7)
C13	0.2456(2)	0.25324(15)	0.64767(15)	0.0597(4)	0.0670(11)	0.0472(8)	0.0582(8)
C14	0.2975(3)	0.15085(17)	0.55700(18)	0.0783(6)	0.1045(16)	0.0460(8)	0.0648(10)
C15	0.4623(4)	0.16402(19)	0.5272(2)	0.0852(6)	0.1126(18)	0.0613(10)	0.0733(12)
C16	0.5855(3)	0.2790(2)	0.58912(18)	0.0734(5)	0.0762(12)	0.0762(11)	0.0687(11)
C17	0.5454(2)	0.38317(15)	0.68335(14)	0.0564(4)	0.0623(10)	0.0541(8)	0.0545(8)
C18	0.6815(3)	0.50893(19)	0.75195(18)	0.0736(5)	0.0722(12)	0.0698(11)	0.0722(11)
C19	0.0586(3)	0.2405(2)	0.6708(2)	0.0881(6)	0.0684(13)	0.0768(12)	0.1008(15)
C21	0.1608(3)	0.45342(15)	0.49675(14)	0.0608(4)	0.0744(11)	0.0568(9)	0.0512(8)
C22	0.1584(2)	0.57460(14)	0.58747(12)	0.0509(4)	0.0743(10)	0.0455(7)	0.0381(7)
C23	-0.0030(3)	0.61981(14)	0.58951(14)	0.0590(4)	0.0836(12)	0.0455(7)	0.0463(8)
N1	0.28650(17)	0.87709(11)	0.84391(11)	0.0478(3)	0.0539(7)	0.0401(5)	0.0478(6)
N2	0.3270(2)	0.47972(12)	0.80023(11)	0.0523(3)	0.0746(9)	0.0366(6)	0.0534(7)
O1	0.25293(16)	0.70594(9)	0.93767(9)	0.0545(3)	0.0831(8)	0.0369(5)	0.0512(5)
O2	0.2827(2)	0.40073(11)	0.93598(12)	0.0830(5)	0.1465(13)	0.0466(6)	0.0711(8)
O3	0.31915(17)	0.64332(11)	0.67208(10)	0.0607(3)	0.0755(8)	0.0500(6)	0.0520(6)

Table 79:- 6.10

Atom label	X	Y	Z	Uiso	Uaniso-U11	Uaniso-U22	Uaniso-U33
C1	0.0560(2)	0.4624(2)	0.19638(17)	0.0629(5)	0.0601(11)	0.0559(11)	0.0613(14)
C2	-0.0382(2)	0.3153(2)	0.1420(2)	0.0646(6)	0.0541(11)	0.0515(11)	0.0829(17)
C3	-0.0212(2)	0.24733(18)	0.04056(19)	0.0601(6)	0.0470(10)	0.0322(8)	0.0891(18)
C4	0.0879(2)	0.32261(16)	-0.01024(16)	0.0487(5)	0.0413(8)	0.0298(7)	0.0626(14)
C5	0.17847(19)	0.47191(16)	0.05151(15)	0.0428(4)	0.0376(8)	0.0309(7)	0.0523(12)
C6	0.1097(2)	0.25904(19)	-0.11614(18)	0.0627(6)	0.0576(11)	0.0323(8)	0.0738(16)
C7	0.2176(3)	0.3374(2)	-0.15949(18)	0.0668(6)	0.0720(13)	0.0488(10)	0.0555(14)
C8	0.3093(2)	0.48593(19)	-0.09933(16)	0.0570(5)	0.0599(11)	0.0438(9)	0.0531(14)
C9	0.2898(2)	0.55236(16)	0.00305(14)	0.0437(4)	0.0437(8)	0.0300(7)	0.0454(12)
C10	0.4847(2)	0.77834(17)	0.02234(14)	0.0472(4)	0.0478(9)	0.0374(8)	0.0473(11)
C11	0.5674(2)	0.93381(17)	0.10055(15)	0.0467(4)	0.0484(9)	0.0362(8)	0.0483(12)
C12	0.5736(2)	1.12854(17)	0.26810(15)	0.0493(4)	0.0571(10)	0.0323(8)	0.0507(11)
C13	0.7314(2)	1.17649(18)	0.33533(16)	0.0564(5)	0.0581(10)	0.0405(9)	0.0605(13)
C14	0.7884(3)	1.3200(2)	0.40879(19)	0.0763(7)	0.0765(14)	0.0484(11)	0.0743(17)
C15	0.6923(4)	1.4111(2)	0.4148(2)	0.0892(8)	0.110(2)	0.0400(11)	0.0879(19)
C16	0.5363(4)	1.3620(2)	0.3479(2)	0.0820(7)	0.1090(19)	0.0514(11)	0.0902(19)
C17	0.4728(3)	1.2186(2)	0.27332(17)	0.0605(5)	0.0711(12)	0.0513(10)	0.0609(14)
C18	0.2998(3)	1.1632(3)	0.2034(2)	0.0865(7)	0.0825(16)	0.0957(18)	0.0894(19)
C19	0.8374(3)	1.0788(2)	0.3314(2)	0.0766(7)	0.0693(13)	0.0608(12)	0.0873(18)
C20	0.4840(3)	0.7543(2)	0.36385(17)	0.0628(5)	0.0752(13)	0.0425(9)	0.0569(14)
C21	0.3913(2)	0.84633(18)	0.36966(14)	0.0495(4)	0.0560(10)	0.0409(9)	0.0425(11)
C22	0.4301(2)	0.98156(18)	0.45890(14)	0.0483(4)	0.0559(10)	0.0406(8)	0.0421(11)
C23	0.3342(3)	1.0782(2)	0.46739(16)	0.0579(5)	0.0644(11)	0.0509(10)	0.0524(13)
C24	0.3777(3)	1.2073(2)	0.55325(18)	0.0693(6)	0.0841(15)	0.0526(11)	0.0680(15)
N1	0.16047(18)	0.53911(15)	0.15398(12)	0.0506(4)	0.0503(8)	0.0382(7)	0.0495(10)
N2	0.50916(19)	0.98015(15)	0.19147(13)	0.0509(4)	0.0546(8)	0.0321(7)	0.0546(10)
O1	0.36951(14)	0.69597(11)	0.06776(9)	0.0481(3)	0.0525(6)	0.0297(5)	0.0471(8)
O2	0.68300(17)	1.01016(13)	0.07456(11)	0.0690(4)	0.0736(9)	0.0464(7)	0.0660(9)
O3	0.26046(17)	0.81937(14)	0.29053(11)	0.0602(4)	0.0643(8)	0.0473(7)	0.0511(9)

Atom label	X	Y	Z	Uiso	Uaniso-U11	Uaniso-U22	Uaniso-U33
C40	0.34289(19)	0.09507(15)	0.54055(12)	0.0469(5)	0.0412(12)	0.0484(12)	0.0509(13)
C20	-0.0987(2)	0.54779(15)	0.12588(12)	0.0495(5)	0.0478(12)	0.0482(12)	0.0515(13)
C12	-0.0810(2)	0.60075(16)	0.05191(13)	0.0521(5)	0.0486(13)	0.0533(13)	0.0577(14)
C32	0.38890(19)	0.11846(15)	0.46535(12)	0.0485(5)	0.0419(12)	0.0533(13)	0.0530(13)
C30	0.6363(2)	0.24282(18)	0.39207(14)	0.0600(6)	0.0509(14)	0.0742(16)	0.0550(15)
C11	0.0424(2)	0.69500(17)	-0.02644(12)	0.0588(6)	0.0626(15)	0.0689(15)	0.0486(13)
C31	0.5313(2)	0.19431(18)	0.38618(12)	0.0590(6)	0.0569(14)	0.0770(16)	0.0432(12)
C36	0.2422(2)	0.04834(16)	0.55093(14)	0.0556(6)	0.0464(13)	0.0516(13)	0.0675(15)
C10	0.1632(2)	0.72594(19)	-0.02423(14)	0.0625(6)	0.0612(15)	0.0817(17)	0.0521(14)
C25	1.0035(2)	0.28274(17)	0.48902(15)	0.0624(6)	0.0552(14)	0.0617(15)	0.0720(17)
C16	-0.2051(2)	0.50743(16)	0.13784(14)	0.0570(6)	0.0465(13)	0.0562(14)	0.0688(15)
C33	0.3366(2)	0.09506(17)	0.40444(13)	0.0602(6)	0.0594(14)	0.0700(15)	0.0542(14)
C22	1.1759(2)	0.39204(17)	0.50455(14)	0.0591(6)	0.0492(14)	0.0600(14)	0.0670(16)
C24	1.0807(2)	0.30647(18)	0.42978(14)	0.0647(6)	0.0582(15)	0.0692(16)	0.0669(16)
C23	1.1670(2)	0.36102(18)	0.43677(14)	0.0656(6)	0.0583(15)	0.0739(16)	0.0616(16)
C4	0.5700(3)	0.76623(19)	0.14987(14)	0.0710(7)	0.0845(19)	0.0805(18)	0.0531(15)
C34	0.2369(2)	0.04927(18)	0.41597(16)	0.0689(7)	0.0707(17)	0.0713(17)	0.0749(18)
C27	1.1005(3)	0.3676(2)	0.56496(15)	0.0762(7)	0.0789(18)	0.101(2)	0.0615(16)
C2	0.7317(2)	0.84387(17)	0.09990(14)	0.0627(6)	0.0537(14)	0.0588(14)	0.0705(16)
C13	-0.1654(2)	0.61123(18)	-0.00638(14)	0.0672(7)	0.0641(16)	0.0834(17)	0.0580(15)
C7	0.6596(2)	0.88461(18)	0.03391(14)	0.0688(7)	0.0686(16)	0.0766(17)	0.0616(15)
C5	0.4928(2)	0.81037(19)	0.08457(14)	0.0691(7)	0.0758(17)	0.0885(18)	0.0538(15)
C39	0.3549(2)	0.0921(2)	0.67045(14)	0.0727(7)	0.0725(17)	0.096(2)	0.0484(14)
C19	-0.0336(2)	0.49094(19)	0.25188(14)	0.0717(7)	0.0666(16)	0.0854(18)	0.0584(15)
C29	0.7713(2)	0.29354(18)	0.47497(15)	0.0667(7)	0.0625(15)	0.0749(16)	0.0705(16)
C37	0.2002(2)	0.02477(19)	0.62653(17)	0.0757(8)	0.0580(16)	0.0762(18)	0.089(2)
C15	-0.2897(2)	0.51963(19)	0.07618(16)	0.0724(7)	0.0537(15)	0.0817(18)	0.088(2)
C8	0.3553(3)	0.79675(19)	0.07611(15)	0.0780(8)	0.096(2)	0.0695(17)	0.0678(17)
C3	0.6871(2)	0.78304(18)	0.15744(14)	0.0694(7)	0.0689(17)	0.0736(17)	0.0598(15)
C17	-0.2212(2)	0.45720(18)	0.21212(16)	0.0732(7)	0.0579(15)	0.0728(17)	0.0843(19)
C35	0.1905(2)	0.02653(17)	0.48628(17)	0.0683(7)	0.0572(15)	0.0592(15)	0.096(2)
C6	0.5416(3)	0.86722(19)	0.02711(14)	0.0740(7)	0.0806(19)	0.0924(19)	0.0553(15)
C28	0.9063(2)	0.22710(19)	0.47975(17)	0.0767(7)	0.0648(16)	0.0724(17)	0.098(2)
C38	0.2564(3)	0.0462(2)	0.68621(16)	0.0820(8)	0.0755(19)	0.103(2)	0.0617(17)
C9	0.3671(3)	0.7050(2)	0.04703(16)	0.0817(8)	0.092(2)	0.0840(19)	0.0685(17)
C18	-0.1362(3)	0.4497(2)	0.26875(16)	0.0810(8)	0.0714(18)	0.097(2)	0.0666(17)
C26	1.0162(3)	0.3139(2)	0.55723(16)	0.0789(8)	0.0766(18)	0.103(2)	0.0677(17)
C21	1.3392(3)	0.4693(2)	0.45797(19)	0.0978(10)	0.0754(19)	0.097(2)	0.129(3)
C14	-0.2695(2)	0.5699(2)	0.00653(16)	0.0804(8)	0.0667(17)	0.105(2)	0.0757(19)
C1	0.8901(3)	0.9313(2)	0.0627(2)	0.1002(10)	0.0755(19)	0.102(2)	0.126(3)
C50	0.29633(18)	0.74708(15)	0.30550(11)	0.0449(5)	0.0445(12)	0.0538(12)	0.0373(11)
C45	0.30795(18)	0.66066(15)	0.27380(11)	0.0451(5)	0.0445(12)	0.0509(12)	0.0403(11)
C46	0.20149(19)	0.65604(15)	0.23131(11)	0.0485(5)	0.0489(13)	0.0537(13)	0.0456(12)
C41	0.4024(2)	0.75281(17)	0.34834(11)	0.0508(5)	0.0546(13)	0.0637(14)	0.0392(11)
C49	0.1818(2)	0.82481(16)	0.29431(12)	0.0538(5)	0.0544(13)	0.0545(13)	0.0537(13)
C48	0.0830(2)	0.81650(17)	0.25304(13)	0.0587(6)	0.0459(13)	0.0591(14)	0.0661(15)
C47	0.0921(2)	0.73201(17)	0.22159(12)	0.0557(6)	0.0469(13)	0.0655(15)	0.0550(13)
C60	0.4162(2)	0.14903(16)	0.17694(11)	0.0517(5)	0.0604(14)	0.0563(14)	0.0375(11)
C42	0.5122(2)	0.67726(18)	0.35884(12)	0.0576(6)	0.0495(13)	0.0724(16)	0.0495(13)

C44	0.4233(2)	0.58334(17)	0.28560(13)	0.0578(6)	0.0530(14)	0.0577(14)	0.0608(14)
C43	0.5213(2)	0.59258(18)	0.32740(14)	0.0643(6)	0.0494(14)	0.0687(16)	0.0660(15)
C55	0.3018(2)	0.21590(17)	0.19672(12)	0.0548(6)	0.0618(15)	0.0626(15)	0.0407(12)
C51	0.5269(2)	0.18464(17)	0.16160(12)	0.0560(6)	0.0610(15)	0.0620(15)	0.0442(12)
C54	0.3018(3)	0.31369(18)	0.20275(13)	0.0651(6)	0.0719(17)	0.0655(16)	0.0583(15)
C59	0.4163(2)	0.05151(17)	0.17183(13)	0.0621(6)	0.0739(16)	0.0553(14)	0.0564(14)
C52	0.5238(2)	0.27919(18)	0.16817(13)	0.0643(6)	0.0716(17)	0.0708(17)	0.0583(14)
C56	0.1897(2)	0.18250(19)	0.20956(13)	0.0625(6)	0.0609(15)	0.0736(17)	0.0532(14)
C58	0.3065(3)	0.02264(19)	0.18502(14)	0.0701(7)	0.0883(19)	0.0624(15)	0.0663(16)
C57	0.1922(3)	0.0885(2)	0.20307(14)	0.0708(7)	0.0719(17)	0.0847(19)	0.0638(16)
C53	0.4108(3)	0.34323(19)	0.18871(14)	0.0698(7)	0.0863(19)	0.0617(16)	0.0671(16)
O6	0.48536(14)	0.16407(11)	0.46044(8)	0.0582(4)	0.0553(9)	0.0826(11)	0.0453(8)
O3	0.02346(14)	0.63822(11)	0.04575(8)	0.0596(4)	0.0634(10)	0.0737(10)	0.0490(9)
O2	0.18897(16)	0.78181(14)	-0.08152(10)	0.0820(5)	0.0818(12)	0.1143(14)	0.0599(11)
O4	1.25668(16)	0.44646(13)	0.51799(11)	0.0787(5)	0.0665(11)	0.0854(12)	0.0909(13)
O5	0.68183(17)	0.27909(15)	0.33277(10)	0.0891(6)	0.0883(13)	0.1313(16)	0.0599(11)
O1	0.84798(17)	0.85865(15)	0.11312(12)	0.1000(7)	0.0610(11)	0.1072(15)	0.1219(17)
O8	0.21653(14)	0.57389(12)	0.19865(10)	0.0653(4)	0.0611(10)	0.0673(10)	0.0743(11)
O7	0.38414(14)	0.83637(12)	0.37919(9)	0.0640(4)	0.0605(10)	0.0781(11)	0.0638(10)
O9	0.63400(15)	0.11951(12)	0.13997(10)	0.0704(5)	0.0628(11)	0.0733(11)	0.0765(12)
O10	0.08259(17)	0.25039(14)	0.22730(12)	0.0882(6)	0.0638(11)	0.0989(14)	0.1040(14)
N4	0.39760(17)	0.11686(14)	0.60113(10)	0.0570(5)	0.0547(11)	0.0727(12)	0.0470(11)
N2	-0.01290(17)	0.53804(13)	0.18355(10)	0.0565(5)	0.0569(11)	0.0625(12)	0.0497(11)
N3	0.67451(19)	0.24529(16)	0.46150(12)	0.0630(5)	0.0597(13)	0.0798(14)	0.0576(13)
N1	0.2372(2)	0.68981(18)	0.03794(13)	0.0751(6)	0.0684(14)	0.1117(18)	0.0587(13)
O11	0.8757(2)	0.1789(2)	0.24377(16)	0.0951(7)	0.0741(14)	0.1314(19)	0.0805(15)

Table 81:- 6.12

Atom label	X	Y	Z	Uiso	Uaniso-U11	Uaniso-U22	Uaniso-U33
C20	0.6167(4)	0.60039(10)	0.02449(8)	0.0426(4)	0.0505(10)	0.0356(10)	0.0418(10)
C12	0.7965(4)	0.64454(11)	0.05141(8)	0.0444(4)	0.0501(10)	0.0420(10)	0.0412(9)
C16	0.6025(4)	0.59676(11)	-0.03961(9)	0.0501(5)	0.0630(12)	0.0424(11)	0.0449(10)
C3	0.3505(4)	0.67817(13)	0.48528(10)	0.0574(6)	0.0484(11)	0.0589(14)	0.0649(14)
C2	0.5201(4)	0.64386(11)	0.52018(9)	0.0492(5)	0.0464(10)	0.0508(11)	0.0504(11)
C15	0.7645(5)	0.63688(13)	-0.07537(10)	0.0595(6)	0.0746(15)	0.0631(14)	0.0408(10)
C4	0.3744(4)	0.67886(14)	0.42304(11)	0.0620(6)	0.0455(11)	0.0779(16)	0.0625(13)
C17	0.4201(5)	0.55294(12)	-0.06411(10)	0.0630(6)	0.0858(17)	0.0564(13)	0.0468(11)
C5	0.5623(4)	0.64656(14)	0.39392(9)	0.0575(6)	0.0444(11)	0.0798(16)	0.0481(11)
C13	0.9485(4)	0.68347(12)	0.01525(10)	0.0556(5)	0.0569(13)	0.0521(12)	0.0579(12)
C14	0.9314(4)	0.67926(14)	-0.04814(11)	0.0633(6)	0.0664(15)	0.0657(14)	0.0578(13)
C21	0.4796(4)	0.35315(12)	0.26484(8)	0.0516(5)	0.0601(12)	0.0560(12)	0.0386(9)
C19	0.2943(4)	0.52366(12)	0.03489(11)	0.0587(6)	0.0614(13)	0.0480(12)	0.0668(14)
C23	0.6114(4)	0.44412(14)	0.19402(11)	0.0618(6)	0.0486(11)	0.0711(15)	0.0657(14)
C18	0.2685(5)	0.51695(13)	-0.02765(11)	0.0660(6)	0.0764(16)	0.0545(14)	0.0671(15)
C7	0.7114(4)	0.61138(13)	0.49219(10)	0.0583(6)	0.0484(11)	0.0737(15)	0.0528(12)
C6	0.7312(4)	0.61272(13)	0.43000(10)	0.0613(6)	0.0481(12)	0.0800(16)	0.0556(13)
C24	0.4182(4)	0.48741(11)	0.20744(9)	0.0493(5)	0.0539(11)	0.0514(12)	0.0426(10)
C26	0.2846(5)	0.39583(13)	0.27708(10)	0.0639(6)	0.0774(16)	0.0608(14)	0.0533(12)
C25	0.2544(4)	0.46303(12)	0.24849(10)	0.0610(6)	0.0617(13)	0.0601(14)	0.0611(13)
C22	0.6416(4)	0.37712(13)	0.22241(11)	0.0615(6)	0.0454(12)	0.0678(15)	0.0714(15)
C1	0.3234(5)	0.67142(17)	0.61295(12)	0.0830(9)	0.096(2)	0.093(2)	0.0602(14)

O1	0.5130(3)	0.63812(10)	0.58202(7)	0.0691(5)	0.0707(10)	0.0896(12)	0.0470(8)
N2	0.4627(3)	0.56310(9)	0.06117(7)	0.0491(4)	0.0577(10)	0.0421(9)	0.0476(9)
O5	0.3867(3)	0.55567(8)	0.18252(7)	0.0623(4)	0.0788(10)	0.0536(9)	0.0544(9)
O4	0.5001(4)	0.28826(9)	0.29527(7)	0.0707(5)	0.0952(12)	0.0626(10)	0.0541(9)
O3	0.7994(3)	0.64432(8)	0.11342(6)	0.0532(4)	0.0599(9)	0.0582(9)	0.0416(7)
C11	0.9752(4)	0.68817(12)	0.14246(10)	0.0535(5)	0.0541(12)	0.0504(12)	0.0561(12)
C8	0.5832(5)	0.6530(2)	0.32564(11)	0.0870(9)	0.0612(15)	0.146(3)	0.0532(13)
C9	0.7866(5)	0.61955(19)	0.29836(11)	0.0839(9)	0.0724(16)	0.132(3)	0.0469(13)
N1	0.8076(4)	0.63422(12)	0.23305(8)	0.0613(5)	0.0561(11)	0.0878(15)	0.0401(9)
C10	0.9633(4)	0.67970(12)	0.21004(10)	0.0545(5)	0.0545(12)	0.0552(12)	0.0538(12)
O2	1.1066(3)	0.71510(10)	0.24101(8)	0.0781(5)	0.0756(11)	0.0862(12)	0.0724(10)



References

1. L. D. Costanzo, H. Wade, S. Geremia, L. Randaccio, V. Pavone, W. F. D. Grado, A. Lombardi, *J. Am. Chem. Soc.* 2001, *123*, 12749
2. J. T. L. Groves, A. Baron, *J. Am. Chem. Soc.* 1989, *111*, 5442
3. G. R. Desiraju, *Angew. Chem. Int. Ed.* 1995, *34*, 2311
4. S. R. Batten, R. Robson, *Angew. Chem. Int. Ed.* 1998, *37*, 1460
5. M. Simonetta, S. Carra, *The Chemistry of Carboxylic Acids and Esters*, Wiley-Interscience, New York, 1969, 1
6. L. Ebersohn, *The Chemistry of Carboxylic Acids and Esters*, Wiley-Interscience, New York, 1969, 211
7. G. R. Desiraju, *Crystal Engineering: The Design of Organic Solids*, Elsevier, New York, 1989
8. R. M. Silverstein, G. C. Bassler, T. C. Morrill, *Spectrometric Identification of Organic Compounds*, John Wiley & Sons, New York, 1981
9. F. A. Cotton, C. Lin, C. A. Murillo, *Acc. Chem. Res.* 2001, *34*, 759
10. R. Murugavel, M. G. Walawalkar, M. Dan, H. W. Roesky, C. N. R. Rao, *Acc. Chem. Res.* 2004, *37*, 763
11. L. Brammer, M. D. Burgard, M. D. Eddleston, C. S. Rodger, N. P. Rath, H. Adams, *CrystEngComm.* 2002, *4*, 239
12. L. Brammer, M. D. Burgard, C. S. Rodger, J. K. Swearingen, N. P. Rath, *Chem. Commun.* 2001, 2468
13. C. M. Rivas, L. Brammer, *Coord. Chem. Rev.* 1999, *183*, 43
14. R. Vaidyanathan, S. Natarajan, C. N. R. Rao, *Cryst. Growth & Des.* 2003, *3*, 47
15. D. Guo, B. Zhang, C. Duan, K. Pang, Q. Meng, *Dalton Trans.* 2002, *20*, 3783
16. M. Eddaouddi, D. B. Moler, H. Li, B. Chen, T. M. Reineke, M. O'Keeffe, O. M. Yaghi, *Acc. Chem. Res.* 2001, *34*, 319
17. A. J. Wu, J. E. Penner-Hahn, V. L. Pecoraro, *Chem. Rev.* 2004, *104*, 903
18. A. E. Tapper, J. R. Long, R. J. Staples, P. Stavropoulos, *Angew. Chem. Int. Ed.* 2000, *39*, 2343
19. S. B. Marr, R. O. Carvel, D. T. Richens, H. -J. Lee, M. Lane, P. Stavropoulos, *Inorg. Chem.* 2000, *39*, 4630
20. K. L. Gurunatha, T. K. Maji, *Inorg. Chim. Acta* 2008, doi:10.1016/j.ica.2008.07.026
21. P. Kopel, Z. Trávníček, J. Marek, J. Mrozinski, *Polyhedron* 2004, *23*, 1573
22. R. Baggio, M. Percec, M. T. Garland, *Acta. Cryst.* 1996, *C52*, 2457

23. J. Kaizer, T. Csay, G. Speier, M. Réglie, M. Giorgi, *Inorg. Chem. Commun.* 2006, 9, 1037
24. A. M. Baruah, R. Sarma, J. B. Baruah, *Inorg. Chem. Commun.* 2008, 11, 121
25. A. M. Baruah, A. Karmakar, J. B. Baruah, *Inorg. Chim. Acta* 2008, 361, 2777
26. R. Sarma, A. Karmakar, J. B. Baruah, *Inorg. Chem.* 2008, 47, 763
27. J. E. Sheats, R. S. Czernuszewicz, G. C. Dismukes, A. L. Rheingold, V. Petrouleas, J. Stubbe, W. H. Armstrong, R. H. Beer, S. J. Lippard, *J. Am. Chem. Soc.*, 1987, 109, 1435
28. K. Wieghardt, V. Bossek, D. Ventur, J. Weiss, *J. Chem. Soc. Chem. Commun.* 1985, 347
29. S. Bhaduri, A. J. Tasiopoulos, M. A. Bolcar, K. A. Abboud, W. E. Streib, G. Christou, *Inorg. Chem.* 2003, 42, 1483
30. D. Coucouvanis, R. A. Reynolds, W. R. Dunham, *J. Am. Chem. Soc.* 1995, 117, 7570
31. B. -H. Yea, I. D. Williams, X. -Y. Li, *J. Inorg. Biochem.* 2002, 92, 128
32. J. Drew, M. B. Hursthouse, P. Thornton, A. J. Welch, *J. Chem. Soc. Chem. Commun.* 1973, 52
33. S. -B. Yu, S. J. Lippard, I. Shweky, A. Bino, *Inorg. Chem.* 1992, 31, 3502
34. U. Turpeinen, R. Hämäläinen, J. Reedijk, *Polyhedron* 1987, 6, 1603
35. K. Geetha, M. Nethaji, A. R. Chakravarty, N. Y. Vasanthacharya, *Inorg. Chem.* 1996, 35, 7666
36. F. A. Mautner, R. Vicente, F. R.Y. Louka, S. S. Massoud, *Inorg. Chim. Acta* 2008, 361, 1339
37. C. Chailuecha, S. Youngme, C. Pakawatchai, N. Chaichit, G. A. van Albada, J. Reedijk, *Inorg. Chim. Acta* 2006, 359, 4168
38. S. Youngme, C. Chailuecha, G. A. van Albada, C. Pakawatchai, N. Chaichit, J. Reedijk, *Inorg. Chim. Acta* 2005, 358, 1068
39. S. Youngme, A. Cheansirisomboon, C. Danvirutai, C. Pakawatchai, N. Chaichit, C. Engkagul, G. A. van Albada, J. S. Costa, J. Reedijk, *Polyhedron* 2008, 27, 1875
40. J. Bickley, R.P. Bonar-Law, M.A. Borrero Martinez, A. Steiner, *Inorg. Chim. Acta* 2004, 357, 891
41. P. M. Selvakumar, E. Suresh, P. S. Subramanian, *Inorg. Chim. Acta* 2008, 361, 1503
42. R. Sarma, A. Karmakar, J. B. Baruah, *Inorg. Chim. Acta* 2008, 361, 2081
43. F. Sapiña, M. Burgos, E. Escrivá, J. -V. Folgado, D. Beltrán, P. Gómez-Romero, *Inorg. Chim. Acta* 1994, 216, 185

44. J. Chen, X. Wang, Y. Zhu, J. Lin, X. Yang, Y. Li, Y. Lu, Z. Guo, *Inorg. Chem.* 2005, 44, 3422
45. P. Christian, G. Rajaraman, A. Harrison, M. Helliwell, J. J. W. McDouall, J. Raftery, R. E. P. Winpenny, *Dalton Trans.* 2004, 2550
46. A. R. E. Baikie, M. B. Hursthouse, D. B. New, P. Thornton, *J. Chem. Soc. Chem. Commun.* 1978, 6
47. A. R. E. Baikie, M. B. Hursthouse, D. B. New, P. Thornton, *J. Chem. Soc. Chem. Commun.* 1980, 684
48. J. B. Vincent, H. -R. Chang, K. Folting, J. C. Huffman, G. Christou, D. N. Hendrickson, *J. Am. Chem. Soc.* 1987, 109, 5703
49. S. W. Zhang, Y. G. Wei, Q. Liu, M. C. Shao, *Polyhedron* 1996, 15, 1041
50. T. C. Stamatatos, D. Foguet-Albiol, C. C. Stoumpos, C. P. Raptopoulou, A. Terzis, W. Wernsdorfer, S. P. Perlepes, G. Christou, *J. Am. Chem. Soc.* 2005, 127, 15380
51. S. -C. Lee, T. C. Stamatatos, S. Hill, S. P. Perlepes, G. Christou, *Polyhedron* 2007, 26, 2225
52. R. L. Rardin, P. Poganiuch, A. Bino, D. P. Goldberg, W. B. Tolman, S. Liu, S. J. Lippard, *J. Am. Chem. Soc.* 1992, 114, 5240
53. K. S. Gavrilenko, S. V. Punin, O. Cador, S. Golhen, L. Ouahab, V. V. Pavlishchuk, *J. Am. Chem. Soc.* 2005, 127, 12246
54. B. -H. Ye, X. -M. Chen, F. Xue, L. -N. Ji, T. C. W. Mak, *Inorg. Chim. Acta* 2000, 299, 1
55. R. A. Reynolds, W. R. Dunham, D. Coucouvanis, *Inorg. Chem.* 1998, 37, 1232
56. W. Clegg, I. R. Little, B. P. Straughan, *Inorg. Chem.* 1988, 27, 1916
57. J. Catterick, M. B. Hursthouse, D. B. New, P. Thornton, *J. Chem. Soc. Chem. Commun.* 1974, 843
58. M. W. Wemple, H. -L. Tsai, S. Wang, J. P. Claude, W. E. Streib, J. C. Huffman, D. N. Hendrickson, G. Christou, *Inorg. Chem.* 1996, 35, 6437
59. N. Aliaga-Alcalde, R. S. Edwards, S. O. Hill, W. Wernsdorfer, K. Folting, G. Christou, *J. Am. Chem. Soc.* 2004, 126, 12503
60. S. Wang, H. -L. Tsai, K. S. Hagen, D. N. Hendrickson, George Christou, *J. Am. Chem. Soc.* 1994, 116, 8376
61. S. Wang, M. S. Wemple, J. Yoo, K. Folting, J. C. Huffman, K. S. Hagen, D. N. Hendrickson, G. Christou, *Inorg. Chem.* 2000, 39, 1501
62. B. Albela, M. S. E. Fallah, J. Ribas, K. Folting, G. Christou, D. N. Hendrickson, *Inorg. Chem.* 2001, 40, 1037

63. H. Andres, R. Basler, H. -U. Güdel, G. Aromí, G. Christou, H. Büttner, B. Rufflé, *J. Am. Chem. Soc.* 2000, *122*, 12469
64. A. K. Boudalis, N. Lalioti, G. A. Spyroulias, C. P. Raptopoulou, A. Terzis, V. Tangoulis, S. P. Perlepes, *J. Chem. Soc. Dalton Trans.* 2001, 955
65. V. I. Ponomarev, L. O. Atovmyan, S. A. Bobkova, K. I. Turté, *Dokl. Akad. Nauk. SSSR*, 1984, *274*, 368
66. W. H. Armstrong, M. E. Roth, S. J. Lippard, *J. Am. Chem. Soc.* 1987, *109*, 6318
67. J. K. McCusker, J. B. Vincent, E. A. Schmitt, M. L. Mino, K. Shin, D. K. Coggin, P. M. Hagen, J. C. Huffman, G. Christou and D. N. Hendrickson, *J. Am. Chem. Soc.* 1991, *113*, 3012
68. P. Chaudhuri, M. Winter, P. Fleischhauer, W. Haase, U. Florke, H. -J. Haupt, *Inorg. Chim. Acta* 1993, *212*, 241
69. K. Dimitrou, A. D. Brown, K. Folting, G. Christou, *Inorg. Chem.* 1999, *38*, 1834
70. K. Dimitrou, K. Folting, W. E. Streib, G. Christou, *J. Am. Chem. Soc.* 1993, *115*, 6432
71. K. Dimitrou, K. Folting, W. E. Streib, G. Christou, *J. Chem. Soc. Chem. Commun.* 1994, 1385
72. A. N. Belyaev, A. I. Fisher, M. Y. Gorlov, S. A. Simanova, *Russ. J. Gen. Chem.* 2004, *74*, 632.
73. A. Tsohos, S. Dionyssopoulou, C. P. Raptopoulou, A. Terzis, E. G. Bakalbassis, S. P. Perlepes, *Angew. Chem. Int. Ed.* 1999, *38*, 983
74. G. S. Papaefstathiou, A. Escuer, M. Font-Bardía, S. P. Perlepes, X. Solans, R. Vicente, *Polyhedron* 2002, *21*, 2027
75. M. Murugesu, R. Clérac, B. Pilawa, A. Mandel, C. E. Anson, A. K. Powell, *Inorg. Chim. Acta* 2002, *337*, 328
76. G. Vučković, M. Antonijević-Nikolić, T. Lis, J. Mroziński, M. Korabik, D. D. Radanović, *J. Mol. Struct.* 2008, *872*, 135
77. Y. Sevryugina, O. Hietsoi, M. A. Petrukhina, *Chem. Commun.* 2007, 3853
78. N. Lah, J. Koller, G. Giester, P. Segedin, I. Leban, *New J. Chem.* 2002, *26*, 933
79. T. Ohshima, T. Iwasaki, K. Mashima, *Chem. Commun.* 2006, 2711
80. J. P. Picart, F. J. Sanchez, J. Casabó, J. Rius, A. Alvarez-Larena, J. Ros, *Inorg. Chem. Commun.* 2002, *5*, 130
81. A. E. Malkov, I. G. Fomina, A. A. Sidorov, G. G. Aleksandrov, I. M. Egorova, N. I. Latosh, O. N. Chupakhin, G. L. Rusinov, Y. V. Rakitin, V. M. Novotortsev, V. N. Ikorskii, I. L. Eremenkoa, I. I. Moiseev, *J. Mol. Struct.* 2003, *656*, 207

82. A. K. Boudalis, C. P. Raptopoulou, V. Psycharis, Y. Sanakis, B. Abarca, R. Ballesteros, M. Chadlaoui, *Dalton Trans.* 2007, 3582
83. T. C. Stamatatos, K. A. Abboud, G. Christou, *J. Mol. Struct.* 2008, doi:10.1016/j.molstruc.2008.04.031.
84. H. Kumagai, Y. Oka, S. Kawata, M. Ohba, K. Inoue, M. Kurmoo, H. Ōkawa, *Polyhedron* 2003, 22,1917
85. A. A. Sidorov, I. G. Fomina, S. S. Talismanov, G. G. Aleksandrov, V. M. Novotortsev, S. E. Nefedov, I. L. Eremenko, *Russ. J. Coord. Chem.* 2001, 27, 548
86. A. Masello, M. Murugesu, K. A. Abboud, G. Christou, *Polyhedron* 2007, 26, 2276
87. C. Lei, J. -G. Mao, Y. -Q. Sun, H. -Y. Zeng, A. Clearfield, *Inorg. Chem.* 2003, 42, 6157
88. D. J. Darensbourg, J. R. Wildeson, J. C. Yarbrough, *Inorg. Chem.* 2002, 41, 973
89. R. P. Feazell, C. E. Carson, K. K. Klausmeyer, *Inorg. Chem. Commun.* 2007, 10, 873
90. N. Lalioti, C. P. Raptopoulou, A. Terzis, A. E. Aliev, S. P. Perlepes, I. P. Gerathanassis, E. Manessi-Zoupa, *Chem. Commun.* 1998, 1513
91. C. Boskovic, J. C. Huffman, G. Christou, *Chem. Commun.* 2002, 2502
92. D. W. Low, D. M. Eichborn, A. Draganescu, W. H. Armstrong, *Inorg. Chem.* 1991, 30, 878
93. R. Sessoli, H. -L. Tsai, A. R. Schake, S. Wang, J. B. Vincent, K. Folting, D. Gatteschi, G. Christou, D. N. Hendrickson, *J. Am. Chem. Soc.* 1993, 115, 1804
94. R. Sessoli, D. Gatteschi, A. Caneschi, M. A. Novak, *Nature* 1993, 365, 141
95. P. Artus, C. Boskovic, J. Yoo, W. E. Streib, L. -C. Brunel, D. N. Hendrickson, G. Christou, *Inorg. Chem.* 2001, 40, 4199
96. C. Lampropoulos, M. Murugesu, K. A. Abboud, G. Christou, *Polyhedron* 2007, 26, 2129
97. Z. Sun, P. Gantzel, D. Hendrickson, *Inorg. Chem.* 1996, 35, 6640
98. J. T. Brockman, J. C. Huffman, G. Christou, *Angew. Chem. Int. Ed.* 2002, 41, 2506
99. M. Soler, W. Wernsdorfer, K. Folting, M. Pink, G. Christou, *J. Am. Chem. Soc.* 2004, 126, 2156
100. J. Tasiopoulos, A. Vinslava, W. Wernsdorfer, K. A. Abboud, G. Christou, *Angew. Chem.Int. Ed.* 2004, 43, 2117
101. M. Soler, E. Rumberger, K. Folting, D. N. Hendrickson, G. Christou, *Polyhedron* 2001, 20, 1365
102. J. C. Goodwin, R. Sessoli, D. Gatteschi, W. Wernsdorfer, A. K. Powell, S. L. Heath, *J. Chem. Soc. Dalton Trans.* 2000, 1835

103. S. L. Heath, A. K. Powell, *Angew. Chem. Int. Ed.* 1992, 31, 191
104. K. Dimitrou, J. -S. Sun, K. Folting, G. Christou, *Inorg. Chem.* 1995, 34, 4160
105. E. K. Brechin, A. Graham, A. Parkin, S. Parsons, A. M. Seddon, R. E. P. Winpenny, *J. Chem. Soc. Dalton Trans.* 2000, 3242
106. M. Murrie, D. Biner, H. Stoeckli-Evans, H. U. Güdel, *Chem. Commun.* 2003, 230
107. A. L. Dearden, S. Parsons, R. E. P. Winpenny, *Angew. Chem. Int. Ed.* 2001, 40, 151
108. R. E. P. Winpenny, *J. Chem. Soc. Dalton Trans.* 2002, 1
109. A. J. Blake, C. M. Grant, C. I. Gregory, S. Parsons, J. M. Rawson, D. Reed, R. E. P. Winpenny, *J. Chem. Soc. Dalton Trans.* 1995, 163
110. M. Murugesu, P. King, R. Clérac, C. E. Anson, A. K. Powell, *Chem. Commun.* 2004, 740
111. A. J. Tasiopoulos, W. Wernsdorfer, B. Moulton, M. J. Zaworotko, G. Christou, *J. Am. Chem. Soc.* 2003, 125, 15274
112. A. Mishra, W. Wernsdorfer, K. A. Abboud, G. Christou, *J. Am. Chem. Soc.* 2004, 126, 15648
113. A. Mishra, K. A. Abboud, G. Christou, *Inorg. Chem.* 2006, 45, 2364
114. K. S. Gavrilenko, S. V. Punin, O. Cador, S. Golhen, L. Ouahab, V. V. Pavlishchuk, *Inorg. Chem.* 2005, 44, 5903
115. X. -M. Chen, Y. -L. Wu, Y. -Y. Yang, S. M. J. Aubin, D. N. Hendrickson, *Inorg. Chem.* 1998, 37, 6186
116. Y. Cui, F. Zheng, Y. Qian, J. Huang, *Inorg. Chim. Acta* 2001, 315, 220
117. C. Janiak, *J. Chem. Soc. Dalton Trans.* 2003, 2781
118. R. Robson, B. F. Abrahams, S. R. Batten, R. W. Gable, B. F. Hoskins, J. P. Liu, *ACS Symp. Ser.* 1992, 499, 256
119. S. Kitagawa, S. Noro, *Compreh. Coord. Chem.* 2004, 7, 231
120. E. Y. Lee, M. P. Suh, *Angew. Chem. Int. Ed.* 2004, 43, 2798
121. H. J. Choi, M. P. Suh, *Inorg. Chem.* 1999, 38, 6309
122. H. R. Moon, J. H. Kim, M. P. Suh, *Angew. Chem. Int. Ed.* 2005, 44, 1261
123. W. J. Belcher, C. A. Longstaff, M. R. Neckenig, J. W. Steed, *Chem. Commun.* 2002, 1602
124. P. J. Nichols, C. L. Raston, J. W. Steed, *Chem. Commun.* 2001, 1062
125. B. Paul, B. Zimmermann, K. M. Fromm, C. Janiak, *Z. Anorg. Allg. Chem.* 2004, 630, 1650.
126. G. -P. Yong, Z. -Y. Wang, Y. Cui, *Eur. J. Inorg. Chem.* 2004, 4317

127. M. Devereux, M. McCann, V. Leon, M. Geraghty, V. McKee, J. Wikaira, *Polyhedron* 2000, 19, 1205
128. D. Sun, R. Cao, Y. Liang, Q. Shi, W. Su, M. Hong, *J. Chem. Soc. Dalton Trans.* 2001, 2335
129. C. D. Ene, F. Tuna, O. Fabelo, C. Ruiz-Pérez, A. M. Madalan, H. W. Roesky, M. Andruh, *Polyhedron* 2008, 27, 574
130. S. G. Baca, I. G. Filippova, N. V. Gerbeleu, Y. A. Simonov, M. Gdaniec, G. A. Timco, O. A. Gherco, Y. L. Malaestean, *Inorg. Chim. Acta* 2003, 344, 109
131. X. -M. Zhang, M. -L. Tong, M. -L. Gong, X. -M. Chen, *Eur. J. Inorg. Chem.* 2003, 138
132. F. Yang, Y. Ren, D. Li, F. Fu, G. Qi, Y. Wang, *J. Mol. Struct.* 2008, doi:10.1016/j.molstruc.2008.05.039.
133. C. Ruiz-Perez, P. Lorenzo-Luis, M. Hernandez-Molina, M. M. Laz, F. S. Delgado, P. Gili, M. Julve, *Eur. J. Inorg. Chem.* 2004, 3873
134. B. O. Patrick, C. L. Stevens, A. Storr, R. C. Thompson, *Polyhedron* 2003, 22, 3025
135. A. M. Baruah, A. Karmakar, J. B. Baruah, *Polyhedron* 2007, 26, 4518
136. A. M. Kutasi, S. R. Batten, A. R. Harris, B. Moubaraki, K. S. Murray, *CrystEngComm.* 2002, 4, 202
137. K. -L. Zhang, Y. Xu, J. -G. Lin, X. -Z. You, *J. Mol. Struct.* 2004, 703, 63
138. M. -S. Wang, G. -C. Guo, M. -L. Fu, L. Xu, L. -Z. Cai, J. -S. Huang, *Dalton Trans.* 2005, 2899
139. B. Conerney, P. Jensen, P. E. Kruger, B. Moubaraki, K. S. Murray, *CrystEngComm.* 2003, 5, 454
140. P. D. C. Dietzel, R. Blom, H. Fjellvåg, *Dalton Trans.* 2006, 586
141. Y. -Z. Zheng, G. -F. Liu, B. -H. Ye, X. -M. Chen, *Z. Anorg. Allg. Chem.* 2004, 630, 296
142. C. Piguet, G. Bernardinelli, G. Hopfgartner, *Chem. Rev.* 1997, 97, 2005
143. X. -M. Chen, G. -F. Liu, *Chem. Eur. J.* 2002, 8, 4811
144. Y. Qi, Y. Wang, C. Hu, M. Cao, L. Mao, E. Wang, *Inorg. Chem.* 2003, 42, 8519
145. O. K. Kwak, K. S. Min, B. G. Kim, *Inorg. Chim. Acta* 2007, 360, 1678
146. H. -T. Zhang, T. Shao, H. -Q. Wang, X. -Z. You, *Acta Cryst.* 2003, C59, m259
147. M. Yuan, E. B. Wang, Y. Lu, S. T. Wang, Y. G. Li, L. Wang, C. W. Hu, *Inorg. Chim. Acta* 2003, 344, 257
148. J. -C Yao, W. Huang, B. Li, S. Gou, Y. Xu, *Inorg. Chem. Commun.* 2002, 5, 711
149. M. P. Suh, H. R. Moon, E. Y. Lee, S. Y. Jang, *J. Am. Chem. Soc.* 2006, 128, 4710

150. J. -Z. Zhang, W. -R. Cao, J. -X. Pan, Q. -W. Chen, *Inorg. Chem. Commun.* 2007, 10, 1360
151. H. Kumagai, Y. Oka, K. Inoue, M. Kurmoo, *J. Chem. Soc. Dalton Trans.* 2002, 3442
152. Z. -Q. Liu, Y. -T. Li, Z. -Y. Wu, S. -F. Zhang, *Inorg. Chim. Acta* 2008, doi:10.1016/j.ica.2008.03.023.
153. M. E. Braun, C. D. Steffek, J. Kim, P. G. Rasmussen, O. M. Yaghi, *Chem. Commun.* 2001, 2532
154. J. Y. Lu, E. E. Kohler, *Inorg. Chem. Commun.* 2002, 5, 600
155. M. Dan, C. N. R. Rao, *Chem. Eur. J.* 2005, 11, 7102
156. Y. Zhao, M. Hong, D. Sun, R. Cao, *J. Chem. Soc. Dalton Trans.* 2002, 1354
157. M. A. Braverman, R. J. Staples, R. M. Supkowski, R. L. LaDuca, *Polyhedron* 2008, 27, 2291
158. D. P. Martin, M. A. Braverman, R. L. LaDuca, *Cryst. Growth & Des.* 2007, 7, 2609
159. C. Qin, X. Wang, E. Wang, C. Hu, L. Xu, *Inorg. Chem. Commun.* 2004, 7, 788
160. D. -X. Hu, P. -K. Chen, F. Luo, L. Xue, Y. Che, J. -M. Zheng, *Inorg. Chim. Acta* 2007, 360, 4077
161. R. H. Groeneman, L. R. MacGillivray, J. L. Atwood, *Chem. Commun.* 1998, 2735
162. L. R. MacGillivray, R. H. Groeneman, J. L. Atwood, *J. Am. Chem. Soc.* 1998, 120, 2676
163. J. Tao, X. -M. Chen, R. -B. Huang, L. -S. Zheng, *J. Solid State Chem.* 2003, 170, 130
164. T. K. Maji, D. Ghoshal, E. Zangrando, J. Ribas, N. R. Chaudhuri, *CrystEngComm.* 2004, 6, 623
165. J. -Y. Zhang, Y. Ma, A. -L. Cheng, Q. Yue, Q. Sun, E. -Q. Gao, *Dalton Trans.* 2008, 2061
166. D. Armentano, G. D. Munno, F. Lloret, M. Julve, J. Curély, A. M. Babb, J. Y. Lu, *New J. Chem.* 2003, 27, 161
167. G. D. Munno, D. Armentano, M. Julve, F. Lloret, R. Lescouëzec, J. Faus, *Inorg. Chem.* 1999, 38, 2234
168. G. D. Munno, M. Julve, F. Nicolò, F. Lloret, J. Faus, R. Ruiz, E. Sinn, *Angew. Chem. Int. Ed.* 1993, 32, 795
169. G. D. Munno, R. Ruiz, F. Lloret, J. Faus, R. Sessoli, M. Julve, *Inorg. Chem.* 1995, 34, 408
170. J. W. Ko, K. S. Min, M. P. Suh, *Inorg. Chem.* 2002, 41, 2151
171. D. -C. Wen, S. -X. Liu, J. Ribas, *Inorg. Chem. Commun.* 2007, 10, 661
172. H. J. Choi, M. P. Suh, *J. Am. Chem. Soc.* 1998, 120, 10622

173. T. -B. Lu, H. Xiang, R. L. Luck, Z. -W. Mao, D. Wang, C. Chen, L. -N. Ji, *CrystEngComm*. 2001, *41*, 168
174. K. E Holmes, P. F. Kelly, M. R. J. Elsegood, *Dalton Trans.* 2004, 3488
175. R. -Q. Zou, Y. Yamada, Q. Xu, *Microporous and Mesoporous Materials* 2006, *91*, 233
176. H. Kim, M. P. Suh, *Inorg. Chem.* 2005, *44*, 810
177. X. Li, R. Cao, D. Sun, W. Bi, Y. Wang, X. Li, M. Hong, *Cryst. Growth & Des.* 2004, *4*, 775
178. Y. -Y. Liu, J. -F. Ma, J. Yang, J. -C. Ma, G. -J. Ping, *CrystEngComm*. 2008, *10*, 565
179. Y. Wei, Y. Yu, K. Wu, *Cryst. Growth & Des.* 2007, *7*, 2262
180. X. -S. Wang, H. Zhao, Z. -R. Qu, Q. Ye, J. Zhang, R. -G. Xiong, X. -Z. You, H. -K. Fun, *Inorg. Chem.* 2003, *42*, 5786
181. O. R. Evans, W. Lin, *Chem. Mater.* 2001, *13*, 2705
182. R. -G. Xiong, J. -L. Zuo, X. -Z. You, B. F. Abrahams, Z. -P. Bai, C. -M. Che, H. -K. Fun, *Chem. Commun.* 2000, 2061
183. W. Lin, L. Ma, O. R. Evans, *Chem. Commun.* 2000, 2263
184. J. Tao, M. -L. Tong, X. -M. Chen, *J. Chem. Soc. Dalton Trans.* 2000, 3669
185. N. Sträter, W. N. Lipscomb, T. Klabunde, B. Krebs, *Angew. Chem. Int. Ed.* 1996, *35*, 2024
186. W. N. Lipscomb, N. Sträter, *Chem. Rev.* 1996, *96*, 2375
187. D. E. Wilcox, *Chem. Rev.* 1996, *96*, 2435
188. G. C. Dismukes, *Chem. Rev.* 1996, *96*, 2909
189. R. P. Hausinger, *Biochemistry of Nickel*, Plenum Press, New York, 1993
190. I. Bertini, H. B. Gray, S. J. Lippard, J. S. Valentine (Eds.), *Bioinorganic Chemistry*, University Science Books, Mill Valley, CA, 1994
191. E. Y. Tshuva, S. J. Lippard, *Chem. Rev.* 2004, *104*, 987
192. J. B. Sumner, *J. Biol. Chem.* 1926, *69*, 435
193. N. E. Dixon, P. W. Riddles, C. Gazzola, R. L. Blakeley, B. Zerner, *Can. J. Biochem.* 1980, *58*, 1335
194. E. Jabri, M. B. Carr, R. P. Hausinger, P. A. Karplus, *Science* 1995, *268*, 998
195. S. J. Lippard, *Science* 1995, *268*, 996
196. M. A. Pearson, L. O. Michel, R. P. Hausinger, P. A. Karplus, *Biochemistry* 1997, *36*, 8164
197. H. E. Wages, K. L. Taft, S. J. Lippard, *Inorg. Chem.* 1993, *32*, 4985
198. S. Benini, W. R. Rypniewski, K. S. Wilson, S. Miletto, S. Ciurli, S. Mangani, *Structure* 1999, *7*, 205

199. P. A. Karplus, M. A. Pearson, R. P. Hausinger, *Acc. Chem. Res.* 1997, 30, 330
200. Z. Kahn, *Indian J. Chem.* 1996, 35A, 1116
201. A. M. Barrios, S. J. Lippard, *J. Am. Chem. Soc.* 2000, 122, 9172
202. W. T. Lowther, B. W. Matthews, *Chem. Rev.* 2002, 102, 4581
203. R. C. Holz, *Coor. Chem. Rev.* 2002, 232, 5
204. M. P. Allen, A. H. Yamada, F. H. Carpenter, *Biochemistry*, 1983, 22, 3778
205. S. K. Burley, P. R. David, A. Taylor, W. N. Lipscomb, *Proc. Natl. Acad. Sci.* 1990, 87, 6878
206. S. K. Burley, P. R. David, R. M. Sweet, A. Taylor, W. N. Lipscomb, *J. Mol. Biol.* 1992, 224, 113
207. N. Sträter, W. N. Lipscomb, *Biochemistry* 1995, 34, 9200
208. N. Sträter, W. N. Lipscomb, *Biochemistry* 1995, 34, 14792
209. S. L. Roderick, B. W. Matthews, *Biochemistry* 1993, 32, 3907
210. W. T. Lowther, D. A. McMillen, A. M. Orville, B. W. Matthews, *Proc. Natl. Acad. Sci.* 1998, 95, 12153
211. B. Chevrier, C. Schalk, H. D'Orchymont, J. -M. Rondeau, D. Moras, C. Tarnus, *Structure* 2, 1994, 283
212. B. C. Antanaitis, P. Aisen, *Adv. Inorg. Biochem* 1983, 5, 111
213. J. B. Vincent, G. L. Olivier-Lilley, B. A. Averill, *Chem. Rev.* 1990, 90, 1447
214. T. Klabunde, N. Sträter, R. Fröhlich, H. Witzel, B. Krebs, *J. Mol. Biol.* 1996, 259, 737
215. N. T. Truong, J. I. Naseri, A. Vogel, A. Rompel, B. Krebs, *Arch. Biochem. Biophys.* 2005, 440, 38
216. N. L. Rosi, J. Kim, M. Eddaoudi, B. Chen, M. O'Keeffe, O. M. Yaghi, *J. Am. Chem. Soc.* 2005, 127, 1504
217. O. M. Yaghi, M. O'Keeffe, N. W. Ockwig, H. K. Chae, M. Eddaoudi, J. Kim, *Nature* 2003, 423, 705
218. M. Eddaoudi, J. Kim, N. Rosi, D. Vodak, J. Wachter, M. O'keeffe, O. M. Yaghi, *Science* 2002, 295, 469
219. H. Li, M. Eddaoudi, M. O'Keeffe, O. M. Yaghi, *Nature* 1999, 402, 276
220. N. L. Rosi, J. Eckert, M. Eddaoudi, D. T. Vodak, J. Kim, M. O'Keeffe, O. M. Yaghi, *Science* 2003, 300, 1127
221. J. L. C. Rowsell, O. M. Yaghi, *Angew. Chem. Int. Ed.* 2005, 44, 4670
222. N. L. Rosi, M. Eddaoudi, J. Kim, Michael O'Keeffe, O. M. Yaghi, *Angew. Chem. Int. Ed.* 2002, 41, 284
223. M. Eddaoudi, H. Li, O. M. Yaghi, *J. Am. Chem. Soc.* 2000, 122, 1391

224. H. K. Chae, D. Y. Siberio-Perez, J. Kim, Y. B. Go, M. Eddaoudi, A. J. Matzger, M. O'Keeffe, O. M. Yaghi, *Nature* 2004, 427, 523
225. A. C. Sudik, A. R. Millward, N. W. Ockwig, A. P. Côté, J. Kim, O. M. Yaghi, *J. Am. Chem. Soc.* 2005, 127, 7110
226. A. C. Sudik, A. P. Côté, A. G. Wong-Foy, M. O'Keeffe, O. M. Yaghi, *Angew. Chem. Int. Ed.* 2006, 45, 2528
227. B. Chen, N. W. Ockwig, A. R. Millward, D. S. Contreras, O. M. Yaghi, *Angew. Chem. Int. Ed.* 2005, 44, 4745
228. B. Chen, M. Eddaoudi, S. T. Hyde, M. O'Keeffe, O. M. Yaghi, *Science* 2001, 291, 1021
229. G. Férey, C. Mellot-Draznieks, C. Serre, F. Millange, J. Cutour, S. Surble, I. Margiolaki, *Science* 2005, 309, 2040
230. G. Férey, C. Serre, C. Mellot-Draznieks, F. Millange, S. Surble, J. Dutour, I. Margiolaki, *Angew. Chem. Int. Ed.* 2004, 43, 6296
231. D. Sun, S. Ma, Y. Ke, D. J. Collins, H. -C. Zhou, *J. Am. Chem. Soc.* 2006, 128, 3896
232. B. Kesanli, Y. Cui, M. R. Smith, E. W. Bittner, C. Bockrath, W. Lin, *Angew. Chem. Int. Ed.* 2005, 44, 72
233. S. Ma, D. Sun, X. -S. Wang, H. -C. Zhou, *Angew. Chem. Int. Ed.* 2007, 46, 2458
234. L. Pan, D. H. Olson, L. R. Ciemnomolonski, R. Heddy, J. Li, *Angew. Chem. Int. Ed.* 2006, 45, 616
235. B. Chen, C. Liang, J. Yang, D. S. Contreras, Y. L. Clancy, E. B. Lobkovsky, O. M. Yaghi, S. Dai, *Angew. Chem. Int. Ed.* 2006, 45, 1390
236. L. A. Christine, E. A. Kirschhock, M. Maes, M. A. vander Veen, V. Finsy, A. Depla, J. A. Martens, G. V. Baron, P. A. Jacobs, J. F. M. Denayer, D. E. De Vos, *Angew. Chem. Int. Ed.* 2007, 46, 4293
237. H. J. Choi, T. S. Lee, M. P. Suh, *Angew. Chem. Int. Ed.* 1999, 38, 1405
238. Y. B. Dong, M. D. Smith, H. C. Z. Loye, *Angew. Chem. Int. Ed.* 2000, 39, 4271
239. M. Kondo, T. Okubo, A. Asami, S. -I. Noro, T. Yoshitomi, S. Kitagawa, T. Ishii, H. Matsuzaka, K. Seki, *Angew. Chem. Int. Ed.* 1999, 38, 140
240. C. Serre, F. Millange, C. Thouvenot, M. Nogues, G. Marsolier, D. Louer, G. Férey, *J. Am. Chem. Soc.* 2002, 124, 13519
241. F. Millange, C. Serre, G. Férey, *Chem. Commun.* 2002, 822
242. R. Matsuda, R. Kitaura, S. Kitagawa, Y. Kubota, R. V. Belosludov, T. C. Kobayashi, H. Sakamoto, T. Chiba, M. Takata, Y. Kawazoe, Y. Mita, *Nature* 2005, 436, 238

243. J. S. Seo, D. Whang, H. Lee, S. I. Jun, J. Oh, Y. J. Jeon, K. Kimoon, *Nature* 2000, *404*, 982
244. J. Bitta, S. Kubik, *Org. Lett.* 2001, *3*, 2637
245. L. Pu, *Chem. Rev.* 2004, *104*, 1687
246. A. P. Davis, L. J. Lawless, *Chem. Commun.* 1999, *1*, 9
247. D. Yang, X. Li, Y. -F. Fan, D. -W. Zhang, *J. Am. Chem. Soc.* 2005, *127*, 7996
248. S. Y. Liu, K. Y. Law, Y. B. Hea, W. H. Chan, *Tetrahedron Lett.* 2006, *47*, 7857
249. C. Schmuck, M. Schwegmann, *J. Am. Chem. Soc.* 2005, *127*, 3373
250. S.R. Batten, *CrystEngCommun.* 2001, *3*, 67
251. S. Mahapatra, J. A. Halfen, W. B. Tolman, *J. Am. Chem. Soc.* 1996, *118*, 11575
252. D. Bradshaw, J. B. Claridge, E. J. Cussen, T. J. Prior, M. J. Rosseinsky, *Acc. Chem. Res.* 2005, *38*, 273
253. B. Zhao, X. Y. Chen, P. Cheng, D. Z. Liao, S. P. Yan, Z. H. Jiang, *J. Am. Chem. Soc.* 2004, *126*, 15394
254. D. Venkataraman, G. F. Gardner, S. Lee, J. S. Moore, *J. Am. Chem. Soc.* 1995, *117*, 11600
255. W. Fujita, K. Awaga, *J. Am. Chem. Soc.* 2001, *123*, 3601
256. M. Fujita, Y. J. Kwon, S. Washizu, K. Ogura, *J. Am. Chem. Soc.* 1994, *116*, 1151
257. X. R. Meng, Y. L. Song, H. W. Hou, Y. T. Fan, G. Li, Y. Zhu, *Inorg. Chem.* 2003, *42*, 1306
258. B. J. Holliday, C. A. Mirkin, *Angew. Chem. Int. Ed.* 2001, *40*, 2023
259. D. Braga, F. Grepioni, G. R. Desiraju, *Chem. Rev.* 1998, *98*, 1375
260. B. -H. Ye, M. -L. Tong, X. -M. Chen, *Coord. Chem. Rev.* 2005, *249*, 545
261. G. -F. Liu, B. -H. Ye, Y. -H. Ling, X. M. Chen, *Chem. Commun.* 2002, 1442
262. A. F. Wells, *Structural Inorganic Chemistry*, 5th ed., Oxford University Press, Oxford, 1984
263. A. F. Wells, *Three-dimensional Nets and Polyhedra*, Wiley, New York, 1977
264. S. Hikichi, M. Yoshizawa, Y. Sasakura, M. Akita, Y. Moro-oka, *J. Am. Chem. Soc.* 1998, *120*, 10567
265. D. M. Kurtz, *Chem. Rev.* 1996, *96*, 585
266. B. N. Figgis, *Introduction to Ligand Fields*, John Wiley, New York, 1966
267. R. W. Corkery, D. C. R. Hockless, *Acta Crystallogr.* 1997, *C53*, 840
268. T. J. Prior, J. C. Burley, *Acta Crystallogr.* 2005, *E61*, m1424
269. W. C. McCrone, *Physics and Chemistry of the Organic Solid State, Vol. 2*, Interscience, New York, 1965, 725

270. J. S. Miller, M. Drillon, *Magnetism: Molecules to Materials II*, Wiley-VCH, Weinheim, 2001
271. W. Jones, *Organic Molecular Solids: Properties and Applications*, CRC Press: Boca Raton, FL, 1997
272. A. Dey, G. R. Desiraju, *CrystEngComm*. 2006, 478
273. J. Bernstein, R. J. Davey, J. -O. Henck, *Angew. Chem. Int. Ed.* 1999, 38, 3440
274. T. Beyer, G. M. Day, S. L. Price, *J. Am. Chem. Soc.* 2001, 123, 5086
275. J. Bernstein, *Polymorphism in Molecular Crystals*, Oxford University Press, 2002
276. J. A. R. P. Sarma, G. R. Desiraju, *Crystal Engineering: The Design and Application of Functional Solids* (Eds.: K. R. Seddon, M. J. Zaworotko), Kluwer, Dordrecht, 1999, 539, 325
277. D. Braga, *Chem. Commun.* 2003, 2751
278. J. A. McMahon, M. J. Zaworotko, J. F. Remenar, *Chem. Commun.* 2004, 278
279. D. Braga, G. Cojazzi, A. Abati, L. Maini, M. Polito, L. Scaccianoce, F. Grepioni, *J. Chem. Soc., Dalton Trans.* 2000, 3969
280. B. Moulton, M. J. Zaworotko, *Chem. Rev.* 2001, 101, 1629
281. J. K. Beattie, T. W. Humbley, J. A. Kelpetko, A. F. Master, P. Turner, *Polyhedron* 1998, 17, 1343
282. T. Ama, M. M. Rashid, T. Yonemura, H. Kawaguchi, A. Takeuchi, T. Yasui, *Coord. Chem. Rev.* 2000, 198, 101
283. R. Chakrabarty, B. K. Das, *J. Mol. Catal. A: Chem.* 2004, 223, 39.
284. Vogel's Textbook of Practical Organic Chemistry, 5th ed, revised by B. S. Furniss, A. J. Hannaford, P. W. G. Smith, A. Tatchell, Longmann Scientific & Technical, UK, 1989
285. G. M. Sheldrick, SHELXS97, *Program for the Solution of Crystal Structures*, Univ. of Gottingen, Germany, 1997
286. G. M. Sheldrick, SHELXL97, *Program for the Refinement of Crystal Structures*. Univ. of Gottingen, Germany, 1997
287. SHELXTL Release 5.10; *The Complete Software Package for Single Crystal Structure Determination*. Bruker AXS Inc., Madison, WI 53719-1173, 1997
288. C. Benelli, A. J. Blake, E. K. Brechin, S. J. Coles, A. Graham, S. G. Harris, S. Meier, A. Parkin, S. Parsons, A. M. Seddon, R. E. P. Winpenny, *Chem. Eur. J.* 2000, 6, 883
289. M. P. Doyle, V. Bagheri, *J. Org. Chem.* 1981, 46, 4806
290. A. M. Barrios, S. J. Lippard, *J. Am. Chem. Soc.* 1999, 121, 11751
291. H. Shim, F. M. Raushel, *Biochemistry* 2000, 39, 7357

292. Y. -H. Liu, H. -L. Tsai, Y. -L. Lu, Y. -S. Wen, J. -C. Wang, K. -L. Lu, *Inorg. Chem.* 2001, *40*, 6426
293. R. Lachicotte, A. Kitaygorodskiy, K. S. Hagen, *J. Am. Chem. Soc.* 1993, *115*, 8883
294. D. W. Christianson, C. A. Fierke, *Acc. Chem. Res.* 1996, *29*, 331
295. B. -H. Ye, X. -Y. Li, I. D. Williams, X. -M. Chen, *Inorg. Chem.* 2002, *41*, 6426
296. F. E. Jacobsen, J. A. Lewis, S. M. Cohen, *J. Am. Chem. Soc.* 2006, *128*, 3156
297. A. Erxleben, *Coord. Chem. Rev.* 2003, *246*, 203
298. M. Super, E. Berluche, C. Costello, E. Beckman, *Macromolecules*, 1997, *30*, 368
299. T. Tsuruta, Y. Kawakami, *Tetrahedron* 1973, *29*, 1179
300. T. Ohmura, W. Mori, T. Takei, T. Ikeda, A. Maeda, *Mater. Sci. Poland* 2005, *23*, 729
301. W. Clegg, D. Harbron, C. Holman, P. Hunt, I. Little, B. Straughan, *Inorg. Chim. Acta* 1991, *186*, 51
302. J. Lewiński, W. Bury, M. Dutkiewicz, M. Maurin, I. Justyniak, J. Lipkowski, *Angew. Chem. Int. Ed.* 2008, *47*, 573
303. H. Kwak, S. H. Lee, S. H. Kim, Y. M. Lee, B. K. Park, E. Y. Lee, Y. J. Lee, C. Kim, S. -J. Kim, Y. Kim, *Polyhedron* 2008, *27*, 3484
304. P. J. Hagrman, D. Hagrman, J. Zubieta, *Angew. Chem. Int. Ed.* 1999, *38*, 2639
305. O. Sato, T. Iyoda, A. Fujishima, K. Hashimoto, *Science* 1996, *271*, 49
306. R. G. Harrison, O. D. Fox, M. O. Meng, N. K. Dalley, L. J. Barbour, *Inorg. Chem.* 2002, *41*, 838
307. L. Pan, E. B. Woodlock, X. Wang, K. -C. Lam, A. L. Rheingold, *Chem. Commun.* 2001, 1762
308. S. M. Kuznicki, V. A. Bell, S. Nair, H. W. Hillhouse, R. M. Jacubinas, C. M. Braunbarth, B. H. Toby, M. Tsapatsis, *Nature* 2001, *412*, 720
309. O. M. Yaghi, H. Li, T. L. Groy, *J. Am. Chem. Soc.* 1996, *118*, 9096
310. L. Pan, H. Liu, X. Lei, X. Huang, D. H. Olson, N. J. Turro, J. Li, *Angew. Chem. Int. Ed.* 2003, *42*, 542
311. G. H. Halder, C. J. Kepert, B. Moubaraki, K. S. Murray, J. D. Cashion, *Science* 2002, *298*, 1762
312. W. Lin, Z. Wang, L. Ma, *J. Am. Chem. Soc.* 1999, *121*, 11249
313. J. Tao, X. Yin, Z. -B. Wei, R. -B. Huang, L. -S. Zheng, *Eur. J. Inorg. Chem.* 2004, 125
314. P. J. Hagrman, D. Hagrman, J. Zubieta, *Angew. Chem. Int. Ed. Engl.* 1999, *38*, 2638
315. S. L. James, *Chem. Soc. Rev.* 2003, *32*, 276
316. A. J. Fletcher, K. M. Thomas, M. J. Rosseinsky, *J. Solid State Chem.* 2005, *178*, 2491

317. E. V. Anokhina, A. J. Jacobson, *J. Am. Chem. Soc.* 2004, *126*, 3044
318. J. Scheerder, J. F. J. Engbersen, A. Casnati, R. Ungaro, D. N. Reinhoudt, *J. Org. Chem.* 1995, *60*, 6448
319. M. Boiocchi, B. L. Del. D. E. Gomez, L. Fabbrizzi, M. Licchelli, E. Monzani, *J. Am. Chem. Soc.* 2004, *126*, 16507
320. T. L. Kurth, F. D. Lewis, *J. Am. Chem. Soc.* 2003, *125*, 13760
321. P. R. Dave, G. Doyle, T. Axenrod, H. Yazdekhashti, H. L. Ammon, *J. Org. Chem.* 1995, *60*, 6946
322. G. Piacenza, C. Beguet, E. Wimmer, R. Gallo, M. Giorgi, *Acta Cryst. Sec. C* 1997, *C53*, 1459
323. B. -C. Tzeng, Y. -C. Huang, B. -S. Chen, W. -M. Wu, S. -Y. Lee, G. -H. Lee, S. -M. Peng, *Inorg. Chem.* 2007, *46*, 186
324. R. -H. Zeng, Z. -Q. Fang, F. Sun, L. -S. Jiang, Y. -W. Tang, *Acta Cryst. Sec. E* 2007, *E63*, m1813
325. W. Huang, H. Qian, S. Gou, C. Yao, *J. Mole. Struct.* 2005, *743*, 183
326. M. Inosako, C. Shimokawa, H. Sugimoto, N. Kihara, T. Takata, S. Itoh, *Chem. Lett.* 2007, *36*, 1306
327. A. M. Bittner, P. Behrens, E. Baeuerlein, *Handbook of Biomineralization: Biomimetic and Bioinspired Chemistry*, 2007, 335
328. A. Nangia, G.R. Desiraju, in: E. Weber (Ed.), *Supramolecular Synthons and Pattern Recognition: Design of Organic Solids*, Springer-Verlag Berlin, Springer-Verlag, Berlin, 1998
329. C. -L. Lin, C. -C. Lai, Y. -H. Liu, S. -M. Peng, S. -H. Chiu, *Chem. A. Eur. J.* 2007, *13*, 4350
330. E. Pardo, K. Bernot, M. Julve, F. Lloret, J. Cano, R. Ruiz-Garcia, J. Pasan, C. Ruiz-Perez, X. Ottenwaelder, Y. Journaux, *Chem. Commun.* 2004, 920
331. M. Fujita, M. Tominaga, A. Hori, B. Therrien, *Acc. Chem. Res.* 2005, *38*, 371
332. S. R. Seidel, P. J. Stang, *Acc. Chem. Res.* 2002, *35*, 972
333. M. D. Pluth, R. G. Bergman, K. N. Raymond, *Science*, 2007, *316*, 85
334. S. Sato, K. L. Suzuki, M. Kawano, T. Ozeki, M. Fujita, *Science*, 2006, *313*, 1273
335. K. M. Anderson, K. Afarikia, H. Yu, A. E. Goeta, J. W. Steed, *Cryst. Growth & Des.* 2006, *6*, 2109
336. X. -L. Wang, C. Qin, E. -B. Wang, L. Xu, Z. -M. Su, C. -W. Hu, *Angew. Chem. Int. Ed. Eng.* 2004, *43*, 5036
337. J. Yoon, S. K. Kim, N. J. Singh, K. S. Kim, *Chem. Soc. Rev.* 2006, *35*, 355

338. C. Miller, *Nature* 2006, 440, 484
339. P. D. Beer, P. A. Gale, *Coord. Chem. Rev.* 2001, 213, 79
340. M. W. Peczuł, A. D. Hamilton, *Chem Rev.* 2000, 100, 2479
341. S. -L. Zheng, P. Coppens, *Cryst. Growth & Des.* 2005, 5, 2050
342. A. Bianchi, K. Bowman-James, E. Garcia-España, *Supramolecular Chemistry of Anions*, Wiley, New York, 1997
343. P. D. Beer, P. A. Gale, *Angew. Chem. Int. Ed.* 2001, 40, 487
344. N. M. Sangeetha, U. Maitra, *Chem. Soc. Rev.* 2005, 34, 821
345. K. Y. Lee, D. J. Mooney, *Chem. Rev.* 2001, 101, 1869
346. I. C. Kwon, Y. H. Bae, S. W. Kim, *Nature* 1991, 354, 291
347. C. Wang, R. J. Stewart, J. Kopeček, *Nature* 1999, 397, 417
348. E. Ostuni, P. Kamaras and R. G. Weiss, *Angew. Chem. Int. Ed. Engl.* 1996, 35, 1324
349. U. Maitra, S. Mukhopadhyay, A. Sarkar, P. Rao, S. S. Indi, *Angew. Chem. Int. Ed.* 2001, 40, 2281
350. S. Bhattacharya, U. Maitra, S. Mukhopadhyay, A. Srivastava, *Molecular Gels*, ed. R. G. Weisse, P. Terech, Springer, Dordrecht, 2006
351. L.R. Pratt, A. Pohorille, *Chem. Rev.* 2002, 102, 2671
352. P. Vishweshwar, A. Nangia, V. M. Lynch, *CrystEngComm.* 2003, 5, 164
353. C. Tamuly, N. Barooah, M. Laskar, R. J. Sarma, J. B. Baruah, *Supramol. Chem.* 2006, 18, 605
354. F. P. Pruchnik, U. Dawid, A. Kochel, *Polyheron*, 2006, 25, 3647
355. P. Rajakumar, A. M. A. Rasheed, *Tetrahedron*, 2005, 61, 5351
356. W. N. Wu, W. B. Yuan, N. Tang, R. D. Yang, L. Yan, Z. H. Xu, *Spectrochim. Acta A*, 2006, 65, 912
357. U. Mukhopadhyay, I. Bernal, *Cryst. Growth & Design*, 2005, 5, 1687
358. S. K. Ghosh, P. K. Bharadwaj, *Inorg. Chem.* 2004, 43, 5180

List of Publications:

Articles/Papers based on this study have appeared in:

1. A. Karmakar, R. J. Sarma, J. B. Baruah, *Eur. J. Inorg. Chem.* **2006**, 4673-4678
2. A. Karmakar, K. Deka, R. J. Sarma, J. B. Baruah, *Inorg. Chem. Commun.* **2006**, 9, 836-838
3. A. Karmakar, R. J. Sarma, J. B. Baruah, *Inorg. Chem. Commun.* **2006**, 9, 1169-1172
4. A. Karmakar, R. J. Sarma, J. B. Baruah, *CrystEngComm.* **2007**, 9, 379-389
5. A. Karmakar, R. J. Sarma, J. B. Baruah, *Eur. J. Inorg. Chem.* **2007**, 643-647
6. A. Karmakar, R. J. Sarma, J. B. Baruah, *Polyhedron*, **2007**, 26, 1347-1355
7. A. Karmakar, J. B. Baruah, *Polyhedron*, **2008**, 27, 3409-3416
8. A. Karmakar, J. B. Baruah, *J. Mol. Struct.* **2008**, 888, 197-203
9. A. Karmakar, J. B. Baruah, *Supramolecular Chemistry*, **2008**, 20, 667-674
10. A. Karmakar, J. B. Baruah, *Inorg. Chem. Commun.* **2009**, 12, 140-144
11. A. Karmakar, J. B. Baruah, R. B. Shankar, *CrystEngComm.* **2009** (Article in press)